

Future Steel Vehicle Phase I



Reduced **CO₂**



95g/km

Environmental



Designed In Steel

Contents

1	Preface	1
1.1	Members of WorldAutoSteel are:	2
1.2	FSV Technology Partners (Phase 1)	2
2	Executive summary	3
2.1	Project Objectives	3
2.1.1	FSV Project Phases Overview	4
2.2	Vehicle Size & Powertrains	5
2.2.1	Vehicle Size	5
2.2.2	FSV Advanced Powertrain Options & Performances	6
2.3	Future Steel Vehicle Design & Layout	7
2.3.1	FSV Front-End	7
2.4	Future Steel Vehicle-1 (FSV-1)	9
2.4.1	FSV1 - (PHEV ₂₀)	9
2.4.2	FSV-1 - BEV	10
2.5	Future Steel Vehicle -2 (FSV-2)	11
2.5.1	FSV-2 (PHEV ₄₀)	11
2.5.2	FSV-2- FCEV	12
2.6	FSV - Estimated Masses	13
2.7	FSV Cost of Ownership	15
2.8	Environmental Impact	17
2.8.1	FSV Fuel Economy and CO ₂ Emissions	17
2.9	Well-to-Pump Assessment	19
2.10	FSV-1 - Environmental Assessment	20
2.10.1	FSV-1 - Pump-to-Wheel CO ₂ Emissions	20
2.10.2	FSV-1 - Well-to-Wheel CO ₂ Emissions	21
2.11	FSV-2 - Environmental Assessment	22
2.11.1	FSV-2 - Pump-to-Wheel CO ₂ Emissions	22
2.11.2	FSV-2 - Well-to-Wheel CO ₂ Emissions	23
2.12	Technology Assessment	24
2.12.1	Future Advanced Powertrains Summary	24
2.12.2	Advanced Powertrain Technologies	25
2.12.3	Automotive Technology Assessment	31
2.13	Future Safety Requirements	34
2.14	Fuel Economy Requirements	35

3	Market Analysis	36
3.1	Global Market Analysis	36
3.1.1	Overview	36
3.1.2	Global Auto Market Analysis	37
3.1.3	Market Overview By Region	39
3.2	OEM Directional Trends	46
3.2.1	Overview	46
3.2.2	Future Forecast of Vehicle Technologies by CARB	47
3.2.3	OEM Announcements	48
3.2.4	Battery Electric Vehicles	49
3.2.5	Fuel Cell Electric Vehicles	51
3.2.6	Plug-in Hybrid Electric Vehicles	52
3.2.7	Toyota	54
3.2.8	General Motors	55
3.2.9	Ford	56
3.2.10	Chrysler	57
3.2.11	Mitsubishi	59
3.2.12	Honda	60
3.2.13	Hyundai	61
3.2.14	Mazda	62
3.2.15	Volvo	63
3.2.16	Nissan	64
3.2.17	TATA Motors	65
3.2.18	Peugeot	66
3.2.19	Newcomers to Plug-ins	67
3.3	Alternate Propulsion Vehicles Benchmark	72
3.3.1	Research Methodology	72
3.3.2	Benchmark Vehicle Selection	73
3.3.3	2009 Mitsubishi i-MiEV	74
3.3.4	2009 Honda FCX Clarity	87
3.3.5	2011 Chevrolet Volt	106
3.3.6	Mercedes Blue-Zero Concept	117
3.3.7	Conclusion	125
3.4	Future Safety Requirements	126
3.4.1	Overview	126
3.4.2	US - Future Safety Requirements	127
3.4.3	Europe - Future Safety Requirements	134
3.4.4	India - Future Regulations	139
3.4.5	Global Technical Regulations	139
3.5	Future Fuel Economy Requirements	141
3.5.1	Overview	141
3.5.2	Future Fuel Economy/CO ₂ Standard	143
3.5.3	United States	143
3.5.4	Europe	146

3.5.5	Japan	147
3.5.6	China	148
3.5.7	India	149
3.6	Future Ozone Emission Standards	150
3.6.1	Kyoto Protocol Overview	150
3.6.2	United States Air Pollution Standards	150
3.6.3	Future HC, NOx Emission Standards	151
3.6.4	United States	151
3.6.5	Green House Gas Emissions Standards	154
3.6.6	Europe Emission Requirements	156
3.6.7	Asia Pacific	157
3.6.8	Vehicle Emissions Test Protocols - Japan	158
3.6.9	Other requirements	158
3.7	Vehicle Classification	159
3.7.1	United States	160
3.7.2	Europe	161
3.7.3	China	162
3.7.4	India	163
4	Future Steel Vehicle Propulsion Systems	164
4.1	Overview	164
4.2	Advanced Powertrain Block Diagrams	165
4.2.1	BEV (Battery Electric Vehicles)	165
4.2.2	FCEV (Fuel Cell Electric Vehicles)	166
4.2.3	PHEV Series Hybrid Vehicle	167
4.2.4	PHEV Parallel Hybrid Vehicle	168
4.2.5	PHEV Parallel-Split Hybrid Vehicle	169
4.3	PHEV Industry Perspectives	170
4.4	Parallel-Split Series Simulation Results	172
4.5	Conclusion	174
5	Future Steel Vehicle - Technology Implementation	176
5.1	Vehicle Classification	176
5.2	Size Comparison	177
5.3	Exterior Dimensions	178
5.4	Interior Dimensions	179
5.5	Occupant and Luggage Carrying Capacity	180
5.6	FSV Front-End	181
5.6.1	Front-End Comparison	182
5.7	FSV Front Rails	183
5.8	FSV Powertrain	184
5.8.1	Options and Performance	184
5.8.2	Mass and Cost Impacts	184
5.9	Battery Electric Vehicle (BEV)	186
5.9.1	Mass Estimates	187

5.9.2	Technical Specification & Performance	188
5.9.3	Layout & Design	192
5.9.4	Benchmark -2009 Mitsubishi i-MiEV	193
5.9.5	Bill of Materials	195
5.10	Plug-In Hybrid with a 32 km (20 mile) All Electric Range(PHEV ₂₀)	198
5.10.1	Mass Estimates	199
5.10.2	Technical Specification & Performance	200
5.10.3	Layout & Design	203
5.10.4	Bill Of Materials (BOM)	205
5.11	Plug-In Hybrid with a 64 km(40 mile) All Electric Range(PHEV ₄₀)	209
5.11.1	Mass Estimates	210
5.11.2	Technical Specification & Performance	211
5.11.3	Layout & Design	214
5.11.4	Bill Of Materials (BOM)	215
5.12	Fuel Cell Electric Vehicle	219
5.12.1	Mass Estimates	220
5.12.2	Technical Specification & Performance	221
5.12.3	Layout & Design	224
5.12.4	Bill Of Materials (BOM)	225
5.13	Vehicle Performance - Results Summary	229
5.14	Powertrain Design Evaluation Results	230
5.15	Fuel Economy and Emissions	231
5.16	FSV-1 Cost of Ownership	232
5.17	FSV-2 Cost of Ownership	233
6	Vehicle Package Development	234
6.1	Synopsis	234
6.2	Electric Drive	235
6.2.1	Motor Vertical - in Line with Axle Centerline	235
6.2.2	Motor Horizontal - Front of Axle Centerline	236
6.2.3	Motor Horizontal - Rear of Axle Centerline	237
6.2.4	Motor Horizontal - Inverter/Controller on Top	238
6.2.5	Motor - Integrated Design Concept	239
6.2.6	Motor - Final Optimised Design	240
6.3	Battery	241
6.3.1	Single Large Underfloor Battery	241
6.3.2	Two Pack Design - Tunnel area and Underhood	242
6.3.3	T-Shaped Pack - Preliminary Design	243
6.3.4	T-Shaped Pack - Refined	244
6.3.5	T-Shaped Pack - Reorganized Cell Arrangement	245
6.3.6	T-Shaped Pack - Under-seat Pods	246
6.3.7	T-Shaped Pack - Refined with Accessories	247
6.3.8	T-Shaped Pack and Sub-Pack - Final design	248
6.3.9	I-Shaped Pack - Packaging Impact	249
6.3.10	Future Battery Pack and its impact to FSV Structure	250

6.4	Fuel Cell and Hydrogen Storage	251
6.4.1	Fuel Cell System in Engine Compartment	251
6.4.2	Fuel Cell Stack under Inverter/Controller	252
6.4.3	Fuel Stack under Rear Seat	253
6.4.4	Fuel Cell Stack in Tunnel Area	254
6.4.5	Fuel Cell System - Final Design with Tonji system	255
6.5	Engine and Generator	256
6.5.1	Engine/Generator in Front	256
6.5.2	Engine/Generator in Rear - Horizontal	257
6.5.3	Engine/Generator in Rear - Vertical	258
6.5.4	Engine/Generator in Rear - 17° tilt	259
6.5.5	Engine/Generator in Rear - 45° tilt	260
6.6	Front Suspension Designs	261
6.6.1	Upper Control Arm / Lower Trailing Arm (sprung)	261
6.6.2	Upper Control Arm (sprung) / Lower Trailing Arm	262
6.6.3	Upper Control Arm (sprung) / Lower Control Arm	263
6.6.4	Upper Control Arm / Lower Control Arm (sprung)	265
6.6.5	Horizontal Leaf Spring Design	266
6.6.6	McPherson Strut / Lower Trailing Arm	267
6.6.7	Conventional McPherson Strut	268
6.7	Rear Suspension Designs	270
6.7.1	Twist Beam or Torsion Beam	270
6.7.2	Passive Wheel	271
6.7.3	Trailing Arm with 2 Camber Links	272
6.7.4	Double Wishbone (SLA)	273
6.7.5	Chapman Strut / McPherson Strut	274
6.7.6	H-Arm with Camber Control Link	275
6.8	FSV Suspension - Decision Matrix	276
6.9	FSV Suspensions - Layout	277
6.10	FSV Suspension Characteristics	278
6.10.1	Camber	278
6.10.2	Toe Change	279
7	Sensitivity Analysis	280
7.1	Synopsis	280
7.2	Battery Technology	281
7.2.1	Battery Energy Density	282
7.2.2	Battery Materials	283
7.2.3	Battery Targets	285
7.2.4	Energy Storage Limits	286
7.2.5	Case Studies	286
7.2.6	Case Study Results	290
7.2.7	Packaging Impact	291
7.2.8	Battery Shape Assessment	292
7.3	Motor Technology and Cooling	293

7.3.1	FSV Recommendation	293
7.3.2	DOE Targets	294
7.3.3	FSV Motor Versus ICE	294
7.3.4	Motor and Transmission Gear Ratio	295
7.3.5	Motor and Power Electronics with Cooling System	296
7.3.6	FSV BEV Energy Balance	297
7.3.7	FSV BEV, Motor Torque versus RPM Curves	298
7.4	Fuel Cell Technology	300
7.4.1	FSV Recommendation	300
7.4.2	Energy Density Comparison	301
7.4.3	FSV Packaging	302
8	Environmental Impact	303
8.1	Overview	303
8.1.1	Fuel Efficiency and CO ₂ Relevance	303
8.1.2	Air Pollution	305
8.1.3	Noise Pollution	305
8.2	Well-to-Wheel Efficiencies	306
8.2.1	Total Life Cycle Assessment	306
8.2.2	Well-to-Pump Assessment - Fuel Cycle	307
8.2.3	Pump-to-Wheel Assessment - FSV	309
8.3	FSV Environmental Assessment	311
8.3.1	FSV-1 - Assessment	311
8.3.2	FSV-2 - Assessment	316
8.4	Well-to-Wheel Energy Usage	318
8.4.1	Conventional Technologies	319
8.4.2	Advanced Technologies	320
8.4.3	FSV Well-to-Wheel Energy Usage	321
9	Advanced Powertrain Technologies	322
9.1	Overview	322
9.2	Fuel Cell Technology	323
9.2.1	Overview	323
9.2.2	Fuel Cell Stack	327
9.2.3	Balance of Plant (BOP)	331
9.2.4	Miscellaneous Parts	338
9.2.5	Operating Pressure	339
9.2.6	Operating Temperature	339
9.2.7	Performance	340
9.2.8	Mass Production Volume Forecast	346
9.2.9	Cost Sensitivity	348
9.2.10	Fuel Cell System Recommendations for FSV	349
9.2.11	Hydrogen Storage Systems	355
9.2.12	Hydrogen Refueling Infrastructure	362
9.3	Battery Technology	366

9.3.1	Overview	366
9.3.2	Nickel-Metal Hydride (NI-MH) Battery	368
9.3.3	Lithium-Ion Battery	369
9.3.4	Packaging	373
9.3.5	Future Trends	374
9.3.6	Recommendations	376
9.4	Ultra-Capacitor Technology	377
9.4.1	Overview	377
9.4.2	Energy and Power Density	377
9.4.3	Performance Industry Targets	379
9.4.4	Packaging	380
9.4.5	Advantages	380
9.4.6	Disadvantages	380
9.4.7	Future Trends (2015-2020)	381
9.4.8	Recommendations	382
9.5	Internal Combustion Engine Technology	383
9.5.1	Overview	383
9.5.2	Gasoline Engine	385
9.5.3	Diesel Engine	387
9.5.4	Future Trends	389
9.5.5	Alternative Energy Sources	390
9.6	Transmission and Transaxle	397
9.6.1	Overview	397
9.6.2	Continuously Variable Transmission (CVT)	399
9.6.3	Dual Clutch Transmission (DCT)	400
9.6.4	6 - 8 Speed Automatic Transmission	402
9.6.5	Future Trends	403
9.6.6	High Voltage Generators and Traction Motors	404
9.6.7	Wheel Motor as Primary or Secondary Drive	408
9.6.8	Traction Motor with Integrated Transaxle	409
9.6.9	Power inverter designs	410
9.6.10	Generator/Motor Recommendations for FSV	411
10	Steel Technologies	412
10.1	Summary	412
10.2	Steel Grades Portfolio - FSV	412
10.3	Processing and Manufacturing Technology Portfolio - FSV	414
10.3.1	Laser Welded Blanks	415
10.3.2	Laser Welded Coil	418
10.4	Laser Welded Rolled Tubes	421
10.5	Multiwall Tube (T ³)	424
10.5.1	MultiWall Tube (T ³ Profiling)	426
10.6	Vibration Damping Steel Sheets and NVH	428
10.6.1	Advantages	429
10.6.2	Automotive Application	429

10.7	Laser Arc Hybrid Welding	431
10.7.1	Advantages	432
10.7.2	Limitations	432
10.8	High Frequency Induction Welded Tubes	432
10.8.1	Automotive Application	434
10.9	Roll Forming	436
10.9.1	Roll Forming Process	436
10.9.2	Advantages	437
10.10	Hot Stamping (Direct and In-Direct)	438
10.10.1	Direct Versus In-Direct Process	438
10.10.2	Properties	439
10.10.3	Material Grades	440
10.10.4	Guidelines	440
10.10.5	Automotive Application	441
10.11	Hydroforming	442
10.11.1	Guidelines	444
10.12	Stamping Advanced High Strength Steel	445
10.12.1	Springback	445
10.12.2	Part Corner Radii	445
10.12.3	Open Ended Profiles	445
10.12.4	Surface Depressions	446
10.12.5	Flanged Holes	446
10.12.6	Surface Transitions	446
10.13	Joining Strategy	447
10.13.1	Resistance Spot Welding	447
10.13.2	Laser Welding	448
10.13.3	Adhesive Bonding	448
10.13.4	Mechanical Joining	449
10.13.5	Hybrid Joining	450
11	Other Advanced Technologies	452
11.1	Drive-by-Wire	452
11.1.1	Overview	452
11.1.2	Types of By-Wire Systems	453
11.1.3	Assessment Scope	455
11.2	Steer-by-Wire	456
11.2.1	Overview	456
11.2.2	General Requirements for Steer-by-Wire	457
11.2.3	Types Of Steer-by-Wire Systems	459
11.2.4	Real Time Performance & Reliability Requirements	462
11.2.5	Mean Time to Failure Greater Than Life of the Vehicle	463
11.2.6	Response Time	464
11.2.7	Tactile Feedback Control	465
11.2.8	Regulatory Requirements for Steering Performance	467
11.2.9	Conclusions	467

11.3	Brake-by-Wire	468
11.3.1	Types Of Brake-by-Wire Systems	468
11.3.2	Advantages Of Brake-by-Wire Systems	468
11.4	Current Challenges to the Auto Industry	470
11.4.1	Costs	470
11.4.2	Application of By-Wire Systems	471
11.4.3	Throttle-by-Wire in Current Cars	471
11.4.4	By-Wire (Active) Suspension Systems In Current Cars	472
11.5	Drive-by-Wire Concept Cars	473
11.5.1	SKF - Bertone	473
11.5.2	Toyota Fine-X	475
11.5.3	Suzuki Ionis	476
11.5.4	FHI - IVX-II	477
11.5.5	Nissan EA2 Concept	478
11.5.6	Mazda Washu	479
11.6	Low Rolling Resistance Tires (LRRT)	480
11.6.1	Overview	480
11.6.2	Role of LRRT in Fuel Consumption	480
11.6.3	Tread Wear, Traction and Temperature Resistance Labeling	481
11.6.4	LRRT - Tread Wear	481
11.6.5	LRRT - Traction	482
11.6.6	LRRT - Temperature Resistance	483
11.6.7	LRRT - Chemical Compound	483
11.6.8	European Emission Rating on Tires	484
11.6.9	North American Emission Rating on Tires	484
11.6.10	Conclusions	486
11.7	Future Lightweight Technologies	487
11.7.1	Overview	487
11.7.2	Automotive Glazing	488
11.7.3	Lighting & Displays	494
11.7.4	LED Lighting – Advantages & Disadvantages	495
11.7.5	Conclusion	496
11.7.6	Lightweight Interior Displays	497
11.7.7	Light Weight Seat Systems	500
11.7.8	Lightweight Seating	501
11.8	Auxiliary Equipment	503
11.8.1	Auxiliary Systems	504
11.8.2	Climate Control	505
11.8.3	Future Technologies to Reduce Climate Control Load	507
12	FSV Structure Design Methodology	516
12.1	Overview	516
12.1.1	FSV Development Process	516
12.1.2	FSV Pilot Project Development Process	517
12.1.3	Objective	518

12.1.4	Optimization Methodology	519
12.2	Baseline Model	520
12.2.1	Baseline Performance	521
12.3	Topology Optimization	525
12.4	3G Optimization	527
12.4.1	Background	527
12.4.2	Load Path Parameterization	528
12.4.3	Problem Statement	531
12.5	Final Design	532
12.6	Final Validation	534
12.6.1	US-NCAP Zero Degree Front Crash	534
12.6.2	IIHS Front Crash 40% ODB	536
12.6.3	Static Stiffness	537
12.7	Conclusion	538
12.8	Manufacturability	539
12.9	3G Optimization Process	542
12.9.1	HEEDS Search Algorithm	542
12.9.2	How HEEDS Works	542
12.9.3	3G Optimization Applied to FSV Pilot Project	545

Bibliography	A
List of Figures	P
List of Tables	U

1.0 Preface

This report documents the results of Phase 1 of the Future Steel Vehicle program.

The Future Steel Vehicle program is the most recent addition to the global steel industry's series of initiatives offering steel solutions to the challenges facing automakers around the world to increase the fuel efficiency of automobiles, reducing Green House Gas emissions, while improving safety, performance and maintaining affordability.

This program follows the Ultra-Light Steel Auto Body (ULSAB) 1998, the Ultra-light Steel Auto Closures (ULSAC) 2000, Ultra-light Steel Auto Suspension (ULSAS) 2000, and ULSAB-AVC (Advanced Vehicle Concepts) 2001.

WorldAutoSteel has commissioned EDAG, Inc., Auburn Hills, Michigan, USA, to conduct an advanced powertrain technology assessment, and to provide vehicle design and program engineering management for the Future Steel Vehicles program. For the Future Steel Vehicle program, EDAG is applying a holistic approach to vehicle layout design using advanced future powertrains and creating a new vehicle architecture that offers mass efficient, steel-intensive solutions. The future advanced powertrains that have major influence on vehicle layout and body structure architecture are: Plug-In Hybrid Electric Vehicle (PHEV), Battery Electric Vehicles, (BEV) and Fuel Cell Electric Vehicles (FCEV).

1.1 Members of WorldAutoSteel are:

- ArcelorMittal - Luxembourg
- Baoshan Iron & Steel Co. Ltd. - China
- China Steel Corporation - Taiwan, China
- Hyundai-Steel Company - South Korea
- JFE Steel Corporation - Japan
- Kobe Steel, Ltd. - Japan
- Nippon Steel Corporation - Japan
- Nucor Corporation - USA
- POSCO - South Korea
- Severstal - Russia/USA
- Sumitomo Metal Industries, Ltd. - Japan
- Tata Steel & Corus - India, UK, Netherlands
- ThyssenKrupp Stahl AG - Germany
- United States Steel Corporation - USA
- Usinas Siderurgicas de Minas Gerais S.A. - Brazil
- Voestalpine Stahl GmbH - Austria

1.2 FSV Technology Partners (Phase 1)

- Quantum Technologies
- Shanghai Fuel Cell Vehicles (SFCV), Tongji University

2.0 Executive summary

2.1 Project Objectives

The future direction of the transportation industry is being influenced by an increasing demand for better fuel economy, and to reduce emissions that result in greenhouse gas induced global warming. Increasing vehicle efficiency and the use of alternate low-carbon content fuels will not only reduce petroleum consumption, but also decrease the carbon footprint associated with the burning of fossil fuels. The use of advanced powertrains will lead to an increased focus on vehicle weight reduction and hence material selection.

This project will illustrate to WorldAutoSteel member companies, the new advanced powertrain technologies that are now being cultivated to fruition towards the year 2020 and beyond. In the Future Steel Vehicle program, EDAG's focus is on a holistic approach to the concept development of innovative vehicle layout and optimized vehicle architecture. The proposed designs will offer advanced high-strength, steel intensive solutions to answer the call of reduced weight vehicles, resulting in a lighter, more fuel and cost efficient vehicle that will reduce the carbon footprint associated with the growing automotive market. Use of advanced high-strength steels and the latest manufacturing processes, which reflect state-of-the-art or future trends, are the primary design objectives. The Future Steel Vehicle development program will focus on the achievement of future crash and safety requirements coupled with the demonstration of low CO₂ emissions, and affordability of a steel intensive vehicle architecture using advanced powertrain technologies.

The main objectives of the FSV program can be broken down into five goals, which encompass the use of advanced high-strength steels:

1. Identify advanced powertrains and their impact on vehicle architecture
2. Investigate steels capability to meet the structural needs of advanced powertrain vehicles
3. Investigate vehicle weight reduction potential with the use of Advanced High-Strength Steels (AHSS), advanced manufacturing processes, and the use of computer aided structural optimization
4. Understand the loads imposed by advanced powertrains on the vehicle structure, thus identifying the requirements for new grades of steel for optimized low-mass vehicle structural applications and design
5. Identify new opportunities for steel uses in advanced powertrains and related infrastructures

2.1.1 FSV Project Phases Overview

The Future Steel Vehicle program is split into the following three phases:

- Phase I: Engineering Study (2008 - July, 2009)
- Phase II: Concept Design (July, 2009 - 2010)
- Phase III: Demonstration of Hardware (2010-2011)

The content of Phase 1 was a comprehensive assessment and identification of advanced powertrains and future automotive technology applicable to year 2020 high volume vehicle production. Other areas to be covered are the impact of future worldwide safety requirements, fuel efficiency mandates, and the total vehicle environmental impact. Worldwide, various countries are pursuing regulations of greenhouse gases and are assessing CO₂ emissions in terms of the well-to-wheel efficiency of advanced powertrains using alternate fuels such as electricity, hydrogen and bio-fuels. The deliverables from Phase 1 include complete vehicle technical specifications and vehicle layout showing major components of advanced powertrain modules, and engineering content, as shown in Figure 2.1.

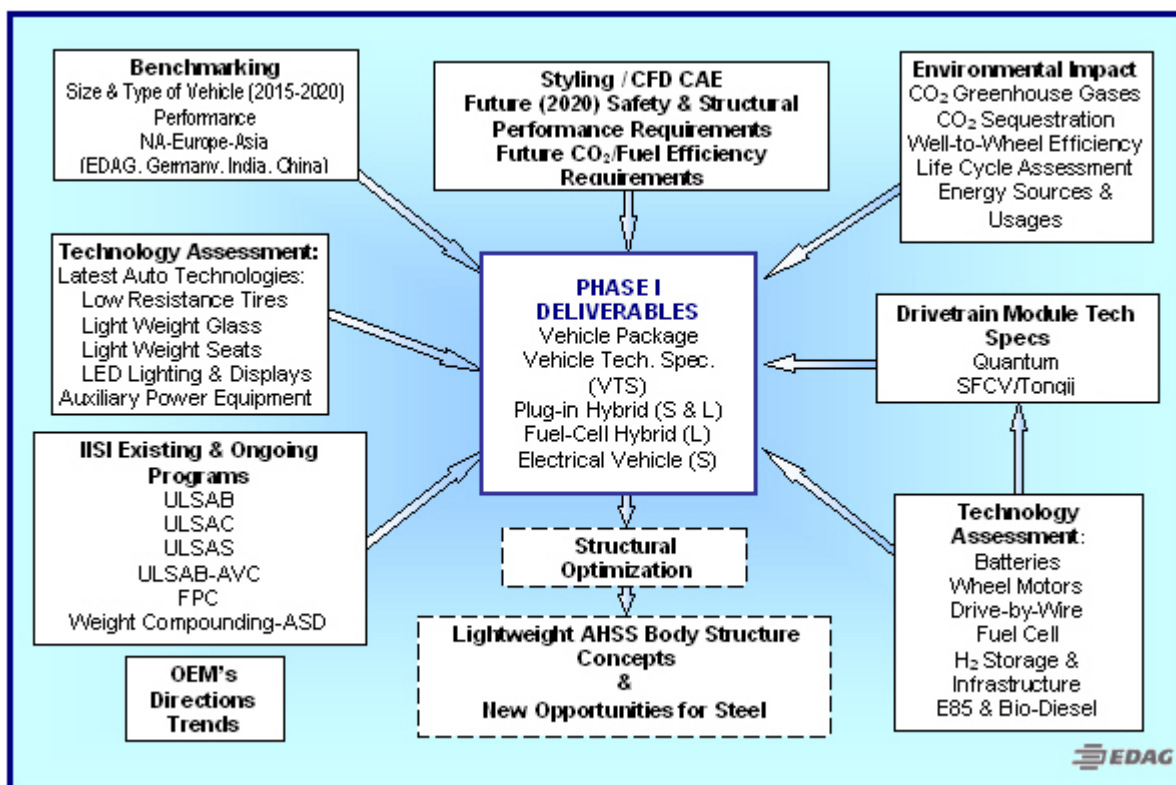


Figure 2.1: Phase 1 - Engineering study: content & methodology

2.2 Vehicle Size & Powertrains

2.2.1 Vehicle Size

Worldwide market analysis shows that over 70% of the cars sold in today's marketplace share two vehicle sizes: the small Car, (A & B Class) up to 4,000 mm long, and the mid-class car, (C & D class) up to 4,900 mm long. To encompass both segments of the worldwide market, the Future Steel Vehicle program includes two vehicle sizes, FSV-1 and FSV-2. The packaging specifications and vehicle performance for each of the vehicles were determined to be acceptable and appropriate for each class of vehicle, in line with worldwide OEM trends.

The determination of vehicle interior dimensions and luggage space requirements were based on each vehicle size and its intended usage. FSV-1 is a small vehicle mainly intended for city and shorter daily driving and, in terms of size, FSV-2 is at the low-end of the mid-size range of vehicles, intended for long range driving with larger luggage carrying capacity. The FSV-1 and FSV-2 layout and capacities are shown in Table 2.1.

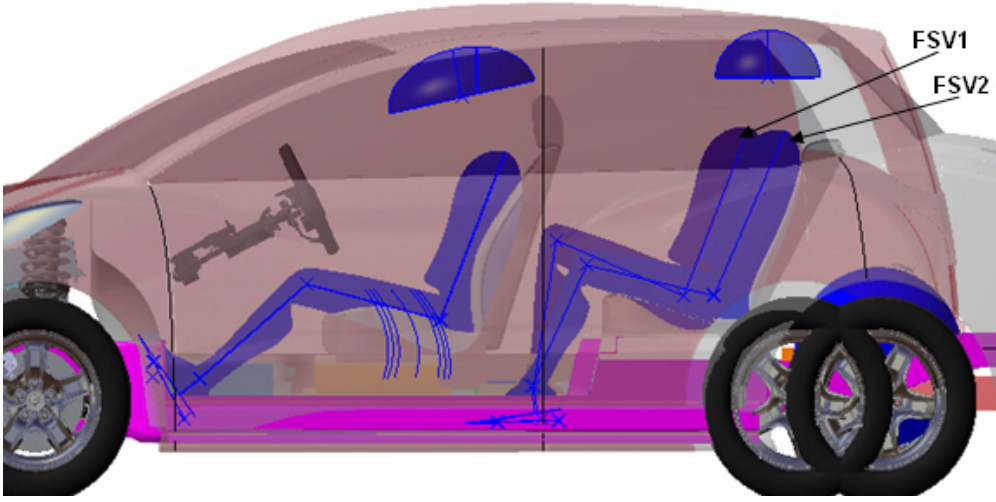
FSV1 Occupants:		FSV2 Occupants:	
Front Row Seating: 2		Front Row Seating: 2	
Rear Row Seating: 2+		Rear Row Seating: 3	
			
Class	Front Leg Room [mm]	Rear Leg Room [mm]	Luggage [Liters]
FSV-1	1070	825	250
FSV-2	1070	925	370
A	1055	760	170
B	1065	850	340
C	1070	877	370
D	1075	961	450

Table 2.1: FSV-1 and FSV-2 vehicle capacity

2.2.2 FSV Advanced Powertrain Options & Performances

The assessment of the announcements from automobile manufacturers shows progress on various technologies that include;

1. Conventional Internal Combustion Engine (ICE) based smaller more efficient gasoline/diesel vehicles
2. Hybrid Electric Vehicles (HEV) predominantly using fossil-based petroleum fuels
3. Plug-in Hybrid Electric Vehicles (PHEV) with a limited range of distance driven in electric mode using electricity from the power grid. This option offers a significant reduction in fossil based petroleum usage, especially when the daily distances driven are close to the vehicle's electric range, the additional distance being driven using fossil based petroleum fuels
4. Battery Electric Vehicles (BEV) with driving range of approximately 200 km
5. Fuel Cell Electric Vehicles (FCEV) using hydrogen gas as a fuel source

Assessment of year 2015 to 2020 powertrain component mass, cost and sizes were taken into account when determining the suitability of each powertrain for each vehicle size. The powertrains chosen for the smaller vehicle (FSV-1) included Plug-in Hybrid (PHEV₂₀) and Battery Electric Vehicle (BEV). For the smaller car, the Fuel Cell Electric Vehicle (FCEV) powertrain was not implemented due to excessive cost and complexity involved with hydrogen storage and fuel stack installation. For the larger vehicle (FSV-2) the BEV option was not included due the larger and more costly battery requirements for larger vehicles. The chosen powertrain options and performance parameters are shown in Table 2.2.

	Plug-in Hybrid (PHEV)	Fuel Cell (FCEV)	Battery Electric (BEV)
FSV 1	PHEV 20 Electric Range - 32km (20mi) Total Range - 500km Max Speed -150km/h 0-100km/h 11-13s		BEV Total Range - 250km Max Speed -150km/h 0-100km/h 11-13s
FSV 2	PHEV 40 Electric Range - 64km (40mi) Total Range - 500km Max Speed - 161km/h 0-100km/h 10-12s	FCEV Total Range - 500km Max Speed - 161km/h 0-100km/h 10-12s	

Table 2.2: *Powertrain options & performance*

2.3 Future Steel Vehicle Design & Layout

Results of technology assessment and powertrain component feasibility studies conducted by Quantum and Shanghai Fuel Cell Vehicles (SFCV), were used for vehicle layout studies. Several layouts were analyzed for each vehicle and powertrain for efficient usage of packaging space and vehicle mass distribution. For the two chosen vehicle sizes, it became apparent that a common platform theme can be developed, utilizing shared technologies in a modular fashion between all four vehicle powertrain variants:

1. FSV-1 - Battery Electric Vehicle (BEV)
2. FSV-1 - Plug-In Hybrid Electric with a 32 km (20 mile) all electric range (PHEV₂₀)
3. FSV-2 - Plug-In Hybrid Electric with a 65 km (40 mile) all electric range (PHEV₄₀)
4. FSV-2 - Fuel Cell Hybrid Electric Vehicle (FCEV)

2.3.1 FSV Front-End

Electrically driven front wheels, applicable to all the powertrains, simplify the front-end layout and leads to a significant reduction in vehicle front-end length. Drivetrains consisting of a traction motor, reduction gearing, and differential as a combined unit yield a more compact space efficient design, as compared to a conventional internal combustion engine (ICE), as shown in Figure 2.2, and Figure 2.3.

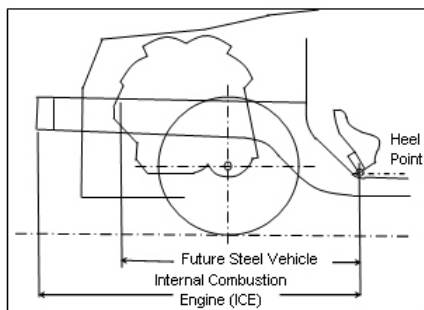


Figure 2.2: Conventional ICE front-end

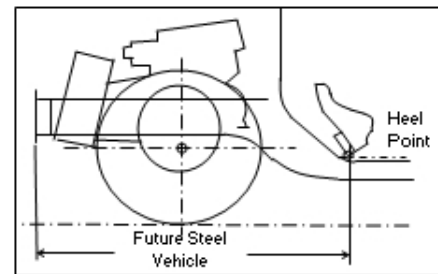


Figure 2.3: FSV Electric drive front-end

The FSV's front-end is 415 mm shorter than a typical mid-size sedan and 205 mm shorter than the 5-star rated Super-Mini Class vehicles. The FSV-1 has similar overall size as the Mini Cooper. However, the FSV-1 realizes 65 mm more legroom and has an additional 80 liters of cargo space. In comparison, the FSV-2 is 500 mm shorter than a Honda Accord yet shares the same interior room.

The electric drive proposed for the FSV vehicles is similar to the drive used on the Honda Clarity FCEV as illustrated in Figure 2.4 ^[1], yet much smaller.

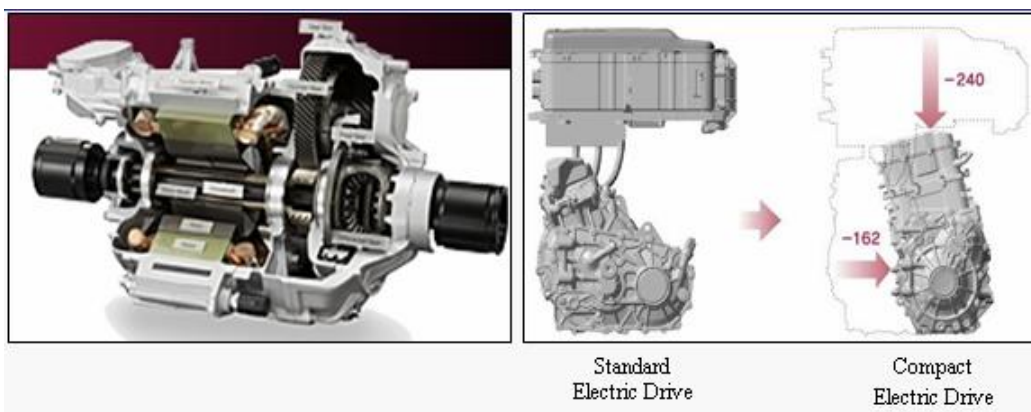


Figure 2.4: *Compact Electric Drive*

The size of a conventional internal combustion engine, and HEV powertrains, generally restrict the size and shape of body structural members in the front end, leading to an inefficient use of materials. The FSV front-end frees up space for an optimized front-end structure. The front-end rails, which play a major role in controlling and absorbing energy in front crashes, can be optimized for section shape, and hence minimizing mass. See Figure 2.5 for the front-end rail structure.

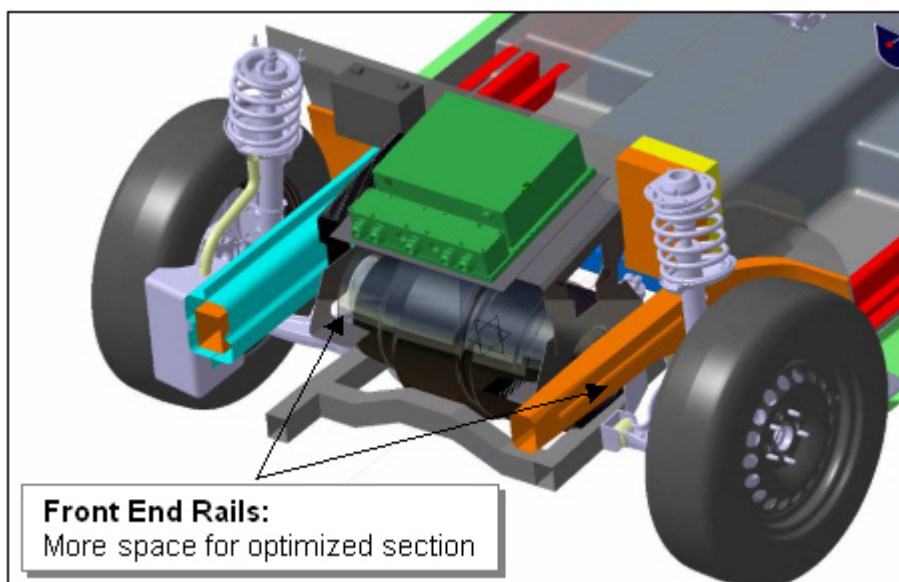


Figure 2.5: *Front-end rail*

¹Source: Honda Motor Company

2.4 Future Steel Vehicle-1 (FSV-1)

FSV-1 is a 4-door hatchback, 3,700 mm long, designed to accept two powertrain options: Plug-In Hybrid Electric Vehicle - PHEV₂₀ and Battery Electric Vehicle - BEV. Both powertrains share a common front-end and common front wheel drive traction motor. The traction motor is rated at peak power of 67 kW (49 kW continuous power).

2.4.1 FSV1 - (PHEV₂₀)

The PHEV₂₀ will have an all electric range of 32 km (20 miles) on a fully charged battery pack. The battery pack is a lithium-ion manganese based cell with a 5 kWh capacity (45 kg mass, 36-liter volume). The battery pack charging time, using a 120 V, 15 amp electric service is 2.5 hours. The extended range of 500 km for PHEV₂₀ is provided by a rear mounted 1.0L-3 cyl gasoline engine/generator set, mounted just ahead of the rear axle, leading to a 50/50 vehicle mass split between front and rear wheels. This packaging arrangement uses the space underneath the rear floor where conventional vehicles place the spare tire. The arrangement is similar to Daimler's Smart-For-Two and Mitsubishi's i-Minicar production vehicles. The FSV installation will be simpler, as the engine does not drive the wheels or any belt driven auxiliary devices.

The under floor structure for the PHEV₂₀ has to be adapted to accommodate the 5 kWh battery pack in the tunnel under the front floor. The engine/generator set mounted under the rear floor will require careful consideration for packaging the rear suspension, and sufficient structure to handle all the dynamic and rear impact crash loading. The layout for PHEV₂₀ is a hydroformed rear sub-frame assembly that can support the engine/generator mounts, and rear multi-link suspension that will form the basis of the rear structure. See Figure 2.6 for PHEV₂₀ layout.

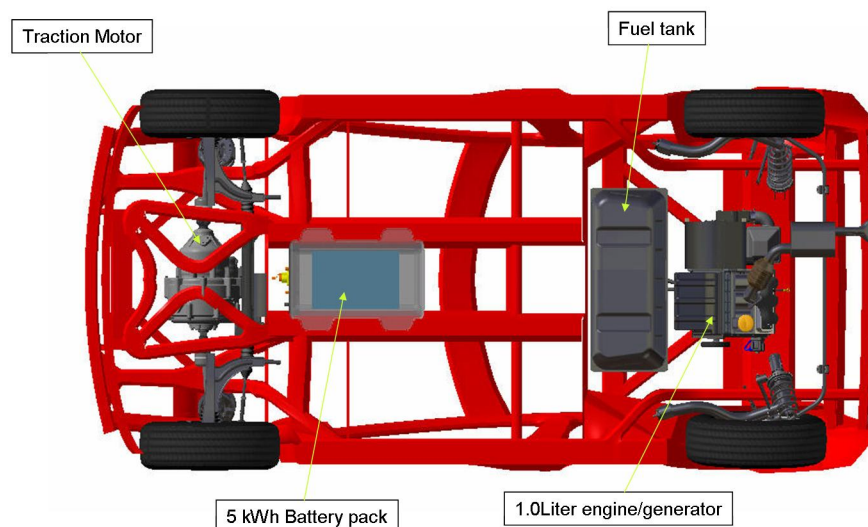


Figure 2.6: PHEV₂₀ powertrain layout

2.4.2 FSV-1 - BEV

The FSV-1 BEV is designed to have a range of 250 km. To achieve this range, the energy storage capacity of the battery pack has to be 35 kWh (347 kg mass, 280 liter volume). Packaging this size of a battery into a small vehicle is a major challenge. The battery extends forward from underneath the rear seat occupants floor into the tunnel and below the front floor. The under floor structures not only have to support the significant weight of the battery during road loading, but also protect it when subjected to frontal, and side and rear crash impact loads. Presently, it is envisioned that a full-size under floor longitudinal member, coupled with several cross members and additional tunnel reinforcements, will be required, leading to a possible application for very high-strength rolled formed martensitic steel sections. See Figure 2.7 for BEV underbody.

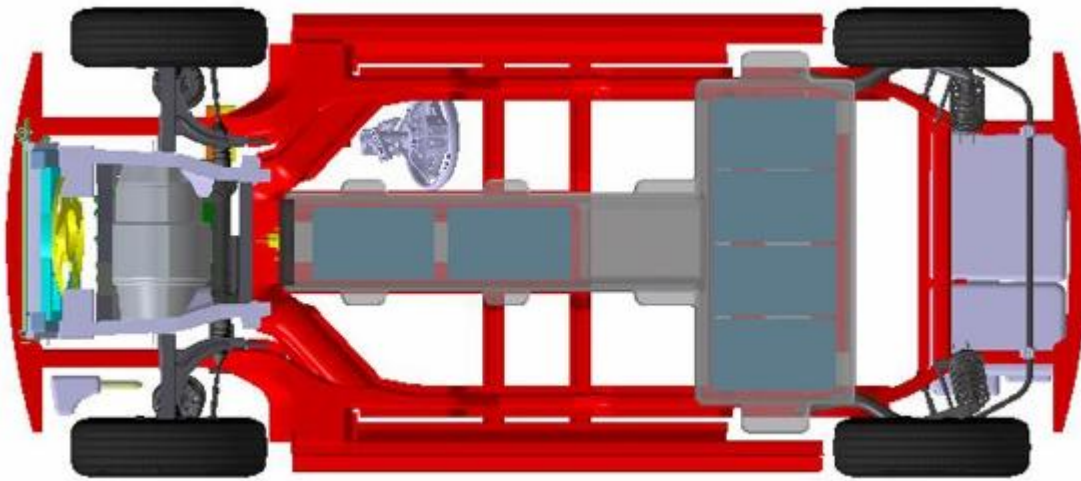


Figure 2.7: BEV underbody

2.5 Future Steel Vehicle -2 (FSV-2)

The FSV-2 is a 4-door sedan, 4,350 mm long, and designed to accept two powertrain options:

- A plug-in hybrid electric vehicle - PHEV₄₀
- A fuel cell electric vehicle - FCEV

Both powertrains share a common front-end and a common front wheel drive traction motor package. The traction motors rated peak power is 75 kw (55 kw of continuous power).

2.5.1 FSV-2 (PHEV₄₀)

The PHEV₄₀ vehicle will have an all-electric range of 64 km (40 miles) on a fully charged battery. The battery pack is a lithium-ion manganese based cell with a 11.7 kWh capacity (105 kg mass, 86 liter volume). The charging time for this battery pack using a 120 V, 15 amp (220 V/13 amp - EU) electric service is 5.5 hours. A rear mounted 1.4 L - 4 cyl gasoline engine/generator set provides the PHEV₄₀ with an extended range of 500 km.

Presently, other driving strategies are being investigated that could considerably reduce the size of the engine/generator.

The component packaging and structural challenges for this vehicle are similar to the PHEV₂₀. See Figure 2.8 for PHEV₄₀ illustration.

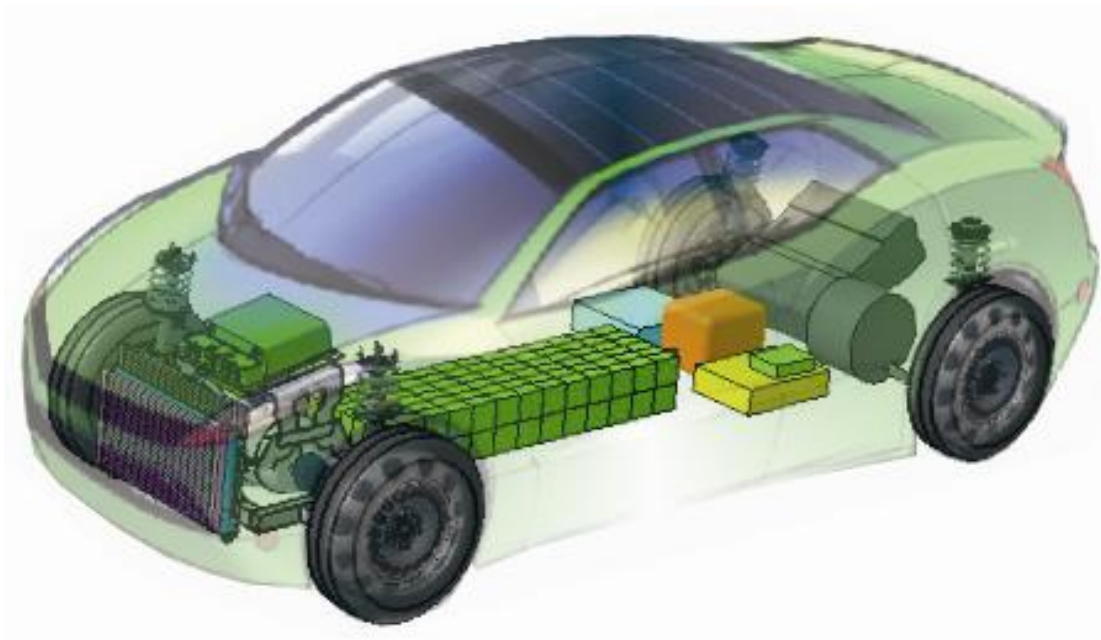


Figure 2.8: *FSV-2 (PHEV₄₀)*

2.5.2 FSV-2- FCEV

The FCEV - Fuel Cell Electric Vehicle has an all-electric driving range of 500 km. The FCEV energy source is electricity generated by the hydrogen fuel cell system. A fuel cell is a device that uses hydrogen (or hydrogen-rich fuel) and oxygen to create electricity by an electro-chemical process. Fuel cells use the chemical energy of hydrogen to cleanly and efficiently produce electricity, with water and heat as by-products. See Figure 2.9 for FCEV illustration.

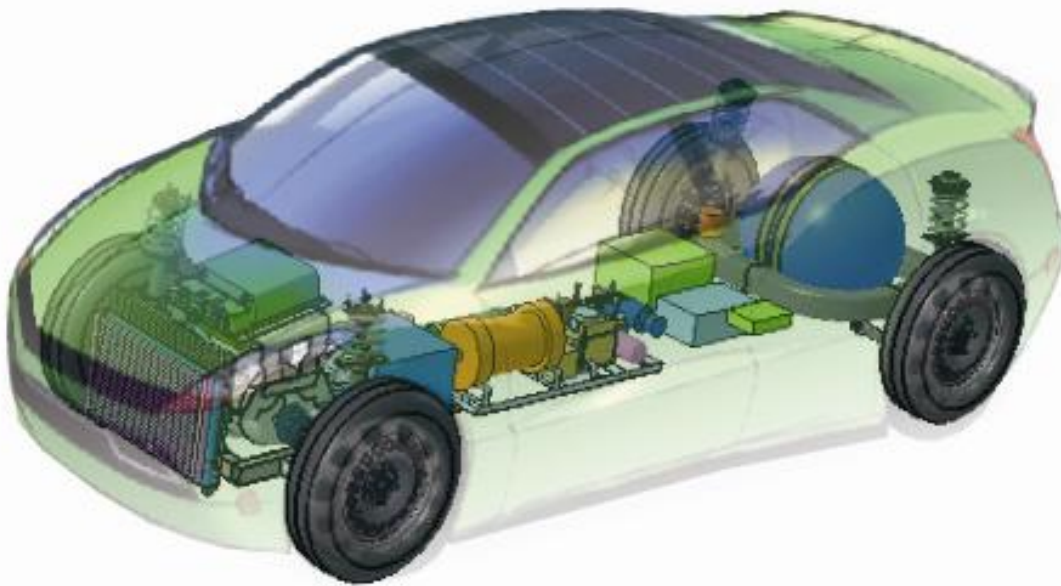


Figure 2.9: FSV-2 - FCEV

The FCEV has a usable hydrogen storage capacity of 3.4 kg, with an internal volume of 95 liters, that is stored at 65 Mpa at 15°C. The fuel-cell stack system has 240 cells, which has a combined weight of 92 kg producing 65 kW of power. The battery pack used in conjunction with this system is a lithium-ion manganese based cell with 2.3 kWh capacity, and weighs 27 kg with a 25-liter volume.

The challenges of the FCEV underbody structure is to provide sufficient support and protection to the fuel stack assembly packaged in the front floor tunnel, and the high-pressure hydrogen tank under the rear floor. The under body-structure will require extensive new structural members to meet stiffness requirements and crash loads.

2.6 FSV - Estimated Masses

The mass estimates, shown in Table 2.3 and Table 2.4 for FSV-1 and FSV-2 were based on the previously described vehicle layouts and calculated using the Mass Compounding Program [34].









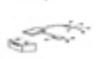




		ICE 1 2010	ICE 1 2020	HEV 1 2010	HEV 1 2020	FSV 1 PHEV ₂₀	FSV 1 BEV
	Body Non-Structure	245	190	215	190	190	190
	Body Structure	272	241	272	237	173	190
	Front Suspension	59	40	62	45	40	45
	Rear Suspension	53	39	61	37	26	35
	Steering	17	17	17	17	16	16
	Brakes	38	31	40	33	29	32
	Drivetrain	222	197	297	252	215	78
	Fuel, Battery, Exhaust	48	55	104	105	98	347
	Wheels and Tires	78	59	68	55	38	44
	Air Conditioning	32	42	27	33	36	36
	Electrical	55	63	55	66	63	58
	Bumpers	26	21	23	24	20	23
	Closures	54	48	49	44	46	46
	TOTAL	1199	1044	1290	1138	990	1,137

Table 2.3: FSV-1 mass estimates (all in kg)














		ICE 2 2010	ICE 2 2020	HEV 2 2010	HEV 2 2020	FSV 2 PHEV ₄₀	FSV 2 FCEV
	Body Non-Structure	302	210	257	210	210	210
	Body Structure	337	298	337	303	198	175
	Front Suspension	73	49	76	55	51	44
	Rear Suspension	65	45	73	44	52	34
	Steering	21	21	21	21	19	19
	Brakes	47	37	49	40	37	34
	Drivetrain	274	244	359	304	261	177
	Fuel, Battery, Exhaust	59	68	125	127	178	114
	Wheels and Tires	96	72	80	73	70	61
	Air Conditioning	40	52	35	46	47	47
	Electrical	68	78	68	82	83	93
	Bumpers	33	25	31	28	26	22
	Closures	67	59	62	55	48	48
TOTAL		1,483	1,260	1574	1388	1279	1079

Table 2.4: FSV-2 mass estimates (all in kg)

The powertrain component masses were obtained from simulations with PSAT (Powertrain System Analysis Toolkit) conducted by Quantum. The estimated masses of a similar (to FSV-1) sized ICE vehicle and a HEV (2010 and 2020) are also shown for comparison purposes.

The mass reductions that can be achieved by other future technologies, smaller vehicle foot print of FSV, and body-structure mass reduction by use of advanced high-strength steels, lead to significant mass reduction of the FSV.

2.7 FSV Cost of Ownership

The following costs were calculated based on vehicle total life of 200,000 km (125,000 miles). Other assumptions include: for PHEV vehicles, - 70% of distance traveled in electric mode, cost of electricity \$0.12 per kWh and 30% of the distance traveled in HEV mode using gasoline at \$1.18 per liter (\$4.50 US per gallon). For hydrogen gas, the cost is \$5.00 /kg, as currently charged by some stations in California on the Hydrogen Highway.

As shown in Table 2.5, and Table 2.6, the advanced powertrains higher costs leads to significantly higher vehicle cost. Although the total cost of ownership is not significantly different between various options except for FCEV, which is 26% higher.

	Petroleum Based				Hydrogen Gas Comp. 70 Mpa FCEV		Electricity & Petroleum PHEV ₄₀	
	ICE 2020 16 $\frac{\text{km}}{\text{l}}$ (38MPG)		HEV2020 19 $\frac{\text{km}}{\text{l}}$ (45MPG)		0.632 $\frac{\text{kgH}_2}{\text{km}}$		119 $\frac{\text{Wh}}{\text{km}}$ & 20 $\frac{\text{km}}{\text{l}}$ (47 MPG)	
	[total \$]	[per km]	[total \$]	[per km]	[total \$]	[per km]	[total \$]	[per km]
Vehicle Cost	21,760	0.110	23,910	0.120	42,153	0.210	31,479	0.160
Overhead	8,160	0.041	8,160	0.041	8,160	0.041	8,160	0.041
Vehicle Cost without Powertrain	10,500	0.053	10,500	0.053	10,500	0.053	10,500	0.053
Powertrain Cost	3,100	0.016	4,350	0.022	22,458	0.112	7554	0.038
Battery Cost			900	0.005	1,035	0.005	5265	0.026
Vehicle Use Cost	15,717	0.080	13,427	0.070	6,320	0.030	6,873	0.030
Gasoline \$1.18 per l (\$4.50 per Gal US)	14,717	0.074	12,427	0.062			4,759	0.024
Oil Change \$40 Per 8050 km	1,000	0.005	1,000	0.005			400	0.002
Electricity \$0.12 per kwh							1,714	0.009
Hydrogen \$5.00 per kg					6,320	0.032		
Total Cost of Ownership	37,477	0.190	37,337	0.190	48,473	0.240	38,352	0.190

Table 2.5: Cost of ownership, FSV-1

	Petroleum Based				FSV-1 Dual Fuel Based Electricity form Grid and Petroleum			
	ICE 2020 18 $\frac{\text{km}}{\text{l}}$ (42.7 MPG)		HEV 2020 27.2 $\frac{\text{km}}{\text{l}}$ (64 MPG)		BEV - EV 114 $\frac{\text{Wh}}{\text{km}}$		PHEV ₂₀ 106 $\frac{\text{Wh}}{\text{km}}$ & 26.7 $\frac{\text{km}}{\text{l}}$ (62.7 MPG)	
	[total \$]	[per km]	[total \$]	[per km]	[total \$]	[per km]	[total \$]	[per km]
Vehicle Cost	16,250	0.081	18,090	0.090	32,535	0.163	22,810	0.114
Overhead	6,094	0.030	6,094	0.030	6,094	0.030	6,094	0.030
Vehicle Cost without Powertrain	7,746	0.039	7,746	0.039	7,746	0.039	7,746	0.039
Powertrain Cost	2,350	0.012	3,350	0.017	2,945	0.015	6,720	0.034
Battery Cost	60		900	0.005	15,750	0.079	2,250	0.011
Vehicle Use Cost	14,097	0.070	9,738	0.050	2,731	0.014	6,232	0.030
Gasoline \$1.18 per l (\$4.50 per gal US)	13,097	0.065	8,738	0.044			4,460	0.022
Oil Change \$40 \$40 per 8,000 km	1,000	0.005	1,000	0.005			500	0.003
Electricity \$0.12per kwh					2,731	0.014	1,272	0.006
Total Cost of Ownership	30,346	0.152	27,828	0.139	35,266	0.176	29,041	0.145

Table 2.6: *Cost of ownership, FSV-2*

For the BEV, comparatively lower energy cost of electricity leads to lower vehicle-use costs compared to the ICE-2020 (\$0.070 and \$0.014 per km traveled for gasoline and electricity respectively).

The fact that the BEV and FCEV vehicle costs are almost double the cost of comparable internal combustion engine vehicles (ICE-2020), will lead to OEMs demands to reduce the powertrain cost as much as possible. The size of powertrain is directly related to the total mass of the vehicle therefore the effect of mass reduction to powertrain cost was determined.

2.8 Environmental Impact

2.8.1 FSV Fuel Economy and CO₂ Emissions

The Pump-to-Wheel fuel economy and CO₂ emissions results achieved for all the FSV variants are well below the future worldwide requirements, as shown in Table 2.7. The most stringent future proposed requirement for CO₂ emissions in the European Union (EU) is 95 $\frac{\text{g}(\text{CO}_2)}{\text{km}}$ (passenger car fleet average), to be met by year 2020. The Pump-to-Wheel emissions for the BEV and FCEV are zero. These powertrains are classed as Zero Emissions Vehicles (ZEV) by the California Air Resources Board (CARB). The CO₂ emissions for PHEV₂₀ and PHEV₄₀ are 23 $\frac{\text{g}(\text{CO}_2)}{\text{km}}$ and 27 $\frac{\text{g}(\text{CO}_2)}{\text{km}}$ respectively, assuming these vehicles will be driven in BEV mode for 70% of the miles driven. Currently, there is no agreed methods for measuring the fuel economy of PHEV vehicles. It will most likely be based on how much petroleum the PHEV is saving by using electricity from the grid, (“Petroleum Displacement” method).

	FSV1		FSV2		Reg. Limit ALL
	BEV	PHEV ₂₀	FCEV	PHEV ₄₀	
European Drive Cycle (NEDC)					
CO2 Emissions g/km	0	23	0	27	95
Fossil Fuel l/100km	0	0.99	0	1.14	4.1
Electricity Usage $\frac{\text{Wh}}{\text{km}}$	89	65	0	75	N/A
Total Energy Usage ** $\frac{\text{Wh}}{\text{km}}$	89	152	211	175	361
2008 US EPA Drive Cycle					
CO2 Emissions (combined) g/km	0	31	0	35	156
Combined MPG	∞	177	∞	157	35
Combined Electricity Usage $\frac{\text{Wh}}{\text{km}}$	109	80	0	92	N/A
Combined Energy Usage ** $\frac{\text{Wh}}{\text{km}}$	109	196	295	224	590
City MPG	∞	177	∞	157	N/A
City Electricity Usage $\frac{\text{Wh}}{\text{km}}$	103	75	0	86	N/A
City Energy Usage ** $\frac{\text{Wh}}{\text{km}}$	103	192	304	218	N/A
Highway MPG	∞	177	∞	157	N/A
Highway Electricity Usage $\frac{\text{Wh}}{\text{km}}$	117	85	0	99	N/A
Highway Energy Usage ** $\frac{\text{Wh}}{\text{km}}$	117	202	295	231	N/A

* Based on Petroleum Displacement method

* Assumption: 70% in EV modes & 30% in Charge Sustaining modes

** Combined fuel energy plus stored electrical energy

Table 2.7: FSV fuel economy and CO₂ emissions table

Figure 2.10 from “Japan - Ministry of Land, Infrastructure, Transport and Tourism” shows how the FSV CO₂ emissions compared with other gasoline, diesel and HEV vehicle technologies. As can be seen, the FSV’s emissions are very close to being in the ZEV class of vehicles.

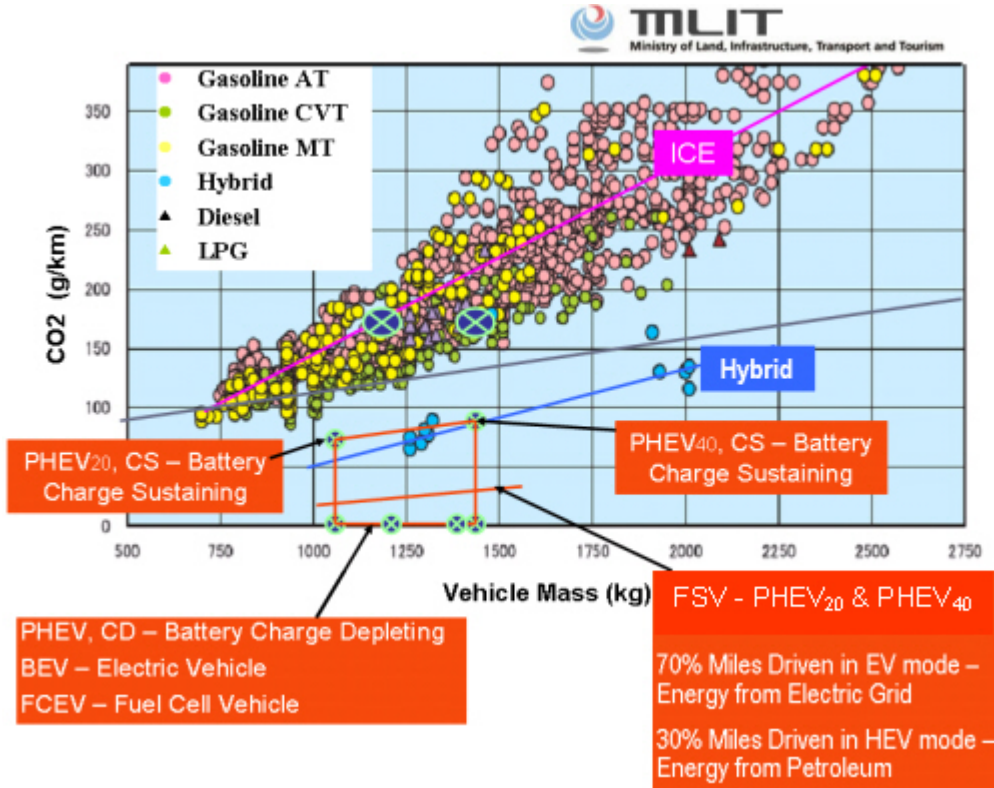


Figure 2.10: FSV fuel economy and CO₂ emissions

It is interesting to note the slope of each technologies data set in the above graph for ICE, HEV, and FSV are progressively trending lower, indicating proportionally lower CO₂ emissions as indicated by the slope of the line, with respect to proportional mass increases, (not to be confused with total mass increases). This is mainly due to future vehicles using regenerative braking systems, whereas the ICE system can not utilize regenerative braking. The FSV has the most effective regenerative braking system due to having a higher power electric motor and larger capacity battery, when compared to the less effective units in the HEV’s.

2.9 Well-to-Pump Assessment

The Well-to-Pump assessment for all possible future sources of FSV vehicle fuels was done using Argonne National Lab programs “Greet 1.8B”. The sources of energy (fuels) considered included the following:

- Electricity (US mix, Europe, China, Japan, India, 100% coal and 100% renewable)
- Gasoline and diesel from petroleum
- Bio-fuels, ethanol and bio-diesel
- Hydrogen gas and liquid made using electrolysis process and from natural gas

Table 2.8 shows electricity generation efficiencies, CO₂ and other emissions during electricity production using various feed-stocks. These results are used to calculate the energy “Well-to-Wheel” quantities shown in results for the FSV in following section.

Feedstocks [%]	USA	Europe	China	Japan	India	Coal	USA Green Mix
Coal	50.7	29.5	79	28.1	68.7	100	0
Natural Gas	18.9	9.9	0	21	8.9	0	0
Oil	2.7	4.5	2.4	13.2	4.5	0	0
Nuclear	18.7	31	2.1	27.7	2.5	0	20
Biomass	1.3	2.1	0	0	0	0	0
Others	7.7	13	16.5	10	15.4	0	80
	100	100	100	100	100	0	100
Electricity Pathway:							
Efficiency [%]	37.9	44.2	35	41.6	35.1	30.7	91.5
CO₂ [g/kWh]	750.6	520.3	973	596.7	923.5	1201.3	0
VOC [g/kWh]	0.07	0.05	0.08	0.06	0.08	0.09	0
Nox [g/kWh]	0.82	0.61	1.05	0.76	1.01	1.26	0
Sox [g/kWh]	1.8	1.25	2.64	1.74	2.46	3.15	0

Table 2.8: *Well-to-Pump results (electricity generation)*

2.10 FSV-1 - Environmental Assessment

2.10.1 FSV-1 - Pump-to-Wheel CO₂ Emissions

The Pump-to-Wheel CO₂ emissions for each FSV vehicle is shown in Figure 2.11. The limit of $95 \frac{\text{g}(\text{CO}_2)}{\text{km}}$ shown in Figure, is the CO₂ regulation proposed for the European Union to come into effect by 2020.

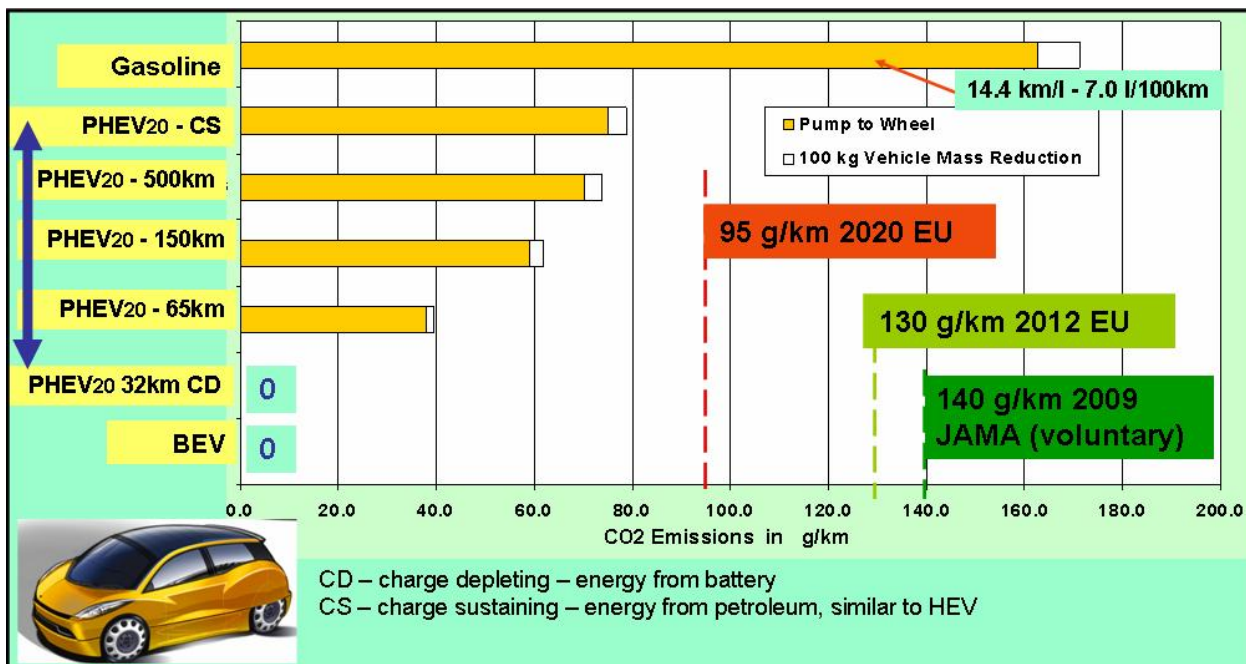


Figure 2.11: FSV-1 Pump-to-Wheel CO₂ emissions

The gasoline representative baseline vehicle shown in Table 2.11 is a conventional vehicle with a gasoline powered internal combustion engine. For each PHEV, both Charge Sustaining (CS) HEV and Charge Depleting (CD) all electric driving modes are also shown. On a Pump-to-Wheel basis, all four FSV Powertrain variants will emit less than $95 \frac{\text{g}(\text{CO}_2)}{\text{km}}$. The PHEVs and BEV produce zero CO₂ from the tailpipe when driven in all-electric mode.

2.10.2 FSV-1 - Well-to-Wheel CO₂ Emissions

There are also CO₂ emissions from the production of fossil fuels, renewable fuel, or electricity. So a Well-to-Wheel analysis is very important for a comprehensive evaluation of vehicle emissions. Adding the Well-to-Pump emissions factor to each vehicle, the Well-to-Wheel CO₂ emissions are attained, as shown in Figure 2.12. It can be observed that the PHEV in Charge Depleting, all electric mode, and the BEV have zero tailpipe CO₂ emissions. However, their carbon footprint is not zero due to emissions from the production of fuel.

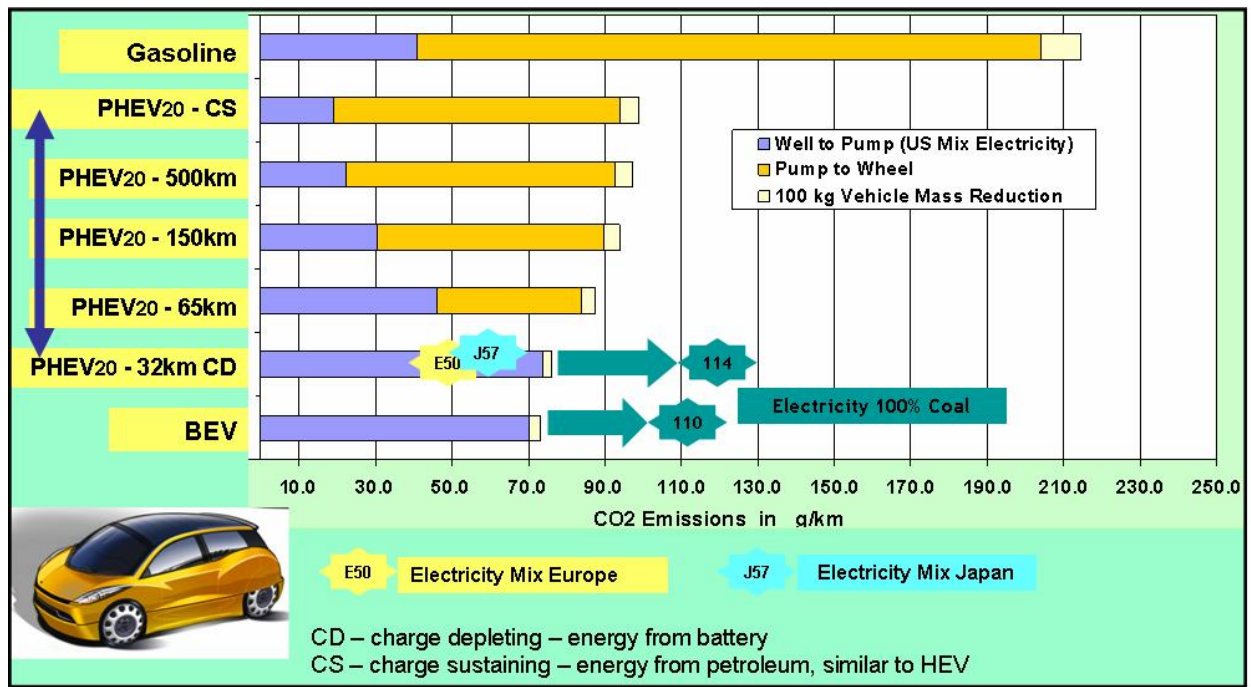


Figure 2.12: FSV-1 Well-to-Wheel CO₂ emissions

2.11 FSV-2 - Environmental Assessment

2.11.1 FSV-2 - Pump-to-Wheel CO₂ Emissions

An environmental assessment of FSV-2 was also conducted using the Well-to-Wheel CO₂ emissions. The results of the assessment are shown in the Figure 2.13 and Figure 2.14.

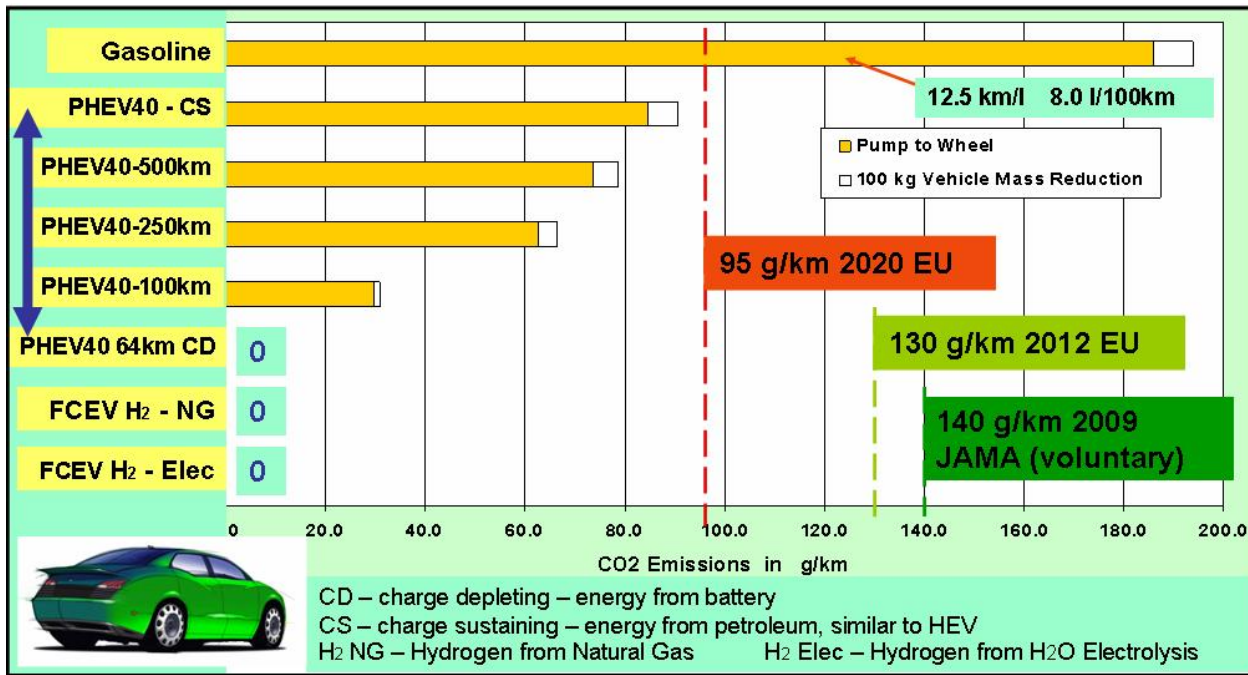
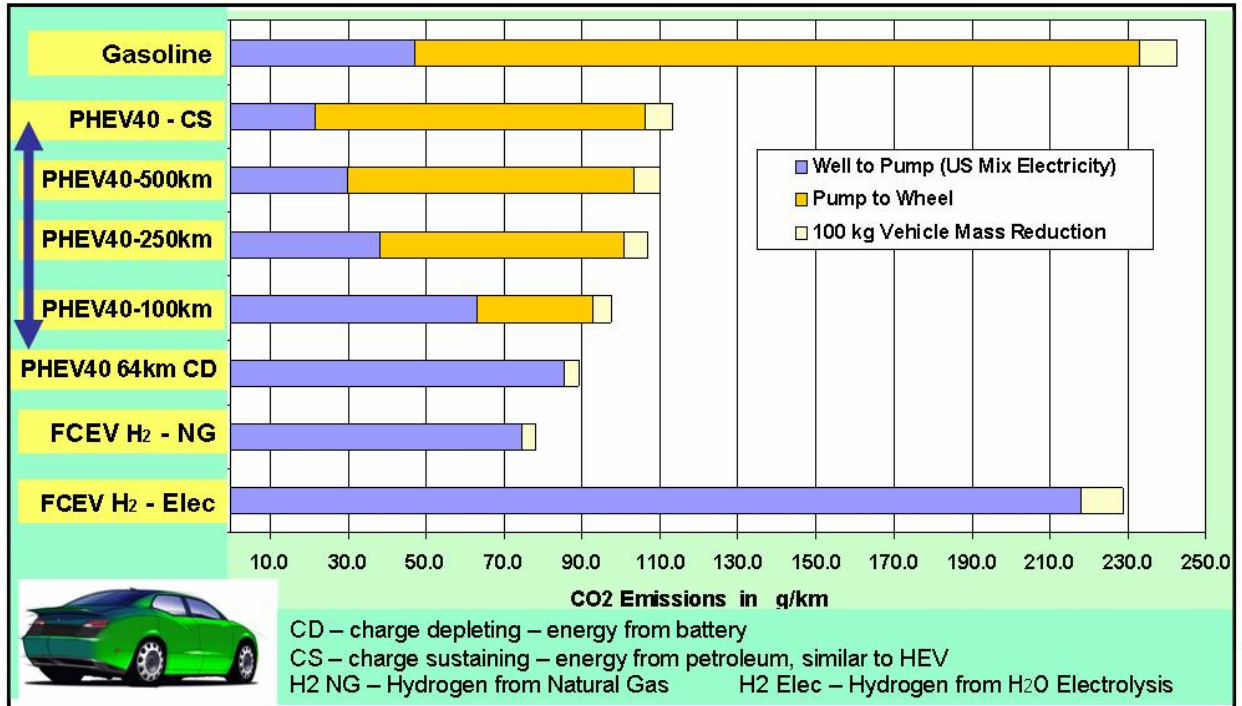


Figure 2.13: FSV-2 Pump-to-Wheel CO₂ emissions

2.11.2 FSV-2 - Well-to-Wheel CO₂ Emissions

 Figure 2.14: FSV-2 Well-to-Wheel CO₂ emissions

Even though FCEV, H₂-NG, and FCEV H₂-elec have zero tailpipe CO₂ emissions, their carbon footprint is not zero due to CO₂ emissions from production of their respective energy source. The H₂ FCEV Well-to-Wheel CO₂ emissions has a strong dependence on where its hydrogen comes from. In the best case scenario, it is only marginally better than the PHEV₄₀ operating in Charge Sustaining mode. It is envisioned that in the 2015 - 2020 time frame, electrical power available for FCEV H₂ electrolytic hydrogen production will come from the utility grid much like today's PHEVs, (power generation infrastructure will not evolve rapidly) and its carbon footprint will be much greater than any of the other PHEV variants.

2.12 Technology Assessment

2.12.1 Future Advanced Powertrains Summary

A feasibility study was performed to determine the powertrain architectures, components, performance, cost, and mass of four powertrain variants predicted to be in volume production by major automotive OEMs in the 2015-2020 timeframe. The study included the evaluation of currently used as well as emerging powertrain technologies. These include high voltage batteries of varying chemistries, ultra-capacitors, traction and wheel motors, and power electronics, as well as hydrogen storage and infrastructure.

For the purpose of the Future Steel Vehicle studies, a common transaxle sub-assembly, consisting of a traction motor, reduction gearing, and differential, were selected. Two different power internal combustion engine/generator assemblies can electrically power the transaxle sub-assembly, by a fuel cell system, or by a large capacity high voltage battery. Each of these powertrain options has its unique fuel storage capacity, high voltage battery size, weight, and cooling configurations resulting in new body-in-white design and structural challenges.

For the complex Fuel Cell System, Shanghai Fuel Cell Vehicles (SFCV) performed a separate powertrain subsystem study in conjunction with Tongji University. The integration studies of the fuel cell sub-system into the vehicle powertrain systems were supported jointly by Quantum Technologies and SFCV. The cost, mass, fuel consumption, and Green-House-Gas (GHG) emission values (Pump-to-Wheel) for the different FSV vehicles are summarized in Table 2.9.

	Mass [kg]	2015 Cost [\$ US]	Consumption, Urban Dynamometer Driving Schedule			
			Depleting Electricity [$\frac{Wh}{km}$]	Charge		Greenhouse Gas (Pump-to-Wheel) [$\frac{g\ CO_2}{km}$]
				Sustaining Gasoline [$\frac{L}{100\ km}$]	Hydrogen [$\frac{Kg}{100\ km}$]	
BEV	449	18.695	88.9	0	0	0
FCEV	326	23.493	N/A	0	0.632	0
PHEV₄₀	469	12.819	107	3.81	0	88.6
PHEV₂₀	343	8.970	92.5	3.31	0	76.9

Table 2.9: Powertrain mass, cost, fuel consumption, and GHG emissions

As a general conclusion, costs of battery technology, fuel cell engines, and hydrogen fuel storage are the greatest challenges. Battery costs are predicted to reduce quicker than both fuel cell and hydrogen storage technology, therefore for 2015 - 2020, PHEV and BEV vehicles will have the highest probability of large volume market acceptance. FCEV vehicles will likely not be in volume production before 2020 and possibly later if cost reductions take longer.

2.12.2 Advanced Powertrain Technologies

Five major topics considered in the evaluation of, and used in advanced powertrain technologies are:

1. Battery technology
2. Fuel cell technology
3. Electric motors
4. Internal combustion engines
5. Advanced powertrain energy sources

2.12.2.1 Battery Technology Assessment

Battery technologies currently used and under development for Hybrid or full electric automotive applications are:

- Nickel Metal Hydride (Ni-MH) - today's mainstream battery technology for automotive traction applications
- Lithium-Ion

In the past 10 years, rechargeable battery energy storage capacities have been rapidly improved upon and costs have been relatively stable due to mature manufacturing processes for consumer products. This is realized by the increase demand in new technologies for consumer products, (cell phones, power tools, etc.). Many of these technologies have proven themselves with excellent product performance and reliability records.

Manufacturing cost and energy storage capacity advantages have caused an industry shift from Ni-MH to Li-Ion battery technology, thus allowing OEM application specific deployment of new chemistry and cylindrical or prismatic cells.

Automotive high-voltage battery technology is typically utilizing this mass production technology for cylindrical cells, which are connected in series (strings) and parallel, to achieve the voltage levels and desired storage capacity. However, these high-voltage energy batteries require safety measures for crash and service.

Temperature control of individual cells and battery packs as a whole has proven to be one of the key areas for automotive battery development in order to increase durability and provide acceptable operation performance under extreme climate conditions (i.e. cold-start or continuous high output at high ambient temperatures).

Ongoing product development and validation cycles paralleled with the ramp-up of manufacturing capacity for large batteries for PHEV deployment is expected in the years 2015 to 2020. However substantial ongoing marketing activity for prototype technology may not be as rapidly turned into large vehicle volume production as might be anticipated. Therefore, new market incentives may be required to offset the high cost of large capacity batteries for plug-in and all-electric vehicle applications.

For phases 2 and 3 of the FSV Program, the FSV engineering team recommends the use of battery technology because it is safe, energy and cost efficient, and lightweight. For the 2015 and forward time frame, lithium-ion batteries using manganese oxide technology shows great potential to meet those requirements. See Table 2.10 for FSV battery recommendations.

Battery Technology Assessment				
		Status 2008	Prediction 2015-2020	Selection FSV
Dominating Technology		Ni-MH	Li-Ion	Li-Ion
Power Density	kW/kg	1.1	1-3	2.0
Energy Density	Wh/kg	45	90 - 170	130

Battery Pack Technology Assessment				
Capacity	kWh	10 (max)	1.5 - 40	2.3 - 35
Cost	\$ USD/ kWh	500	400-700	450

Future Steel Vehicle Concept				
	Capacity (kWh)	Weight (kg)	Volume (Liters)	Cost (\$ USD)
PHEV₂₀	5	58.2	47	\$2,346
PHEV₄₀	11.7	136.5	103	\$5,365
BEV	35	346.5	280	\$15,895
FCEV	2.3	27.3	25	\$1,503

Table 2.10: Battery recommendation for FSV

2.12.2.2 Fuel cell Technology Assessment

The Shanghai Fuel Cell Vehicle Company (SFCV) in cooperation with Tongji University, Shanghai China, studied the fuel cell engine, its sub-systems, and its components separately.

The fuel cell engine technical assessment results and recommendations were documented in separate reports that are part of the combined Future Steel Vehicle Phase 1 effort. Close attention was given to integration of those results into the vehicle and powertrain packaging, weight and costs analysis. The necessary fuel cell engine performance parameters, established to meet vehicle performance requirements were co-developed with Quantum Technologies while utilizing the Powertrain System Analysis Toolkit (PSAT).

In recent years, fuel cell system development has proven more challenging in solving the technical and commercial viability of a large-scale production deployment. Substantial efforts are still required in cost efficient on-board hydrogen storage as well as fuel cell engine development. Integration of hydrogen fuel cell and storage technology in existing vehicle platforms yields unsatisfactory vehicle packaging compromises leading to potential consumer dissatisfaction.

Large-scale production volumes to justify dedicated hydrogen fuel cell vehicle platforms cannot be achieved due to high manufacturing cost and unfavorable market pricing of such vehicles. Therefore, published production forecasts are based either on limited short and mid-term plans published by OEMs, or far reaching estimates by industry and financial analysts. In either case, fuel cell vehicle production by 2015 and 2020, is going to be very limited compared to overall vehicle production. See Figure 2.15 for fuel stack assembly. The fuel cell recommendations for the FSV program is shown in Table 2.11.

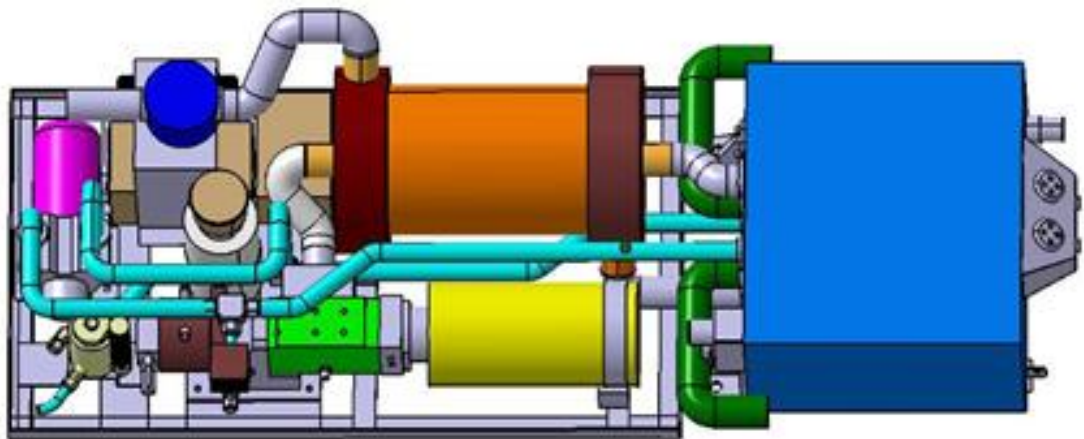


Figure 2.15: Fuel stack assembly

Fuel Cell Technology Assessment				
		Status 2008	Prediction 2015-2020	Selection FSV
Dominating Technology		PEM	PEM	PEM
Power Output (net)	kW	40 - 100	50 - 170	65
Efficiency	%	45 - 56	50 - 62	50 - 62
Power Density	kW/kg	0.8 - 1.9	~2.0	2
Cost [\$USD]	\$ USD/ kW	1,500-2,900	~100 - 200	155

Hydrogen Storage Technology Assessment				
		Status 2008	Prediction 2015-2020	Selection FSV
Dominating Technology		Compressed Gas		Compressed
Pressure	MPa	35	50 - 70	70
Tank Material	Carbon Composite	Aluminum Liner	Plastic Liner	Plastic Liner
H₂O Volume Capacity	Liters	80 - 220	70 - 150	95
Hydrogen Capacity (net)	kg	1.7 - 5.0	1.6 - 5.4	3.4

Future Steel Vehicle Concept				
	Capacity (net)	Weight [kg]	Volume [Liters]	Cost [\$ USD]
Without Cooling System				
Fuel Cell Engine	65 kW	92	67	\$10,081
Hydrogen Storage	3.4 kg	87	120	\$7,919

Table 2.11: Fuel cell recommendation for FSV

2.12.2.3 Electric Motor Technology Assessment

Electric motor development is shifting from industrial designs to meet customized automotive durability, weight, and cost requirements. Electrification of powertrains, allows fossil fuel energy recovery for a substantial reduction in fuel consumption and CO₂ emissions. However, plug-in technology requires bigger electric motors and battery capacity suitable for all electric operation in normal drive cycles.

Electric motors/generators are very efficient relative to an ICE, but they are at their maximum operating efficiency only in a narrow rpm range. Electric motor efficiency improvements are primarily extending the efficient operating range and power density. By focusing on magnet arrangement and coil designs, motor efficiency is optimized for the operating range the unit will be spending most of its service life in. For larger speed ranges, multi-speed transmissions are typically used, especially if the motor is used as an auxiliary power supply in typical hybrid vehicle configurations. If the motor is required to provide full traction power, a single speed gear reduction may be sufficient.

Electric motor/generators are closely coupled with DC power inverter hardware and software for optimized performance, efficiency and electro-magnetic emission resistance. For power and speed regulation, permanent magnets are used to electronically commutate (converts alternating electric current to direct current or vice versa) using variable voltage and variable frequency.

To ensure optimized efficiency of the generator and traction motors, the motor manufacturer matches the set to their respective power inverters. High efficiency allows the simplification or complete elimination of transmissions in series architectures based on performance, weight, cost and packaging considerations. The integrated traction drive concept, (series integrated generator/traction motor set without a transmission), offers the best compromise for the Future Steel vehicle. With internal scaling of the motor, the size of the motor components are engineered to operate at their maximum efficiency for the mass and power requirements of the vehicle application. By using internal scaling of the motor in addition to optimal gear reductions, it will be possible to support a modular powertrain design concept, and therefore reduce development and potential tooling cost at the same time. The recommendations for the FSV program are summarized in Table 2.12.

	Units	Current	BEV	PHEV ₂₀	FCEV	PHEV ₄₀
Peak Power	kW	Varies	67	67	75	75
Continuous Power	kW	Varies	49	49	55	55
Max Torque	Nm	Varies	270	270	240	240
Max Efficiency	%	95	96	96	95	95
Specific Cost	\$/kW	40	26	26	26	26
Specific Power	kW/kg	1.2	1.63	1.63	1.63	1.63
Specific Power	kW/l	3.2	4.8	3.3	3.3	3.3
Physical Volume	l	Varies	14	14	23	23

Table 2.12: Electric motor recommendations for FSV

2.12.2.4 Advanced Internal Combustion Engines

Internal combustion engine technology is a mature technology with incremental potential for efficiency improvements. The current fuels of choice for the light-duty vehicle market are gasoline and diesel, used with their respective engine type (Otto and Diesel Cycle). See Table 2.13 for Internal Combustion Engine Recommendations for FSV.

PHEV₂₀	PHEV₄₀
1.0 L , 3-cylinder , water cooled	1.4 L , 4-cylinder , water cooled
Gasoline fuel	Gasoline fuel
Normally aspirated	Normally aspirated
Direct fuel injection	Direct fuel injection
50kW Peak Power	70kW Peak Power
Cylinder orientation tilted to approach horizontal	Cylinder orientation tilted to approach horizontal
Torque and power curves matched with generator for maximum fuel efficiency and CO ₂ emission reduction	Torque and power curves matched with generator for maximum fuel efficiency and CO ₂ emission reduction
All accessories electric powered (no belt drive)	All accessories electric powered (no belt drive)
Generator used for Engine Start (no starter motor required)	Generator used for Engine Start (no starter motor required)

Table 2.13: *Internal Combustion Engine Recommendations - PHEV₂₀ and PHEV₄₀*

2.12.3 Automotive Technology Assessment

2.12.3.1 Drive-by-Wire

As a part of the engineering assessment on drive-by-wire systems as viable options for mainstream production on FSV-1 and FSV-2 by 2020, three types of drive-by-wire systems were looked at:

1. Brake-by-Wire
2. Throttle-by-Wire
3. Steer-by-Wire

Based on the research, the FSV engineering team strongly believes that of the three systems, only Brake-by-Wire and Throttle-by-Wire are viable production oriented technologies, as these provide a mass savings of approximately 3 kgs, and packaging advantages that significantly change the front-end structure of the vehicle while overcoming its current design challenges. “By-Wire-Systems” require robust and reliable 42V battery systems, and since both FSV-1 and FSV-2 have high-performance and high-voltage batteries as standard options, this technology provides a means for the FSV team to engineer optimized front-end packaging while reaping many other benefits of such a system.

At present, there are “partial” brake-by-wire systems that have some type of fail-safe hydraulic backup built into the system that provides minimal braking (limp home condition) in case of a complete electrical failure in the vehicle and/or the Brake-by-Wire system. However, all future development work currently being undertaken in terms of fault tolerant electronics in this regard, lead us to conclude that a complete Brake-by-Wire system with no hydraulic backup will be a production technology of the future (2020).

With the timeframe that FSV-1 and FSV-2 vehicles are targeted for production, The FSV engineering team believes that Steer-by-Wire is not a viable technology due to its inherent challenges in terms of safety and reliability of the system and its fault tolerance. The sizes of the components required are similar to a conventional steering system and the use of steer-by-wire does not lead to any significant mass saving. It is understood that at present, the use of a steering wheel is essential for regular high-speed driving. This necessitates similar structural mounting requirements as a conventional steering system to minimize vibrations, in addition to stiffness requirements, which in turn leads to locating the airbag in the steering wheel.

On the FSV structure, the positioning of the steering rack will not yield any additional packaging gains as the front length has been reduced to the minimum required to meet the 5-star NCAP crash rating.

2.12.3.2 Lightweight Components - Technical Assessment

Investigations of new automotive technologies on the horizon were investigated to assess the impact of mass reduction and packaging space implications without sacrificing vehicle function or safety. The reduction in trim and component mass generally leads to a total reduction in the vehicle's mass and also a reduction of body-structure mass (Mass Compounding).

The following automotive technologies were investigated:

- Glazing
- LED lighting
- Instrument panel displays
- Light weight seating

Table 2.14 illustrates the compared component weight savings between conventional vehicles and the proposed Future Steel Vehicle, thus proving the FSV's considerable weight advantage.

Item	Generic Weight [kg]	FSV Weight [kg]	Mass Savings [%]
Glazing	44	31	29.5
Lighting	10	6.3	37
I/P Display	2.2	0.2	91
Seating	65	42	35.4
Totals	121.2	79.5	

Mass Savings [kg]	41.7
--------------------------	-------------

Table 2.14: *Component weight savings - conventional vehicles versus Future Steel Vehicle*

The compounding effect of a 41.7 kg weight savings on the vehicle and body is a mass reduction of 10 kg on the body-structure.

2.12.3.3 FSV Wheels and Tires

The FSV-1 and FSV-2 are designed to accept a 15-inch wheel. The specific tire size, wheel and mass for both the vehicles are shown in Table 2.15.

Vehicle	Tire Size	Wheel Type	Mass [kg]	Mass [lbs]
FSV1	P175/65R15	Steel	14.1	31
FSV2	P175/65R15	Steel	14.1	31

Table 2.15: *FSV wheels & tires*

Low-rolling resistance tires are designed to improve the fuel efficiency of a vehicle by minimizing the energy wasted as heat as the tire rolls down the road. Tire companies are conducting significant research and development in this area as approximately 5-15% of the fuel consumed by a typical car is used to overcome rolling resistance of the tires.

A 2003 California Energy Commission (CEC) preliminary study estimated that adoption of low-rolling resistance tires could save 1.5-4.5% of all gasoline consumption.

Rolling Resistance Coefficient (RRC) is the value of the rolling resistance force divided by the wheel load. A lower coefficient means the tires will use less energy to travel. The Society of Automotive Engineers (SAE) has developed test practices to measure the RRC of tires. These tests (SAE J1269 and SAE J2452) are usually performed on new tires. When measured by using these standard test practices, most new passenger tires have reported RRCs ranging from 0.008 to 0.014.

All calculations for FSV are assuming a RRC target equal to 0.007.

2.12.3.4 Auxiliary Equipment & Power Management Systems

As a part of the engineering assessment on new automotive technologies that are viable for production by the year 2020, the FSV engineering team assessed the impact of auxiliary equipment power demand loads on the vehicles performance and all-electric range (AER).

A major portion of the auxiliary energy demand comes from the vehicle's air conditioning system, and our research has revealed that reducing this load significantly affects vehicle performance and range. A number of new technologies will be available for mainstream production for FSV-1 and FSV-2 by 2020 that will help reduce this parasitic load and provide FSV-1 and FSV-2 with enhanced performance and range.

The study has also led the team to conclude that reducing and optimizing A/C load may be the most efficient way of designing the propulsion system and battery to arrive at a very balanced (in terms of cost and size) design while achieving the set performance targets. Studies conducted by

leading national labs have shown that peak A/C loads reduce the range of an electric vehicle by as much as 38%.

In this study, a combination of proven methods and systems for FSV-1 and FSV-2 were used to achieve performance targets while maintaining optimized propulsion and power management systems. These methods and systems include the following:

- Advanced glazing (solar reflective glass)
- Solar reflective paint
- Cabin recirculation strategies (active sunroof ventilation)

2.13 Future Safety Requirements

The FSV engineering team conducted an assessment of proposed future (2010-2020) global safety regulations in comparison to the current requirements, with the intention to understand the implication of new regulations on the design of the FSV-1 and FSV-2, and to incorporate all the necessary structural changes on the FSV to meet and exceed these upcoming regulatory specifications by a comfortable safety margin.

The estimated mass, cost and fuel economy impacts of these new requirements (over vehicle lifetime) are shown in Table 2.16.

Regulation	Timeline	Mass	Cost [\$ US]	Fuel Used
Roof Crush/Rollover	2016	~ 2 kg	N/A	N/A
Electronic Stability Control (ESC)	2011	~ 1 kg	92.00	9.8 l (2.6 ga)
Pole Impact	2011	~ 6-8 kg	208.00	N/A
Frontal Impact	TBD	TBD	N/A	N/A
Bumper Impact	2008	1 kg	N/A	N/A
Ped-Pro	2011	1-2 kg	N/A	N/A

Table 2.16: *Estimated mass, cost and fuel economy impacts*

2.14 Fuel Economy Requirements

2.14 Fuel Economy Requirements

The results from our research into future fuel economy requirements have shown that all countries are currently working on regulations that mandate the amount of CO₂ emissions allowed for passenger cars.

The US passed regulations that mandate the average passenger car fuel economy shall be at least 35.7 $\frac{\text{miles}}{\text{gallon}}$. The average fleet fuel economy shall be 31.6 $\frac{\text{miles}}{\text{gallon}}$ by 2015, and this requirement will further increase to 35.0 $\frac{\text{miles}}{\text{gallon}}$ by the year 2020.

European regulations demand that the average passenger car fleet CO₂ emissions be within 130 $\frac{\text{g}(\text{CO}_2)}{\text{km}}$ by 2012, and proposals to reduce this number to 95 $\frac{\text{g}(\text{CO}_2)}{\text{km}}$ by the year 2020 are currently being discussed by the European Commission.

Summary of future fuel economy requirements is shown in Table 2.17.







CO ₂ Emissions			Fuel Economy			
year		$[\frac{\text{g}(\text{CO}_2)}{\text{km}}]$	Gasoline		Diesel	
			[mpg]	[km/l]	[mpg]	[km/l]
2008		200	27.46	11.67	31.51	13.39
2008		160	34.33	14.59	39.39	16.74
2015		153	35.70	15.17	41.19	17.51
2012		130	42.25	17.96	48.48	20.60
2012		120	45.77	19.45	52.52	22.32
2020		95	57.82	24.57	66.34	28.20

Table 2.17: CO₂ emission requirements

Data source: US EPA^[2]

²CO₂ emissions from a gallon of **gasoline** = 2,421 g x 0.99 x (44/12) = 8,788 g = 8.8 kg/gallon = 19.4 lbs/gallon
CO₂ emissions from a gallon of **diesel** = 2,778 g x 0.99 x (44/12) = 10,084 g = 10.1 kg/gallon = 22.2 lbs/gallon

3.0 Market Analysis

3.1 Global Market Analysis

3.1.1 Overview

As part of the Phase 1 - engineering study for determining the size of the FSV, extensive research was conducted on the global automotive trends projected to 2015 and beyond. The results of the investigation revealed that a major shift appears to be taking place globally towards small and mid-size cars due to the global concern about rising fuel costs and affordability. Worldwide, over 70% of the cars sold in today's marketplace share two vehicle sizes; the Small Car (A & B Class) up to 4,000 mm long and the Mid-Class car (C & D class) up to 4,900 mm long. To encompass both segments of the worldwide market, the FSV Steering Team made the decision to include two vehicle sizes as a part of this study.

The packaging specifications and vehicle performance for each of the vehicles were determined to be acceptable and appropriate for each class of vehicle in line with worldwide OEM trends. The determination of vehicle interior dimensions and luggage space requirements were based on each vehicle size and its intended usage.

FSV-1: A small vehicle mainly intended for city and shorter range driving

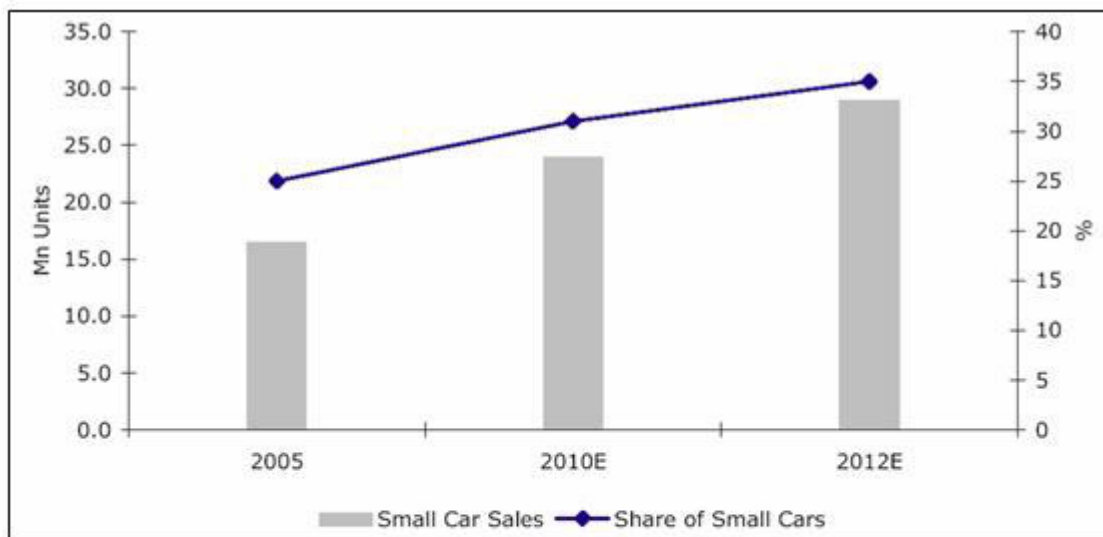
FSV-2: A lower - mid-size vehicle for long range driving with larger luggage carrying capacity

This document presents data that relates to the FSV Steering Team's decision and also presents data that shows the vehicle market is indeed headed towards a shift in its focus towards significant growth in the small car segment driven by growth in developing countries.

3.1.2 Global Auto Market Analysis

In the next decade, the majority of the growth in the global auto industry will come from countries with developing economies such as India, China, and Eastern Europe. The fastest growing segment will be small cars, the size most affordable to the expanding middle classes in those countries.

Demand for small cars is expected to rise globally with emerging markets representing special growth areas. In developed countries, stricter environmental standards are increasing the need for decreased fuel consumption, while in emerging markets, the escalating level of disposable income has increased demand for small cars. In 2005, small cars represented 25% of new car sales globally, but this ratio is predicted to rise to 35% by 2012 as shown in Figure 3.1.



Source: Konzept Analytics Copyright ©



Figure 3.1: Global Auto Market - small car sales & share

By 2014, India and China are expected to lead the expansion of the global output of low-cost cars by 11% and 34% respectively, with 80% of the demand expected to be in those rapidly developing economies.

By the year 2012, global sales of small cars are expected to be around 29 million per year, an increase of 65% from a decade earlier. In Western Europe, the market for micro-cars is projected to rise nearly 50% by 2012. Even in the United States, sales of small cars are expected to grow 25% by 2012 to 3.4 million.

Major companies developing low-cost cars include Renault, Fiat, Peugeot, Daewoo (GM), Hyundai and Daihatsu (Toyota), as well as Chinese firms Geely and Chery and Indian companies Tata and Maruti.

Mini-cars account for more than one-third of the total volume sales in the Japanese auto market. In Japan, Suzuki and Daihatsu are the market leaders in the small car market.

Key Findings:

- Small cars represented 25% of new car sales globally in 2005, but this ratio is expected to rise to 31% in 2010
- 80% of this demand is expected to come from the developing economies of India and China
- India and China are expected to lead the growth trend with 11% and 34% of the global output of low-cost cars by 2014
- By 2012, consumers around the world are expected to buy a record 29 million small cars annually, up 65% from a decade earlier
- Small cars account for more than 70% of the Indian car market
- Mini cars account for 35% of total volumes in Japan. The demand for mini vehicles in the Japanese market is expected to grow, eventually pushing sales past 2 million units per year
- A large number of Japanese consumers are moving from luxury cars to mini-cars due to environmental standards and increasing gas prices

3.1.3 Market Overview By Region

3.1.3.1 India

In India, only 0.7% of the total population own private vehicles. The Indian ownership rate is less than China, with 1.2 vehicles per 100 inhabitants, and to Germany, Japan and the U.S., where at least one in two people own a car. Thus, the Indian market potential for small cars is huge.

India is expected to be among the top six countries in the global auto industry - along with the U.S., Germany, China, Japan and Korea - that will account for 60% of worldwide production in 2012.

By the end of 2016, India will become the fourth largest producer of passenger cars and light vehicles from its current position of being the 12th largest player. However, India is the world's fastest growing automotive market in these categories with an annual growth rate of 14% compared with 9% in China.

India is the third largest producer of small cars after Japan and Brazil. Small cars account for more than 70% of the total Indian car market share, as can be seen in Figure 3.2.

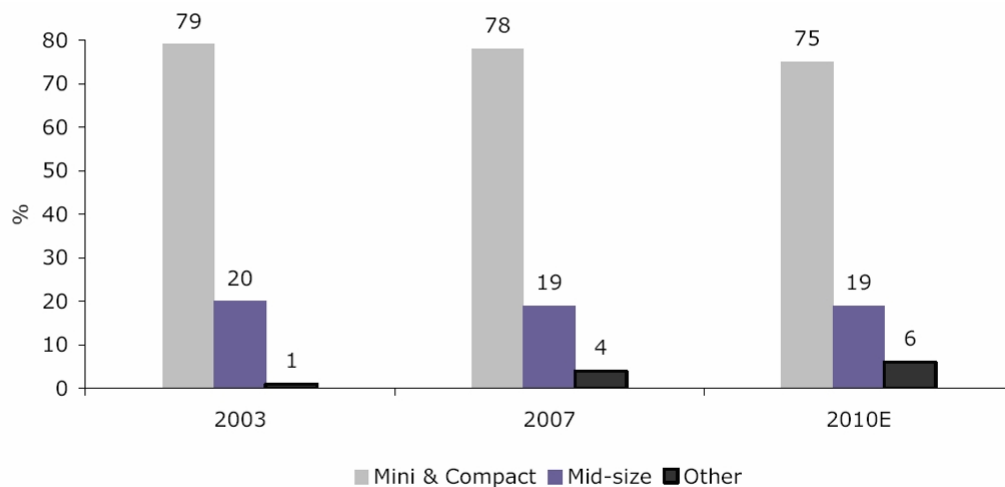


Figure 3.2: Breakdown of car market by segments (India)

3.1.3.2 China

The market share of the upper-medium segment surpassed the small car segment for the first time in the second quarter of 2007, thus becoming the second-biggest segment in the passenger car market. In the meantime, market share of the medium segment also increased, eventually seizing a lot of the small segment's share. See Figure 3.3 for a breakdown of vehicle ownership by market segment.

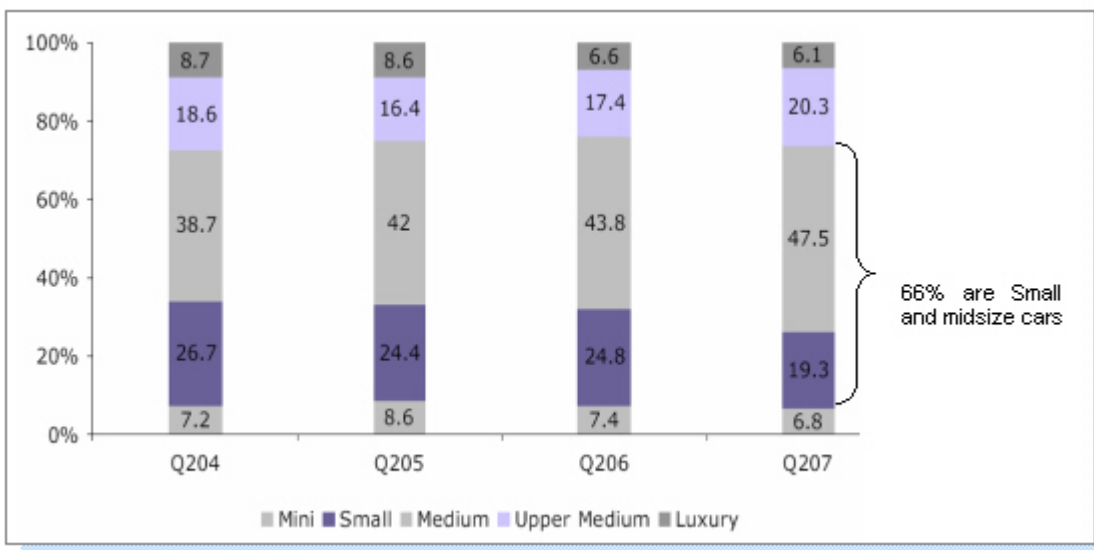


Figure 3.3: Breakdown of car market by segments (China)[20]

First-time car owners represent 80% of the total car buyers in China which drives this phenomenal growth. The growth is virtually the opposite of more mature markets like the United States, Europe and Japan, where first time car buyers are below 15%.

3.1.3.3 Japan

Mini cars (known as Kei cars in Japan) have engine sizes of 660 cc or less, and account for 35% of total volumes in Japan. Suzuki leads the Japanese car industry with more than 30% of the total market share in the small car segment. The 1997 revision of emission standards in Japan has made all makers believe that launching mini-vehicles will prove helpful in recovering the declining domestic demand for new cars, improving fuel consumption and safety, and meeting consumer desire for more economical cars with a lower sticker price and tax rate. See Figure 3.4 for Mini-vehicle market share and sales.

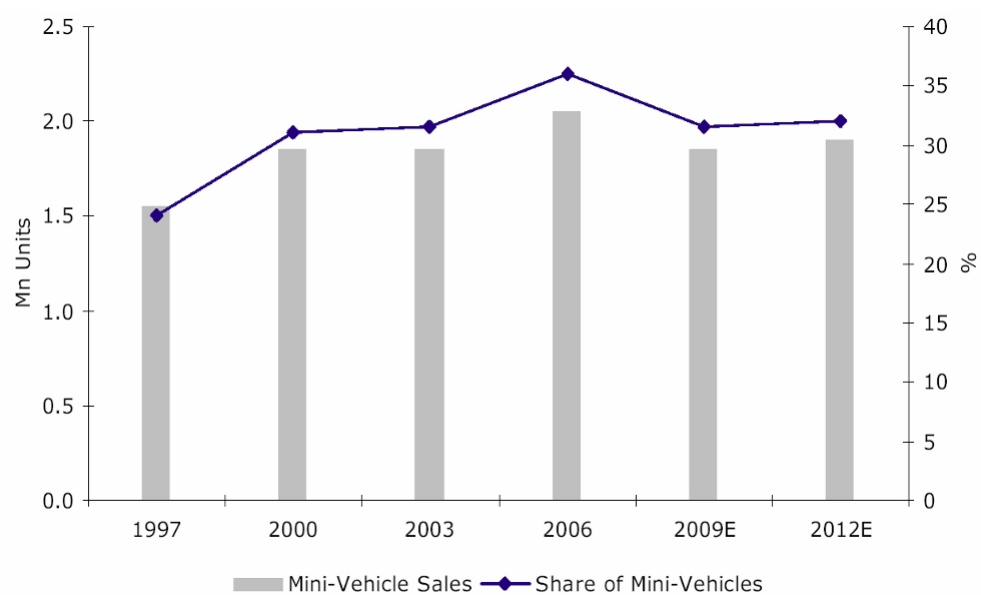


Figure 3.4: *Mini-Vehicle market in Japan*

Japanese mini car statistics are shown on the next page.

Kei Cars (Mini Cars)

Engine displacement: 0.66 liters

Maximum power: 47 kW, 63 hp

Length: 3.4 m; Height: 2 m

Width: 1.48 m

Kei Cars are required to have special black and yellow license plates.



They were **originally exempt** from emissions testing, insurance requirements and even parking regulations that required people to show that they own or rent a legal parking space before they can register the vehicle.

“Rules are the same now for everybody”

Average Cost

A new Kei Car costs around one million yen (\$9,000)

Displacement	Yen [¥]
under 661	7,200
661 - 1,000	29,500
1,001 - 1,500	34,500
1,501 - 2,000	39,500
2,001 - 2,500	45,000

Table 3.1: Japan 2008 car taxation



Figure 3.5: Suzuki WagonR - most popular mini car in Japan

3.1 Global Market Analysis

3.1.3.4 Europe

Annual vehicle sales in Europe are approaching 15,000,000 units as can be seen from the graph in Figure 3.6.

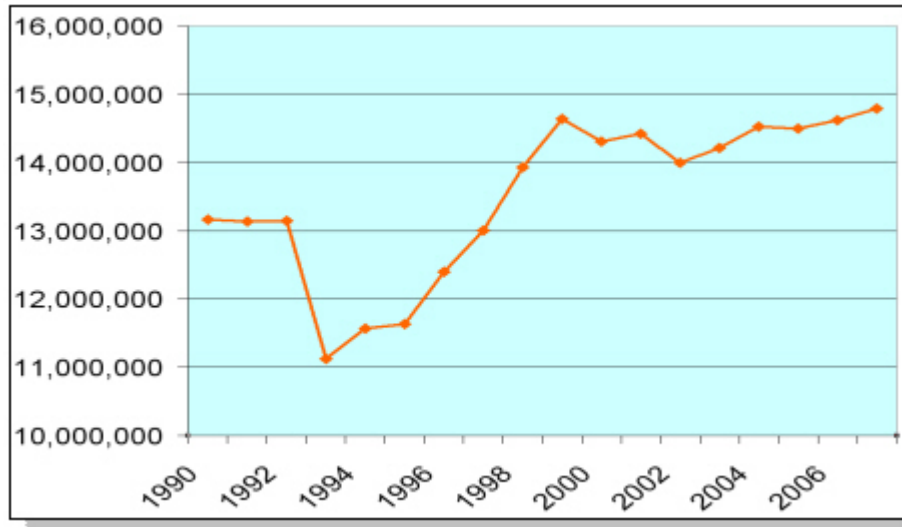


Figure 3.6: Annual vehicle sales in Europe

The graph in Figure 3.7 shows the European car market is also seeing a significant shift in small car sales since 2006 and continues to move in that direction. The total share between small and lower medium cars adds up to approximately 70%.

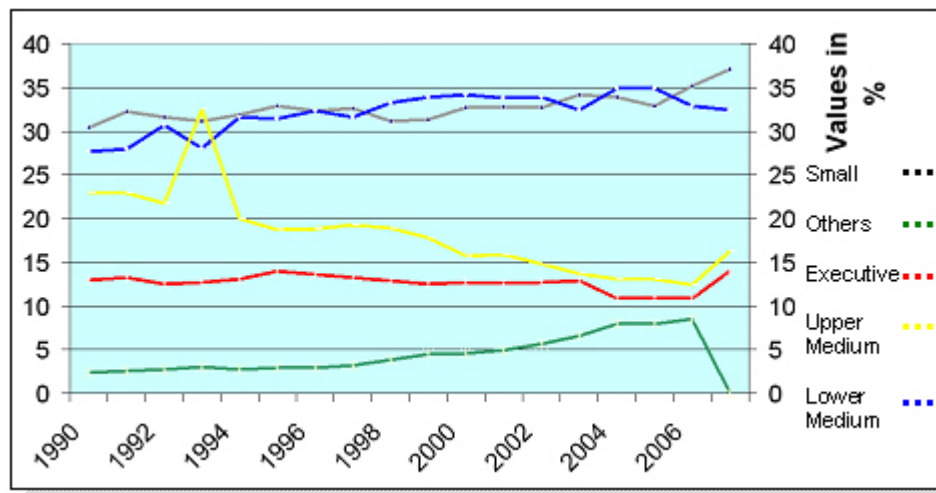


Figure 3.7: New passenger car registration

3.1.3.5 North America

For many years, the United States had been the single largest car market in the world. But now the US represents less than one-quarter of the global industry with an expected decline in its current market share. Some industry observers believe that the American car market has already reached its saturation point at approximately 16 to 17 million unit sales annually.

The graph in Figure 3.8 shows the US market split between light-duty trucks and Cars. As can be seen, since 1980 the percentage of truck sales rose while cars declined. This trend is reversed in 2004 in line with an increase in gasoline prices.

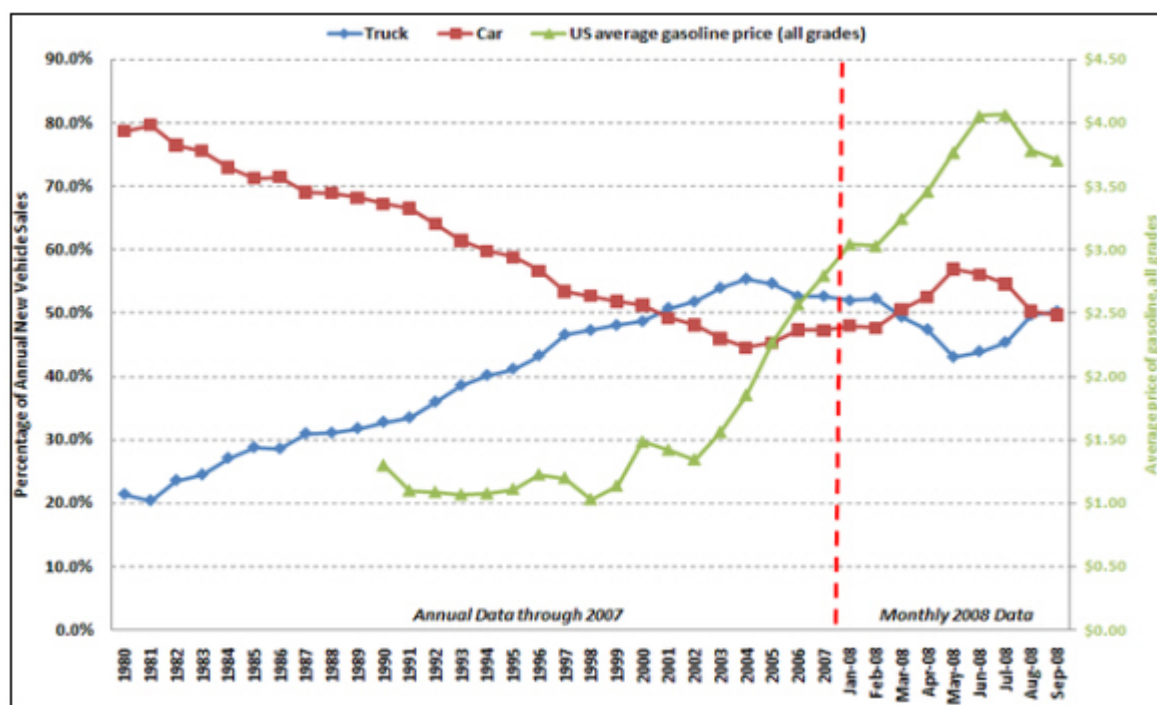


Figure 3.8: US car and light truck sales (new vehicle) with average gasoline price [35]

3.1 Global Market Analysis

The graph in Figure 3.9 from Toyota, shows a radical demand shift towards fuel-efficient vehicles and away from large SUV's and pick-up trucks for the US market. The greatest increase in sales during 2008 is of the new entry, sub-compact class of cars.

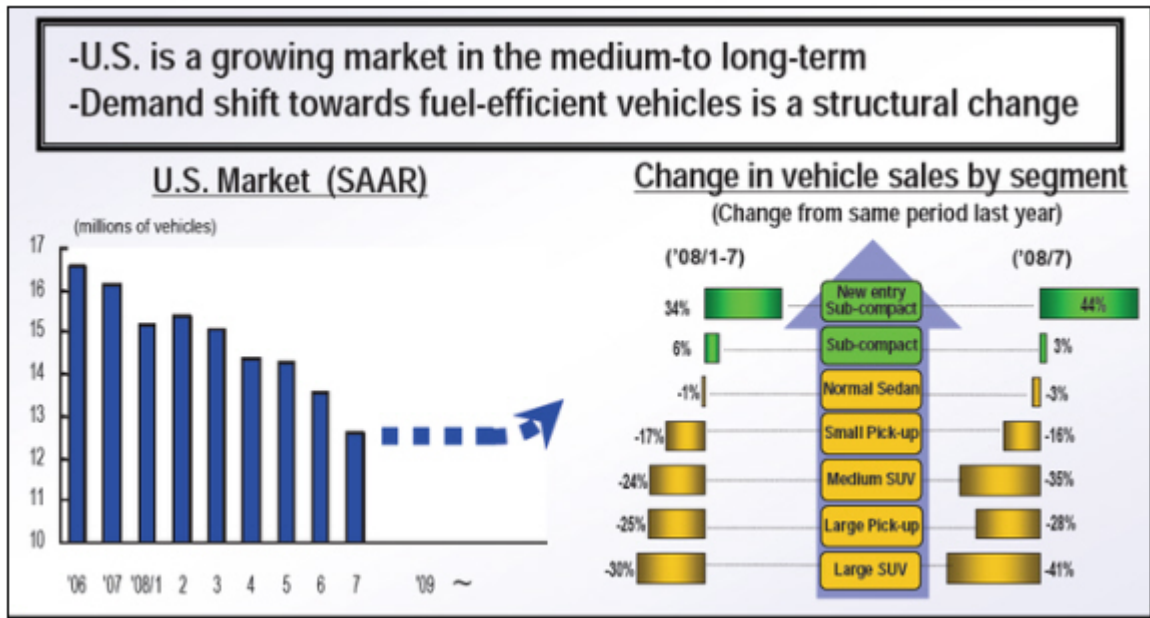


Figure 3.9: Rapid change in market structure [23]

3.2 OEM Directional Trends

3.2.1 Overview

With the increasing worldwide demand for oil and the increased need to create environmentally cleaner cars and reduce consumer fuel costs, the global automobile manufactures are striding towards implementing new advanced powertrain technologies. The assessment of the announcements from automobile manufacturers shows progress with various technologies which includes:

1. Conventional internal combustion engine (ICE) based vehicles that are smaller, and utilize more efficient gasoline/diesel engines
2. Higher-efficiency hybrids (HEV) predominantly using fossil based petroleum fuels
3. Plug-in hybrids (PHEV) with limited range of miles driven in electric mode. This option offers a significant reduction in fossil based petroleum usage, especially when the daily miles driven are close to the vehicle's electric range. The additional miles being driven above the vehicle's electric range, using petroleum or bio-fuels
4. Battery Electric Vehicles (BEV) with a driving range of approximately 200 km
5. Fuel Cell Electric Vehicles (FCEV) using hydrogen gas as a fuel source

3.2.2 Future Forecast of Vehicle Technologies by CARB

The bar chart in Figure 3.10 published by CARB (California Air Resources Board) shows future projections for advanced powertrain technologies. During the time frame for FSV's of the years 2015-2020, PHEV technology is forecast to be at mass commercialization while FCEV's are further out to year 2025, and various EV technologies are further out to year 2030.

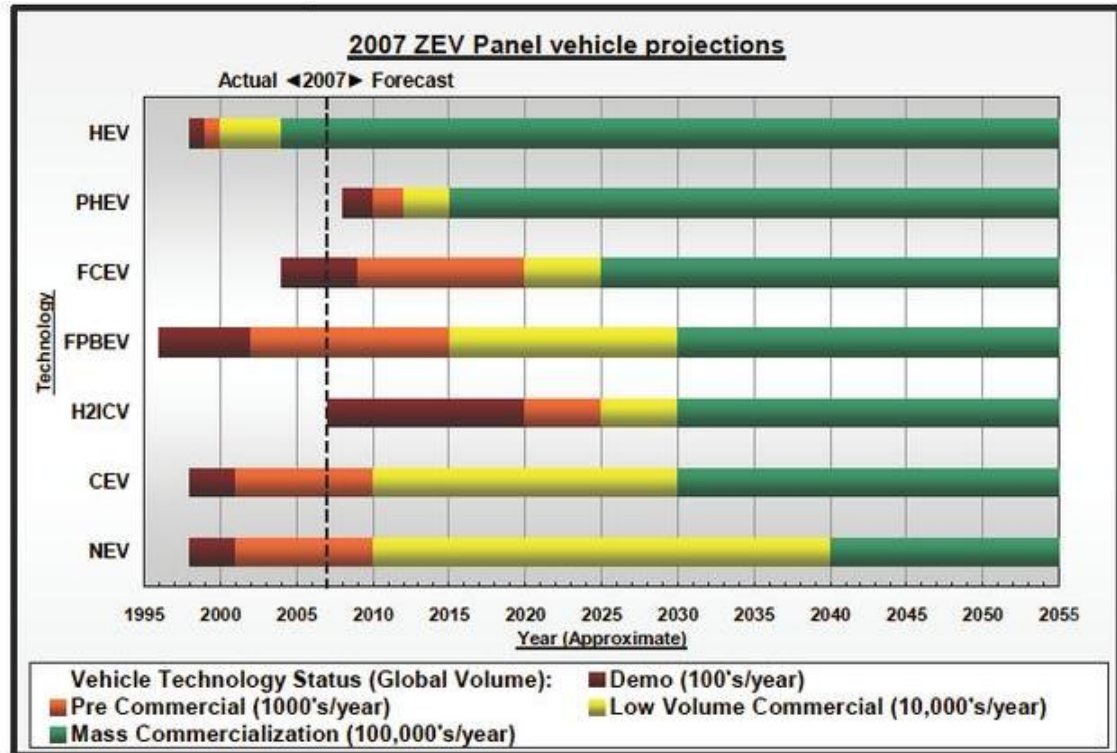


Figure 3.10: Future forecast of vehicle technologies

3.2.3 OEM Announcements

A market survey study was undertaken to research and document all of the alternate propulsion vehicles (prototype and production) that were announced by the various automakers. These were compiled and classified based on the vehicles' similarity to the Future Steel Vehicle concept of a battery electric, plug-in hybrid and a fuel cell vehicle. Table 3.2 shows the number of vehicles announced and their expected production year.

OEM Announcements (2009-2020)					
Type		Electric only	Plug-in Hybrid	Fuel Cell	
Future Steel Vehicles	BEV	18	-	-	
	PHEV	-	9	-	
	FCEV	-	-	4	Honda (2009) GM (C) Hyundai (C) Mercedes (C)

Mitsubishi (2009)	Subaru (C)
Mercedes (2011)	Th!nk (2009)
BMW (2015)	Tesla (2009)
BMW (2009)	Nissan (2010)
NICE (2009)	Dodge (2010)
Toyota (2012)	REVA (C)
BYD(2011)	TATA (2011)
Ford (2011)	Magna (C)

GM (2011)
GM (2010)
Fisker (2010)
Chrysler (2012)
Toyota (2010)
Mercedes (2012)
BYD (2009)
Volvo (C)

(XXXX) – Proposed year of production
(c) – Concept Vehicle

Table 3.2: OEM announcements

Hybrid electric vehicles have been omitted from this benchmark exercise based on research results from the FSV team that it may not be the most preferred technology by 2015-2020. Hence, only the Battery Electric Vehicles (BEV), Plug-in Hybrid Electric Vehicles (PHEV) and Fuel Cell Electric Vehicles (FCEV) were considered in this research.

The following areas on the vehicle were compiled into the list:

1. Exterior dimensions
2. Luggage volumes
3. Seating capacities
4. Performance
 - a) Vehicle range (km)
 - b) 0-100 $\frac{\text{km}}{\text{h}}$ performance
 - c) Top speed performance
 - d) Drivetrain specifications
 - e) Material of choice for body-structure, closures and sub-frames

3.2 OEM Directional Trends

3.2.4 Battery Electric Vehicles

Vehicle		Manufacturer	FSV	Mitsubishi	Mercedes	BMW	Toyota
		Name	BEV	I Miev	E cell	Mini-e	EV
		Production year	2020	2009	2011	2009	2012
Picture							
Exterior Dimensions		Length (mm)	3700	3395	4220	3714	3048
		Width (mm)	1680	1475	1890	1683	1676
		Height (mm)	1518	1600	1590	1407	1498
		Wheel base (mm)	2524	2550	unknown	2467	1998
		Curb Weight (kg)	1234	1080	unknown	1465	unknown
		Seating capacity	4+	4+	5	2	3+1
		Luggage volume (L)	250	246	500	60	unknown
Performance		All Electric Range(km)	250	160	190	250	80
		0-100kmph (secs)	10-12	9	10.8	8.4	unknown
		Top Speed (kmph)	150	155	150	152	112
Drive Train	Battery	Battery Technology	Li-ion	Li-ion	Li-ion	Li-ion	Li-ion
		Battery Capacity (kwh)	35	16	35	35	11
		Battery Weight (kg)	345	200	unknown	260	unknown
	Motor	Electric motor PP (kw)	67	47	100	150	45
Material Usages		Body Structure	Steel	Steel	Aluminum	Steel	Steel
		Closures	Steel	Steel	Aluminum	Steel	Steel
		Sub Frames	Steel	Steel	Aluminum	Steel	Steel
Estimated Cost		purchase cost (USD)		28000		60000	
		lease cost (USD/month)		NA		850	

Table 3.3: Battery electric vehicles

Vehicle		Manufacturer	Think	Nissan	NICE	NICE	Subaru
		Name	City	Nuvu	Ze-0	Mega City	R1e
		Production year	2009	2010	2009	2009	
Picture							
Exterior Dimensions		Length (mm)	3120	3000	3560	2897	unknown
		Width (mm)	1604	1700	1670	1474	unknown
		Height (mm)	1548	1550	1600	1600	unknown
		Wheel base (mm)	1970	1980		1960	unknown
		Curb Weight (kg)	1397		1350	725	unknown
		Seating capacity	2	2+1	5	2	2
		Luggage volume (L)	unknown	unknown	unknown	800	unknown
Performance		All Electric Range(km)	203 (city)	125	64	80	80
		0-100kmph (secs)	16+	unknown	unknown	unknown	unknown
		Top Speed (kmph)	100	120	88	64	104
Drive Train	Battery	Battery Technology	Li-Ion	Li-ion	lead-Acid	lead-Acid	Li-Ion (Mn)
		Battery Capacity (kWh)	28.3	unknown	18	8.2	unknown
		Battery Weight (kg)	260	unknown	unknown	unknown	unknown
	Motor	Electric motor PP (kw)	30	unknown	15	4	40
Material Usages		Body Structure	Steel	unknown	Aluminum	Aluminum	unknown
		Closures	Plastic	unknown	Acrylic ABS	Acrylic ABS	unknown
		Sub Frames	Steel	unknown	unknown	unknown	unknown
Estimated Cost		purchase cost (USD)	49500		28000	15600	
		lease cost (USD/month)	NA			NA	

Table 3.4: Battery electric vehicles

Vehicle		Manufacturer	Subaru	Tesla	BYD	Dodge	TATA	REVA
		Name	Stella	EV	E6	Circuit EV	Indica EV	NXG
		Production year	2009	2009	2011	2010	2009	TBD
Picture								
Exterior Dimensions		Length (mm)	3395	3946	4554	3900	3795	2620
		Width (mm)	1475	1851	1822	1714	1695	1640
		Height (mm)	1660	1126	1630	1150	1550	1550
		Wheel base (mm)	unknown	2351	2830	2330	2470	1810
		Curb Weight (kg)	1060	1238	2020	1360	unknown	825
		Seating capacity	4	2	5	2	4	2
		Luggage volume (L)	unknown	0	unknown	unknown	unknown	unknown
Performance		All Electric Range(km)	80	392	400	250-320	200	200
		0-100kmph (secs)	unknown	3.9	8	5	10	unknown
		Top Speed (kmph)	100	201	160	193	80	120
Drive Train	Battery	Battery Technology	Li-ion	Li-ion	Li-Ion	Li-ion	Li-ion	Zebra
		Battery Capacity (kWh)	9.2	53	65	26	unknown	18
		Battery Weight (kg)	unknown	450	590	unknown	unknown	unknown
	Motor	Electric motor PP (kw)	40	185	150/40	200	60	37
Material Usages		Body Structure	unknown	Aluminum	unknown	unknown	Steel	unknown
		Closures	unknown	Carbon Fiber/ Kevlar composite	unknown	unknown	Steel	unknown
		Sub Frames	unknown	unknown	unknown	unknown	Steel	unknown
Estimated Cost		purchase cost (USD)	20000	50000		109000	15000	
		lease cost (USD/month)		NA		NA	NA	

Table 3.5: Battery electric vehicles

3.2.5 Fuel Cell Electric Vehicles





Vehicle		Manufacturer	FSV	Honda	Mercedes	Hyundai
		Name	FCEV	Clarity	F cell	I blue
		Production year	2020	2009	concept	2015
Picture						
Physical Dimensions		Length (mm)	4300	4833	4220	4800
		Width (mm)	1780	1580	1890	1500
		Height (mm)	1518	1468	1590	
		Wheel base (mm)	2800	2799	unknown	2800
		Curb Weight (kg)	1174	1682	unknown	
		Seating capacity	5	4	5	
		Luggage volume (L)	350	370	500	
Performance		All Electric Range(km)	500	435	400	576
		0-100kmph (secs)	10-12	10	10.8	
		Top Speed (kmph)	160	160	145	160
Drive Train	Battery	Battery Technology	Li-ion	Li-ion	Li-ion	
		Battery Capacity (Kwh)	2.3	unknown	unknown	
		Battery Weight (kg)	27	unknown	unknown	
	Fuel Cell	max Output (Kw)	74	100	90	100
	Motor	Peak power (Kw)	75	100	111	
	H2 storage	Type of Storage	compressed	compressed	compressed	compressed
		Pressure (BAR)	700	350	700	700
Storage Capacity (kg)		3.4	4.1	unknown	4-5	
Material		Body Structure	Steel	Aluminum + Aluminum	Aluminum	
		Closures	Steel	Aluminum	Aluminum	
		Sub Frames	Steel	Aluminum	Aluminum	
Estimated Cost		purchase cost (USD)		500000+		
		lease cost (USD/month)		600		

Table 3.6: Fuel cell electric vehicles

3.2.6 Plug-in Hybrid Electric Vehicles


Vehicle		Manufacturer	FSV	Chevy	Mercedes	Fiskar	Toyota
		Name	PHEV	Volt	E cell +	Karma	Prilus plug-in
		Production year	2020	2010	2011	2010	2011
Picture							
Physical Dimensions		Length (mm)	4300	4495	4220	4987	4445
		Width (mm)	1780	1778	1890	1984	1725
		Height (mm)	1518	1422	1590	1330	1490
		Wheel base (mm)	2800	2710	unknown	3160	2700
		Curb Weight (kg)	1380	1530	unknown	2358	1360
		Seating capacity	5	4	5	4	5
		Luggage volume (L)	350	301	500	160	unknown
Performance		All Electric Range(km)	64	64	100	80	11.2
		Extended Range (km)	500	480	600	560	unknown
		0-100kmph (secs)	10-12	9	10.8	6	unknown
		Top Speed (kmph)	160	160	145	201	67
Drive Train	Battery	Battery Technology	Li-ion	Li-ion	Li-ion	Li-ion	Ni-Mh
		Battery Capacity (Kwh)	11.7	16	17.5	22.6	2.6
		Battery Weight (kg)	137	170	unknown	unknown	272
	motor	Peak Power (kw)	75	111	100	300	50
	IC Engine	capacity (l)	1.4	1.4	1.0	2.0T	1.4
		# of Cylinders	4	4	3	4	4
	Peak Power (kw)	75	75	50	186	56	
Material Usages		Body Structure	Steel	Steel	Aluminum	Aluminum	Steel
		Closures	Steel	Steel + Aluminum	Aluminum*	Aluminum + composites	Aluminum + steel
		Sub Frames	Steel	Steel	Aluminum *	Aluminum	Steel
Estimated Cost		purchase cost (USD)		40000		88000	
		lease cost (USD/month)		NA		NA	

Table 3.7: Plug-in hybrid electric vehicles






Vehicle	Manufacturer	BYD	Jeep	Chrysler	GM	Volvo	
	Name	F3Dm	EV	EV	Saturn Vue	C30	
	Production year	2008	TBD	TBD	2011	TBD	
Picture							
Physical Dimensions	Length (mm)	4533	4409	5144	4574	unknown	
	Width (mm)	1705	1755	1953	1854	unknown	
	Height (mm)	1490	1669	1750	1701	unknown	
	Wheel base (mm)	2600	2634	3078	2707	unknown	
	Curb Weight (kg)	1560	unknown	unknown	unknown	unknown	
	Seating capacity	5	5	7	5	4	
	Luggage volume (L)	unknown	unknown	unknown	unknown	unknown	
Performance	All Electric Range(km)	100	64	64	16	100	
	Extended Range (km)	unknown	640	640	unknown	unknown	
	0-100kmph (secs)	10.5	8	8.7	unknown	9	
	Top Speed (kmph)	150	144+	160+	unknown	160	
Drive Train	Battery	Battery Technology	Li-Fe-Ph	Li-ion	Li-ion	Li-ion	
		Battery Capacity (kwh)	16	27	22	unknown	unknown
		Battery Weight (kg)	unknown	unknown	unknown	unknown	unknown
	motor	Peak Power (kw)	50	150	190	190	unknown
	IC Engine	capacity (l)	1.0	unknown	unknown	3.6	1.6
		# of Cylinders	3	unknown	unknown	6	4
Peak Power (kw)		50	45	50	unknown	unknown	
Material Usages	Body Structure	unknown	Steel	Steel	Steel	unknown	
	Closures	unknown	steel	steel	steel	unknown	
	Sub Frames	unknown	Steel	Steel	Steel	unknown	
Estimated Cost	purchase cost (USD)	21900	32000				
	lease cost (USD/month)	NA					

Table 3.8: Plug-in hybrid electric vehicles

3.2.7 Toyota



Toyota has announced intentions to build a test fleet of Prius plug-in hybrids by 2010, but has said it will focus on traditional hybrids, including the next generation of its Prius sedan. The chief executive of Toyota Motor Corporation said that he is pushing his company's engineers to develop a plug-in hybrid electric vehicle with a lithium-ion battery before 2010, raising the stakes in a race with General Motors.

On PHEV's Toyota's argument is that the costs and trade-offs of deploying an extended range electric vehicle architecture at this time outweigh the benefits, and that blended systems have a greater benefit at this point in time. See Figure 3.11 for Toyota's Prius PHEV.



Figure 3.11: *Toyota Prius plug-in hybrid*

On March 5th, 2008 in Geneva, Toyota's president Katsuaki Watanabe told Automotive News that sometime in the 2020s, every Toyota will be available with a hybrid engine. For Toyota, hybrids are the future as it continues to build on the success of the Prius.

"When we first started the research and development of fuel-cell cars, some people predicted that they may be commercialized by around 2010. But that's difficult", Toyota Motor Corp. President Katsuaki Watanabe said.

In June of 2008, Toyota announced that they will release their new FCHV-adv model, which reportedly has a maximum cruising range of 830 km (516 miles), (compared with 330 km (205 miles) for Toyota's previous fuel cell vehicle). This improved model uses both the hydrogen powered fuel cell and an electric motor, and has improved performance partially due to better braking efficiency. See Figure 3.12 for Toyota's FCHV.



Figure 3.12: *Toyota's new 516-mile range fuel cell vehicle*

3.2.8 General Motors



GM has pledged to produce plug-in hybrid vehicles, the Saturn Vue Green Line SUV parallel-split PHEV by 2010, as well as the Chevrolet Volt, an Extended Range Electric Vehicle (E-REV) slated for production by Sept 2010. See Figure 3.13 for GM's E-REV Chevrolet Volt.

The PHEV Vue is based on the two-mode hybrid Vue also launching in 2009. If GM makes their target of having the plug-in Vue on sale for 2010, it will likely be the first commercially available plug-in hybrid in the world. See Figure 3.14 for GM's late 2009 PHEV Saturn Vue.



Figure 3.13: *Sept 2010 - Chevrolet Volt*



Figure 3.14: *Late - 2009 Saturn Vue*

Chevrolet Equinox is part of GM's Fuel Cell program. The FSV team drove this vehicle in Costa Mesa, California at Quantum. See Figure 3.15 for GM's Chevrolet Equinox Fuel Cell Vehicle.



Figure 3.15: *Chevrolet Equinox*

3.2.9 Ford



Ford will build 20 plug-in hybrids as part of a test fleet, but has not announced any plans for production.

First flex-fuel plug-in hybrid electric vehicle - As part of a push by the US Department of Energy (DOE) to make Plug-in Hybrid Electric Vehicles (PHEV) cost competitive with other cars by 2014, Ford has delivered a flex-fuel PHEV Escape to the DOE to join its test fleet of other PHEVs currently undergoing research and testing.

The vehicle is equipped with a 10 kWh lithium-ion battery that can take it up to 30 miles at speeds under $65 \frac{\text{km}}{\text{h}}$ ($40 \frac{\text{m}}{\text{h}}$) before needing to fire up its fuel-fed engine. After that, the hybrid electric engine kicks in and can deliver fuel economy of $\frac{37 \text{ km}}{\text{l}}$ ($88 \frac{\text{m}}{\text{g}}$) in the city and $\frac{21 \text{ km}}{\text{l}}$ ($50 \frac{\text{m}}{\text{g}}$) on the highway when using E85 (85% ethanol / 15% gasoline blend). See Figure 3.16 for Ford's flex-fuel PHEV.

“This vehicle offers Ford the ultimate in flexibility in researching advanced propulsion technology”, said Gerhard Schmidt, VP for Ford research and advanced engineering. “We could take the fuel cell power system out and replace it with a downsized diesel, gasoline engine or any other powertrain connected to a small electric generator to make electricity like the fuel cell does now.”



Figure 3.16: *Ford flex-fuel plug-in hybrid electric vehicle*

3.2.10 Chrysler



Chrysler Vice-Chairman and President Jim Press says some dealers have seen advanced prototypes of the company's plug-in hybrids, and according to the Los Angeles Times, Press claims to have actually driven "producible prototypes" that have a range of 483 km (300 miles) and can do 0-100 $\frac{\text{km}}{\text{h}}$ (0-62 $\frac{\text{m}}{\text{h}}$) in less than four seconds. Chrysler should have its first product in showrooms within three to five years.



Figure 3.17: Dodge EV

On Sept 24th 2008, Chrysler LLC unveiled working prototypes of an electric vehicle and two plug-in electric hybrids and announced plans to bring one of the vehicles to market in the United States by 2010.

The Dodge EV (Electric Development Vehicle), as shown in Figure 3.17, is a two-passenger, rear-wheel drive, all electric sports car that combines a lithium-ion battery pack with a 200 kW motor, capable of generating 200 kW (268 hp) and 650 Nm (480 foot-pounds) of torque. Most notably, Chrysler claims that the Dodge EV has a driving range of 240-320 km, approaching the range and performance of the all electric Tesla Roadster.

The Jeep EV Development Vehicle, as shown in Figure 3.18, is a range extended electric vehicle that uses an electric motor, a 27 kWh lithium-ion battery pack, and a small gasoline engine with an integrated electric generator to produce additional energy to power the electric drive system when needed. The 200 kW (268 hp) electric motor generates 400 Nm of torque. With approximately 30 l (eight gallons) of gasoline, the Jeep EV has a range of 650 km, including 65 km of zero fuel consumption, zero emissions, all electric operation. The Jeep EV accelerates from 0-100 $\frac{\text{km}}{\text{h}}$ in 9.0 seconds, and has a top speed of more than 153 $\frac{\text{km}}{\text{h}}$. Chrysler says that it is also exploring four wheel drive, in-wheel electric motors to demonstrate the full reach of ENVI's ^[1] advanced electric-drive technologies.

¹ENVI - Chrysler's Electric Vehicle Division - derived from **ENV**ironmental



Figure 3.18: *Jeep EV*

The Chrysler EV development vehicle is a range-extended electric vehicle that demonstrates another possible application of the ENVI electric drive technology in the segment leading Chrysler Town & Country minivan. The Chrysler EV uses a 190 kW (255 hp) motor, producing 350 Nm (258 lb-ft) of torque, providing 0-100 $\frac{\text{km}}{\text{h}}$ acceleration in approximately 9.0 seconds. Top speed is more than 160 $\frac{\text{km}}{\text{h}}$. Featuring a 22 kWh lithium-ion battery pack, the Chrysler EV range extended electric vehicle can drive 65 km on all electric power, and offers a range of 650 km on approximately 30 l (eight gallons) of gasoline. The knowledge and experience gained from the Chrysler EV will be applied to other front-wheel-drive applications in Chrysler's portfolio. See Figure 3.19 for the Chrysler EV Town & Country minivan.

Chrysler LLC has launched a Web site - www.chryslergoeselectric.com - to allow consumers to view the latest updates on electric vehicles and range extended electric vehicles from the company.

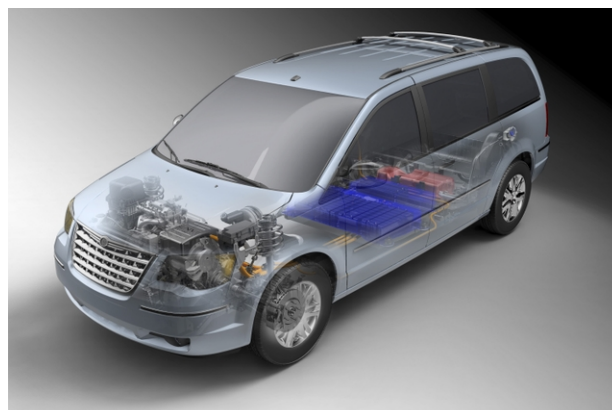


Figure 3.19: *Chrysler EV*

3.2.11 Mitsubishi



Mitsubishi plans to introduce an all electric vehicle (i-MiEV) in Japan using lithium-ion batteries in 2010, with some discussion of bringing it to the United States. See Figure 3.20 for Mitsubishi’s i-MiEV all electric vehicle.

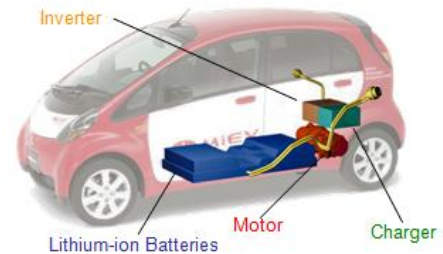


Figure 3.20: Mitsubishi innovative Electric Vehicle (i-MiEV)

The Mitsubishi i-MiEV is a test bed for an electric vehicle scheduled to be introduced for 2009. Mitsubishi has about 30 vehicles in a test fleet that are running around Tokyo right now, under study for power company usage. See Table 3.9 for Mitsubishi’s i-MiEV specifications.

Overall Length x Width x Height		3385x1475x1600 mm
Curb Weight		1080 kg
Seating Capacity		4
Max Speed		130 $\frac{\text{km}}{\text{h}}$
Range Driving Pattern: Japan 10-15 mode		160 km
Motor	Type	Permanent magnet synchronous
	Max Power	47 kW
	Max Torque	180 Nm
Drive System		Rear-wheel drive
Battery	Type	Lithium-ion
	Total Voltage	330 V
	Total Energy	16 kWh

Table 3.9: i-MiEV data table

3.2.12 Honda



Honda top executives have questioned the need for plug-in hybrids, and the company has focused on developing regular hybrids and hydrogen powered fuel cell vehicles.

In this summer of 2008, Honda released its fuel cell vehicle, the FCX Clarity, targeting southern California, which is one of the very few states in the US with hydrogen refueling stations in some numbers. While the Clarity is not immediately available for purchase, it will be available for a 36 month lease at \$600 per month. See Figure 3.21 for 2008 Honda FCX Clarity.



Figure 3.21: 2008 Honda FCX Clarity

3.2.13 Hyundai



On February 7th 2008, Hyundai's new hydrogen powered, zero-emission concept, the "i-Blue Fuel Cell Electric Vehicle" (FCEV), debuted in North America at the 100th edition of the Chicago Auto Show. Developed at Hyundai's Design and Technical Center in Chiba, Japan, the i-Blue concept illustrates the design direction for a future FCEV production model. The all-new i-Blue platform features Hyundai's third generation fuel cell technology, currently being developed at Hyundai's Eco-Technology Research Institute in Mabuk, Korea. See Figure 3.22 for Hyundai's i-Blue fuel cell electric vehicle.

Unlike its predecessors, which were built on production SUV platforms, the i-Blue features a new purpose-built 2+2 crossover architecture. Hyundai is making tremendous efforts to achieve mass production of i-Blue between 2012 and 2015.

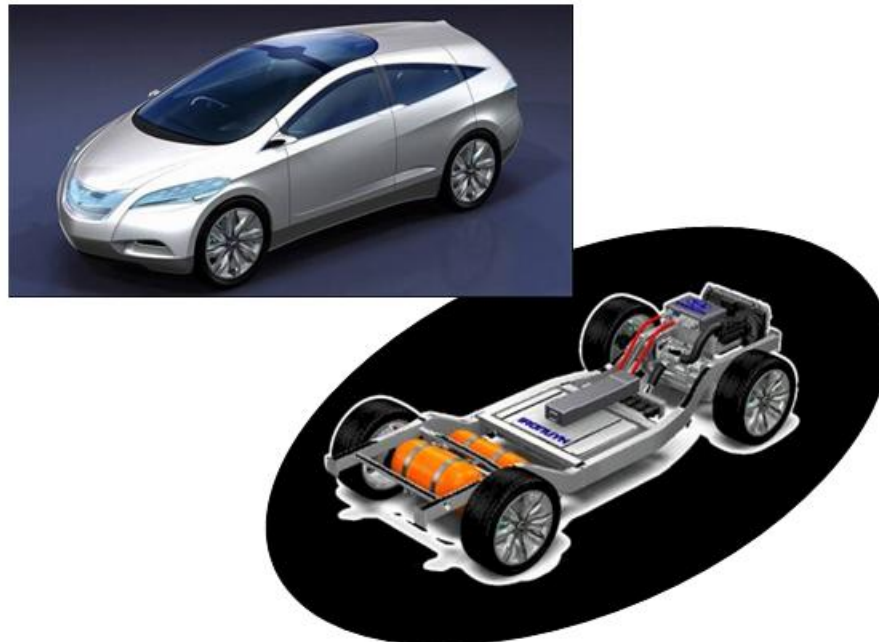


Figure 3.22: Hyundai i-Blue fuel cell electric vehicle

3.2.14 Mazda



In March 2007, Mazda announced that it will begin commercial leasing of the Premacy Hydrogen RE hybrid in 2008. The hybrid's power will be increased by 40%, and it will offer a hydrogen range of 200 km (124 miles), double the 100 km of the first version of the concept hybrid. Mazda will follow that with an improved hydrogen hybrid system shortly after 2010. Mazda's newest hydrogen rotary engine will take to public roads in Japan for testing this year (2008). The company says the vehicle is the world's first hydrogen hybrid car with a dual-fuel system, enabling the use of either hydrogen or gasoline.

In the Premacy Hydrogen RE hybrid, the hydrogen-fueled rotary engine and the 30 kW electric motor are incorporated into a power unit that is transversely mounted at the front of the car in a front-forward layout. A NiMH battery pack is located under the second row seats, and a high capacity hydrogen tank is located in the space that would otherwise be occupied by a third row seat. See Figure 3.23 for 2010 Mazda Premacy Hydrogen RE hybrid.

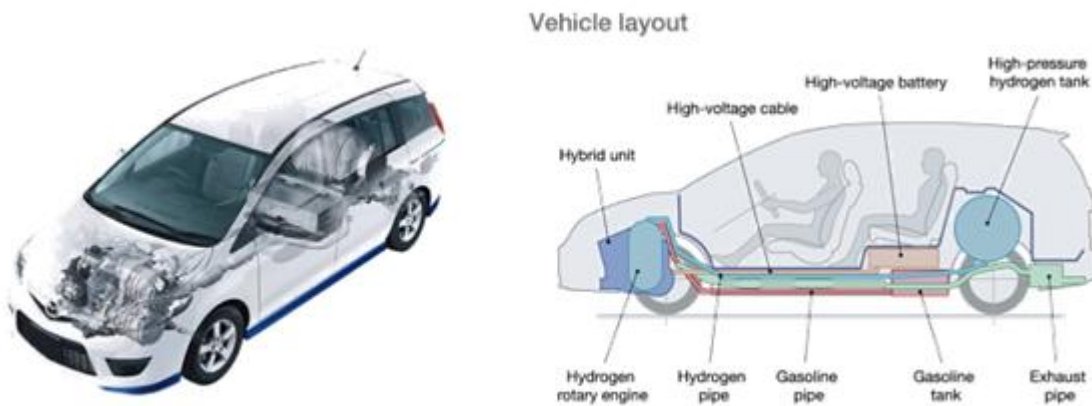


Figure 3.23: 2010 Mazda Premacy Hydrogen RE hybrid

3.2.15 Volvo



Together with electricity provider Vattenfall, automobile manufacturer Saab, Swedish battery maker ETC and the Sweden government itself, Volvo is launching a joint broad based research venture to spearhead technology development in the area of PHEVs. Sweden will be the location for the field testing of PHEVs.

Volvo's investment in the project will be over 11 billion SEK (USD \$1.8 billion) for the next five years, even though Volvo is not totally committed to bringing this vehicle on the road.

The Volvo ReCharge concept shown at the 2008 Detroit NAIAS, combines a number of the latest technological innovations in a "Series hybrid" where there is no mechanical connection between the engine and the wheels. See Figure 3.24 for the Volvo C30 ReCharge concept, and Figure 3.25 for its powertrain layout.

- The battery pack integrated into the luggage compartment uses lithium-polymer battery technology. The batteries are designed to have a useful life beyond that of the car itself
- EV range of 100 km
- Four electric motors, one at each wheel, provide independent traction power
- Four cylinder, 1.6 L turbo-diesel 81.3 kW (109 hp) engine, drives an advanced generator that efficiently powers the wheel motors when the battery is depleted



Figure 3.24: Volvo C30 ReCharge concept

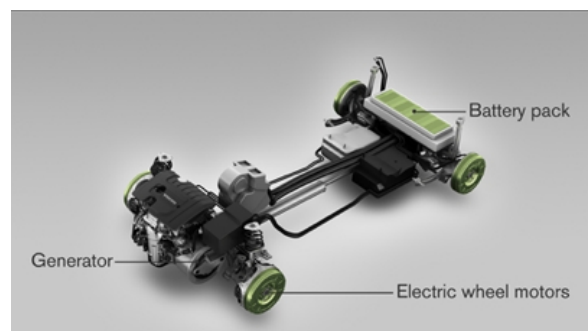


Figure 3.25: Volvo C30 concept powertrain

3.2.16 Nissan



Hybrids are yesterday's news according to Nissan's standards. Although the Japanese automaker does plan to embrace hybrid technology, it is banking on plug-in electric vehicles as the next big thing.

In August of 2008, Nissan Motor unveiled all electric and original hybrid electric prototype vehicles, both powered by advanced lithium-ion batteries. Under the Nissan GT 2012 business plan, the company has committed to zero emission vehicle leadership, and has announced plans to introduce an all electric vehicle in 2010 and mass market it globally in 2012. See Figure 3.26 for Nissan's EV prototype.

3.2.16.1 Electric Vehicle (EV)

Powered by advanced lithium-ion batteries, the EV prototype is part of Nissan's substantial research and development program on zero emission vehicles (ZEV). This latest generation vehicle features a front wheel drive layout and uses a newly developed 80 kW motor and inverter. The advanced laminated compact lithium-ion batteries are installed under the floor, without sacrificing either cabin or cargo space.



Figure 3.26: Nissan EV - Electric Vehicle

The production vehicle to be introduced in 2010 will have a unique body style and is not based on any existing Nissan model. Nissan has not released the production volume numbers for the EV, but the first American version of the EV-02 will be limited to fleet applications.

3.2.16.2 Hybrid Electric Vehicle (HEV)

The Nissan original HEV delivers two breakthrough technologies - a high performance rear wheel drive hybrid system and a parallel-hybrid powertrain system. The hybrid employs Nissan's own originally developed hybrid technology and its first rear wheel drive hybrid power train. Nissan will have a line up of electric cars, as well as plug-in hybrids and fuel cell cars, which will not be available until "no earlier than 2015".

3.2.17 TATA Motors



The company is working on a gas-electric hybrid vehicle capable of delivering about 20 km per liter complying with BS III and IV emission norms that could be applicable to Tata's Indica and its variants, and a possible adaptation of the concept to other platforms in future.

Moreover, the sources said TATA Motors is also working on five prototype electric vehicles using lithium-ion batteries to be produced on the TATA Indica platform, which could have a range of 200 km per charge and may be introduced by 2011. See Figure 3.27 for Tata's Indica.



Figure 3.27: TATA Indica

The new car is expected to hit Indian roads in 2008, said chairman Ratan Tata, but Tata has not disclosed the possible price range for the electric car. Although, quoted to be launched in Europe in "large production volumes", the exact number of these vehicles TATA plans to build is unknown.

3.2.18 Peugeot



Scheduled to enter the market in 2010, the new Peugeot 308 diesel hybrid continues development on a commercially viable hybrid drive system, in its present form the 308 is now capable of $\frac{35 \text{ km}}{\text{l}}$ ($83 \frac{\text{m}}{\text{g}}$) on the combined city/highway cycle and emissions of only $90 \frac{\text{g}}{\text{km}}$ of CO_2 . See Figure 3.28 for Peugeot 308.

Focusing on the commercialization of the 308 hybrid HDi, the number of specific parts associated with the “hybridization” of the new model has been reduced by 30% over its predecessor, while concentration on the hybrid’s packaging into the 308’s structure and its Euro V compliancy have become key priorities.

Powered by a 82 kW (110 hp) 1.6 L HDi engine, coupled with a 16 kW (22 hp) electric motor and a 6 speed electronically-controlled manual gearbox, the 308 hybrid HDi is able to trump existing models in the 308 range.

A new generation Nickel Metal Hydride (NiMH) battery pack has been developed which delivers an output of 200 V. It is housed in the spare wheel well and does not reduce the available trunk volume.



Figure 3.28: Peugeot

3.2.19 Newcomers to Plug-ins

3.2.19.1 BYD



China's car manufacturer and battery specialist BYD will launch its F3DM PHEV in China by the end of 2008. The BYD Dual Mode F3, known as the F3DM plug-in hybrid, uses an iron based battery instead of a lithium battery to reduce high production costs, which according to BYD should be good for 600,000 km. See Figure 3.29 for BYD's F3DM plug-in hybrid.

BYD says that the battery pack can be recharged about 2,000 times, sufficient for up to 10 years of operation. BYD claims that F3DM is capable of traveling 100 km (62 miles) on electric power provided by the battery, with combined total mileage of 300 km (186.4 miles).

F3DM plug-in hybrid can be 50% recharged in just 10 min and fully recharged within 7 hours. Top speed is over 150 $\frac{\text{km}}{\text{h}}$ (93.2 $\frac{\text{m}}{\text{h}}$) and it takes less than 13.5 s to accelerate from 0-100 $\frac{\text{km}}{\text{h}}$ (62 $\frac{\text{m}}{\text{h}}$).



Figure 3.29: F3DM plug-in hybrid

The F3DM will be on sale in China by the end of November, mainly available to fleet operators. The company also has plans to sell inexpensive hybrids and electric vehicles in the U.S., Israel and Europe by 2010. Expected volumes of the F3DM is unknown.

In the Fall of 2008, Warren Buffet, MidAmerican Energy Holdings Co., a Berkshire Hathaway Inc. subsidiary, announced that it would spend US \$230 million to buy a 10% stake in BYD.

3.2.19.2 Fisker Automotive



Capable of hitting $200 \frac{\text{km}}{\text{h}}$ and $0-100 \frac{\text{km}}{\text{h}}$ in under 6 s, Fisker Automotive claims the Karma will be able to drive 80 km (50 miles) on electric power and another 570 km on gasoline.

The car is a series plug-in hybrid based on technology developed by Quantum Technologies. The Q-DRIVE consists of a gasoline engine, which in turn charges the lithium battery packs in the car. See Figure 3.30 for Fisker's Karma. The first Fisker Karmas are expected to roll off of the line in late 2009, and Valmet Automotive, the contract company that will build these vehicles in Finland, can produce 15,000 cars annually.



Figure 3.30: Fisker Karma

3.2.19.3 Tesla



The Tesla Roadster is the first production car powered solely by lithium-ion batteries. Its structure is constructed from an extruded aluminum space frame which is similar in design and construction to the Lotus Elise. See Figure 3.31 for Tesla's Roadster.

Tesla has also announced that its White Star, a high performance electric sedan competing with such cars as the BMW 5-series, will be a US \$60,000 car, but that it was also working on a sub-\$30,000 all electric car that could be available within four years.

The Tesla Roadster is currently in production as of September 2008. Tesla's Roadster production volumes are only expected to hit a maximum of about 2,000 cars a year.

A new sedan model, called the Model S, is a plug-in electric vehicle, designed from the ground up. Unlike the Roadster, which has a starting price of \$109,000, the Model S will be priced beginning at \$57,400 and Tesla hopes to see as many as 15000 sedans a year.

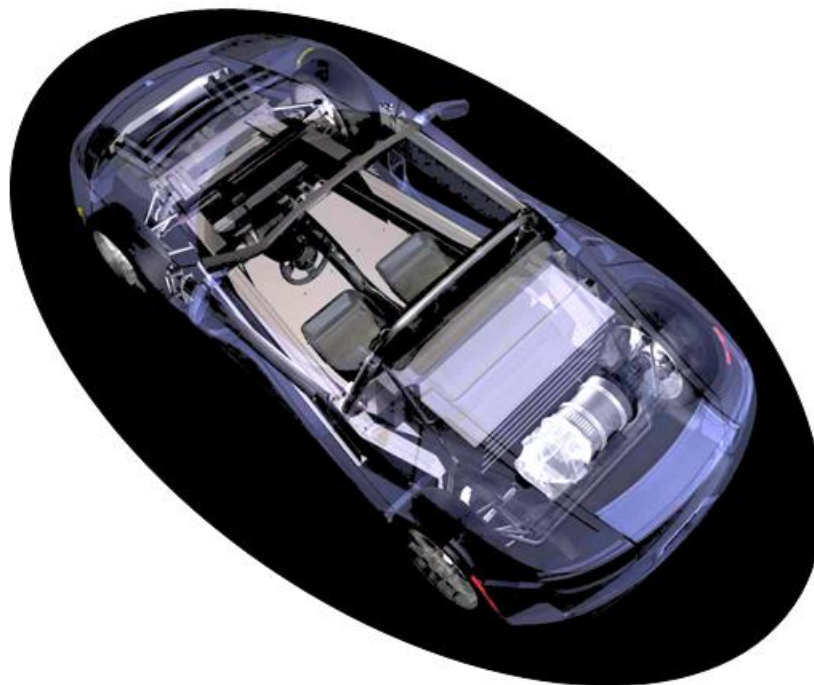


Figure 3.31: Tesla Roadster

3.2.19.4 Project Better Place



Project Better Place is a venture backed company aiming to reduce global dependency on oil by creating a transportation infrastructure supporting electric vehicles, while providing consumers with a cleaner, sustainable, personal transportation alternative. Shai Agassi publicly launched the company, headquartered in Palo Alto, CA on October 11, 2007. See Figure 3.32 for Project Better Place business plan.

Key Goals

1. Infrastructure setup for a universal battery charging and/or replacement station
2. Manufacturers will provide the vehicle and design the vehicle to accommodate a universal replaceable battery pack
3. Catalyze mass market deployment of electric vehicles
4. Implement a new ownership model (same strategy as cell phone providers)

Business Plan

The Project Better Place business plan can be compared to a mobile phone system.

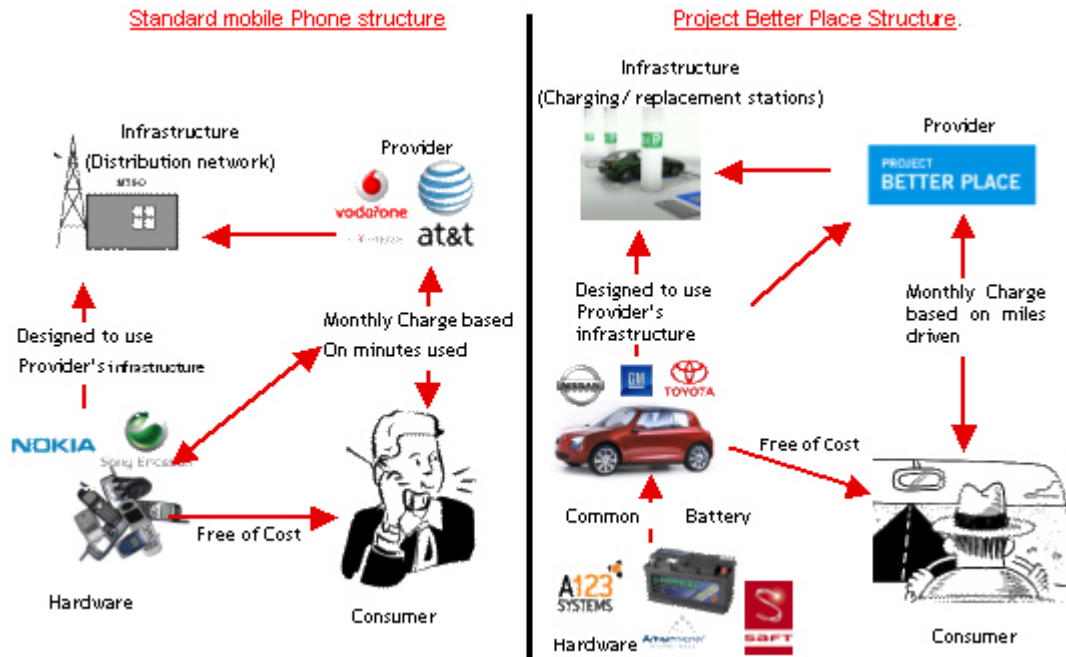


Figure 3.32: *Project Better Place business plan*

Project Better Place: Prototype Vehicle

Their first prototype (a modified Renault Megane) was unveiled in Tel Aviv in May 2008. See Figure 3.33 for Project Better Place powertrain, and Figure 3.34 for Project Better Place prototype car during evaluation tests. Project Better Place prototype vehicle specifications are listed in Table 3.10.



Figure 3.33: Project Better Place powertrain



Figure 3.34: Project Better Place mule vehicle

Platform	Renault Megane
EV Range	200 km (124 mi)
Performance	0-100 kph in 13 s
Start of Production	2010
Projected Volume	100,000 units

Table 3.10: Prototype vehicle specifications

In The News

1. Successful partnerships have been reached early in 2008 to launch the program in Denmark and Israel (for cars on the market by 2011)
 - ⇒ Project Better place has claimed it will build 500,000 charging stations and 100,000 electric cars in Israel by 2010
2. Better Place CEO Shai Agassi, on Oct 24th 2008, announced a deal with Australia's AGL Energy Ltd. and Macquarie Capital Group to raise \$1 billion (US \$670 mil) to develop the program in Australia, with the first mass-market cars expected to be available for the 2012 model year, including:
 - a. More than 200,000 charge stations in Brisbane, Sydney and Melbourne
 - b. About 150 battery exchange stations at about 40 km intervals on major freeways
3. Project Better Place is currently in conversation with 15 other countries

3.3 Alternate Propulsion Vehicles Benchmark

3.3.1 Research Methodology

Data compiled in this benchmarking report is a combination of research data obtained by the following sources.

- Los Angeles Auto Show (Nov 24-25, 2008)
At the Los Angeles Auto Show, the production Mitsubishi i-Miev was on display. FSV team members were provided exclusive up close contact with the vehicle to study the material of choice for the body-structure and closures, along with some useful comments from the manufacturer technical representative
- North American International Auto show, Detroit, MI (Jan 14-15, 2009)
The North American International Auto Show provided some useful insights into the latest alternate fuel vehicles from Mercedes, the Blue-Zero series. The FSV team gathered useful information on the technology, and some general information during this auto show
- Manufacturer's press releases
A majority of the information in this report relies on press releases from the respective manufacturers. These were collected from the auto shows, and the respective manufacturer websites
- Secondary research
Secondary research is an additional method of conducting marketing research, however it differs from primary research as the information found has already been compiled by someone else. Extensive materials were collected from various sources that have considerable experiences in research of new green technologies and future concepts in automotive design and manufacturing
- Word of mouth
Some of the information compiled in this report was obtained through word of mouth. This mode of data collection was given the least priority in terms of credibility of the information received

3.3.2 Benchmark Vehicle Selection

Based on the similarities in the powertrain layout, overall vehicle size or advanced technologies, the following vehicles, shown in Figure 3.35 were chosen for a detailed benchmark study against the Future Steel Vehicles.

1. 2009 Mitsubishi i-MiEV
2. 2011 Chevrolet Volt
3. 2009 Honda Clarity FCX
4. Mercedes Blue-Zero concepts

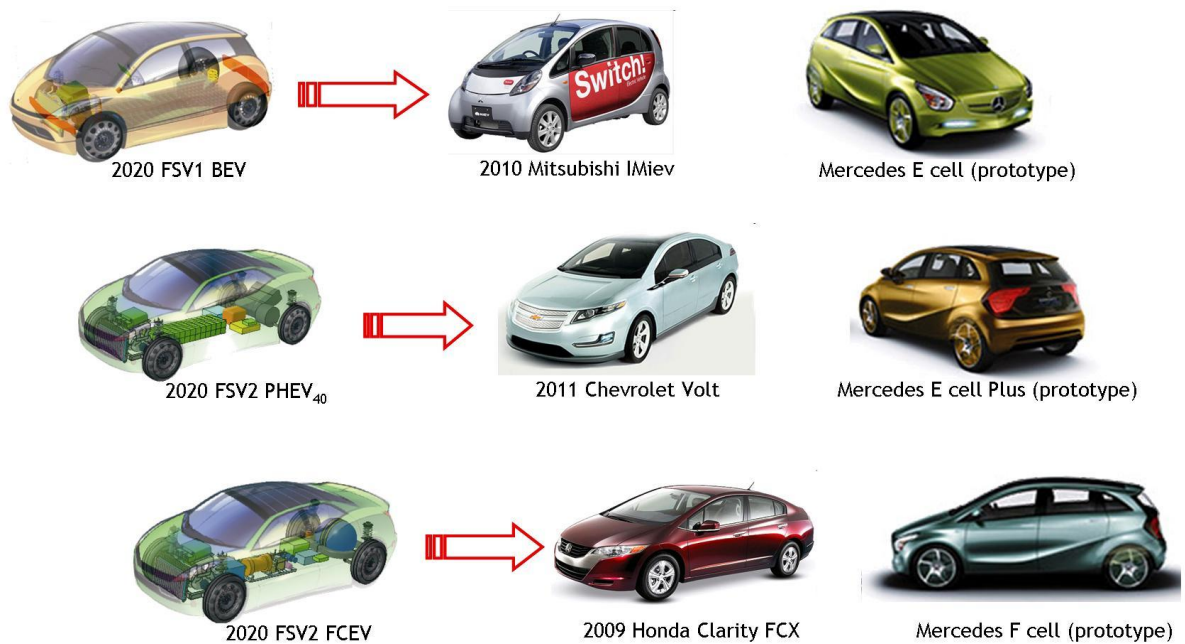


Figure 3.35: *Vehicles selected for benchmark*

3.3.3 2009 Mitsubishi i-MiEV

3.3.3.1 Synopsis

The 2020 Future Steel Vehicle-1, as shown in Figure 3.37 is a B-class hatchback, designed completely using steel, and provides packaging for a battery electric vehicle and a PHEV₂₀ vehicle.

The 2009 Mitsubishi i-MiEV, shown in Figure 3.36, was chosen for this benchmark study since it is the first production electric vehicle, meets all the relevant Japanese and European safety and crashworthiness requirements and is available for purchase in Japan starting mid year 2009.

This report compares the two vehicles in terms of powertrain sizes and performance, packaging and material usages on various body-structure parts and closures. The general specifications of the two vehicles are compared in Table 3.11.



Figure 3.36: 2009 Mitsubishi i-Miev



Figure 3.37: Future Steel Vehicle-1

General Specifications	2009 IMiEV	2020 FSV
Type	BEV	BEV
AER [km]	160	250
Extended range [km]	NA	NA
Curb Weight [kg]	1080	1232
Drive Type	RWD	FWD
0-60mph [sec]	9	10-12
Top Speed [kmph]	130	150
Model Year	2009	2020
Apprx Cost [USD]	\$TBD	\$32,500

Table 3.11: General specifications - FSV & Mitsubishi i-Miev

Since the Mitsubishi i-MiEV was not available to the general public at the time of this report being generated, all data obtained on this vehicle is through media sources and limited interaction with the vehicle at the various auto shows. Currently built mostly from steel, the i-MiEV is based on the i-minicar platform.

3.3.3.2 Exterior Dimensions

The i-MiEV is approximately 305 mm shorter in length than the Future Steel Vehicle, and is higher than the FSV by approximately 60 mm. The FSV is 205 mm wider than the i-MiEV and thus provides more shoulder room for passengers. i-MiEV is narrower than the Smart Fortwo by 84 cms and 225 cms shorter than a Ford Ka. Despite this good packaging and a cab forward design, it will seat four adults with head and leg room to spare. The dimensions of the i-MiEV are shown in Figure 3.38 and compared with the FSV-1 shown in Figure 3.39

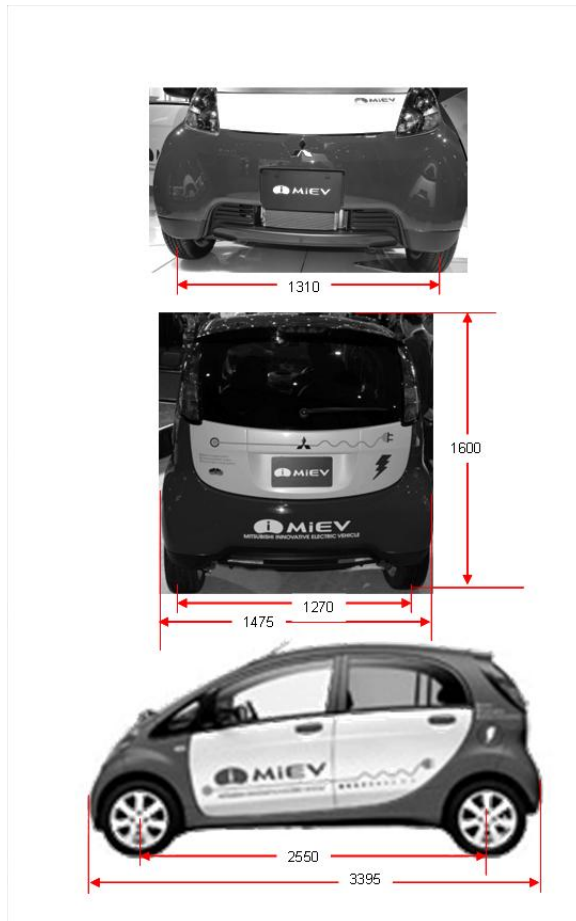


Figure 3.38: 2009 Mitsubishi i-MiEV

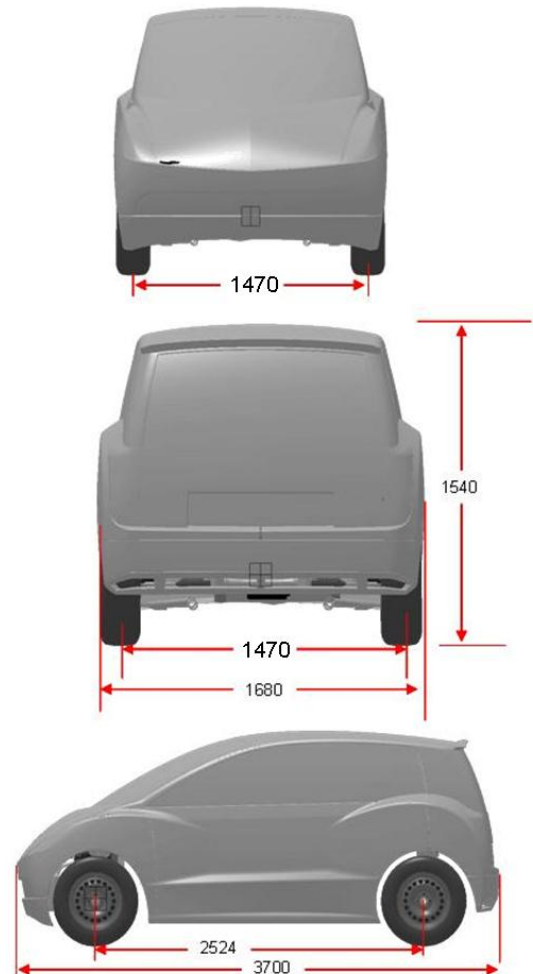


Figure 3.39: Future Steel Vehicle 1

3.3.3.3 Material Usage

The i-MiEV predominantly uses steel on all the body closures and the pillars. The rockers are steel and are covered by a plastic trim panel. Figure 3.40 shows the type of materials used on the i-MiEV.



Figure 3.40: Material usage

3.3.3.4 Powertrain Packaging

The key difference between the two vehicles, in terms of powertrain packaging, is that the motor, inverter, and charger are packaged in the front on the FSV-1 as opposed to the rear on the i-MiEV. A higher energy density battery (35 kWh) is packaged under the floor of the FSV-1, while the i-MiEV has a 16 kWh battery pack in the same location. The wheelbase of the FSV-1 is shorter than the i-MiEV by approximately 25 mm. Figure 3.41 and Figure 3.42 show the packaging of powertrain components on the i-MiEV and FSV-1 BEV respectively.

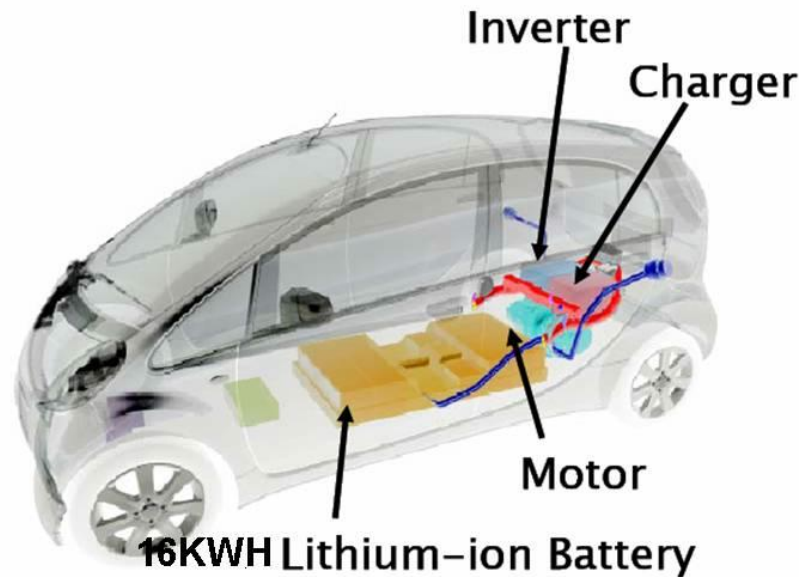


Figure 3.41: 2009 Mitsubishi i-MiEV

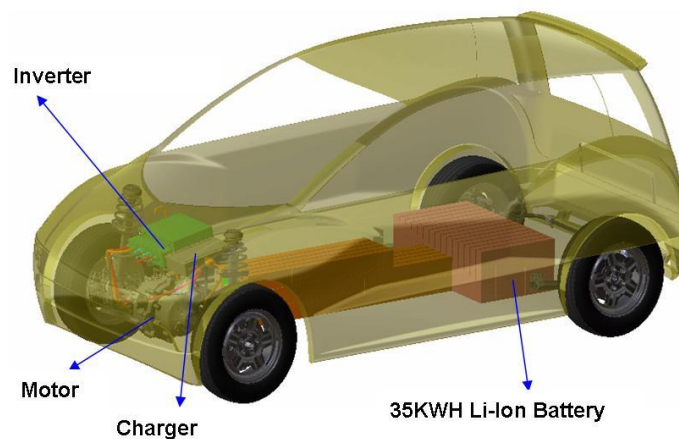


Figure 3.42: FSV-1 BEV

3.3.3.5 Electric Drive Components

The electric drive components on the i-MiEV and the FSV-1 comprise of the following components:

- Battery Module
- Traction Motor
- Inverter and DC/DC converter

Figure 3.43 shows the battery, traction motor and inverter of the i-MiEV.

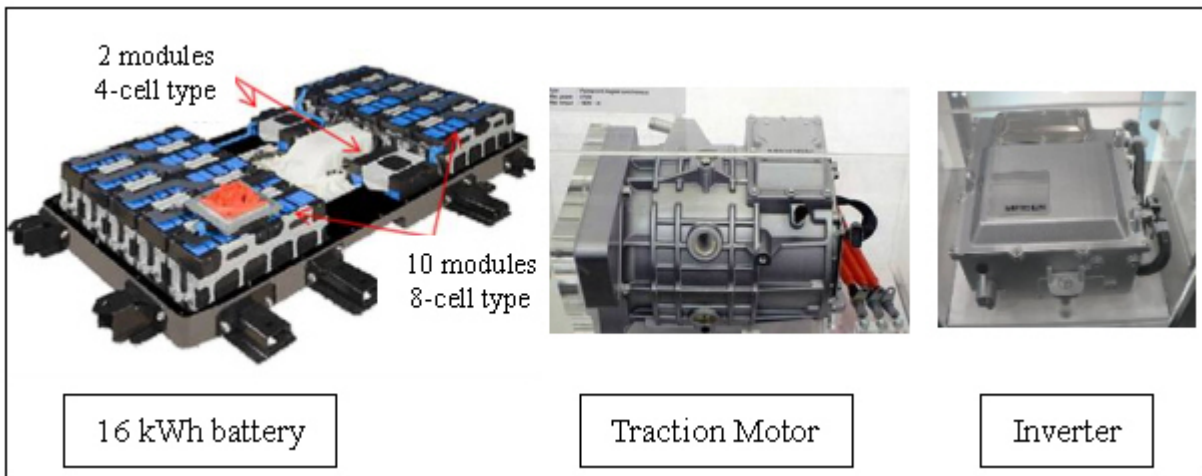


Figure 3.43: *i-MiEV electric drive components*

Figure 3.44 shows the battery, traction motor and inverter of the FSV-1.

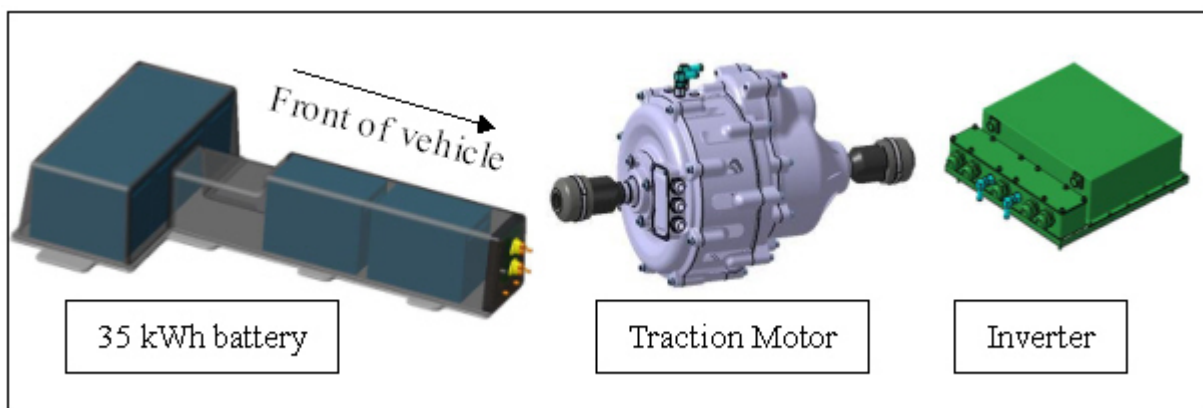


Figure 3.44: *FSV-1 electric drive components*

Lithium-Ion Battery

On the i-MiEV, the battery cell is a GS Yuasa's LIM series Li-ion based LEV50 with modifications in cell-structure and electrode materials to deliver improved energy and power densities. The LEV50 is a 3.7 V, 50 Ah cell that weighs 1.7 kg and has a volume of 0.85 liter, yielding a nominal $109 \frac{\text{Wh}}{\text{kg}}$ or a peak $218 \frac{\text{Wh}}{\text{kg}}$. The i-MiEV battery pack weighs approximately 200 kg. The 16 kWh i-MiEV battery pack, as shown in Figure 3.45 is installed under the base floor. The pack consists of 22 cell modules connected in series at the nominal voltage of 330 V (high voltage helps deliver high power). Two types of modules are packaged to allow efficient usage of the limited space. Two 4-cell modules are vertically placed at the center of the pack and ten 8-cell modules are placed horizontally. With the above configuration, the battery pack occupies almost the entire floor space underneath the vehicle. FSV-1 BEV battery, shown in Figure 3.46, weighs 346 kg, but packs more than twice the energy capacity at 35 kWh. The T-shaped battery pack utilizes the area under the tunnel and the rear seat effectively. This allows the interior to be more spacious and the pack also acts as a load carrying component.

The battery specifications from the two vehicles are compared in Table 3.12.

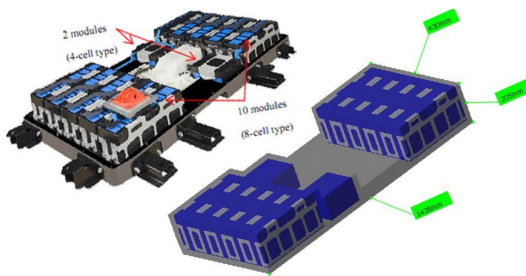


Figure 3.45: i-MiEV 16 kWh Li-ion battery

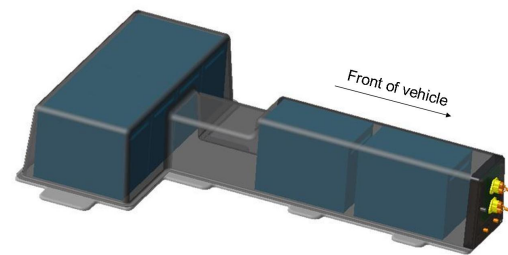


Figure 3.46: FSV 35 kWh Li-ion battery

Battery Specifications	2009 i-MiEV	2020 FSV
Capacity [KWh]	16	35
Voltage [Volt]	330	334
Energy Density [wh/kg]	80	130
weight [kg]	200	348.5
Type	Li-ion	Li-ion
Volume [liter]	NA	280

Table 3.12: Battery specifications

Traction Motor

The i-MiEV's motor, shown in Figure 3.47 along with the inverter and charger is located under the floor of the luggage area behind the rear seat. The electric inverter and traction motor are packaged into the space where the I minicar's (i-MiEV's predecessor) three-cylinder engine was packaged. The FSV-1 BEV has the motor and inverter packaged in the front under the hood leading to a shorter front-end as compared to the i-MiEV. The FSV-1 BEV also packages a higher peak power motor (67kW), shown in Figure 3.48. The BEV motor is an integrated design with the differential and the gearbox contained within the motor housing. This provides significant packaging advantages. The motor specifications of the two vehicles are compared in Table 3.13.



Figure 3.47: *i-MiEV traction motor*



Figure 3.48: *FSV-1 BEV traction motor*

Motor	2009 i-MiEV	2020 FSV
Type	Perm Magnet	Perm Magnet
Drive Type	Direct	Direct
Peak power [kW]	47	67
Continuous power [kW]	31	49
Peak torque [Nm]	108	220

Table 3.13: *Motor specifications*

3.3 Alternate Propulsion Vehicles Benchmark

3.3.3.6 Packaging

Underhood Packaging

Under the hood of the i-MiEV are the brake reservoir, coolant bottle, the ABS valve and the 12 V battery. Since all the powertrain components are packaged in the rear, additional crush space is obtained in the front with only minimal components packaged under the hood.

The FSV-1 BEV underhood packaging has the traction motor and the inverter/controller packaged to allow for a significant reduction in the front-end length of the vehicle. This also helps keep this front-end common between other FSV variants.

Figure 3.49 and Figure 3.50 show the underhood packaging on the i-MiEV and the FSV-1 BEV respectively. Figure 3.51 and Figure 3.52 show the rear trunk packaging on the i-MiEV and the FSV-1 BEV respectively.



Figure 3.49: *i-MiEV underhood*

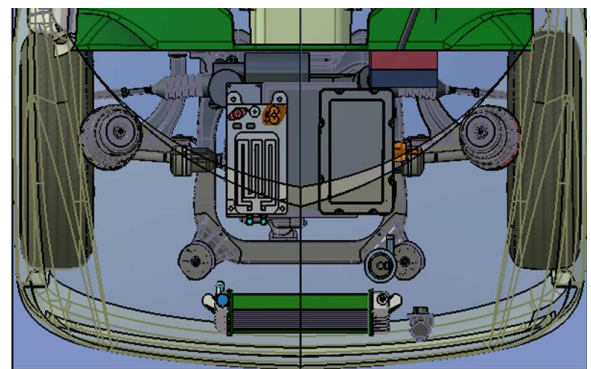


Figure 3.50: *FSV underhood*

Rear Packaging



Figure 3.51: *i-MiEV rear*

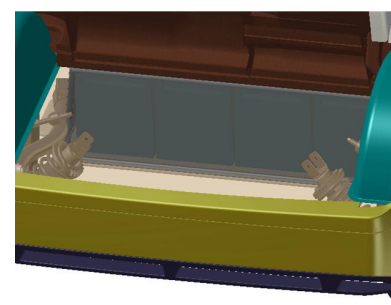


Figure 3.52: *FSV rear*

3.3.3.7 Suspension

Front

The i-MiEV uses McPherson struts in the front as shown in Figure 3.53. The absence of the engine at the front has allowed for optimization of the front suspension configuration and stroke. This, and the longer wheelbase combine to deliver well-balanced and well-mannered handling with a smooth ride and with good straight line stability.

The front suspension on the FSV is also a conventional McPherson strut design as shown in Figure 3.54.

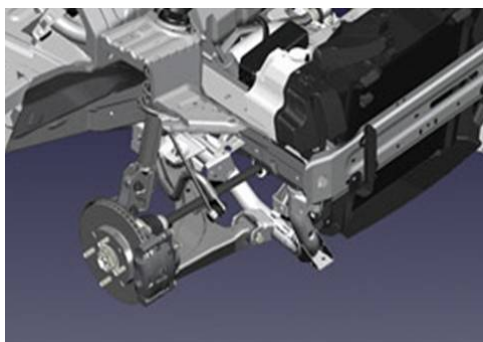


Figure 3.53: *i-MiEV front suspension*

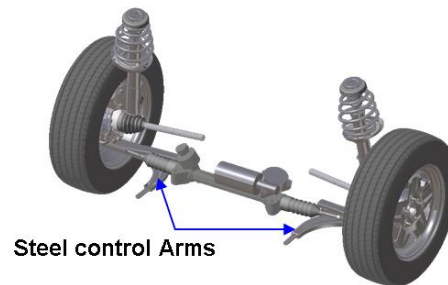


Figure 3.54: *FSV front suspension*

Rear

The i-MiEV features a 3-link De-Dion suspension at the rear as shown in Figure 3.55. The FSV, as shown in Figure 3.56, uses a H-arm camber control link independent suspension in the rear. Because the majority of the loads are in the lower arm, the camber link can be very lightweight, resulting in an overall lightweight setup.



Figure 3.55: *i-MiEV rear suspension*



Figure 3.56: *FSV rear suspension*

3.3.3.8 Tires and Wheels

The i-MiEV rides on 15-inch wheels but uses different tread widths and profiles front and rear: 145/65 R15 at the front and 175/55 R15 at the rear. As commonly seen in many other mid or rear engine configuration vehicles, the fifteen inch wheels with uneven sized tires, minimize oversteer caused by the rear-biased weight distribution. The FSV rides on light weight steel wheels and 175/65 R15 tires.

Figure 3.57 and Figure 3.58 shows the wheels on the i-MiEV and the FSV-1 respectively. The specifications of the two wheels are compared in Table 3.14.



Aluminum

Figure 3.57: i-MiEV wheel



Steel

Figure 3.58: FSV-1 wheel

	2009 i-MiEV	Future Steel Vehicle-1
Size - Front	145/65 R15	175/65 R15
Size - Rear	175/55 R15	175/65 R15
Material	Aluminum	Steel
Rolling Resistance	Low	Low - 0.007

Table 3.14: Tire & wheel specifications - i-MiEV and FSV-1

3.3.3.9 Interior

Passenger Compartment

Table 3.15 compares the interior specifications on the i-Miev and the FSV-1.

Dimensions		2009 i-MiEV	2020 FSV 1
Headroom	(Front/Rear) [mm]	990/960	997/950
Legroom	(Front/Rear) [mm]	NA	1064/063
Shoulder Room	(Front/Rear) [mm]	NA	1493/1386
Hip Room	(Front/Rear) [mm]	NA	1828/1592
Seating Capacity		4	4+
Cargo Volume	[liter]	246	250

Table 3.15: *Interior specifications*

Figure 3.59 through Figure 3.64 show the front, rear and cargo areas on the i-Miev and FSV-1 BEV.

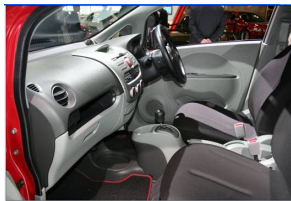


Figure 3.59: *i-MiEV front*



Figure 3.60: *i-MiEV rear*



Figure 3.61: *i-MiEV cargo space*



Figure 3.62: *FSV-1 front*



Figure 3.63: *FSV-1 rear*



Figure 3.64: *FSV-1 cargo space*

Instrument Cluster

Simple instrumentation indicates the charge level of the battery pack and the rate at which the vehicle is consuming it. The instrument cluster on the i-Miev, as shown in Figure 3.65 features a digital speedometer (with values shown in $\frac{\text{km}}{\text{h}}$), a digital fuel gauge that shows the state of the battery, and a digital odometer. The needle at the center of the analog gauge indicates the power usage.

During acceleration, the needle arcs up and to the right. During coasting, the needle dips down to the area indicating that the battery is charging via the car's regenerative braking system.

The FSV cluster utilizes a paper-thin Organic Light Emitting Diode (OLED) that allows a weight savings of 2.0 kg over a conventional instrument cluster.



Figure 3.65: i-MiEV instrument cluster

Shifter

In addition to the standard drive range, the i-MiEV transmission (shift lever shown in Figure 3.66), features an ECO (Economy) range and brake range which applies the regenerative braking more aggressively during descents.



Figure 3.66: i-MiEV transmission shifter

3.3.3.10 Safety

The rear-midship layout of the i-MiEV allows a generous front crumple zone and provides a roomier interior space. i-MiEV uses a frame structure that delivers improved multi-directional impact safety. Large cross-sectional longitudinal rails running the length of the body, absorb and diffuse impact energy in a frontal crash. Strong cross members linking these longitudinal rails effectively absorb energy during a side impact, while the floor and engine together absorb and diffuse energy during a rear impact.

Also, the additional space under the hood obtained by using a rear-midship layout and energy-absorbing wiper pivots, reduce impact energy transmission in the event of a pedestrian impact.

Figure 3.67 shows the underbody structure of the i-MiEV and the FSV-1 BEV.

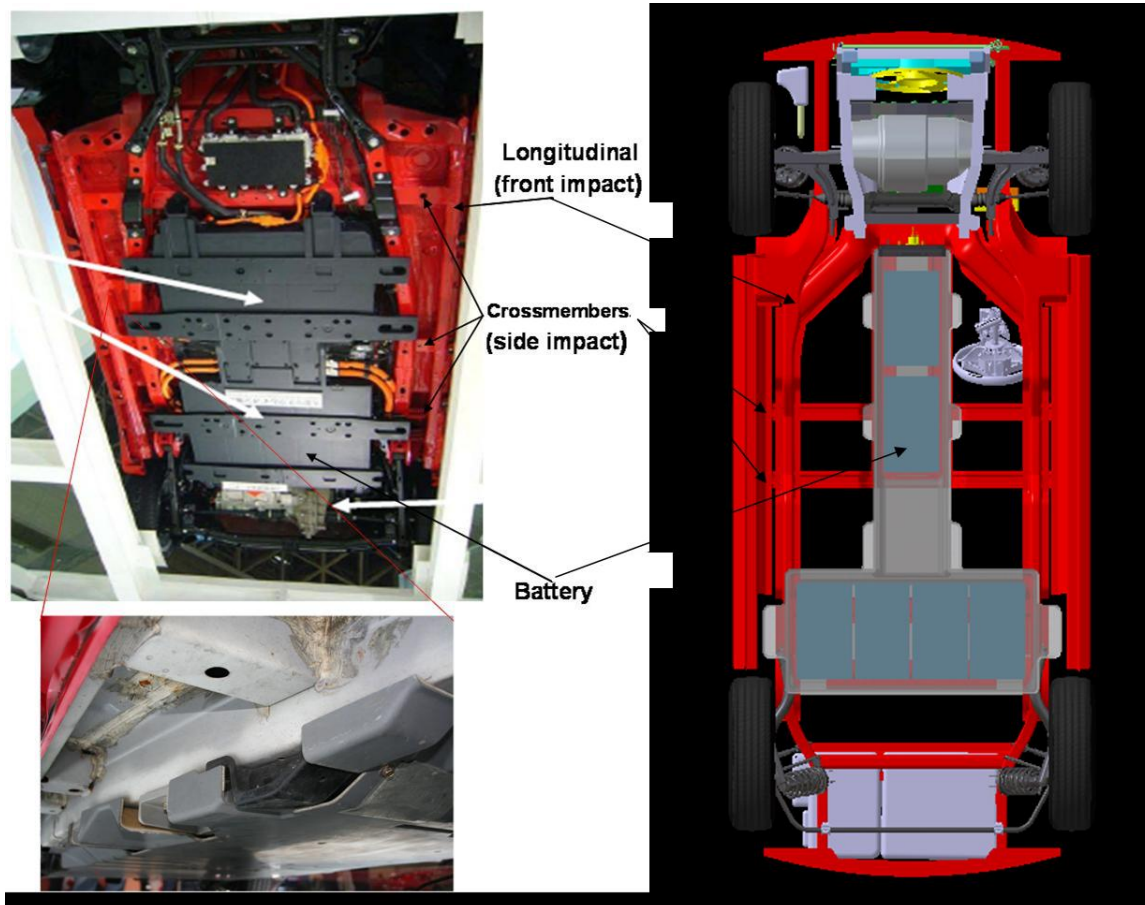


Figure 3.67: *Underbody structure*

3.3.4 2009 Honda FCX Clarity

3.3.4.1 Synopsis

The 2009 Honda FCX Clarity, shown in Figure 3.68, was chosen for this benchmark study as this is the first production fuel cell electric vehicle that belongs to the same vehicle class as the FSV-2 FCEV, shown in Figure 3.69. This vehicle meets all the relevant US safety and crashworthiness requirements (FMVSS, NCAP, IIHS) and is made available (although in limited numbers) to "eligible" customers as a short term (36 months) lease using Honda's discretionary selection methods and criteria. The overall specifications of the Honda Clarity is compared with the FSV-2 FCEV in Table 3.16.



Figure 3.68: 2009 Honda FCX Clarity



Figure 3.69: Future Steel Vehicle-2

General Specifications	2009 Clarity	2020 FSV
Type	FCEV	FCEV
AER [km]	450	500
Extended range [km]	NA	NA
Curb Weight [kg]	1624	1174
Drive Type	FWD	FWD
0-60mph [sec]	10	10-12
Top Speed [kmph]	160	161
Model Year	2009	2020
Apprx Cost [USD]	\$500,00+	\$42,150

Table 3.16: General specifications - FSV & Honda FCX Clarity

This report compares the two vehicles in terms of powertrain size and performance, packaging and material usages on the structure and closures.

Since the FCX Clarity was not available to the general public at the time this report was generated, all data obtained on this vehicle is through media sources and limited interaction with the vehicle at the various autoshow. Production numbers for the FCX Clarity are not known but Honda has planned to produce 200 vehicles within the next 3 years

3.3.4.2 Exterior Dimensions

The Future Steel Vehicle with the fuel cell package is approximately 500 mm shorter and 72 mm taller than the Honda Clarity. The Clarity is wider than the FSV-2 by 66 mm. The wheelbases of the two vehicle are similar and the track width of the FSV-2 is smaller than that of the Clarity by 29 mm. The exterior dimensions of the two vehicles are shown in Figure 3.70 and Figure 3.71 respectively.

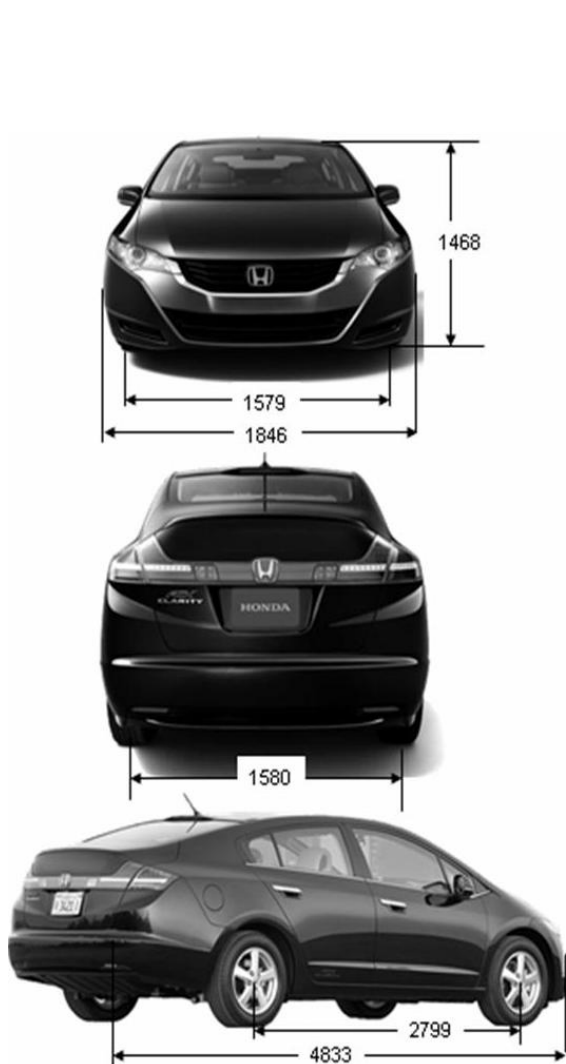


Figure 3.70: *Honda Clarity exterior dimensions*

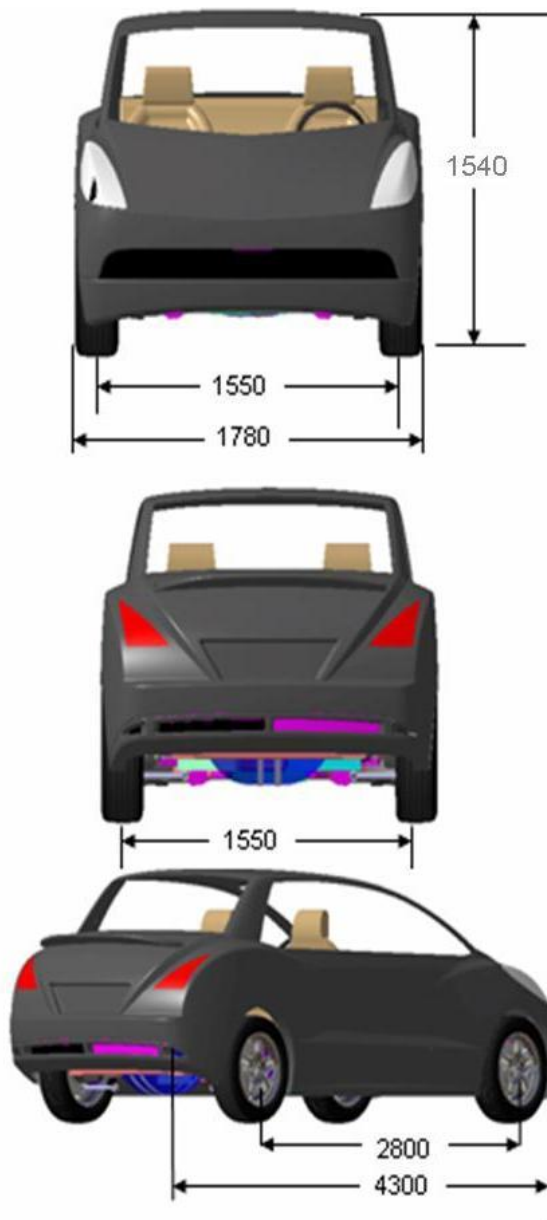


Figure 3.71: *FSV-2 exterior dimensions*

3.3.4.3 Material Usage

The FCX uses a multi-material body structure, with steel and aluminum as primary materials. The new Clarity uses the Honda Advanced Compatibility Engineering (ACE) body structure concept. The ACE body structure technology incorporates a front-end frame structure that helps absorb and disperse crash energy over a large area in a frontal impact. ACE also makes the vehicle more crash compatible in frontal impacts with vehicles of differing ride heights. Figure 3.72 shows Honda's choice of materials for the structure and closures:

- The hood, trunk, doors and fenders of the 2009 Honda FCX Clarity are made of aluminum.
- The front and rear sub-frames of 2009 Honda FCX Clarity are made from extruded aluminum.

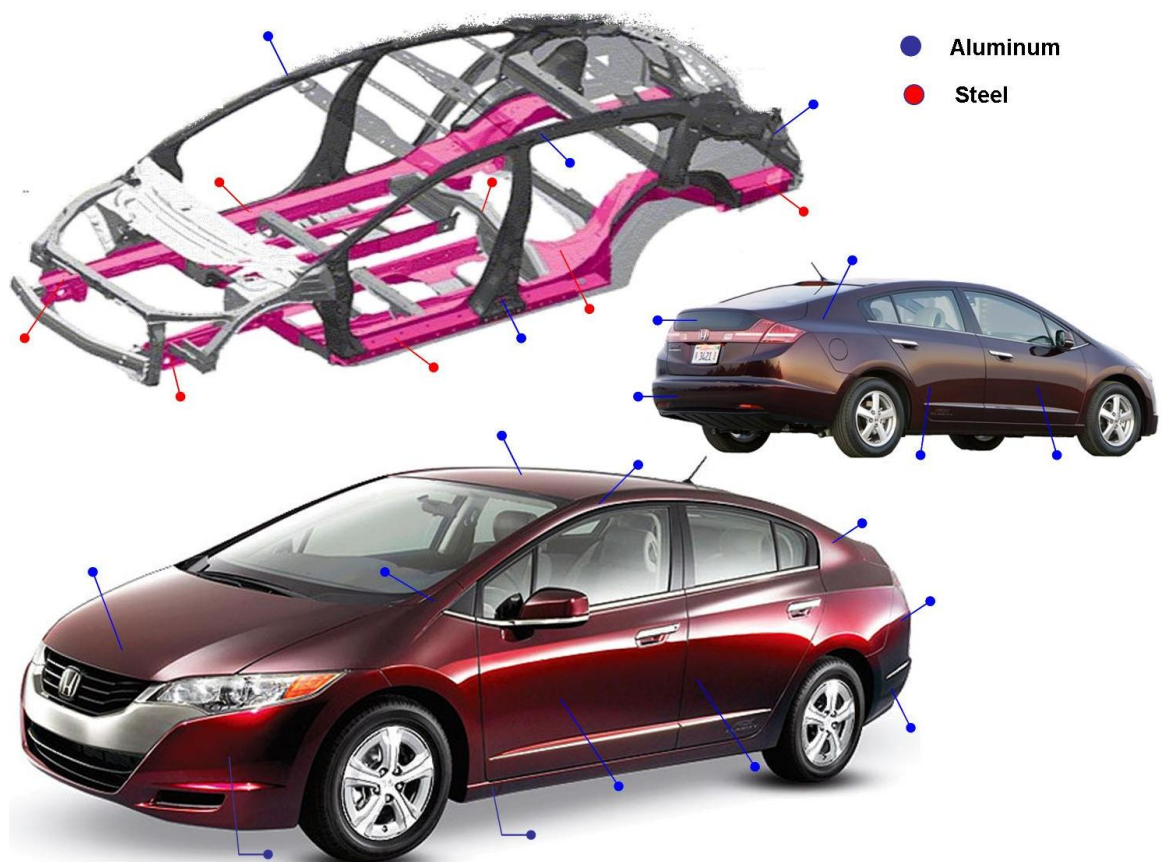




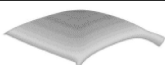



Figure 3.72: Honda Clarity material usages

3.3.4.4 Mass Estimates

The Honda Clarity, by using aluminum as a primary material for all closures and sub-frames, appears to save approximately 44 kg in weight as opposed to steel being used in these applications.

The Future Steel Vehicle uses steel as primary material of choice for all areas of the vehicle and manages to be lighter than the FCX by a margin of 450 kg. Table 3.17 shows the amount of mass savings Honda may have achieved on the body-structure, closures and suspension of the Clarity by using aluminum as the material of choice over conventional steel.

Part	Description	Honda Clarity	Appox Weight** [kg]	Comparative All Steel Vehicle	Weights [kg*]	Difference
	Front Door Panels	Aluminum	20.15	Steel	31.00	10.85
	Rear Door Panels	Aluminum	16.06	Steel	24.70	8.65
	Front Fenders	Aluminum	4.36	Steel	6.70	2.35
	Rear Decklid Panels	Aluminum	7.35	Steel	11.30	3.96
	Roof Panel	Aluminum	7.81	Steel	12.02	4.21
	Hood Panels	Aluminum	10.53	Steel	16.20	5.67
	Subframe (front)	Extruded Al	6.31	Steel	9.70	3.40
	Subframe (rear)	Extruded Al	10.92	Steel	16.80	6.88
		Al Total:	83.47	Steel Total:	128.42	44.95

** Calculated Values assuming aluminum provides atleast 35% weight gain over steel

Table 3.17: Honda Clarity - mass savings

3.3.4.5 Vehicle Layout

The vehicle layout on the Honda Clarity and the FSV-2 FCEV are shown in Figure 3.73 and Figure 3.74.

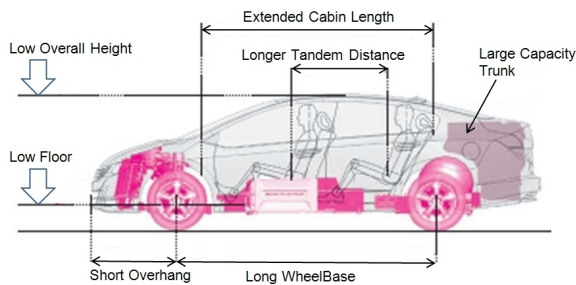


Figure 3.73: Honda Clarity layout

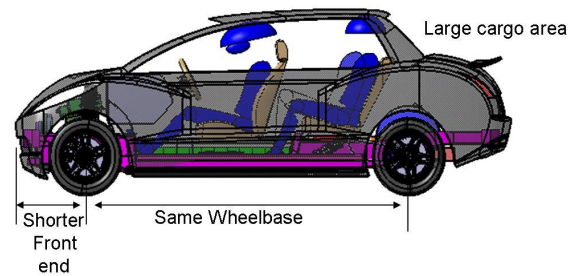


Figure 3.74: FSV-2 layout

Table 3.18 documents some key points on the layout of each vehicle.

2009 Honda FCX clarity	2020 Future Steel vehicle
The V Flow stack is located inside the center tunnel, and the lithium ion battery is placed under the rear seat. The result is a free-flowing, full-cabin design with a long wheelbase.	The fuel cell pack is also placed in the tunnel areas and li-ion battery is underneath the rear seat resulting in the same full-cabin design with a long wheelbase.
The drive motor, gearbox and PDU are combined for major space savings in the drive train system. A more compact radiator unit contributes to the short-nose design.	The motor and gearbox are combined on the FSV and results in a front end that is 415 mm shorter than a typical midsize sedan.
Reducing the number of parts in the hydrogen tank and modifying its shape result in a more efficient use of space, creating ample room in the rear seating and trunk areas. Improvements both to the hydrogen tank and the FC stack layout result in a low floor and low overall height.	The FSV tank is capable of storing Hydrogen at much higher pressures (10000psi), resulting in a smaller tank capable of providing a range of 500 km.

Table 3.18: Layout - key points

3.3.4.6 Electric Drive Components

The electric drive components on the Honda Clarity and the FSV-2 FCEV comprise of the following components:

- Battery module
- Fuel cell module
- Traction motor
- Hydrogen tank

Figure 3.75, Figure 3.76 and Figure 3.77 shows the battery, fuel cell stack and traction motor of the Honda Clarity.

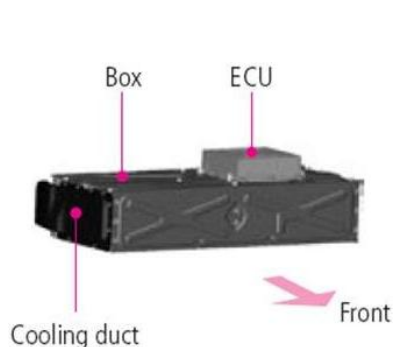


Figure 3.75: *Honda Clarity battery*



Figure 3.76: *Honda Clarity fuel cell module*



Figure 3.77: *Honda Clarity traction motor*

Figure 3.78, Figure 3.79 and Figure 3.80 shows the Battery, Fuel Cell Stack and Traction motor of the FSV-2 FCEV.



Figure 3.78: *FSV-2 FCEV battery*

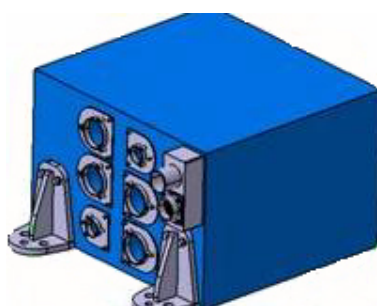


Figure 3.79: *FSV-2 FCEV fuel cell module*



Figure 3.80: *FSV-2 FCEV traction motor*

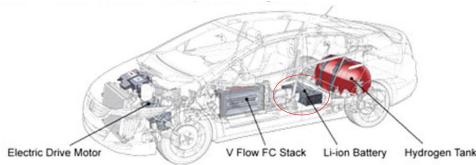
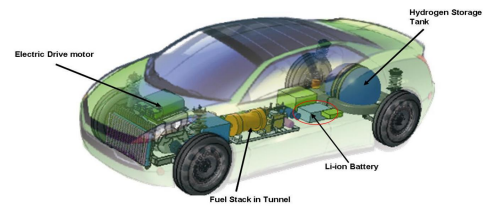
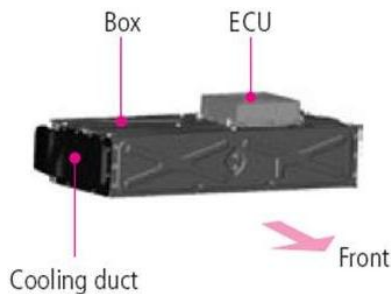
Lithium-Ion Battery

Figure 3.81: Honda Clarity battery location

Figure 3.82: FSV-2 FCEV battery location

Figure 3.83: Honda Clarity battery

Figure 3.84: FSV-2 FCEV battery

Located under the rear seat as shown in Figure 3.81, Honda Clarity's new lithium-ion battery (shown in Figure 3.83), delivers improved performance and energy recovery in a lightweight, compact package. The new battery is light and small, allowing it to be located under the rear seat as shown in Figure 3.82. This gives the car additional passenger space and a larger trunk. The FSV-2 FCEV uses a dimensionally smaller 2.3 kWh battery (Figure 3.84) is packaged in a similar location as the Clarity's battery pack and weighs 27 kg.

The battery specifications on these two vehicles are compared in Table 3.19.

Battery Specifications		2009 Clarity	2020 FSV-2
Capacity	[KWh]	NA	2.3
Voltage	[Volt]	288	334
weight	[kg]	NA	27
Type		Li-ion	Li-Ion
Volume	[liter]	NA	25

Table 3.19: Battery specifications

Fuel Cell Stack

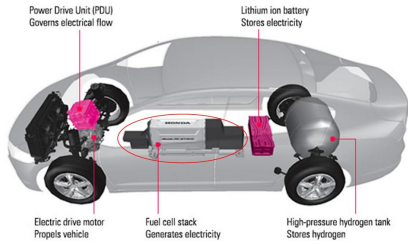


Figure 3.85: Honda Clarity fuel cell stack location

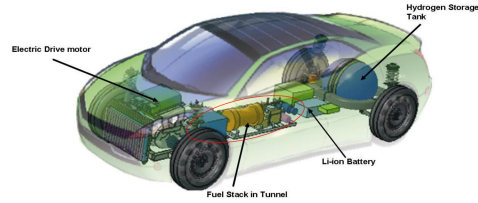


Figure 3.86: FSV-2 FCEV fuel cell stack location

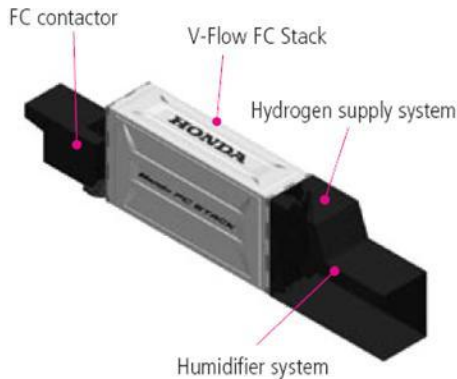


Figure 3.87: Honda Clarity fuel cell stack

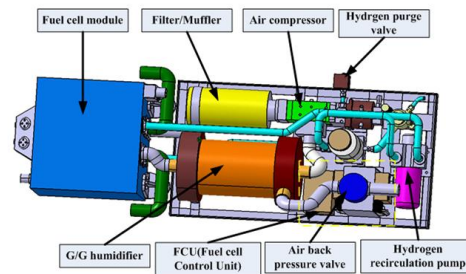


Figure 3.88: FSV-2 FCEV fuel cell stack

The FSV-2 FCEV fuel stack is mounted under the floor (Figure 3.86) but does not sacrifice any interior space while the Clarity packages its fuel stack under the front floor, in the tunnel, as shown in Figure 3.85. The FSV-2 FCEV fuel stack, shown in Figure 3.88, is 25 kg lighter and produces 25 kW less power than the Honda fuel stack (shown in Figure 3.87).

Honda’s design uses stamped stainless-steel generating plates that are grooved with vertical gas channels formed in a wave pattern that increases surface area and allows gravity to drain waste water. The fuel cell specifications of the clarity and the FSV-2 are compared in Table 3.20.

Fuel Cell Specifications		2009 Clarity	2020 FSV-2
Output	[kW]	100	65
Volume	[Liter]	52	38
Weight	[kg]	67	42
Type		PEMFC	PEMFC

Table 3.20: Fuel Cell specifications

Hydrogen Storage

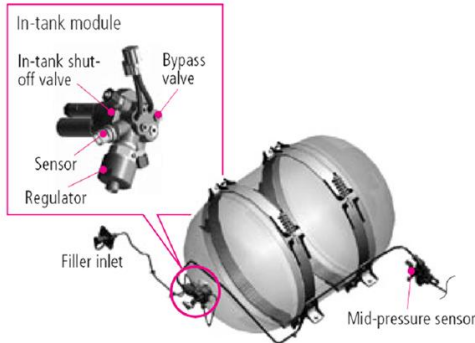


Figure 3.89: Honda Clarity hydrogen tank

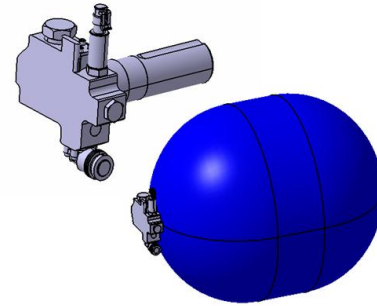


Figure 3.90: FSV-2 FCEV hydrogen tank

The Clarity features a 171 liter tank, shown in Figure 3.89, located behind the rear seats that stores hydrogen gas at up to 350 bar (5000 psi) while the FSV-2 FCEV has a 95 liter tank, shown in Figure 3.90, that stores hydrogen gas at a higher pressure of 700 bar (10000 psi). Since the FSV-2 FCEV tank is capable of storing hydrogen at such a high pressure, it allows for the tank to be of smaller volume.

The FCX hydrogen tank is made up of aluminum and carbon fiber and can store up to 4.1 kg of compressed hydrogen gas allowing a maximum range of 450 km (270 miles) on one tank. The FSV-2 FCEV tank is also made of carbon fiber and allows a higher range of 500 km.

On the Honda Clarity, the shut-off valve, regulator, pressure sensor and other components in the refueling and supply system are integrated into a single in-tank module, reducing the number of components and the same is applied to the Future Steel Vehicle.

Table 3.21 compares the specifications of the hydrogen tank on the two vehicles.

Hydrogen Tank Specifications		2009 Clarity	2020 FSV
Volume	[Liter]	171	95
Pressure	[bar]	350	700
Weight	[kg]	NA	87.1
Type		Compressed gas	Compressed gas
Capacity	[kg]	4.1	3.4

Table 3.21: Hydrogen tank specifications

Traction Motor

On the Honda Clarity motor assembly shown in Figure 3.91, the innovative shape and layout of the magnets in the rotor results in high-output, high-torque, high-rpm performance, according to Honda.

A newly designed rotor features an Interior Permanent Magnet (IPM) to lower inductance, improving reluctance torque for high-torque performance. The magnet's high-energy characteristics also contribute to a compact design.

The number of poles has also been reduced and the magnets widened to better withstand stress, allowing the yoke to wrap around the outside of the IPM. A center rib has been installed for greater rigidity. This more robust construction allows for operation at higher rpm. A new stator features a low iron-loss electrical steel sheet and higher density windings that decrease resistance and contribute to high torque and higher output. Honda reduced the number of poles from 12 to 8 to eliminate resonance points and produce quieter operation within the operating rpm range.

The FSV-2 FCEV traction motor, shown in Figure 3.92, includes the drive gear and the differential inside the housing similar to the Honda Clarity. The specifications of the two motors are compared in Table 3.22.



Figure 3.91: *Honda Clarity motor*

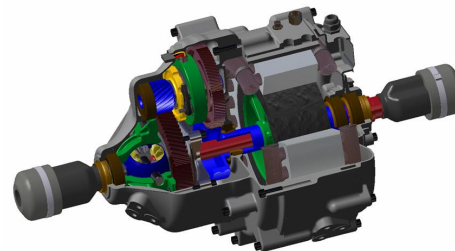


Figure 3.92: *FSV-2 FCEV Traction motor*

Motor	2009 Clarity	2020 FSV
Type	Perm Magnet	Perm Magnet
Drive Type	Direct	Direct
Peak power [kW]	100	75
Continuous power [kW]	NA	55
Peak torque [Nm]	256	220

Table 3.22: *Motor specifications*

Radiator

The FCX incorporates the fuel cell radiator, drive train radiator and the A/C condenser into one unit, as shown in Figure 3.93 which results in a 40% reduction in space typically taken by a conventional setup. This allows the FCX to have a shorter front-end when compared to similar vehicles in its class.

The FSV-2 uses the different radiators as shown in Figure 3.94, for cooling the traction motor, drivetrain and the A/C condenser which are stacked in the front, but still manages a shorter front-end when compared with the Clarity.

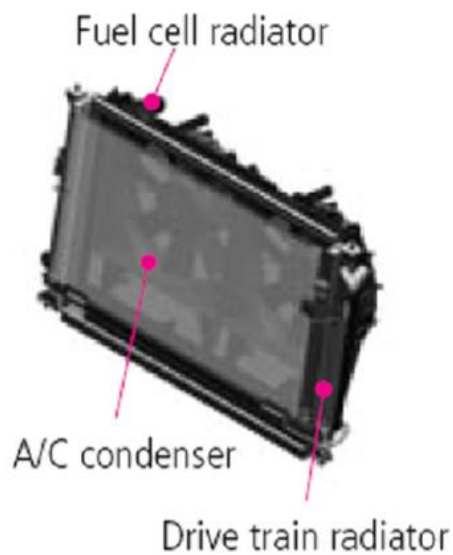


Figure 3.93: *Honda Clarity radiator*

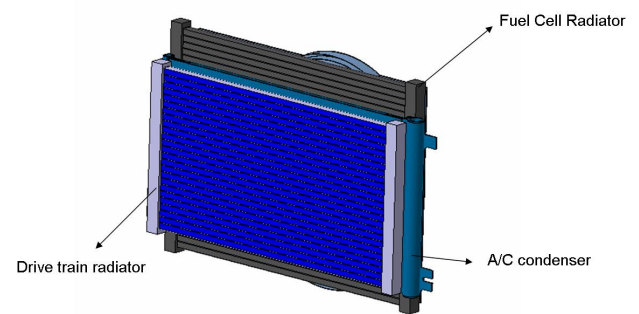


Figure 3.94: *FSV-2 radiator*

3.3.4.7 Powertrain Packaging

Figure 3.95 and Figure 3.96 show the powertrain packaging layout on the Honda Clarity and the FSV-2 FCEV . Both the Honda Clarity and the Future Steel Vehicle have similar packaging in terms of the powertrain components. The major differences among the two vehicles are that the Future Steel Vehicle packages a higher pressure hydrogen tank (700 bar) as opposed to the Honda Clarity's 350 bar hydrogen tank. Even though the Honda Clarity and FSV-2 FCEV package the fuel stack under the tunnel area, the seating capacity of the Honda Clarity is limited to four while the FSV-2 can seat five.

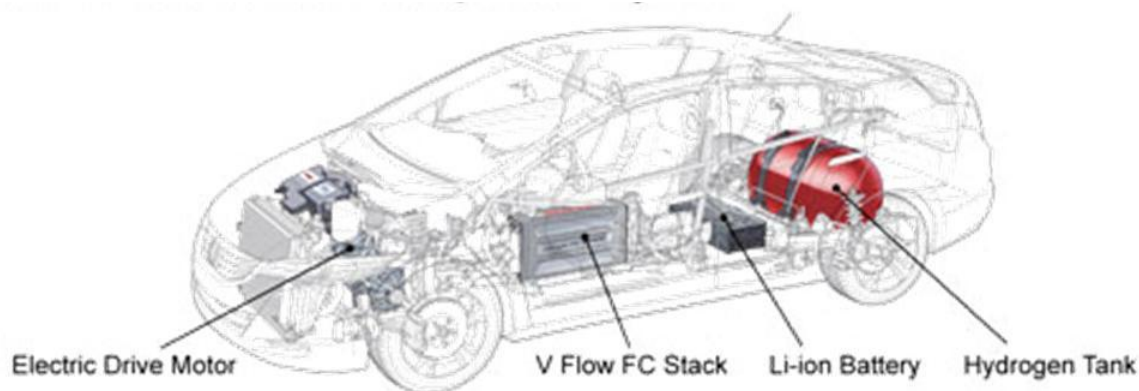


Figure 3.95: *Honda Clarity - packaging*

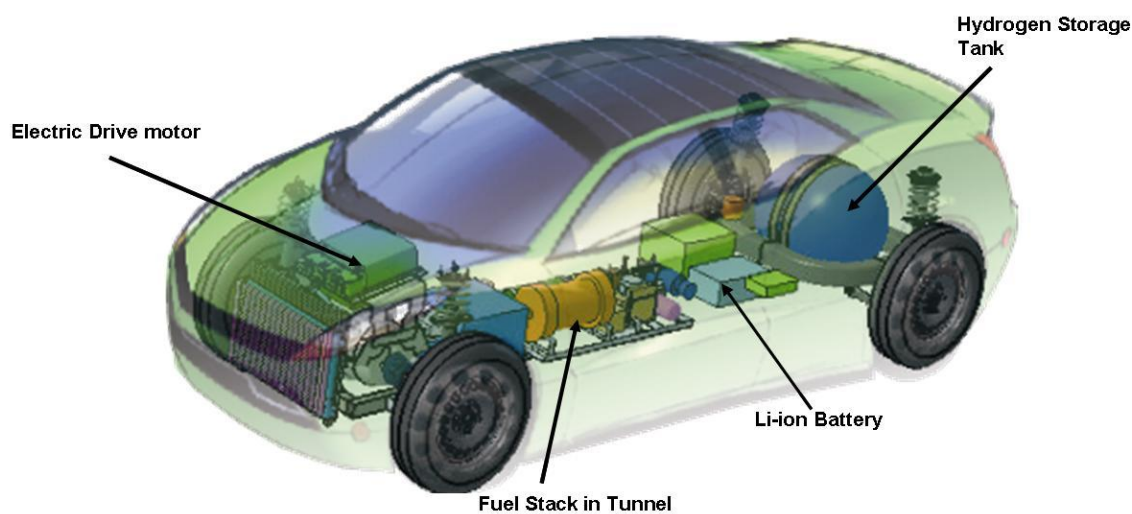


Figure 3.96: *FSV-2 - packaging*

3.3.4.8 Underhood Packaging

Under the hood of the FCX clarity, as shown in Figure 3.97, there is an air intake, air filter, and an air pump to move the air through the fuel cell. Underneath this is the traction motor which connects directly to the front (drive) wheels. There is just a single gear transmission, which is packaged within the motor housing. This is an inexpensive option when compared to that of a conventional ICE vehicle, where the transmission is one of the most expensive components.



Figure 3.97: *Honda Clarity underhood*

Under the hood of the FSV-2 FCEV is the traction inverter, AC condenser and the motor, directly connected to the front wheels as shown in Figure 3.98. Similar to the Clarity, a single gear transmission, housed inside the motor compartment on the FSV-2 FCEV results in a significantly shorter front-end, common between all the variants of the Future Steel Vehicle (BEV and PHEV).

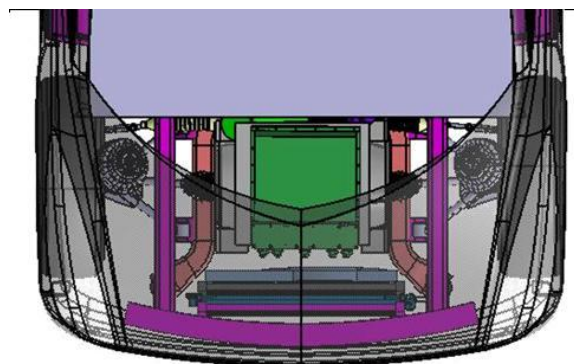


Figure 3.98: *FSV-2 FCEV underhood*

3.3.4.9 Suspension

Front

The FCX Clarity features a double wishbone suspension in the front as shown in Figure 3.99. The suspension sub-frame assembly is produced using extruded aluminum. The FSV-2 FCEV features a conventional McPherson strut suspension in the front as shown in Figure 3.100 with low-profile steel control arms resulting in a lightweight, but robust design.

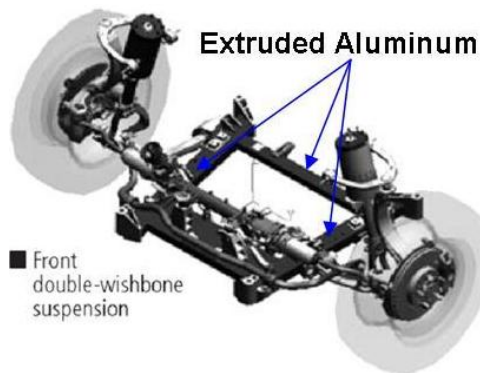


Figure 3.99: *Honda Clarity front suspension*

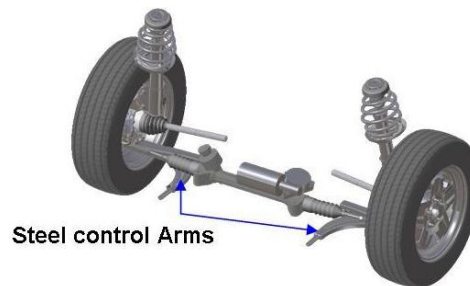


Figure 3.100: *FSV-2 FCEV front suspension*

Rear

The FCX features an optimized 5 link double wishbone suspension in the rear as shown in Figure 3.101, allowing additional space for a large hydrogen tank. The forged aluminum lower arms, high-capacity trailing arm bushings and reduced unsprung weight provides an improved ride. The rear suspension sub-frame is produced using extruded aluminum.

The FSV uses an H-arm camber control link independent suspension in the rear as shown in Figure 3.102. Because the majority of the loads are in the lower arm, the camber link can be very lightweight resulting in an overall lightweight setup.

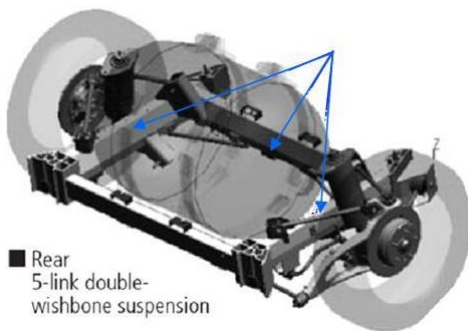


Figure 3.101: *Clarity rear suspension*

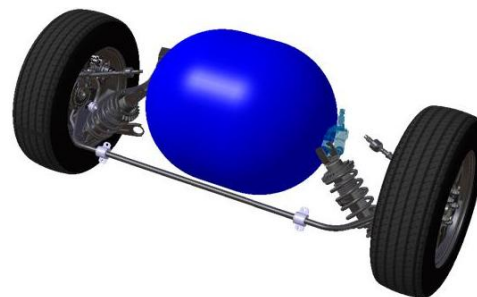


Figure 3.102: *FSV-2 FCEV rear suspension*

3.3.4.10 Tires and Wheels

The 2009 Honda Clarity rides on 215/55R16 low rolling resistance tires with 5-spoke "ultra light" forged aluminum wheels, and a special drag-reducing plastic trim to suppress turbulence and drag.

The FSV-2 rides on light weight steel wheels and 175/65 R15 tires with a rolling resistance value of 0.007. The tire and wheel specifications for the two vehicles are compared in Table 3.23.



Figure 3.103: Honda Clarity wheel



Figure 3.104: FSV-2 Wheel

	2009 Clarity	Future Steel Vehicle-2
Size - Front	215/55 R16	175/65 R15
Size - Rear	215/55 R16	175/65 R15
Material	Aluminum	Steel
Rolling Resistance	Low	Low - 0.007

Table 3.23: Tire & wheel specifications - 2009 Honda Clarity and FSV-2

3.3.4.11 Interior

Passenger compartment

Table 3.24 compares the interior specifications of the Honda Clarity and the FSV-2 FCEV.

Interior Measurements		2009 Honda Clarity	2020 FSV 2
Headroom	(Front/Rear) [mm]	980/941	997/950
Legroom	(Front/Rear) [mm]	1064/963	1070/925
Shoulder Room	(Front/Rear) [mm]	1493/1386	1465/1440
Hip Room	(Front/Rear) [mm]	1828/1592	1484/1484
Seating Capacity		4	5
Cargo Volume		370	370
	[liter]		

Table 3.24: *Interior specifications*

Figure 3.105 through Figure 3.110 shows the front, rear and cargo spaces on the Honda clarity and the FSV-2 .



Figure 3.105: *Honda Clarity front*



Figure 3.106: *Honda Clarity rear*



Figure 3.107: *Honda Clarity cargo space*



Figure 3.108: *FSV-2 front*



Figure 3.109: *FSV-2 rear*



Figure 3.110: *FSV-2 cargo Space*

Instrument Cluster

Honda Clarity's instrument cluster, shown in Figure 3.111, features a ball on the dashboard that indicates relative fuel economy by changing color and shape (see "Chapter - Other advanced technologies for details"). A small, blue ball indicates efficient driving, amber signifies poor economy during heavy acceleration, yellow indicates average fuel consumption periods, and bright electric-blue to signify good economy.



Figure 3.111: Honda Clarity instrument cluster

The FSV cluster is a paper thin Organic Light Emitting Diode(OLED) that allows a weight savings of 2.0 Kg over a conventional instrument cluster.

Shifter

The FCX Clarity uses the latest Shift-By-Wire technology with the use of a compact electronic shifter (shown in Figure 3.112) that is built into the display.



Figure 3.112: Honda Clarity shifter

3.3.4.12 Alternate Materials

In keeping with its theme as an environmentally advanced automobile, the FCX Clarity features seat upholstery and door trim made from Honda Bio-Fabric - a newly developed, plant-based material that offers CO₂ reductions as an alternative to traditional interior materials, along with outstanding durability and resistance to wear, stretching, and damage from sunlight.

- Areas where Honda Bio-Fabric (PTT) is used
- ① Seat coverings
- ② Front/rear armrests
- ③ Front/rear door linings (middle section)
- ④ Door armrests
- ⑤ Console tray
- Areas where another bio-fabric (PLA) is used
- ⑥ Roof lining
- ⑦ Pillar coverings
- ⑧ Floor carpets
- ⑨ Piece mats
- ⑩ Trunk lining

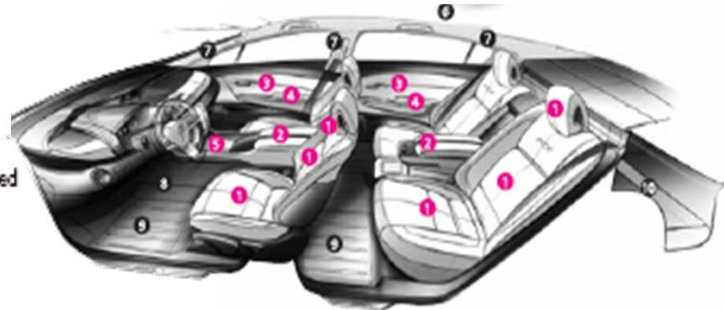


Figure 3.113: *Honda Clarity interior materials*

Climate Controlled Seats

The FCX Clarity features climate controlled seats (both front and rear) . Fans draw air into the seats where a thermo-electric device cools or heats the air before blowing it through pores in the seat cushions. The end result is greatly reduced demand on the climate control system by decreasing the A/C loads.



Figure 3.114: *Honda Clarity climate controlled seats*

The FSV-2 FCEV also features Climate Controlled Seats (CCS).

3.3.4.13 New Technology Implementation

The FCX introduces some new and future technology into the vehicle such as:

1. Honda Bio-Fabric: the world's first automotive interior covering made from plant-based materials
2. Climate controlled seats (front and rear)
3. Compact, easy-to-operate transmission featuring Shift-by-Wire technology
4. An extra rear window that enhances rearward visibility-privacy
5. Fuel cell powertrain

The FSV-2 FCEV introduces some new and future technologies that achieve significant advantages in terms of weight and performance of the vehicle such as:

1. Brake-By-Wire, Shift-By-Wire and Throttle-By-Wire.
2. LED lighting
3. OLED instrument cluster
4. Polycarbonate side and rear glass.
5. Low resistance tires (value of 0.007)
6. Climate Controlled Seats (CCS)
7. Solar reflective glazing and active parked car ventilation

3.3.5 2011 Chevrolet Volt

3.3.5.1 Synopsis

The 2011 Chevrolet Volt, shown in Figure 3.115 was chosen for this benchmark study since it is the first high volume production plug-in electric vehicle (Extended range electric Vehicle or E-REV) that belongs to the same vehicle class as that of the FSV-2 PHEV₄₀, shown in Figure 3.116 and will meet all the relevant US FMVSS safety and crashworthiness requirements and is available to the general public in late 2010 as MY2011. Chevrolet Volt utilizes GM's E-Flex platform, which can accept various powertrain variations depending on the intended market.

This report compares Chevrolet Volt and FSV-2 PHEV₄₀, in terms of powertrain sizes and performance, packaging and material usages on various body-structure parts and closures. The overall specifications of the two vehicles are compared in Table 3.25.



Figure 3.115: 2010 Chevrolet Volt



Figure 3.116: FSV-2 PHEV₄₀

General Specifications	2011 Volt	2020 FSV-2 PHEV ₄₀
Classification	E-REV	E-REV
Type	Series	Series
AER [km]	64	64
Extended range [km]	480	500
Curb Weight [kg]	1530	1380
Drive Type	FWD	FWD
0-60mph [sec]	8-9	10-12
Top Speed [kmph]	160	161
Apprx Cost [USD]	\$40,000	\$31,500

Table 3.25: General specifications - FSV-2 PHEV₄₀ & Chevrolet Volt

Since the Chevrolet Volt was not available to the general public at the time of this report being generated, all data obtained on this vehicle was through available media sources and limited interaction with the vehicle at the various auto shows.

3.3.5.2 Exterior Dimensions

The Chevrolet Volt is 104 mm longer in length than the FSV-2. The Volt is shorter than the FSV by 110 mm which translates to more headroom in the FSV than in the Volt. The wheelbase on the FSV is longer than the Volt by 115 mm.

Figure 3.117 and Figure 3.118 show the exterior dimensions of the 2011 Chevrolet Volt and the FSV-2 respectively.

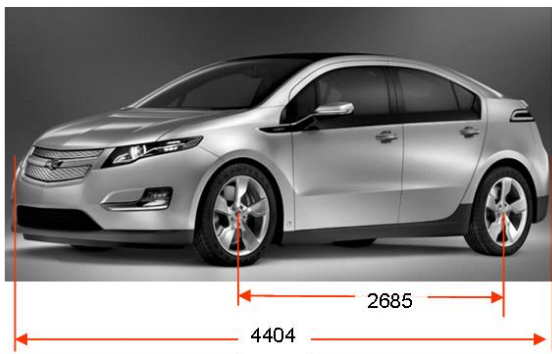


Figure 3.117: Chevrolet Volt exterior dimensions

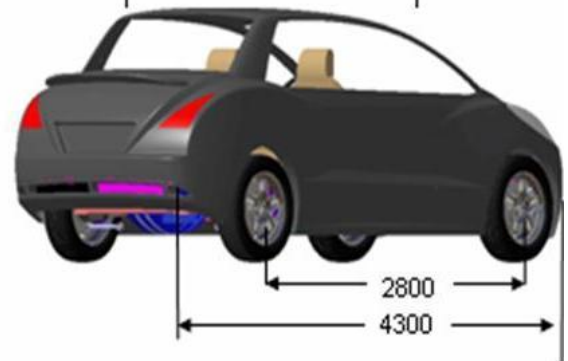
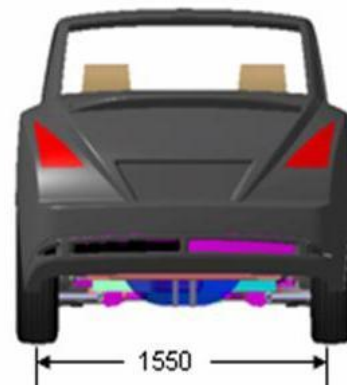
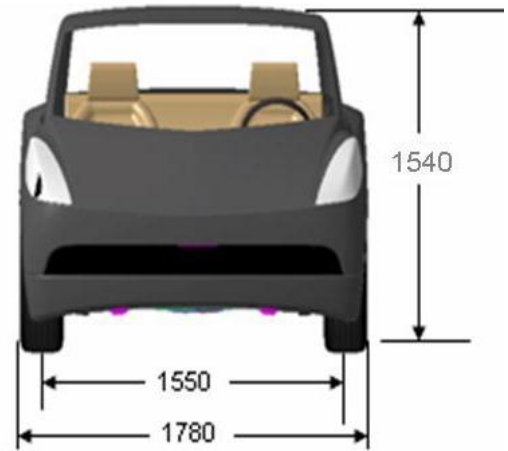


Figure 3.118: FSV-2 PHEV₄₀ exterior dimensions

3.3.5.3 Material Usage

The Chevrolet Volt predominantly uses steel for all the closures except for the hood, which is aluminum. The body structure is also steel.

Figure 3.119 shows the material usage on the Volt (closures).

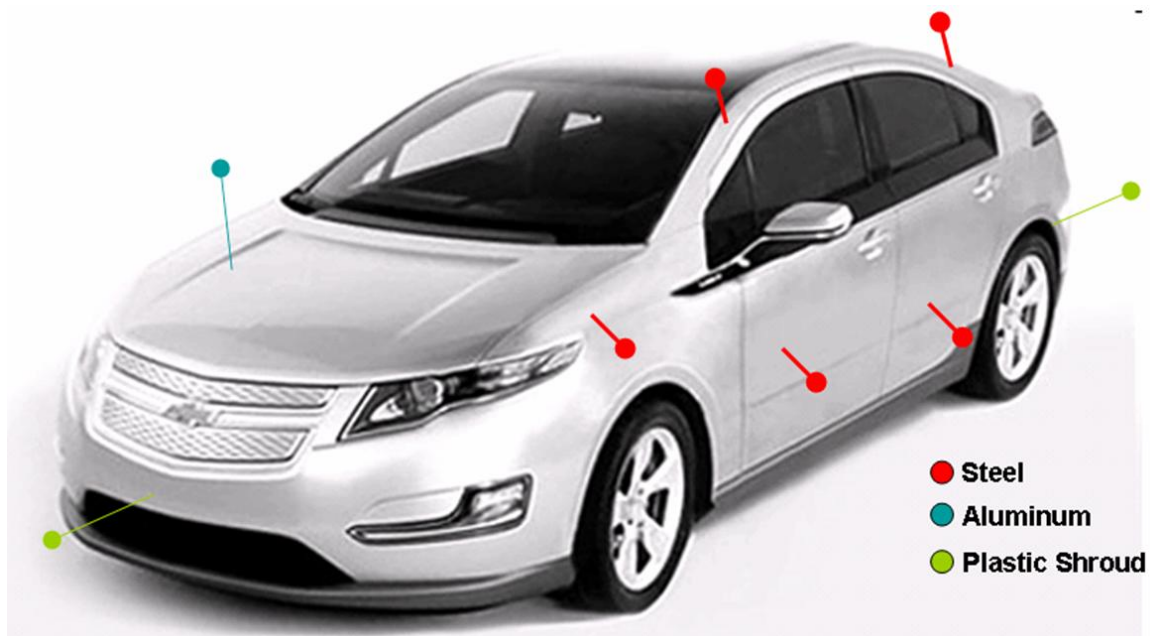


Figure 3.119: Chevrolet Volt - material usages

3.3.5.4 Powertrain Packaging

The Chevrolet Volt is based on GM's E-flex platform that allows easy configuration changes from the powertrain side without any major changes to the body structure. Figure 3.120 shows the packaging layout on the Volt and the FSV-2 PHEV₄₀.

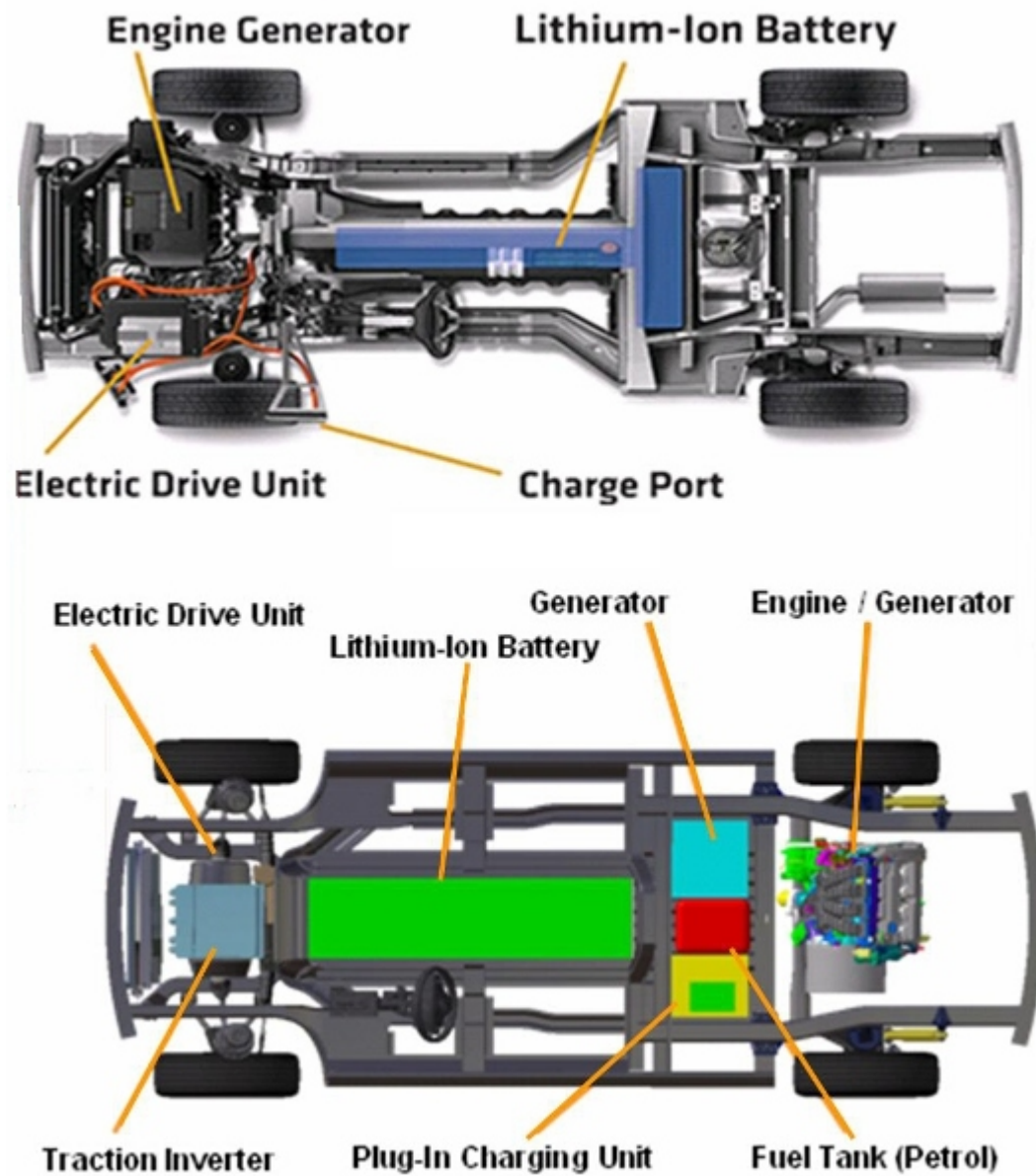


Figure 3.120: Powertrain packaging - Chevrolet Volt (top) & FSV-2 (bottom)

3.3.5.5 Electric Drive Components

The electric drive components on the Chevrolet Volt and the FSV-2 PHEV₄₀ have the following components:

- Battery module
- Internal Combustion Engine (ICE)
- Traction motor and inverter
- Fuel storage (tank)

Figure 3.121, Figure 3.122 and Figure 3.123 shows the battery, traction motor and engine/generator of the Chevy Volt.

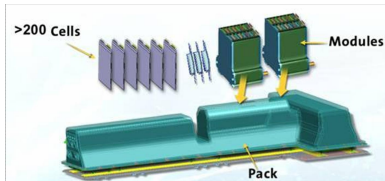


Figure 3.121: *Chevrolet Volt 16 kWh battery*



Figure 3.122: *Chevrolet Volt 111 kW motor*



Figure 3.123: *Chevrolet Volt 1.4 L IC engine*

Figure 3.124, Figure 3.125 and Figure 3.126 shows the Battery, traction motor and engine/generator of the FSV-2 PHEV₄₀ .

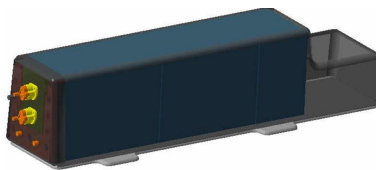


Figure 3.124: *FSV-2 PHEV₄₀ 11.7 kWh battery*



Figure 3.125: *FSV-2 PHEV₄₀ 75 kW motor*

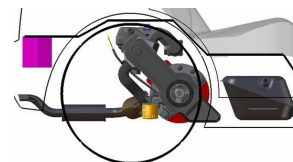
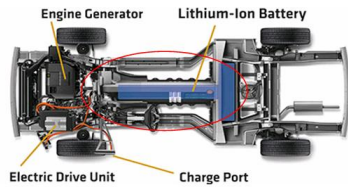
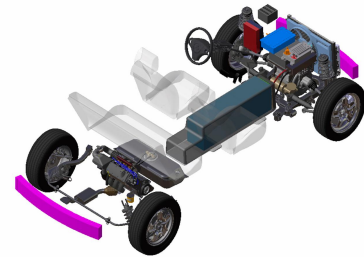
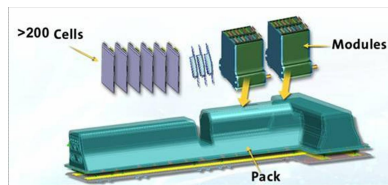
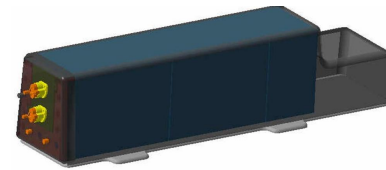


Figure 3.126: *FSV-2 PHEV₄₀ 1.4 L IC engine*

Li-Ion battery

Figure 3.127: Chevrolet Volt battery location

Figure 3.128: FSV-2 PHEV₄₀ battery layout

Figure 3.129: Chevrolet Volt 16 kWh battery

Figure 3.130: FSV-2 11.7 kWh battery

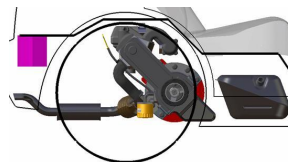
The Chevrolet Volt's battery pack, shown in Figure 3.129, is T-shaped, with the vertical leg running longitudinally between the seats and under the rear seats, as shown in Figure 3.127. This reduces the occupant space so that only four passengers can be accommodated in the vehicle. The FSV-2 PHEV₄₀ has a 11.7 kWh battery, shown in Figure 3.130, that fits underneath the tunnel, as shown in Figure 3.128, and provides enough room in the passenger compartment to seat five adults.

The battery specifications of the two vehicles are compared in Table 3.26.

Battery Specifications		2011 Volt	2020 FSV-2 PHEV ₄₀
Capacity	[kWh]	16	11.7
Voltage	[Volt]	320-350	297-378
weight	[kg]	175	105
Type		Li-Ion	Li-Ion
Volume	[liter]	NA	86
Cost	[\$/kWh]	800-1000	450
Energy Density	[wh/kg]	91	130

Table 3.26: Battery specifications - FSV-2 PHEV₄₀ & Chevrolet Volt

Engine/Generator

Figure 3.131: *Chevrolet Volt 1.4 L ICE*

Figure 3.132: *FSV-2 1.4 L ICE*

Both the Chevrolet Volt and FSV-2 PHEV₄₀ feature a 1.4 L four-cylinder ICE as shown in Figure 3.132 and Figure 3.131 respectively. This ICE drives the generator and is packaged in the rear on the FSV-2 PHEV₄₀, while in the Chevrolet Volt, it is packaged in the front (underhood). This rear packaging design allows the FSV-2 PHEV₄₀ to be designed with a significantly shorter and common (with other FSV variants) front-end. The engines on both vehicles do not power the wheels of the car. They drive a generator while operating in three very narrow RPM ranges (to be announced) to recharge the batteries while the car is in motion.

The base engine on the Volt consists of a cast iron cylinder block and an aluminum cylinder head with the block designed with a hollow frame to keep the weight down while maintaining strength. The gasoline engine on the volt is connected to a fuel tank that holds 19-22 liters of gasoline (unconfirmed data) but, working with the car's batteries, should be sufficient to give it a 480 km (300 mile) range. The FSV-2 PHEV₄₀ also has a 19 liter fuel tank which provides a range of 500 km in charge sustaining mode.

The ICE specifications of these two vehicles are compared in Table 3.27.

ICE	2011 Volt	2020 FSV-2 PHEV ₄₀
Capacity [Liter]	1.4	1.4
Cylinders	4	4
Peak power [kW]	75	75
Fuel Tank Capacity [Liter]	19-22	19
fuel Type	Gasoline/E85	Gasoline

Table 3.27: *ICE specifications - FSV-2 PHEV₄₀ & Chevrolet Volt*

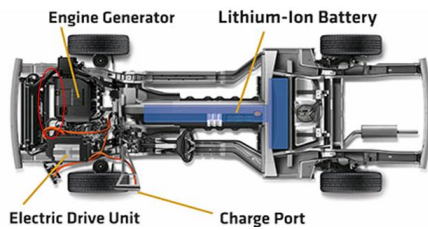
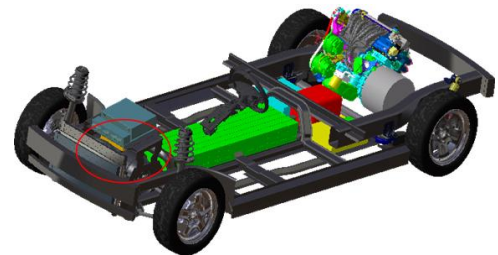
Traction Motor

Figure 3.133: Chevrolet Volt motor location

Figure 3.134: FSV-2 PHEV₄₀ motor location

Figure 3.135: Chevrolet Volt- 111 kW motor

Figure 3.136: FSV-2 75 kW motor

Both the Volt and the FSV-2 PHEV₄₀ use the electric drive motors shown in Figure 3.135 and Figure 3.136, as the primary means of propulsion. Both vehicles have the traction motors packaged in the front as shown in Figure 3.133 and Figure 3.134. The wheels are directly connected to the traction motors and carry one drive gear thus eliminating the need for a complex transmission.

The specifications of the Chevrolet Volt and FSV-2 PHEV₄₀ motors are compared in Table 3.28.

Motor Specifications	2011 Volt	2020 FSV
Type	Perm Magnet	Perm Magnet
Drive Type	Direct	Direct
Peak power [kW]	111	75
Continuous Power [kW]	45	55
Peak Torque [Nm]	370	220

Table 3.28: Motor specifications - FSV-2 PHEV₄₀ & Chevrolet Volt

3.3.5.6 Suspension

Front

The Volt features an independent McPherson strut front suspension, shown in Figure 3.137. The FSV-2 PHEV₄₀ also features a McPherson strut front suspension as shown in Figure 3.138, but uses a low profile steel control arm which provides lightweight, but robust characteristics.

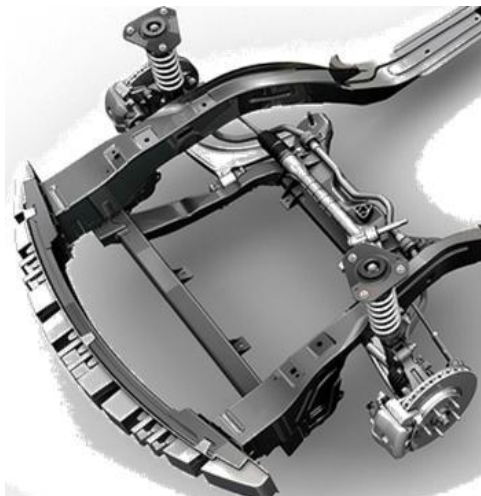


Figure 3.137: *Chevrolet Volt front suspension*

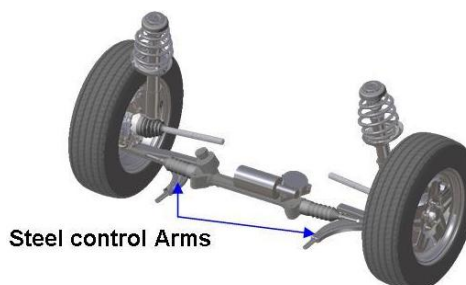


Figure 3.138: *FSV-2 front suspension*

Rear

The Chevrolet Volt features a semi-independent torsion beam suspension system in the rear as shown in Figure 3.139. The FSV, as shown in Figure 3.140, proposes a H-arm camber control link fully independent suspension in the rear. Because the majority of the loads are in the lower arm, the camber link can be very lightweight resulting an overall lightweight setup.

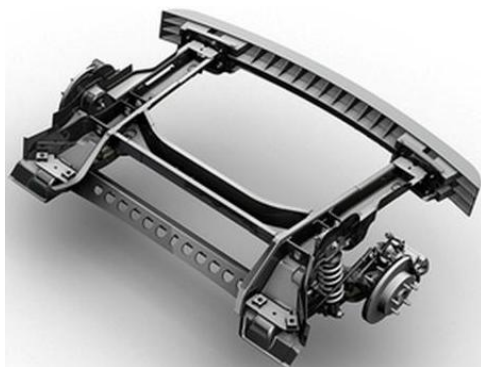


Figure 3.139: *Volt rear suspension*



Figure 3.140: *FSV-2 rear suspension*

3.3.5.7 Tires and Wheels

The 2011 Chevrolet Volt rides on 17 inch wheels and 215/55R17 low-rolling resistance tires (shown in Figure 3.141). 6-spoke forged aluminum wheels are proposed to be used on the production version.

The FSV-2 as shown in Figure 3.142, rides on 15 inch lightweight steel wheels, and 175/65 R15 tires with a rolling resistance value of 0.007. The tire and wheel assembly specifications of the two vehicles are compared in Table 3.29.



Figure 3.141: Volt wheel



Figure 3.142: FSV-2 wheel

	Chevrolet Volt	Future Steel Vehicle-2
Size - Front	215/55 R17	175/65 R15
Size - Rear	215/55 R17	175/65 R15
Material	Aluminum	Steel
Rolling Resistance	Low	Low - 0.007

Table 3.29: Tire & wheel specifications - 2009 Chevy Volt and FSV-2

3.3.5.8 Interior



Figure 3.143: *Chevrolet Volt rear*

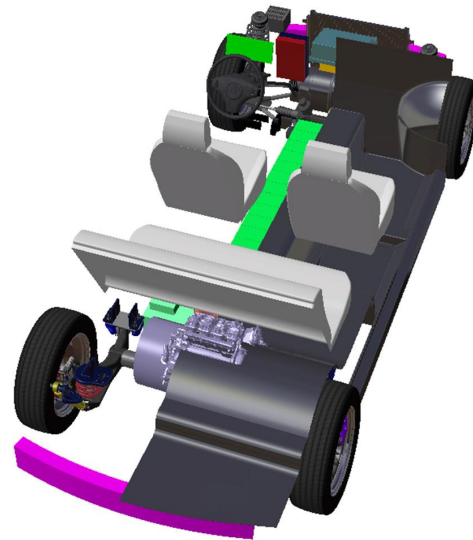


Figure 3.144: *FSV-2 rear*

The Chevrolet Volt, due to the fact that the battery is located inside the tunnel area, restricts the passenger compartment space in the rear to two seating positions as shown in Figure 3.143, whereas the FSV-2 PHEV₄₀ battery pack is packaged in the tunnel area which allows full usage of the rear floor space enabling comfortable seating for three as shown in Figure 3.144.

The interior specifications of the Chevy Volt and FSV-2 PHEV₄₀ are shown in Table 3.30.

Interior Measurements		2011 Chevrolet Volt	2020 FSV 2
Headroom	(Front/Rear) [mm]	NA	997/950
Legroom	(Front/Rear) [mm]	NA	1070/925
Shoulder Room	(Front/Rear) [mm]	NA	1465/1440
Hip Room	(Front/Rear) [mm]	NA	1484/1484
Seating Capacity		4	5
Cargo Volume	[liter]	NA	370

Table 3.30: *Interior specifications - - FSV & Chevrolet Volt*

3.3.6 Mercedes Blue-Zero Concept

3.3.6.1 Synopsis

At the 2009 Detroit auto show, Mercedes-Benz announced three new concept vehicles. All the three vehicles are built on the same platform and based on a modular concept which allows the three models with different drive configurations.

The E-CELL version is battery-electric, the E-CELL PLUS is similar but has a small internal combustion engine to act as a range-extender (like on the BYD F3DM or GM Volt), and the F-CELL is a hydrogen fuel cell model. Figure 3.145 shows the three Blue-Zero concept vehicles announced by Mercedes.



Figure 3.145: Mercedes Blue-Zero concept vehicles

While Mercedes concept is similar to the FSV's concept with a BEV, FCEV and PHEV, Mercedes concepts have a single body style design (midsize) for all its variants while the FSV's concept incorporates four vehicles with two body styles (small and midsize) variants.

Production Numbers

Mercedes will produce the first fuel cell cars on a small scale in 2009. Small-scale production of Mercedes-Benz cars with battery electric drive alone will commence in 2010.

3.3.6.2 Vehicle Dimensions

The exterior difference, as noted previously, between the Mercedes concept vehicles and the FSV variants is the common body style on all three Mercedes variants. Table 3.31 shows the major exterior dimensions of the Mercedes Blue-Zero concept vehicles and also compares them with the FSV exterior dimensions.

The vehicle lengths of the Blue-Zero concepts are similar to that of the FSV-2 variant and can be considered a midsize vehicle. The Mercedes vehicle are taller and wider than the FSV variants, mainly as a result of the raised floor height on the Mercedes vehicle (discussed in later sections).

Mercedes has 500 liters of luggage space available which is 26% more than that of the FSV variants.

Dimensions	Mercedes BlueZero	FSV 1	FSV 2
Length [m]	4.22	3.7	4.3
Width [m]	1.89	1.68	1.78
Height [m]	1.59	1.54	1.54
Luggage Volume [Liters]	500	250	370

Table 3.31: Mercedes Blue-Zero Dimensions comparison with FSV

3.3.6.3 Vehicle Range

Figure 3.146 shows the range of the Mercedes vehicles compared with the FSV variants. The FSV vehicles (BEV and FCEV) have higher All Electric Range (AER) when compared to the Mercedes variants.

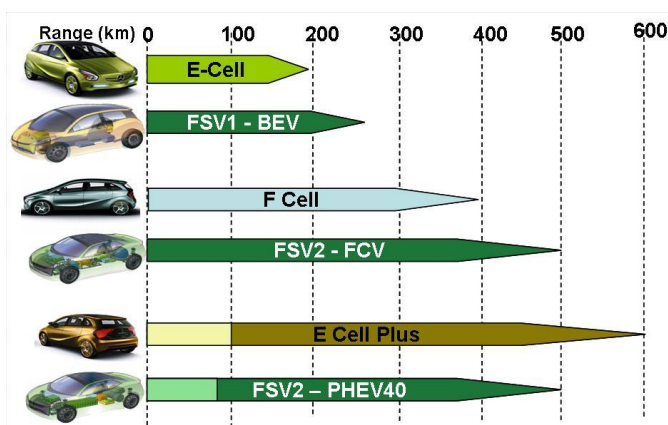


Figure 3.146: Vehicle Range Comparison - FSV & Mercedes Blue-Zero

3.3.6.4 Vehicle Architecture

The three Mercedes-Benz Blue-Zero variants are based on the unique sandwich-floor architecture as shown in Figure 3.147. This floor packages all the powertrain components for all the 3 variants. A few features of this powertrain layout on the Blue-Zero variants are similar to the FSV concept design such as:

1. Common front-end among between all the variants with the electric motor packaged in the front
2. On the E cell+ (plug-in), the ICE is packaged in the rear similar to the PHEV₂₀ and PHEV₄₀ variants of the FSV

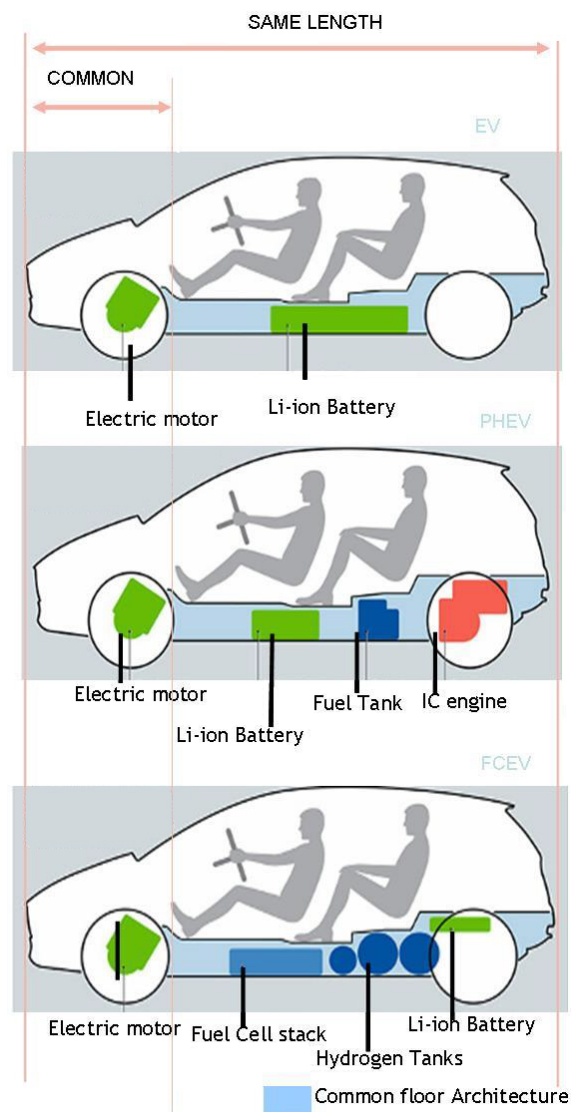


Figure 3.147: Mercedes Blue-Zero powertrain layout

This common floor architecture concept has its own advantages and disadvantages.

Advantages

1. Interior space above the floor is unrestricted by drivetrain, fuel tank or mechanical components which allows passenger and luggage volume
2. Better stability and handling characteristics due to the low center of gravity
3. High-floor design allows for a better frontal field of view for driver
4. Floor structure acts a major load carrying member in case of a high speed impact, protecting the battery from intrusion

Disadvantages

1. Raised floor leads to a taller vehicle, increasing the aerodynamic drag of the vehicle which has negative impacts of the fuel economy

Figure 3.148 shows the height of the floor on the concept vehicle unveiled at the Detroit auto show.

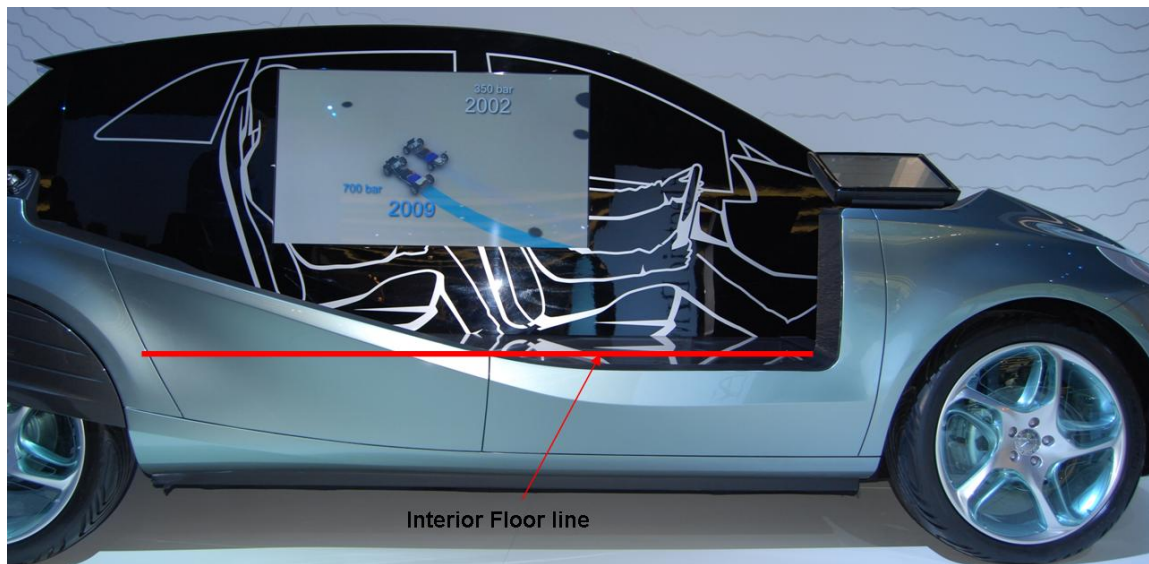


Figure 3.148: Mercedes Blue-Zero floor height

3.3.6.5 E-Cell (Battery Electric Vehicle)

The E-Cell version is the simplest of the three variants with a battery pack and electrical motor packaged under the floor and underhood respectively. The E-cell's 35 kWh liquid-cooled Li-ion battery pack is capable of propelling the vehicle to a range of 152 km which is 30% less than that of the FSV-1 BEV which is capable of a range of 250 km with the same energy capacity of 35 kWh. The FSV battery pack is packaged under the tunnel area which is an advantage in terms of a not requiring a high floor as in the case of the E-Cell. The motor is packaged in the front similar to the FSV design. The unique feature of the Blue-Zero series is that the motor is common between all the variants. FSV packages a larger capacity motor on its PHEV and FCEV variants. Figure 3.149 shows the powertrain packaging of the E-Cell.

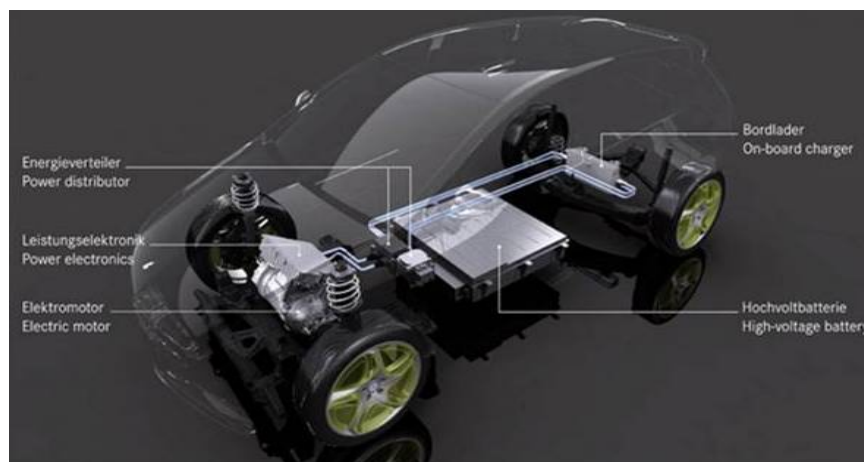


Figure 3.149: Mercedes E-Cell - powertrain layout

Table 3.32 compares the general specifications of the Mercedes E-Cell with that of the FSV BEV.

General Specifications	Mercedes E Cell	2020 FSV (BEV)
Type	BEV	BEV
All Electric Range [km]	192	250
Curb Weight [kg]	unknown	1232
Drive Type	FWD	FWD
0-60mph [sec]	10.8	10-12
Top Speed [kmph]	150	150
Model Year	TBD	2020
Apprx Cost [USD]	TBD	\$32,500

Table 3.32: General specifications - FSV (BEV) & Mercedes E-Cell

3.3.6.6 F-cell (Fuel Cell Electric Vehicle)

This is the fuel cell variant of the Blue-Zero series. This concept, as mentioned before, uses the same floor space to package the fuel cell stack, three hydrogen tanks (compressed gas at 700 bar) and the Li-ion battery pack. The total range of this vehicle as specified by Mercedes is 400 km. The FSV-2 variant has a single hydrogen tank and is capable of propelling the vehicle to a range of 500 km. The packaging layout of the F-Cell variant is shown in Figure 3.150.

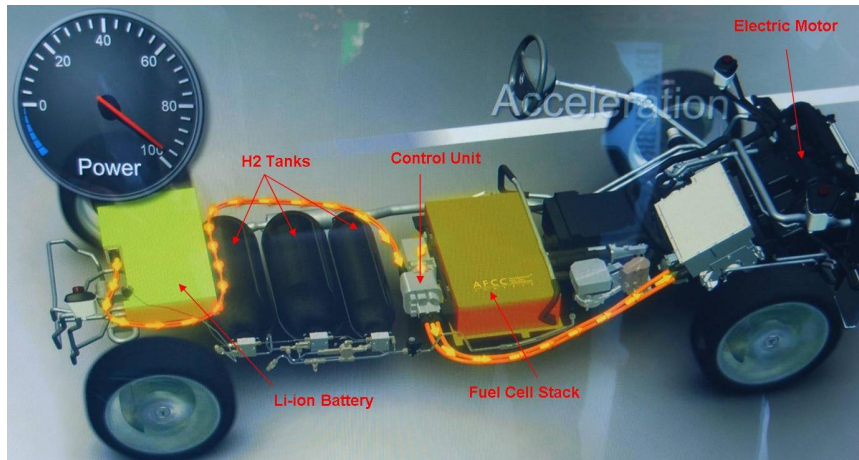


Figure 3.150: Mercedes F-Cell - powertrain layout

A comparison of the specifications of the F-Cell and the FSV-2 FCEV is shown in Table 3.33.

General Specifications	Mercedes F Cell	2020 FSV (FCEV)
Type	FCEV	FCEV
AER [km]	400	500
Fuel cell power [kW]	90	65
Curb Weight [kg]	unknown	1174
Drive Type	FWD	FWD
0-60mph [sec]	10.8	10-12
Top Speed [kmph]	150	161
Model Year	TBD	2020

Table 3.33: General specifications - FSV (FCEV) & Mercedes F-cell

3.3.6.7 E-Cell + (Plug-in Hybrid)

The E-Cell+ is the plug-in version of the Blue-Zero series. The E-cell+ has a CD (Charge Depleting) range of 100 km (62 miles) and with a full charge and a full tank (and using regenerative braking), the E-Cell+ can extend the range up to 600 km (373 miles) powered by a small 1.0 liter turbocharged engine. Figure 3.151 shows the layout of the powertrain components on the E-Cell+. The placement of the ICE and the electric motor is similar to that of the FSV, with the Li-ion battery placed in the floor as opposed to the tunnel area on the FSV.

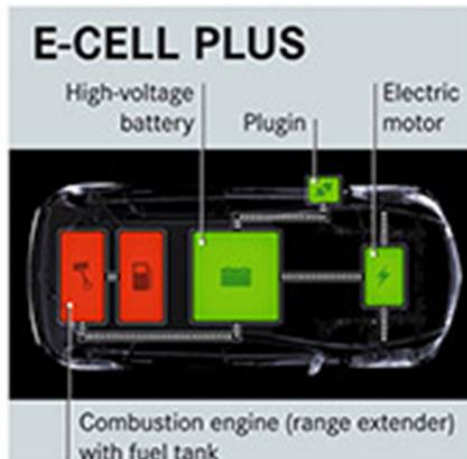


Figure 3.151: Mercedes E-Cell+ - powertrain layout

A comparison of the specifications of the F-Cell and the FSV-2 PHEV₄₀ is shown in Table 3.34.

General Specifications	Mercedes E Cell+	2020 FSV (PHEV ₄₀)
Type	EREV	EREV
All Electric Range [km]	100	64
Extended Range [km]	600	500
Configuration	Series	Series
Curb Weight [kg]	unknown	1380
ICE [Liter]	1.0TC	1.4
ICE power [kW]	50	75
Drive Type	FWD	FWD
0-60mph [sec]	10.8	10-12
Top Speed [kmph]	150	161
Model Year	TBD	2020

Table 3.34: General specifications - FSV (PHEV₄₀) & Mercedes E Cell+

3.3.6.8 Material Usage

Body-Structure

The tailgate is made completely from lightweight, but highly robust Lexan and the vehicle frame is completely made out of aluminum. The Blue-Zero series rides on 20-inch aluminum wheels which have also been aerodynamically optimized, while low-friction tires reduce rolling resistance.

3.3.6.9 Aerodynamics

The Mercedes Blue-Zero vehicles also have the rear wheels partially covered, as shown in Figure 3.152, to improve the coefficient of drag, reducing the energy required to keep the car moving at higher speeds.



Figure 3.152: Mercedes Blue-Zero wheel covers

3.3.7 Conclusion

Researching the alternate powertrain vehicles that have been announced by OEMs worldwide have led to the following conclusions:

- Alternate materials are already being used on production electric and fuel cell vehicles (Clarity, Tesla) with further need to reduce body-structure mass
- Electric vehicles scheduled for production in the next two years are drive technology validation vehicles, based on existing vehicle platforms (i-MiEV, BMW mini E, Toyota EV, TATA Indica)
- OEMs are already working on next generation versions of these technology tryout vehicles with a goal of weight savings on the vehicle
- Vehicles announced for production have already made the choice of using lighter materials (Al, composites) for body-structure (Mercedes, Fisker, Honda)
- For OEMs, bolt-on parts (closures) is a easy target for any weight reduction on the vehicle while meeting all the required safety regulations (Honda, Th!nk, Toyota, Mercedes, NICE)
- Closures / bolt-on assemblies are the most immediate and valid threat to steel, in terms of OEM's choice for weight reduction

3.4 Future Safety Requirements

3.4.1 Overview

The FSV engineering team conducted an assessment of proposed future (2010-2020) global safety regulations in comparison to the current requirements, with the intention to understand the implication of new regulations on the design of the FSV-1 and FSV-2, and to incorporate all the necessary structural changes on the FSV to meet and exceed these upcoming regulatory specifications by a comfortable safety margin.

The FSV engineering team also estimated the mass, cost and fuel economy impacts these new requirements pose to the FSV structure. See Table 3.35 for regulatory impact statistics.

Regulation	Timeline	Mass	Cost	Fuel Used
Roof Crush/Rollover (FMVSS 216)	2016	~ 2 kg	\$54	N/A
Roof Crush/Rollover (IIHS)	2016	~ 2 kg	N/A	N/A
Electronic Stability Control (ESC)	2011	~ 1 kg	\$92.00	9.8 l (2.6 ga)
Pole Impact	2012	~ 6-8 kg	\$208.00	N/A
Frontal Impact	TBD	N/A	N/A	N/A
Bumper Impact	2008	1 kg	N/A	N/A
Ped-Pro	2011	1-2 kg	N/A	N/A

Table 3.35: *Estimated mass, cost and fuel economy impacts*

Proposed changes to current and new safety regulations are being implemented, with the US and EU taking a lead role in defining these new regulations.

3.4.2 US - Future Safety Requirements

3.4.2.1 Mandatory Regulations

The National Highway Traffic Safety Administration (NHTSA) has a legislative mandate under Title 49 of the United States Code, Chapter 301, Motor Vehicle Safety, to issue Federal Motor Vehicle Safety Standards and Regulations (FMVSS/FMVSR) to which manufacturers of motor vehicles and motor vehicle equipment must conform to, and certify compliance.

Occupant Protection (FMVSS 208)

Current Requirement:

1. $56 \frac{\text{km}}{\text{h}}$ (35 mph) 0° frontal impact using belted 50th percentile male ATD.

Future Proposed Requirement:

1. $56 \frac{\text{km}}{\text{h}}$ (35 mph) 0° frontal impact using belted 5th percentile female ATD

Figure 3.153 shows the FMVSS 208 test mode. The test mode remains the same except that a 5th percentile female dummy (shown in Figure 3.154) replaces the current 50th percentile male ATD (shown in Figure 3.155).

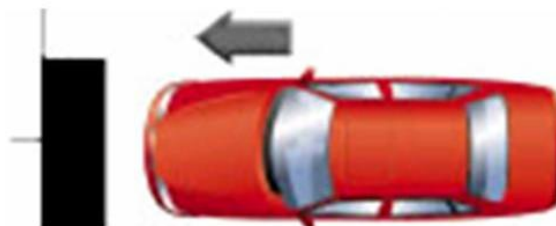


Figure 3.153: FMVSS 208 - $56 \frac{\text{km}}{\text{h}}$ (35 mph) 0-degree frontal impact

The impact of such a regulation is primarily focused on restraint system calibration (to account for the different injury pattern of a female) and is thought to have a minimal impact on the vehicle structure.



Figure 3.154: *FMVSS 208 - Hybrid III 5th female*



Figure 3.155: *FMVSS 208 - Hybrid III 50th male*

Dynamic Side Pole Impact (FMVSS 214P)

Current Test standard:

1. The current test standard for dynamic side impact protection with a moving deformable barrier is $54 \frac{\text{km}}{\text{h}}$
2. Uses a 90° pole impact test at $29 \frac{\text{km}}{\text{h}}$ ($18 \frac{\text{m}}{\text{h}}$) with a SID-H3 ATD

Future Proposed standard:

1. Adds a new 75° rigid pole test conducted at $32 \frac{\text{m}}{\text{h}}$
2. Replaces the 50th percentile male Side Impact Dummy - Anthropomorphic Test Device (SID ATD) with the Euro SID-2 with Rib Extensions (ES-2re) ATD
3. change to a 75° oblique - $32 \frac{\text{km}}{\text{h}}$ ($20 \frac{\text{m}}{\text{h}}$) pole impact test with a $31 \frac{\text{km}}{\text{h}}$ ($19 \frac{\text{m}}{\text{h}}$) lateral component.
4. Mandates that vehicles comply with a 5th percentile female ATD when tested.

The proposed rule adopts a 4 year phase-in period starting September 2009. By September 2012, all vehicles must meet these new requirements.

These proposed changes will need vehicle structural changes, especially in the B-pillar areas, in terms of increasing material gauge (weight impact) or using advanced high strength steels (cost impact). The impact would be approximately 6-8 kg and \$208 in added weight and cost per vehicle.

See Figure 3.156 for ATD's used in FMVSS 214P testing. See Figure 3.157 for current side impact testing, and Figure 3.158 for an additional future proposed side impact test.

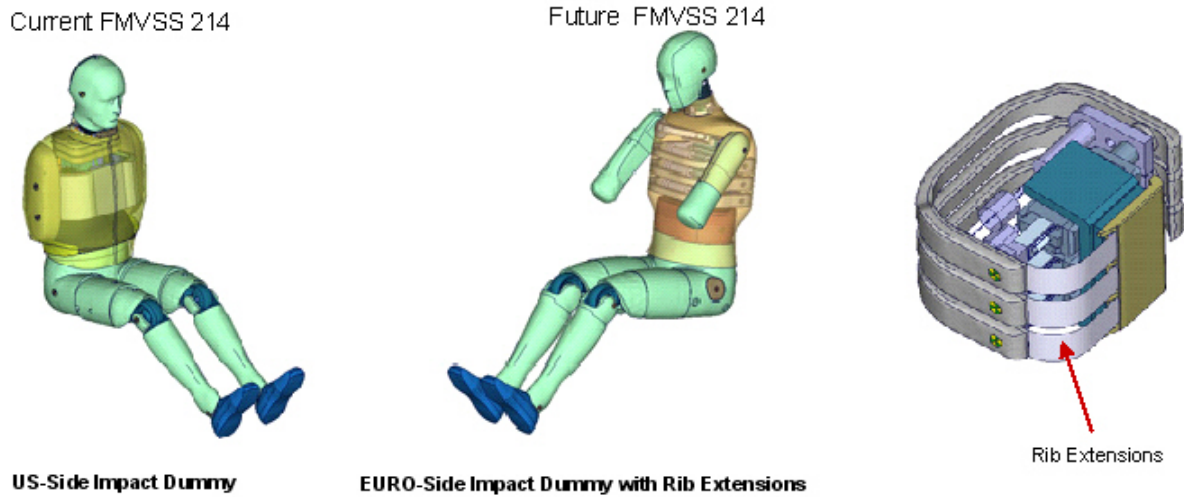


Figure 3.156: FMVSS 214P Anthropomorphic Test Device (ATD)

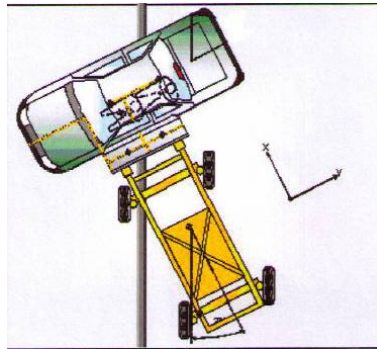


Figure 3.157: Current - 54 $\frac{\text{km}}{\text{h}}$ side crabbed barrier



Figure 3.158: Additional - 32 $\frac{\text{km}}{\text{h}}$ 75 degree rigid pole test

Roof Crush Resistance (FMVSS 216)

Current Requirements:

1. For all passenger cars and multipurpose vehicles less than 2,722 kg, the standard requires that when a large steel test plate (sometimes referred to as a platen) is placed in contact with the roof of a vehicle and then pressed downward, with steadily increasing force until a force equivalent to 1.5 times the unloaded weight of the vehicle is reached
2. Test mandates either driver side OR passenger side to be tested
3. The distance that the test plate (platen) has moved from the point of contact (also referred to as “platen travel”), must not exceed 127 mm (5 inches)
4. Application of force is limited to 22,240 Newtons (5,000 pounds) for passenger cars, even if the unloaded weight of the car times 1.5 is greater than that amount

Future Requirements:

By September 2015, all passenger cars and multipurpose passenger vehicles, trucks and buses with a Gross Vehicle Weight Rating (GVWR) of 2,722 kg (6,000 lb) or less are subject to the new FMVSS 216, which:

1. Doubles the amount of force the vehicle’s roof structure must withstand to three times the vehicle’s unloaded weight
2. Requires testing on driver and passenger side. The same vehicle must meet the force requirements when tested first on one side and then on the other side of the vehicle.
3. Establishes a new requirement for maintenance of headroom, i.e., survival space, during testing, in addition to the existing limit on the amount of roof crush
4. Eliminates the force limitation to 22,400 N and retains the same “platen travel” requirements
5. Uses a Headform Positioning Fixture (HPF) to position a headform (16.5 cm (6.5 inch) diameter metallic hemisphere) at the location of a 50th percentile male inside the vehicle (FMVSS 214 seating position) to determine if and when contact (when 222 N is measured on the HPF load cell) is made between the interior roof and the top of the headform

Figure 3.159 shows the new requirement phase-in schedule.

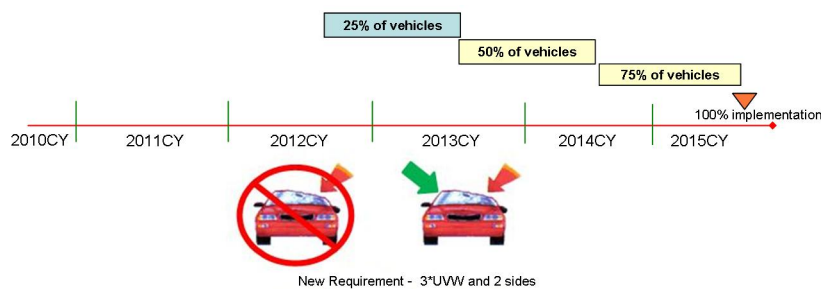


Figure 3.159: Roof crush resistance

Electronic Stability Control System (ESC) (FMVSS 126)

Starting 2011, NHTSA will mandate the installation of Electronic Stability Control (ESC) systems on light-duty vehicles with GVWR up to 4,536 kg (10,000 pounds) and specifies performance requirements for those ESC systems. The rule also provides a thorough definition of ESC, including the requirement for closed-loop, over-steer and under-steer control.

Electronic Stability Control (ESC) has been found to be highly effective in preventing single-vehicle loss-of-control, run-off-the road crashes, of which a significant portion are rollover crashes.

An ESC system utilizes computers to control individual wheel brakes and assists the driver in maintaining control of the vehicle by keeping the vehicle headed in the direction the driver is steering even when the vehicle nears or reaches the limits of road traction. ESC ensures there is sufficient over and/or under steer intervention to prevent spin-out and maintain lateral stability. See Figure 3.160 for an ESC illustration.

The average weight gain for this improvement is approximately 1 kg (2.1 lbs) resulting in 9.8 l (2.6 gallons) more of fuel being used over the lifetime of the vehicle.

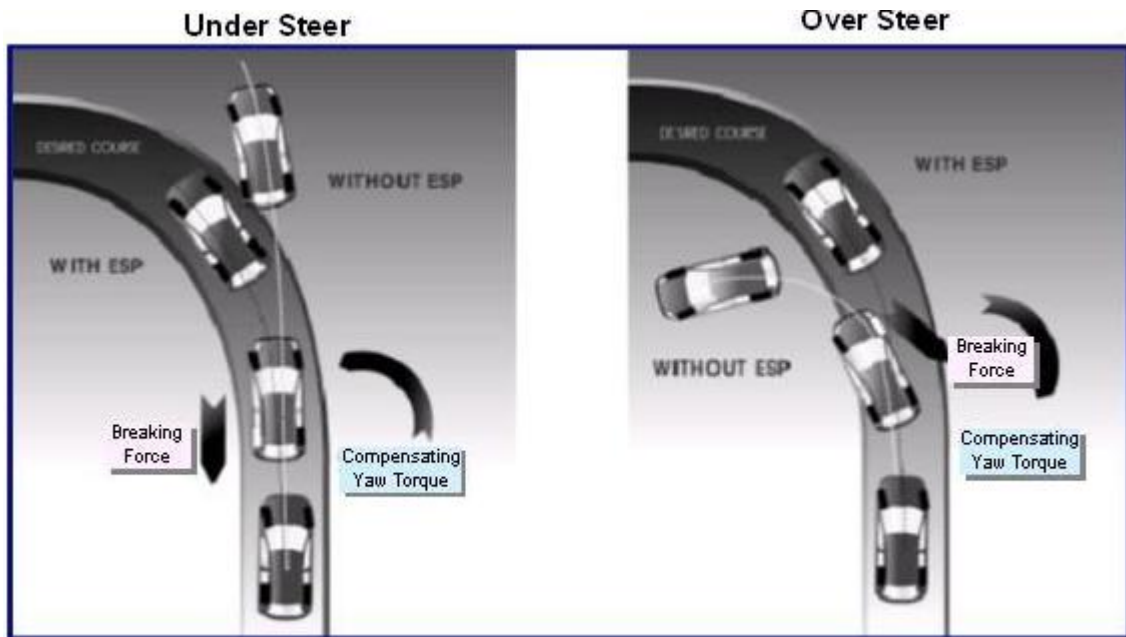


Figure 3.160: Electronic Stability Control system (ESC)

3.4.2.2 Consumer Metrics Tests (non government mandated, but OEM followed)

Consumer metrics tests are more severe (than FMVSS) and are non government mandated with the sole purpose of providing real world comparison data to consumers in terms of vehicle passenger safety and insurance costs. These requirements are aggressively pursued by automakers who treat these as a mandatory requirement and design the vehicle structure and systems to meet these regulations.

Consumer metric tests in the US are typically classified into two categories:

1. High-speed Impact test - administered by NHTSA under the New Car Assessment Program (NCAP)
2. Low speed impact tests - administered by the Insurance Institute for Highway Safety (IIHS)

The Insurance Institute for Highway Safety (IIHS) is an independent, nonprofit, scientific and educational organization and is wholly supported by auto insurers.

Insurance Institute Requirements

Side Impact

The US based Insurance Institute for Highway Safety (IIHS) was the first to revamp its tests to replicate collisions with SUV's and trucks in 2003. The IIHS test is a $50 \frac{\text{km}}{\text{h}}$ (31 mph) perpendicular impact into the driver side of a passenger vehicle. The moving deformable barrier that strikes the test vehicle weighs 1,500 kg (3,300 pounds) and has a front-end shaped to simulate the typical front-end of a pickup or SUV as shown in Figure 3.161. In each side-struck vehicle are two instrumented SID-II dummies representing a small (5th percentile) female or a 12-year-old adolescent. These dummies are positioned in the driver seat and the rear seat behind the driver.

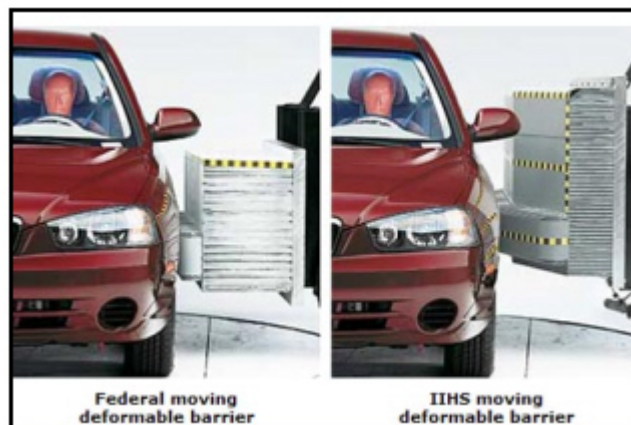


Figure 3.161: IIHS - New side barrier to simulate crash into a SUV

Low Speed Bumper Impact

Bumper impacts tests are conducted with full width contact at $9.66 \frac{\text{km}}{\text{h}}$ ($6 \frac{\text{m}}{\text{h}}$) frontal/rear impact, or at $4.83 \frac{\text{km}}{\text{h}}$ ($3 \frac{\text{m}}{\text{h}}$) with corner impacts. See Figure 3.162 for IIHS new bumper impact tests.

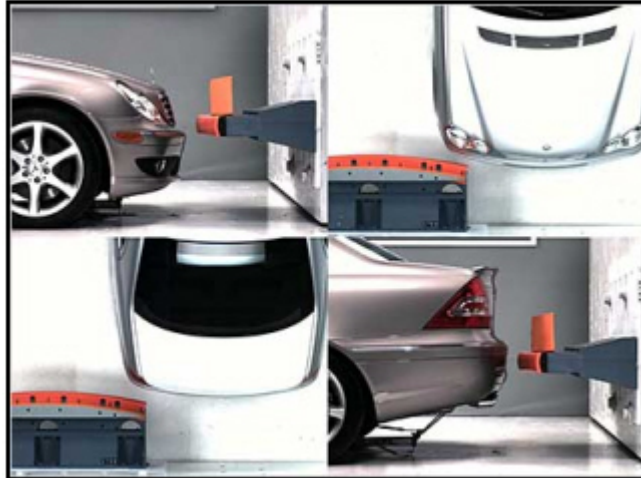


Figure 3.162: IIHS - New bumper impact tests

Roof Crush

On February 19, 2009, IIHS met with NHTSA representatives to provide the agency information about a new roof strength consumer information program that organization is initiating.

The IIHS test is similar to the previously discussed FMVSS 216 requirement with the following changes:

1. Only one side of the vehicle will be tested
2. A minimum Strength to Weight Ratio (SWR) of 3.25 (3.25x vehicle unloaded weight) is required to receive an "acceptable" rating
3. Does not include vehicles over 2,722 kg
4. Rating system will be according to below mentioned SWR ratio
 - Good rating (SWR of 4.0)
 - Marginal rating (SWR of 3.25)
 - Poor rating (SWR < 2.5)

New Car Assessment Program (US-NCAP)

NHTSA plans to continue enhancing its NCAP crash worthiness and crash avoidance activities by challenging manufacturers and by providing consumers with relevant information to aid them in their new car purchasing decisions. Safety enhancements for frontal impact include maintaining the current $56.33 \frac{\text{km}}{\text{h}}$ ($35 \frac{\text{m}}{\text{h}}$) test protocol with the hybrid III 50th percentile male dummy, and incorporate KTH (Knee/Thigh/Hip) injuries into the rating. Lower speed tests will also be evaluated. For side impact evaluations, IIHS can use NCAP to encourage head protection by using the pole test proposed for FMVSS No. 214 until such time as the rule is fully phased-in. A new barrier test protocol calls for increased speed and barrier weight, and the use of new ATD's such as the "WorldSID". The agency will also develop additional lateral injury criteria.

3.4.3 Europe - Future Safety Requirements

3.4.3.1 Mandatory Requirements

The EC Whole Vehicle Type-Approval (WVTA) system applies to passenger cars on a mandatory basis since January 1998. In order to meet the European Union's safety and environmental objectives, there is a continual need to update the various regulations that apply to new vehicle construction. Directive 2007/46/EC, the new framework Directive for motor vehicles, was adopted in 2007. It entered into force on October 29, 2007. Member States have to implement its provisions by April 29, 2009. From then on, it will make EC WVTA mandatory for all the remaining categories of motor vehicles in stages from 2009 to 2014. Key areas of concentration are emissions (EURO 5 and 6 introduction), pedestrian protection implementation, electronic stability control, and tire noise (low rolling resistance tires).

Future hydrogen powered vehicle regulations will address impact protection, electrical safety, hydrogen components designed for M and N class motor vehicles, and hydrogen systems designed for storage and usage with a 36 month from date of entry enforcement timeline.

Pedestrian Protection Requirements

Pedestrian protection is achieved by designing the front of a vehicle so that pedestrians and other vulnerable road users are less likely to be injured if they are hit. European legislation has now been introduced to ensure that all cars offer some level of protection. The tests are being introduced in two phases with the second set of tests being more stringent than the first, resulting in an estimated additional weight impact of 1-2 kg per vehicle.

See Figure 3.163, Figure 3.164, and Figure 3.165 for phase 1 & 2 pedestrian protection requirements.

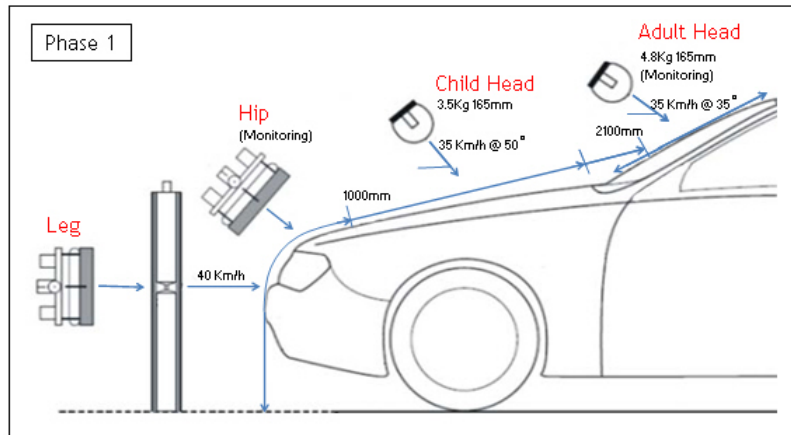


Figure 3.163: Pedestrian protection requirements Phase 1

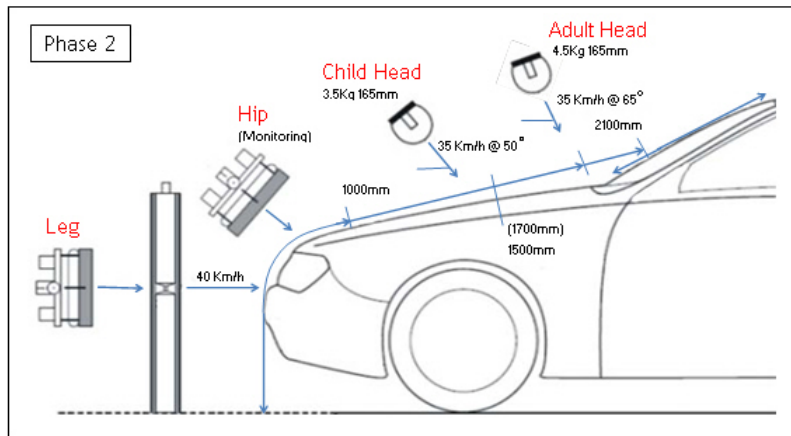


Figure 3.164: Pedestrian protection requirements Phase 2

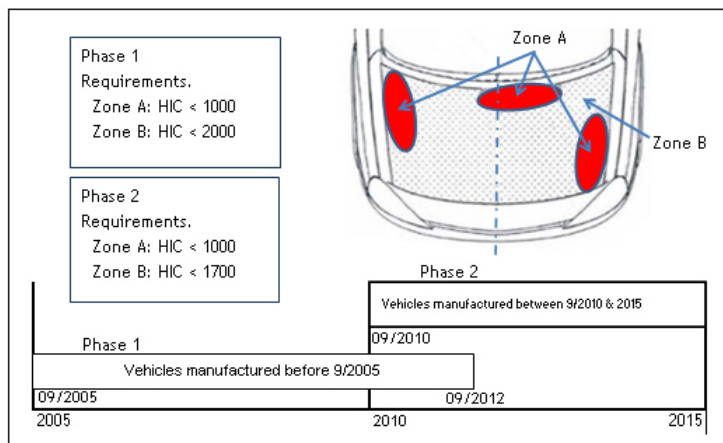


Figure 3.165: Pedestrian protection requirements Phase 1 and 2

3.4.3.2 Non-mandatory Requirements (Consumer Metrics)

EU - New Car Assessment Program (NCAP)

The Euro-NCAP is set to receive an overhaul in the year 2010 its rating safety system performance and will challenge vehicle manufacturers to make all-round safer cars.

Current Regulations

The current system provides 3 separate ratings based on injury criteria (passive safety) from the below mentioned tests:

1. Adult Occupant Safety (shown in Figure 3.166) - 5 stars

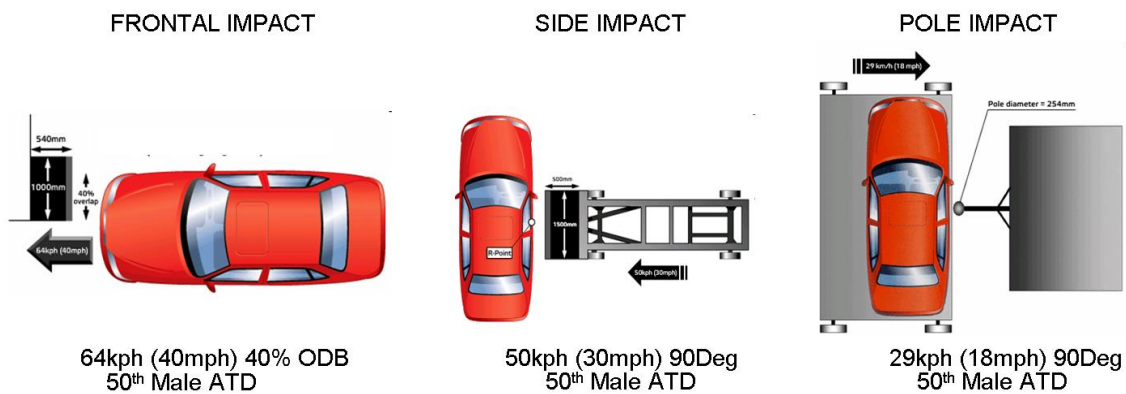


Figure 3.166: Adult occupant protection

2. Child Occupant Safety (shown in Figure 3.167) - 5 stars

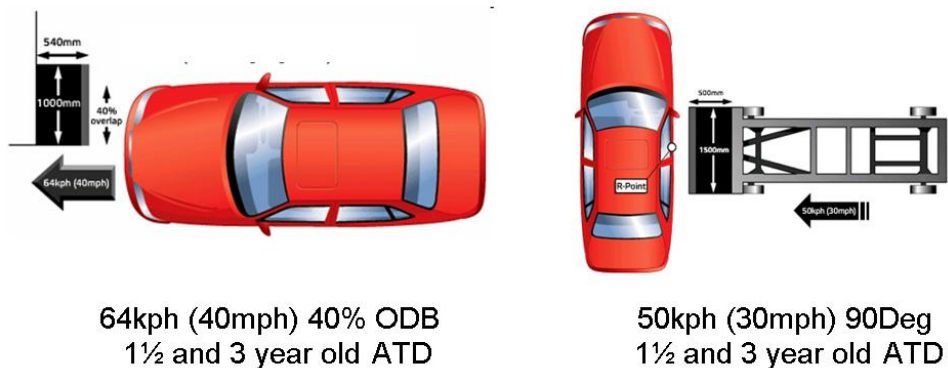


Figure 3.167: Child occupant protection

3. Pedestrian Protection (shown in Figure 3.168) - 4 stars

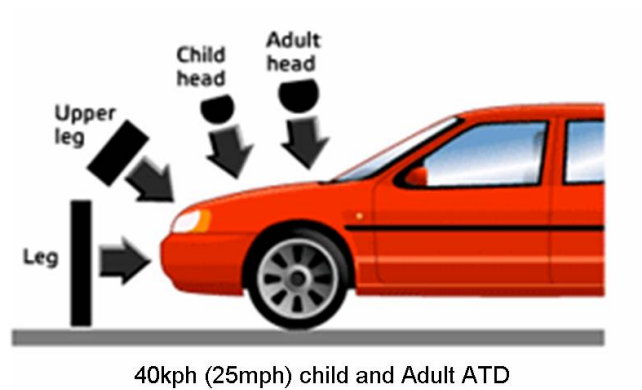


Figure 3.168: *Pedestrian impact protection*

Although there are three different tests, this system enabled automakers to claim a five-star result even though the car's pedestrian or child safety performance was inadequate.

Proposed Rating System

The new proposed system provides a single point based rating which will cover adult occupant protection, Child occupant protection, pedestrian protection and a new area of assessment: safety assist (electronic stability control, speed limitation, seat belt reminders).

1. Adult occupant protection - 32 points
2. Rear whiplash protection (shown in Figure 3.169) - 4 points

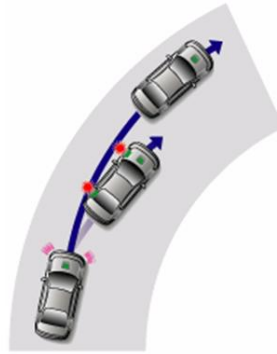


Figure 3.169: *Rear Impact - Whiplash protection*

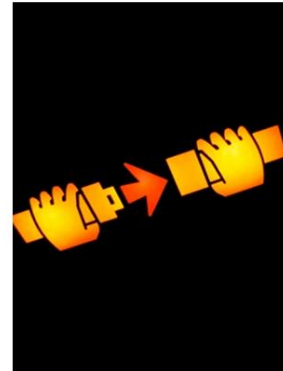
- 3. Child occupant protection - 49 Points
- 4. Pedestrian protection - 36 Points
- 5. Safety assist (shown in Figure 3.170)- 7 points



Speed Limiters



Electronic Stability Control



Seat Belt Reminder

Figure 3.170: *Safety assist*

This new rating system will impose additional requirements on the manufacturer to obtain a better rating which will drive structural changes and in turn, the cost of the vehicle itself because manufacturers have to account for better performance on those areas that they did not have to focus on earlier but still managed to obtain a good rating.

3.4.4 India - Future Regulations

Since 2000, European regulations have been used as basis for Indian regulations and increased efforts are being made to technically align the Indian vehicle regulations with the respective EU regulations.

Alignment of Indian regulations (AIS/ BIS) with ECE is being attempted as per the broad roadmap drafted by automobile manufacturers based in India.

The main changes being implemented are the adoption of the EU occupant protection standards.

Table 3.36 below outlines the time-frame of its adoption into the Indian regulatory standards.

SI No.	ECE/EFC	AIS/IS	Subject	Date of Implementation
20	94	IS 11939 - 1996	Occupant protection in case of frontal offset impact	April 2010
21	95	IS 11939 - 1996	Occupant protection in case of side impact	April 2010
22	33	IS 11939 - 1996	Behavior of the structure in case of frontal impact	April 2010

Table 3.36: *Timeframe of adoption into the Indian regulatory standards*

3.4.5 Global Technical Regulations

The UN's Global Technical Regulation, also known as WP29, is a global arrangement that aims at harmonizing or developing technical regulations for improving vehicle safety, protecting the environment, promoting energy efficiency and anti-theft technology.

The UN/ECE 1958 agreement includes mutual recognition of governmental certifications based on the ECE regulations, while the purpose of the 1998 global agreement is to internationally harmonize the regulations:

- New regulations in the areas of vehicle safety are being implemented in the US and EU
- Most of the countries around the world are adopting the EU safety regulations
- Significant effort in the daunting task of harmonizing the Global Technical Regulations (GTR) are underway. Most countries have already adopted the GTRs
- Advanced technologies in terms of “crash and rollover avoidance” are being standardized all over the world

3.4.5.1 Electric hybrid or hydrogen Fuel Cell Vehicle GTR Action Plan

In order to develop the Global Technical Regulation in the context of an evolving hydrogen technology, the Trilateral Commission^[2] proposes to develop the GTR in two phases:

Phase 1

- Establish a GTR by 2010 for hydrogen powered vehicles based on component level, sub-systems, and a whole vehicle crash test approach
- Existing crash tests (front, side and rear) already applied in all jurisdictions
- Electrical isolation - safety and protection against electric shock (post crash)

Phase 2

- Amend the GTR to maintain its relevance with new findings based on new research and the state of the technology beyond 2010
- Harmonize crash test requirements for FCEV's regarding whole vehicle crash testing for fuel system integrity

²The Trilateral Commission is a private organization, established to foster closer cooperation between the United States, Europe and Japan.

3.5 Future Fuel Economy Requirements

3.5.1 Overview

An assessment was conducted by the FSV engineering team to research into future (2010-2020) global regulations that mandate emissions and fuel economy that are either being researched or are proposed to be changed from the current requirement. These new or proposed changes are required to be complied with after a certain grace period as deemed necessary by the respective regulatory division of the government.

The intention of this exercise is to understand the implication of new regulations on the design of the FSV-1 and FSV-2 propulsion system, and to study and incorporate all the necessary changes on the FSV to meet and exceed these upcoming regulatory specifications by a comfortable safety margin. Typically, most of the fuel economy regulations are rated on a fleet basis and since most manufacturers would want to sell large sized vehicles, the FSV-1 & FSV-2 must exceed these regulations by a considerable margin to offset and support these larger vehicles.

Table 3.37 summarizes the outcome of the research exercise.








CO ₂ Emissions		Fuel Economy				
year		[$\frac{g(CO_2)}{km}$]	Gasoline [mpg]	[km/l]	Diesel [mpg]	[km/l]
2008		200	27.46	11.67	31.51	13.39
2008		160	34.33	14.59	39.39	16.74
2015		153	35.70	15.17	41.19	17.51
2012		130	42.25	17.96	48.48	20.60
2012		120	45.77	19.45	52.52	22.32
2020		95	57.82	24.57	66.34	28.20

Table 3.37: CO₂ emission requirements

Data source: US EPA^[3]

³CO₂ emissions from a gallon of **gasoline** = 2,421 g x 0.99 x (44/12) = 8,788 g = 8.8 kg/gallon = 19.4 lbs/gallon
CO₂ emissions from a gallon of **diesel** = 2,778 g x 0.99 x (44/12) = 10,084 g = 10.1 kg/gallon = 22.2 lbs/gallon

A comparison of the implementation schedules of Green House Gas (GHG) emissions and fuel economy standards around the world[12] is shown in the following figures in Figure 3.171.

Solid lines denote actual performance or projected performance due to adopted regulations; dotted lines denote proposed standards. All values are normalized to the NEDC test cycle in $\frac{\text{g}(\text{CO}_2)}{\text{km}}$.

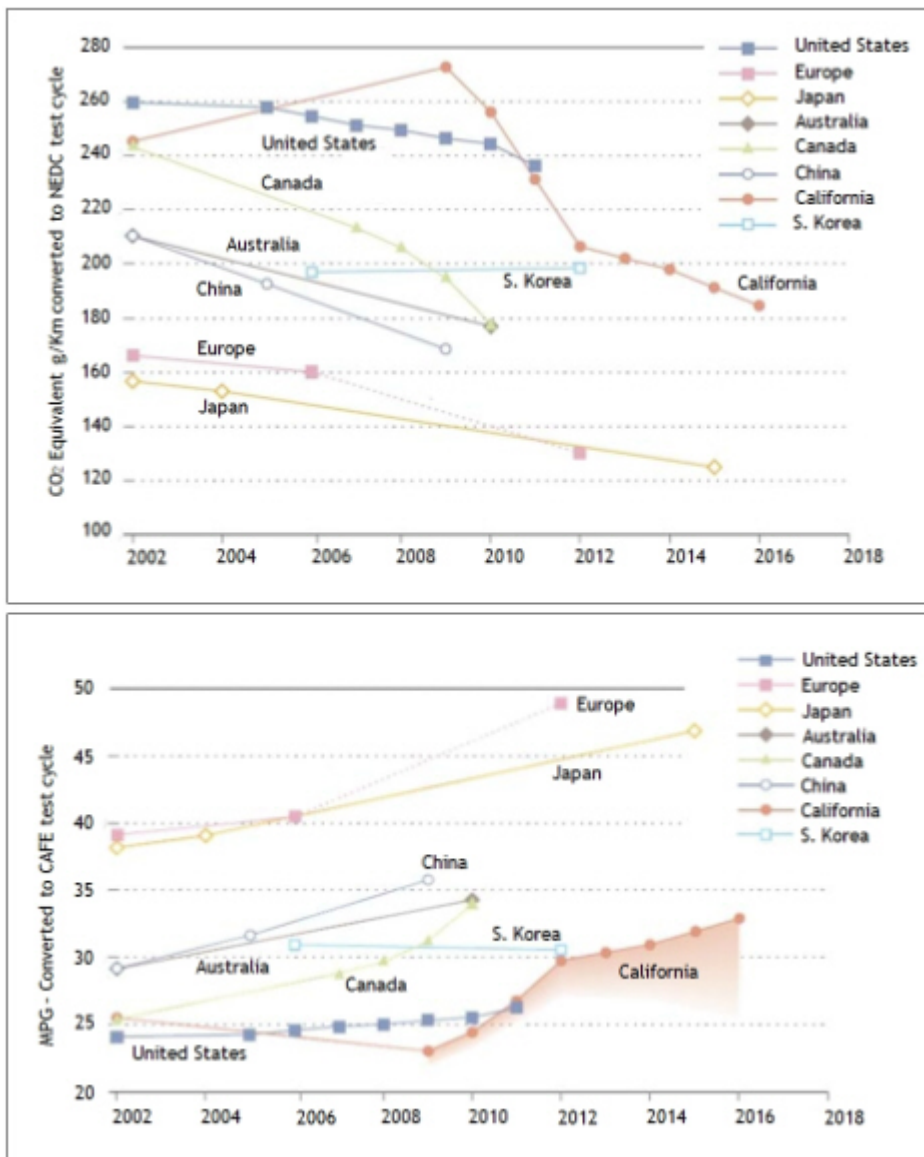


Figure 3.171: Actual and projected GHG emissions for new passenger vehicles: 2002-2018

3.5.2 Future Fuel Economy/CO₂ Standard

3.5.3 United States

Fuel economy standards and its testing methods in the United States is mandated by the Environmental Protection Agency (EPA) operating under the Department of Transportation (DOT).

Fuel economy data is also used by:

1. The U.S. Department of Energy (DOE) to publish the annual Fuel Economy Guide
2. The U.S. Department of Transportation (DOT) to administer the Corporate Average Fuel Economy (CAFE) program, and
3. The Internal Revenue Service (IRS) to collect gas guzzler taxes

Fuel Economy Guide: Is an annual publication containing the fuel economy estimates for all cars and light trucks. The guide includes information about alternative fueled vehicles, the range of fuel economy for different classes of vehicles, a list of fuel economy leaders, and tips for improving fuel economy.

Corporate Average Fuel Economy (CAFE): Requires vehicle manufacturers to comply with the gas mileage, or fuel economy standards, set by the Department of Transportation (DOT).

The Gas Guzzler Tax: Imposed on manufacturers of new cars that do not meet required fuel economy levels to discourage the production and purchase of fuel-inefficient vehicles. The tax is collected by the Internal Revenue Service and paid by the manufacturer.

Fuel Economy Labels: Every new car and light truck sold in the U.S. is required to have a fuel economy window sticker label. The label contains the city and highway mpg estimates that are designed to help consumers compare and shop for vehicles. See Figure 3.172 for an example of the EPA mandated fuel economy label.

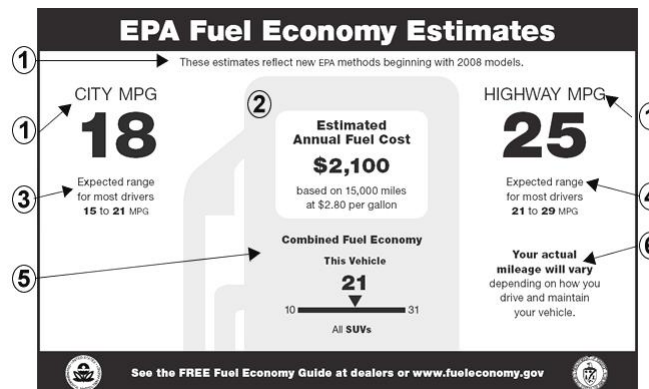


Figure 3.172: New proposed fuel economy label

3.5.3.1 Corporate Average Fuel Economy Standards (CAFE)

The United States Transportation Department proposes a change to the fuel economy standards for 2011 - 2015.

The United States Transportation Secretary, Mary Peters, announced April 22, 2008 a proposed change in federal fuel economy standards for cars and light trucks. The aim of this new proposal is to reduce the average fuel consumption of automobiles, which will save consumers money and in turn will prevent millions of tons of GHG emissions from being expelled into the environment.

The goal, by 2015, is to have the fuel economy standards reach 15.2 $\frac{\text{km}}{\text{l}}$ (35.7 $\frac{\text{m}}{\text{g}}$) for passenger cars, up from the current 11.7 $\frac{\text{km}}{\text{l}}$ (27.5 $\frac{\text{m}}{\text{g}}$) and 12.2 $\frac{\text{km}}{\text{l}}$ (28.6 $\frac{\text{m}}{\text{g}}$) for light trucks, an increase from the existing standard of 9.6 $\frac{\text{km}}{\text{l}}$ (22.5 $\frac{\text{m}}{\text{g}}$). Combined, average fuel economy for cars and light trucks would be 13.4 $\frac{\text{km}}{\text{l}}$ (31.6 $\frac{\text{m}}{\text{g}}$) by 2015.

The proposal would raise fuel economy requirements for model years 2011 to 2015, as the Transportation Department begins to implement the requirements in the Energy Independence and Security Act. The energy law mandated a combined average standard for cars and light trucks of 14.9 $\frac{\text{km}}{\text{l}}$ (35 $\frac{\text{m}}{\text{g}}$) by 2020. The current combined average is about 10.6 $\frac{\text{km}}{\text{l}}$ (25 $\frac{\text{m}}{\text{g}}$), according to the department. The new standards must be in place by April 2009 in order to take effect with the 2011 model year.

The proposed rule would phase in the higher standards over a five-year period, with the standards rising 4.5% a year. That is greater than the 3.3% annual increase mandated in the 2007 energy law.

The proposed new standards would be implemented according to the following schedule in Table 3.38.

Year	Cars	Trucks	Average
2011	30.2	24.1	27.1
2012	32.8	26.4	29.2
2013	34.0	27.8	30.5
2014	34.8	28.2	31.0
2015	35.7	28.6	31.6

Table 3.38: *Average miles per gallon*

3.5 Future Fuel Economy Requirements

The new standards would save 208 billion liters (55 billion gallons) of fuel over the lifetime of vehicles produced during those model years and prevent emissions of an estimated 521 million metric tons of carbon dioxide. These standards also would save consumers US \$100 billion in lower fuel costs over the life of those vehicles.

The increase for passenger cars only, is the first since 1990 when the standard rose from 11.27 $\frac{\text{km}}{\text{l}}$ (26.5 $\frac{\text{m}}{\text{g}}$) to the current 11.69 $\frac{\text{km}}{\text{l}}$ (27.5 $\frac{\text{m}}{\text{g}}$).

The Transportation Department's National Highway Traffic Safety Administration increased the fuel economy standard for light trucks in 2006. The standard for trucks is to rise from 9.57 $\frac{\text{km}}{\text{l}}$ (22.5 $\frac{\text{m}}{\text{g}}$) in 2008 to about 10 $\frac{\text{km}}{\text{l}}$ (23.5 $\frac{\text{m}}{\text{g}}$) in 2010, according to the department.

The Energy Independence and Security Act requires the Transportation Department to institute increases in the average fuel economy standards for cars and light trucks beginning with model year 2011 and ending with model year 2020.

3.5.4 Europe

On December 12th 2007, The European Commission (EC) proposed legislation to reduce the average CO₂ emissions of new passenger cars to 130 $\frac{\text{g}(\text{CO}_2)}{\text{km}}$ by 2012 (14 $\frac{\text{km}}{\text{l}}$).

Support for research efforts is aimed at further reducing emissions from new cars to an average of 95 $\frac{\text{g}(\text{CO}_2)}{\text{km}}$ of by 2020. See Figure 3.173 for CO₂ emissions vs. vehicle mass.

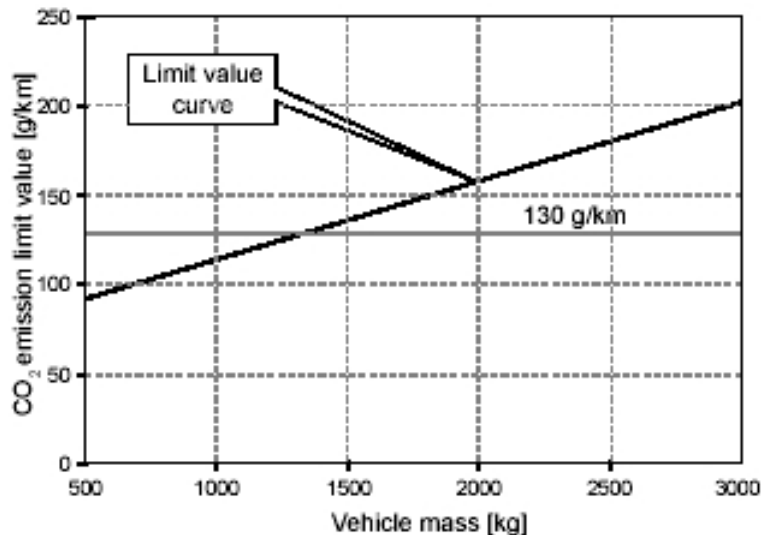


Figure 3.173: CO₂ emission vs. vehicle mass

The main characteristics of the EU regulations are:

- Possibility for a manufacturer to form a “pool” with other manufacturers to jointly meet their combined target
- Independent manufacturers who sell < 10,000 vehicles per year can apply to the EU Commission for an individual target
- Binding limits for average emissions on all new cars sold in the EU from 2012
- Special purpose vehicles are excluded from the scope of the proposal
- A further 10 $\frac{\text{g}(\text{CO}_2)}{\text{km}}$ to 120 $\frac{\text{g}(\text{CO}_2)}{\text{km}}$ reduction by 2012
- Minimum efficiency requirements are expected for car components (tires, air conditioning)
- Also expected are legislative proposals to encourage greater use of bio-fuels
- If a manufacturer’s average emissions levels are above the limit value curve, excess emissions premium will be applied:
 - In 2012: 20 $\frac{\text{g}(\text{CO}_2)}{\text{km}}$ and in 2014: 60 $\frac{\text{g}(\text{CO}_2)}{\text{km}}$
 - In 2013: 35 $\frac{\text{g}(\text{CO}_2)}{\text{km}}$ and in 2015: 95 $\frac{\text{g}(\text{CO}_2)}{\text{km}}$

3.5.5 Japan

The Japanese government first established fuel economy standards for gasoline and diesel powered light-duty passenger and commercial vehicles in 1999.

Fuel economy targets in Japan are based on weight class, with automakers allowed to accumulate credits in one weight class for use in another, subject to certain limitations.

In 2006, Japan increased the stringency of its fuel economy standards by expanding the number of weight bins from nine to sixteen. As a result, Japan's standards are expected to lead to the lowest fleet average greenhouse gas emissions for new passenger vehicles in the world, of 16.8 $\frac{\text{km}}{\text{l}}$ in 2015.

Each manufacturer has to achieve the fuel efficiency in $\frac{\text{km}}{\text{l}}$ as a weighted average (range) in each weight (kg) class. New regulation will consider diesel and gasoline vehicles together.

In 2010 Japan will introduce a new test cycle, the JC08, to measure progress toward meeting the revised 2015 targets and should be applicable from March 2011. See Table 3.39 for the JC08 test cycle, and Table 3.40 for 2015 fuel economy for all fuels. The JC08 cycle's higher average speed, quicker acceleration, and new cold start have increased the stringency of the test by 9%.

Gasoline Passenger Cars - Target for 2015								
Curb weight	≤ 600	601	741	856	971	1081	1195	1311
		-	-	-	-	-	-	-
		740	855	970	1080	1195	1310	1420
$\frac{\text{km}}{\text{l}}$	22.5	21.8	21.0	20.8	20.5	18.7	17.2	15.8
Curb weight	1421	1531	1654	1761	1871	1991	2101	
	-	-	-	-	-	-	-	
	1530	1650	1760	1870	1990	2100	2270	≥ 2271
$\frac{\text{km}}{\text{l}}$	14.6	13.2	12.2	11.1	10.2	9.4	8.7	7.4

Table 3.39: Test cycle - JC08 (cold and hot), applicable from March 2011

Vehicle Class	2004 Avg value [km/l]	2015 Avg value [km/l]	Change [%]
PC	13.6	16.8	23.5
Small buses	8.3	8.9	7.2
LCV	13.5	15.2	12.6

Table 3.40: 2015 fuel economy requirement for all fuels

3.5.6 China

China is one of the newest entrants to the field of regulating vehicle fuel economy. Since 2005, China's rapidly growing new passenger vehicle market has been subjected to the country's fuel economy standards.

The new standards set up maximum fuel consumption limits by weight category and are implemented in two phases:

Phase 1: Started on July 1, 2005 for new models and a year later for previous model year vehicles.

Phase 2: Will take effect on January 1, 2008 for new models and January 1, 2009 for previous model year vehicles.

The standards will be classified into 16 weight classes, ranging from 16.2 $\frac{\text{km}}{\text{T}}$ (38 $\frac{\text{m}}{\text{g}}$) in 2005, to 18.3 $\frac{\text{km}}{\text{T}}$ (43 $\frac{\text{m}}{\text{g}}$) in 2008, for the lightest vehicles, to 8 $\frac{\text{km}}{\text{T}}$ (19 $\frac{\text{m}}{\text{g}}$) in 2005, (9 $\frac{\text{km}}{\text{T}}$ / 21 $\frac{\text{m}}{\text{g}}$ in 2008) for vehicles weighing over approximately 2,495 kg (5,500 lbs).

In a recent study conducted by China Automotive Technology and Research Center (CATARC), the introduction of Phase 1 has increased overall passenger vehicle fuel efficiency by approximately 9%, from 11.7 $\frac{\text{km}}{\text{T}}$ (26 $\frac{\text{m}}{\text{g}}$) in 2002 to 12.07 $\frac{\text{km}}{\text{T}}$ (28.4 $\frac{\text{m}}{\text{g}}$) in 2006. See Figure 3.174 for Chinese fuel economy standards.

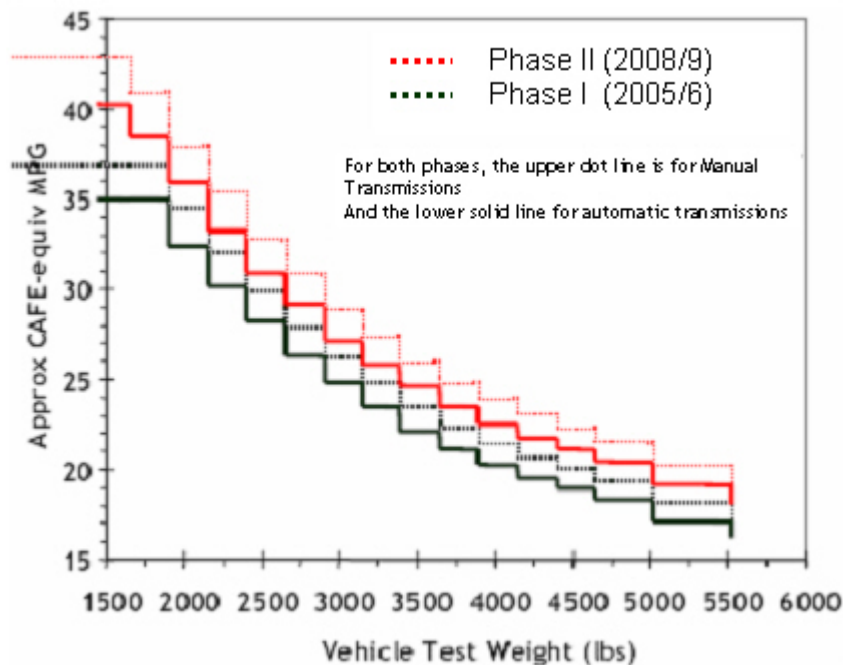


Figure 3.174: *Chinese fuel economy standards*

3.5.7 India

In August 2008, India commenced the development of fuel economy regulations with two autonomous bodies, the Bureau of Energy Efficiency (BEE) and Petroleum Conservation Research Association of India (PCRA), each developing regulations.

It is not yet clear which body has the government mandate for fuel economy even as two more bodies, Ministry of Shipping, Road Transport and Highways (MOSRTH), the key regulator for vehicular emissions which administers the Central Motor Vehicles Act, and the Ministry of Heavy industries, aim to also develop fuel economy rules.

After a voluntary agreement with the automotive industry failed, the government now hopes to improve fuel efficiency 50% by 2030 with mandatory measures.

3.6 Future Ozone Emission Standards

Ozone is a colorless, odorless reactive gas comprised of three oxygen atoms. It is found naturally in the earth's stratosphere, where it absorbs the ultraviolet component of incoming solar radiation that could be harmful to life on earth. Ground-level ozone is an air pollutant with harmful effects on the respiratory systems of animals. The ozone layer in the upper atmosphere filters potentially damaging ultraviolet light from reaching the surface of the earth.

3.6.1 Kyoto Protocol Overview

The Kyoto Protocol is an international agreement linked to the United Nations Framework Convention on climate change. The major feature of the Kyoto Protocol is that it sets binding targets for 37 industrialized countries and the European Community for reducing greenhouse gas (GHG) emissions. This amounts to an average reduction of 5% compared with 1990 levels over the five year period 2008-2012.

3.6.2 United States Air Pollution Standards

On March 12, 2008, the U.S. EPA (Environmental Protection Agency) finalized a new national outdoor air quality standard for ground-level ozone, a component of smog.

Ground-level ozone is not emitted directly into the air, but forms when emissions of nitrogen oxides (NO_x) and volatile organic compounds (VOC's) "cook" in the sun. The new standard is the most stringent standard ever set for ozone at 75 parts per billion.

See Table 3.41 for implementation timeline.

2009	States submit recommendations for county designations to US EPA
2010	US EPA designates non-attainment areas.
2013	States submit state implementation plans to US EPA.
2013-2030	States have up to 20 years to comply with the standard. Areas with dirtier air have longer to comply than those with lower pollution levels.

Table 3.41: *Implementation timeline*

US air pollution standards for cars have historically been stricter than in Europe. This situation was reinforced with the introduction of US "Tier 2" emission standards in 2007.

3.6.3 Future HC, NOx Emission Standards

3.6.4 United States

3.6.4.1 Environmental Protection Agency (EPA)

Two sets, or Tiers, of emission standards for light-duty vehicles in the US were defined as a result of the Clean Air Act Amendments of 1990. See Table 3.42 for the EPA Tier 2 emission limits.

- Tier 1 standard was adopted in 1991 and was phased in from 1994 to 1997
- Tier 2 standards are being phased in from 2004 to 2009
 - Tier 2 is subdivided into 8 Bins or categories (Bin 1, Bin 2, Bin 3, ... Bin 8).
 - Bin 1 is the cleanest and Bin 8 is the dirtiest category.

g/mi	Durab.	Bin 8	Bin 7	Bin 6	Bin 5	Bin 4	Bin 3	Bin 2
NMOG	50 k	0.100	0.075	0.075	0.075			
	120 k	0.125	0.090	0.090	0.090	0.070	0.055	0.010
CO	50 k	3.400	3.400	3.400	3.400			
	120 k	4.200	4.200	4.200	4.200	2.100	2.100	2.100
NOx	50 k	0.140	0.110	0.080	0.050			
	120 k	0.200	0.150	0.100	0.070	0.040	0.030	0.020
PM	120 k	0.020	0.020	0.010	0.010	0.010	0.010	0.010
HCHO	50 k	0.015	0.015	0.015	0.015			
	120 k	0.018	0.018	0.018	0.018	0.011	0.011	0.004

Table 3.42: US EPA - emission limits

3.6.4.2 California Air Resources Board (CARB)

CARB classifies vehicles into the following categories based on the levels of emissions of each vehicle. See Table 3.43 for CARB emissions limits.

1. Low Emission Vehicle (LEV)
2. Ultra Low Emission Vehicle (ULEV)
3. Super Ultra Low Emission Vehicle (SULEV)
4. Zero Emission Vehicle (ZEV)

These standards specifically restrict emissions of carbon monoxide (CO), nitrogen oxides (N₂O), particulate matter (PM), formaldehyde (HCHO), and non-methane organic gases (NMOG) or non-methane hydrocarbons (NMHC). Confusingly, the limits are defined in the mixed-system unit of grams per mile ($\frac{g}{mi}$).

g/mi	Durab.	LEV₂	ULEV₂	SULEV₂	ZEV₂
NMOG	50 k	0.075	0.040	-	0
	120 k	0.090	0.055	0.010	0
CO	50 k	3.400	1.700	-	0
	120 k	4.200	2.100	1.000	0
NOx	50 k	0.050	0.050	-	0
	120 k	0.070	0.070	0.020	0
PM	50 k	-	-	-	0
	120 k	0.010	0.010	0.010	0
HCHO	50 k	0.015	0.008	-	0
	120 k	0.018	0.011	0.004	0

Table 3.43: CARB emission limits

3.6.4.3 US/California Emission Implementation Timeline

Table 3.44 outlines the timeline for implementation of the each of these emission regulations (US tier II and CARB).

Timeline	'98	'99	'00	'01	'02	'03	'04	'05	'06	'07	'08	'09	'10	'11
Federal	Tier 1		Tier 1 and NLEV			Tier 2 phase-in					Tier 2			
California	LEV					LEV 2 phase-in			LEV 2					
States opting into California LEV program	NY MA	NY MA VT	NY, MA VT, ME			Other states may choose to adopt the LEV 2 program								
1. The NLEV program began in 1998. 2. The Clean Air Act allows states to adopt the California Low Emissions Vehicle Program														

Table 3.44: US/CARB implementation timeline

Figure 3.175 shows the distribution of the type of emission regulations enforced by each individual state within the United States. Currently only 4 of the 50 states in the US require vehicles to be compliant to the US Tier 2 Bins 1-4. This essentially means that manufacturers have to comply with the Bin 1-4 standards in order to be able to legally sell vehicles in these four states.

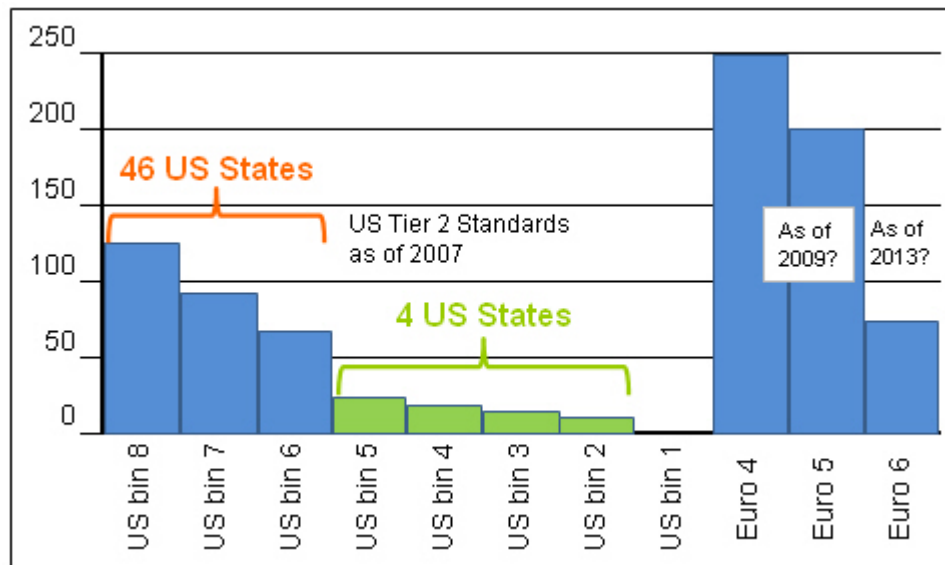


Figure 3.175: US emissions

3.6.5 Green House Gas Emissions Standards

3.6.5.1 California

California adopted greenhouse gas emissions standards for new passenger vehicles, effective with 2009 models. Manufacturers have flexibility in meeting these standards through a combination of reducing tailpipe emissions of carbon dioxide (CO₂), nitrous oxide (N₂O), and methane (CH₄) and receive credit for systems demonstrated to mitigate fugitive emissions of hydro-fluorocarbons (HFCs) from vehicle HVAC systems.

The emission standards become increasingly more stringent through the 2016 model year (Pavley regulation). California is also committed to further strengthening these standards beginning in 2017 to obtain a 45% greenhouse gas reduction from the 2020 model year vehicles. As allowed by the federal Clean Air Act, 12 additional states have adopted California's standards and other states, as well as Canadian provinces, have also expressed interest in doing so.

California standards regulate Green House Gas (GHG) emissions whereas federal CAFE standards aim to reduce the nation's fuel consumption.

The apples-to-apples comparison of total tons of GHG emissions reduced under the new federal CAFE standards versus those that would occur with full implementation of the California rules, also reveal the following results:

- **California's Rules Are More Stringent Earlier**

In calendar year 2016, the state standards (referred to as the California standards or the Pavley rules) will reduce California's GHG emissions by 16.4 million metric tons (MMT) of carbon dioxide equivalents (CO₂E). This is more than double the 7.5 MMT reduction produced by the federal rules.

- **California's Rules Are More Stringent Later**

By 2020, California is committed to implement revised, more stringent GHG emission limits (the Pavley Phase 2 rules). California's requirements would reduce California GHG emissions by 31.7 MMT CO₂E in 2020, 69% more than the 18.8 MMT's reductions under the federal rules in that year.

- **There Are Greater Fuel Savings Under California Rules**

The analysis estimates the effects of the federal CAFE standards on GHG emission rates. This also allows a comparison of the impact of the two programs on vehicle efficiency. Since the California rules are significantly more effective at reducing GHG's than the federal CAFE program, they also result in better fuel efficiency - roughly 18.3 $\frac{\text{km}}{\text{l}}$ ($43 \frac{\text{m}}{\text{g}}$) in 2020 for the California vehicle fleet as compared to the new CAFE standard of 14.9 $\frac{\text{km}}{\text{l}}$ ($35 \frac{\text{m}}{\text{g}}$).

□ **The Cumulative Greenhouse Gas Benefit is Greater under California Rules**

The cumulative GHG emission reductions of the California standards have also been estimated. Between 2009 and 2016, the California standards will prevent emissions of 55 MMT's of CO₂ equivalents in California. This is more than twice the 22 MMT's prevented if only the new federal CAFE standards were implemented. By 2020, the California rules would prevent 158 MMT's CO₂ equivalents emissions, double the 79 MMT's reductions of CO₂E expected if only the federal standards were implemented in California.

□ **Other States Magnify the California Rules**

There are also significant benefits for other states that adopt the California standards. Twelve states have done so to date. By 2020, California's more stringent limits will reduce cumulative GHG emissions in California and those 12 states by 434 MMT's CO₂ equivalents, an 89% improvement over the federal standards.

The US Environmental Protection Agency (EPA) and NHTSA are working together to comprehend the California Proposal into US national law.

3.6.6 Europe Emission Requirements

European emission standards are sets of requirements defining the acceptable limits for exhaust emissions of new vehicles sold in EU member states. See Table 3.45 for European emission standards for gasoline.

Tier	Date	CO	HC	NOx	HC+NOx	PM
EM1	1989	2.72 (3.16)	-	-	0.97 (1.13)	-
Euro 2	1993	2.20	-	-	0.50	-
Euro 3	1997	2.30	0.2	0.15	-	-
Euro 4	2003	1.00	0.1	0.08	-	-
Euro 5 (Future)	2009	1.00	0.1	0.06	-	0.0055
Euro 6 (Future)	2014	1.00	0.1	0.06	-	0.0055

Table 3.45: European emission standards for gasoline

In the year 2016, The European emission standard will be aligned with the US Federal (Tier 2) emissions standard. See Figure 3.176 for implementation of EURO standards.

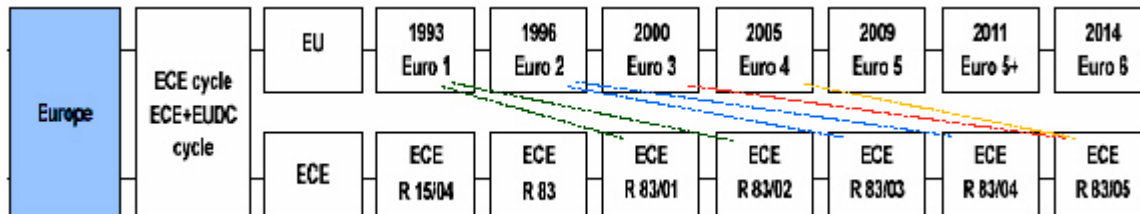


Figure 3.176: Year of implementation of each of the EURO standards

3.6.7 Asia Pacific

Currently, all but three Asian countries (Japan, South Korea and Taiwan) have adopted the EU standard(s). The Asia Pacific region implements only the EU Standards. Countries with minimal or no emissions standards like India and China are adopting the EU standards by 2010. See Figure 3.177 for EURO emissions standards implementation timeline in Asia.

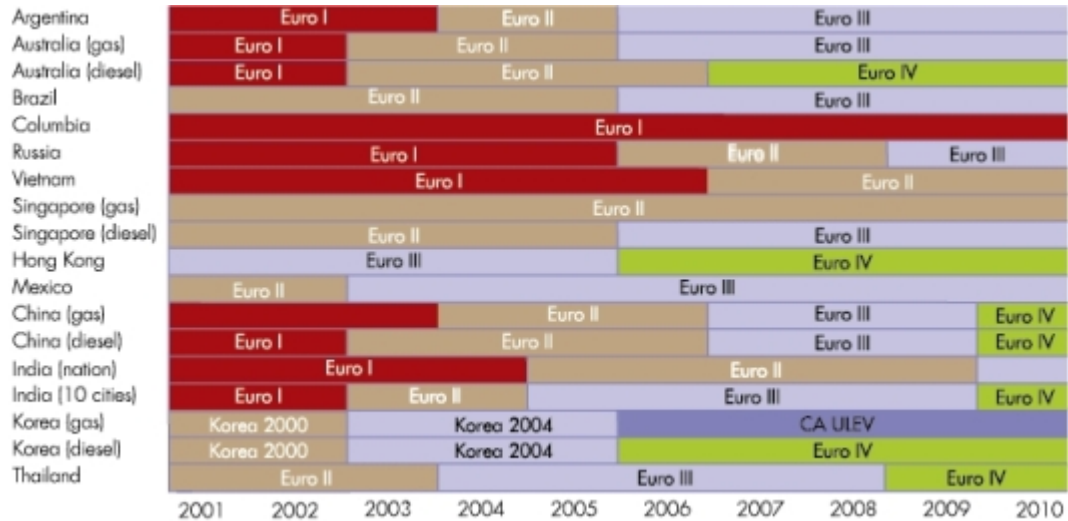


Figure 3.177: Year of implementation of each of these EURO standards in Asia

3.6.8 Vehicle Emissions Test Protocols - Japan

Ministry of Land, Infrastructure, Transport and Tourism (MLIT) has announced that the existing emission test mode for passenger cars and mini and mid-sized cars will be replaced by the new test mode (JC08) and that the installation of On Board Diagnostics (OBD) will be made mandatory.

3.6.8.1 Effective Dates of Implementation of the new test protocol

Change from 11 mode to JC08C mode	Sept. 1, 2010
Change from 10-15 mode to JC08H mode	March 11, 2011
Mandatory installation of J-OBD II	Sept. 1, 2010
Partial change in measuring method of fuel evaporative emission	March 1, 2011

3.6.9 Other requirements

For vehicles powered by fuels other than gasoline, LPG or diesel:

- Test Method is JC08H + JC08C after 31 March 2011
- Emission limits are similar to the relevant 2009 vehicle regulation
- Application date: Domestic vehicle - 01 Oct 2009
- Application date : Imported vehicle - 01 Sep 2010

Test Mode (from Oct. 2009)

The new JC08 test mode that will be implemented starting in 2011 and 2013 will have the emissions levels calculated as indicated below.

The Total emission level of a vehicle would be 75% of the levels measured under the JC08 Hot Start Mode and 25% of the levels measured under the JC08 Cold Start Mode.

$$(JC08 \text{ Hot Start Mode} \times 0.75 + JC08 \text{ mode cold start} \times 0.25)$$

3.7 Vehicle Classification

There are a set of classification systems for passenger cars which are widely understood in North America, another set for Europe, and other systems prevalent in China and India.

Vehicle classification is somewhat subjective, as many vehicles fall between classes or even outside all of them. Not all car types are sold in all countries and names differ in some cases between British and American English. See Table 3.46 for commonly used vehicle classification. Where applicable, the relevant Euro-NCAP classifications are shown.

American	British	Segment	Euro NCAP	Vehicle Example
MicroCar	Microcar	N/A	N/A	Smart For Two
N/A	City Car	A	Super Mini	Renault Twingo
Sub-compact	Super Mini	B		Hyundai Accent
Compact	Small family	C	Small family	Ford Focus
Mid-size	Large Family	D	Large family	VW Passat
Entry level Luxury	Compact Executive			Audi A4
Full-size	Executive	E	Executive	Chrysler 300
Mid-size Luxury				BMW 5-Series
Full-size Luxury	Luxury	F	N/A	Mercedes S-Class
N/A	Leisure Activity	B	Small MPV	Peugeot Partner
N/A	Mini MPV			Opel Meriva
Compact Mini Van	Compact MPV	C		Mazda 5
Mini Van	Large MPV	D	MPV	Toyota Previa
Mini SUV	Mini 4x4	B	Small	Suzuki SX4
Compact SUV	Compact 4x4	C/D	Off-Roader	Honda CR-V
Mid-size Crossover SUV	Large 4x4	E	Large Off-Roader	BMW X5
Mid-size SUV	Off-Roader			Jeep Cherokee
Full-size SUV		N/A	Cadillac Escalade	

SUV=Sports Utility Vehicle, **MPV**=Multi Purpose Vehicle, **N/A**=No comparable classification

Table 3.46: *Vehicle Classification*

3.7.1 United States

In the US, passenger cars are classified on the basis of the interior volume index or seating capacity, except those classified as a special vehicle. Interior volume index is the sum, rounded to the nearest .0028 m³ (0.1 ft³), of the front and rear seat volume, and the luggage capacity. A two seater is classified as a car with no more than two designated seating positions. See Table 3.48 for US passenger vehicle classifications.

Class	Vehicle Examples	Interior Volume	
		[ft ³]	[m ³]
Mini-Compact	VW Beetle Lexus SC-340 Mitsubishi Eclipse Porsche Carrera	< 85.0	< 2.41
Sub-Compact	Chrysler Sebring Honda Civic Audi A4 Toyota Scion tC	85.0 - 99.9	2.41 - 2.83
Compact	BMW 3-Series Mazda 3-Series Ford Focus Pontiac G6	100.0 - 109.9	2.83 - 3.11
Mid-size	BMW 5-Series Cadillac CTS Ford Fusion Toyota Camry	110.0 - 119.9	3.11 - 3.40
Large	BMW 7 -Series Cadillac DTS Ford Taurus Chevrolet Impala	> 120.0	> 3.40
Small Station Wagon	BMW 3-Wagon Pontiac Vibe Volvo V50 Audi A3 Wagon	< 130.0	< 3.68
Mid-Size Station Wagon	VW Passat Saab 9-5 Volvo V70 Audi A6 Wagon	130.0 - 160.0	3.68 - 4.53

Table 3.48: USA vehicle classification

3.7.2 Europe

Vehicle segments in Europe do not follow any formal characterization or regulations generally. The European New Car Assessment Program (Euro-NCAP) uses the following nine categories:

1. Super minis
2. Small family cars
3. Large family cars
4. Executive cars
5. Roadsters
6. Small off-road (similar to crossover SUV category)
7. Large off-road (similar to SUV category)
8. Small multipurpose vehicles
9. Large multipurpose vehicles

3.7.3 China

In China, passenger cars are categorized as follows in Table 3.49.

Class	Length [mm]	Capacity		Current Modes	
		Engine	Seating		
A00 (Sub-Compact)	3400	< 1.2 l	NA	Chery QQ Changhe-Suzuki Beidouxing	Changan-Suzuki Alto
A0 (Small Cars)	3401-4000	< 1.2 l	NA	Chevrolet Lova AVEO Citroen C2 Fiat Palio Kia Rio	Honda Fit VW Polo Peugeot 206 Chevrolet Lova
A (Mid-Size)	4001-4500	1.2-1.6 l	NA	Hyundai Cerato Hyundai Elantra Peugeot 307 Nissan Tilda	Buick Excele Honda Civic Toyota Corolla
B (Mid-High)	4501-4700	> 1.6 l	NA	Chevrolet Epica Hyundai Sonata Kia Optima	S-MAX Mazda 6 Audi A4
C (Luxury)	> 5000	> 1.6 l	NA	BMW 5 series Benz E	

Table 3.49: *China vehicle classification*

3.7.4 India

Car Classification in India (by length in mm) can be seen in Table 3.50.

Class	Length [mm]	Engine Capacity	Current Modes		
A1 (Mini)	3400	< 1.2 l	Maruti 800 Tata Nano Reva		
A2 (Compact)	3401-4000	1.2-1.6 l	Maruti Alto Chevy Spark Hyundai i10 Fiat Palio	Tata Indica Maruti Swift Hyundai Getz Hyundai Santro	Maruti WagonR
A3 (Mid-Size)	4001-4500	1.6-2.2 l	Ford Focus Ambassador Maruti esteem Ford Ikon	Ford Fiesta Tata Indig Opel Astra Hyundai Accent	Renault Logan Hyundai Verna Maruti SX4 Maruti Baleno
A4 (Executive)	4501-4700	V6 Engines > 2.2 l	Ford Mondeo Honda City Toyota Corolla Chevy Aveo	Mitsubishi Lancer Honda Civic BMW 3 series Audi A4	
A5 (Premium)	4701-5000	V6 Engines > 2.2 l	Honda Accord Toyota Camry Hyundai Elantra	Chevy Optra Scoda Octavia Hyundai Sonata	
A6 (Luxury)	> 5000	V6 Engines > 2.2 l	Audi A6, A8 BMW 7 series Volvo S80	Mercedes Benz Bently	

Table 3.50: *India vehicle classification*

4.0 Future Steel Vehicle Propulsion Systems

4.1 Overview

This section defines the preliminary design of powertrain options for the Future Steel Vehicle.

A feasibility study was performed to determine the powertrain architectures, components, performance, cost, and mass of four powertrain variants predicted to be in volume production by major automotive OEMs in the 2015 - 2020 timeframe. The four powertrain variants studied were:

- Plug-In Hybrid Electric with a 32 km (20 mile) all electric range (PHEV₂₀)
- Plug-In Hybrid Electric with a 64 km (40 mile) all electric range (PHEV₄₀)
- Battery Electric Vehicle (BEV)
- Fuel Cell Electric Vehicle (FCEV)

The study included the evaluation of currently used, as well as emerging powertrain technologies. These include high voltage batteries of varying chemistries, ultra-capacitors, traction and wheel motors, and power electronics, as well as hydrogen storage and infrastructure.

For typical drive cycles, the well documented fuel efficiency and green house reduction advantages of the parallel-split hybrid architecture were confirmed. To achieve compact modular design for vehicle packaging and platform cost optimization, the series architecture offers advantages. Along with potentially changing driving habits and the opportunity of mostly shorter distance all electric operation, life cycle greenhouse emissions and fuel consumption may not be impacted significantly by the occasional deployment of the less efficient series powertrain option.

For the purpose of the Future Steel Vehicle studies, a virtually common transaxle sub-assembly was selected, consisting of a traction motor, reduction gearing, and differential. Two different power internal combustion engine/generator assemblies electrically power the transaxle sub-assembly, by a fuel cell system, or by a large capacity high voltage battery. Each of these powertrain options has its unique fuel storage, high voltage battery size, weight and cooling configurations resulting in new body-structure design and challenges.

For the complex fuel cell system, Shanghai Fuel Cell Vehicles (SFCV) performed a separate powertrain sub-system study in conjunction with Tongji University. The integration studies of the fuel cell sub-system into the vehicle powertrain systems were supported jointly by Quantum and SFCV.

4.2 Advanced Powertrain Block Diagrams

The major powertrain components were integrated into an architecture functional block diagram. This, in a high-level fashion, defines the electrical and mechanical transmission of power to both drive the vehicle and supply power to vehicle loads.

A common feature among all vehicles is the electrification of the powertrain based on a high voltage DC Bus (at battery voltage). Any high power electrical loads, whether from traction motors or on-vehicle, use high voltage in order to keep the amperage at a reasonable level so as to keep component efficiency high ^[1].

4.2.1 BEV (Battery Electric Vehicles)

Electric Vehicles (EV) do not have on board power generation and instead rely on stored electrical energy supplied by a large battery. The battery system is charged primarily from the utility electrical grid but may also be charged using distributed forms of power generation. The architecture recommended for the FSV BEV can be seen in Figure 4.1.

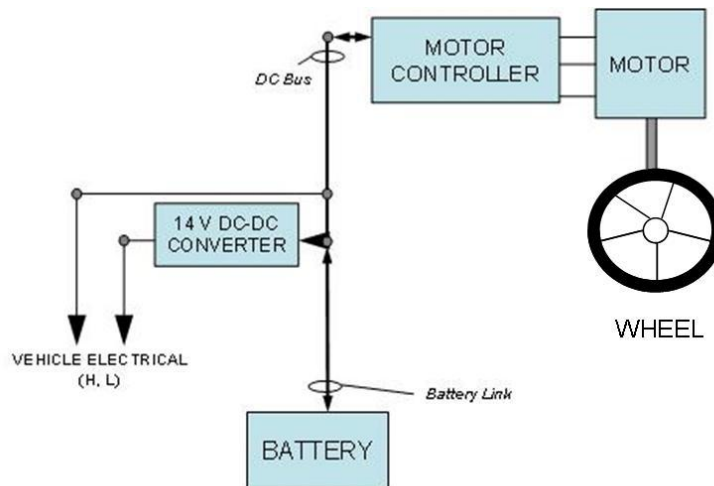


Figure 4.1: BEV

An EV powertrain configuration consists of the following major components:

- Traction motor
- Traction motor controller/inverter
- DC/DC converter
- Battery energy storage

¹Electrical component efficiency is inversely proportional to the current (amperes) it carries. Current is inversely proportional to voltage, high voltage translates to less current. The same principle is used in high-voltage power transmission from generating stations to the electrical grid, to lower transmission losses.

4.2.2 FCEV (Fuel Cell Electric Vehicles)

Fuel Cell Electric Vehicles (FCEV) are similar to PHEVs but they substitute a fuel cell system in place of an IC engine/generator. The fuel cell directly converts fuel and air into DC electrical power, which is then regulated by a fuel cell DC/DC converter. The architecture recommended for the FSV FCEV configuration is shown in Figure 4.2.

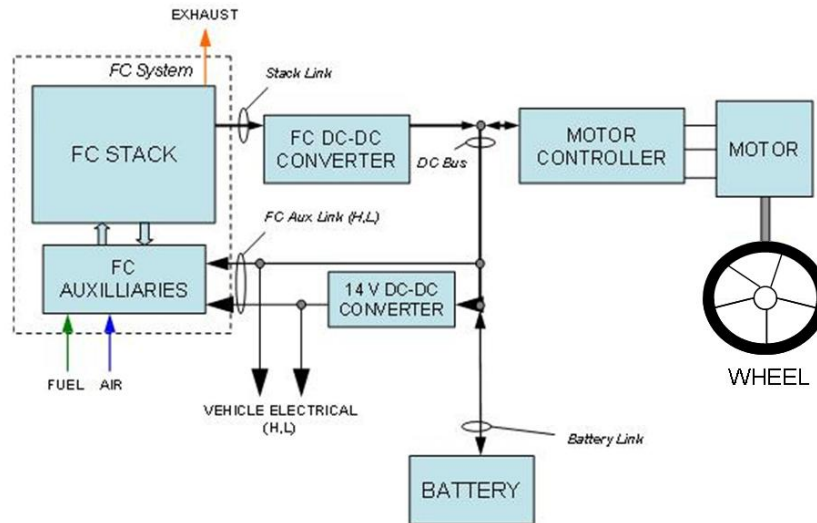


Figure 4.2: FCEV

A FCHEV Series powertrain configuration consists of the following major components:

- Fuel cell stack
- Fuel cell auxiliary equipment (compressor, recirculator, etc.)
- Fuel cell DC/DC converter
- Traction motor with controller/inverter
- AC/DC converter^[2]
- Battery energy storage

²DC/DC converters are designed to regulate the output voltage from the fuel cell stack to the final load so that you can get steady, reliable operation from the fuel cell.

4.2.3 PHEV Series Hybrid Vehicle

In a series hybrid system shown in Figure 4.3, the ICE drives an electric generator instead of directly driving the wheels. The generator charges the battery, and powers an electric motor that propels the vehicle. Series Plug-In Hybrid Electric Vehicles (PHEV) are similar to today's hybrid electric vehicles in that they have both have an Internal Combustion Engine (ICE) as well as electrical energy storage, and drive motors.

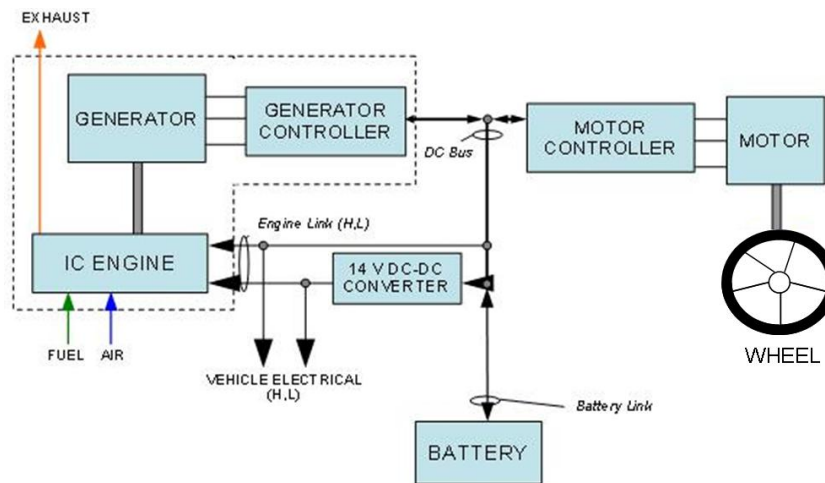


Figure 4.3: PHEV Series hybrid vehicle

4.2.3.1 Advantages

- ICE can be run at a constant and efficient rate at all vehicle speeds
- Platform architecture can be common among variants
- A complex transmission is not needed

4.2.3.2 Disadvantages

- Lower efficiency on long highway drives (less than 30% of driving is in this mode)

The architecture recommended for the FSV PHEV is the series hybrid configuration due to the following reasons:

1. Platform flexibility
2. Primary criteria for design of the FSV is Charge Depleting (electric) mode and the series configuration offers the best efficiency in this mode (70% driving is in electric mode)

4.2.4 PHEV Parallel Hybrid Vehicle

Parallel hybrid systems as shown in Figure 4.4, which are most commonly produced at present, have both an internal combustion engine (ICE) and an electric motor connected to a mechanical transmission.

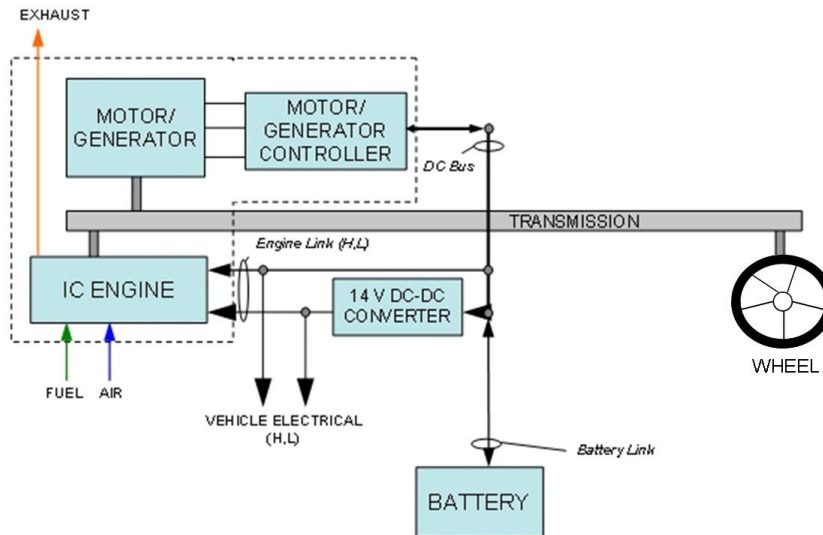


Figure 4.4: PHEV Parallel hybrid vehicle

4.2.4.1 Advantages

- Better performance can be achieved with a discharged battery

4.2.4.2 Disadvantages

- Requires a complex transmission
- ICE cannot be run at an efficient RPM
- Platform flexibility cannot be achieved

4.2.5 PHEV Parallel-Split Hybrid Vehicle

Power-split hybrid or series-parallel hybrid systems, as shown in Figure 4.5, have features of both series and parallel hybrids. In a parallel-split hybrid, both the ICE and the traction motor are connected to the wheel with a power-split device^[3] that allows the power path from the engine to the wheels to be either mechanical or electrical (The ICE can operate independently of the vehicle speed, charging the batteries or providing power to the wheels as needed).

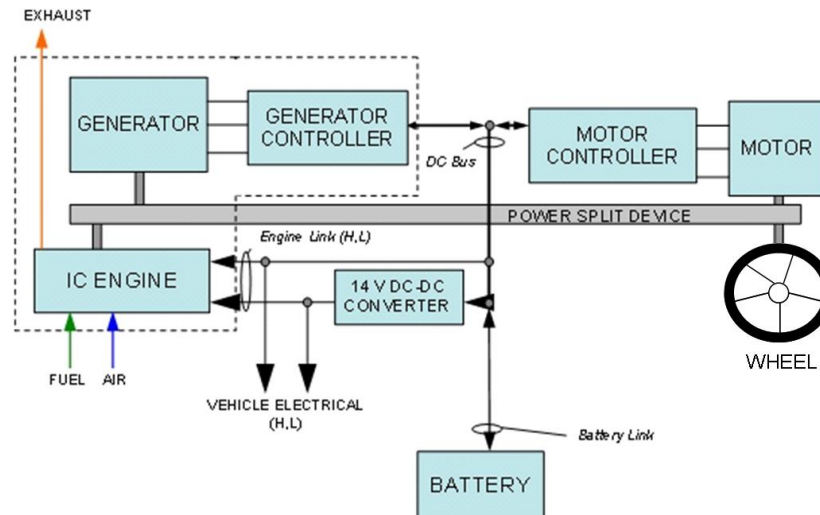


Figure 4.5: PHEV Parallel-Split hybrid vehicle

4.2.5.1 Advantages

- Smaller ICE using a more efficient cycle^[4] contributes significantly to the higher overall efficiency of the vehicle
- Power-split device acts as a continuously variable transmission, thus eliminating the need for a conventional transmission
- Power-split device allows the generator to start the car, thus eliminating the starter

4.2.5.2 Disadvantages

- This system incurs higher costs than a parallel hybrid since it needs a generator, a larger battery pack and more advanced electronics to manage the dual system

³Planetary gear system (Toyota Prius) or dual mode transmission (GM)

⁴Atkinson/Miller cycle: lower power density, less low-rpm torque, higher fuel efficiency

4.3 PHEV Industry Perspectives

Future plug-in hybrid vehicles may be one of the following architectures:

- Parallel
- Series
- Parallel-split

The parallel architecture, used in vehicles like the current Honda Civic, is not appropriate for PHEV applications due to the inability to operate in electric only mode without running the IC engine. Although a clutch disconnect system can be used to allow all electric operation, previous independent studies determined the fuel economy for this architecture is the lowest of the three PHEV designs. In terms of tank-to-wheel fuel efficiency, the parallel-split configuration is the most appropriate architecture for reducing overall vehicle CO₂ emissions when driven in charge sustaining mode (all energy from petroleum), provided this is the primary criteria for vehicle design. This position is supported by Quantum Technologies as well as Argonne National Laboratory (ANL)[45][44], Directed Technologies, Inc. (DTI)[54][63] and General Motors (GM)[42].

In selected cases, series architectures are being employed by OEMs, most likely for technology development strategies. Tooling and development costs of dedicated hybrid vehicle platforms are still hard to justify at volumes below hundreds of thousands of vehicles produced. The series configuration will sacrifice some fuel economy and increase CO₂ output levels, with respect to the parallel-split, in an effort to optimize vehicle manufacturing cost over multiple configurations.

Although the benefit of plug-in battery power is for a limited driving range, for a significant number of people it is well within their daily driving needs. At present the EPA (Environmental Protection Agency - USA) is not sure how to rate series PHEV vehicles like Chevrolet Volt's fuel economy. The confusion stems from the EPA's classification of series PHEV. Is it an Electric Vehicle (EV) with an on board generator, or a hybrid vehicle that relies heavily on its electric drive? The driving habits and battery charging routines of the operator will play a huge role in the fuel economy attained by such vehicles. Methods for measuring fuel economy, potential petroleum displacement and overall reduction in CO₂ emissions due to miles driven in EV modes, are at present, under review.

4.3 PHEV Industry Perspectives

If specific driver profiles, travel distances and terrain conditions are given, optimizations of power-train architectures can be made, possibly giving series plug-in hybrid vehicles an advantage. The following in Table 4.1 summarizes the PHEV architecture trade-offs.

Hybrid Type	Series	Parallel	Parallel Split
Example	Chevy Volt, garbage trucks, buses	Honda Hybrids	Toyota hybrids, Ford hybrids, GM Dual Mode hybrids
Complexity	Low	Medium	High
Acceleration and Top Speed	Disadvantage: Traction motor power dictates peak performance. Engine is not mechanically connected to the wheels.	Good - Advantage in that engine and electric motor can be combined for better acceleration.	Good - Advantage in that engine and electric motor can be combined for better acceleration.
Stop and Go Traffic	Best - Cost and regenerative braking	Medium regenerative capability	GM Two Mode: Large regenerative capability; Single Planetary: Medium Regenerative capability
Highway Cruise	Poor - Mechanical to electrical to mechanical conversion inefficiencies, heavy battery.	Best - Mechanical efficiency / light weight electric motor and battery. Approaches conventional mechanical efficiency.	Good - Mechanical efficiency / light to medium weight motor and battery.
City and highway combined	Poor - Mechanical to electrical to mechanical conversion inefficiencies.	Good - Electrical and mechanical efficiency. Engine / motor speed matching reduces efficiency.	Best - Electrical and mechanical efficiency.
PHEV	Advantage: Traction motor is properly sized for electric vehicle operation; Disadvantage: In highway efficiency and possible acceleration.	Typically smaller traction motor size limits acceleration and top speed performance in electric operation.	GM Two Mode: Advantage with electric motor power allowing 'normal driving' performance, engine providing heavy duty performance; Single Planetary: Typically smaller traction motor size limits acceleration and top speed performance in electric operation.
Flexibility between Power Units (IC engine, Fuel Cell)	Best - Preferred configuration, fuel cell and battery only.	Poor - Must use a mechanical power supply (IC engine) in addition to fuel cell. Fuel cell is usually auxiliary.	Poor - Must use a mechanical power supply (IC engine) in addition to fuel cell. Fuel cell is usually auxiliary.

Table 4.1: Industry perspectives

4.4 Parallel-Split Series Simulation Results

A summary of parameters used in the analysis as well as the required power and energy consumption can be seen in Table 4.2. For the Parallel-split, “E” signifies IC Engine, “G” signifies the Generator, and “M” signifies the Traction Motor. Peak and continuous power requirements for fuel economy drive cycles, grade climb ability for short and very steep hills, long uphill grades at high speed also have to be considered to achieve driver satisfaction with adequate performance.

Vehicle Design Parameters (comparable to OEM Standards)	PHEV ₄₀				
		Series		Parallel-Split	
		Curb+ Driver	GVW	Curb+ Driver	GVW
Front wheel drive	yes	yes		yes	
Wheel base [mm]	2578	2578		2578	
Weight distribution [%/%]	50/50				
Center of gravity height [M]	0.53				
Coefficient of drag (Cd)	0.25	0.25		0.25	
Vehicle frontal area [m ²]	2.25	2.25		2.25	
Tire size and specifications		P205/60R16		P205/60R16	
Tire rolling resistance	0.007	0.007		0.007	
Auxiliary power demand, Max. continuous [W]	2500				
Auxiliary power demand, Test [W]		700	700	700	700
Mechanical accessory losses [W]		1000	1000	1000	1000
Road condition, brake + acceleration	Dry asphalt	Dry asphalt		Dry asphalt	
Passenger capacity	4+				
Cargo volume [Liters]	370				
Curb weight [kg]	1300	1300		1300	
Payload [kg]	437.5		437.5		437.5
Driver weight [kg]	75	75		75	
Vehicle test weight [kg]	-	1375	1737.5	1375	1737.5
Max. grade capability, at 40 Km/h (25mph) with peak motor @ GVW [%/km/h/s] [%/mph/s]	22/40/30 22/25/30 Target		22% 44KW		10% E41KW M31KW G27KW
Max. grade capability, at 73 Km/h (45mph) with continuous motor @ GVW [%/km/h] [%/mph]	10/73 10/45 Target		10% 42KW		10% E42KW M21KW G20KW
Max. grade capability, at 90 Km/h (56mph) with continuous motor @ GVW [%/km/h] [%/mph]	10/90 10/56 Target		10% 54KW		10% E54KW M24KW G23KW

Max. grade capability, at 100/112 Km/h (62/70mph) with continuous motor @ GVW	[%/km/h] [%/mph]	10/112 10/70 Target		10% 71KW 7% 55KW		10% E66KW M32KW G27KW
0-100 km/h (0-62 mph) with peak motor @ acceleration test weight	[sec] [Peak KW]	10-12	11.4sec 75KW		9.4sec E62KW M47KW G26KW	
Top speed	[km/h/mph] [Cont.KW]	161/100	161/100 37KW		161/100 E20KW M 0KW G18KW	
Vehicle electric range (UDDS w/Regen)	[km/miles]	64/40	77/48		76/47	
Vehicle range (UDDS w/Regen)	[km]	500	77+500		76+540	
Ambient operating temperatures	[Deg C]	-40/+52				

Table 4.2: Vehicle design parameters for PHEV₄₀ series & parallel-split

The PSAT model considers dynamic component performance such as torque and power efficiency curves of components, as well as cooling requirements for critical components such as the high voltage battery packs. Identical vehicle size and weights were used to showcase the powertrain performance differences under comparable circumstances.

The simulation outputs are engine power ratings required to meet the various driving conditions. The Parallel-split powertrain requires lower engine power in most driving conditions while in charge-sustaining operating mode. This manifests itself in lower fuel consumption and CO₂ emissions values as well. In addition, the combination of mechanical and electrical power to drive the vehicle results in significant performance improvements for a given vehicle size when factors like acceleration and grade-ability are considered.

Another factor not considered in this study is that the Parallel-split powertrain will have a lower mass (up to 20%). This will improve fuel efficiency compared to the series configuration of similar size and performance.

After examining the electrical and fuel consumption charts, the FSV team concluded that:

1. Parallel-split configuration consumes less fuel in charge sustaining mode, and is especially more significant when driven under aggressive driving and travel conditions
2. Series configuration consumes slightly less electricity in charge depleting mode, but only enough to extend the range by 1-2 km
3. When the powertrain mass difference is considered (mass was assumed to be constant in this study), the efficiency of the parallel-split configuration would increase

4.5 Conclusion

While the fuel economy and CO₂ emissions play key roles in future vehicle technology concept selection, other factors have to be considered as well before a vehicle and powertrain design concept finds OEM approval.

Performance targets must be met under all typical driving conditions to satisfy expectations of a large percentile of potential vehicle operators. Likewise, market segment typical passenger and cargo accommodations must be satisfied as primary design goals. Platform or powertrain sharing within vehicle families is essential to reduce the substantial development and tooling costs for new vehicle variants. In order to meet commercial targets, especially emerging technologies like hybrid electric drive systems, vehicles have to be built with modular sub-systems.

Table 4.3 shows the matrix based on which the FSV team arrived at the final design concept for the PHEV₄₀.

FSV Medium Car PHEV Architecture Decision Matrix	Priority	Series	Parallel Split
Fuel Economy / CO ₂ Emission (70% CD, 30% CS)	5	+	
Driving Range and Performance	2	+	+
Powertrain Weight	4		+
Powertrain System Cost	4		+
Powertrain complexity	3	+	
Platform Sharing with ICE/Transmission Powertrains	1		+
Platform commonality among FSV Variants	4	+	
Score		14	11
		+ Advantageous	

Table 4.3: PHEV decision matrix

After reviewing the advantages and disadvantages of the two systems, a joint decision to select the series powertrain configuration for both plug-in vehicle derivatives (PHEV₂₀ and PHEV₄₀) for the FSV project was made by WorldAutoSteel, EDAG, Quantum Technologies and Shanghai Fuel Cell Vehicle Company.

4.5 Conclusion

Under the conclusion based on research data that a majority of daily driving would be within 64 km (40 miles) for the PHEV₄₀ and within 32 km (20 miles) for the PHEV₂₀, 70% of the driving would be in Charge Depleting (CD) mode for the FSV. The series design concept provides more advantages in this mode when compared to the parallel-split configuration. An opportunity to commonize the packaging on the BEV, FCEV and the PHEVs, keeping the front-end and drivetrain common and better fuel economy are major advantages that a series system has to offer for the FSV application. Vehicle weight distribution can be optimized for both traction and handling improvements. Placement of the internal combustion engine under the rear cargo compartment does present a number of challenges for thermal management and serviceability, which have been overcome by a significant number of OEMs.

Based on this design decision, a modular concept based analysis for all vehicles was conducted to determine key design parameters and specifications. The data was then transferred into the common design requirements for Phase 2 of the Future Steel Vehicle program.

5.0 Future Steel Vehicle - Technology Implementation

5.1 Vehicle Classification

Results of technology assessment and powertrain component feasibility studies conducted by Quantum and Shanghai Fuel Cell Vehicles (SFCV) were used for vehicle layout studies. Several layouts were analyzed for each vehicle and powertrain, for efficient usage of packaging space and vehicle mass distribution. For the two chosen vehicle sizes, it soon became apparent that a common platform theme can be developed by utilizing shared technologies in a modular fashion between all four vehicle powertrain variants.

1. FSV-1 - (BEV) Battery Electric Vehicle
2. FSV-1 - (PHEV₂₀) Plug-In Hybrid Electric with a 32km (20 mile) All Electric Range(AER)
3. FSV-2 - (PHEV₄₀) Plug-In Hybrid Electric with a 64km (40 mile) All Electric Range(AER)
4. FSV-2 - (FCEV) Fuel Cell hybrid Electric Vehicle

Table 5.1 shows the matrix of the Future Steel vehicle variants.

	PHEV (Plug-In Electric Vehicle)	FCEV (Fuel Cell Electric Vehicle)	EV (Electric Vehicle)
FSV1 (Small Vehicle)	X		X
FSV2 (Large Vehicle)	X	X	

Table 5.1: *Future Steel Vehicle*

Worldwide market analysis (refer Chapter - Market Analysis) show that over 70% of the cars sold in today's marketplace share two vehicle sizes; the small car (A & B Class) up to 4,000 mm long and the mid-class car (C & D class) up to 4,900 mm long. To encompass both segments of the worldwide market, the Future Steel Vehicle program includes two vehicle sizes, FSV-1 and FSV-2. The packaging specifications and vehicle performance for each of the vehicle were determined to be acceptable and appropriate for each class of vehicle and in line with OEM trends worldwide.

5.2 Size Comparison

5.2 Size Comparison

The size comparisons between the FSV-1 & FSV-2 is shown in Figure 5.1. The FSV-1 has similar overall size as the Mini Cooper, however, the FSV-1 realizes 65 mm more rear leg room than that of its competitive size vehicle and has an additional 80 liters of cargo space, as illustrated in Figure 5.2. In comparison, the FSV-2 is 500 mm shorter than a Honda Accord yet shares the same interior room.

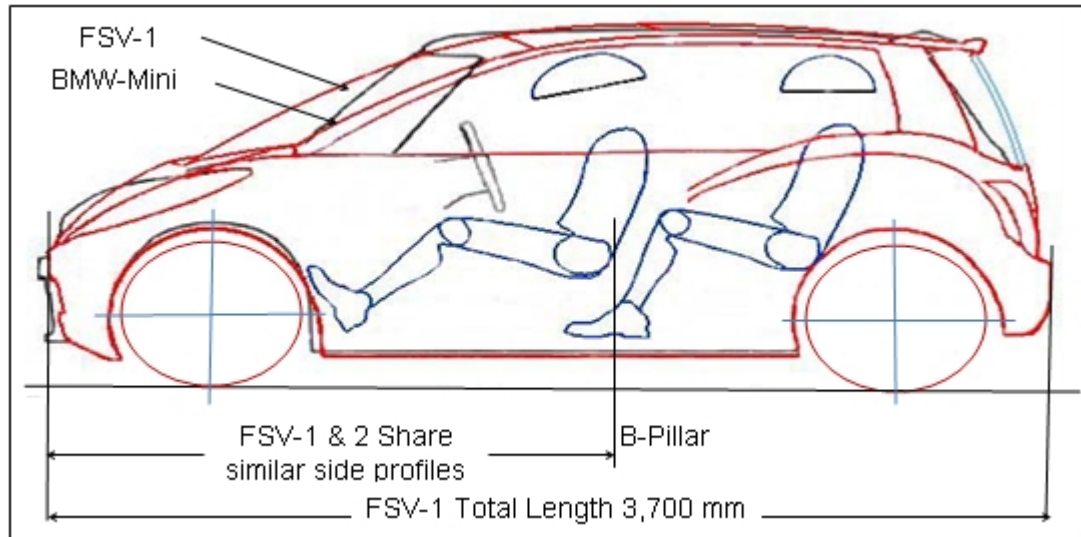


Figure 5.1: Future Steel Vehicle size comparisons

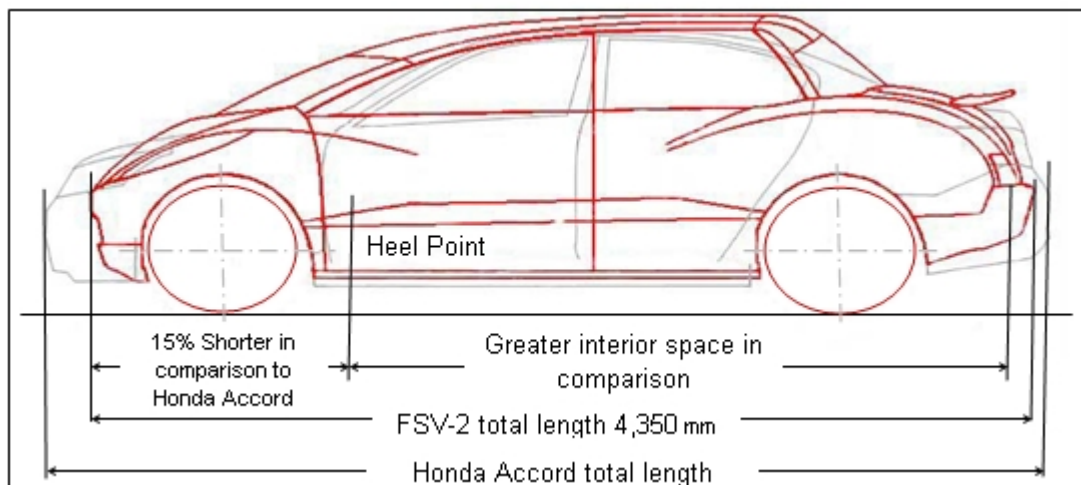


Figure 5.2: Future Steel Vehicle size comparison with competitive vehicles

5.3 Exterior Dimensions

The exterior dimensions of the vehicles are referenced in Figure 5.3 and values are tabulated in Table 5.2.

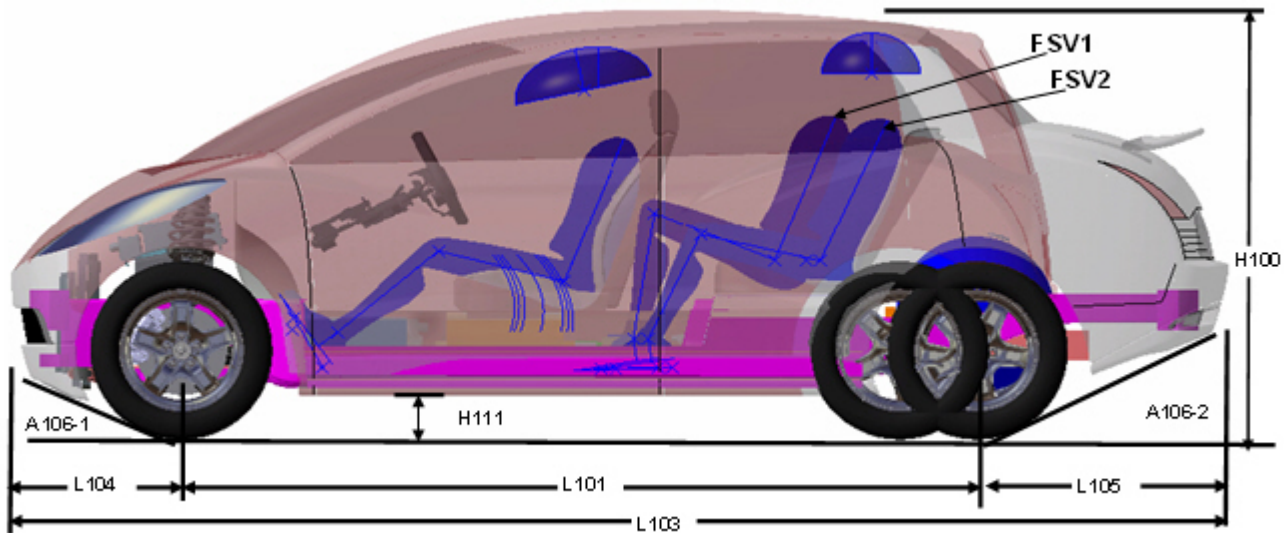


Figure 5.3: *FSV exterior dimensions*

		FSV1	FSV2
L101	Wheel Base	2524	2800
L103	Total Length	3700	4350
L104	Front Overhang	600	600
L105	Rear Overhang	576	950
H100	Total Height	1540	1540
W103	Total Width	1680	1780
W102	Front Track	1470	1570
W101	Rear Track	1470	1570
H111		150	150
A106-1		23	23
A106-2		25	26

Table 5.2: *FSV vehicle dimensions*

5.4 Interior Dimensions

The interior dimension of the vehicle as referenced in Figure 5.4 and values are tabulated in Table 5.3.

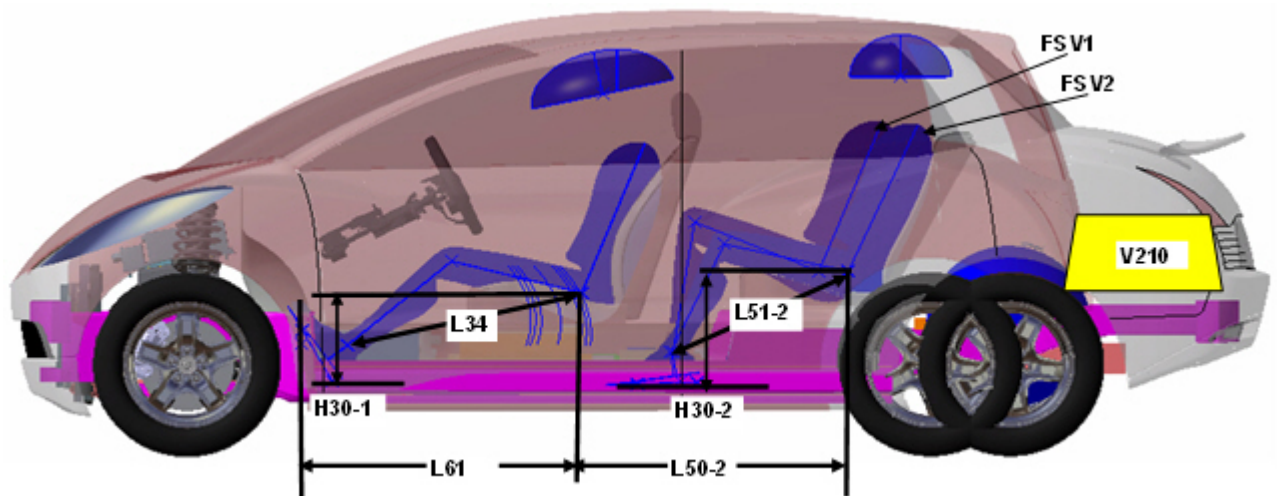


Figure 5.4: *FSV interior dimensions*

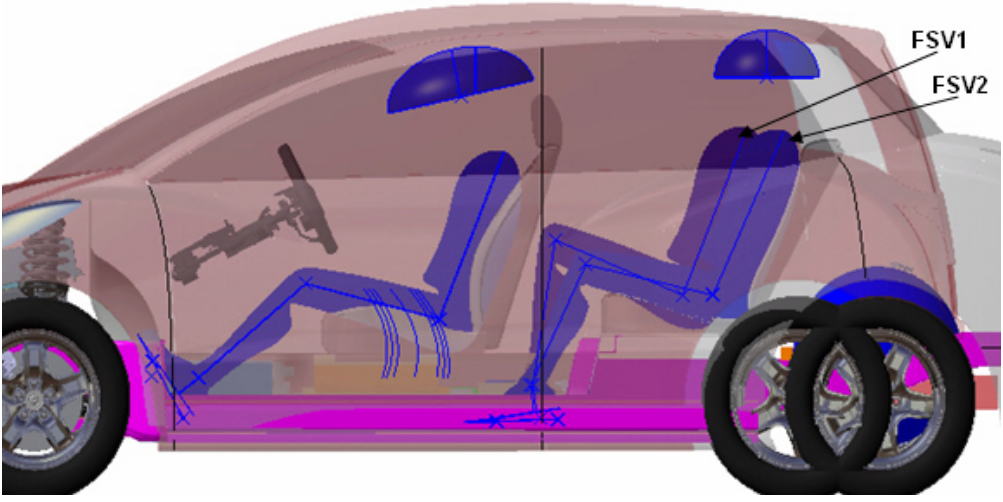
	L34	L61	H30-1	L50-2	L51-2	H30-2	V210
FSV1	1070	945	325	780	825	375	250 L
FSV2	1070	945	325	780	925	375	350 L

Table 5.3: *FSV vehicle dimensions*

5.5 Occupant and Luggage Carrying Capacity

The determination of vehicle interior dimensions and luggage space requirements were based on each vehicle size and its intended usage. FSV-1 is a small vehicle mainly intended for city and lower daily driving, whereas FSV-2 is a mid-size vehicle for long range driving with larger luggage carrying capacity. Table 5.4 shows the capacity of the FSV-1 and FSV-2 in terms of luggage (cargo) volume and comparison with average numbers from cargo volume on different classes of vehicles (A,B,C,D).

FSV1 Occupants:		FSV2 Occupants:	
Front Row Seating: 2		Front Row Seating: 2	
Rear Row Seating: 2+		Rear Row Seating: 3	



Class	Front Leg Room [mm]	Rear Leg Room [mm]	Luggage [Liters]
FSV-1	1070	825	250
FSV-2	1070	925	370
A	1055	760	170
B	1065	850	340
C	1070	877	370
D	1075	961	450

Table 5.4: *FSV-1 and FSV-2 vehicle capacity*

5.6 FSV Front-End

Drivetrains consisting of a traction motor, reduction gearing, and differential as a combined unit yield a more compact space-efficient design when compared with regular internal combustion engine (ICE) as shown in Figure 5.5. Electrically driven front wheels, applicable to all the powertrains, simplify the front-end layout and leads to significant reduction in vehicle front-end length, as shown below in Figure 5.6

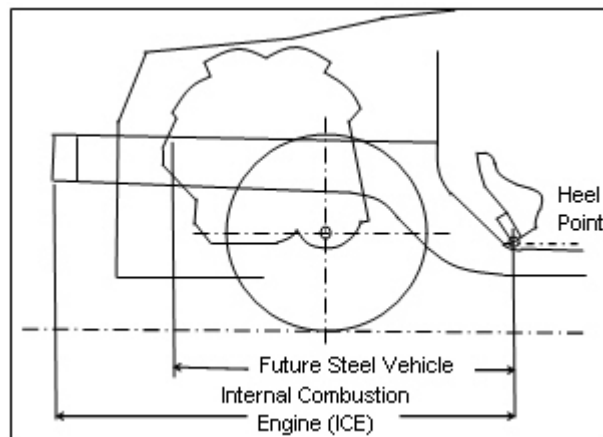


Figure 5.5: *Conventional ICE front-end*

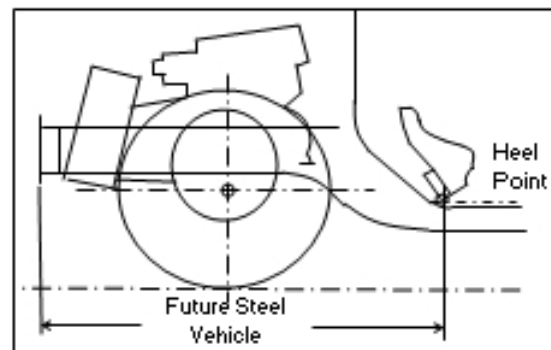


Figure 5.6: *FSV - electric drive front-end*

5.6.1 Front-End Comparison

Figure 5.7 shows the comparison of the FSV front-end with that of a typical mid-size sedan of its class, the ULSAB AVC and the super-mini class of vehicles.

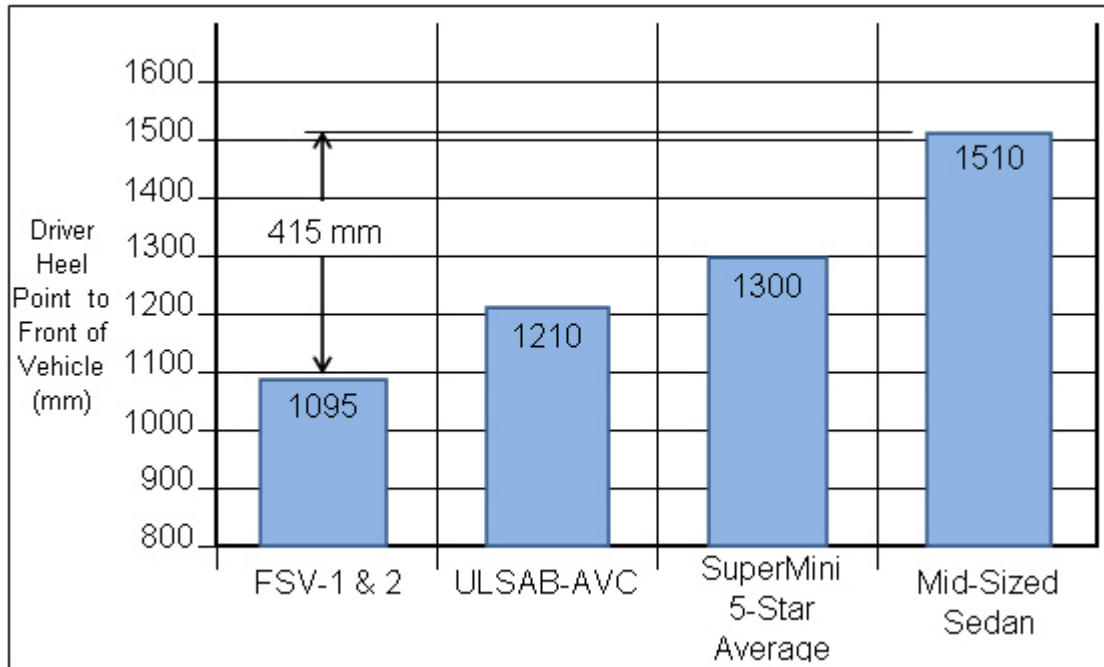


Figure 5.7: FSV- front-end comparison

The FSV's front-end is 415 mm shorter than that of a typical mid-size sedan and 205 mm shorter than that of the 5-star rated Super-Mini Class vehicles. The FSV-1 has similar overall size as the Mini Cooper. However, the FSV-1 realizes 65 mm more legroom and has an additional 80 liters of cargo space. In comparison, the FSV-2 is 500 mm shorter than a Honda Accord yet shares the same interior room as shown in Figure 5.8.

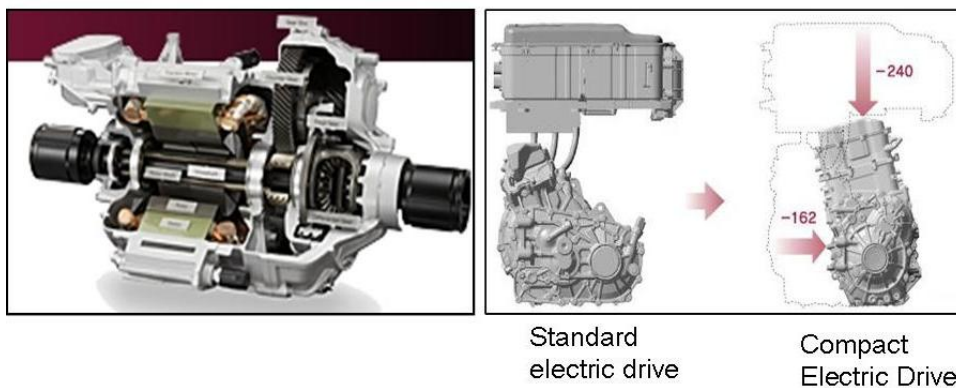
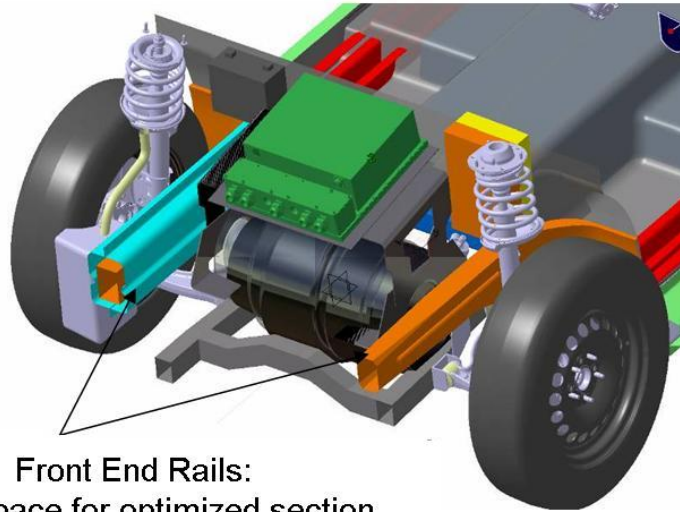


Figure 5.8: Honda Clarity electric drive

5.7 FSV Front Rails

The size of conventional internal combustion engine and Hybrid Electric Vehicle (HEV) powertrains generally restrict the size and shape of body-structural members in the front-end, leading to inefficient use of materials. The FSV's front-end frees up space for an optimized structure. The front-end rails, which play a major roll in controlling and absorbing energy in front crashes, can be optimized for section shape and hence minimizing mass as shown in Figure 5.9.



Front End Rails:
More space for optimized section

Figure 5.9: FSV front rail

5.8 FSV Powertrain

5.8.1 Options and Performance

The assessment of announcements from automobile manufacturers shows progress in various technologies that include:

1. Conventional Internal Combustion Engine (ICE) based on smaller and more efficient gasoline/diesel vehicles
2. Higher efficiency Hybrid Electric Vehicles(HEV) predominantly using fossil-based petroleum fuels
3. Plug-in hybrids (PHEV) with limited distance driven in electric mode with battery energy obtained from the electric grid. This option offers significant reduction in fossil-based petroleum usage, especially when the daily distances driven are close to the vehicle's electric range
4. Battery Electric Vehicle (BEV) with driving range of approximately 200 km
5. Fuel Cell Electric Vehicles (FCEV) using hydrogen gas as fuel source

Assessment of powertrain component mass, cost and sizes for the years 2015–2020 were taken into account when determining the suitability of a powertrain for each vehicle size. The powertrain chosen for the smaller FSV-1 included the Plug-in Hybrid with 32 km(20 miles) electric range (PHEV₂₀) and Battery Electric Vehicle (BEV) with a total driving range of 250 km. The Fuel Cell Electric Vehicle (FCEV) powertrain for the small car was not implemented due to excessive cost and complexity involved with hydrogen storage and fuel stack installation. For the larger vehicle FSV-2 the BEV option was not included due to the larger and more expensive battery requirements for larger vehicles. The chosen performance parameters and powertrain type for the FSV are as shown in Table 5.5.

	Plug-in Hybrid (PHEV)	Fuel Cell (FCEV)	Battery Electric (BEV)
FSV 1	PHEV 20 Electric Range - 32km (20mi) Total Range - 500km Max Speed -150km/h 0-100km/h 11-13s		BEV Total Range - 250km Max Speed -150km/h 0-100km/h 11-13s
FSV 2	PHEV 40 Electric Range - 64km (40mi) Total Range - 500km Max Speed -161km/h 0-100km/h 10-12s	FCEV Total Range - 500km Max Speed -161km/h 0-100km/h 10-12s	

Table 5.5: *Powertrain options & performance*

5.8.2 Mass and Cost Impacts

Future powertrains will be heavier and more expensive than conventional powertrain systems. It can be noted that the major part of the cost and mass impact is from the Li-ion battery pack (for

5.8 FSV Powertrain

BEV and PHEV) and the fuel cell system for the FCEV, followed by the large capacity generators and traction motors. The mass and cost impact of the varying powertrain configurations are displayed in Figure 5.10 and Figure 5.11 respectively.

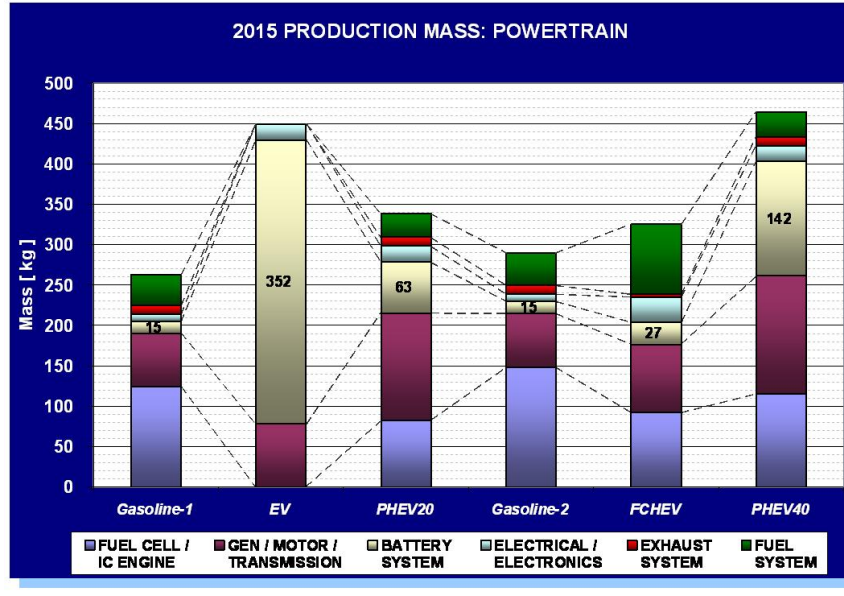


Figure 5.10: Powertrain mass

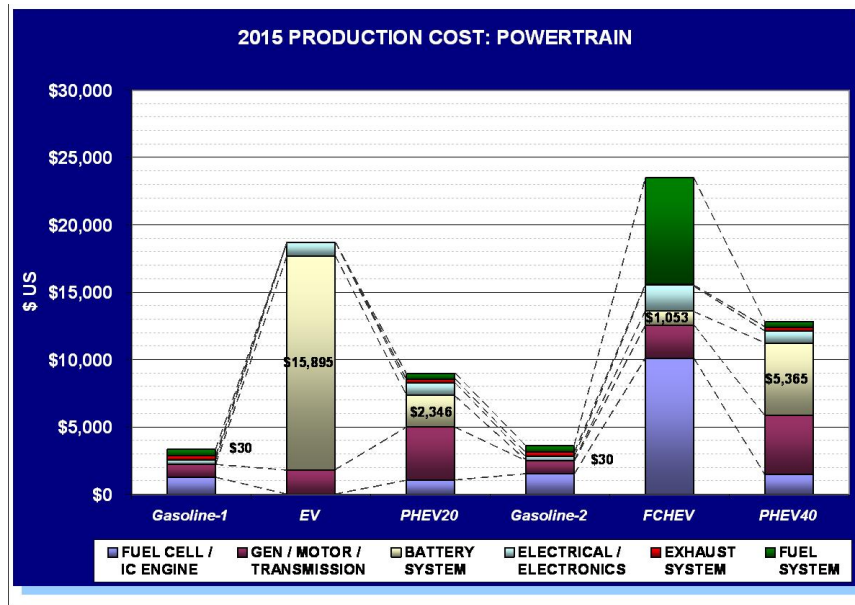


Figure 5.11: Powertrain sub-system cost

5.9 Battery Electric Vehicle (BEV)

The all electric variant of the FSV-1 abbreviated as BEV is shown in Figure 5.12. This is a four door hatchback designed mostly for urban usage. It is the smaller of the two FSV variants, measures 3700 mm in length and is a pure electric vehicle.

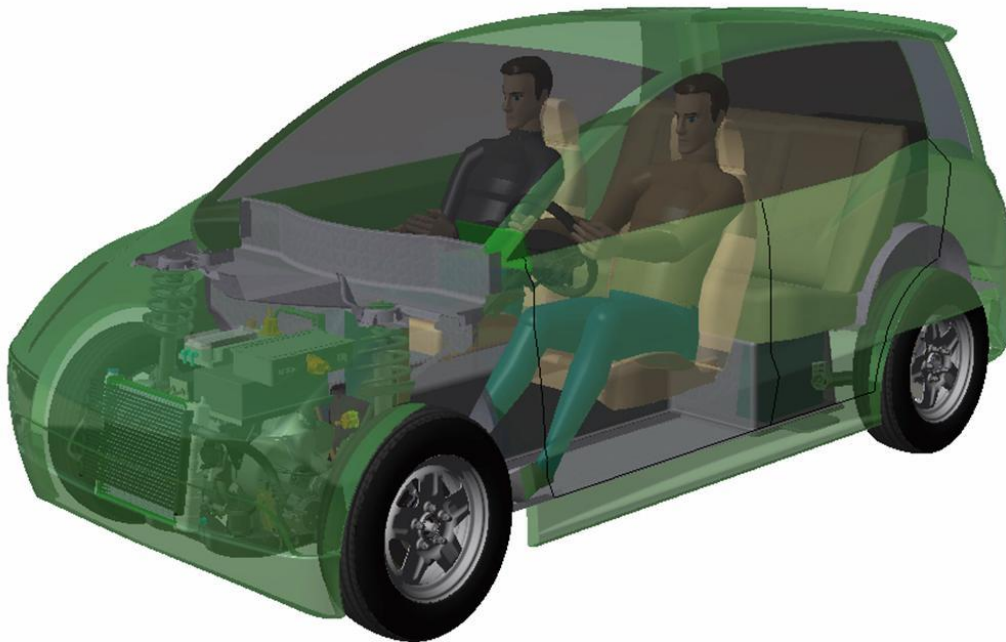


Figure 5.12: FSV-1 Battery Electric Vehicle

This vehicle is powered by a high performance 35 kWh lithium-ion battery pack. The mass of the BEV is estimated to be 1232 kg and rides on light weight steel wheels and 175/65 R15 tires with a rolling resistance of 0.007. The BEV interior is large enough to seat 5 passengers comfortably.

5.9.1 Mass Estimates

The mass estimates of the BEV in comparison with a similar sized 2010 and 2020 ICE vehicle and Hybrid Electric Vehicle (HEV) are as shown in Table 5.6. Future technologies, body-structure mass reduction by use of Advanced High Strength Steels (AHSS) and smaller vehicle foot print of FSV, all lead to significant mass reduction of the BEV. The body-structure mass target of 190 kg for BEV is 30% lower than the body-structure mass of the 2010 ICE vehicle, even though the powertrain masses for FSV are higher. Similar comparisons can be derived between the BEV and the 2010 HEV, 2020 ICE vehicle and 2020 HEV.













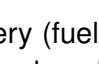
	ICE 1 2010	ICE 1 2020	HEV 1 2010	HEV 1 2020	FSV 1 BEV
 Body Non-Structure	245	190	215	190	190
 Body Structure	272	241	272	237	190
 Front Suspension	59	40	62	45	45
 Rear Suspension	53	39	61	37	35
 Steering	17	17	17	17	16
 Brakes	38	31	40	33	32
 Drivetrain	222	197	297	252	78
 Fuel, Battery, Exhaust	48	55	104	105	347
 Wheels and Tires	78	59	68	55	44
 Air Conditioning	32	42	27	33	36
 Electrical	55	63	55	66	58
 Bumpers	26	21	23	24	23
 Closures	54	48	49	44	46
TOTAL	1199	1044	1290	1138	1,137

Table 5.6: FSV-1 BEV estimated mass (kg)

The battery (fuel storage) and the powertrain system (traction motor and accessories) constitute a significant portion of the added mass and cost for the BEV. Table 5.7 shows the forecasted (2015–2020) mass and cost premium for this vehicle.

Powertrain components	Mass [kg]	Cost [US \$]
Li-ion Battery and controller	346.5	15,895
Traction Motor System (67kW)	78	1,742

Table 5.7: BEV - Powertrain and fuel system mass & cost

5.9.2 Technical Specification & Performance

The performance targets data shown in the previous sections was the basic input used by Quantum to perform the feasibility study. Powertrain System Analysis Toolkit (PSAT) software was used to model the BEV variant with outputs such as vehicle performance and fuel economy. PSAT, developed by Argonne National Labs, is a simulation tool based on Matlab/Simulink software and specifically designed for transient performance evaluation of vehicle powertrains. Each configuration was repeatedly designed to select the correct size of the powertrain components and then compared with each other.

It is expected that the actual total vehicle design would be a recursive process in which:

- Inputs such as vehicle total mass, auxiliary power, etc. would be assumed
- Characteristics of powertrain components (mass, volume, efficiency, etc.) are incorporated into the vehicle design
- Vehicle design is iterated to accommodate the necessary powertrain and a new mass is determined
- Updated vehicle total mass, auxiliary power, etc. are returned back to the powertrain designers for verification of vehicle performance

Based on vehicle weight, size, and performance targets, the power requirements for typical OEM operation conditions were calculated. If the mass deviations are big enough to affect performance, the whole cycle is repeated until the final vehicle configuration is determined.

5.9.2.1 Powertrain Performance

For the BEV and PHEV₂₀, it can be observed that almost identical power requirements exist for shorter term (peak) driving situations as well as for the longer term (continuous) driving conditions. Traction motor sizing can be solely based on continuous power performance, which typically will allow offering better than required peak performance and/or keep powertrain components at lower, more cost efficient, ratings. The simulation results also show that minor compromises in grade climbing speed will allow keeping overall component power rating lower, thus benefiting powertrain and vehicle weight, cost and efficiency. Using the basic vehicle performance specifications/targets, a series of PSAT simulations were performed and the results are tabulated in Table 5.8 and Table 5.9.

Vehicle Design Parameters (comparable to OEM standards)		BEV	
		Curb +Driver	GVW
Front wheel drive		yes	yes
Wheel base	[mm]	2461	2461
Weight distribution	[%/%]	50/50	
Center of gravity height	[mm]	530	
Coefficient of drag (Cd)		0.25	0.25
Vehicle frontal area	[m ²]	2.1	2.1

Continued on next page

5.9 Battery Electric Vehicle (BEV)

Vehicle Design Parameters (comparable to OEM standards)	BEV		
		Curb +Driver	GVW
Tire size and specifications		P175/65R15	
Tire rolling resistance	0.007	0.007	
Auxiliary power demand, Max. continuous [W]	2200		
Auxiliary power demand, Test [W]		700	
Mechanical accessory losses [W]		0	
Road condition, Brake + Acceleration	Dry Asphalt	Dry Asphalt	
Passenger capacity	4+		
Cargo volume [Liters]	250		
Curb weight [kg]	1100	1100	
Payload [kg]	360		360
Driver weight [kg]	75	75	
Vehicle test weight [kg]	-	1175	1460
Max. grade capability, at 40 Km/h (25mph) with peak motor @ GVW [%/km/h/s] [%/mph/s]	22/30/30 22/18.6/30 Target		10% 28kW
Max. grade capability, at 73 Km/h (45mph) with continuous motor @ GVW [%/km/h] [%/mph]	10/73 10/45 Target		10% 36kW
Max. grade capability, at 90 Km/h (56mph) with continuous motor @ GVW [%/km/h] [%/mph]	10/90 10/56 Target		10% 46kW
Max. grade capability, at 100/112 Km/h (62/70mph) with continuous motor @ GVW [%/km/h] [%/mph]	10/100 10/62 Target		10% 52kW 9% 49kW
0-100 km/h (0-62 mph) with peak motor @ acceleration test weight [sec] [Peak kW]	11-13	12.4 s 49kW	
Top speed [km/h/mph] [Cont kW]	150/93	150/93 31kW	
Vehicle Electric range (UDDS w/Regen) [km/miles]	250/155	296/183	
Vehicle range (UDDS w/Regen) [km]	n/a		
Ambient operating temperatures [Deg C]	-40/+52		

Table 5.8: Vehicle design parameters for BEV

Powertrain Design Parameters (comparable to OEM standards)		BEV	
		Curb +Driver	GVW
Regenerative braking	yes	yes	
Peak engine power (mechanical)	[kW]	n/a	
Fuel cell power (electrical)	[kW]	n/a	
Battery capacity	[kWh]		35.1
Traction motor mechanical capacity (Continuous/ Peak/ Max RPM)	[kW]		49 / 49 / 8700 rpm
Peak motor power (mechanical)	[kW]		49
Peak generator power (electrical)	[kW]		n/a
Final drive/differential	[ratio]		6.44
Powertrain weight	[kg]		441
Battery weight	[kg]		347
Fuel tank capacity	[kg]		n/a
Type of PHBEV	Series		n/a

Table 5.9: BEV - Powertrain design parameters

5.9 Battery Electric Vehicle (BEV)

5.9.2.2 Vehicle Performance - Simulation Results

Simulation results, at the vehicle level, based on PSAT analysis, were tabulated and compared with the targets for the BEV. The BEV meets all requirements except for the 10% hill climb ability requirements at 100 $\frac{\text{km}}{\text{h}}$ (GVW). However, the BEV meets this target at a lower speed. The BEV overall vehicle performance results and capabilities are shown in Table 5.10.

IC Engine, Peak (mechanical)	N/A
Generator, Peak (electrical)	N/A
Traction Motor, Peak (mechanical)	49 kW

	Units	Specs	Traction Power				Capability
			Peak 49 kW		Continuous 49 kW		
			Curb + Driver	GVW	Curb + Driver	GVW	
Performance							
Acceleration							
0 - 100 km/h, Curb + Driver	sec.	11-13	12.4 @ 49 kW	—	—	—	
Peak Grade							
30 km/h - 30 sec., GVW	%	22	—	22 @ 28 kW	—	—	
Continuous Grade							
73 km/h - Continuous, GVW	%	10	—	—	—	10 @ 36 kW	
90 km/h - Continuous, GVW	%	10	—	—	—	10 @ 46 kW	
100 km/h - Continuous, GVW	%	10	—	—	—	9 @ 49 kW	
Top Speed							
Continuous, GVW	km/h	150	—	—	—	150 @ 31 kW	
Range							
Curb + Driver, UDDS	km	250	—	—	296	—	

Limited Performance =

Unable to Perform =

Table 5.10: BEV - Vehicle performance results

5.9.3 Layout & Design

The FSV-1 BEV is designed to have a range of 250 km. To achieve this range, the energy storage capacity of the battery pack has to be 35 kWh (347 kg mass, 264 liter volume). Packaging this size of a battery into small vehicle is the major challenge. The battery extends forward from underneath the rear seat occupant floor, into the tunnel, and below the front floor. The under-floor structure, shown in Figure 5.13 not only has to support the significant weight of the battery during road loading, but also protect it when subjected to frontal, side and rear crash impact loads. At present it is envisioned that a full size under-floor longitudinal member, coupled with several cross members and additional tunnel reinforcements will be required. Figure 5.14 shows the powertrain packaging of the BEV with the battery pack and the traction motor.

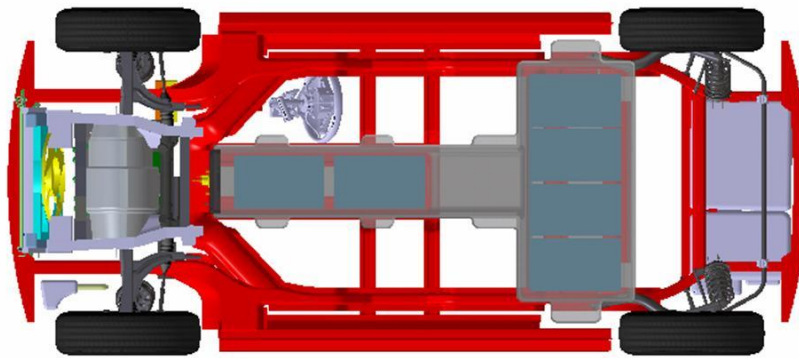


Figure 5.13: *BEV underbody*

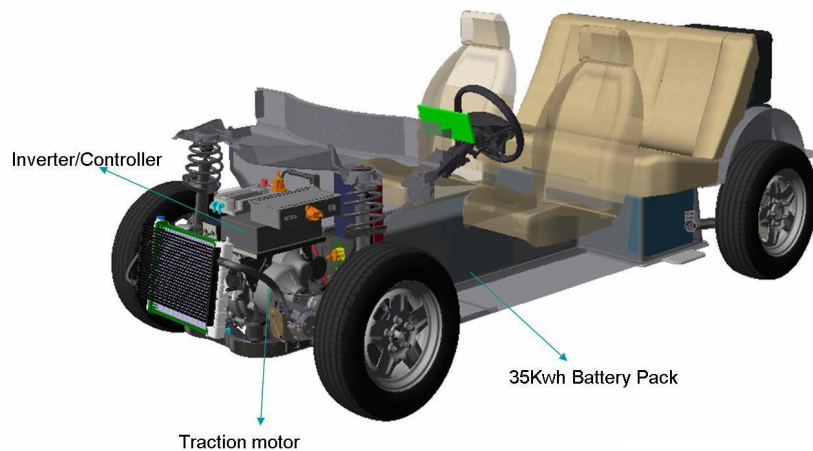


Figure 5.14: *BEV packaging*

5.9 Battery Electric Vehicle (BEV)

5.9.4 Benchmark -2009 Mitsubishi i-MiEV

Mitsubishi i-MiEV - an electric vehicle with range of 160 km (tested under Japan 10-15 drive cycle), has been under development and is intended for production release in Japan in 2009.

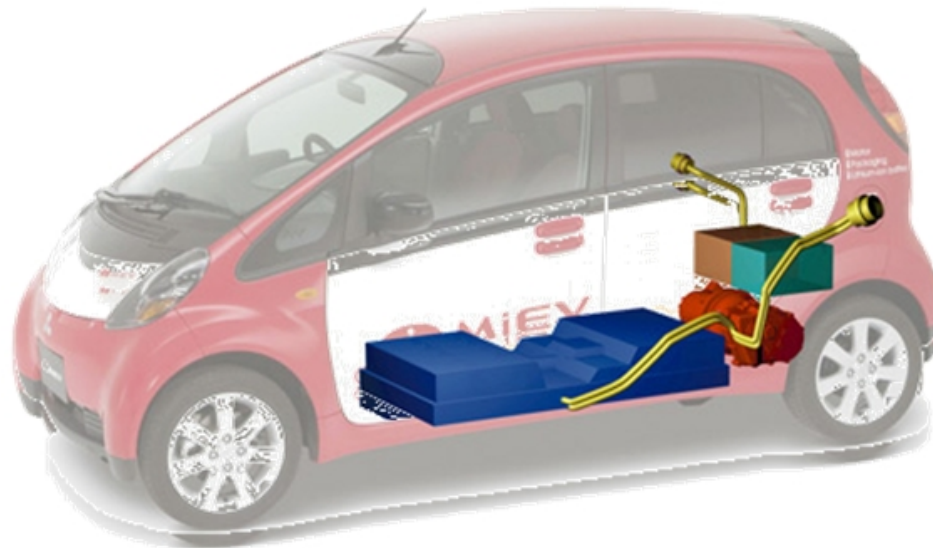


Figure 5.15: 2009 Mitsubishi i-Miev

The vehicle has been displayed at various auto-shows worldwide and has been driven by members of the press and has generally received very good feed back.

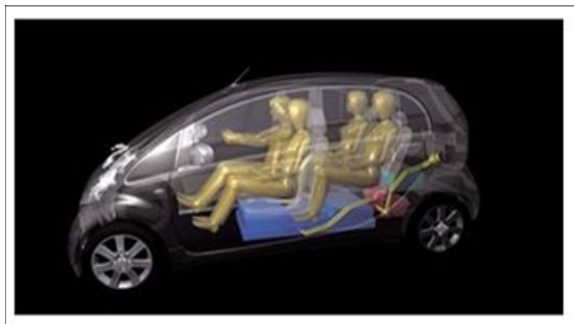


Figure 5.16: 2009 Mitsubishi i-MiEV

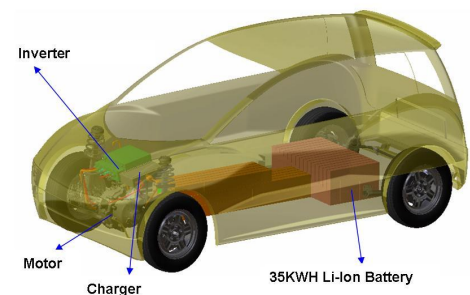


Figure 5.17: Future Steel Vehicle

The specifications of the i-MiEV and the FSV-1 BEV are compared in Table 5.11.

		MIEV	FSV1	FSV1	
				MIEV	MIEV2
Length	[mm]	3395	3700	3700	3395
Width	[mm]	1475	1680	1680	1475
Height	[mm]	1600	1540	1540	1600
Curb Weight	[kg]	1080	1232	928	750
Seat Capacity		4	4+	4+	4
Drive System		rear wheel drive	front wheel drive	front wheel drive	rear wheel drive
Assumptions					
Battery					
Type		Li-ion	Li-ion	Li-ion	Li-ion
Voltage	[V]	330	334	334	334
Total Energy	[kWh]	16.4	35	16.4	16.4
Motor					
Type		permanent magnet	permanent magnet	permanent magnet	permanent magnet
Cont. Power	[kW]	31	49	31	31
Max. Power	[kW]	47	67	47	47
Max. Torque	[Nm]	180	220	180	180
Drag Coefficient		0.25	0.25	0.25	0.25
Rolling Resistance		0.007	0.007	0.007	0.007
Torque Coupling Ratio		1.2	1.2	1.2	1.2
Differential Ratio		3.1	3.1	3.1	3.1
Frontal Area	[m ²]	1.9	2.1	2.1	1.9
Tire Size		195/65R14	175/65R15	175/65R15	195/65R14
Results					
Range for 70% SOC (Japan 10-15)	[km]	125	247	133	150
Range for 85% SOC (Japan 10-15)	[km]	157	308	166.7	182
Electr. Consumption	[Wh/km]	88.7	96.6	83.6	74
Acceleration (0- 60km/h)	[s]	10.6	8.7	9.5	7.7
Acceleration (0-100km/h)	[s]	18	14.6	16.1	13
Top Speed	[$\frac{km}{h}$]	180	198	180	180

Table 5.11: Mitsubishi i-MiEV data

Columns 2 & 3 in this table show the comparison of the FSV-1 BEV with that of the 2009 i-MiEV. If the FSV-1 BEV just used a battery pack that is of the same capacity as that on the i-MiEV (column 4), the total vehicle mass of the FSV-1 BEV would be 928 kg (14% lower than i-MiEV). On the other hand, if the FSV-1 BEV were to be designed to the exact specifications (column 5) as that of the i-MiEV, the weight of the FSV-1 BEV would be 750 kg (30% lower than i-MiEV).

5.9.5 Bill of Materials

The BEV variant of the FSV has particular component needs for its powertrain. As such, a detailed Bill of Materials (BOM) was generated for the BEV. This BOM includes only the major components required to fulfill the powertrain needs. The powertrain BOM for the BEV is shown in Table 5.12.

Item #	BOM Level	ASSEMBLY / COMPONENT	VENDOR	QTY ASM	U/M	Size LxWxH [mm]	Item Mass [kg]	Extended Weight [kg]	USD - 2015 Price - (100K/year)	Comments
1		POWERTRAIN-EV	Q	1	EA			449.2	\$18,575	
2		TRACTION DRIVE INSTALLATION	Q	1	EA			78.0	\$1,796	
3		TRACTION MOTOR- 67 kW Peak; 49 KW, continuous		1	EA	216xØ288	40.6	40.6	\$1,256	Base Motor 8 L/min WEG 50/50, 55C max inlet
3		T-MOTOR INVERTER/CONTROLLER - 67 kW Peak; 49 KW; continuous		1	EA	282x282x130	14.2	14.2	—	8 L/min WEG 50/50, 55C max inlet
3		TRANSAXLE / DIFFERENTIAL		1	EA	250xØ250	15.0	15.0	\$300	
3		HALF-SHAFTS		2	EA	230xØ94	4.1	8.2	\$240	Based on GKN Type 102 / Joint 10
3		TRACTION BATTERY SYSTEM	Q	1	EA			351.5	\$15,895	
3		BATTERY PACK(LI ION) & CONTROLLER		1	EA	Varies: 0.28 m3	346.5	346.5	\$15,795	334 Volt Nominal, 378 Volt Max., 297 Volt Min.
4		CONTROLLER / WIRING / THERMAL MGMT		1	EA	—	31.5	—	—	
4		BATTERY PACK		1	EA	—	315.0	—	—	35 kW-h
5		BATTERY MODULE		450	EA	100x60x95	0.7	—	—	
6		BATTERY CELLS		6	EA	—	0.1	—	—	130 W-h / kg; 13 W-h / cell
3		PLUG-IN CHARGING SYSTEM		1	EA	406x305x100	5.0	5.0	\$100	Input: 110/220 VAC; 45 - 75 Hz; 16 A
4		ELECTRICAL AND ELECTRONICS	Q	1	EA			19.7	\$884	

Continued on next page

Item #	BOM Level	ASSEMBLY / COMPONENT	VENDOR	QTY ASM	U/M	Size LxWxH [mm]	Item Mass [kg]	Extended Weight [kg]	USD - 2015 Price - (100K/year)	Comments
	3	DC-DC CONVERTER	Q	1	EA	253x257x79	4.9	4.9	\$429	DC input voltage: 250 to 425, 10A Max DC output voltages: 13.8 @ 2.2 kW (157 A) @ 90% Eff. 10L/min WEG 50/50 75C Max Inlet
	3	HARNESS LOW VOLTAGE	Q	1	EA	Varies	0.2	0.2	\$80	
	4	HIGH VOLTAGE CABLE	Q	30	M	—	0.01	—	—	18 AWG Copper 4.92 lb/1000 ft
	3	HARNESS HIGH VOLTAGE	Q	1	EA	Varies	5.7	5.7	\$150	
	4	HIGH VOLTAGE CABLE	Q	6	M	—	1.0	—	—	4/0 AWG Copper 641 lb/1000 ft
	3	FUSE BLOCK	E	1	EA	150x150x100	0.2	0.2	\$25	
	3	MISC. ELECTRICAL	Q	1	EA		8.0	8.0		
5	2	COOLING SYSTEM	E	1	EA			0.0	\$0	
	3	FAN - ELECTRIC COOLING		1	EA			0.0		
	3	FAN CONTROLLER		1	EA			0.0		
	3	ELECTRIC COOLANT PUMP		1	EA			0.0		42 L/min (10 L/min DC/DC Converter, 32 L/min Motor-Controller)
	3	RADIATOR-ELECTRONICS		1	EA			0.0		10.2 kW Heat Rejection (0.2 kW DC/DC, 5 kW Motor Inverter, 5 kW Motor), 42 L/min, 55C max Outlet @ 58C max Inlet, 40C Ambient
6	2	DRIVER - DRIVETRAIN INTERFACE	E	1	EA			1.1	\$0	
	3	THROTTLE PEDAL/SENSOR ASSEMBLY		1	EA	193x49x275	0.3	0.3	\$0	
	3	BRAKE PEDAL/ SWITCH ASSEMBLY		1	EA	193x49x275	0.3	0.3	\$0	

Continued on next page

5.9 Battery Electric Vehicle (BEV)

Item #	BOM Level	ASSEMBLY / COMPONENT	VENDOR	QTY ASM	U/M	Size LxWxH [mm]	Item Mass [kg]	Extended Weight [kg]	USD - 2015 Price - (100K/year)	Comments
	3	GEAR SELECTION ASSEMBLY		1	EA	75x50x50	0.3	0.3	\$0	
	3	DRIVER INFORMATION DISPLAY		1	EA	10x305x125	0.2	0.2	\$0	OLED Technology

VENDOR CODE: Q = QUANTUM; U = UQM; E = EDAG; S = SFCV

Table 5.12: Bill of materials : FSV-1 - EV

5.10 Plug-In Hybrid with a 32 km (20 mile) All Electric Range(PHEV₂₀)

The PHEV₂₀ variant of the FSV-1 is also a four door hatchback capable of a driving range of 32 km(20 miles) and 500 km (310 miles) using a combination of the 1.0 L 3-cylinder internal combustion engine and a smaller 5 kWh lithium-ion battery pack.

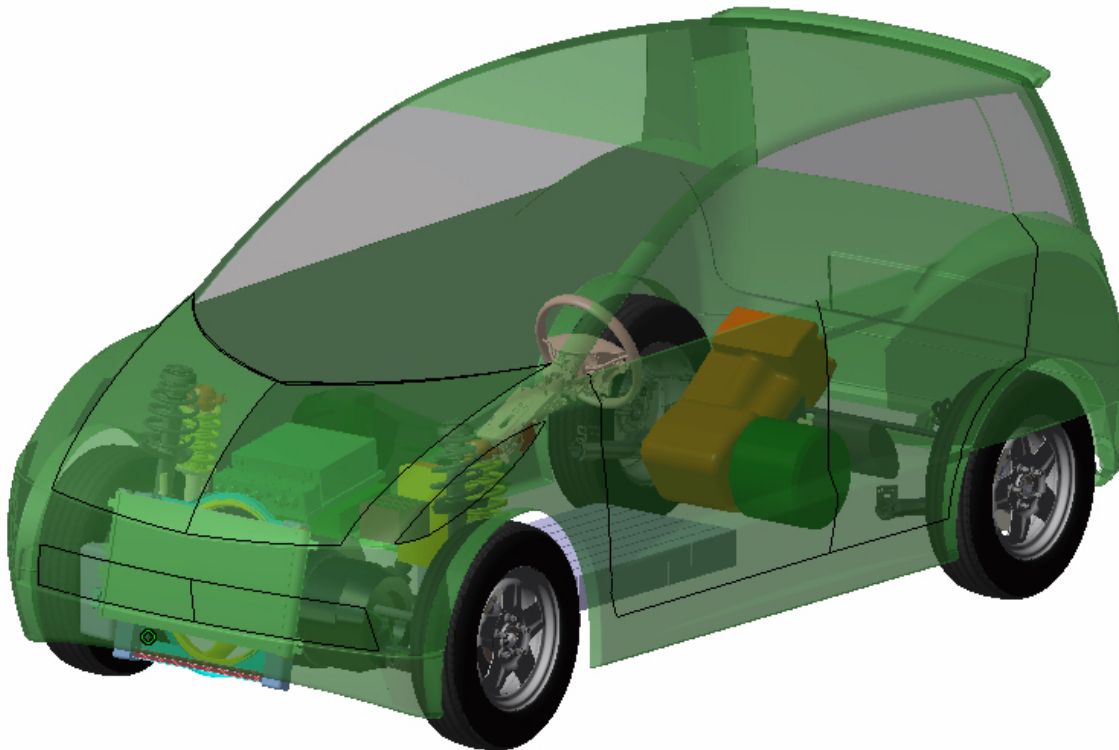


Figure 5.18: FSV-1 PHEV₂₀

The PHEV₂₀ is a series hybrid vehicle, which means that the rear mounted 1.0 L 3-cylinder internal combustion engine is not connected to the driving wheels but acts only as a generator for providing power to the drive motor and charging the battery when needed. The compact packaging of an advanced traction motor in the front allows the vehicle to sport a significantly shorter front-end (same as that of the BEV). The PHEV₂₀ rides on the same wheels and tires as that of the BEV . This vehicle will also be designed to meet the US and EU fuel economy requirements of the future, similar to the other FSV variants.

5.10.1 Mass Estimates

The mass estimates of the PHEV₂₀ in comparison with a similar sized 2010 and 2020 ICE vehicle and Hybrid Electric Vehicle (HEV) are as shown in Table 5.13. Future technologies, body-structure mass reduction by use of Advanced High Strength Steels (AHSS), and smaller vehicle foot print of FSV, all lead to significant mass reduction on the PHEV₂₀. The body-structure mass target of 173 kg for PHEV₂₀ is 36% lower than the body-structure mass of the 2010 ICE vehicle, even though the powertrain masses for FSV are higher. Similar comparisons can be derived between the PHEV₂₀ and the 2010 HEV, 2020 ICE vehicle and 2020 HEV.













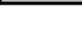
	ICE 1 2010	ICE 1 2020	HEV 1 2010	HEV 1 2020	FSV 1 PHEV ₂₀
 Body Non-Structure	245	190	215	190	190
 Body Structure	272	241	272	237	173
 Front Suspension	59	40	62	45	40
 Rear Suspension	53	39	61	37	26
 Steering	17	17	17	17	16
 Brakes	38	31	40	33	29
 Drivetrain	222	197	297	252	215
 Fuel, Battery, Exhaust	48	55	104	105	98
 Wheels and Tires	78	59	68	55	38
 Air Conditioning	32	42	27	33	36
 Electrical	55	63	55	66	63
 Bumpers	26	21	23	24	20
 Closures	54	48	49	44	46
TOTAL	1199	1044	1290	1138	990

Table 5.13: FSV-1 PHEV₂₀ estimated mass (kg)

The powertrain and battery system (fuel storage) mass and cost numbers, as forecasted for the years 2015–2020, are as shown in Table 5.14.

Powertrain components	Mass [kg]	Cost [US \$]
Li-ion Battery and controller	58.2	2,346
Generator/Traction Drive (75kW)	132.8	3,975
IC Engine(1.0L)	82.5	1,050
Fuel system	29.3	415
Exhaust System	10.8	300

Table 5.14: FSV-1 PHEV₂₀ - Powertrain and fuel system mass & cost

5.10.2 Technical Specification & Performance

5.10.2.1 Powertrain

The targets data shown in the previous section was the basic input used by Quantum to perform the feasibility study. Powertrain System Analysis Toolkit (PSAT) software was used to model the PHEV₂₀ variant with outputs such as vehicle performance and fuel economy.

Based on the continuous power demand at $112 \frac{\text{km}}{\text{h}}$ of the PHEV₂₀, the traction motor would have to be rated slightly higher. This motor would typically be sufficiently sized to handle the peak acceleration power demand without overheating. Using the basic vehicle performance specifications, a series of PSAT simulations were performed and the results are tabulated in Table 5.15 and Table 5.16.

Vehicle Design Parameters (comparable to OEM Standards)	PHEV ₂₀		
		Curb +Driver	GVW
Front wheel drive	yes	yes	
Wheel base [mm]	2461	2461	
Weight distribution [%/%]	50/50		
Center of gravity height [mm]	530		
Coefficient of drag (Cd)	0.25	0.25	
Vehicle frontal area [m ²]	2.1	2.1	
Tire size and specifications		P205/60R16	
Tire rolling resistance	0.007	0.007	
Auxiliary power demand, Max. continuous [W]	2200		
Auxiliary power demand, Test [W]		700	
Mechanical accessory losses [W]		715	
Road condition, Brake + Acceleration	Dry Asphalt	Dry Asphalt	
Passenger capacity	4		
Cargo volume [Liters]	250		
Curb weight [kg]	1000	1000	
Payload [kg]	360		360
Driver weight [kg]	75	75	
Vehicle test weight [kg]	-	1075	1360
Max. grade capability, at 40 Km/h (25mph) with peak motor @ GVW	[%/km/h/s] [%/mph/s]	22/30/30 22/18.6/30 Target	22% 26kW
Max. grade capability, at 73 Km/h (45mph) with continuous motor @ GVW	[%/km/h] [%/mph]	10/73 10/45 Target	10% 33kW
Max. grade capability, at 90 Km/h (56mph) with continuous motor @ GVW	[%/km/h] [%/mph]	10/90 10/56 Target	10% 43kW
Max. grade capability, at 100/112 Km/h (62/70mph) with continuous motor @ GVW	[%/km/h] [%/mph]	10/100 10/62 Target	10% 49kW

Continued on next page

Vehicle Design Parameters (comparable to OEM standards)		PHEV ₂₀		
			Curb +Driver	GVW
0-100 km/h (0-62 mph) with Peak Motor @ Acceleration Test Weight	[sec] [Peak kW]	11-13	11.3 s 49kW	
Top Speed	[km/h/mph] [Cont kW]	150/93	150/93 28kW	
Vehicle Elec Rance (UDDS w/Regen)	[km/miles]	32/20	41/26	
Vehicle Range (UDDS w/Regen)	[km]	500	41+515	
Ambient Operating Temperatures	[Deg C]	-40/+52		

Table 5.15: Vehicle design parameters for PHEV₂₀

Powertrain Design Parameters (comparable to OEM standards)		PHEV ₂₀	
		Curb +Driver	GVW
Regenerative braking		yes	yes
Peak engine power (mechanical)	[kW]		53
Fuel cell power (electrical)	[kW]	n/a	n/a
Battery capacity	[kWh]		5.1
Traction motor mechanical capacity (Continuous/ Peak/ Max RPM)	[kW]		49 / 49 / 8700 rpm
Peak motor power (Mechanical)	[kW]		49
Peak generator power (Electrical)	[kW]		48
Final drive/differential	[ratio]		6.44
Powertrain weight	[kg]		335
Battery weight	[kg]		58
Fuel tank capacity	[kg]		13
Type of PHEV		Series	Series

Table 5.16: Powertrain design parameters - PHEV₂₀

5.10.2.2 Vehicle Performance - Simulation Results

Simulation results based on PSAT analysis were tabulated and compared with the targets for the PHEV₂₀. The PHEV₂₀ overall vehicle performance results and the capability of this vehicle to meet its targets are identified in Table 5.17. The PHEV₂₀ meets all preset performance requirements of the FSV.

IC Engine, Peak (mechanical)	50 kW
Generator, Peak (electrical)	48 kW
Traction Motor, Peak (mechanical)	49 kW

	Units	Specs	Traction Power				Capability
			Peak 49 kW		Continuous 49 kW		
			Curb + Driver	GVW	Curb + Driver	GVW	
Performance							
Acceleration							
0 - 100 km/h, Curb + Driver	sec.	11-13	11.3 @ 49 kW	—	—	—	
Peak Grade							
30 km/h - 30 sec., GVW	%	22	—	22 @ 26 kW	—	—	
Continuous Grade							
73 km/h - Continuous, GVW	%	10	—	—	—	10 @ 33 kW	
90 km/h - Continuous, GVW	%	10	—	—	—	10 @ 43 kW	
112 km/h - Continuous, GVW	%	10		—	—	10 @ 49 kW	
Top Speed							
Continuous, GVW	km/h	150	—	—	—	150 @ 28 kW	
Range							
Curb + Driver, UDDS	km	500	—	—	556	—	



Limited Performance = 
 Unable to Perform = 

Table 5.17: Vehicle performance results - PHEV₂₀

5.10.3 Layout & Design

The PHEV₂₀ vehicle will have an all-electric range of 32 km (20 miles) on a fully charged battery pack. The battery pack is a lithium-ion manganese based cell with a 5 kWh capacity (45 kg, 36 liter). The charging time for this battery pack is 2.5hrs using a 120 V, 15 amp (220 V/13 amp(EU)) outlet. The extended range of 500 km for PHEV₂₀ is provided by a rear mounted 1.0L-3cyl gasoline engine/generator set. The rear mounted engine/generator set is just ahead of the rear axle, leading to 50/50 vehicle mass split between front and rear wheels. The layout on the FSV PHEV₂₀ is shown in Figure 5.19.

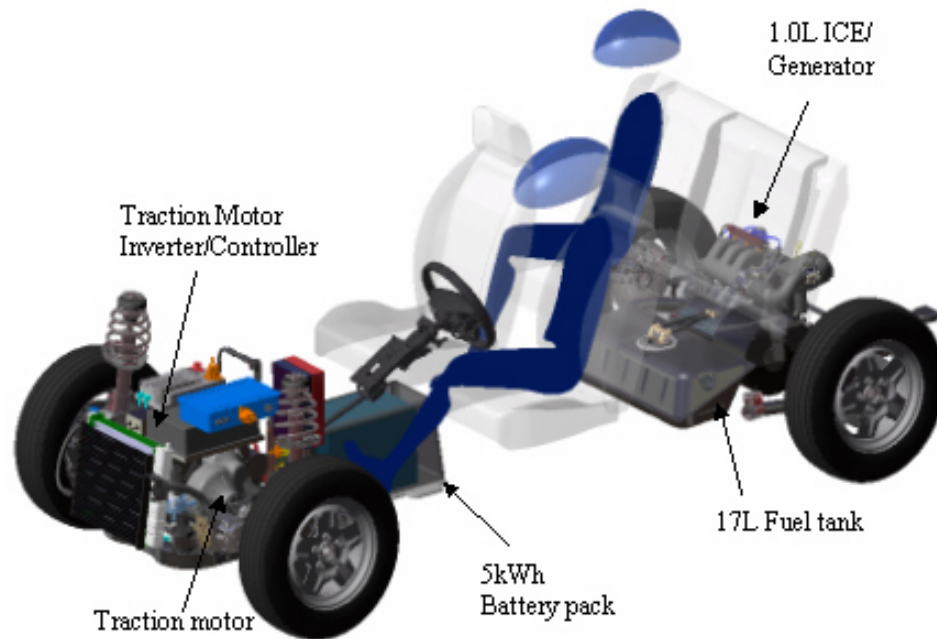


Figure 5.19: PHEV₂₀ layout

This above shown packaging arrangement makes use of space underneath the rear floor. Some of this space on conventional vehicles would be taken up by the spare tire. The arrangement is similar to Daimler Smart-For-Two and Mitsubishi i-Minicar production vehicles. On the FSV, the installation will be simpler as the engine does not drive the wheels and does not carry all of the belt driven auxiliary devices.

The under-floor structure as shown in Figure 5.20 for the PHEV₂₀ has to be adapted to accommodate the 5 kWh battery pack in the tunnel under the front floor. The engine/generator set mounted under the rear-floor will require careful consideration of packaging the rear suspension and sufficient structure to handle all the dynamic and rear impact crash loading. The body-structure sub-frame assembly that can support the engine/generator mounts and the multi-link suspension will form the base of rear structure.

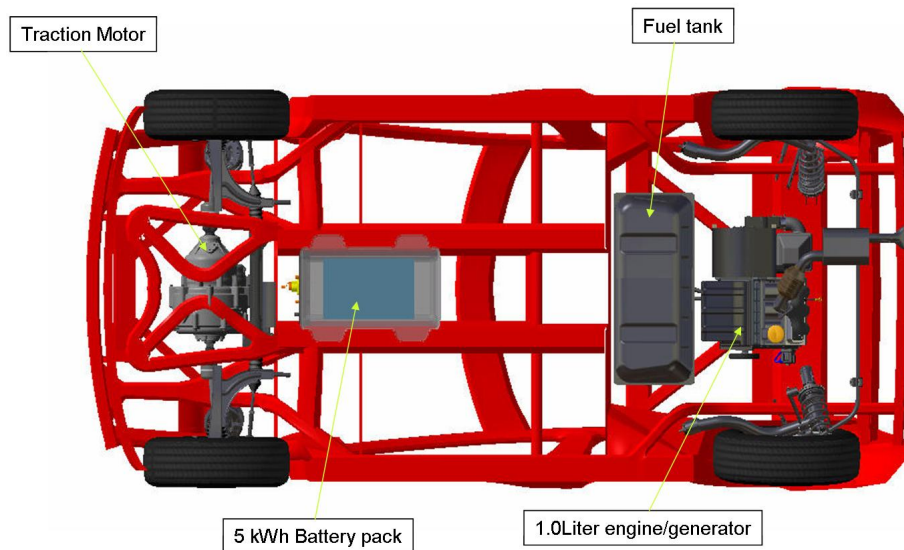


Figure 5.20: PHEV₂₀ underbody

5.10.4 Bill Of Materials (BOM)

The PHEV₂₀ variant of the FSV has particular component needs for its powertrain. As such, a detailed Bill of Materials (BOM) was generated for the PHEV₂₀. This BOM includes only the major components required to fulfill the powertrain needs. Table 5.18 shows the powertrain BOM for the PHEV₂₀.

Item #	BOM Level	ASSEMBLY / COMPONENT	VENDOR	QTY ASM	U/M	Size LxWxH [mm]	Item Mass [kg]	Extended Weight [kg]	USD - 2015 Price - (100K/year)	Comments
1		POWERTRAIN-PHEVs	Q	1	EA			343.4	\$8,970	
2		ENGINE INSTALLATION	Q	1	EA			82.5	\$1,050	
3		IC ENGINE 1.0L 3-cylinder		1	EA	381x229x610	82.5	82.5	\$1,050	Gasoline NA DI, 50kW Shaft Power Peak; No Accessory Belt Drive
2		GENERATOR/ TRACTION DRIVE INSTALLATION	Q	1	EA			132.8	\$3,975	
3		GENERATOR- 67 kW Peak; 49 KW, continuous		1	EA	216xØ288	40.6	40.6	\$1,718	8 L/min WEG 50/50, 55C max inlet
3		GENERATOR INVERTER/ CONTROLLER- 67 kW Peak; 49 KW, continuous		1	EA	282x282x130	14.2	14.2	—	8 L/min WEG 50/50, 55C max inlet
3		TRACTION MOTOR- 67 kW Peak; 49 KW, continuous		1	EA	216xØ288	40.6	40.6	\$1,718	8 L/min WEG 50/50, 55C max inlet
3		T-MOTOR INVERTER/ CONTROLLER - 67 kW Peak; 49 KW, continuous		1	EA	282x282x130	14.2	14.2	—	8 L/min WEG 50/50, 55C max inlet
3		TRANSAXLE / DIFFERENTIAL		1	EA	250xØ250	15.0	15.0	\$300	
3		HALF-SHAFTS		2	EA	230xØ94	4.1	8.2	\$240	Based on GKN Type 102 / Joint 10
2		TRACTION BATTERY SYSTEM	Q	1	EA			63.2	\$2,346	
3		BATTERY PACK(Li ION) & CONTROLLER		1	EA	Varies: 0.047 m3	58.2	58.2	\$2,246	245 Volt Nominal, 277 Volt Max., 218 Volt Min.

Continued on next page

Item #	BOM Level	ASSEMBLY / COMPONENT	VENDOR	QTY ASM	U/M	Size LxWxH [mm]	Item Mass [kg]	Extended Weight [kg]	USD - 2015 Price - (100K/year)	Comments
	4	CONTROLLER / WIRING / THERMAL MGMT		1	EA	—	13.4	—	—	
	4	BATTERY PACK		1	EA	—	44.8	—	—	5 kW-h
	5	BATTERY MODULE		64	EA	100x60x95	0.7	—	—	
	6	BATTERY CELLS		6	EA	—	0.1	—	—	130 W-h / kg; 13 W-h / cell
	3	PLUG-IN CHARGING SYSTEM		1	EA	406x305x100	5.0	5.0	\$100	Input: 110/220 VAC; 45 - 75 Hz; 16 A
4	2	ELECTRICAL AND ELECTRONICS	E	1	EA			19.7	\$884	
	3	DC-DC CONVERTER	Q	1	EA	253x257x79	4.9	4.9	\$429	DC input voltage: 250 to 425 DC output voltages: 13.8 @ 2.2 kW @ 90% Eff. 10L/min WEG 50/50 75C Max Inlet
	3	HYBRID CONTROLLER	Q	1	EA	200x150x50	0.6	0.6	\$200	
	3	HARNESS LOW VOLTAGE	Q	1	EA	Varies	0.2	0.2	\$80	
	4	HIGH VOLTAGE CABLE	Q	30	M	—	0.01	—	—	18 AWG Copper 4-92 lb/1000 ft
	3	HARNESS HIGH VOLTAGE	Q	1	EA	Varies	5.7	5.7	\$150	
	4	HIGH VOLTAGE CABLE	Q	6	M	—	1.0	—	—	4/0 AWG Copper 641 lb/1000 ft
	3	FUSE BLOCK	E	1	EA	150x150x100	0.2	0.2	\$25	
	3	MISC. ELECTRICAL	Q	1	EA		8.0	8.0		
5	2	EXHAUST SYSTEM	Q	1	EA			10.8	\$300	
	3	IC ENGINE-TO-TAILPIPE TUBING		3	M	Varies xØ50	1.1	3.2	\$60	0.36 kg/m 50mm OD, 0.3 mm wall
	3	3-WAY CATALYTIC CONVERTER		1	EA		3.0	3.0	\$150	
	3	O2 SENSOR		2	EA		0.3	0.6	\$60	
	3	MUFFLER		1	EA		4.0	4.0	\$30	
6	2	FUEL SYSTEM	Q	1	EA			34.3	\$415	

Continued on next page

Item #	BOM Level	ASSEMBLY / COMPONENT	VENDOR	QTY ASM	U/M	Size LxWxH [mm]	Item Mass [kg]	Extended Weight [kg]	USD - 2015 Price - (100K/year)	Comments
	3	FUEL TANK - 17L		1	EA	Varies: 0.017 m3	9.0	9.0	\$150	
	3	FUEL PUMP		1	EA	In-Tank	2.0	2.0	\$25	
	3	FUEL SUPPLY LINES		4	M	Varies xØ6	0.8	3.0	\$40	0.19 kg/m 13mm OD, 0.6 mm wall
	3	FUEL RETURN LINES		4	M	Varies xØ6	0.8	3.0	\$40	
	3	FILL LINE		1	M	Varies xØ20	0.2	0.2	\$35	0.19 kg/m 13mm OD, 0.6 mm wall
	3	EVAP CANISTER AND ACCESSORIES		1	EA	90xØ50	2.0	2.0	\$100	
	3	BRACKETS AND WIRING		1	EA	Varies	10.0	10.0	\$25	
7	2	COOLING SYSTEM	E	1	EA			0.0	\$0	
	3	FAN - ELECTRIC COOLING		1	EA			0.0		
	3	FAN CONTROLLER		1	EA			0.0		
	3	ELECTRIC COOLANT PUMP		1	EA			0.0		50 L/min (IC Engine)
	3	RADIATOR-ENGINE COOLANT		1	EA			0.0		75 kW Heat Rejection, 50 L/min, 80C max Outlet @ 102C max Inlet, 40C Ambient
	3	ELECTRIC COOLANT PUMP		1	EA			0.0		42 L/min (10 L/min DC/DC Converter, 32 L/min Motor-Inverter)
	3	RADIATOR-ELECTRONICS		1	EA			0.0		20.2 kW Heat Rejection (0.2 kW DC/DC, 10 kW Motor Inverter, 10 kW Motor), 42 L/min, 55C max Outlet @ 62C max Inlet, 40C Ambient
8	2	DRIVER - DRIVETRAIN INTERFACE	E	1	EA			1.1	\$0	
	3	THROTTLE PEDAL/SENSOR ASSEMBLY		1	EA	193x49x275	0.3	0.3	\$0	

Continued on next page

Item #	BOM Level	ASSEMBLY / COMPONENT	VENDOR	QTY ASM	U/M	Size LxWxH [mm]	Item Mass [kg]	Extended Weight [kg]	USD - 2015 Price - (100K/year)	Comments
	3	BRAKE PEDAL/ SWITCH ASSEMBLY		1	EA	193x49x275	0.3	0.3	\$0	
	3	GEAR SELECTION ASSEMBLY		1	EA	75x50x50	0.3	0.3	\$0	
	3	DRIVER INFORMATION DISPLAY		1	EA	10x305x125	0.2	0.2	\$0	OLED Technology

VENDOR CODE: Q = QUANTUM; U = UQM; E = EDAG; S = SFCV

Table 5.18: Bill of materials : FSV-1 - PHEV₂₀

5.11 Plug-In Hybrid with a 64 km(40 mile) All Electric Range(PHEV₄₀)

The PHEV₄₀ is the one of the variants of the FSV-2 which is new 4-door sedan with a US size classification as a C/D-Class vehicle and is 4300 mm in length. This vehicle is for in-city as well as longer duration trip use. This vehicle has an All Electric Range (AER) of 64 km (40 miles), and 500 km(310 miles) using the combination of its 1.4 Liter 4 Cylinder Internal Combustion Engine and a 11.7 kWh Battery. Figure 5.21 shows the FSV-2 PHEV₄₀ vehicle with its powertrain.

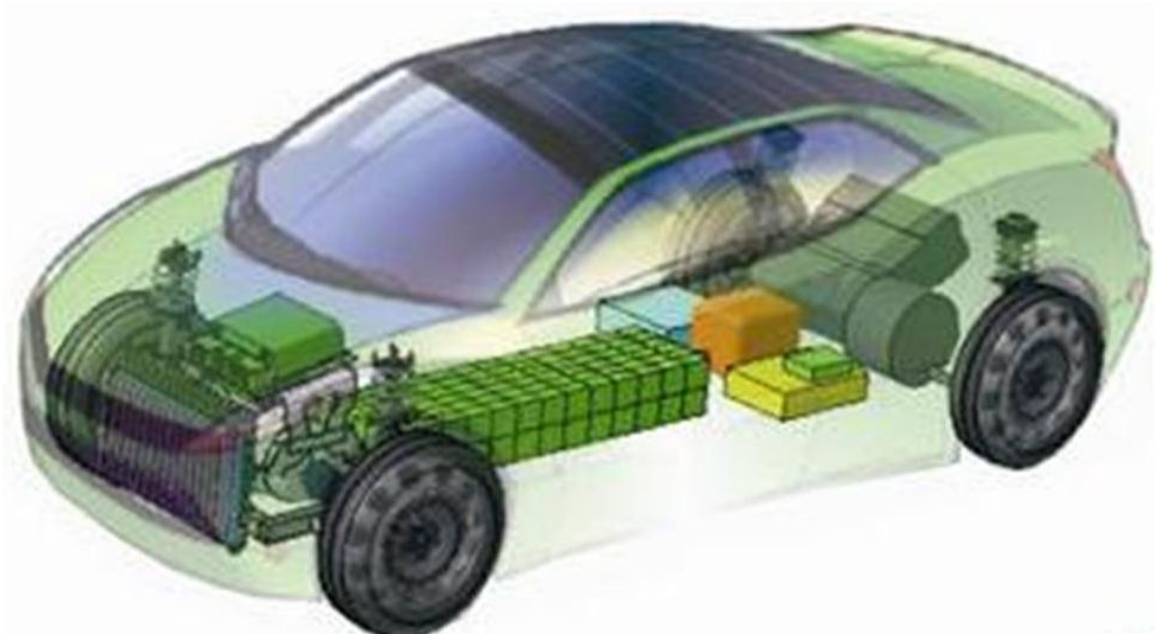


Figure 5.21: FSV-2 PHEV₄₀

The PHEV₄₀ gets the upgraded 1.4 L 4-Cylinder engine and similar to the PHEV₂₀, it is rear mounted and thus provides an opportunity to maintain the same design feature of the BEV and PHEV₂₀ of shorter and common front-end. The PHEV₄₀ rides on the same wheels as that of the BEV and PHEV₂₀, using a 15 in wheel with 175/65/R15 tires. Designed completely in steel, using the future technology in Li-ion battery, motor and ICE, the PHEV₄₀ just like the other FSV variants, meets all future fuel economy requirements.

5.11.1 Mass Estimates

The mass estimates of the PHEV₄₀ in comparison with a similar sized 2010 and 2020 ICE vehicle and Hybrid Electric Vehicle (HEV) are as shown in Table 5.19. Future technologies, body-structure mass reduction by use of Advanced High Strength Steels (AHSS) and smaller vehicle foot print of FSV, all lead to significant mass reduction on the PHEV₄₀. Estimated total vehicle mass for PHEV₄₀ is 1,279 kg and is 14% less than the vehicle mass of a comparable size conventional 2010 ICE vehicle. The body-structure mass target of 198 kg for PHEV₄₀ is 41% lower than the body-structure mass of the 2010 ICE vehicle, even though the powertrain masses for FSV are higher. Similar comparisons can be derived between the PHEV₄₀ and the 2010 HEV, 2020 ICE vehicle and 2020 HEV.












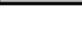

	ICE 2 2010	ICE 2 2020	HEV 2 2010	HEV 2 2020	FSV 2 PHEV ₄₀
 Body Non-Structure	302	210	257	210	210
 Body Structure	337	298	337	303	198
 Front Suspension	73	49	76	55	51
 Rear Suspension	65	45	73	44	52
 Steering	21	21	21	21	19
 Brakes	47	37	49	40	37
 Drivetrain	274	244	359	304	261
 Fuel, Battery, Exhaust	59	68	125	127	178
 Wheels and Tires	96	72	80	73	70
 Air Conditioning	40	52	35	46	47
 Electrical	68	78	68	82	83
 Bumpers	33	25	31	28	26
 Closures	67	59	62	55	48
TOTAL	1,483	1,260	1574	1388	1279

Table 5.19: FSV-2 PHEV₄₀ estimated mass (Kg)

The mass and cost breakdown of this new powertrain and fuel storage (battery) system for the PHEV₄₀ is shown in Table 5.20. These numbers are forecasted for the year 2015–2020.

Powertrain components	Mass [kg]	Cost [US \$]
Li-ion Battery and controller	136.5	5,365
Generator/Traction Drive (75kW)	145.9	4,385
IC Engine(1.4L)	115.5	1,470
Fuel system	30.3	415
Exhaust system	10.8	300

Table 5.20: FSV-2 PHEV₄₀ - Powertrain and fuel system mass & cost

5.11.2 Technical Specification & Performance

5.11.2.1 Powertrain

The targets outlined in the previous section was used as the primary input into PSAT to conduct the feasibility study. Using these basic vehicle performance specifications/targets, a series of PSAT simulations were performed and the results are tabulated in Table 5.21 and Table 5.22.

Vehicle Design Parameters (comparable to OEM standards)	PHEV ₄₀		
		Curb +Driver	GVW
Front wheel drive	yes	yes	
Wheel base [mm]	2578	2578	
Weight distribution [%/%]	50/50		
Center of gravity height [M]	0.53		
Coefficient of drag (Cd)	0.25	0.25	
Vehicle frontal area [m ²]	2.25	2.25	
Tire size and specifications		P175/65R15	
Tire rolling resistance	0.007	0.007	
Auxiliary power demand, Max. continuous [W]	2500		
Auxiliary power demand, Test [W]		700	
Mechanical accessory losses [W]		1000	
Road condition, Brake + Acceleration	Dry Asphalt	Dry Asphalt	
Passenger capacity	4+		
Cargo volume [Liters]	370		
Curb weight [kg]	1300	1300	
Payload [kg]	437.5		437.5
Driver weight [kg]	75	75	
Vehicle test weight [kg]	-	1375	1737.5
Max. grade capability, at 40 Km/h (25mph) with peak motor @ GVW [%/km/h/s] [%/mph/s]	22/40/30 22/25/30 Target		22% 44kW
Max. grade capability, at 73 Km/h (45mph) with continuous motor @ GVW [%/km/h] [%/mph]	10/73 10/45 Target		10% 42kW
Max. grade capability, at 90 Km/h (56mph) with continuous motor @ GVW [%/km/h] [%/mph]	10/90 10/56 Target		10% 54kW
Max. grade capability, at 100/112 Km/h (62/70mph) with continuous motor @ GVW [%/km/h] [%/mph]	10/112 10/70 Target		10% 71kW 7% 55kW
0-100 km/h (0-62 mph) with peak Motor @ acceleration test weight [sec] [Peak kW]	10-12	11.4 sec 75kW	

Continued on next page

Vehicle Design Parameters (comparable to OEM standards)		PHEV ₄₀		
			Curb +Driver	GVW
Top Speed	[km/h/mph] [Cont. kW]	161/100	161/100 37kW	
Vehicle electric range (UDDS w/Regen)	[km/miles]	64/40	77/48	
Vehicle range (UDDS w/Regen)	[km]	500	77 + 500	
Ambient operating temperatures	[Deg C]	-40/+52		

Table 5.21: Vehicle design parameters PHEV₄₀

Powertrain Design Parameters (comparable to OEM standards)		PHEV ₄₀	
		Curb +Driver	GVW
Regenerative braking		yes	yes
Peak engine power (mechanical)	[kW]		67
Fuel cell power (electrical)	[kW]	n/a	n/a
Battery capacity	[kWh]		11.7
Traction motor mechanical capacity (Continuous/ Peak/ Max RPM)	[kW]		54 / 75 / 7600 rpm
Peak motor power (mechanical)	[kW]		75
Peak generator power (electrical)	[kW]		60
Final drive/differential	[ratio]		5.38
Powertrain weight	[kg]		461
Battery weight	[kg]		137
Fuel tank capacity	[kg]		14
Type of PHEV		Series / Parallel	Series


Table 5.22: Powertrain design parameters - PHEV₄₀

5.11.2.2 Vehicle Performance - Simulation Results

Simulation results based on PSAT analysis were tabulated and compared with the preset targets for the PHEV₄₀. The PHEV₄₀ overall vehicle performance results are shown and capabilities measured in Table 5.23. The PHEV₄₀ meets all preset performance requirements except for the continuous 10% hill climb at 112 $\frac{\text{km}}{\text{h}}$ (GVW). However, the PHEV₄₀ meets this performance requirement at a lower speed.

IC Engine, Peak (mechanical)	70 kW
Generator, Peak (electrical)	60 kW
Traction Motor, Peak (mechanical)	75 kW

	Units	Specs	Traction Power				Capability
			Peak 75 kW		Continuous 55 kW		
			Curb + Driver	GVW	Curb + Driver	GVW	
Performance							
Acceleration							
0 - 100 km/h, Curb + Driver	sec.	10-12	11.4 @ 75 kW	—	—	—	Green
Peak Grade							
40 km/h - 30 sec., GVW	%	22	—	22 @ 44 kW	—	—	Green
Continuous Grade							
73 km/h - Continuous, GVW	%	10	—	—	—	10 @ 42 kW	Green
90 km/h - Continuous, GVW	%	10	—	—	—	10 @ 54 kW	Green
112 km/h - Continuous, GVW	%	10	—	10 @ 71 kW	—	7 @ 54 kW	Yellow
Top Speed							
Continuous, GVW	km/h	161	—	—	—	161 @ 75 kW	Green
Range							
Curb + Driver, UDDS	km	500	—	—	577	—	Green

Limited Performance = 


Unable to Perform = 

Table 5.23: Vehicle performance results - PHEV₄₀

5.11.3 Layout & Design

The PHEV₄₀ vehicle will have an all-electric range of 64 km (40 miles) on a fully charged battery pack. The battery pack is a lithium-ion manganese based cell with 11.7 kWh capacity (105 kg mass, 86 liter volume). The charging time for this battery pack using an 120 V, 15 amp (220 V/13 amp - EU) outlet is 5.5 hours. The extended range of 500 km for PHEV₄₀ is provided by a rear mounted 1.4 L-4cylinder gasoline engine/generator. Figure 5.22 shows the layout of the PHEV₄₀ powertrain.

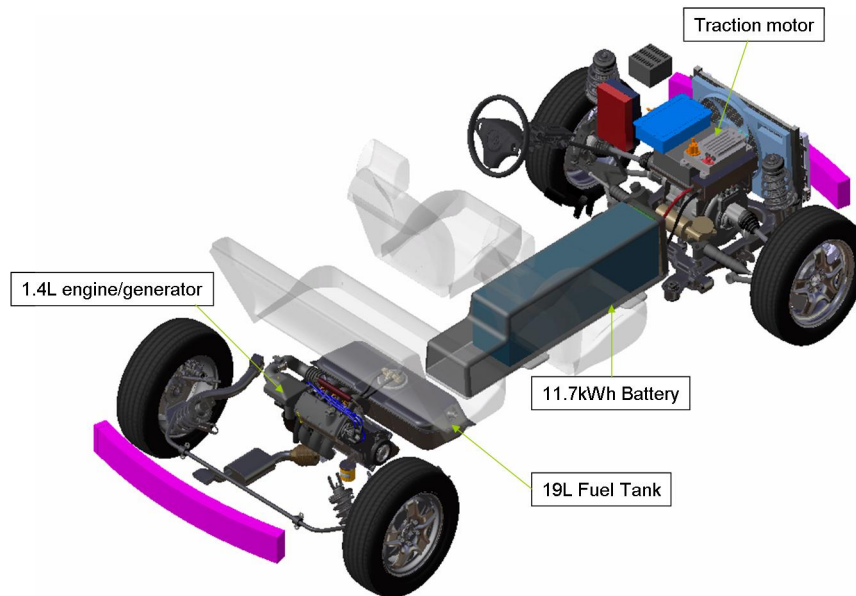


Figure 5.22: *PHEV₄₀ layout*

At present, other driving strategies that could considerably reduce the size of the engine/generator are being investigated.

The component packaging and structural challenges for this vehicle are similar to the PHEV₂₀ as previously discussed.

5.11.4 Bill Of Materials (BOM)

The PHEV₄₀ variant of the FSV has particular component needs for its powertrain. As such, a detailed Bill of Materials (BOM) was generated for the PHEV₄₀. This BOM includes only the major components required to fulfill the powertrain needs. Table 5.24 shows the powertrain BOM for the PHEV₄₀.

Item #	BOM Level	ASSEMBLY / COMPONENT	VENDOR	QTY ASM	U/M	Size LxWxH [mm]	Item Mass [kg]	Extended Weight [kg]	USD - 2015 Price - (100K/year)	Comments
1		POWERTRAIN-PHEVs	Q	1	EA			468.7	\$12,819	
2		ENGINE INSTALLATION	Q	1	EA			115.5	\$1,470	
3		IC ENGINE 1.4L 4-cylinder		1	EA	533x229x610	115.5	115.5	\$1,470	Gasoline NA DI, 70kW Shaft Power Peak; No Accessory Belt Drive
2		GENERATOR/TRACTION DRIVE INSTALLATION	Q	1	EA			145.9	\$4,385	
3		GENERATOR- 75 kW Peak, 55 kW Cont.		1	EA	241xØ350	45.5	45.5	\$1,923	8 L/min Coolant, 55C max inlet
3		GENERATOR INVERTER/CONTROLLER- 75 kW Peak, 55 kW Cont.		1	EA	380x365x119	15.9	15.9	—	8 L/min Coolant, 55C max inlet
3		TRACTION MOTOR- 75 kW Peak, 55 kW Continuous		1	EA	241xØ350	45.5	45.5	\$1,923	8 L/min Coolant, 55C max inlet
3		T-MOTOR INVERTER/CONTROLLER- 75 kW Peak, 55 kW Cont.		1	EA	380x365x119	15.9	15.9	—	8 L/min Coolant, 55C max inlet
3		TRANSAXLE / DIFFERENTIAL		1	EA	250xØ250	15.0	15.0	\$300	
3		HALF-SHAFTS		2	EA	230xØ94	4.1	8.2	\$240	Based on GKN Type 102 / Joint 10
3		TRACTION BATTERY SYSTEM	Q	1	EA			141.5	\$5,365	
3		BATTERY PACK(Li ION) & CONTROLLER		1	EA	Varies: 0.103 m3	136.5	136.5	\$5,265	334 Volt Nominal, 378 Volt Max., 297 Volt Min.

Continued on next page

Item #	BOM Level	ASSEMBLY / COMPONENT	VENDOR	QTY ASM	U/M	Size LxWxH [mm]	Item Mass [kg]	Extended Weight [kg]	USD - 2015 Price - (100K/year)	Comments
4	4	CONTROLLER / WIRING / THERMAL MGMT		1	EA	—	31.5	—	—	
4	4	BATTERY PACK		1	EA	—	105.0	—	—	11.7 kW-h
5	5	BATTERY MODULE		150	EA	100x60x95	0.7	—	—	
6	6	BATTERY CELLS		6	EA	—	0.1	—	—	130 W-h / kg; 13 W-h / cell
3	3	PLUG-IN CHARGING SYSTEM		1	EA	406x305x100	5.0	5.0	\$100	Input: 110/220 VAC; 45 - 75 Hz; 16 A
4	2	ELECTRICAL AND ELECTRONICS	E	1	EA			19.7	\$884	
3	3	DC-DC CONVERTER	Q	1	EA	253x257x79	4.9	4.9	\$429	DC input voltage: 250 to 425 DC output voltages: 13.8 @ 2.2 kW @ 90% Eff. 10L/min WEG 50/50 75C Max Inlet
3	3	HYBRID CONTROLLER	Q	1	EA	200x150x50	0.6	0.6	\$200	
3	3	HARNESS LOW VOLTAGE	Q	1	EA	Varies	0.2	0.2	\$80	
4	4	HIGH VOLTAGE CABLE	Q	30	M	—	0.01	—	—	18 AWG Copper 4-92 lb/1000 ft
3	3	HARNESS HIGH VOLTAGE	Q	1	EA	Varies	5.7	5.7	\$150	
4	4	HIGH VOLTAGE CABLE	Q	6	M	—	1.0	—	—	4/0 AWG Copper 641 lb/1000 ft
3	3	FUSE BLOCK	E	1	EA	150x150x100	0.2	0.2	\$25	
3	3	MISC. ELECTRICAL	Q	1	EA		8.0	8.0		
5	2	EXHAUST SYSTEM	Q	1	EA			10.8	\$300	
3	3	IC ENGINE-TO-TAILPIPE TUBING		3	M	Varies xØ50	1.1	3.2	\$60	0.36 kg/m 50mm OD, 0.3 mm wall
3	3	3-WAY CATALYTIC CONVERTER		1	EA		3.0	3.0	\$150	
3	3	O2 SENSOR		2	EA		0.3	0.6	\$60	
3	3	MUFFLER		1	EA		4.0	4.0	\$30	
6	2	FUEL SYSTEM	Q	1	EA			30.3	\$415	

Continued on next page

Item #	BOM Level	ASSEMBLY / COMPONENT	VENDOR	QTY ASM	U/M	Size LxWxH [mm]	Item Mass [kg]	Extended Weight [kg]	USD - 2015 Price - (100K/year)	Comments
	3	FUEL TANK - 19L		1	EA	Varies: 0.019 m3	10.0	10.0	\$150	
	3	FUEL PUMP		1	EA	In-Tank	2.0	2.0	\$25	
	3	FUEL SUPPLY LINES		4	M	Varies xØ6	0.8	3.0	\$40	0.19 kg/m 13mm OD, 0.6 mm wall
	3	FUEL RETURN LINES		4	M	Varies xØ6	0.8	3.0	\$40	
	3	FILL LINE		1	M	Varies xØ20	0.2	0.2	\$35	0.19 kg/m 13mm OD, 0.6 mm wall
	3	EVAP CANISTER AND ACCESSORIES		1	EA	90xØ50	2.0	2.0	\$100	
	3	BRACKETS AND WIRING		1	EA	Varies	10.0	10.0	\$25	
7	2	COOLING SYSTEM	E	1	EA			0.0	\$0	
	3	FAN - ELECTRIC COOLING		1	EA			0.0		
	3	FAN CONTROLLER		1	EA			0.0		
	3	ELECTRIC COOLANT PUMP		1	EA			0.0		68 L/min (IC Engine)
	3	RADIATOR-ENGINE COOLANT		1	EA			0.0		105 kW Heat Rejection, 68 L/min, 80C max Outlet @ 102C max Inlet, 40C Ambient
	3	ELECTRIC COOLANT PUMP		1	EA			0.0		42 L/min (10 L/min DC/DC Converter, 32 L/min Motor-Inverter)
	3	RADIATOR-ELECTRONICS		1	EA			0.0		28.2 kW Heat Rejection (0.2 kW DC/DC, 14 kW Motor Inverter, 14 kW Motor), 42 L/min, 55C max Outlet @ 65C max Inlet, 40C Ambient
8	2	DRIVER - DRIVETRAIN INTERFACE	E	1	EA			1.1	\$0	
	3	THROTTLE PEDAL/SENSOR ASSEMBLY		1	EA	193x49x275	0.3	0.3	\$0	

Continued on next page

Item #	BOM Level	ASSEMBLY / COMPONENT	VENDOR	QTY ASM	U/M	Size LxWxH [mm]	Item Mass [kg]	Extended Weight [kg]	USD - 2015 Price - (100K/year)	Comments
	3	BRAKE PEDAL/ SWITCH ASSEMBLY		1	EA	193x49x275	0.3	0.3	\$0	
	3	GEAR SELECTION ASSEMBLY		1	EA	75x50x50	0.3	0.3	\$0	
	3	DRIVER INFORMATION DISPLAY		1	EA	10x305x125	0.2	0.2	\$0	OLED Technology

VENDOR CODE: Q = QUANTUM; U = UQM; E = EDAG; S = SFCV

Table 5.24: Bill of materials : FSV-2 - PHEV₄₀

5.12 Fuel Cell Electric Vehicle

The FCEV variant of the FSV is the second of the two bigger vehicles (FSV-2) and is a compressed-hydrogen powered fuel cell electric vehicle. Approximately 3.4 kg of compressed hydrogen at 700 bar (10,000 psi) is stored in a single 95 L tank, which allows for a vehicle range of about 500 km (310 miles). The FSV-2 FCEV is shown in Figure 5.23.



Figure 5.23: FSV-2 FCEV

The FCEV fuel cell system including the stack and its components, designed by Tongji incorporates the future technological advances in fuel cell system and is designed to compliment the other variants of the FSV in terms of its design cues of a common and shorter front-end.

5.12.1 Mass Estimates

For the FSV-2 FCEV, the calculated vehicle masses of 1,079 kg is 27% lower than that of a comparable size 2010 ICE vehicle. The body-structure mass estimate of 175 kg for the FCEV is 48% lower than a comparable internal combustion engine vehicle as illustrated in Table 5.25.









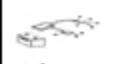




	ICE 2 2010	ICE 2 2020	HEV 2 2010	HEV 2 2020	FSV 2 FCEV
 Body Non-Structure	302	210	257	210	210
 Body Structure	337	298	337	303	175
 Front Suspension	73	49	76	55	44
 Rear Suspension	65	45	73	44	34
 Steering	21	21	21	21	19
 Brakes	47	37	49	40	34
 Drivetrain	274	244	359	304	177
 Fuel, Battery, Exhaust	59	68	125	127	114
 Wheels and Tires	96	72	80	73	61
 Air Conditioning	40	52	35	46	47
 Electrical	68	78	68	82	93
 Bumpers	33	25	31	28	22
 Closures	67	59	62	55	48
TOTAL	1,483	1,260	1574	1388	1079

Table 5.25: FSV-2 FCEV estimated mass (Kg)

The mass and cost of the powertrain and fuel storage system, which constitute the majority of the added mass to the vehicle, is shown in Table 5.26. These masses and cost are forecasted for the year 2015–2020.

Powertrain components	Mass [kg]	Cost [US \$]
Li-ion Battery and controller	27.3	1,503
Traction Motor (75kW)	84.6	2,463
Fuel Cell system (65kW)	92	10,081
Hydrogen Storage(3.4L)	87	7,919

Table 5.26: FSV-2 FCEV - Powertrain and fuel system mass & cost

5.12.2 Technical Specification & Performance

5.12.2.1 Powertrain

The targets data shown in the previous section was the basic input used by Quantum to perform the feasibility study. Powertrain System Analysis Toolkit (PSAT) software was used to model the FCEV variant with outputs such as vehicle performance and fuel economy.

For the bigger and heavier FCEV, power demand goes up as continuous power is gradually increased, with high-speed grade climbing ability being the most power demanding operation mode. Ultimate peak power demand is governed by short-term acceleration goals.

Based on the continuous power demand at $70 \frac{\text{km}}{\text{h}}$ of the FCEV, the traction motor would have to be rated slightly higher. This motor would typically be sufficiently sized to handle the peak acceleration power demand without overheating. In the case of the FCEV, the high-speed hill climbing capability of 10% at $112 \frac{\text{km}}{\text{h}}$ is going to be the capacity-determining factor for the traction motor and transmission. Using the basic vehicle performance specifications, a series of PSAT simulations were performed and the results are tabulated in Table 5.27 and Table 5.28.

Vehicle Design Parameters (comparable to OEM Standards)	FCEV		
		Curb +Driver	GVW
Front wheel drive	yes	yes	
Wheel base [mm]	2578	2578	
Weight distribution [%/%]	50/50		
Center of gravity height [mm]	530		
Coefficient of drag (Cd)	0.25	0.25	
Vehicle frontal area [m ²]	2.25	2.25	
Tire size and specifications		P175/55R15	
Tire rolling resistance	0.007	0.007	
Auxiliary power demand, Max. continuous [W]	2500		
Auxiliary power demand, Test [W]		700	
Mechanical accessory losses [W]		0	
Road condition, Brake + Acceleration	Dry Asphalt	Dry Asphalt	
Passenger capacity	4+		
Cargo volume [Liters]	370		
Curb weight [kg]	1300	1300	
Payload [kg]	437.5		437.5
Driver weight [kg]	75	75	
Vehicle test weight [kg]	-	1375	1737.5
Max. grade capability, at 40 Km/h (25mph) with peak motor @ GVW [%/km/h/s] [%/mph/s]	22/40/30 22/25/30 Target		22% 44kW

continued on next page

Vehicle Design Parameters (comparable to OEM standards)		FCEV		
			Curb +Driver	GVW
Max. Grade capability, at 73 Km/h (45mph) with continuous motor @ GVW	[%/km/h] [%/mph]	10/72.5 10/45 Target		10% 42kW
Max. grade capability, at 90 Km/h (56mph) with continuous motor @ GVW	[%/km/h] [%/mph]	10/90 10/56 Target		10% 54kW
Max. grade capability, at 100/112 Km/h (62/70mph) with continuous motor @ GVW	[%/km/h] [%/mph]	10/112 10/70 Target		10% 71kW 7% 55kW
0-100 km/h (0-62 mph) with peak motor @ acceleration test weight	[sec] [Peak kW]	10-12	11.4 sec 75kW	
Top speed	[km/h/mph] [Cont. kW]	161/100	161/100 37 kW	
Vehicle electric range (UDDS w/Regen)	[km/miles]	n/a	n/a	
Vehicle range (UDDS w/Regen)	[km]	500	540	
Ambient operating temperatures	[Deg C]	-30/+52		

Table 5.27: Vehicle design parameters FCEV

Powertrain Design Parameters (comparable to OEM standards)		FCEV		
			Curb +Driver	GVW
Regenerative braking		yes		yes
Peak engine power (mechanical)	[kW]			n/a
Fuel cell power (electrical)	[kW]			65
Battery capacity	[kWh]			2.3
Traction motor mechanical capacity (Continuous/ Peak/ Max RPM)	[kW]			54 / 75 / 7600 rpm
Peak motor power (mechanical)	[kW]			75
Peak generator power (electrical)	[kW]			n/a
Final drive/differential	[ratio]			5.38
Powertrain weight	[kg]			318
Battery weight	[kg]			27
Fuel tank capacity	[kg]			3.4
Type of PHEV				n/a

Table 5.28: Powertrain design parameters - FCEV

5.12.2.2 Vehicle Performance - Simulation Results

Simulation results based on PSAT analysis were tabulated and compared with the performance targets for the FCEV. Table 5.29, which is an overall performance results and capabilities compilation, shows that the FCEV meets all its targets except the 10% hill climb at 112 $\frac{\text{km}}{\text{h}}$ (gross weight condition). However, the FCEV is meets this performance requirement at a lower speed.

FC Stack, Peak (gross electrical)	74 kW
FC Engine, Peak (net electrical)	62 kW
Traction Motor, Peak (mechanical)	75 kW

	Units	Specs	Traction Power				Capability
			Peak 75 kW		Continuous 55 kW		
			Curb + Driver	GVW	Curb + Driver	GVW	
Performance							
Acceleration							
0 - 100 km/h, Curb + Driver	sec.	10-12	11.4 @ 75 kW	—	—	—	
Peak Grade							
40 km/h - 30 sec., GVW	%	22	—	22 @ 44 kW	—	—	
Continuous Grade							
73 km/h - Continuous, GVW	%	10	—	—	—	10 @ 42 kW	
90 km/h - Continuous, GVW	%	10	—	—	—	10 @ 54 kW	
112 km/h - Continuous, GVW	%	10	—	10 @ 71 kW	—	7 @ 55 kW	
Top Speed							
Continuous, GVW	km/h	161	—	—	—	161 @ 75 kW	
Range							
Curb + Driver, UDDS	km	500	—	—	577	—	

 Limited Performance =

 Unable to Perform =
Table 5.29: Vehicle performance results - FCEV

5.12.3 Layout & Design

The FCEV - Fuel Cell Electric Vehicle has an all-electric driving range of 500 km. The energy source for FCEV is electricity generated by the hydrogen fuel cell system. A fuel cell is a device that uses hydrogen (or hydrogen-rich fuel) and oxygen to create electricity by an electrochemical process. Figure 5.24 shows the FCEV powertrain design layout.

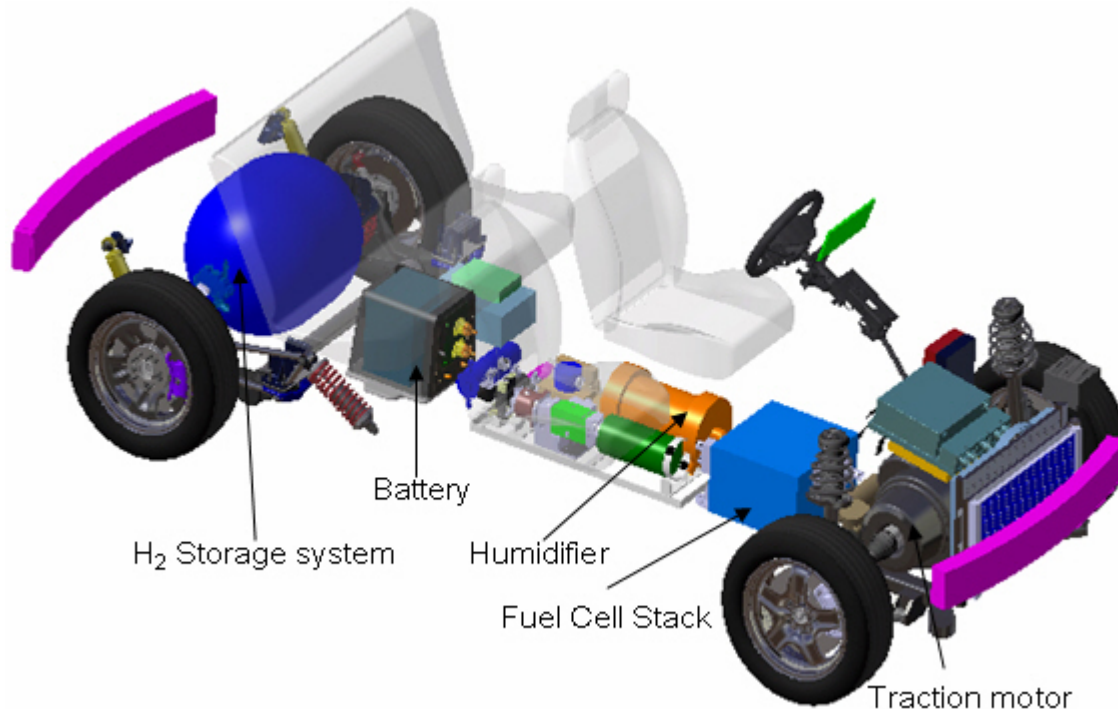


Figure 5.24: FCEV layout

The FCEV has a hydrogen usable storage capacity of 3.4 kg with an internal volume of 95 liters that is stored at 70 Mpa at 15°C. The fuel cell stack system has 240 cells, which has a combined weight of 92 kg producing 65 kW of power. A battery pack used in conjunction with this system is a lithium-ion manganese based cell with a 2.3 kWh capacity weighing in at 27 kg with 25 liter volume.

More details on the design and packaging of the fuel cell system into the FSV-2 can be found in “Chapter - Vehicle Package Development”.

5.12.4 Bill Of Materials (BOM)

The FCEV variant of the FSV has particular component needs for its powertrain. As such, a detailed Bill of Materials (BOM) was generated for the FCEV. This BOM includes only the major components required to fulfill the powertrain needs. Table 5.30 shows the powertrain BOM for the FCEV.

Item #	BOM Level	ASSEMBLY / COMPONENT	VENDOR	QTY ASM	U/M	Size LxWxH [mm]	Item Mass [kg]	Extended Weight [kg]	USD - 2015 Price - (100K/year)	Comments
1		POWERTRAIN-FC EV	Q	1	EA			325.7	\$23,493	
2		ENGINE INSTALLATION	S	1	EA			92.0	\$10,081	
3		FUEL CELL STACK		1	EA	403x372x252	42.5	42.5	\$7,667	74 KW gross out, maximum, Water Cooled, 47 KW heat generated, 85C max Outlet, 70C max Inlet
3		FUEL CELL SYSTEM CONTROLLER		1	EA	437x93x102	0.5	0.5	—	12 V, 5 A
3		AIR COMPRESSOR		1	EA	146x180x30	8.8	8.8	\$1,076	BLDC 12 V 40 A
3		COMPRESSOR CONTROLLER		1	EA	190x100x120	10.0	10.0	—	Powered by High Voltage Bus 9.5 kW max
3		AIR MUFFLER / FILTER ASSY		1	EA	280xØ140	2.0	2.0	\$20	
3		H2 RECIRCULATION PUMP		1	EA	266xØ88	10.0	10.0	\$458	BLDC, 12V, 40A
3		RECIRC PUMP CONTROLLER		1	EA	100x150x100	0.5	0.5	—	Powered by High Voltage Bus 1 kW max
3		FUEL REGULATOR 1		1	EA	300xØ100	1.0	1.0	\$70	
3		FUEL REGULATOR 2 / METER		1	EA	119xØ63	2.7	2.7	\$150	12 V, 0.4 A
3		AIR BACK-PRESSURE VALVE		1	EA	65xØ100	2.0	2.0	\$70	
3		G/G HUMIDIFIER		1	EA	411 xØ200	6.1	6.1	\$300	
3		H2 PURGE VALVE		1	EA	50x50x97	0.5	0.5	\$70	12 V, 0.8 A
3		CONNECTORS		1	EA	1617xØ32	5.4	5.4	\$200	
2		TRACTION DRIVE INSTALLATION	Q	1	EA			84.6	\$2,463	

Continued on next page

Item #	BOM Level	ASSEMBLY / COMPONENT	VENDOR	QTY ASM	U/M	Size LxWxH [mm]	Item Mass [kg]	Extended Weight [kg]	USD - 2015 Price - (100K/year)	Comments
	3	TRACTION MOTOR- 75 kW Peak, 55 kW Continuous		1	EA	241xØ350	45.5	45.5	\$1,923	8 L/min WEG 50/50, 55C max inlet
	3	T-MOTOR		1	EA	380x365x119	15.9	15.9	—	8 L/min WEG 50/50, 55C max inlet
	3	INVERTER/CONTROLLER- 75 kW Peak, 55 kW Cont.		1	EA	250xØ250	15.0	15.0	\$300	
	3	TRANSAXLE / DIFFERENTIAL		2	EA	230xØ94	4.1	8.2	\$240	Based on GKN Type 102 / Joint 10
	3	HALF-SHAFTS		1	EA			27.3	\$1,053	
3	2	TRACTION BATTERY SYSTEM	Q	1	EA			27.3	\$1,053	334 Volt Nominal, 378 Volt Max., 297 Volt Min.
	3	BATTERY PACK(Li ION) & CONTROLLER		1	EA	Varies: 0.025 m3	27.3	27.3	—	
	4	CONTROLLER / WIRING / THERMAL MGMT		1	EA	—	6.3	—	—	
	4	BATTERY PACK		1	EA	—	21.0	—	—	2.3 kW-h
	5	BATTERY MODULE		30	EA	100x60x95	0.7	—	—	
	6	BATTERY CELLS		6	EA	—	0.1	—	—	130 W-h / kg; 13 W-h / cell
4	2	ELECTRICAL AND ELECTRONICS	E	1	EA			31.5	\$1,918	
	3	FC POWER ELECTRONICS DC-DC	Q	1	EA	230x330x120	11.8	11.8	\$1,034	DC input voltage: Variable 330 to 440 V, 225 A Max DC output voltages: Constant 400 V Max: 74 kW Input; 71 kW, (178 A) Output. Water Cooled, 3.0 kW heat generated. 55C max inlet

Continued on next page

Item #	BOM Level	ASSEMBLY / COMPONENT	VENDOR	QTY ASM	U/M	Size LxWxH [mm]	Item Mass [kg]	Extended Weight [kg]	USD - 2015 Price - (100K/year)	Comments
3		DC-DC CONVERTER	Q	1	EA	253x257x79	4.9	4.9	\$429	DC input voltage: 250 to 425, 10A Max DC output voltages: 13.8 @ 2.2 kW (157 A) @ 90% Eff. 10L/min WEG 50/50 75C Max Inlet
3		HYBRID CONTROLLER	Q	1	EA	200x150x50	0.6	0.6	\$200	
3		HARNESS LOW VOLTAGE	Q	1	EA	Varies	0.2	0.2	\$80	
4		HIGH VOLTAGE CABLE	Q	30	M	—	0.01	—	—	18 AWG Copper 4-92 lb/1000 ft
3		HARNESS HIGH VOLTAGE	Q	1	EA	Varies	5.7	5.7	\$150	
4		HIGH VOLTAGE CABLE	Q	6	M	—	1.0	—	—	4/0 AWG Copper 641 lb/1000 ft
3		FUSE BLOCK	E	1	EA	150x150x100	0.2	0.2	\$25	
3		MISC. ELECTRICAL	Q	1	EA		8.0	8.0		
5		EXHAUST SYSTEM	S	1	EA			3.2	\$60	
3		FC STACK-TO-TAILPIPE TUBING		3	M	Varies xØ50	1.1	3.2	\$60	0.36 kg/m 50mm OD, 0.3 mm wall
6		FUEL SYSTEM	Q	1	EA			87.1	\$7,919	
3		FUEL TANK ASSEMBLY, 95 L , 3.4 kg H2		1	EA	710xØ560	62.0	62.0	\$6,000	70 mPa system
3		FUEL SUPPLY LINES		4	M	Varies xØ6	0.8	3.0	\$400	0.19 kg/m 13mm OD, 0.6 mm wall
3		FILL LINE		1	M	Varies xØ6	0.2	0.2	\$150	0.19 kg/m 13mm OD, 0.6 mm wall
3		PRESSURE REGULATOR		1	EA	90xØ100	2.0	2.0	\$80	
3		TANK VALVES		1	EA	50xØ150	3.0	3.0	\$1,019	
3		TUBING		3	M	Varies xØ13	0.3	0.9	\$60	0.09 kg/m 6 mm OD, 0.6 mm wall
3		SHUT-OFF VALVE		1	EA	50x50x100	1.0	1.0	\$60	

Continued on next page

Item #	BOM Level	ASSEMBLY / COMPONENT	VENDOR	QTY ASM	U/M	Size LxWxH [mm]	Item Mass [kg]	Extended Weight [kg]	USD - 2015 Price - (100K/year)	Comments
3		BRACKETS AND WIRING		1		Varies	15.0	15.0	\$150	
7	2	COOLING SYSTEM	E	1	EA			0.0	\$0	
	3	FAN - ELECTRIC COOLING		1	EA			0.0		
	3	FAN CONTROLLER		1	EA			0.0		
	3	ELECTRIC COOLANT PUMP		1	EA			0.0		45 L/min (FC Stack)
	3	RADIATOR - FC STACK COOLANT		1	EA			0.0		47 kW Rejection, 45 L/min, 85C max Inlet, 70C max Outlet @ 40C Ambient
	3	ELECTRIC COOLANT PUMP		1	EA			0.0		42 L/min (10 L/min DC/DC Converter, 32 L/min Motor-Controller)
	3	RADIATOR-ELECTRONICS		1	EA			0.0		14.2 kW Heat Rejection (0.2 kW DC/DC, 7 kW Motor Inverter, 7 kW Motor), 42 L/min, 55C max Outlet @ 60C max Inlet, 40C Ambient
8	2	DRIVER - DRIVETRAIN INTERFACE	E	1	EA			1.1	\$0	
	3	THROTTLE PEDAL/SENSOR ASSEMBLY		1	EA	193x49x275	0.3	0.3	\$0	
	3	BRAKE PEDAL/ SWITCH ASSEMBLY		1	EA	193x49x275	0.3	0.3	\$0	
	3	GEAR SELECTION ASSEMBLY		1	EA	75x50x50	0.3	0.3	\$0	
	3	DRIVER INFORMATION DISPLAY		1	EA	10x305x125	0.2	0.2	\$0	OLED Technology

VENDOR CODE: Q = QUANTUM; U = UQM; E = EDAG; S = SFCV

Table 5.30: Bill of materials : FSV-2 - FCEV

5.13 Vehicle Performance - Results Summary

The summary Table 5.31 shows that all four Future Steel Vehicle variants meet the expected vehicle performance targets. However, the continuous hill climb capability at higher speeds was allowed to deviate to some extent. Most drivers do not often encounter this driving condition, therefore the limited performance in terms of vehicle speed, while ascending, could to be allowed as it does not affect the ability of the vehicle to get to the top of a hill. The benefit of this decision is that all powertrain components can remain smaller lighter and more efficient, having a significant benefit in fuel consumption and green house gas emissions for the typical driving patterns of most drivers.

	Capability			
	FCEV	PHEV ₄₀	EV	PHEV ₂₀
Performance				
Acceleration				
0 - 100 $\frac{\text{km}}{\text{h}}$, Curb + Driver				
Peak Grade				
30/40 $\frac{\text{km}}{\text{h}}$ - 30 sec., GVW				
Continuous Grade				
73 $\frac{\text{km}}{\text{h}}$ - Continuous, GVW				
90 $\frac{\text{km}}{\text{h}}$ - Continuous, GVW				
100/112 $\frac{\text{km}}{\text{h}}$ - Continuous, GVW				
Top Speed				
Continuous, GVW				
Range				
Curb + Driver, UDDS				



Limited Performance = 
 Unable to Perform = 

Table 5.31: Vehicle simulation results summary

5.14 Powertrain Design Evaluation Results

The powertrain components were selected and sized using the PSAT simulation tool for optimized performance and fuel efficiency. In the vehicle performance, ultimate grade climbing speed, not ability, was sacrificed to some extent, which allowed the use of smaller, lighter components and their ability to perform closer to their peak efficiency ratings for longer durations.

With cost and weight of new technologies remaining to be key vehicle design impacting parameters, the conclusion for the Future Steel Vehicle study is that hybridization and plug-in technology deployment is going to be the commercially viable industry trend for 2015 and even 2020.

Fuel cost or government incentives or subsidies, may accelerate the rate of new technology evolution for battery and fuel cell technologies, as well as cause a shift in driving behavior patterns, regionally, nationally and globally.

A comparison of the key parameters and characteristics of all four FSV variants is shown in Figure 5.25.

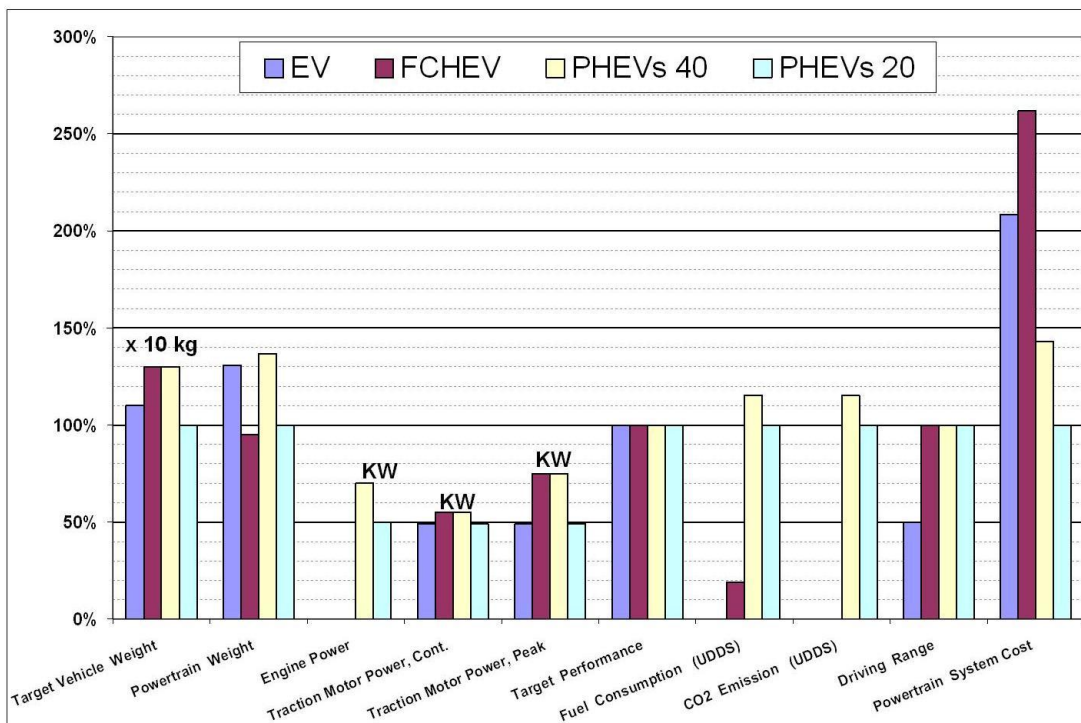


Figure 5.25: FSV powertrain key parameters comparison

5.15 Fuel Economy and Emissions

As part of the PSAT powertrain and vehicle simulations, fuel consumption and emission values for each of the FSV variants were predicted. A comparison between drive cycles typically used in North America, Europe and Japan was conducted to evaluate the vehicle's sensitivity to different regional certification standards. For each charge depleting operation, the drive cycle used for the simulations study, was repeated multiple times back-to-back until the charge in the battery was depleted. For charge sustaining operation, the drive cycle was repeated two times. The results of the Tank-to-Wheel fuel and electrical economy on the FSV variants analyzed using PSAT are tabulated in Table 5.32. This table also shows that the fuel economy and CO₂ values from the vehicle operation are extremely favorable when compared to today's hybrid vehicle.

		UDDS	Japan 10-15	NEDC
PHEV₄₀ Series Mid-size: 1300kg Vehicle + 75kg driver				
Charge Depleting	[Wh / km]	107	110	111
	[L / 100km]	0	0	0
	[g CO ₂ / km]	0	0	0
Charge Sustaining	[Wh / km]	0	0	0
	[L / 100km]	3.8	3.79	3.79
	[g CO ₂ / km]	88.4	88	88
PHEV₂₀ Series Small-size: 1000kg Vehicle + 75kg driver				
Charge Depleting	[Wh / km]	92.5	94.9	96.9
	[L / 100km]	0	0	0
	[g CO ₂ / km]	0	0	0
Charge Sustaining	[Wh / km]	0	0	0
	[L / 100km]	3.3	3.27	3.43
	[g CO ₂ / km]	76.7	76	79.8
EV Series Small-size: 1100kg Vehicle + 75kg driver				
	[Wh / km]	88.9	92.8	96.4
	[g CO ₂ / km]	0	0	0
FCEV Series Mid-size: 1300kg Vehicle + 75kg driver				
	[kg / 100km]	0.632	0.669	0.653
	[g CO ₂ / km]	0	0	0

Table 5.32: Fuel economy and emissions

For each PHEV, both Charge Sustaining (CS) and Charge Depleting (CD) modes are also shown. The FCEV is displayed as fueled by hydrogen from two sources: Natural Gas reformation (NG) and US average utility grid electrolysis. On a Tank-to-Wheel basis, all four FSV powertrain variants will emit less than $95 \frac{\text{g}(\text{CO}_2)}{\text{km}}$.

Further details on this topic can be found in "Chapter 7 - Environmental impact", of this report.

5.16 FSV-1 Cost of Ownership

The cost of ownership of a vehicle is divided into the cost of the vehicle itself and the cost of the fuel. The Table 5.33 shows the breakdown of these costs for the FSV-1 when compared to a similar sized 2020 gasoline driven ICE vehicle and a 2020 hybrid electric vehicle. The cost of the vehicle for FSV-1 variants are higher than the ICE and the HEV variants, driven mainly by the high cost of the battery (\$15,750 and \$2250) for the BEV and PHEV₂₀. However, the cost of fuel (electricity) for the FSV-1 vehicles are much lower (\$0.12 per kWh) than the ICE and HEV fuel (gasoline) at \$1.18 per liter.

	Petroleum Based				FSV-1 Dual Fuel Based Electricity form Grid and Petroleum			
	ICE 2020 18 $\frac{\text{km}}{\text{l}}$ (42.7 MPG)		HEV 2020 27.2 $\frac{\text{km}}{\text{l}}$ (64 MPG)		BEV - EV 114 $\frac{\text{Wh}}{\text{km}}$		PHEV ₂₀ 106 $\frac{\text{Wh}}{\text{km}}$ & 26.7 $\frac{\text{km}}{\text{l}}$ (62.7 MPG)	
	[total \$]	[per km]	[total \$]	[per km]	[total \$]	[per km]	[total \$]	[per km]
Vehicle Cost	16,250	0.081	18,090	0.090	32,535	0.163	22,810	0.114
Overhead	6,094	0.030	6,094	0.030	6,094	0.030	6,094	0.030
Vehicle Cost without powertrain	7,746	0.039	7,746	0.039	7,746	0.039	7,746	0.039
Powertrain Cost	2,350	0.012	3,350	0.017	2,945	0.015	6,720	0.034
Battery Cost	60		900	0.005	15,750	0.079	2250	0.011
Vehicle Use Cost	14,097	0.070	9,738	0.050	2,731	0.014	6,232	0.030
Gasoline \$1.18 per l (\$4.50 per gal US)	13,097	0.065	8,738	0.044			4,460	0.022
Oil Change \$40 \$40 per 8,000 km	1,000	0.005	1,000	0.005			500	0.003
Electricity \$0.12per kwh					2,731	0.014	1,272	0.006
Total Cost of Ownership	30,346	0.152	27,828	0.139	35,266	0.176	29,041	0.145

Table 5.33: Cost of ownership - FSV-2

The conclusion derived from the above table is that even though the initial costs of the vehicle is high for the PHEV₂₀, the operating cost per kilometer over the life of the vehicle (200,000 km) is \$0.14 which is lower than the ICE operating costs of \$0.15 per kilometer. The BEV costs per kilometer at \$0.17 is significantly higher than the HEV and ICE operating costs per kilometer at (\$0.13) & (\$0.15) respectively. The PHEV₂₀ is the most cost effective solution in this case study.

5.17 FSV-2 Cost of Ownership

5.17 FSV-2 Cost of Ownership

Similar to the previous analysis for the FSV-1, Table 5.34 shows the breakdown of these costs for the FCEV and PHEV₄₀. In this case, the cost of the vehicle for FSV-2 variants are higher than the ICE and the HEV variants. Primary reason is the high cost of the powertrain for the PHEV₄₀ and FCEV (\$22,458 and \$7554) versus those of the ICE and HEV (\$3100 and \$4350). High battery costs also factors into the total vehicle cost for the PHEV₄₀. However, the cost of fuel for the FSV-2 variants are lower than the ICE and HEV variants primarily due to the low cost of electricity (\$0.12 per kWh) versus the cost of gasoline for the ICE and HEV (\$1.18 per liter).

	Petroleum Based				Hydrogen Gas Comp. 70 Mpa FCEV 0.632 $\frac{\text{kgH}_2}{\text{km}}$		Electricity & Petroleum PHEV ₄₀ 119 $\frac{\text{Wh}}{\text{km}}$ & 20 $\frac{\text{km}}{\text{l}}$ (47 MPG)	
	ICE 2020 16 $\frac{\text{km}}{\text{l}}$ (38MPG)		HEV2020 19 $\frac{\text{km}}{\text{l}}$ (45MPG)		[total \$]	[per km]	[total \$]	[per km]
Vehicle Cost	21,760	0.110	23,910	0.120	42,153	0.210	31,479	0.160
Overhead	8,160	0.041	8,160	0.041	8,160	0.041	8,160	0.041
Vehicle Cost without Powertrain	10,500	0.053	10,500	0.053	10,500	0.053	10,500	0.053
Powertrain Cost	3,100	0.016	4,350	0.022	22,458	0.112	7554	0.038
Battery Cost			900	0.005	1,035	0.005	5265	0.026
Vehicle Use Cost	15,717	0.080	13,427	0.070	6,320	0.030	6,873	0.030
Gasoline \$1.18 per l (\$4.50 per Gal US)	14,717	0.074	12,427	0.062			4,759	0.024
Oil Change \$40 Per 8050 km	1,000	0.005	1,000	0.005			400	0.002
Electricity \$0.12 per kwh							1,714	0.009
Hydrogen \$5.00 per kg					6,320	0.032		
Total Cost of Ownership	37,477	0.190	37,337	0.190	48,473	0.240	38,352	0.190

Table 5.34: Cost of ownership - FSV-1

The conclusion from the above table is that even though the initial costs of the vehicle is high for the PHEV₄₀, the operating cost per kilometer over the life of the vehicle (200,000 km) is similar to that of the ICE and HEV variants. The total operating costs of PHEV₄₀ is \$0.19 per kilometer. The FCEV is significantly higher at \$0.24 per kilometer.

6.0 Vehicle Package Development

6.1 Synopsis

This section of the report focuses on the developmental history of the FSV electric drive (electric motor, inverter and controller), Fuel cell system (fuel cell stack, hydrogen storage, humidifiers, etc) and the engine/generator. Design studies were undertaken to achieve the best possible packaging for the FSV application without sacrificing the vehicle performance and design targets established early during the course of the project.

6.2 Electric Drive

6.2.1 Motor Vertical - in Line with Axle Centerline

Very early design and packaging of the electric drive assembly started with motor assembly packaging studies. The initial position of the motor was vertical with the motor centerline in line with the front axle centerline of the vehicle as shown in Figure 6.1.

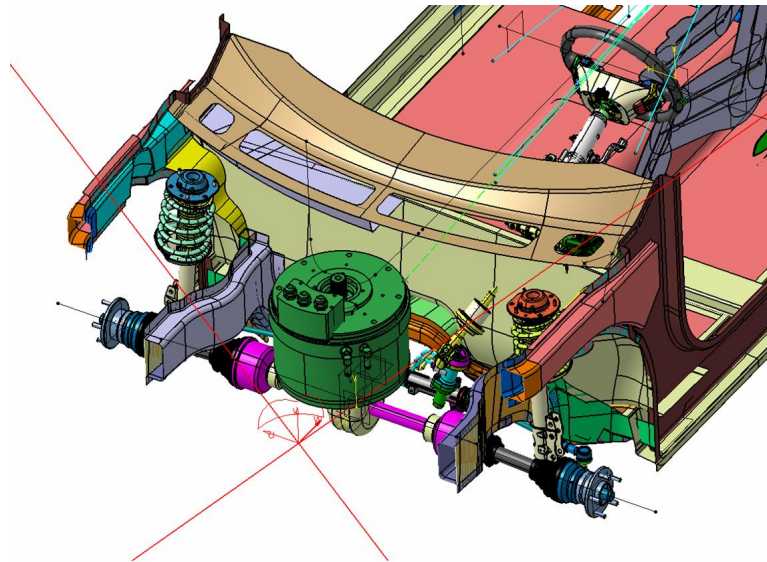


Figure 6.1: Motor vertical

6.2.1.1 Design Study Outcome

This design study revealed some inherent issues with the orientation of the motor in its current state. The related torque that it developed would induce undue stress on the body structure and did not optimize the packaging in the vehicle. The differential and gearbox assembly would have to be modified to accommodate this type of motor packaging and the next set of design studies focused on this aspect.

6.2.2 Motor Horizontal - Front of Axle Centerline

Lessons learned from the previous packaging study led the team to the conclusion that the motor would be more effectively packaged in the horizontal position with the motor centerline in front of the axle centerline as shown in Figure 6.2. In this design for the PHEV₂₀ variant of the FSV, the IC engine is also packaged along with the electric motor.

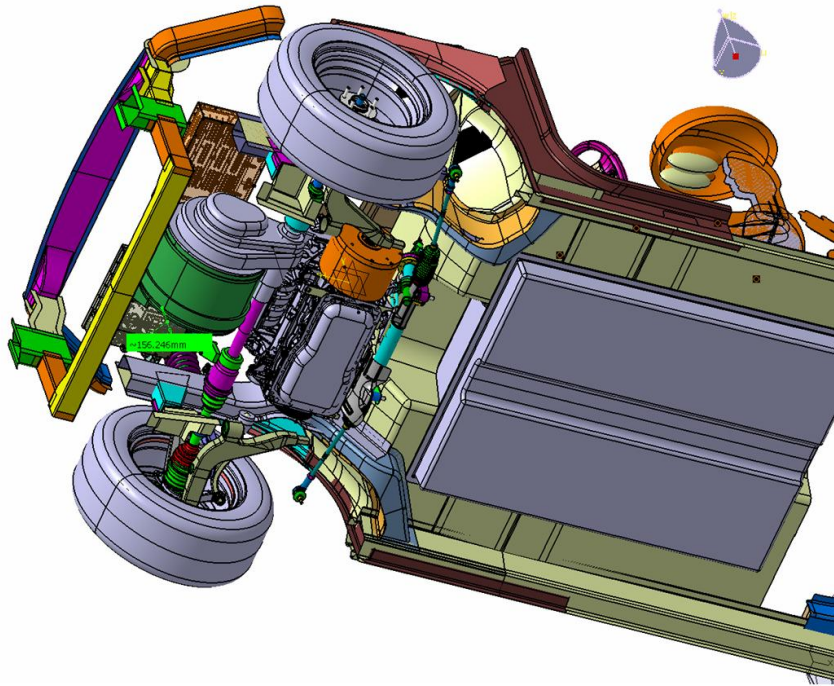


Figure 6.2: Motor Horizontal in front of axle

6.2.2.1 Design Study Outcome

This design package resulted in better utilization of packaging space as compared to the earlier vertical placement design, but at the same time became a disadvantage in terms of front crush space. Since the motor is a rigid body and was in the direct line of the stack-up, in case of a high speed frontal impact, it was not advisable to package the motor in this location in terms of front-end crush management which is critical during the first few milliseconds of the crash event. One more negative outcome of this packaging of the engine behind motor was that it led to a longer front-end of the vehicle. This led to further design studies to optimize the front-end for crush space and also reduce the front-end length for the PHEV variants.

6.2.3 Motor Horizontal - Rear of Axle Centerline

Using the lessons learned from earlier designs, the motor was now placed in the horizontal position but now with the motor centerline rearward to the vehicle front axis and the inverter/controller was packaged towards the front of the vehicle, just behind the radiator, as shown in Figure 6.2 and Figure 6.3 respectively.

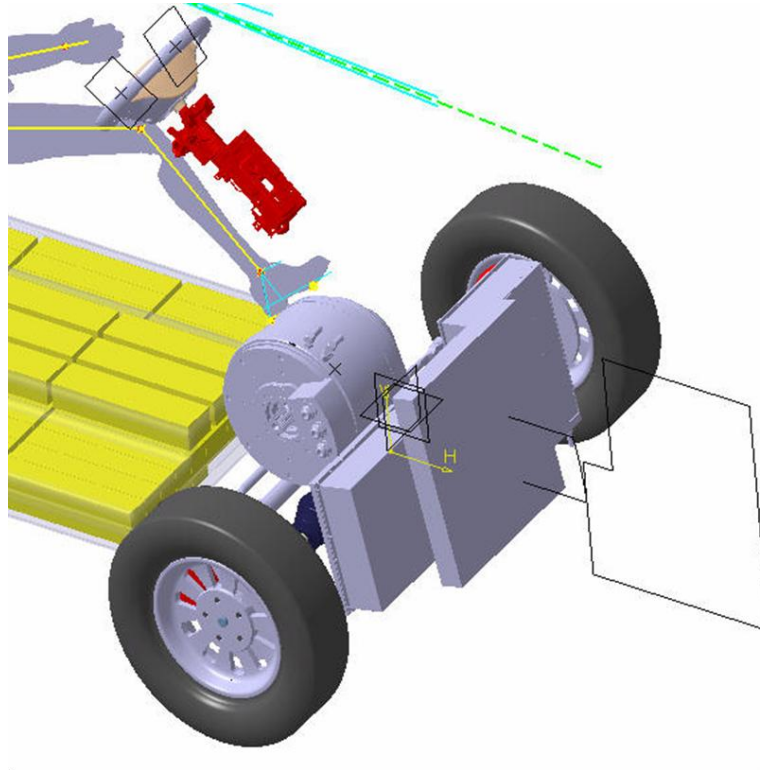


Figure 6.3: *Inverter and controller - front*

6.2.3.1 Design Study Outcome

From this design study, the motor location was better optimized in terms of crash energy management, however, the location of the controller/inverter, which was behind the radiator could possibly hinder the crush space in the event of a frontal impact. The next iteration of the design study was to optimize the controller/inverter locations.

6.2.4 Motor Horizontal - Inverter/Controller on Top

From the previous design study and its outcome, the location of the controller and inverter was redesigned and moved on top of the motor as shown in Figure 6.4 resulting in an optimized front-end packaging with an adequate crumple zone in the event of a frontal impact and leading to a much more efficient management of underhood space as compared to previous designs.

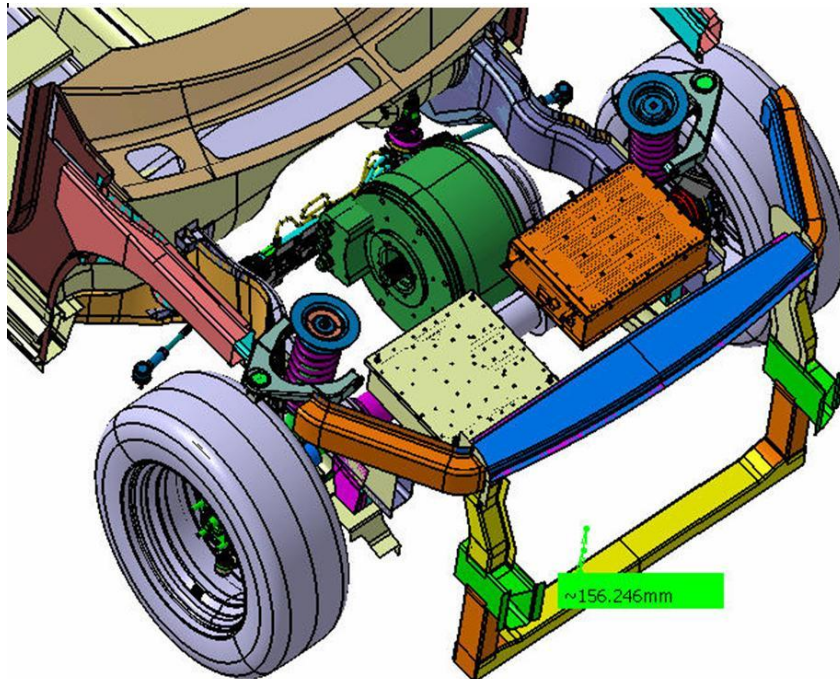


Figure 6.4: Motor- Rear of axle, inverter - on top

6.2.4.1 Design Study Outcome

After the completion of this design study, the inverter/controller was mounted on to the top side of the motor assembly. However, the location of the motor and the motor itself needed further optimization for more efficient management of underhood space, since the current motor required a gearbox and a differential to be coupled to it. The next few design studies focused on the motor assembly and integration of its accessories in the vehicle.

6.2.5 Motor - Integrated Design Concept

As a part of this study, the electric motor as an assembly was reviewed and redesigned based on the following:

- Quantum supplied motor assembly interfaced with a differential and gearbox and did not make use of available package space efficiently
- Research on the 2009 Honda FCX Clarity motor assembly revealed an integrated differential and parking brake, based on which, a generic FSV motor was designed as shown in Figure 6.5
- This generic motor model then evolved into a real design concept for the FSV as shown in Figure 6.6

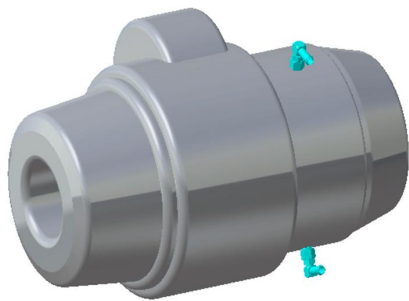


Figure 6.5: *Integrated motor - generic*

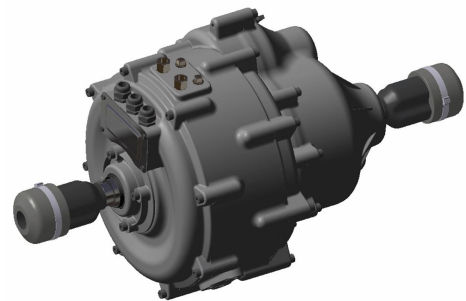


Figure 6.6: *Integrated motor - evolved*

6.2.5.1 Design Study Outcome

After the completion of this design study, a good center of gravity along with the most efficient usage of packaging space could be achieved as the differential and other accessories of the motor were now a part of the motor assembly. Further studies were conducted to refine the packaging of this new motor design.

6.2.6 Motor - Final Optimised Design

This packaging study was mainly focused on the design and packaging of the new integrated motor for the FSV. Since this new motor did not require a separate differential and gearbox assembly, it was placed in line with the axle and the inverter/controller assembly packaged on top of the motor. The final optimized design packaging of the electric drive assembly for the Future Steel Vehicles is shown in Figure 6.7.

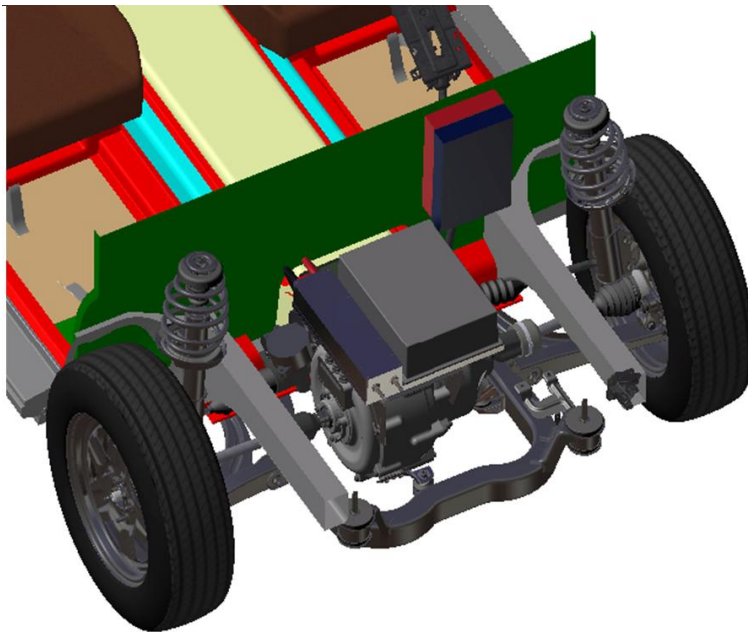


Figure 6.7: *Electric drive- final design and packaging*

6.2.6.1 Design Study Outcome

After the completion of this design study, the electric drive on the FSV had achieved:

- Optimized utilization of underhood space resulting in a significantly short front-end (compared to vehicles in its class)
- Integrated motor assembly
- Optimized vehicle balance achieved due to optimized location of the vehicle's center of gravity

6.3 Battery

6.3.1 Single Large Underfloor Battery

The preliminary battery studies on the FSV were focused on a single large rectangular pack under the floor of the vehicle. Since the battery technology research activity was in its infancy at this time, the main intension of this phase of study was to ascertain if such a large battery pack could be packaged within the physical boundaries of the vehicle structure. This was starting point for all future studies on the battery. Figure 6.8 shows the location of the 35 kWh battery pack for BEV.

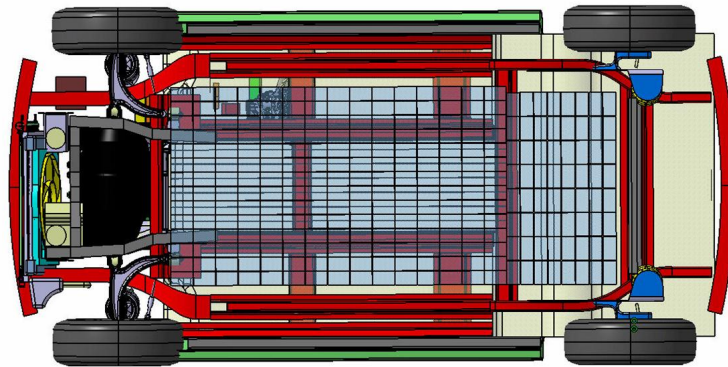


Figure 6.8: *Single large rectangular battery pack*

6.3.1.1 Design study outcome

This preliminary study revealed that even though such a large battery pack setup was theoretically possible to be packaged, it interfered with the structure of the vehicle to a large extent resulting in loss of ability to design a robust vehicle structure. This design also raised the floor height of the vehicle more than a 75 mm, which in turn raised the overall vehicle height and also increased drag, which is undesirable for a vehicle of this type and size.

6.3.2 Two Pack Design - Tunnel area and Underhood

This study focused on the different battery module packaging variations. One of the design studies added an additional battery pack under the hood of the vehicle up against the firewall, essentially creating a T-section as shown in Figure 6.9. The tunnel area was now used a lot more than in earlier designs and the battery pack itself was narrow enough to eliminate the constraints faced with the structure of the vehicle.

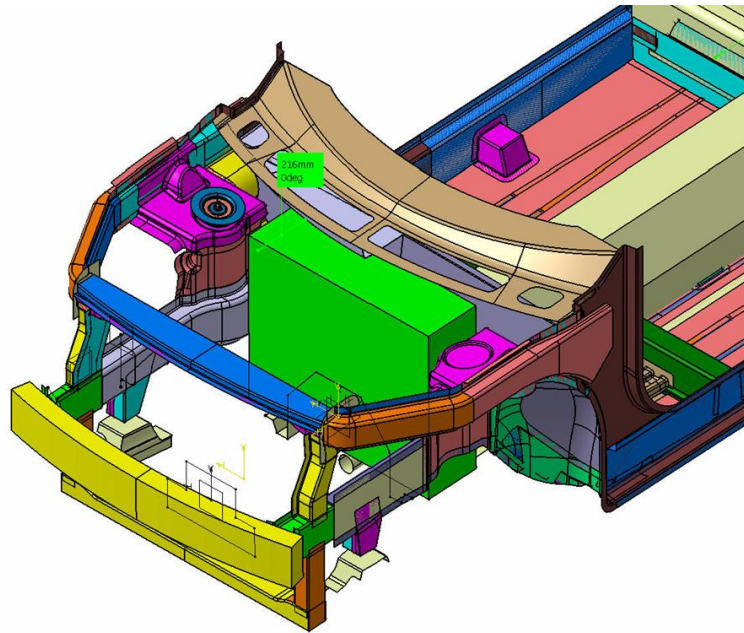


Figure 6.9: *additional pack under the hood*

6.3.2.1 Design Study outcome

While this battery pack design and packaging seemed to relieve the constraints placed on the design of the vehicle structure, a new problem in terms of vehicle crush zones were identified. The battery pack was now a part of the front-end stack-up, and now seemed like an inefficient package in terms of vehicle safety. This design led a decision that the right location for the battery pack is under the tunnel area, between the firewall and the rear seat back. Future design studies were focused on achieving this.

6.3.3 T-Shaped Pack - Preliminary Design

Previous design packaging studies revealed that a T-shaped battery pack would be an appropriate shape for the FSV application. The first step was to remove the additional battery pack previously packaged in the engine compartment and package it under the rear seats, thus creating a perfect T-shaped battery pack. This made use of the tunnel space more effectively and did not interfere with any of the vehicle structures. The pack is shown in Figure 6.10 and location of the battery pack in the vehicle is shown in Figure 6.11.

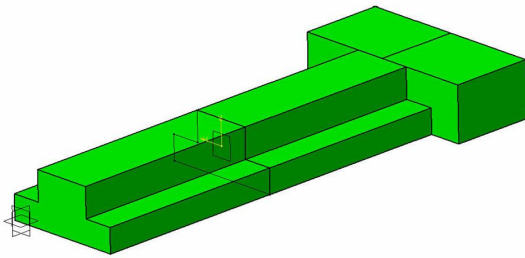


Figure 6.10: *T shaped battery pack*

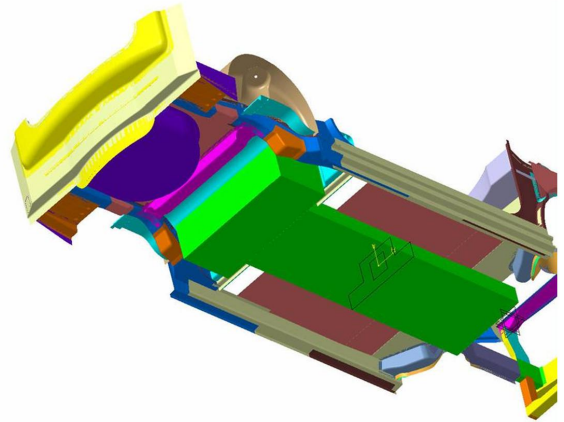


Figure 6.11: *Packaging in vehicle*

6.3.3.1 Design Study Outcome

This above design of the battery met most of the critical packaging requirements for the FSV battery pack. The H point of the rear passenger was lowered and the battery pack was not in the way of any load carrying structures on the vehicle. However, this design of the battery pack had some disadvantages in terms of the 5th passenger seating and needed some refinements in that area.

6.3.4 T-Shaped Pack - Refined

Additional design iterations models of the T-shaped battery pack discussed in the previous section were run and Figure 6.12 is one of them. In this particular design, individual modules have been rearranged with a few of them stacked up under the rear seats. Some modules have been distributed around the tunnel area with the intension of maximizing the battery pack structure so that the battery pack could also act as a load path in the event of a side impact. The packaging of this battery in the vehicle is as shown in Figure 6.13.

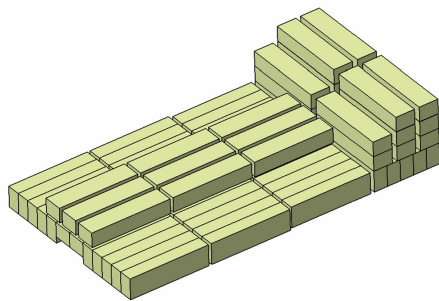


Figure 6.12: *More refined T-shaped battery*

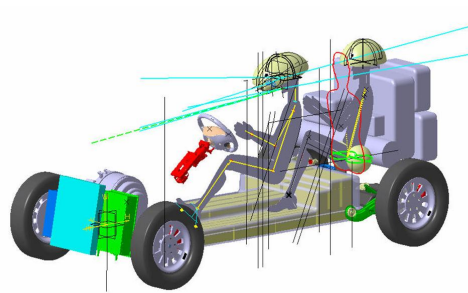


Figure 6.13: *Packaging in vehicle*

6.3.4.1 Design Study Outcome

This design of the battery pack resulted in the rear passenger seating position to be raised by about 50 mm. The next set of design studies focused on optimizing the rear floor space to provide a more comfortable seating position for the rear passengers, particularly the middle seat occupant.

6.3.5 T-Shaped Pack - Reorganized Cell Arrangement

The T-section battery was further revised based on the rear middle seat passenger space and also Quantum's new 450 cell count requirement for the BEV battery pack. The battery pack shown in Figure 6.14 has cells reorganized within the outer T-shell. The pack has been minimized in 2 locations under the rear passenger seating areas. Figure 6.15 shows the location of this battery in vehicle position.

1. Foot well
2. Seat mount area

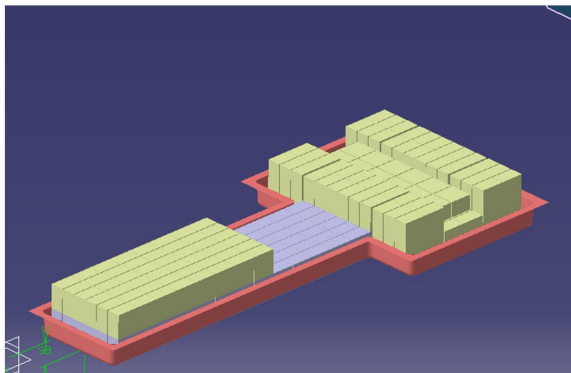


Figure 6.14: Battery pack with minimized areas

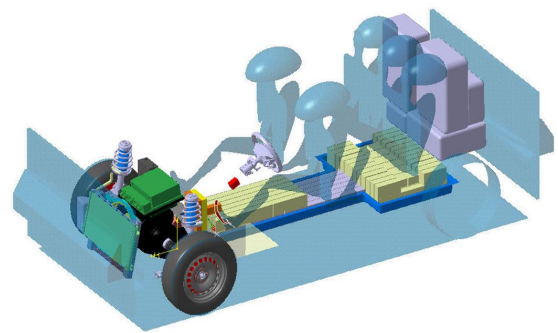


Figure 6.15: Packaging in vehicle

6.3.5.1 Design Study Outcome

This design indicated that minimizing the battery pack underneath critical areas provided additional interior passenger space. Further refinements were needed to distribute the individual modules evenly throughout the pack. The next design study concentrated on these refinements.

6.3.6 T-Shaped Pack - Under-seat Pods

This design study focused on the refinements on the distribution of individual battery modules discussed in the previous section. Additional space beneath the front seats were utilized to package some battery modules creating underseat pods as shown in Figure 6.16. This design resulted in reduced height of the battery pack underneath the rear seats, resulting in lowering the H-point of rear seat passengers. The location of this battery pack in the vehicle is shown in Figure 6.17.

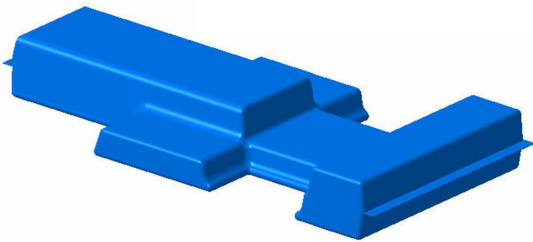


Figure 6.16: *Battery pack w/under seat pods*

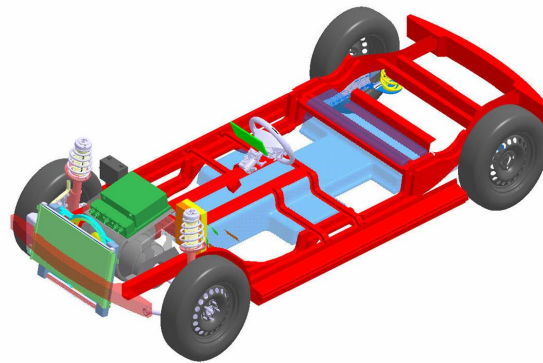


Figure 6.17: *Packaging in vehicle*

6.3.6.1 Design Study Outcome

This design posed a formidable challenge in terms of cooling characteristics (FSV battery pack is air cooled) particularly in those areas under the front seat mounts. This modular setup shown in Figure 6.16, did not allow for effective packaging of the individual cell modules, and thus the fins were deleted in the next design.

6.3.7 T-Shaped Pack - Refined with Accessories

Based on previous design package exercises and Quantum's input, the battery pack underwent some final refinements and the outcome was a T-section with minimized modules under the rear passenger foot well area. With the shape and location of the battery pack frozen in design, focus was placed on the other aspects of a battery pack design as shown in Figure 6.18. This included addition of the following:

1. Coverplate - for protection of battery components
2. Tray - for protection and attachment to the vehicle
3. Bulk heads - to provide additional stiffness
4. Separators - Protection from environment
5. Aero package - to smooth air flow underneath the battery

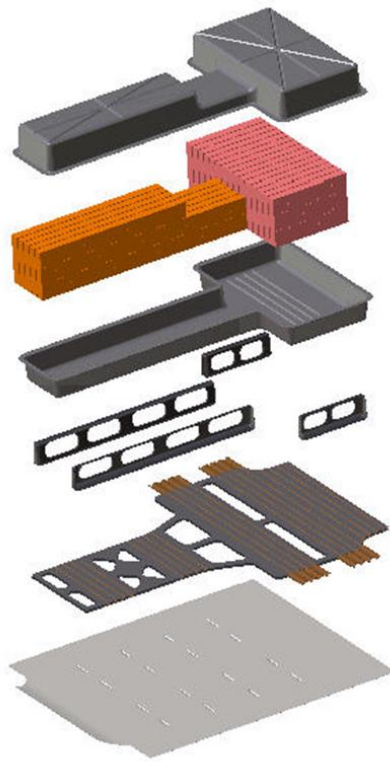


Figure 6.18: Battery pack - Assembly

6.3.8 T-Shaped Pack and Sub-Pack - Final design

A final refinement to the FSV battery pack was undertaken to assess the possibility of packaging of individual battery cells into the FSV battery pack design. In this design, modules based on future (2015–2020) Lithium ion technology, were packaged into the FSV battery pack. The size, mass, capacity and energy density at the cell, sub-pack and battery pack level for FSV-1 BEV is shown in the Table 6.1. These numbers are calculated for battery end-of-life, assuming a 20% degradation in battery performance over the life of the vehicle (200,000 km).

FSV Battery Pack	Cell	Sub-Pack	Battery Pack
	468	6	1
Size [l]	0.28	34.5	271
Mass [kg]	0.55	49.1	345
Capacity [kWh]	0.075	5.8	34.9
Energy Density [kWh/kg]	0.14	0.12	0.10

Table 6.1: FSV-1 BEV battery specifications

This sub-pack, shown in Figure 6.19 has 78 individual cells, the battery pack shown in Figure 6.19 has 6 sub-packs and packs the energy capacity required for the FSV-1 BEV. This battery pack, when assembled on the FSV-1 is as shown in Figure 6.20.

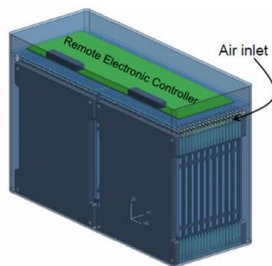


Figure 6.19: FSV-1 sub-pack (78 cells)

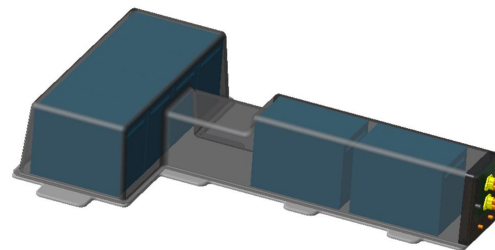


Figure 6.20: 35 kWh pack(6 sub-packs)

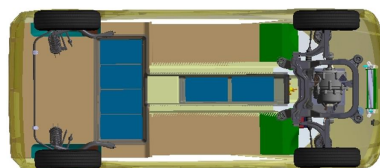


Figure 6.21: FSV-1 battery pack in vehicle

6.3.9 I-Shaped Pack - Packaging Impact

With the battery pack for the FSV-1 BEV defined, an additional study attempting to further reduce the physical foot print of the battery pack was conducted. In this study, an I-shaped battery pack and its impact on the previous battery specifications was identified.

If the FSV-1 retained the 250 km range, a 35 kWh battery pack would need the energy density at the cell level to be at $228 \frac{\text{Wh}}{\text{kg}}$.

If the FSV-1 increased the range to 500 km, cell energy density needed to be at $433 \frac{\text{Wh}}{\text{kg}}$ and a 66 kWh battery pack would be needed (within the same I-shaped physical foot print).

The design of this type of single length 35 kWh battery pack for the FSV-1 and its packaging into the vehicle is shown in Figure 6.22 and Figure 6.23 respectively.

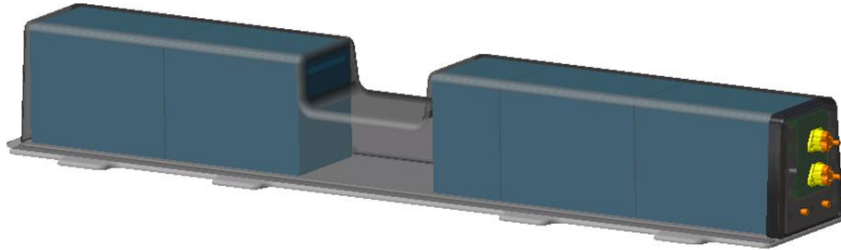


Figure 6.22: FSV-1 35 kWh /66 kWh I pack

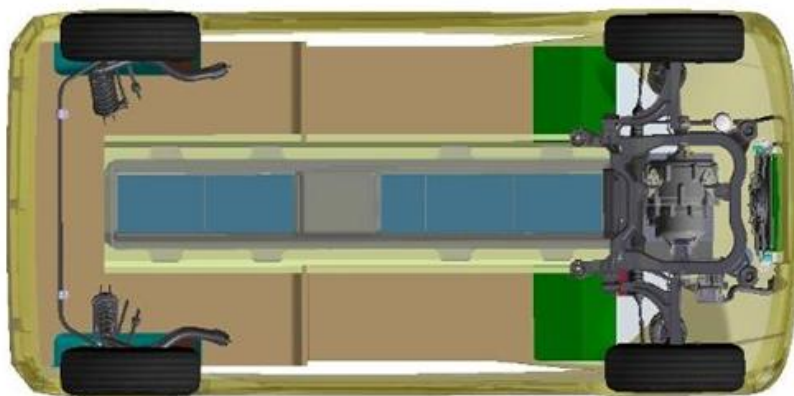


Figure 6.23: Packaging in vehicle

6.3.10 Future Battery Pack and its impact to FSV Structure

This is a study focused on increasing the range of the FSV-1 BEV and assessment of its impact to the battery design. This study also focused on studying the implications of this futuristic battery design on the structure of the vehicle.

If the range of the FSV-1 were to increase to 500 km, battery capacity of the FSV-1 would need to increase to 66 kWh with energy density at the cell level to be at $500 \frac{\text{Wh}}{\text{kg}}$. This energy density number is also the target of NEDO (New Energy and industrial technology Development Organization) for the year 2030. Achieving these target numbers at the cell level would reduce the overall footprint of the battery pack to a large extent. This would essentially allow displacement the current Internal Combustion Engine powertrain on the vehicle with no mass or performance impact on the vehicle.

The Table 6.2 shows the specifications of the FSV battery using the NEDO3 target numbers.

FSV Battery Pack (Same Energy as NEDO3 Target)	Cell	Sub-Pack	Battery Pack
	240	4	1
Size [l]	0.28	25.4	133
Mass [kg]	0.55	37.8	177
Capacity [kWh]	0.275	16.5	66
Energy Density [kWh/kg]	0.5	0.44	0.37

Table 6.2: *FSV-1 Battery specs with NEDO3 targets*

The design of this futuristic battery pack for the FSV-1 and its packaging into the vehicle is shown in Figure 6.24 and Figure 6.25 respectively.

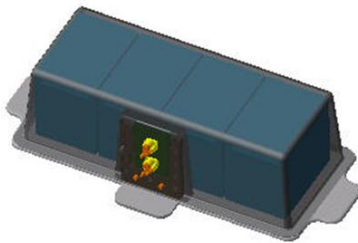


Figure 6.24: *FSV-1 66 Kwh (500 km) pack*

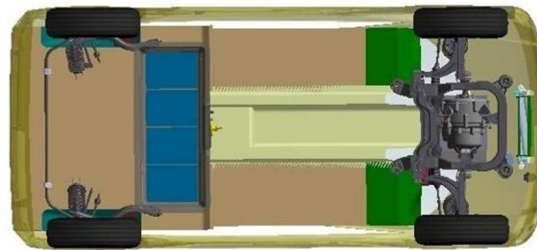


Figure 6.25: *FSV-1 Packaging in vehicle*

The impact of such a design on the structure of the vehicle would not require a tunnel in the vehicle.

6.4 Fuel Cell and Hydrogen Storage

6.4.1 Fuel Cell System in Engine Compartment

The earliest design on the FCEV was to try and package all the fuel cell components (stack, battery, humidifier, hydrogen pump, compressor, etc) in the engine compartment as shown in Figure 6.26. Two hydrogen tanks, each of 61 L capacity, were placed on either side of the rear axle as shown in Figure 6.27.

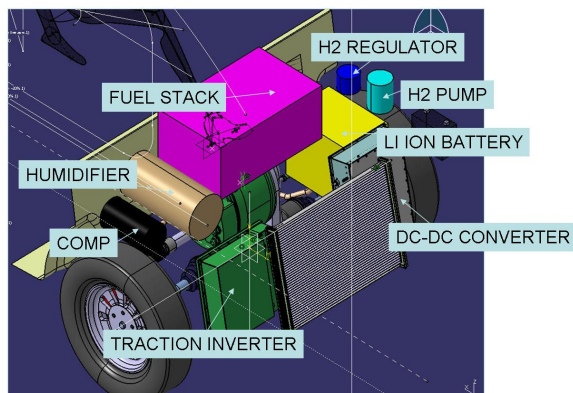


Figure 6.26: Fuel cell components

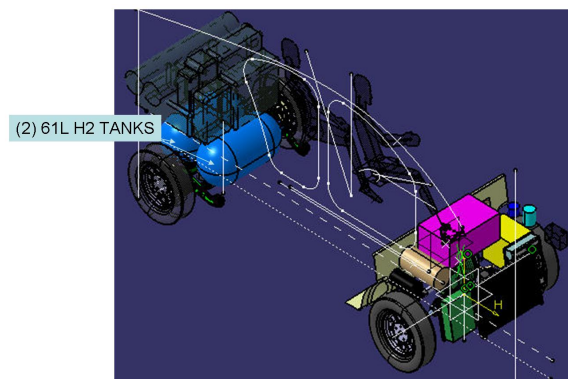


Figure 6.27: Packaging overview with tanks

6.4.1.1 Design Study Outcome

This design had some serious implications on the crash energy management of the vehicle since all the components were now a part of the stack-up during a front-end impact. The position of the fuel cell stack in the current position raised the front-end height and may have required a taller hood with a negative impact on the front field of view. This was an ineffective design and the stack needed repackaging.

6.4.2 Fuel Cell Stack under Inverter/Controller

This design exercise focused on some repackaging of the fuel cell components to reduce the height of the front-end. The fuel stack was now moved underneath the inverter/controller. The Li-ion battery pack was repositioned behind the firewall and in front of the tunnel. The humidifiers were also moved outward closer to the firewall. Smaller, modified hydrogen tanks (61 L each) were now packaged in front of the rear axle under the rear passenger seats. Figure 6.28 shows this type of packaging layout on the FSV.

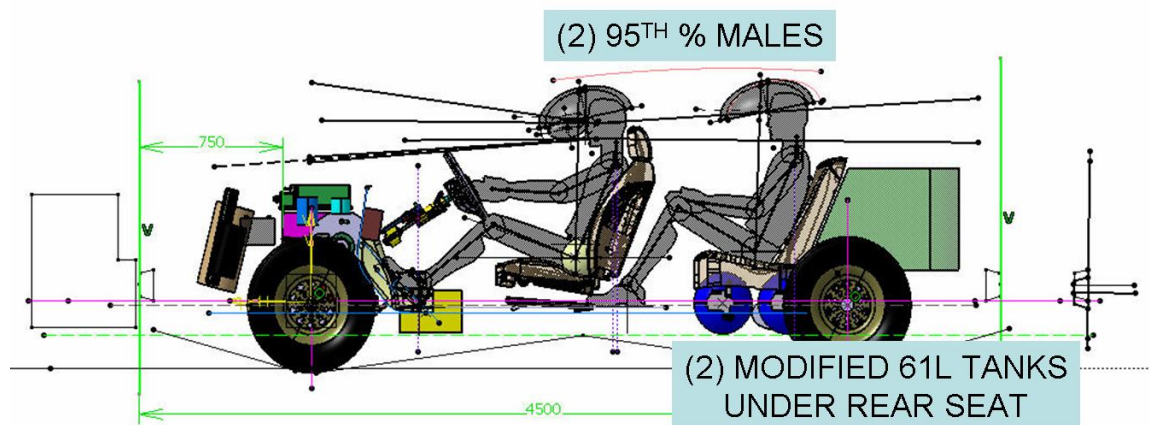


Figure 6.28: *Stack repositioned with modified tanks*

6.4.2.1 Design Study Outcome

This design did reduce the front-end height but did not help improve the vehicle crash energy management characteristics. The front-end (with the stack and all other components) were still a major part of the stack-up and was not an efficient design in terms of energy management during a high-speed frontal impact. The fuel cell components needed to be in close proximity to each other. The hydrogen tanks also altered the weight distribution in an adverse way and needed repackaging. The next design studies focused on a comprehensive packaging of the fuel cell components away from the engine compartment.

6.4.3 Fuel Stack under Rear Seat

Based on the lessons learned from previous studies, this design study repositioned the fuel cell stack, humidifiers and the pump under the rear seat, as shown in Figure 6.29. The front-end of the vehicle was now populated with only the electric drive components. This packaging design allowed for a common front-end with the BEV variant of the FSV which is a huge advantage in terms of manufacturing and design of the vehicle itself.

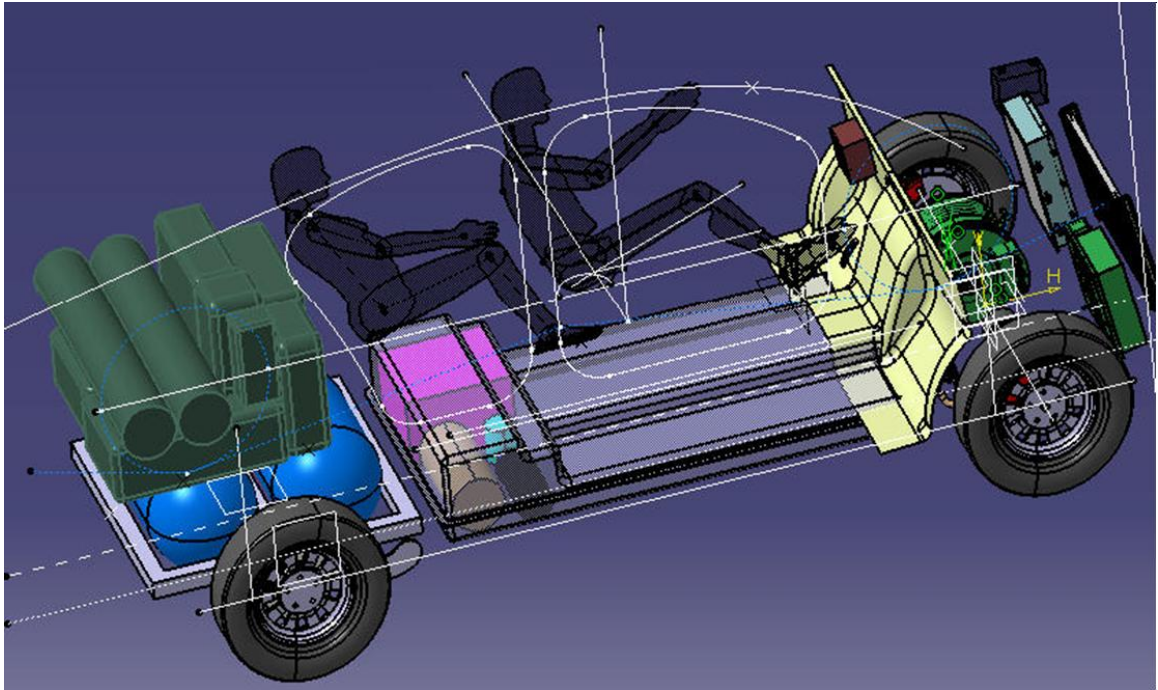


Figure 6.29: Fuel cell stack under the rear seat

6.4.3.1 Design Study Outcome

This concept enabled the FSV BEV and FCEV variants to have a common front-end. However, the placement of the stack under the rear seat did not allow for efficient positioning of the Li-ion battery pack. One of the options considered was to use the same battery case as that of the PHEV variant of the FSV. Further design studies used this concept to refine the position of the fuel cell system and the Li-ion battery pack.

6.4.4 Fuel Cell Stack in Tunnel Area

The fuel cell stack and its accessories were now stacked up in the tunnel area as shown in Figure 6.30. The tunnel area was now widened to accommodate the fuel cell system. The dual tanks were now replaced with one larger 95 L tank with hydrogen stored at higher pressure (700 bar). This larger hydrogen tank had a lower mass and occupied less space in the vehicle, than the dual 61 L tanks. This type of packaging allowed the FSV-2 FCEV to have a larger cargo volume (370 L).

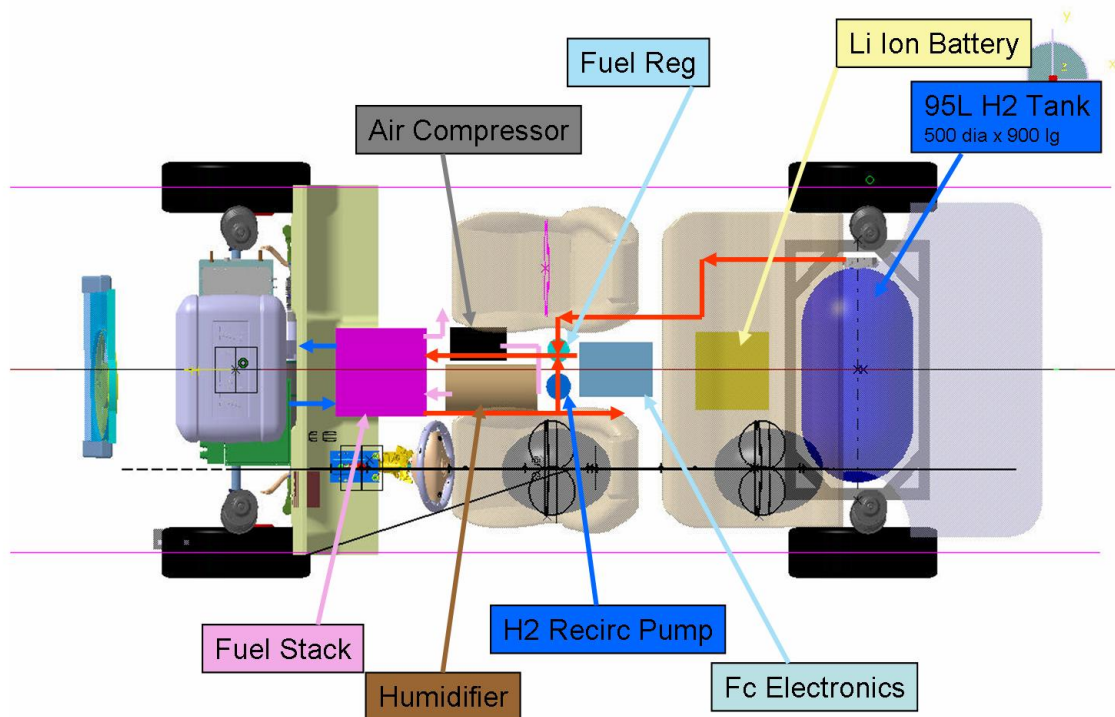


Figure 6.30: *Fuel cell stack in the tunnel*

6.4.4.1 Design Study Outcome

This design proved to be most efficient way for the packaging of the fuel cell system on the FCEV and allowed a common architecture with the BEV. This design was also in line with the working fuel cell bench model specifications provided by Tongji for the FSV. The next final design study was to incorporate this new working model into the FSV and provide the final underbody structure.

6.4.5 Fuel Cell System - Final Design with Tonji system

This design study was to package the working model of the Tongji system into the FSV. The design concept identified in previous studies were conducive to Tongji's fuel cell system and its integration into the FSV. Figure 6.31 shows the Tongji fuel cell system. Figure 6.32 shows the final design layout of the FCEV with the Tongji system.

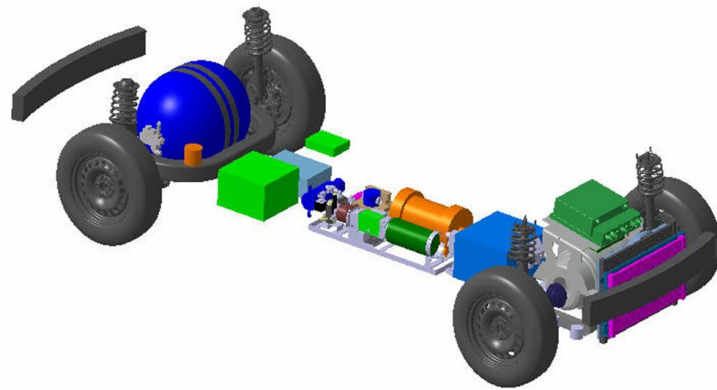


Figure 6.31: FCEV with Tongji fuel cell model

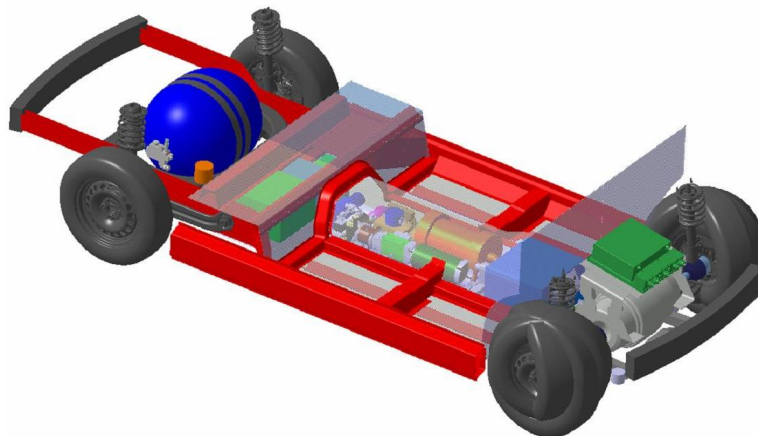


Figure 6.32: Design of the FCEV with structure

6.5 Engine and Generator

6.5.1 Engine/Generator in Front

Initial packaging studies on the PHEV variant of the FSV were focused on the packaging of the Internal Combustion Engine (ICE) and the generator. As with other design packages, the first iteration showed the engine and generator assembly in the front of the vehicle mainly due to the fact that a majority of the vehicles are produced with this type of a configuration. In case of the FSV-1, PHEV₂₀, the engine was a 1.0 L 3-cylinder. The packaging of this engine, in the above mentioned configuration, is shown in Figure 6.33.

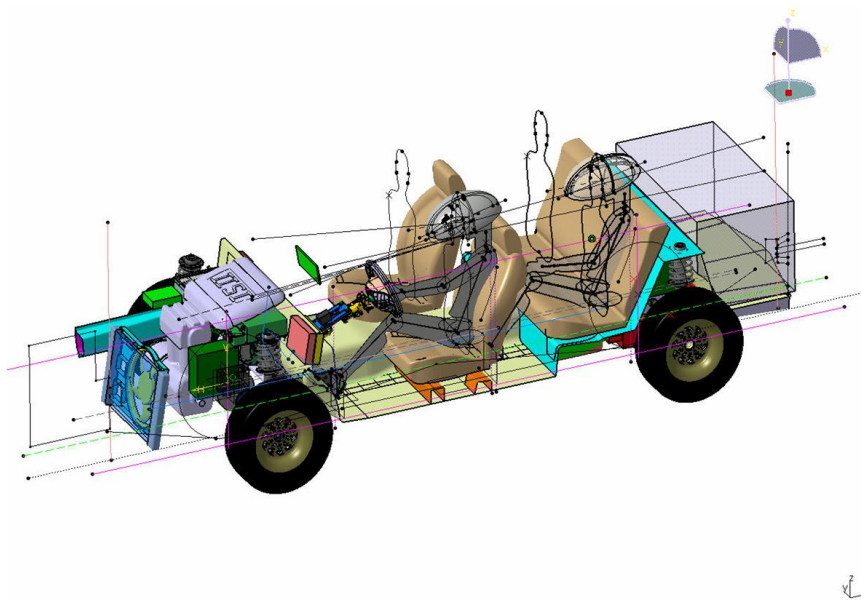


Figure 6.33: *Front engine/generator configuration*

6.5.1.1 Design Study Outcome

This design, although a very common configuration, did not allow for a shorter front-end which was now a distinct characteristic of the FSV BEV and FCEV variants. It also meant that the PHEV variant of the FSV would have a different front-end length and could not be commonized with the its other variants.

6.5.2 Engine/Generator in Rear - Horizontal

The second iteration of the study focused on the relocation of the engine/generator to the rear of the vehicle based on the FSV goal of a common and shorter front-end for all variants. The 54 L fuel tank and the 16 kWh battery pack were also incorporated into the vehicle. The engine/generator was packaged in the rear in a horizontal position while trying to make use of the FCEV's hydrogen tank cradle as mounts for the engine/generator. The battery pack was packaged under the tunnel with the fuel tank under the rear seat. Figure 6.34 shows this rear engine configuration and Figure 6.35 shows the fuel tank and battery placement locations.

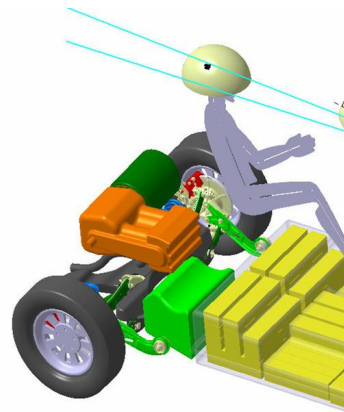


Figure 6.34: *Rear Engine - Horizontal*

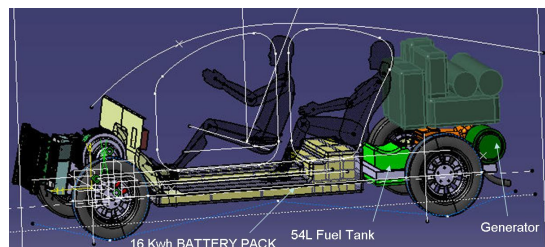


Figure 6.35: *Fuel tank and battery locations*

6.5.2.1 Design Study Outcome

This study comprehended the common short front-end requirement. However, the placement of the engine/generator in the horizontal position did not account for efficient utilization of the engine characteristics in terms of the lubrication (Oil could possibly enter the combustion chamber) and a vertical position was the probable solution or a tilted position would be desired. The next few design iterations focused on this concept and further enhanced the rear engine design concept.

6.5.3 Engine/Generator in Rear - Vertical

The main focus of this study was to refine the position of the engine/generator in the vehicle. Since it was determined that the ICE could not be placed horizontally in the vehicle, vertical placement was attempted. This was an acceptable position for the engine and generator as shown in Figure 6.36 and its relative location with the fuel tank and battery is shown in Figure 6.37.

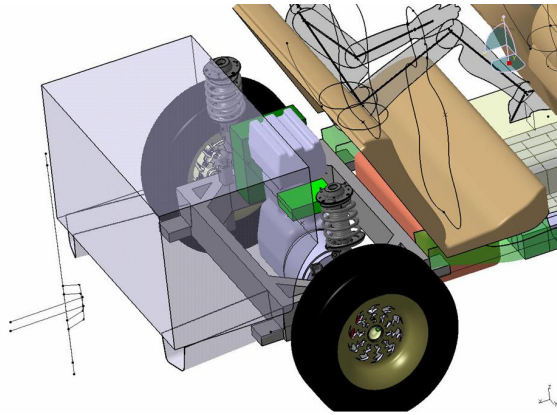


Figure 6.36: *Rear engine - vertical*

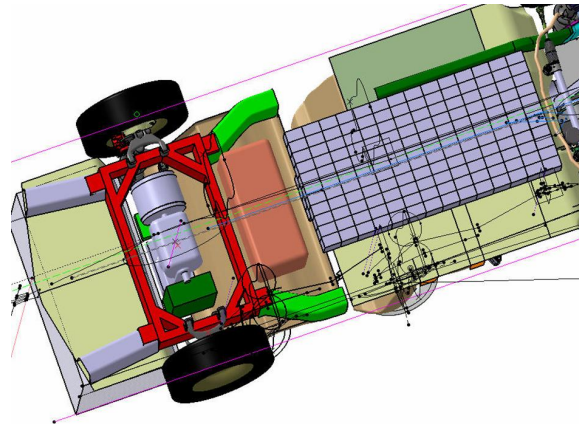


Figure 6.37: *Rear engine with fuel tank and battery*

6.5.3.1 Design Study Outcome

This configuration accommodated the FSV goals and also the engine/generator efficiency was not compromised (due to lubrication challenges as discussed in previous section). This vertical placement of the engine negatively impacted the cargo volume and the next few iterations were conducted to refine this design and increase cargo volume.

6.5.4 Engine/Generator in Rear - 17° tilt

This design study was primarily undertaken to refine the placement of the engine and generator to maximize the cargo volume of the vehicle. The engine was tilted certain degrees to the vertical plane as it allowed for better utilization of the space and also provided more opportunity to increase the cargo volume. After many iterations with the engine at various different angles to the vertical, maximum cargo volume could be obtained by tilting the engine to 17°. Figure 6.38 shows the location of the engine with the 17° tilt.

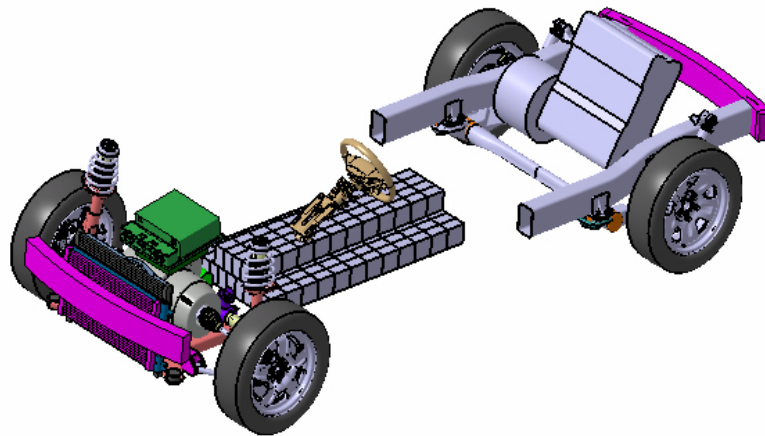


Figure 6.38: Rear Engine - 17° tilt

6.5.4.1 Design Study Outcome

This design study achieved all the FSV target goals in terms of design but lacked performance. The next iteration of the design was to accommodate a bigger engine and a smaller battery pack based on the technology assessment results.

6.5.5 Engine/Generator in Rear - 45° tilt

Technical assessments showed that the PHEV₄₀ required a higher powered ICE. The engine was upgraded to a 1.4 L 4-cylinder variant for the PHEV₄₀. Studies also showed that a 11.7 kWh battery pack and a smaller 19 L fuel tank was sufficient to meet all the requirements on the PHEV₄₀ and these changes were incorporated into the previous design in this study. Further design iterations of the engine/generator and its orientation with respect to the vehicle packaging, identified that a 45° tilt would produce a more refined and optimized powertrain layout. Figure 6.39 shows the PHEV₄₀ 1.4 L engine (without accessories) and Figure 6.40 shows the packaging of the 45° oriented engine/generator along with the drivetrain and suspension for the PHEV₄₀. A 1.0 L 3-cylinder low power variant of this engine/generator is used on the PHEV₂₀.

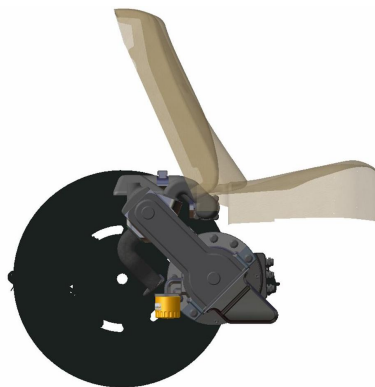


Figure 6.39: *New 1.4 L 4-cylinder engine/generator*

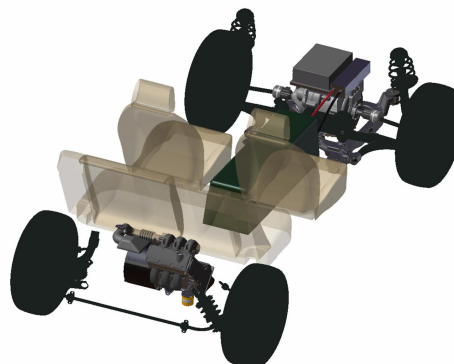


Figure 6.40: *PHEV₄₀ 45° orientation layout*

6.5.5.1 Design Study Outcome

Both the FSV PHEV variants have adopted this above engine/generator packaging method. With further minor refinements on the design and packaging of an upgraded 1.4 L engine, both the PHEV₂₀ and PHEV₄₀ variants have achieved the design and performance target goals set for each of these vehicles.

6.6 Front Suspension Designs

6.6.1 Upper Control Arm / Lower Trailing Arm (sprung)

6.6.1.1 Concept Overview

This concept design, as shown in Figure 6.41, consists of an upper control arm (shown in pink) and a lower trailing arm (shown in green). The mass of the vehicle is sprung by a horizontal coil spring (shown in red). The roll stability of the vehicle is obtained by the horizontal anti-roll bar (shown in orange) connecting the two (left and right) trailing arms. The damper (not shown) could be mounted either vertically or longitudinally (using a fulcrum) on the lower arm which translates to efficient usage of the available space.

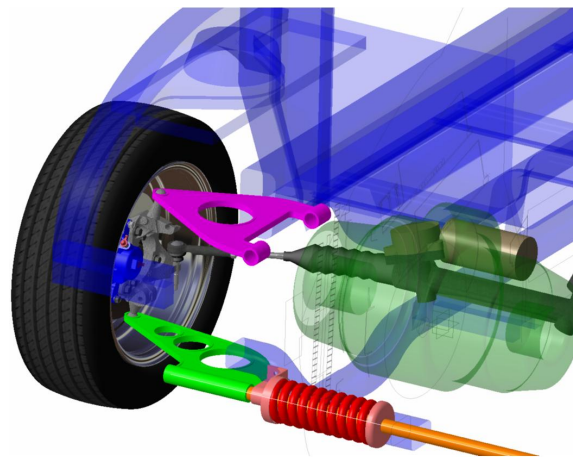


Figure 6.41: Upper control arm / Lower trailing arm (sprung)

6.6.1.2 Advantages

1. Integrated anti-roll bar leads to fewer parts
2. Structural shock tower not required (exterior styling can be more flexible)
3. System geometry is similar to Short and Long Arm (SLA) suspension (favorable kinematics)

6.6.1.3 Disadvantages

1. Coil spring takes up more space and increases mass
2. Unproven coil spring usage concept
3. Upper control arm protrudes into the motor compartment
4. Multiple arms
5. Vertical reaction loads must be taken by arm mounts ie., bigger structures

6.6.1.4 Conclusions

This suspension package provides unique packaging flexibility due to the integrated roll bar and also because the shock tower is not required (vehicle styling advantage). The horizontal spring may not be the most effective design and would need to be replaced with a horizontal torsion bar (Early Volkswagen Beetles had a similar design for its front suspension). This type of suspension concept is typical of a high performance vehicle (with higher cost penalty) and would be an over-engineered for the FSV application.

6.6.2 Upper Control Arm (sprung) / Lower Trailing Arm

6.6.2.1 Concept Overview

This design, as shown in Figure 6.42, consists of the upper control arm (shown in pink) and the lower trailing arm (shown in green) which provide the upper and lower tire control respectively. The vehicle sprung mass is now supported by the horizontally placed coil spring (shown in red) which is secured to the upper control arm on one end and to an additional central cross-member on the other. Vehicle roll stability is maintained by the horizontal torsion bar (shown in orange) which connects the two trailing arms (left and right). The damper (not shown) could be coil over shock (shown in red) or could be mounted on the lower trailing arm either vertically or longitudinally.

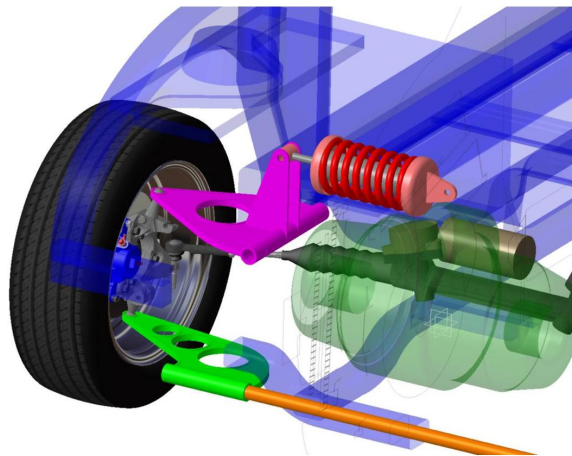


Figure 6.42: *Upper control arm (sprung) / Lower trailing arm*

6.6.2.2 Advantages

1. Integrated anti-roll bar leads to fewer parts
2. Structural shock tower not required (exterior styling can be more flexible)
3. System geometry is similar to Short and Long Arm (SLA) suspension (favorable kinematics)
4. Multiple spring rates can be quickly achieved by varying the shock mount locations on the control arm (typical race car feature)

6.6.2.3 Disadvantages

1. Coil spring and upper control arm intrude into the motor compartment, reducing the packaging space for powertrain components
2. Additional structure like a center cross member would be needed to mount the shock/damper, limiting access to the powertrain components

6.6.2.4 Conclusions

This concept sacrifices valuable underhood space to achieve typical race car suspension characteristics (at a cost premium to redesign and relocate) and would be unnecessary for the FSV application.

6.6.3 Upper Control Arm (sprung) / Lower Control Arm

6.6.3.1 Concept Overview

This concept, as shown in Figure 6.43 is similar in construction to that of the previous design except for the fact that lower trailing arm is replaced by a lower control arm (shown in green). Vehicle mass is supported by the coil spring over shock (shown in red) mounted horizontally to the upper control arm. This design requires a stabilizer bar (not shown) to provide roll stability for the vehicle.

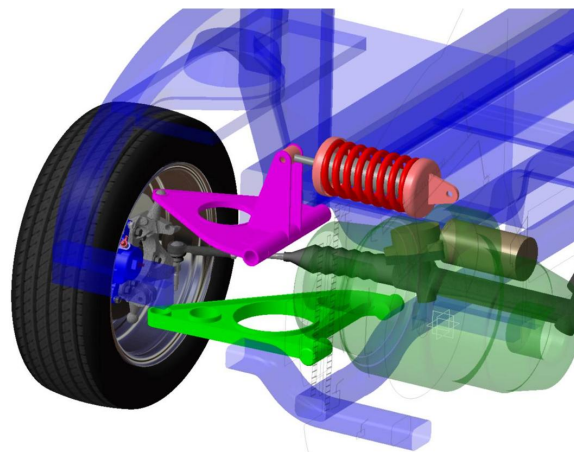


Figure 6.43: Upper Control Arm (sprung) / Lower control arm

6.6.3.2 Advantages

1. Structural shock tower not required (exterior styling can be more flexible)

2. This is a Short and Long Arm (SLA) suspension design (favorable kinematics for high performance application)
3. Multiple spring rates can be quickly achieved by varying the shock mount locations on the control arm (typical race car feature)

6.6.3.3 Disadvantages

1. Coil spring and upper control arm intrude into the motor compartment, reducing the packaging space for powertrain components
2. Additional structure like a center cross member would be needed to mount the shock/damper, limiting access to the powertrain components
3. Cost premium for higher performance

6.6.3.4 Conclusions

This suspension design with the horizontally mounted coil spring on to the upper control arm has no practical advantages over having a spring attached to the lower control arm as in the case of a conventional SLA suspension design. This concept also sacrifices valuable underhood space to achieve typical race car suspension characteristics (at a cost premium) and would be unnecessary for the FSV application.

6.6.4 Upper Control Arm / Lower Control Arm (sprung)

6.6.4.1 Concept Overview

This suspension design concept shown in Figure 6.44 uses two control arms, one on the top side of the knuckle (shown in pink) and one on the bottom side of the knuckle (shown in green). The vehicle sprung mass is supported by the torsion bar (shown in red) connecting the lower control arm to the vehicle body. This design also requires a stabilizer bar (not shown in the figure) to provide roll stability for the vehicle. The damper (not shown in the figure) would be located on the lower arm.

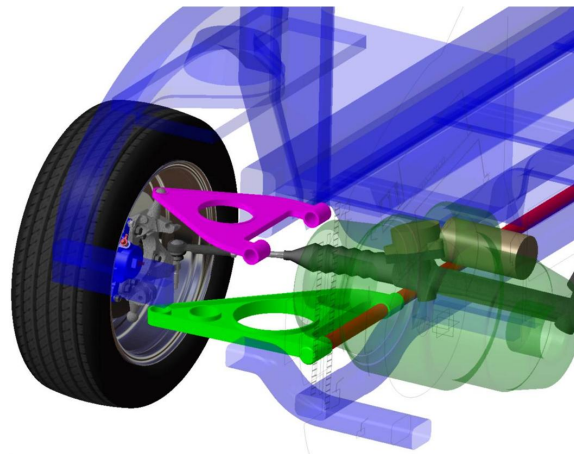


Figure 6.44: *Upper control arm / Lower control arm (sprung)*

6.6.4.2 Advantages

1. This is a typical Short and Long Arm (SLA) suspension and has better kinematics suited for high performance applications
2. Torsion bar is less expensive than a coil spring
3. Lower overall system cost

6.6.4.3 Disadvantages

1. Inability to pitch the lower arm restricts anti-dive kinematics
2. Torsion bars cannot provide a progressive spring rate

6.6.4.4 Conclusions

This suspension design provides the best cost effective solution for implementing the Short and Long Arm (SLA) suspension design which provides the best performance in terms of kinematics.

This would be a feasible design only if race car type performance was ever desired of the FSV.

6.6.5 Horizontal Leaf Spring Design

6.6.5.1 Concept Overview

In this design shown in Figure 6.45, the conventional coil spring is replaced with a leaf spring (shown in red). The upper control arm (shown in pink) and the lower control arm (shown in green) provide upper and lower tire controls respectively. The mass of the vehicle is now supported by the leaf spring placed in between the two (left and right) lower control arms. The damper and the anti-roll (not shown) would be located on the lower arm.

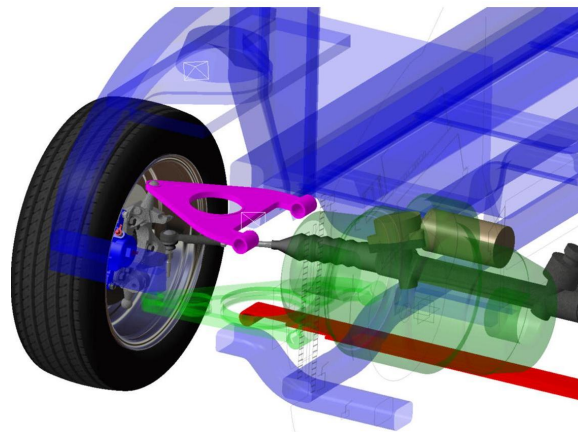


Figure 6.45: *Leaf spring design*

6.6.5.2 Advantages

1. This is a typical Short and Long Arm (SLA) suspension and thus has better kinematics suited for high performance applications

6.6.5.3 Disadvantages

1. High spring costs
2. Leaf spring would require larger clearances that take up motor compartment space

6.6.5.4 Conclusions

This does not provide a feasible packaging solution for the FSV, due to the fact that it interferes with the location of the electric motor of the vehicle. This suspension design is currently used on the Chevrolet Corvette.

6.6 Front Suspension Designs

6.6.6 McPherson Strut / Lower Trailing Arm

6.6.6.1 Concept Overview

In this concept design as shown in Figure 6.46, the upper control arm function is provided by the McPherson strut (shown in red). The mass of the vehicle is also sprung by McPherson struts. The lower Trailing Arm (shown in green) provides lower tire control. The vehicle's roll stability is achieved by the horizontal torsion bar connecting the two (left and right) trailing arms (shown in orange).

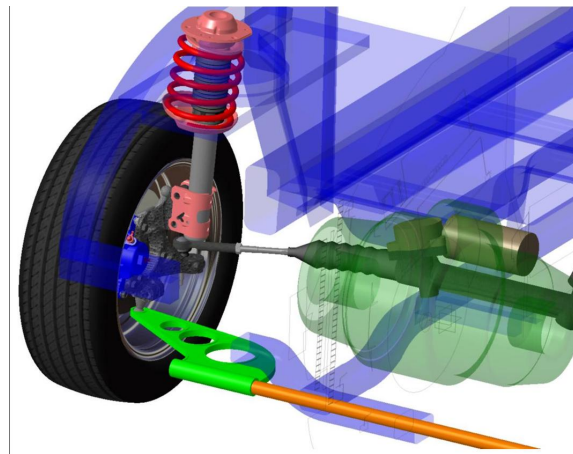


Figure 6.46: *McPherson strut (sprung) / Lower trailing arm*

6.6.6.2 Advantages

1. Integrated roll bar design required fewer parts
2. Lightweight design
3. Lower cost design
4. Minimal space required in the engine compartment

6.6.6.3 Disadvantages

1. This design requires a structural shock tower which dictates the exterior surface theme of the vehicle
2. Unproven strut and trailing arm configuration
3. Minimal camber gain, reducing performance

6.6.6.4 Conclusions

This design, with the strut and the roll bar, constitutes a suspension with the least amount of individual parts. This could have been a feasible design for the FSV application but the minimal advantage of having an integrated roll bar did not justify the developmental risk over choosing a conventional McPherson strut suspension.

6.6.7 Conventional McPherson Strut

6.6.7.1 Concept Overview

This suspension design as shown in Figure 6.47 comprises of the McPherson strut (shown in grey) with the coil spring (shown in red) with the lower control arm (shown in green) for upper and lower tire control respectively. The vehicle mass is supported by the strut (with the coil spring). A stabilizer bar (not shown) is required for roll stability.

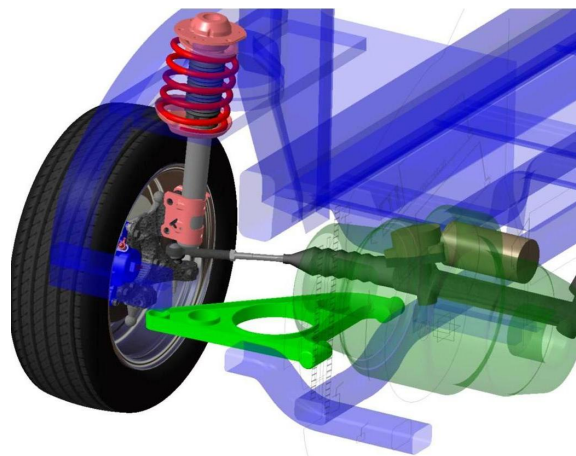


Figure 6.47: *Conventional McPherson strut*

6.6.7.2 Advantages

1. Most compact, lightweight and cost effective suspension design
2. Provides easy packaging solutions
3. More than 80% of passenger vehicles use this type of suspension
4. Additional unsprung mass saving potential have been realized by research

6.6.7.3 Disadvantages

1. Minimal camber gain reducing performance
2. Requires a structural shock tower limiting exterior styling possibilities

6.6.7.4 Conclusions

This is the most popular and conventional system used on automobiles worldwide. A study conducted by Thyssenkrupp-Bilstein of America shows that further weight reduction of about 7 kg in unsprung weight can be reduced from this system by using lightweight struts and stabilizer bars, high strength springs and monotube shocks instead of the conventional twin tube ones. Using these above mentioned facts about this type of suspension, the McPherson strut was the choice of choice for the Future Steel Vehicles.

6.7 Rear Suspension Designs

6.7.1 Twist Beam or Torsion Beam

6.7.1.1 Design concept

Torsion beam suspension, also known as a twist beam suspension has a long metal bar attached firmly between the right and left trailing arms. This horizontal bar functions as the anti-roll bar and also induces camber and toe kinematics when the two wheels have different rates. Vertical motion of the wheel causes the bar to rotate along its axis and is resisted by the bar's torsion resistance. The mass of the vehicle is supported by the damper (shown in yellow).



Figure 6.48: *Twist Beam or Torsion Beam*

6.7.1.2 Advantages

1. Simple, inexpensive and effective design
2. Low loads at mounting points
3. Anti-roll bar not required, thus reducing the number of parts

6.7.1.3 Disadvantages

1. Does not handle lateral loads well
2. Not a true independent suspension

6.7.1.4 Conclusion

The clearance required to the twist beam did not allow for a common suspension design on all FSV variants. The suspension could not be packaged into the vehicle without significant redesign required on the battery layout for the BEV and FCEV.

6.7.2 Passive Wheel

6.7.2.1 Design concept

This concept design packages all the suspension components (spring, knuckle, damper) inside the wheel assembly. The whole wheel assembly bolts onto the vehicle body. Siemens VDO and Michelin each have a similar concept. The FSV design concept is completely passive with no power required (unlike the 2 other concepts).



Figure 6.49: *Passive wheel*

6.7.2.2 Advantages

1. Compact
2. Light weight

6.7.2.3 Disadvantages

1. Low wheel travel
2. Minimal kinematic control (camber, toe)
3. Unproven technology

6.7.2.4 Conclusion

High developmental costs are involved in commercializing this design and the this suspension's design articulation range does not meet FSV targets. Thus, this design concept was not considered for the FSV.

6.7.3 Trailing Arm with 2 Camber Links

6.7.3.1 Design concept

The two crosscar links (shown in grey) are for controlling the camber and also handles lateral loads. The trailing arms (shown in black) are sprung to support the weight of the vehicle.



Figure 6.50: *Trailing arm with 2 camber links*

6.7.3.2 Advantages

1. High performing kinematics could be achieved
2. Packages into all FSV variants

6.7.3.3 Disadvantages

1. Design would end up very heavy to be able to transfer loads
2. Higher part count
3. High complexity

6.7.3.4 Conclusion

The coil over shocks were packaged under the rear seats to take advantage of the unused space. This package on the FSV would result in increasing the weight of the vehicle due to added unsprung weight of the suspension itself.

6.7.4 Double Wishbone (SLA)

6.7.4.1 Design concept

This design consists of a Short and Long Arm (SLA wishbones) and provides independent vertical wheel movement. The horizontal coil over shock (shown in purple) control this vertical movement.

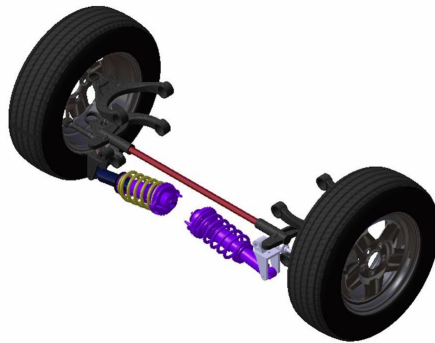


Figure 6.51: Double wishbone

6.7.4.2 Advantages

1. High performance kinematics can be achieved
2. Does not intrude into luggage compartment
3. Can be used on all FSV variants

6.7.4.3 Disadvantages

1. High cost premium
2. Additional fulcrums and links needed, increasing the number of parts
3. High level of design complexity

6.7.4.4 Conclusion

The horizontal coil over shock was designed to maximize the luggage compartment space. However, due to the battery pack location on the FSV, the arms had to be very short resulting in an undesirable high track change rate when the suspension articulates.

6.7.5 Chapman Strut / McPherson Strut

6.7.5.1 Design concept

A strut (shown in grey) is designed to act as both a shock absorber (with an integrated coil spring) and a wheel location device. When a McPherson strut is located in the rear, its referred to as a Chapman strut. The difference is that the tie rods are mounted to the body instead of the rack and pinion. The mass of the vehicle is also sprung by this Chapman strut while lower tire control is provided by the lower control arm.



Figure 6.52: *Chapman strut / McPherson strut*

6.7.5.2 Advantages

1. Cost effective
2. Acceptable performance in terms of kinematics
3. Light weight

6.7.5.3 Disadvantages

1. Requires a large shock mount
2. Intrudes into the luggage compartment

6.7.5.4 Conclusion

This design, although provided a low cost and weight solution, was not considered for the FSV due to the fact that it required a rear shock tower and intruded into the luggage compartment space.

6.7.6 H-Arm with Camber Control Link

6.7.6.1 Design concept

In the H-arm, Independent rear suspension, all driving and braking loads are reacted by the lower lateral H-arm in torsion and bending. Reactions to all wheel center inputs in the longitudinal direction result in torsional loading of the H-arm. The upper camber control link controls the front view instant center. In this H-arm suspension, the forward bushing (shown in grey) on the arm is positioned very far forward to reduce mounting loads. Because the mount is so far forward, it can easily be mistake for a trailing arm.



Figure 6.53: *H-arm with camber control link*

6.7.6.2 Advantages

1. By adding one more pivot point on the lower arm, two additional degrees of freedom are constrained - lower control arm now controls 4 degrees of freedom
2. Compact and lightweight
3. Packages well with all FSV variants (BEV, PHEV and FCEV)

6.7.6.3 Disadvantages

6.7.6.4 Conclusion

In this H-arm suspension, the forward bushing (shown in grey) on the arm is positioned very far forward to reduce mounting loads. Because the majority of the loads are in the lower arm, the camber link can be very light weight resulting an overall light weight set-up. This suspension also packages well with all FSV variants and thus was the rear suspension of choice for the FSV.

6.8 FSV Suspension - Decision Matrix

Each of these above mentioned suspension designs and their parameters with advantages and disadvantages were studied. Table 6.3 and Table 6.4 show the matrix used as a tool to weight out each front and rear suspension design respectively against the few predetermined set of parameters to help arrive at a cost effective, lightweight design for the future Steel Vehicle.

In the front, both the McPherson strut suspension options shown in Table 6.3 are feasible designs for the FSV, but the conventional McPherson strut was chosen for the FSV as it is the most efficient design that required minimal developmental investment cost and time.

		Suspension Parameters						
		Kinematics	Packaging	Mass	Cost	number of parts	Design Complexity	Ranking
Potential FSV Suspension Designs	Upper Control Arm / Lower Trailing Arm (sprung)	++	○	-	-	+	-	3
	Upper Control Arm (sprung) / Lower Trailing Arm	++	-	-	-	○	-	6
	Upper Control Arm (sprung) / Lower Control Arm	++	-	-	-	-	-	7
	Upper Control Arm / Lower Control Arm (sprung)	+	○	-	○	○	-	4
	Leaf Spring	++	-	○	-	○	-	5
	McPherson Strut / Lower Trailing Arm	+	+	+	+	++	+	1
	Conventional McPherson strut	+	+	+	+	+	+	2

Table 6.3: Front suspension design - Decision matrix

The H-arm with camber control link suspension was the suspension of choice in the rear for the FSV. This suspension package design is simple, light weight, cost effective, has a low part count, has acceptable kinematics for our vehicle and most importantly, allowed for a common rear suspension on all the FSV variants (BEV, FCEV and PHEV).

		Suspension Parameters						
		Kinematics	Packaging	Mass	Cost	number of parts	Design Complexity	Ranking
Potential FSV Suspension Designs	Twist Beam or Torsion Beam	○	-	○	+	+	+	3
	Passive Wheel	-	++	++	--	+	-	5
	Trailing Arm concept with 2 Camber links	+	+	-	○	○	-	6
	Double Wishbone	+	+	○	○	○	-	4
	Chapman strut / McPherson strut	○	+	+	+	+	+	2
	H-Arm with Camber Control Link	+	+	+	+	+	+	1

Table 6.4: Rear suspension design - Decision matrix

6.9 FSV Suspensions - Layout

Figure 6.54 shows the FSV suspension design in the front and in the rear. The FSV front suspension design is a conventional McPherson strut design which was further refined in terms of reducing the size and mass of the lower control arm. This lower control arm (shown in inset) is a two piece design (hydroformed and stamped) made from light weight steel of 2 mm gauge thickness, weighs about 1.56 kg which is only about 6% heavier than a similar sized aluminum lower control arm.

The H-arm with camber control link suspension was the suspension of choice in the rear for the FSV. This suspension package design is simple, light weight, cost effective, has a low part count has acceptable kinematics for our vehicle and most importantly, allowed for a common rear suspension on all the FSV variants (BEV, FCEV and PHEV).

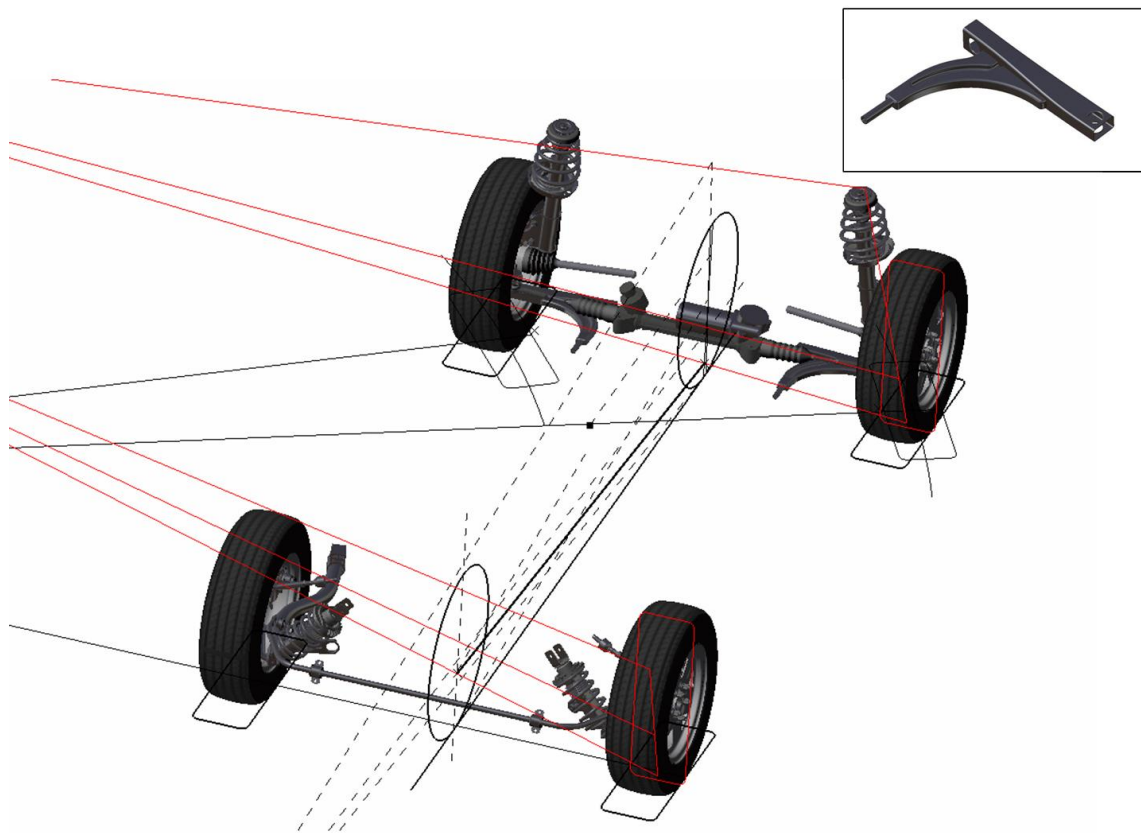


Figure 6.54: FSV suspension - front and rear

6.10 FSV Suspension Characteristics

6.10.1 Camber

Camber is the angle of the tire in relation to the road surface. During a turn, the body rolls and the outboard suspension compresses towards jounce. Negative camber counteracts the effect of body roll by bringing the top of tire inboard maintaining a large contact patch with the ground. In Figure 6.55, the wheel travel (jounce and rebound) is plotted against the camber angle in degrees and as the wheel travels towards jounce, the camber angles moves into the negative range.

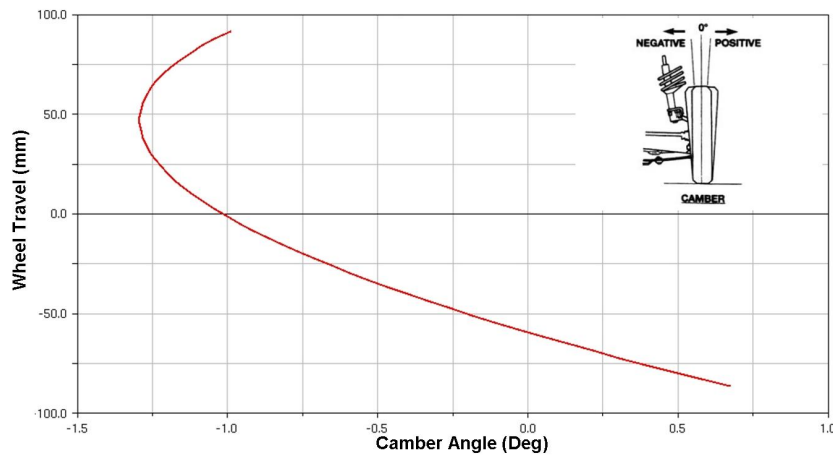


Figure 6.55: *Camber angle versus wheel travel*

6.10.2 Toe Change

Toe change is designed into a suspension to promote understeer, providing the driver with a more stable feel. During a turn, this is accomplished by having the outboard front tire increase toe and the rear tire decrease toe. Figure 6.56 shows an ADAMS plot of the front toe increase negatively as the wheel travels towards jounce and Figure 6.57 shows the rear toe increase positively when the wheel travel towards jounce.

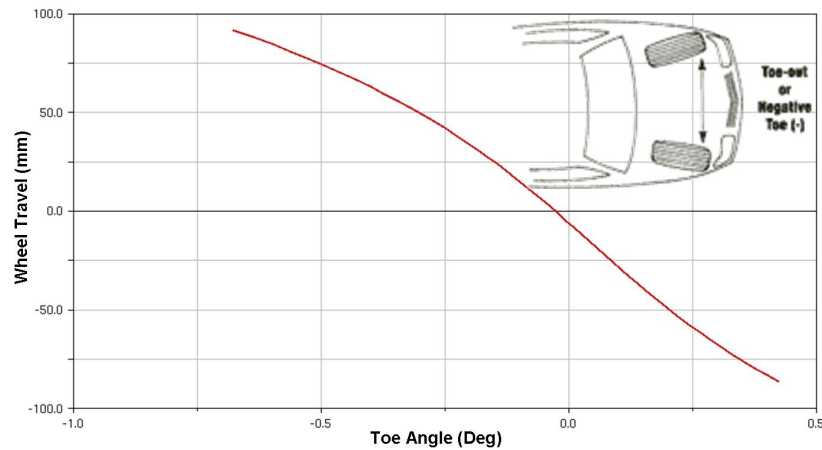


Figure 6.56: *Toe change versus wheel travel- front*

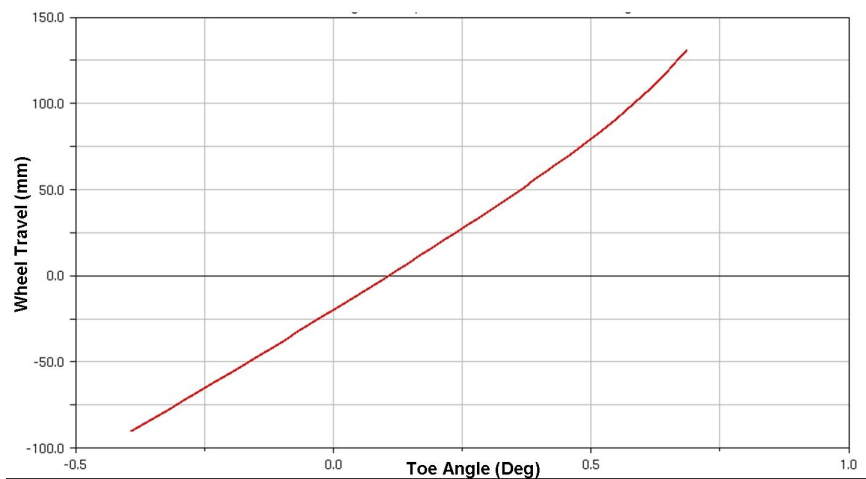


Figure 6.57: *Toe change versus wheel travel - rear*

7.0 Sensitivity Analysis

7.1 Synopsis

Lithium-Ion technology is evolving at a greater pace than previously possible due to the large amount of time and money spent on research into new materials and cell chemistries. New avenues to harness the promising potential of lithium-ion and fuel cells, with the goal of ultimately replacing fossil fuels completely, have been discovered.

Various government bodies like the United States Department of Energy (US-DOE) and New Energy and Industrial Technology Development Organization (NEDO) have internally funded development projects that have helped them arrive at targets in terms of battery cell technology for automotive applications.

The FSV project conducted a study to analyze these new technological developments in Lithium-Ion cells and targets set by these government bodies to assess the effect it would have on current FSV design recommendations in terms of its battery and motor technology. Such radical changes in technology could possibly have a significant impact on the structural design of the vehicle.

7.2 Battery Technology

During the course of the project, the FSV team researched battery technologies that would be production viable by years 2015-2020, and provided recommendations for the type and specifications of the battery pack on the FSV variants. Table 7.1 shows the FSV battery recommendations.

Battery Technology Assessment				
		Status 2008	Prediction 2015-2020	Selection FSV
Dominating Technology		Ni-MH	Li-Ion	Li-Ion
Power Density	kW/kg	1.1	1-3	2.0
Energy Density	Wh/kg	45	90 - 170	130

Battery Pack Technology Assessment				
Capacity	kWh	10 (max)	1.5 - 40	2.3 - 35
Cost	\$ USD/ kWh	500	400-700	450

Future Steel Vehicle Concept				
	Capacity (kWh)	Weight (kg)	Volume (Liters)	Cost (\$ USD)
PHEV₂₀	5	58.2	47	\$2,346
PHEV₄₀	11.7	136.5	103	\$5,365
BEV	35	346.5	280	\$15,895
FCEV	2.3	27.3	25	\$1,503

Table 7.1: Battery recommendation for FSV

Table 7.2 shows the energy densities of the battery packs used in some of the current (2009) vehicle applications.

	Battery Capacity	Mass	Energy Density		Year
			Pack	Cell	
			kWh	Kg	
Mini e	35	260	135		2009
Tesla	53	430	123	200	2004
EnerDel	27	283	95		2009
I MiEV	16	200.0	80	150	2007
GM Volt	16	170.1	94		2010

Table 7.2: Current cell technology

The energy density (cell level), taking into account the technological advancements in the field

of Lithium-ion during the period between years 2015 - 2020, is in the range of 90-170 $\frac{Wh}{kg}$. The energy density of the FSV battery as recommended by Quantum is 130 $\frac{Wh}{kg}$ at the battery-pack level.

7.2.1 Battery Energy Density

Figure 7.1^[1] shows a comparison of the energy densities and specific energy of different types of cell chemistries (Li-ion, Ni-Cd, Ni-MH, Zn-Air). The specific energy of these types of batteries are plotted on the Y-axis. The higher the value, the lighter the battery pack (mass). The energy density is plotted on the X-axis. The higher the value, smaller the pack in terms of its volume.

The red star on the chart represents the FSV battery pack assumptions for year 2015-2020.

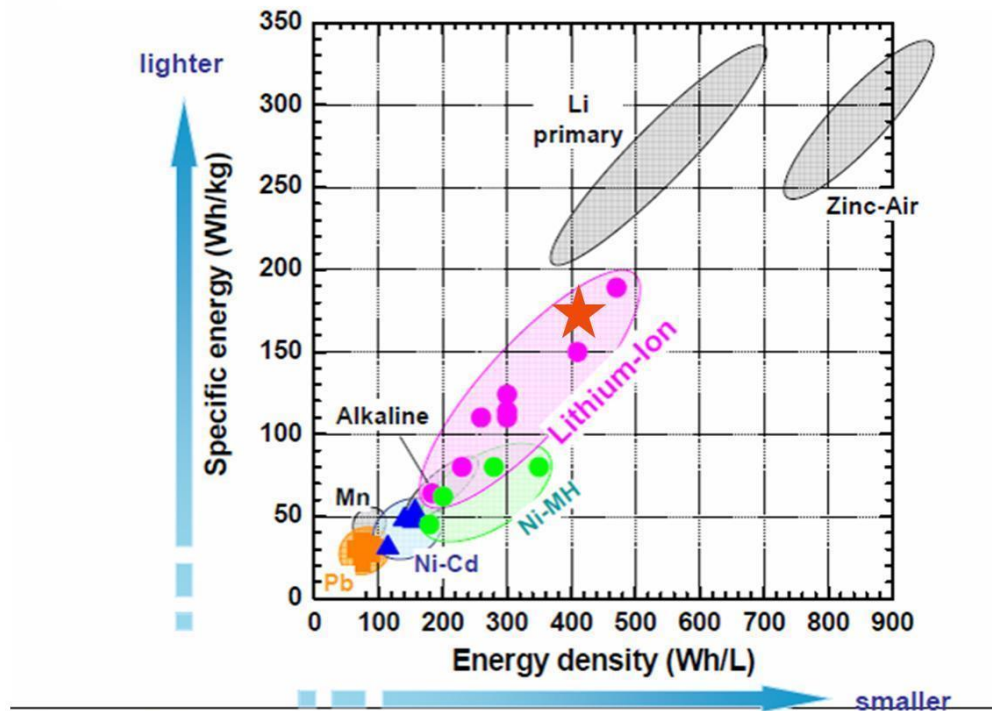


Figure 7.1: Battery energy density versus specific energy

¹TLD Workshop, IEA, 07/6/11-12, Paris

7.2.2 Battery Materials

The basic elements of a battery consists of a cathode material (positive terminal) and an anode material (negative terminal). Electrons collect on the negative terminal of the battery. Figure 7.2 shows the redox potential ^[2] of various elements typically used in the construction of batteries.

Lithium metal, amongst all other materials, shows the lowest redox potential (retains more electrons) which relates to a high-cell voltage and high-energy density.

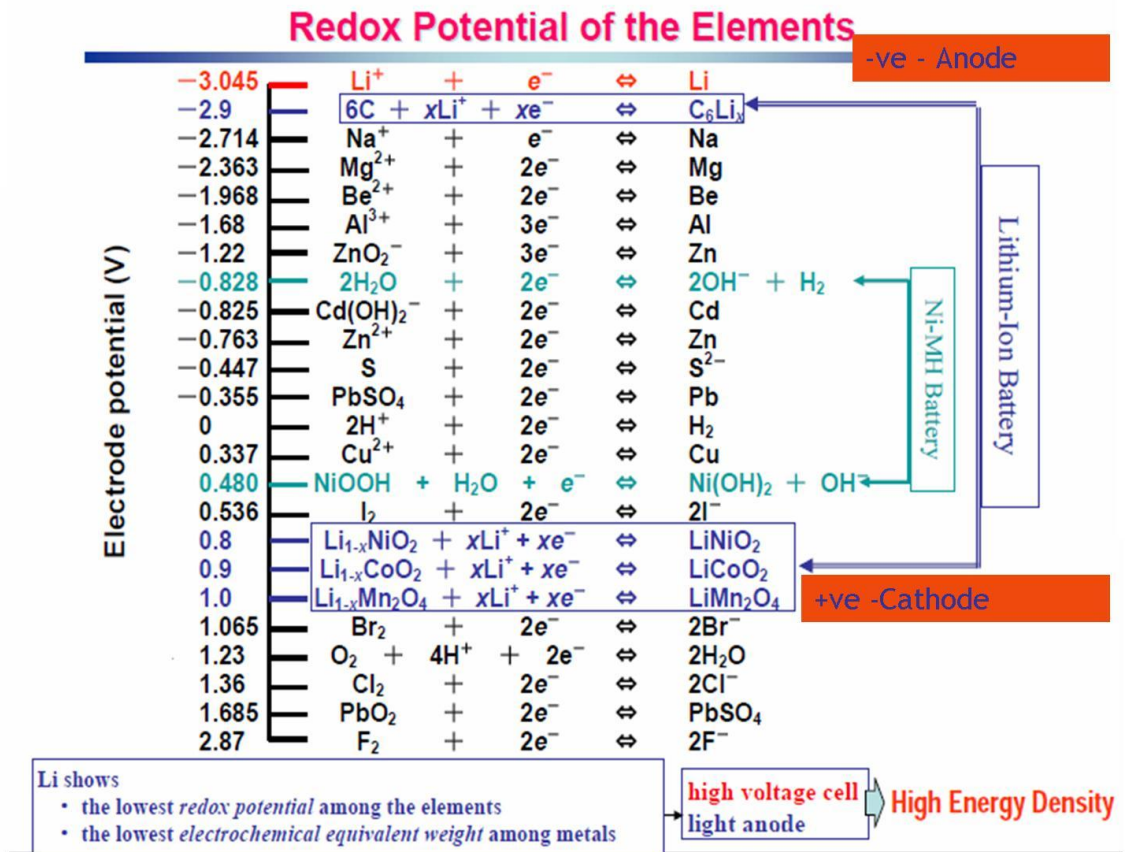


Figure 7.2: Redox potential of elements [64]

²Reduction potential (also known as redox potential) is the tendency of a chemical species to acquire electrons and thereby be reduced.

7.2.2.1 Lithium-Ion Battery - Positive and Negative Electrodes

Figure 7.3 and Figure 7.4 show the negative electrode (anode) and positive electrode (cathode) materials for the rechargeable lithium cells. There are certain anode materials possessing high specific energy capacity. However, materials possessing such high specific energy generally show large volume change during the charge-discharge cycle. On the cathode side, there are a few materials that possess higher specific energy capacity. High Lithium content materials such as Li_2MO_3 , have been studied.

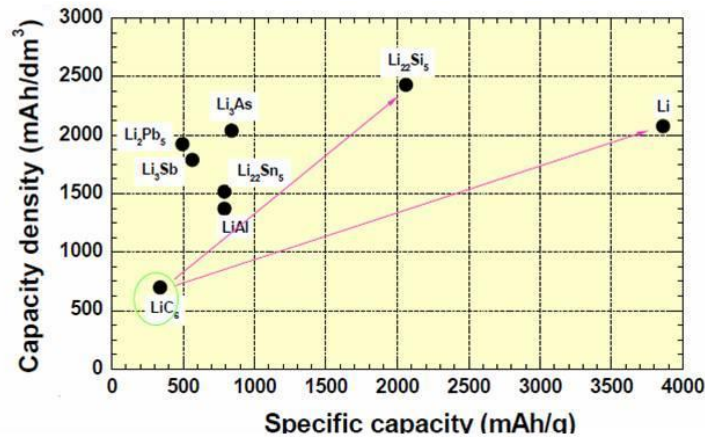


Figure 7.3: Negative electrode materials for rechargeable Li-cells

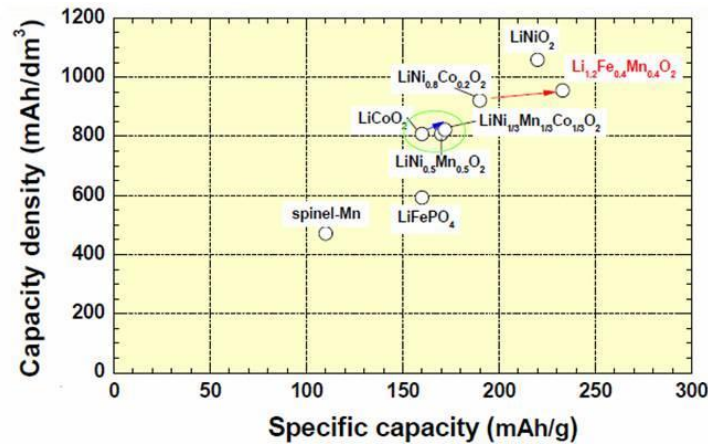


Figure 7.4: Positive electrode materials for rechargeable Li-cells

7.2 Battery Technology

7.2.3 Battery Targets

The United States Department of Energy (USDOE) and the New Energy and Industrial Technology Development Organization (NEDO) have set specific targets that they intend the Li-ion battery technology to meet in future. The targets (cell level) for the DOE are two fold:

1. Short term (2015) goal of $150 \frac{\text{Wh}}{\text{kg}}$
2. Long term (2020) goal of $200 \frac{\text{Wh}}{\text{kg}}$

NEDO targets, similar to the DOE, have set up their targets, but have three steps as opposed to two on the DOE:

1. Short term (2015) goal of $150 \frac{\text{Wh}}{\text{kg}}$
2. Near long term (2020) goal of $200 \frac{\text{Wh}}{\text{kg}}$
3. Long term (2030) goal of $500 \frac{\text{Wh}}{\text{kg}}$

The FSV recommended cell level energy density of $170 \frac{\text{Wh}}{\text{kg}}$ is in line with DOE and NEDO goals.

Figure 7.5 shows the NEDO Li-ion battery goals and timeline with FSV targets plotted along the timeline (red star).

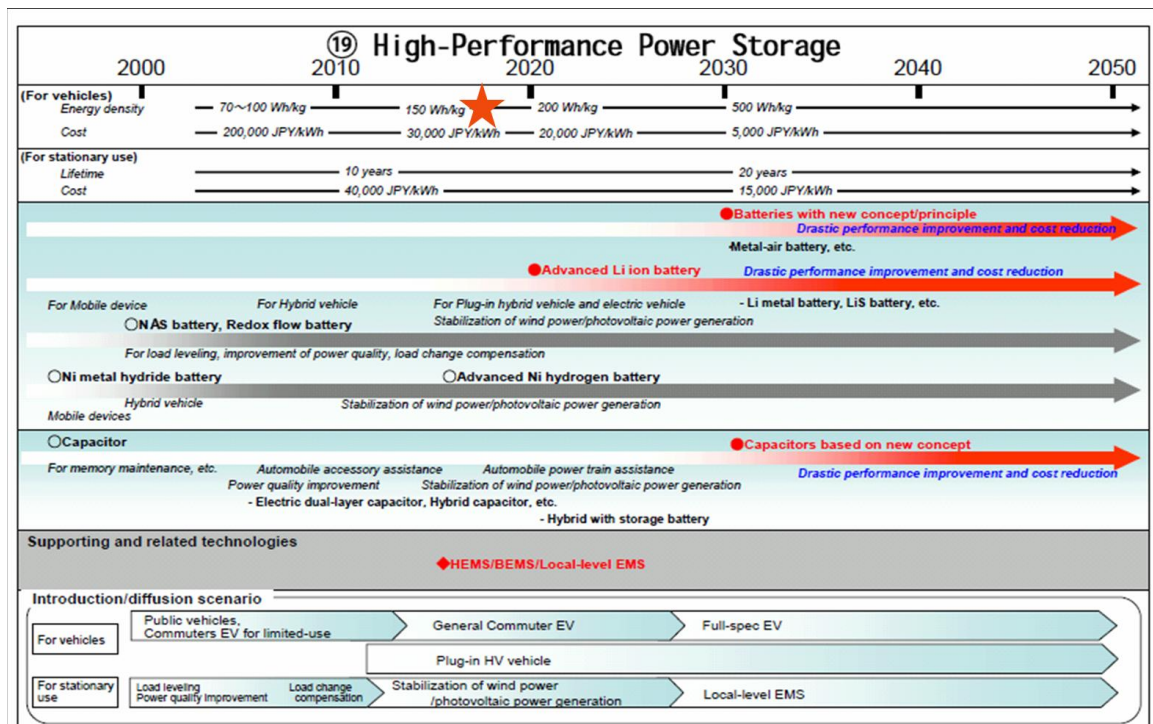


Figure 7.5: NEDO Li-ion battery targets

7.2.4 Energy Storage Limits

Energy stored in lithium-ion batteries, like other sources of energy storage, has its limits. Table 7.3 shows the limits of lithium-ion. Currently, Li-ion cells can store $140 \frac{\text{Wh}}{\text{kg}}$ of energy with a theoretical limit of $560 \frac{\text{Wh}}{\text{kg}}$. Replacing carbon anode with silicon anode increases the energy storage capacity to $830 \frac{\text{Wh}}{\text{kg}}$ and an ultra-advanced Li-ion cell could store up to $1390 \frac{\text{Wh}}{\text{kg}}$. The FSV battery sensitivity studies were conducted at 80% of these limits.

			kwh/kg	
			Cell	Pack
				75%
Lead Acid Present	0.1	MJ/kg	0.03	0.02
Lead Acid Limit	0.7	MJ/kg	0.19	0.15
Li Ion Present	0.5	MJ/kg	0.14	0.10
Li Ion Limit	2.0	MJ/kg	0.56	0.42
Li Ion - silicon instead of carbon	3.0	MJ/kg	0.83	0.63
Li Ion - Ultra Advanced	5.0	MJ/kg	1.39	1.04
Hydrogen at 700 bar	6.0	MJ/liter	1.67	kwh/l
3.4 kg Hydrogen at 700 bar+ 87 kg tank	4.6	MJ/kg	1.267	kwh/kg
Hydrogen at 700 bar	121.3	MJ/kg	33.70	kwh/kg
Gasoline	34.0	MJ/liter	9.44	kwh/l
Gasoline	50.0	MJ/kg	13.89	kwh/kg

Table 7.3: Energy storage limits [49]

7.2.5 Case Studies

Based on the limits of energy storage and the targets set by DOE and NEDO, different case studies were created to analyze the effect of these variables on the mass of the battery and powertrain for the FSV. These results were compared against the current technology as well as FSV recommendations for years 2015-2020, which was the basis for all the calculations.

The effect of these variables on the vehicle range was also studied.

7.2.5.1 Current Technology

With the cell energy density at $140 \frac{\text{Wh}}{\text{kg}}$ (current technology), a 35 kWh battery with a mass of 335 kg would be required to drive 250 km, resulting in a total powertrain mass of 469 kg.

7.2.5.2 Case 1 - FSV Recommendation (2015-2020)

The baseline for this case study is the FSV technology recommendation for years 2015-2020 with an assumed cell energy density value of $170 \frac{\text{Wh}}{\text{kg}}$. For a vehicle range of 250 km, a 35 kWh battery

7.2 Battery Technology

weighing only 274 kg, a total powertrain mass of 408 kg would be required.

Table 7.4 shows recommended battery specs (new pack) for the FSV BEV with the cell energy density of $170 \frac{\text{Wh}}{\text{kg}}$ and $130 \frac{\text{Wh}}{\text{kg}}$ at the pack level, yielding a total energy capacity of 34.7 kWh.

FSV Battery Pack	Cell	Sub-Pack	Battery Pack
	372	6	1
Size [l]	0.28	27.4	215
Mass [kg]	0.55	39	274
Capacity [kWh]	0.093	5.8	34.7
Energy Density [kWh/kg]	0.17	0.15	0.13

Table 7.4: FSV-1 BEV battery specifications (new pack)

Since batteries degrade over the life of the vehicle, the performance will not be the same at its end of life. In order to achieve the expected performance from the battery at its end of life, a degradation factor is applied, and the battery is designed with this degradation factor. For the FSV, with a degradation factor of 20%, energy density at the cell level reduces to $140 \frac{\text{Wh}}{\text{kg}}$ and the total energy capacity is reduced to 27.8 kWh as shown in Table 7.5.

FSV Battery Pack	Cell	Sub-Pack	Battery Pack
	372	6	1
Size [l]	0.28	27.4	215
Mass [kg]	0.55	39.0	274
Capacity [kWh]	0.075	4.6	27.8
Energy Density [kWh/kg]	0.14	0.12	0.10

Table 7.5: FSV-1 BEV battery specifications (end of life)

In order to achieve a battery pack with total energy capacity of 34.9 kWh while keeping the energy density at the cell level at $140 \frac{\text{Wh}}{\text{kg}}$, the number of cells within a sub-pack has to be increased to 468 from 372, which in turn increases the mass of the battery pack from 274 kg to 345 kg. Table 7.6 shows the final specifications of the FSV BEV battery pack at its end of life (200,000 km).

FSV Battery Pack	Cell	Sub-Pack	Battery Pack
	468	6	1
Size [l]	0.28	34.5	271
Mass [kg]	0.55	49.1	345
Capacity [kWh]	0.075	5.8	34.9
Energy Density [kWh/kg]	0.14	0.12	0.10

Table 7.6: FSV-1 BEV final battery specifications (end of life)

Figure 7.6 shows the FSV BEV battery at the cell, sub-pack and pack level.

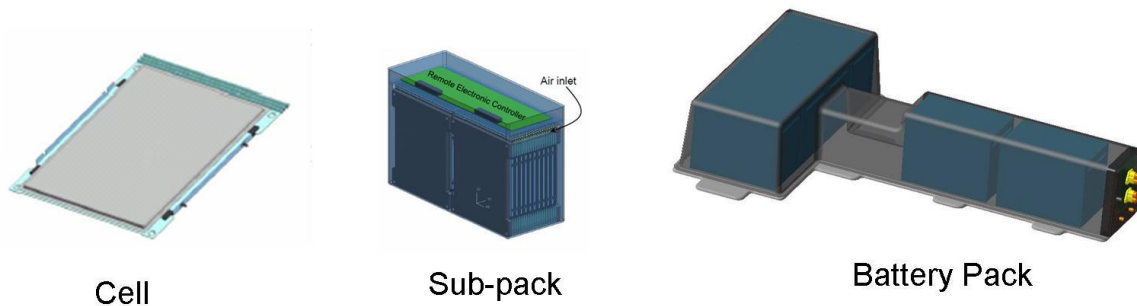


Figure 7.6: *FSV BEV recommended specification*

7.2.5.3 Case 2 - 80% of Lithium-Ion Limit

Assuming the lithium-ion technology would reach 80% of its storage capacity limits, the energy density at the cell level would be at $1110 \frac{\text{Wh}}{\text{kg}}$. With this type of technological advancement, a 66 kWh FSV battery would weigh only 79 kg (70% reduction from baseline), resulting in a powertrain mass of 213 kg (47% reduction from baseline) and the vehicle would be capable of achieving twice the current range (500 km).

7.2.5.4 Case 3 - Compete with Gasoline

Conventional ICE based powertrain including fuel storage on the FSV, would weigh around 316 kg. If this exact same mass were to be achieved with the FSV electric powertrain and battery, for a 500 km range, the Li-ion battery would have to weigh 182 kg (34% reduction from baseline) and would need 69.9 kWh of energy. This translates to a cell energy density of $510 \frac{\text{Wh}}{\text{kg}}$. This means that the battery technology would have to increase by a factor of three ($170 \frac{\text{Wh}}{\text{kg}} * 3$) if the electric powertrain and battery can completely displace the conventional ICE and fuel storage systems.

7.2.5.5 Case 4 - Compete with Hydrogen at 700 bar

For lithium-ion to compete with hydrogen at 700 bar (same powertrain mass), the cell energy density of the li-ion battery at the cell level has to be at least $460 \frac{\text{Wh}}{\text{kg}}$, keeping the battery mass at 203 kg (25% lower than baseline) with 69.9 kWh required for a range of 500 km.

7.2.5.6 Case 5 - NEDO and DOE targets

If DOE and NEDO targets of $150 \frac{\text{Wh}}{\text{kg}}$ and $200 \frac{\text{Wh}}{\text{kg}}$ for years 2015 and 2020 were met, the FSV-1 BEV would need a 34.9 kWh battery (for a 250 km range) with a mass of 310 kg (12% higher than baseline) and 233 kg (15% lower than baseline) respectively. The total powertrain mass of the FSV would be 444 kg (8% higher than baseline) and 367 kg (10% lower than baseline).

7.2.5.7 Case 6 - NEDO Step 3 targets

If NEDO's step 3 cell energy density target of $500 \frac{\text{Wh}}{\text{kg}}$ for the year 2030 were to be met, the FSV-1 BEV would be able to achieve a range of 500 km using a 66.2 kWh battery weighing 176 kg (36% lower than baseline) and a total powertrain mass of 310 kg (25% lower than baseline). This essentially is the same as displacing the conventional ICE with an electric powertrain while achieving the same performance characteristics.

Table 7.7 shows the specifications of such a battery pack for the FSV BEV and Figure 7.7 is a physical representation of the battery pack itself.

FSV Battery Pack (Same Energy as NEDO3 Target)	Cell	Sub-Pack	Battery Pack
	240	4	1
Size [l]	0.28	25.4	133
Mass [kg]	0.55	37.8	177
Capacity [kWh]	0.275	16.5	66
Energy Density [kWh/kg]	0.5	0.44	0.37

Table 7.7: FSV-1 Battery specs with NEDO3 targets

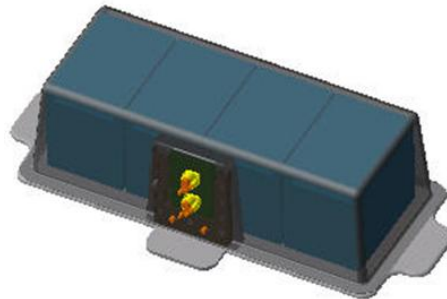


Figure 7.7: FSV BEV battery pack (NEDO3 target)

7.2.6 Case Study Results

Table 7.8 shows the results of the case studies.

	Energy density kWh/kg		Useful energy at Wheels		Energy Required to Drive 1 km	Battery Size (DOD 80%)	Fuel (or battery) Mass to Drive 500 km (200)	Electric Power train (motor, converter/ controller, transmission,	Total Powertrain Mass for 500 km (250 km) Driving
	Cell	Pack	Efficiency	kWh/kg	kWh	kWh	kg	kg	kg
Li-ion Batteries Current Technology 2008	0.14	0.10	85%	0.09	0.095	34.9	335	134	469
Case 1 - FSV Technology (2015-2020)	0.17	0.13	85%	0.11	0.095	34.9	274	134	408
Case 2 - 80% of Li Ion Limit	1.11	0.83	85%	0.71	0.090	66.2	79	134	213
Case 3 - Li-ion to compete with Gasoline for Cars (same powertrain mass)	0.51	0.38	85%	0.33	0.095	69.9	182	134	316
Case 4 - Li-ion to compete with H2 at 700 bar for Cars (same powertrain mass)	0.46	0.34	85%	0.29	0.095	69.9	203	134	337
Case 6 - NEDO & DOE Step 1 (2015)	0.15	0.11	85%	0.10	0.095	34.9	310	134	444
Case 7 - NEDO & DOE Step 2 (2020)	0.20	0.15	85%	0.13	0.095	34.9	233	134	367
Case 8 - NEDO Step 3 (2030)	0.50	0.38	85%	0.32	0.090	66.2	176	134	310

Table 7.8: Battery case study results

7.2.7 Packaging Impact

Figure 7.8 shows the packaging of the current FSV recommended battery pack into the vehicle. If this battery pack were to be reduced to an "I" section, for a 35 kWh battery pack, the cell energy density would have to be $228 \frac{\text{Wh}}{\text{kg}}$ (250 km Range), and for a 500 km range the same "I" section battery would have to be 66 kWh, with cell energy density at $433 \frac{\text{Wh}}{\text{kg}}$.

Figure 7.9 shows the impact this "I" section pack would have on packaging into the vehicle. Both these batteries would need a tunnel, possibly a Ultra-High-Strength (1.6 GPa) roll formed steel (UHSS).

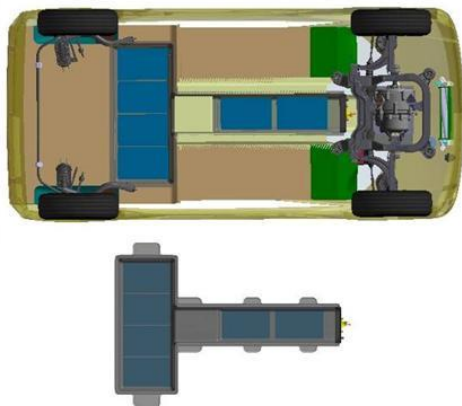


Figure 7.8: 35 kWh, 250 km range FSV 2015-2020

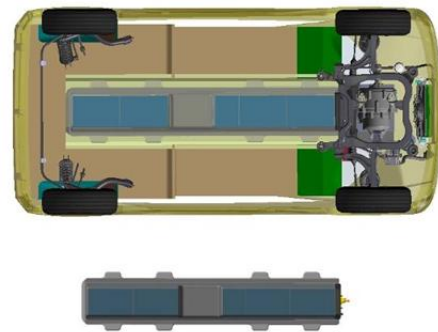


Figure 7.9: 35 kWh (250 km) or 66 kWh (500 km)

Using the battery pack from NEDO3 target case study, a 66 kWh battery packaged into the vehicle is shown in Figure 7.10. In this case, the structure could be as radical as not requiring the tunnel area at all. This powertrain would be of the same mass as that of a conventional ICE or hydrogen fuel cell powertrain at 700 bar.

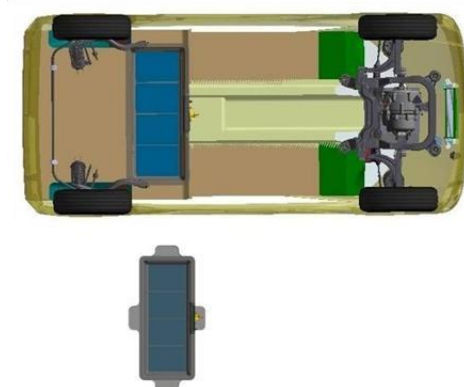





Figure 7.10: 66 kWh (500 km) NEDO3 2030 target battery pack

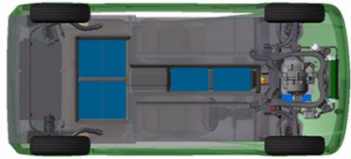

7.2.8 Battery Shape Assessment


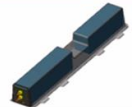
An assessment study on the battery shape, the available volume for packaging (assuming the same $170 \frac{\text{Wh}}{\text{kg}}$ cell level energy density) and its impact on the vehicle's crash energy management revealed some interesting results. The recommended FSV battery shape of a T-section has total available volume of 300 liters, capable of achieving a total energy of 43 kWh (end of life) and 360 km driving range. This design poses a medium risk in the case of a side impact due to the cross car section of the battery.

With an "I" shaped battery, the available volume is 175 liters, achieving a total energy capacity of 24 kWh and capable of a 200 km range. This design poses a medium risk during a high speed rear impact.

A new "flat" design provides an available volume of 260 liters, 37 kWh total energy density and is capable of a range of 310 km. This flat design can pack a higher number of individual cells spread out evenly, reducing the height of the pack to 150 mm. This requires the floor of the vehicle to be raised by at least 100 mm to be able to package this battery into the FSV in contrast to the "T" design which packages inside the tunnel area. The increased height of the vehicle leads to a higher frontal area, less efficient aerodynamics due to the increase in drag at higher speeds. Table 7.9 tabulates the results of this design exercise.

Battery Shape	Available Under-Floor Volume (l)	Battery Capacity kWh New (End of life)	Range (km)	Damage/Risk due to Crash Tests		
				Frontal	Rear	Side
	300	54 (43)	455 (360)	Low	Low	Medium
	175	30 (24)	250 (200)	Low	Medium	Low
	260	46 (37)	385 (310)	Low	Low	Medium

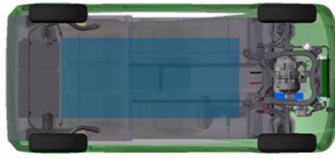




Table 7.9: FSV battery shape assessment

7.3 Motor Technology and Cooling

7.3.1 FSV Recommendation

The motor technology recommendations are based on the following factors:

1. The motor is sized to provide maximum acceleration, grade ability and top speed
2. Peak efficiency is only available in a small operating range
3. Smaller motor is more efficient due to higher operating speed, but torque falls more rapidly as speed increases

The motor specifications recommended for the four FSV variants are as shown in Table 7.10 and Figure 7.11 shows the FSV motor with cooling cavity.

	Units	Current	BEV	PHEV ₂₀	FCEV	PHEV ₄₀
Peak Power	kW	Varies	67	67	75	75
Continuous Power	kW	Varies	49	49	55	55
Max Torque	Nm	Varies	270	270	240	240
Max Efficiency	%	95	96	96	95	95
Specific Cost	\$/kW	40	26	26	26	26
Specific Power	kW/kg	1.2	1.63	1.63	1.63	1.63
Specific Power	kW/l	3.2	4.8	3.3	3.3	3.3
Physical Volume	liters	Varies	14	14	23	23

Table 7.10: *Electric motor recommendations for FSV*

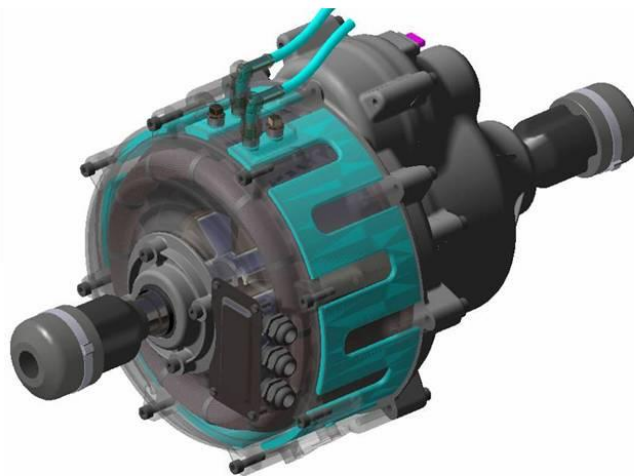


Figure 7.11: *FSV motor with cooling cavity*

7.3.2 DOE Targets

The United States Department of Energy has set motor and power electronics technological development targets in terms of its power density ($\frac{kW}{kg}$) for the years 2010, 2015 and 2020, as shown in Table 7.11.

Year	Power Density (kW/Kg)
2010	1.06
2015	1.2
2020	1.4

Table 7.11: DOE motor and power electronics targets

The FSV motor with its power density at 1.32 is close to the DOE's 2020 goal of 1.4 $\frac{kW}{kg}$.

7.3.3 FSV Motor Versus ICE

Table 7.12 shows the FSV motor specifications compared with the current gasoline ICE. The FSV motor power density is 123% better which leads to a 55% lower mass compared to the ICE at the same power capacity. The volume of the FSV motor is reduced by 80% compared to that of the ICE.

	Power density kW/kg		Motor Peak Power	Motor & Controller Mass	Motor Size		
	kW/kg	kW/l	kW	kg	Volume (l)	Diameter (mm)	Length (mm)
Gasoline Engine	0.59	0.9	75.0	127.1	79.5		
EV Drive Motor 2015-2020 *	1.32	4.80	75.0	56.9	15.6	280.0	253.0
Improvements from Gasoline Engine to Electric Motor	123%	409%		-55%	-80%		

Table 7.12: FSV motor and gasoline ICE

7.3.4 Motor and Transmission Gear Ratio

The size of the motor and transmission gear ratio for the FSV were determined based on the following vehicle specifications:

1. Vehicle acceleration performance (0-100 $\frac{\text{km}}{\text{h}}$) - peak power
2. 10% grade climb at 100 $\frac{\text{km}}{\text{h}}$ - continuous power
3. Vehicle top speed ($\frac{\text{km}}{\text{h}}$)- continuous power
4. Motor efficiency (%)

In case of the FSV, the vehicle top speed of 158 $\frac{\text{km}}{\text{h}}$ and the acceleration of 0-100 $\frac{\text{km}}{\text{h}}$ in 11.6 s were initial specifications. In order to size up the FSV motor, a number of case studies were conducted to arrive at an efficient gear ratio for the motor. Table 7.13 shows the results of these studies and only one of these different ratios selected, is within the FSV required specification.

gear ratio	total ratio	acceleration					NEDC		grade test
		acceleration	top speed	power motor	torque	speed	motor bidirectional efficiency	10% 100km/h	
		0-100km/h	km/h	peak/continuous	Nm	rpm	%	cont. kW motor	
1	3.9	14.8	197	67 / 67	220 / 95	6760	89.23	49	
1.2	4.68	12.8	183	67 / 55	220 / 70	7550	89.47	49	
1.4	5.46	11.6	158	67 / 37	220 / 46	7600	89.08	49	
1.5	5.85	11.2	148	67 / 31	220 / 39	7620	88.88	49	
1.6	6.24	10.8	138	67 / 26	220 / 33	7630	88.73	49	
1.8	7.02	10.4	123	67 / 20	220 / 24	7650	87.84	49	

Table 7.13: FSV motor & transmission case studies

As the gear ratios increased, the acceleration (0-100 $\frac{\text{km}}{\text{h}}$) times decreased and the vehicle top speed ($\frac{\text{km}}{\text{h}}$) decreased. For an acceleration time of 11.6 s, the motor with a peak power capacity of 67 kW and a single ratio of 5.46 is sufficient. Higher ratios, although providing better acceleration times, do not meet the FSV top speed specification of 158 $\frac{\text{km}}{\text{h}}$. PSAT results have shown that a motor with a continuous power rating of 49 kW is required for meeting the FSV’s top speed requirements. The only ratio on the motor that met the continuous power and top speed requirement was 5.46.

Another component of motor sizing is the efficiency of the motor itself. With varying ratios, efficiency varies. As ratio increases, efficiency decreases. The best efficiency values were obtained for the first three cases and 5.46 was the only ratio with the efficiency close to 89% and meet the other two requirements.

If the acceleration time for the FSV was desired to be higher than specified (say in the 8-10 s range), it may be beneficial to have two different gear ratios for the FSV motor (higher gear ratio for satisfying peak power requirements (0-100 $\frac{\text{km}}{\text{h}}$) and a lower ratio for satisfying continuous power requirements (top speed)). But since a single ratio of 5.46 satisfied all FSV requirements, it was the gear ratio chosen for the FSV.

Figure 7.12 shows the cutaway of the FSV motor & transmission assembly.

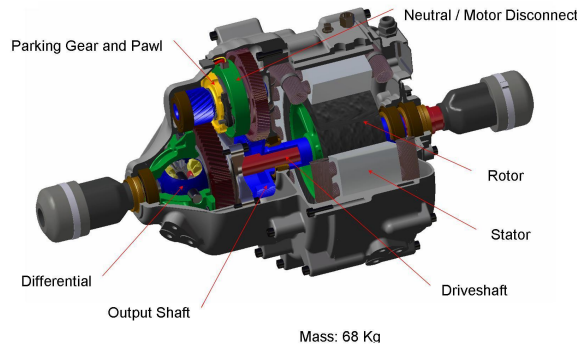


Figure 7.12: FSV motor & transmission cutaway

The transmission consists of a hollow output shaft (blue) connected to the rotor which drives the counter gear (brown) to obtain a ratio of 1.3:1. The counter gear and the differential drive gear (small blue gear) are on the same shaft and are decoupled with a neutral gear (green). The flip side of this neutral gear houses the parking gear (yellow). The smaller differential gear drives the larger brown gear achieving a ratio of 4:1. The red output shaft (or drive shaft) from the differential is concentric to the input shaft. This allows the motor center of gravity to be low when compared to conventional a motor/transmission design.

7.3.5 Motor and Power Electronics with Cooling System

The FSV motor along with the power electronics (DC-DC inverter, motor controller) and the radiator with its hoses are shown in Figure 7.13. Figure 7.14 shows the coolant flow diagram for the FSV.

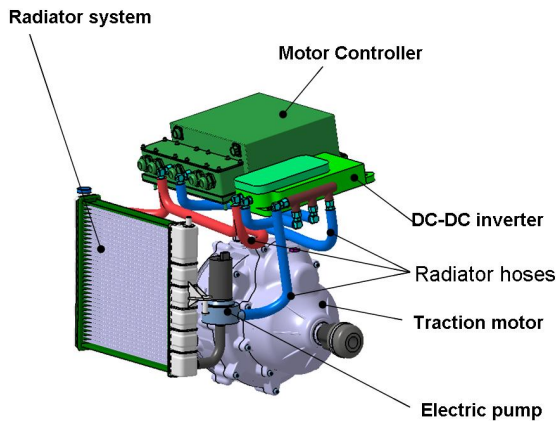


Figure 7.13: FSV motor with cooling

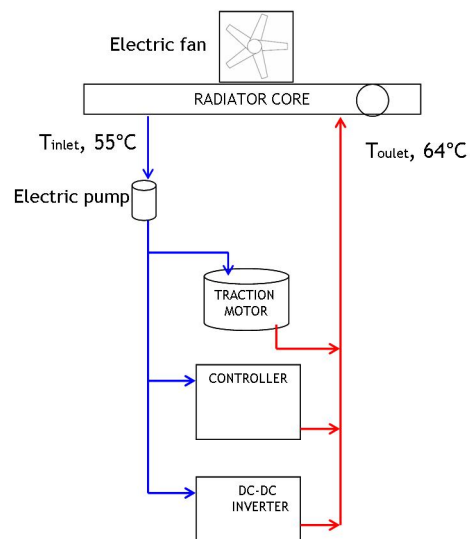


Figure 7.14: FSV motor cooling flow diagram

7.3.6 FSV BEV Energy Balance

Figure 7.15 is a PSAT representation of the energy balance on the FSV BEV for one NEDC drive cycle (11 km).

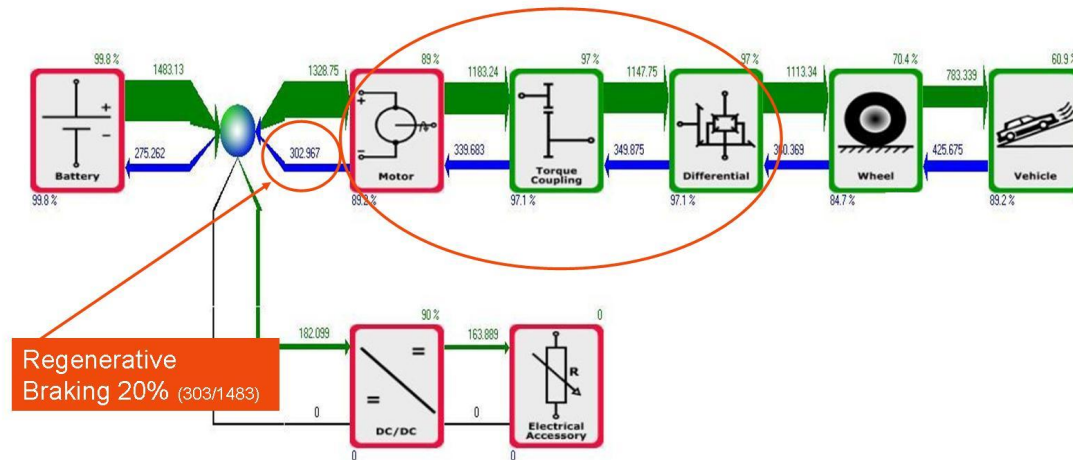


Figure 7.15: FSV BEV energy balance

Figure 7.15 shows the energy travel path starting from the battery to the electric motor, torque coupler (transmission), differential and finally to the wheel. The amount of energy ultimately propelling the vehicle is considerably less than the initial energy available from the battery. A fair amount of energy is lost during transmission due to the inefficiencies of these components.

This energy lost is far less than that of a ICE vehicle due to the higher efficiencies of the electric components (motor, transmission, differential).

Another significant portion of this energy balance is regenerative braking. A small amount of energy travels back from the wheels, through the same channel (with the motor now acting as a generator) and is fed back into this battery. PSAT analysis results for the BEV have shown that 1483 Wh of energy is available in the battery for propulsion and about 302 Wh is recovered through regenerative braking, which translates to about 20% of the initial energy available.

This 20% is calculated assuming that the efficiencies of the motor, transmission and differential are about 89%, 97% and 97% respectively. Since the FSV transmission is a single gear design, the efficiency assumed in PSAT studies is on the conservative side.

7.3.7 FSV BEV, Motor Torque versus RPM Curves

7.3.7.1 1 NEDC Cycle (11 km)

Figure 7.16 shows a plot of the BEV motor torque versus RPM for 1 cycle of the NEDC driving cycle.

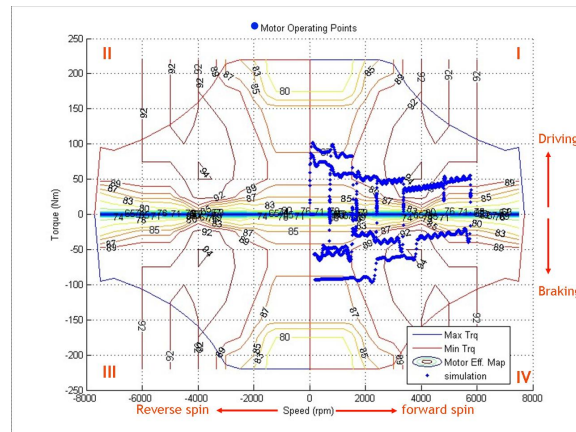


Figure 7.16: FSV BEV motor torque versus RPM

It can be noted that most of these points are along the lines of high efficiencies (brown lines). The same applies to the regenerative braking phase where the motor is operating at high efficiency for the entire phase.

7.3.7.2 0-100 $\frac{\text{km}}{\text{h}}$

Figure 7.17 shows a plot of the BEV motor torque versus RPM during acceleration from 0-100 $\frac{\text{km}}{\text{h}}$.

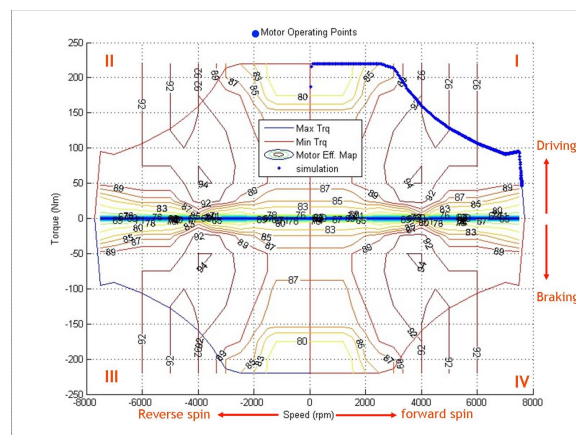


Figure 7.17: FSV BEV motor torque versus RPM - Acceleration

7.3 Motor Technology and Cooling

The motor torque reaches peak power almost instantaneously at a very low RPM and upon reaching $100 \frac{\text{km}}{\text{h}}$ gradually drops down as the motor RPM increases. The blue dots are still in the high efficiency area.

7.3.7.3 10% grade at $100 \frac{\text{km}}{\text{h}}$

Figure 7.18 shows a plot of the BEV motor torque versus RPM during climbing a 10% grade at $100 \frac{\text{km}}{\text{h}}$.

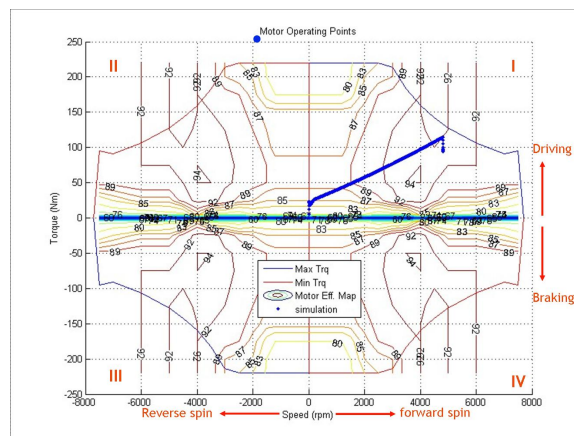


Figure 7.18: FSV BEV motor torque versus RPM - Constant speed grade climb

In this phase, the motor torque and RPM increase until the vehicle reaches a constant speed of $100 \frac{\text{km}}{\text{h}}$ and once reached, the torque drops to a lower value and RPM remains constant for the rest of the grade climb. The motor operating range is still in the high efficiency area.

7.3.7.4 Power demand at 10% grade

Figure 7.19 shows a plot of the vehicle power demand versus time. The motor power demand increases with time and as soon as the speed reaches $100 \frac{\text{km}}{\text{h}}$ evens out and remains constant at 49 kW for the rest of the time the vehicle is on this grade.

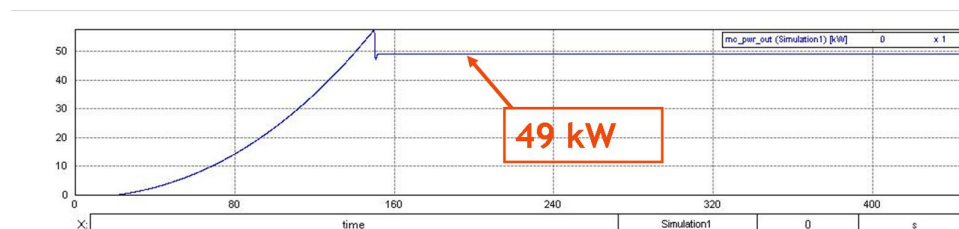


Figure 7.19: FSV BEV power demand at 10% grade

7.4 Fuel Cell Technology

7.4.1 FSV Recommendation

The FSV recommendations for the FCEV is shown in Table 7.14.

Fuel Cell Technology Assessment				
		Status 2008	Prediction 2015-2020	Selection FSV
Dominating Technology		PEM	PEM	PEM
Power Output (net)	kW	40 - 100	50 - 170	65
Efficiency	%	45 - 56	50 - 62	50 - 62
Power Density	kW/kg	0.8 - 1.9	~2.0	2
Cost [\$USD]	\$ USD/ kW	1,500-2,900	~100 - 200	155
Hydrogen Storage Technology Assessment				
		Status 2008	Prediction 2015-2020	Selection FSV
Dominating Technology		Compressed Gas		Compressed
Pressure	MPa	35	50 - 70	70
Tank Material	Carbon Composite	Aluminum Liner	Plastic Liner	Plastic Liner
H₂O Volume Capacity	Liters	80 - 220	70 - 150	95
Hydrogen Capacity (net)	kg	1.7 - 5.0	1.6 - 5.4	3.4
Future Steel Vehicle Concept				
	Capacity (net)	Weight [kg]	Volume [Liters]	Cost [\$ USD]
Without Cooling System				
Fuel Cell Engine	65 kW	92	67	\$10,081
Hydrogen Storage	3.4 kg	87	120	\$7,919

Table 7.14: Fuel Cell recommendation for FSV

The 95 liter tank stores 3.4 kg of hydrogen at a pressure of 700 bar, allowing for a vehicle range of 500 km before having to be refilled. This technology, in terms of hydrogen storage, is state-of-the-art compared to the current capability of storing hydrogen at only about 350 bar.

The FSV's higher output fuel cell stack allows it to be compact enough with efficient packaging within the vehicle.

7.4.2 Energy Density Comparison

Figure 7.20 and Figure 7.21 show the current levels of energy densities in terms of weight ($\frac{kW}{kg}$) and volume ($\frac{kW}{l}$) respectively, achieved by fuel cells from various sources and projected numbers for the year 2015 and beyond. The FSV's fuel cell has the energy density of $2.0 \frac{kW}{kg}$ and $2.25 \frac{kW}{l}$, which are both in line with the technological advancements predicted in this field for year 2015 and beyond.

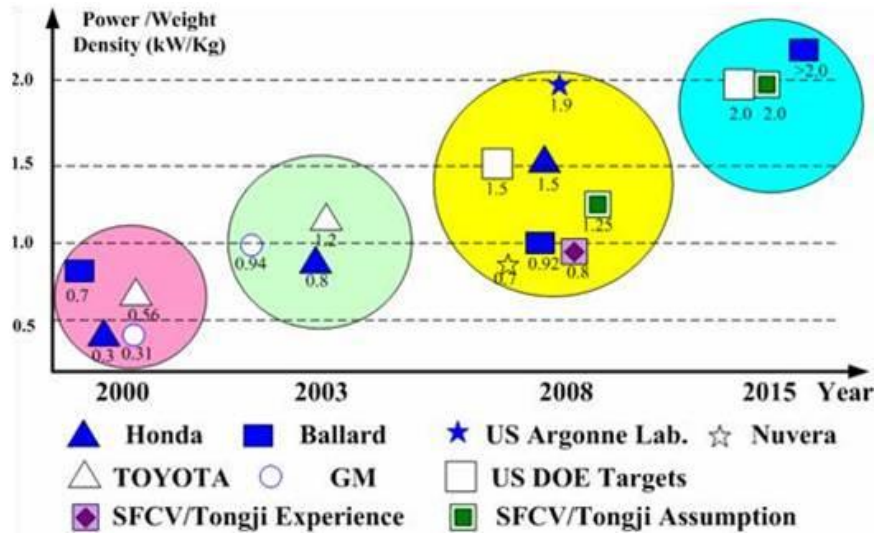


Figure 7.20: Energy density (power/weight)

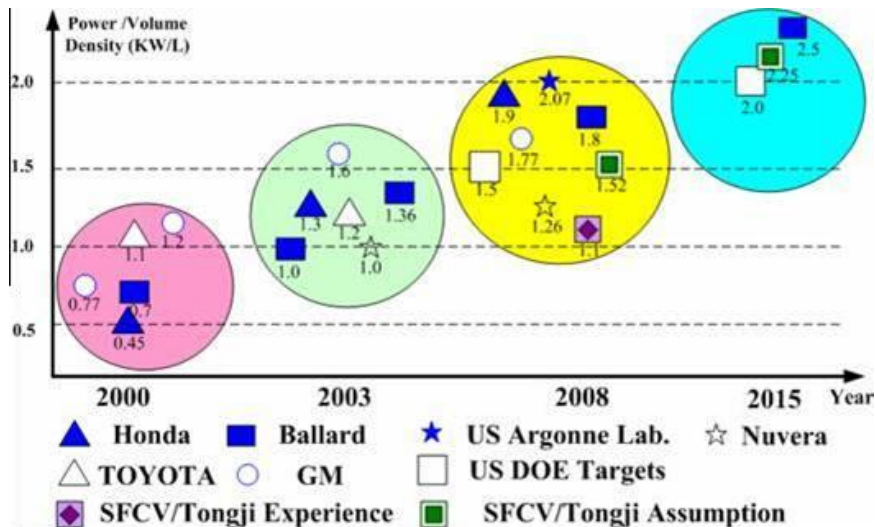


Figure 7.21: Power density (power/Volume)

7.4.3 FSV Packaging

The FSV FCEV achieves an efficient packaging of the fuel cell components due to the inherent design advantages posed by each of its components.

The hydrogen tank is packaged in between the rear wheels. The FSV hydrogen tank has a much smaller volume as compared to some of the current technology hydrogen tanks used by OEMs. This packaging allows the FSV to retain more luggage space.

The fuel stack itself is packaged under the tunnel area, which is an efficient packaging strategy. This allows the FSV to have a low center of gravity and does not require significant changes to the underbody of the vehicle. This higher capacity fuel stack allows the FSV achieve the its performance requirements.

Figure 7.22 shows the packaging of the fuel cell system on the FSV.

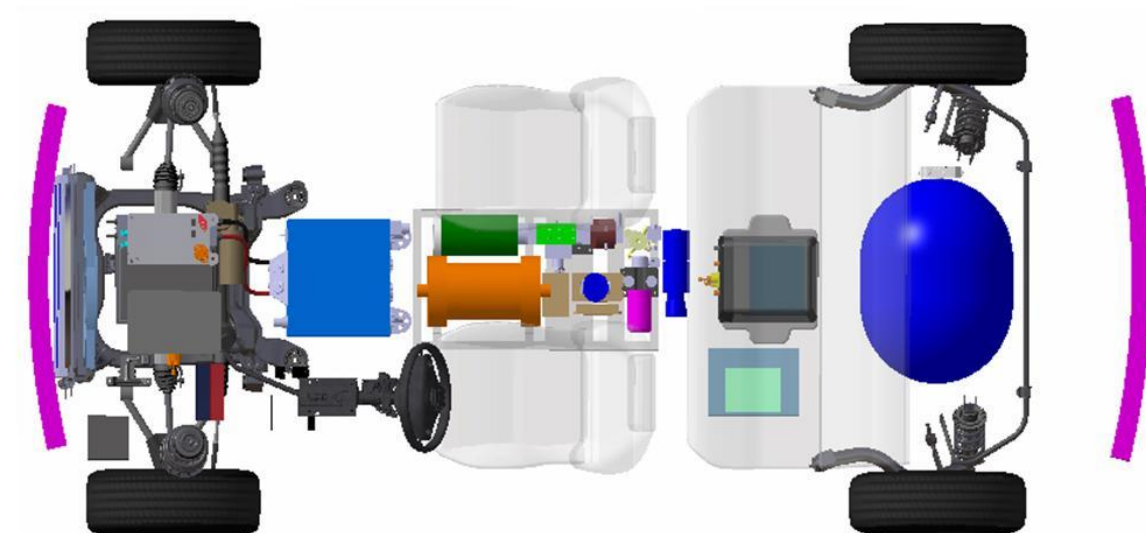


Figure 7.22: *FSV fuel cell system packaging*

8.0 Environmental Impact

8.1 Overview

Automobiles affect the environment in many ways, impacts begin from the point automobiles are manufactured (considering the production of the parts and materials that the automobile is made of) until the end when the automobiles are scrapped in a junkyard (considering the wastes to be disposed in spite of recycling many parts). However, much of the environmental damage occurs during the driving of vehicles, due to pollution from the exhaust and pollution associated with supplying the fuel.

In the United States, the majority of the vehicles use gasoline as the fuel. When gasoline and diesel fuels are burned in car engines, combustion is never perfect, and so mixes of hazardous pollutants come out the tailpipe. If combustion were perfect, the exhaust would contain only water vapor and carbon dioxide. Carbon dioxide (CO₂) is not harmful to health directly, at least not in low concentrations. However, CO₂ from fossil fuels like gasoline and diesel is very harmful to the environment because it has been identified a source of global warming.

Regulatory bodies across the globe are addressing global warming due to CO₂ emissions by imposing stricter targets to limit the emissions: the United States Transportation Department proposed a combined average standard for cars and light trucks of 35 mpg by 2020, the European Commission (EC) proposed legislation to reduce average CO₂ emissions to 130 g by 2012, and Japan's standards are expected to lead to lowest fleet average emissions for new vehicles to be 125 $\frac{\text{g}}{\text{km}}$ in 2015.

8.1.1 Fuel Efficiency and CO₂ Relevance

- CO₂ is directly proportional to fuel economy with carbon-based fuels
- Gasoline vehicle emission - 1 l ~ 2325 g CO₂
- CO₂ is decreased when the fuel efficiency increases or when carbon based fuels are not used (i.e. hydrogen, electricity, bio-fuels)

Currently, 96% of the automobiles are dependent on petroleum based fuels^[1]. The number of

¹gasoline and diesel

vehicles produced in 2008 was 82 million globally resulting in a daily petroleum consumption of over 30 million barrels. So, the amount of CO₂ released into the atmosphere from the vehicles is 12.5 million tons on a daily basis (one barrel of oil releases 370 kg of CO₂), assuming all the produced vehicles are on the road, and ignoring the emissions from current vehicles already on the road. Further, the global production of vehicles is projected to increase to 1 billion by 2020, which implies proportional increase in the CO₂ emissions into the environment.

The reduction of green house gas emissions can only be achieved by utilizing more fuel-efficient vehicles with advanced powertrains thus lowering petroleum consumption. As hybrid, plug-in hybrids and all electric vehicles become dominant over the next ten to twenty years, they will play a major role in reducing the environmental impact.

Currently, Hybrid Electric Vehicle (HEV) is the most effective solution to reduce fuel consumption (Toyota Prius - $109 \frac{\text{g}(\text{CO}_2)}{\text{km}}$, $4.7 \frac{\text{l}}{100\text{km}}$), as compared to conventional vehicles. Current HEVs reduce petroleum consumption under certain circumstances, compared to otherwise similar conventional vehicles, primarily by using three mechanisms:

1. Reducing wasted energy during idle/low output, generally by turning the engine off
2. Recapturing vehicles inertial energy through regenerative braking
3. Reducing the size and power of the engine, and hence inefficiencies from under-utilization, by using the added power from the electric motor to compensate for the loss in peak power output from the smaller engine

Combinations of the above three primary hybrid advantages form the basis of various HEV powertrains in production at present. The ICE (internal combustion engine) in an HEV can be smaller, lighter, and more efficient than the one in a conventional vehicle, because the combustion engine can be sized for slightly above average power demand rather than peak power demand.

Future advanced powertrains that will lead to additional fuel efficiencies, green house gases reduction and petroleum independence by use of alternate fuels are:

- Electricity - BEV (Battery Electric Vehicle)
- Electricity & Gasoline - PHEV (Plug-in HEV)
- Hydrogen Gas - FCEV (Fuel Cell Electric Vehicle)

8.1.2 Air Pollution

Although great strides have been made at reducing air pollution from automobile exhaust over the past 30 years, motor vehicles still account for a significant proportion of air pollution in urban areas worldwide as shown in Table 8.1.

Air Pollutant	Proportion from Vehicles	Note
Oxides of Nitrogen (NO _x)	34%	Precursor to ground-level ozone (smog), which damages the respiratory system and injures plants
Volatile Organic Compounds (VOC)	34%	Precursor to ground-level ozone (smog), which damages the respiratory system and injures plants
Carbon Monoxide (CO)	51%	Contributes to smog production; poisonous in high concentrations
Particulate Matter (PM ₁₀)	10%	Does not include dust from paved and unpaved roads, which are the major source of particulate matter pollution (50% of the total)
Carbon Dioxide (CO ₂)	33%	Thought to be primary contributor to global warming

Table 8.1: Selected facts and figures 2002 (Source: US Department of Transportation - Federal Highway Administration)

By reducing fuel consumption and the use of alternate carbon free fuels, there will be lower air pollution and lead to improved human health. Advanced powertrains BEV, PHEV in EV mode and FCEV are zero emissions vehicles and will play great role in urban pollution reduction.

8.1.3 Noise Pollution

Car and truck noise has become perhaps the primary source of noise pollution in urban environments worldwide. The Organization for Economic Cooperation and Development (OECD) estimates that 37% of the US population was exposed to “annoying” levels of highway noise (greater than 55 dB), while 7% were exposed to levels that made conversation difficult (> 65 dB).

In comparison to conventional gasoline or diesel powered engine vehicles, BEV, PHEV and FCEV vehicles are considerably quieter and will lead to reduction in roadway noise.

8.2 Well-to-Wheel Efficiencies

8.2.1 Total Life Cycle Assessment

Currently, vehicles produced worldwide are only being evaluated on the basis of their performance known as “Pump-to-Wheel” fuel consumption and corresponding CO₂ emissions. This only accounts for the CO₂ emissions arising from the usage of fuel by the vehicles from the point the fuel is filled into the fuel tank. For comprehensive assessment of green-house gas emissions, the following two cycles are also to be considered:

1. Fuel production cycle also known as “Well-to-Pump”
2. Vehicle manufacturing cycle

“Well-to-Pump” cycle denotes the efficiency of the fuel source net energy retention left over from the refining and transportation process. Vehicle manufacturing cycle considers the steps involved during the production of materials and end of life recycling. Hence, total life cycle assessment refers to the assessment starting from the raw material used for production of a product, respective usage of the product, and finally the disposal. The sum of all those steps - or phases - is the life cycle of the product. The total life cycle assessment based on all the factors is shown in Figure 8.1.

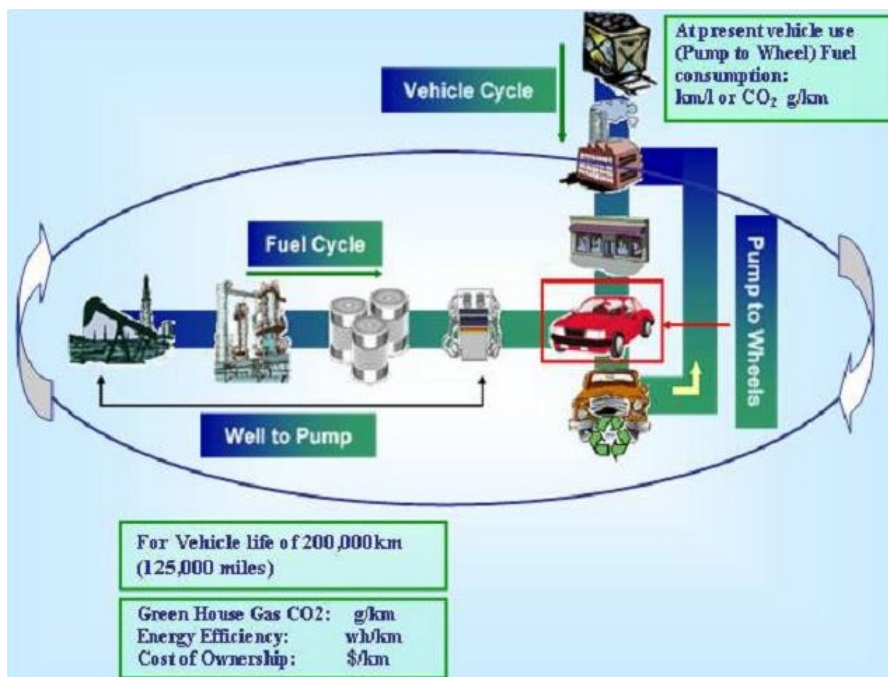


Figure 8.1: Total life cycle assessment

8.2.2 Well-to-Pump Assessment - Fuel Cycle

The Well-to-Pump assessment for all possible future sources of FSV vehicle fuels was done using Argonne National Lab programs “Greet 1.8B”. The sources of energy (fuels) considered included the following:

- Electricity (US Mix, Europe, China, Japan, India, 100% coal and 100% renewable)
- Gasoline and diesel from petroleum
- Bio-fuels, ethanol and bio-diesel
- Hydrogen (gas and liquid), made using electrolysis process, and from natural gas

Electricity generation efficiencies vary from one country to the other due the different feedstocks used. Each feedstock has a different efficiency for generating electricity. The electricity generation distribution using various feedstocks, and the corresponding emissions, are shown in Table 8.2.

It can be observed that the CO₂ and NO_x emissions due to electricity generation are higher in the US than Europe, due to the difference in feedstocks used. However, the emissions will be zero and the efficiency will be higher, if a green mix of feedstocks is used for the electricity generation (91.5% efficiency for USA, as shown in the figure).

Feedstocks [%]	USA	Europe	China	Japan	India	Coal	USA Green Mix
Coal	50.7	29.5	79	28.1	68.7	100	0
Natural Gas	18.9	9.9	0	21	8.9	0	0
Oil	2.7	4.5	2.4	13.2	4.5	0	0
Nuclear	18.7	31	2.1	27.7	2.5	0	20
Biomass	1.3	2.1	0	0	0	0	0
Others	7.7	13	16.5	10	15.4	0	80
	100	100	100	100	100	0	100
Electricity Pathway:							
Efficiency [%]	37.9	44.2	35	41.6	35.1	30.7	91.5
CO2 [g/kWh]	750.6	520.3	973	596.7	923.5	1201.3	0
VOC [g/kWh]	0.07	0.05	0.08	0.06	0.08	0.09	0
Nox [g/kWh]	0.82	0.61	1.05	0.76	1.01	1.26	0
Sox [g/kWh]	1.8	1.25	2.64	1.74	2.46	3.15	0

Table 8.2: Well-to-Pump results (electricity generation)

The Well-to-Pump efficiencies for the different fuels used by US vehicles are shown in Figure 8.2 and the corresponding CO₂ emissions for the respective fuels are shown in Figure 8.3. It can be seen that the CO₂ footprint is more prominent for electricity generation and production of hydrogen.

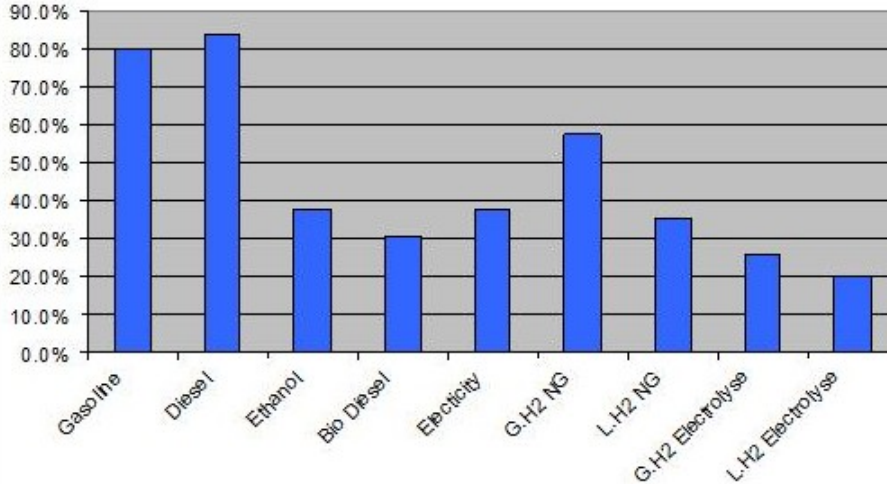


Figure 8.2: Well-to-Pump efficiency fuel production cycle (US)

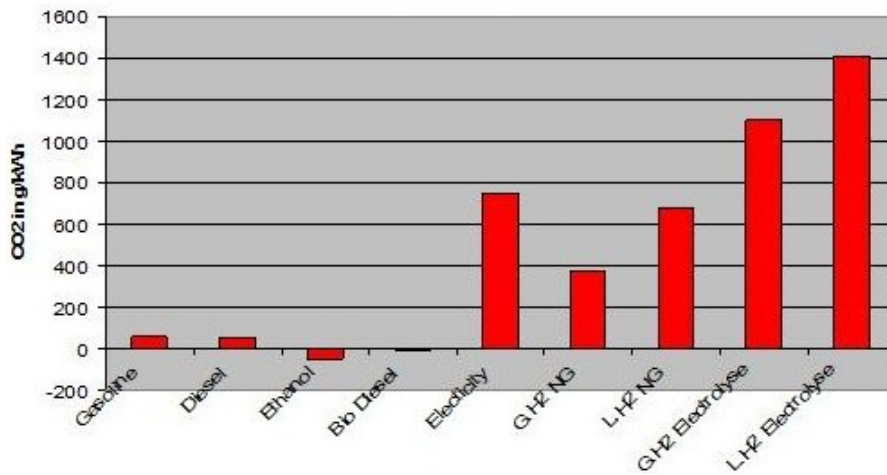


Figure 8.3: Well-to-Pump fuel production GHG CO₂ emissions (US)

8.2.3 Pump-to-Wheel Assessment - FSV

The Pump-to-Wheel fuel economy and CO₂ emissions for all the variants of the FSV are shown in Table 8.3.

	FSV1		FSV2		Reg. Limit ALL
	BEV	PHEV ₂₀	FCEV	PHEV ₄₀	
European Drive Cycle (NEDC)					
CO2 Emissions g/km	0	23	0	27	95
Fossil Fuel l/100km	0	0.99	0	1.14	4.1
Electricity Usage $\frac{Wh}{km}$	89	65	0	75	N/A
Total Energy Usage ** $\frac{Wh}{km}$	89	152	211	175	361
2008 US EPA Drive Cycle					
CO2 Emissions (combined) g/km	0	31	0	35	156
Combined MPG	∞	177	∞	157	35
Combined Electricity Usage $\frac{Wh}{km}$	109	80	0	92	N/A
Combined Energy Usage ** $\frac{Wh}{km}$	109	196	295	224	590
City MPG	∞	177	∞	157	N/A
City Electricity Usage $\frac{Wh}{km}$	103	75	0	86	N/A
City Energy Usage ** $\frac{Wh}{km}$	103	192	304	218	N/A
Highway MPG	∞	177	∞	157	N/A
Highway Electricity Usage $\frac{Wh}{km}$	117	85	0	99	N/A
Highway Energy Usage ** $\frac{Wh}{km}$	117	202	295	231	N/A

* Based on Petroleum Displacement method

* Assumption: 70% in EV modes & 30% in Charge Sustaining modes

** Combined fuel energy plus stored electrical energy

Table 8.3: FSV fuel economy and CO₂ emissions table

The Pump-to-Wheel fuel economy and CO₂ emissions results achieved for all variants of the FSV are well below the future worldwide requirements. The most stringent future proposed requirement for CO₂ emissions is 95 $\frac{g(CO_2)}{km}$ (passenger car fleet average) in the European Union (EU), to be met by year 2020.

The Pump-to-Wheel emissions for the BEV and FCEV are zero. These powertrains are classified as Zero Emissions Vehicles (ZEV) by California Air Resources Board (CARB). The CO₂ emissions for PHEV₂₀ and PHEV₄₀ are 23 $\frac{g(CO_2)}{km}$ and 27 $\frac{g(CO_2)}{km}$ respectively, assuming these vehicles will be driven in EV mode for 70% of the miles driven. Currently, there are no agreed methods for measuring the fuel economy for the PHEV vehicles. It will most likely be based on how much petroleum

the PHEV is saving by using electricity from the grid, (“Petroleum Displacement” method).

The graph from “Japan - Ministry of Land, Infrastructure, Transport and Tourism”, in Figure 8.4, shows how the FSV CO₂ emissions compared with other gasoline, diesel and HEV vehicle technologies.

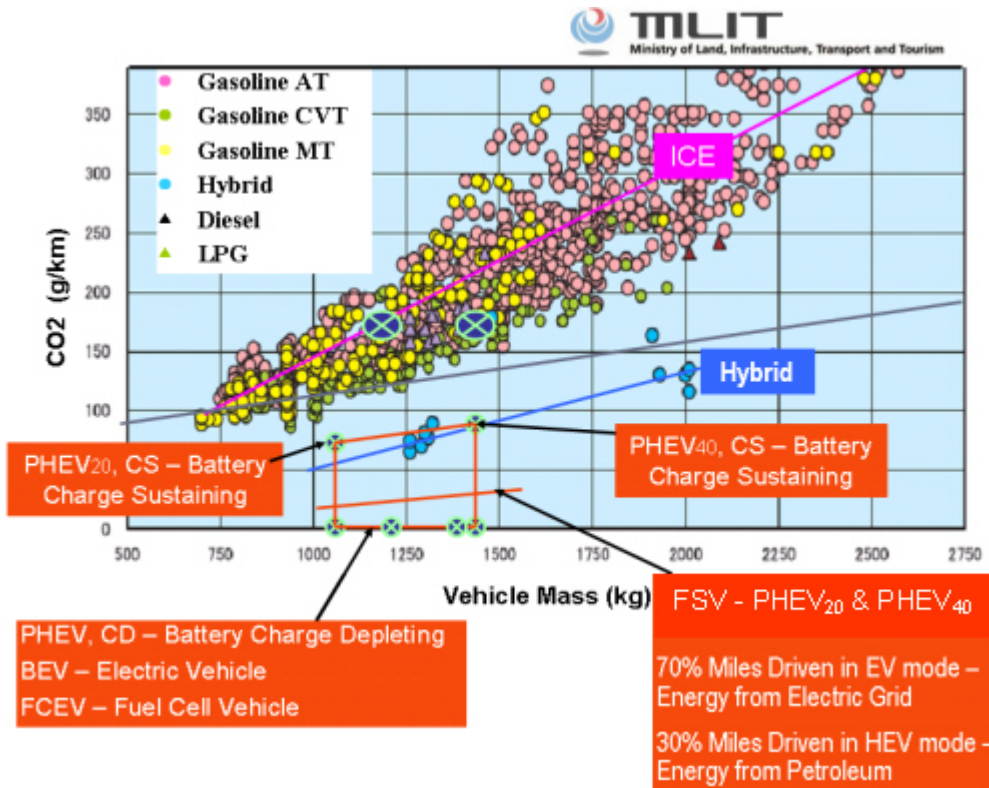


Figure 8.4: FSV fuel economy and CO₂ emissions versus other technologies

It can be clearly seen from Figure 8.4 that the FSVs emissions are very close to those in the Zero Emission Vehicle (ZEV) class of vehicles. It can be observed that the slope of each technologies data set, in the above graph, for ICE, HEV, and FSV are progressively trending lower, indicating proportionally lower CO₂ emissions as indicated by the slope of the line, with respect to proportional mass increases, (not to be confused with total mass increases). This is mainly due to future vehicles using regenerative braking systems, whereas the ICE system can not utilize regenerative braking. The FSV has the most effective regenerative braking system due to having a higher power electric motor and larger capacity battery, when compared to the less effective units in the HEVs.

8.3 FSV Environmental Assessment

8.3.1 FSV-1 - Assessment

8.3.1.1 FSV-1 Pump-to-Wheel CO₂ Emissions

The Pump-to-Wheel fuel economy was analyzed using the Powertrain System Analysis Toolkit (PSAT). In order to evaluate the FSV vehicles and represent worldwide markets, each vehicle was put through standard drive cycles from North America, Japan, and Europe. The cycles used were the following:

1. US EPA UDDS (shown in Figure 8.5)
2. Japan 10-15 (shown in Figure 8.6)
3. EU NEDC (shown in Figure 8.7)

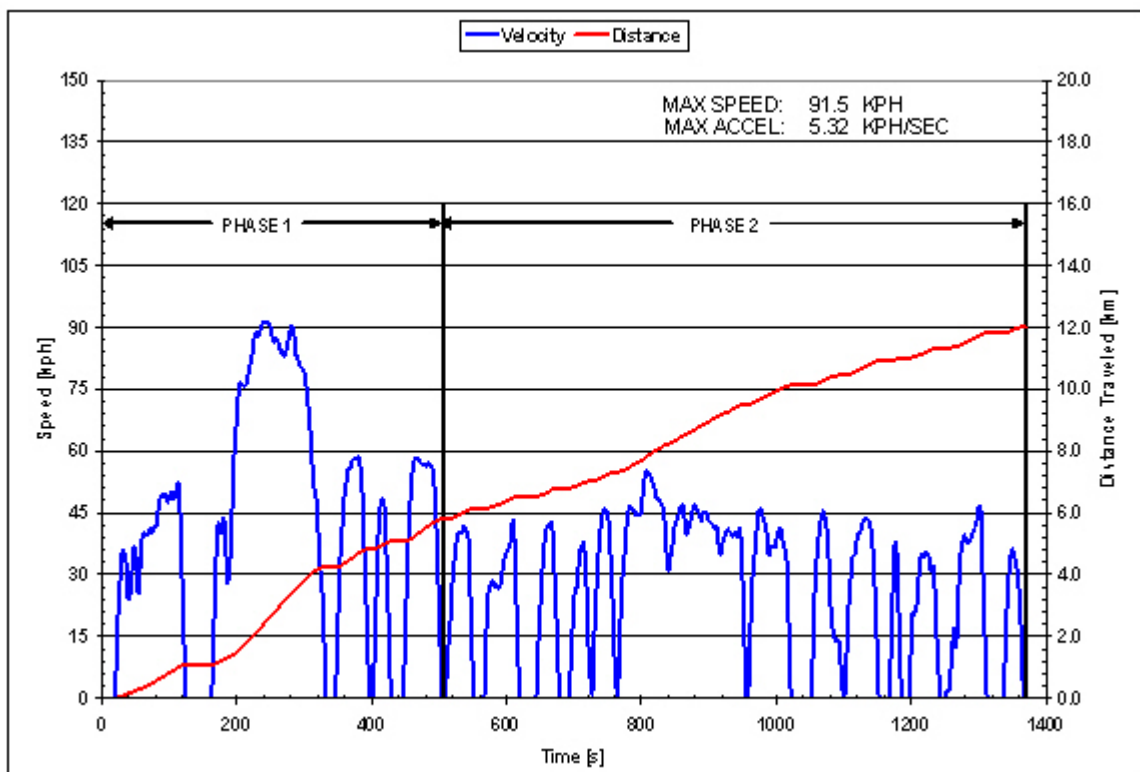


Figure 8.5: US EPA UDDS cycle

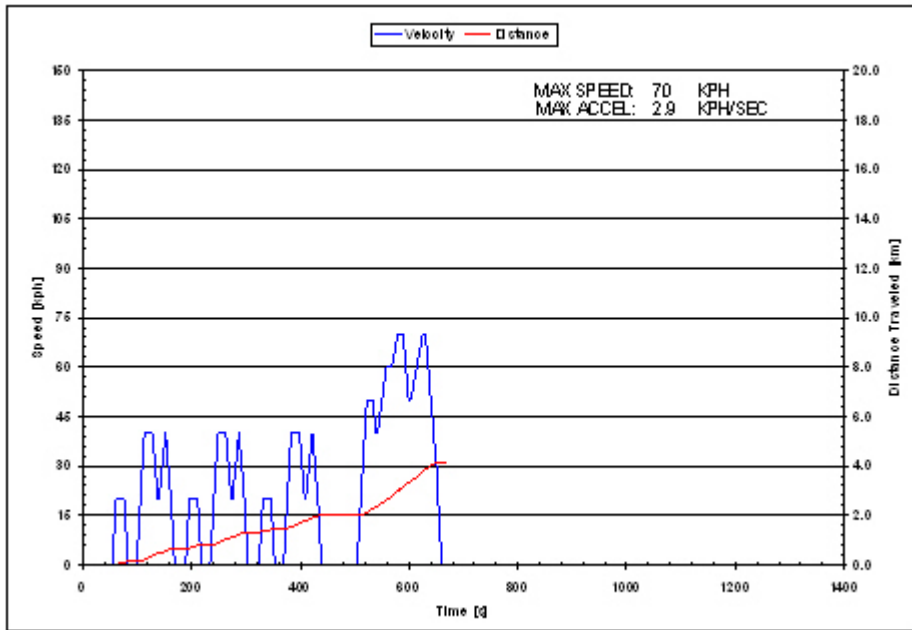


Figure 8.6: *Japan 10-15 cycle*

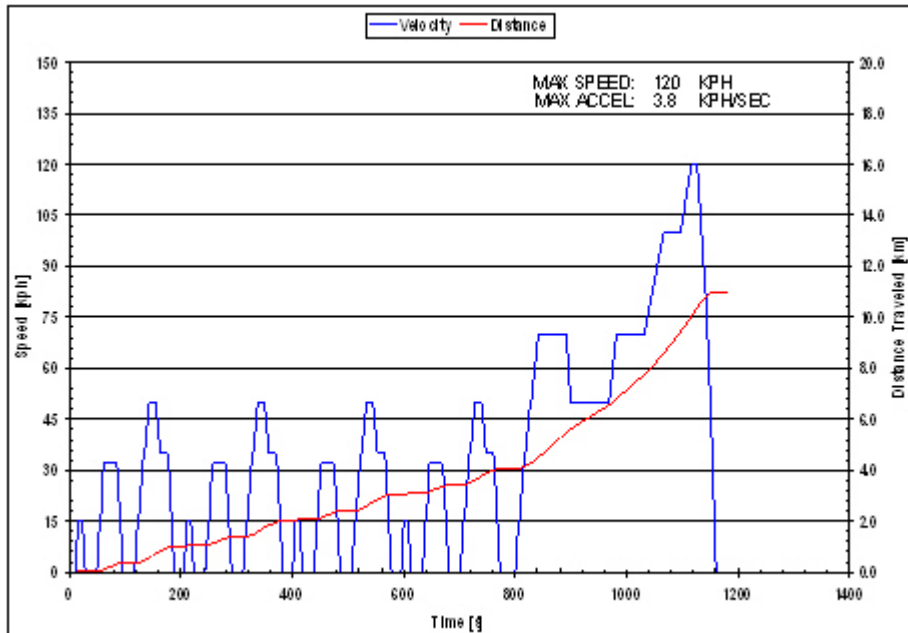


Figure 8.7: *EU NEDC Drive cycle*

Drive cycles used on different continents are designed to simulate the regional driving patterns and behaviors. Most optimizations in a development cycle can be made with any one of the indicated standards, while regional verification and fine tuning can be left towards the end of the

development phase. For vehicle comparison purposes, the UDDS cycle was selected for the FSV.

In the PSAT simulations, for each Charge Depleting operation, the cycle being evaluated was repeated multiple times back-to-back until the charge in the battery was depleted. For Charge Sustaining operation, each cycle was repeated two times. The PSAT analysis results are shown in Table 8.4.

		UDDS	Japan 10-15	NEDC
PHEV₄₀ Series Mid-size: 1300kg Vehicle + 75kg driver				
Charge Depleting	[Wh / km]	107	110	111
	[L / 100km]	0	0	0
	[g CO ₂ / km]	0	0	0
Charge Sustaining	[Wh / km]	0	0	0
	[L / 100km]	3.8	3.79	3.79
	[g CO ₂ / km]	88.4	88	88
PHEV₂₀ Series Small-size: 1000kg Vehicle + 75kg driver				
Charge Depleting	[Wh / km]	92.5	94.9	96.9
	[L / 100km]	0	0	0
	[g CO ₂ / km]	0	0	0
Charge Sustaining	[Wh / km]	0	0	0
	[L / 100km]	3.3	3.27	3.43
	[g CO ₂ / km]	76.7	76	79.8
EV Series Small-size: 1100kg Vehicle + 75kg driver				
	[Wh / km]	88.9	92.8	96.4
	[g CO ₂ / km]	0	0	0
FCEV Series Mid-size: 1300kg Vehicle + 75kg driver				
	[kg / 100km]	0.632	0.669	0.653
	[g CO ₂ / km]	0	0	0

Table 8.4: Pump-to-Wheel GHG CO₂ emissions

The Pump-to-Wheel CO₂ emissions for each FSV vehicle is shown in Figure 8.8. The limit of 95 $\frac{g(CO_2)}{km}$ shown in Figure, is the CO₂ regulation proposed for the European Union to come into effect by 2020.

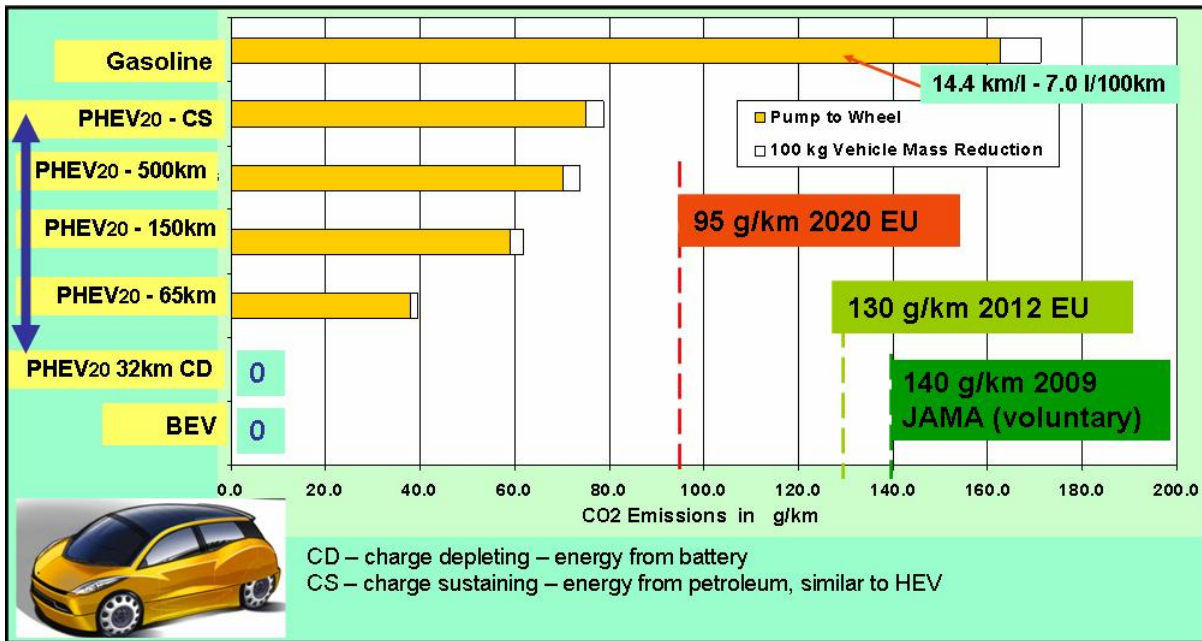


Figure 8.8: FSV-1 Pump-to-Wheel CO₂ emissions

The Gasoline representative baseline vehicle shown in Figure 8.8 is a conventional vehicle with gasoline powered internal combustion engine. For each PHEV, both Charge Sustaining (CS) HEV and Charge Depleting (CD) all-electric driving modes are also shown. On a Pump-to-Wheel basis, all four FSV powertrain variants will emit less than 95 $\frac{g(CO_2)}{km}$. The PHEVs and BEV produce zero CO₂ from the tailpipe when driven in all-electric mode.

8.3.1.2 FSV-1 Well-to-Wheel CO₂ Emissions

As mentioned earlier there are CO₂ emissions also from the production of fossil fuels, renewable fuel, or electricity. So a Well-to-Wheel analysis is very important for a comprehensive evaluation of vehicle emissions. Adding the Well-to-Pump emissions factor to each vehicle, the Well-to-Wheel CO₂ emissions are attained, as shown in Figure 8.9.

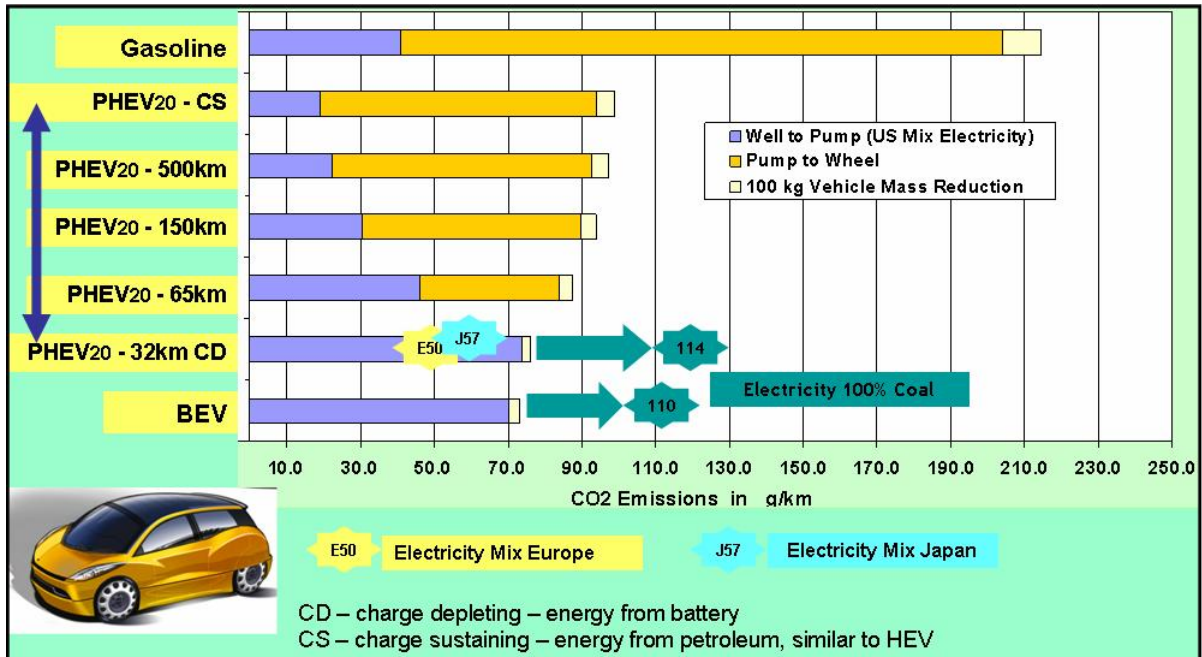


Figure 8.9: FSV-1 Well-to-Wheel CO₂ emissions

It can be observed from Figure 8.9 that, the PHEV in Charge Depleting all electric mode and BEV have zero tailpipe CO₂ emissions. However, their carbon footprint is not zero due to emissions from the production of fuel.

8.3.2 FSV-2 - Assessment

An environmental assessment of FSV-2 was also conducted using the Well-to-Wheel CO₂ emissions as explained earlier in Section 8.3.1.2. The results of the assessment are shown in the Figure 8.10 and Figure 8.11.

8.3.2.1 FSV-2 Pump-to-Wheel CO₂ Emissions

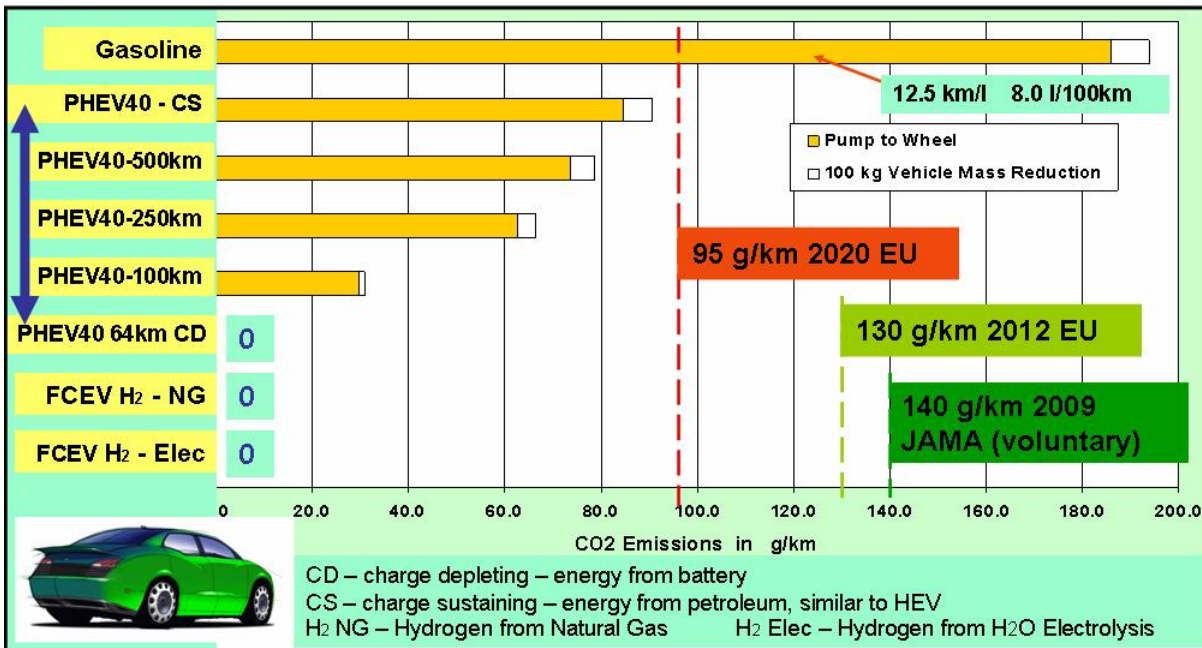
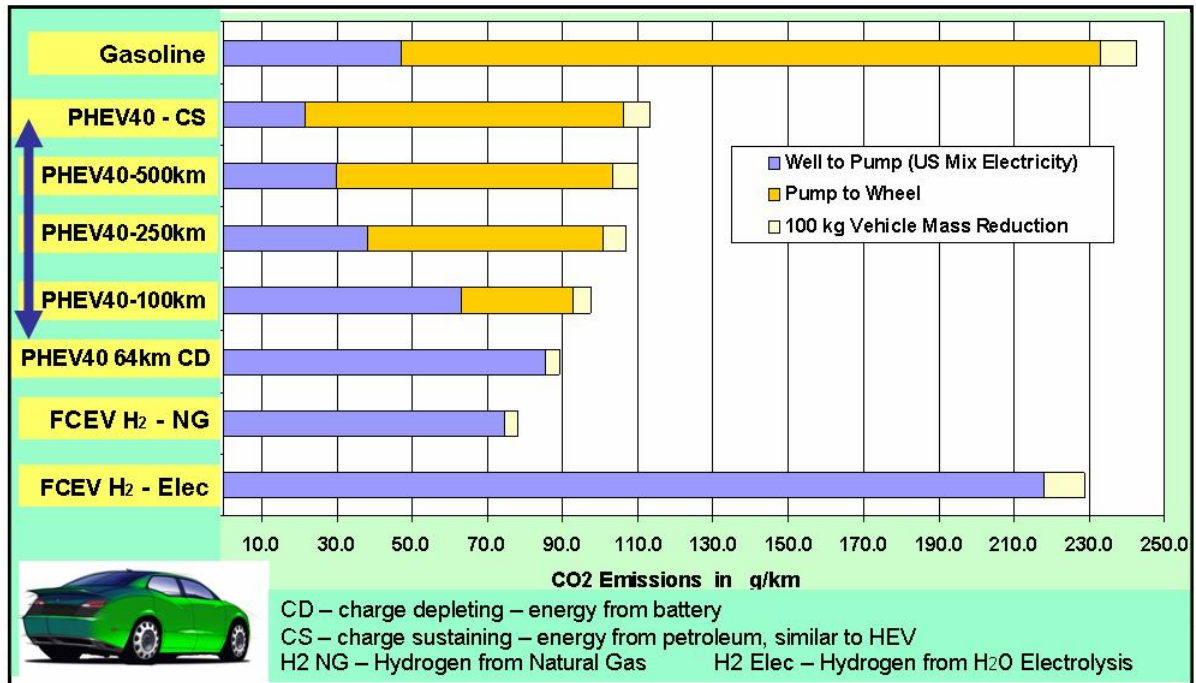


Figure 8.10: FSV-2 Pump-to-Wheel CO₂ emissions

8.3.2.2 FSV-2 Well-to-Wheel CO₂ Emissions

 Figure 8.11: FSV-2 Well-to-Wheel CO₂ emissions

Even though FCEV H₂-NG, FCEV H₂-electric have zero tailpipe CO₂ emissions, their carbon footprint is not zero due to production of their respective energy source. The FCEV H₂ has a strong dependence on where its hydrogen comes from. In the best case scenario it is only marginally better than the PHEV₄₀ operating in Charge Sustaining mode. It is envisioned that in the 2015 - 2020 timeframe, electrical power available for FCEV H₂ electrolytic hydrogen production will come from a utility grid much like today's (power generation infrastructure will not evolve rapidly) and its carbon footprint is much greater than any of the other PHEV variants.

8.4 Well-to-Wheel Energy Usage

“Well-to-Wheel” efficiency is the overall energy cost utilized in the production of fuel (from the well to...) and use of fuel in a vehicle (...the wheel). If the amount of energy is available at the production source for the different fuels, the amount of energy that is ultimately utilized varies according to the respective efficiencies of the respective production process and the respective engines.

Figure 8.12 shows the different fuels and the corresponding “Well-to-Pump - Pump-to-Wheel” efficiency showing the net energy available at the vehicle wheels when starting with 100 units of feedstock energy.

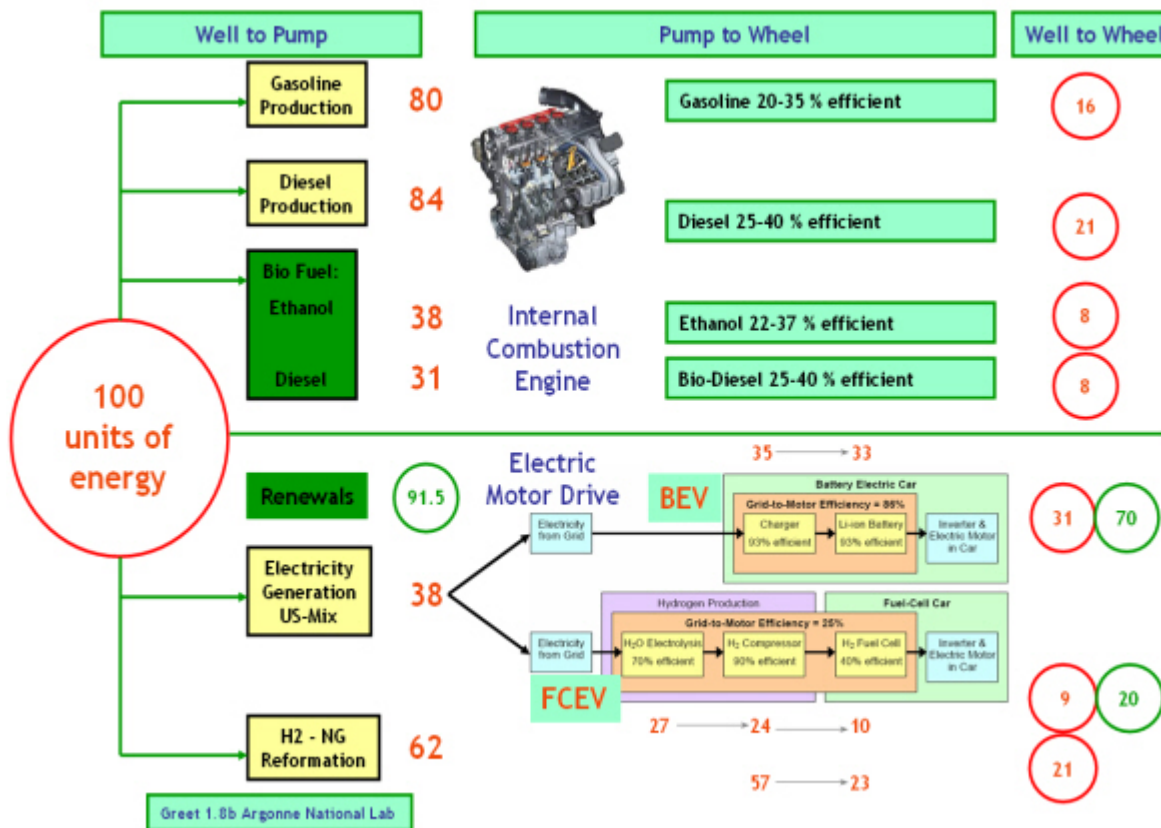


Figure 8.12: Well-to-Wheel Energy Efficiency

8.4.1 Conventional Technologies

Considering the case of gasoline production if one hundred units are available at source, there is a net loss of 20 energy units in the transformation process due to the energy consumed by the drilling process, refining process and ultimately by transportation of gasoline to the gas pump. Further, from the 80 units available after the gasoline production, the internal combustion engine (ICE) consumes 65%-80% of that energy through combustion induced heat loss with approximately 16 units of energy remaining for the vehicle propulsion.

As shown in Figure 8.13, for the conventional ICE drive systems, diesel offers the highest efficiency of 21%. The bio-fuels (first generation corn based) are only 8% efficient due to most of the 100 energy units being consumed during its production process.

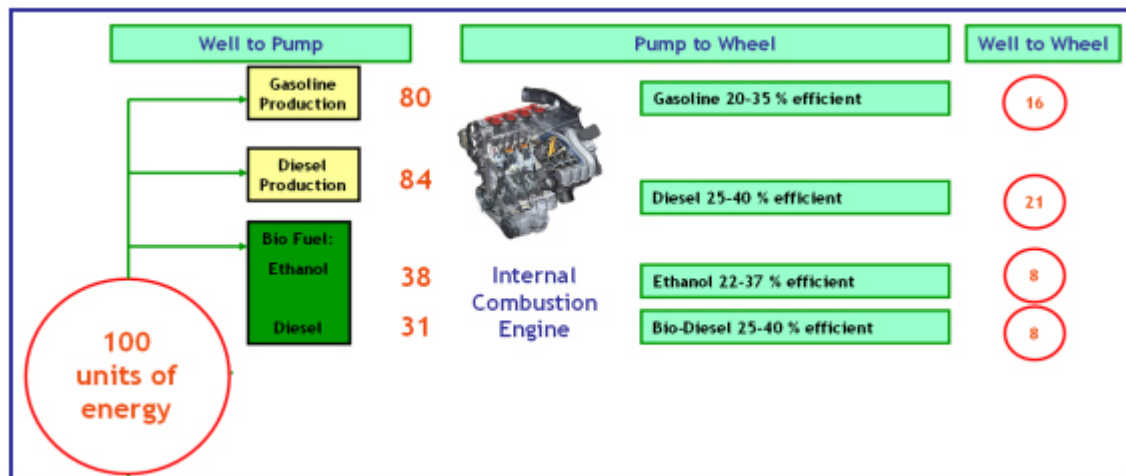


Figure 8.13: Conventional technologies Well-to-Wheel energy efficiency

8.4.2 Advanced Technologies

The production process of electricity is not as efficient as gasoline production. As seen in Figure 8.14, only 38 units of energy is available from the 100 units of energy fed into the electricity generation process (US-mix). However, due to the higher efficiency of BEVs, only 7 units are lost, resulting in 31 units for vehicle propulsion. The losses in BEV are due to battery charging/discharging, and electric motor loss.

FCEV is not as efficient as the BEV, resulting in only 9 units for vehicle propulsion out of the initially available 38 units. The energy lost in the FCEV is due to losses during H₂O electrolysis, H₂ compression, fuel cell losses, and finally electric motor loss. However, the Well-to-Wheel efficiency of FCEV is much higher if the source of hydrogen is natural gas. As can be seen in Figure 8.14, 21 units are available if natural gas is the feedstock for the hydrogen used in the FCEV.

Further, if renewable sources of energy such as solar, wind etc., are used to produce electricity, BEV proves to be the most efficient with an impressive 70 units remaining for propulsion (shown in Figure 8.15).

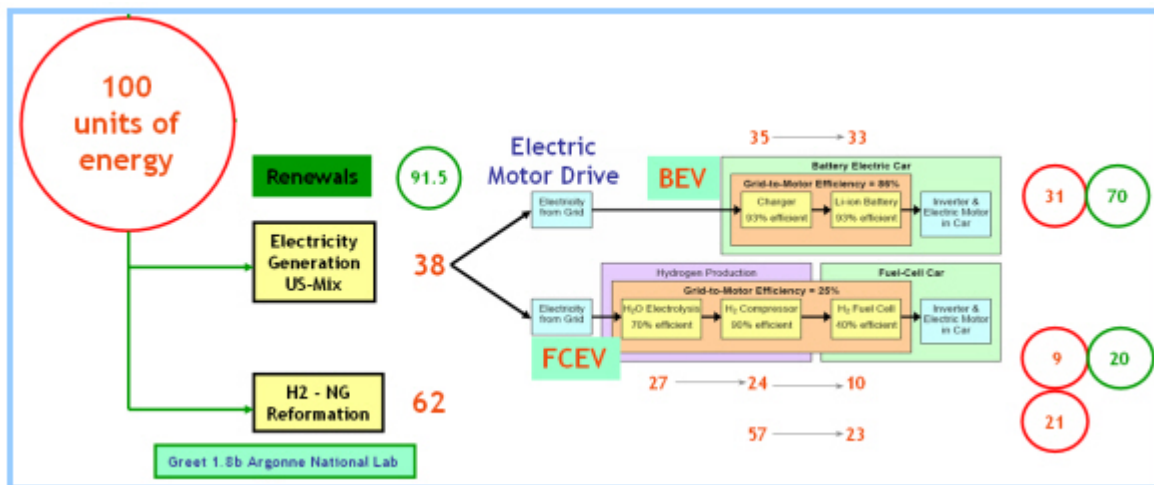


Figure 8.14: Advanced technologies Well-to-Wheel energy efficiency (non-renewable energy source)

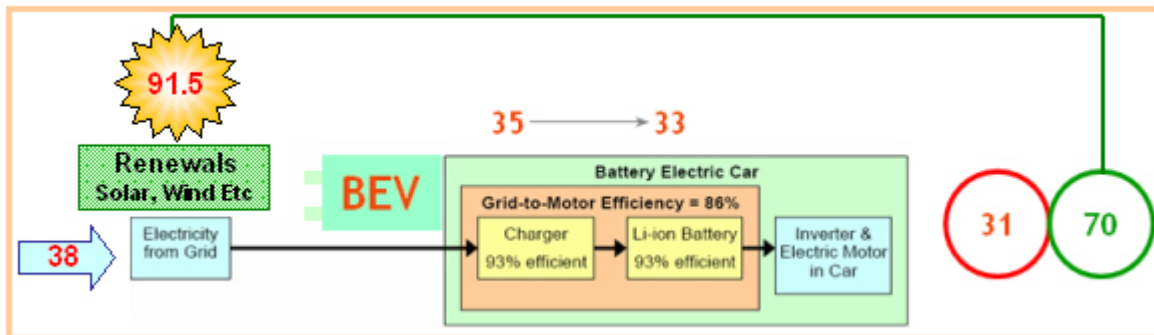


Figure 8.15: BEV Well-to-Wheel energy efficiency (renewable energy source)

8.4 Well-to-Wheel Energy Usage

8.4.3 FSV Well-to-Wheel Energy Usage

The Well-to-Wheel energy usage was calculated for FSV-1 and compared to a baseline gasoline vehicle within the same class. As shown in Figure 8.16, all of the FSV-1 vehicles are more efficient compared to a vehicle with ICE engine.

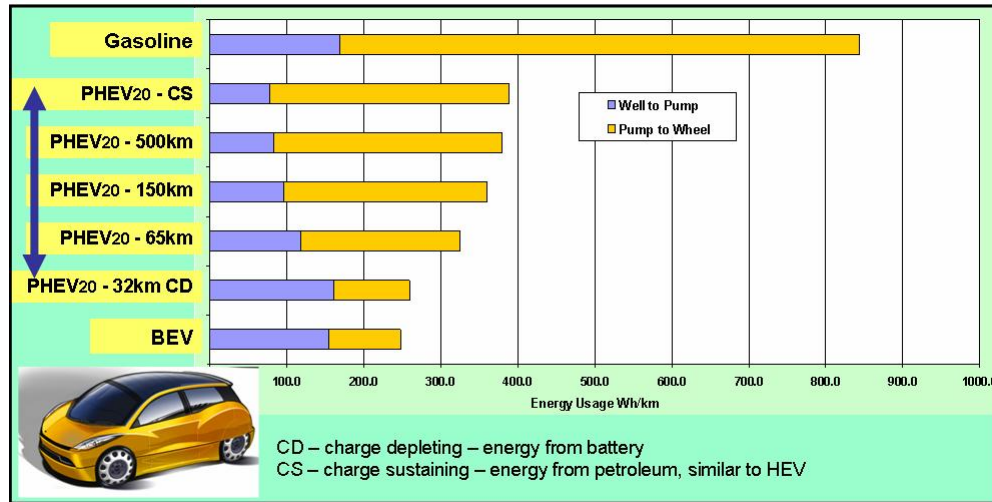


Figure 8.16: FSV-1 Well-to-Wheel energy usage

Similarly, Figure 8.17 shows the comparison between FSV-2 and a baseline gasoline vehicle within similar class.

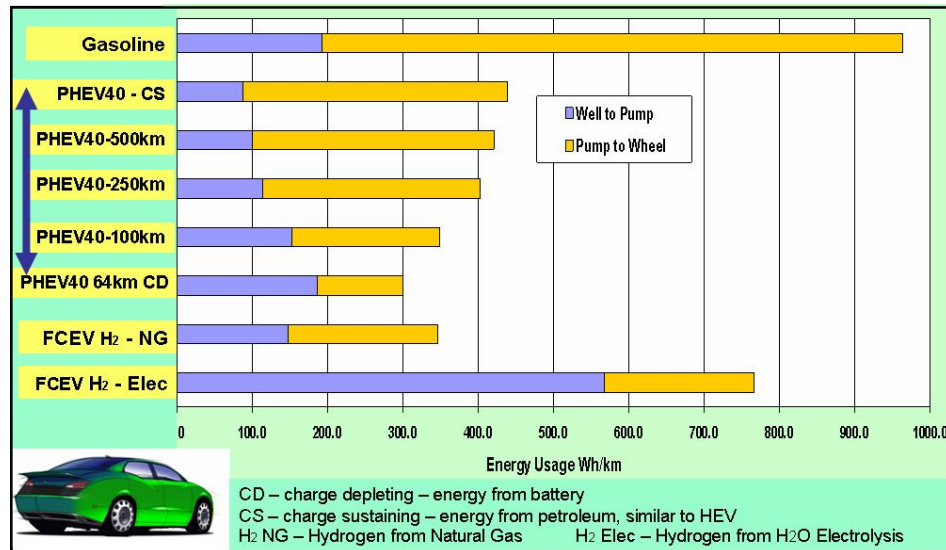


Figure 8.17: FSV-2 Well-to-Wheel energy usage

9.0 Advanced Powertrain Technologies

9.1 Overview

For the purpose of conceptualizing the Future Steel Vehicle, a technical assessment of currently applied hybrid powertrain component and sub-system technologies was conducted. In addition new technologies under development were evaluated with a focus on 2015 to 2020 deployment. In order to establish comparison data for further analysis, gains from technical advancements and scaling of production were taken into consideration.

Based on technical performance, durability, and commercial cost viability, potential large scale OEM deployment forecasts of competing technologies were made for the 2015 and 2020 time frames. Material availability, manufacturability, and product reliability were the key focus areas in making recommendations for the particular components/sub-systems design concepts.

The study included the evaluation of currently used as well as emerging powertrain technologies. These include high voltage batteries of varying chemistries, ultra-capacitors, traction and wheel motors, and hydrogen storage solutions.

For the purpose of the Future Steel Vehicle studies, a virtually common transaxle sub-assembly was selected. The common transaxle assembly consists of a traction motor, reduction gearing, and differential. The internal combustion engine/generator assemblies can electrically power the transaxle subassembly, either by a fuel cell system, or by a large capacity high voltage battery. Each of these powertrain options has its unique fuel storage and high voltage battery. The specific fuel storage/energy storage size, weight and cooling configurations resulted in further body-in-white design and structural challenges.

For the complex Fuel Cell System, Shanghai Fuel Cell Vehicles (SFCV) performed a separate powertrain sub-system study in cooperation with Tongji University. The integration studies of the fuel cell sub-system into the vehicle powertrain systems were also supported by Quantum Technologies and SFCV.

9.2 Fuel Cell Technology

9.2.1 Overview

Fuel cell technologies are an attractive alternative to oil dependency. Fuel cells give off no pollution, and in fact produce pure water as a by-product. Several countries are partnering to advance research and development efforts in fuel cell technologies. One partnership is The International Partnership for the Hydrogen Economy [13].

A comprehensive fuel cell technology assessment was conducted by the Shanghai Fuel Cell Vehicle Company (SFCV) in cooperation with Tongji University, Shanghai China. The study involved the Fuel Cell Engine along with its sub-systems and components.

Proton Exchange Membrane or Polymer Electrolyte Membrane (PEM) fuel cell is the most widely applied type of fuel cell in automotive application due to its many advantages. Recent breakthroughs in PEM fuel cells have turned the technology into a potential consumer product with applications such as replacements for rechargeable batteries, remote power for houses, and powertrain for automobiles. The PEM Fuel Cells (PEMFC) can be categorized into five types depending on the allowable working conditions (pressure and temperature) or the membrane materials:

- High Temperature (HT)
- Low Temperature (LT)
- Self Breathing
- High Pressure
- Low Pressure

Table 9.1 shows the detail information about the mentioned five types and the specific applications.

Types	Advantages	Disadvantages	Application
HT-PEMFC (90-120°C)	More tolerance to CO; Low requirement on thermal management system	Difficult fabrication process; Corrosion of metal stack components	Laboratory testing only
LT-PEMFC (<90°C)	Rapid start-up; High current density	High requirement on thermal management system	Prototype level, Highly developed
Self-breathing	No air compressor; High system efficiency; Low cost; Simple structure	Low power output; Less applications in transportation	Prototype level only with small power output (<10kW)
High Pressure Fuel Cell (>0.2MPa)	High power density; Easy cold start	More parasitic losses; High requirement on sealing	Prototype level
Low Pressure Fuel Cell (<0.2MPa)	Low requirement on sealing; Simple structure	Low power density and efficiency	Prototype level

Table 9.1: *Types of fuel cells and applications*

Low temperature and high air pressure fuel cell systems are applied mostly by OEMs in developed industrial countries. The low pressure PEM fuel cell can also be applied in vehicles. Following are some examples of current fuel cell system applications:

- Passat fuel cell car developed by Tongji and Shanghai Volkswagen (VW) powered by a low pressure fuel cell engine
- VW has adopted the high temperature fuel cell as the propulsion system in VW HY-motion prototype sport utility vehicle

It is hard to find the self-breathing fuel cell application in the current automotive industry due to its small power output. Tongji has attempted to equip this kind of fuel cell on a mini car because of its simple structure, system level and ease of operation.

Many fuel cell stack and system suppliers are dedicated to R&D activities and commercial efforts oriented to various markets. Table 9.2 lists some of the main fuel cell suppliers with corresponding products, rated powers, as well as applications with a quasi-commercial level of production with stable demands from different automotive OEMs. [38]

Fuel cell stack Suppliers/countries	Products	Rated Power (kW)	Application
Ballard/Canada	Mark902	85	Transportation
	Mark1030	1.32	Residential
	HD series	150	Transportation
Nedstack/Netherlands	P8	8	Auxiliary Power Unit
UTC/USA	-	85	Hyundai, Nissan, BMW fuel cell cars
Nuvera/Italy	HDL-82	82	Fiat prototype vehicle
Hydrogenics/Canada	HyPX-1-27	21	Auxiliary Power Unit
	HyPM-HD	65	Supplied for lift trucks
Nucellsys/Germany	HY-80	68	DaimlerChrysler's NECAR5
Honda/Japan	-	100	Honda FCX clarity
Toyota/Japan	-	90	Supplied for FCHV
GM/USA	GM2000	80	E-Flex fuel cell vehicle

Table 9.2: *Main suppliers of fuel cell stack and system*

9.2.1.1 Assessment Scope

Direct hydrogen PEM fuel system is considered as the most promising innovative fuel cell power system for automotive applications. Therefore, SFCV/Tongji's working scope focused on the direct hydrogen PEM fuel cell system, as shown in Figure 9.1. The fuel cell system studied included low pressure (<2.5 MPa) hydrogen delivery, air supply, fuel cell stack, compressor and humidifier. The heat rejection unit, hydrogen storage and DC electric power inverter were not taken into account.

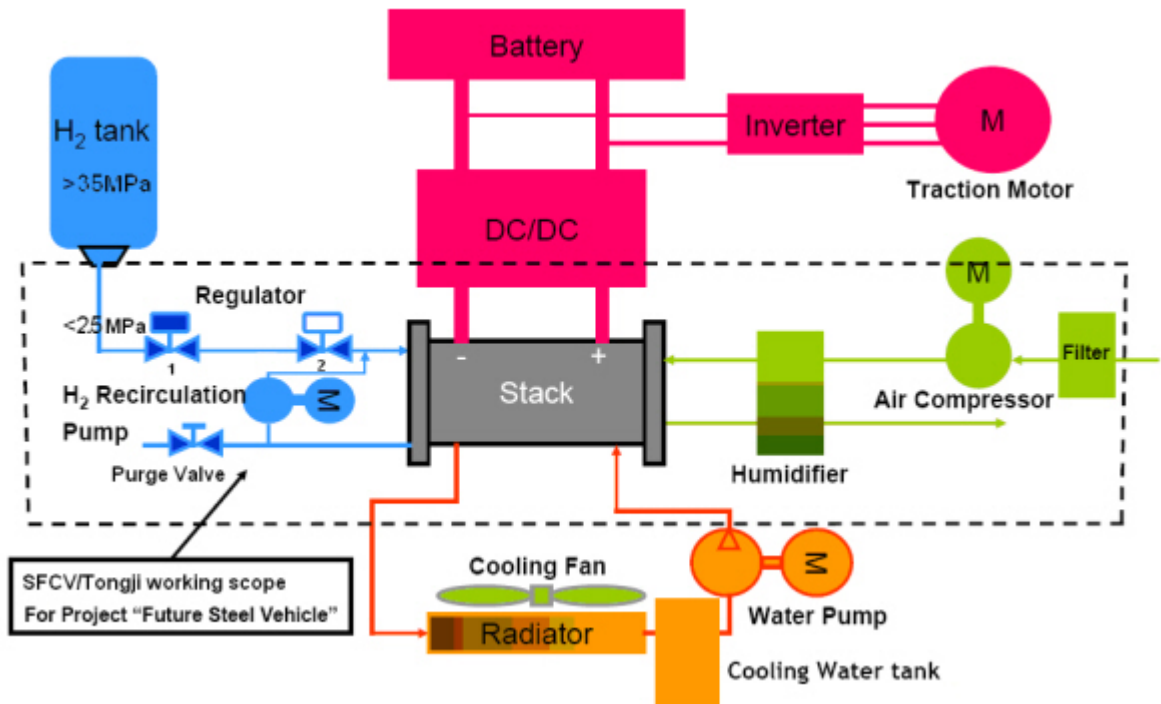


Figure 9.1: SFCV/Tongji's working scope

9.2.1.2 Recommendations for FSV

Based on the technical assessment of fuel cell and hydrogen storage technology, a recommendation was made for the FSV program by Tongji University and SFCV. The highlights of the technical assessment and the recommendations are shown in Table 9.3.

Fuel Cell Technology Assessment				
		Status 2008	Prediction 2015-2020	Selection FSV
Dominating Technology		PEM	PEM	PEM
Power Output (net)	kW	40 - 100	50 - 170	65
Efficiency	%	45 - 56	50 - 62	50 - 62
Power Density	kW/kg	0.8 - 1.9	~2.0	2
Cost [\$USD]	\$ USD/ kW	1,500-2,900	~100 - 200	155

Hydrogen Storage Technology Assessment				
		Status 2008	Prediction 2015-2020	Selection FSV
Dominating Technology		Compressed Gas		Compressed
Pressure	MPa	35	50 - 70	70
Tank Material	Carbon Composite	Aluminum Liner	Plastic Liner	Plastic Liner
H₂O Volume Capacity	Liters	80 - 220	70 - 150	95
Hydrogen Capacity (net)	kg	1.7 - 5.0	1.6 - 5.4	3.4

Future Steel Vehicle Concept				
	Capacity (net)	Weight [kg]	Volume [Liters]	Cost [\$ USD]
Without Cooling System				
Fuel Cell Engine	65 kW	92	67	\$10,081
Hydrogen Storage	3.4 kg	87	120	\$7,919

Table 9.3: Fuel cell recommendation for FSV

9.2.2 Fuel Cell Stack

Most of the fuel cells designed for commercial use produce less than enough to power a vehicle. Multiple cells must be assembled into a Fuel Cell Stack (FCS) to meet the power requirements of a vehicle. Fuel cell stack is the key component in a fuel cell system, serving the purpose of generating electrical power through chemical reactions. Fuel cell stack consists of the electrode, membrane, Gas Diffuse Layer (GDL, also called backing layer), bipolar plate, end plate and miscellaneous parts. The arrangement of major components of a fuel cell stack is shown in Figure 9.2. Herein, the electrode, membrane and GDL are integrated into a Membrane Electrode Assembly (MEA). MEA is the core component in a stack.

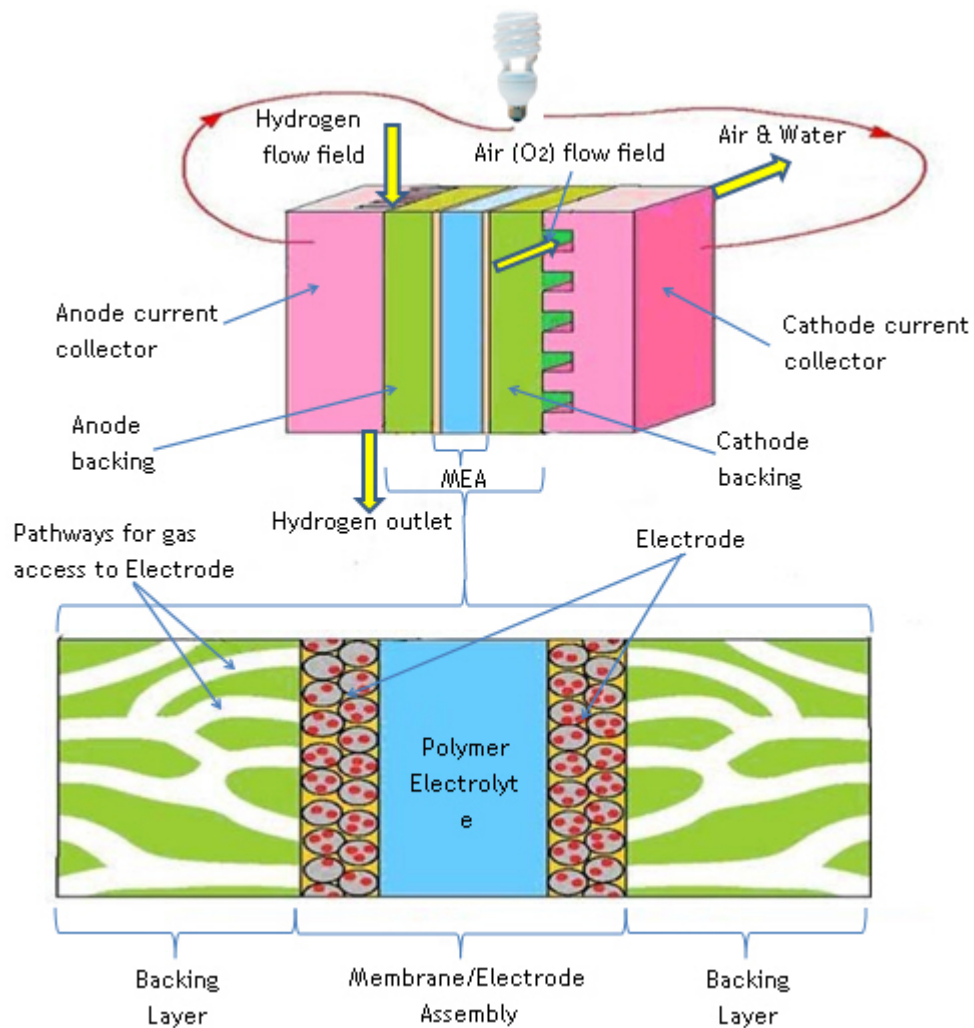


Figure 9.2: Arrangement of major cell components in a fuel cell stack [16]

9.2.2.1 Membrane Electrode Assembly

The MEA consists of electrodes (anode and cathode sides), as shown in Figure 9.2. The MEA's performance (cost, degradation, durability, etc.) directly determines the overall stack performance.

Each electrode in a MEA is a thin catalyst layer sandwiched between the ionomer membrane and the GDL. Platinum (Pt) is the most common catalyst in PEMFCs for both oxygen reduction and hydrogen oxidation reactions. In the early days of PEMFC development, large amounts of catalyst were used (up to $28 \frac{\text{mg}}{\text{cm}^2}$) [38]. In the late 1990s with the use of supported catalyst structure the amounts of catalyst was reduced to 0.6-1.0 $\frac{\text{mg}}{\text{cm}^2}$. As of 2007, the current status was a total of 0.4 $\frac{\text{mg}}{\text{cm}^2}$ Pt loading. [61]

The membrane is a thin film between cathode catalyst layer and anode catalyst layer. It serves the dual purpose of preventing mixing of the reactant gases at each electrode, and also provides ion conduction that makes fuel cell operation possible. The research indicates the water content is a key factor in determining the proton conductivity. The requirements on the membrane are following [58]:

- It must exhibit relatively high proton conductivity
- It must present an adequate barrier to mixing of fuel and reactant gases
- It must be chemically and mechanically stable in the fuel cell environment

Perfluorinated polymeric membrane and perfluorosulfonated (PFSA) membranes are the most commonly used membranes in PEMFC applications. Nafion, made by Dupont, is the best known PFSA membrane. Typically, the thickness of this membrane ranges between 25 μm and 175 μm . In contrast to the perfluorinated polymeric membranes, PFSA membranes have longer lifetime and less degradation during operation. But PFSA membranes also have disadvantages of high cost and limited temperature operation. The Gore Company developed expanded Polytetrafluoroethylene (PTFE) to be applied in fuel cell application. Expanded PTFE is a core technology with multiple forms and varied structures to improve the performance of the membranes. Polybenzimidazole (PBI) membrane is often used in high temperature fuel cell system due to its good performance under low humidity and high temperature operation conditions. [52]

9.2.2.2 Gas Diffuser Layer

The gas diffuser layer is a porous, electrically conductive substrate that permits the reactant gas to access the catalyst surface. The GDL is commonly made of an electrically conductive carbon cloth or carbon paper treated with hydrophobic Polytetrafluoroethylene (PTFE) coating so that water does not accumulate within its layers. Following are the requirements of a GDL:

- It must be sufficiently porous to allow flow of both reactant gases and by-product water
- It must be both electrically and thermally conductive
- Pores of the gas diffusion layer facing the catalyst layer must be big enough since the catalyst layer is made of discreet small particles
- It must be rigid enough to support the MEA

9.2.2.3 Bipolar Plate

The bipolar plates that support the MEA are one of the main challenging components hindering fuel cell development. Generally, most PEM fuel cells are constructed utilizing multiple cells connected in series with bipolar plates. The MEA for PEM fuel cells is very thin, so the bipolar plate actually comprises most of the mass of the fuel cell stack, typically about 80% of the mass. [43]

In general, two materials have been used for PEMFC bipolar plates, namely graphite and metal. Graphite composites have been challenged by metals since the graphite composites have high specific volume, low durability, and high manufacturing cost. The key characteristics of bipolar plate material suitable for transportation applications are as follows [53]:

- High corrosion resistance with corrosion current at 0.1 V and H₂ purge < 16 μAcm^{-2}
- High corrosion resistance with corrosion current at 0.6 V and air purge < 16 μAcm^{-2}
- Interfacial contact resistance (ICR), $140 \text{ Ncm}^{-2} = 20 \text{ m}\Omega^{-2}$
- Does not dissolve and produce metal ions
- Possess steady low ohmic resistance throughout the operation
- High surface tension with water contact angle close to 90°, i.e. high dehydration
- Light weight
- Maximal allowable mechanical pressure: 200 N m⁻²

The thickness of the bipolar plate and the manufacturing technology used for its production vary according to the particular bipolar-plate material. Alternative materials such as stainless steel, aluminum, titanium and nickel, as shown in Figure 9.3, are used in the recent related researches.

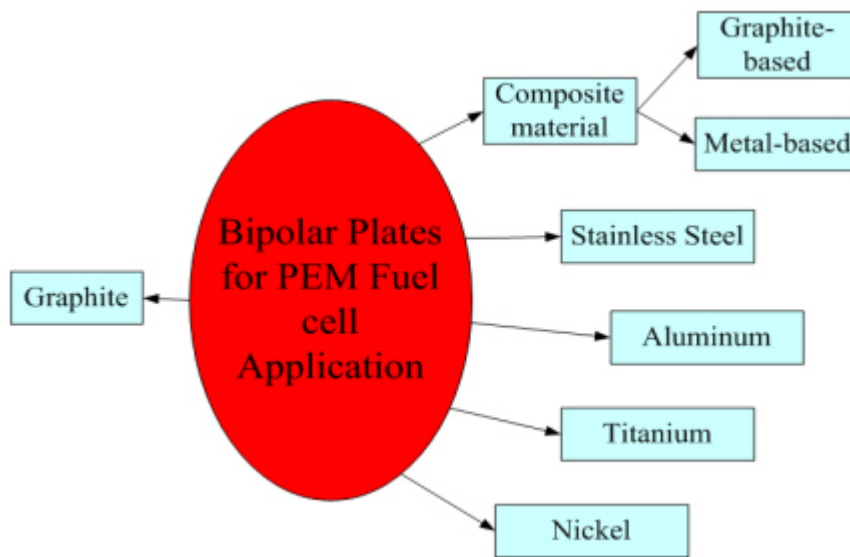


Figure 9.3: Bipolar plates alternative materials for PEM fuel cell application

The flow field on the bipolar plate has many shapes and designs. A variety of different designs are known for graphite plate; the traditional designs mainly include pin, straight or serpentine designs. In a metallic plate application, the stamped metal sheet provides channels for hydrogen, air and coolant depending on the particular shapes. A sample metallic plate is shown in Figure 9.4.

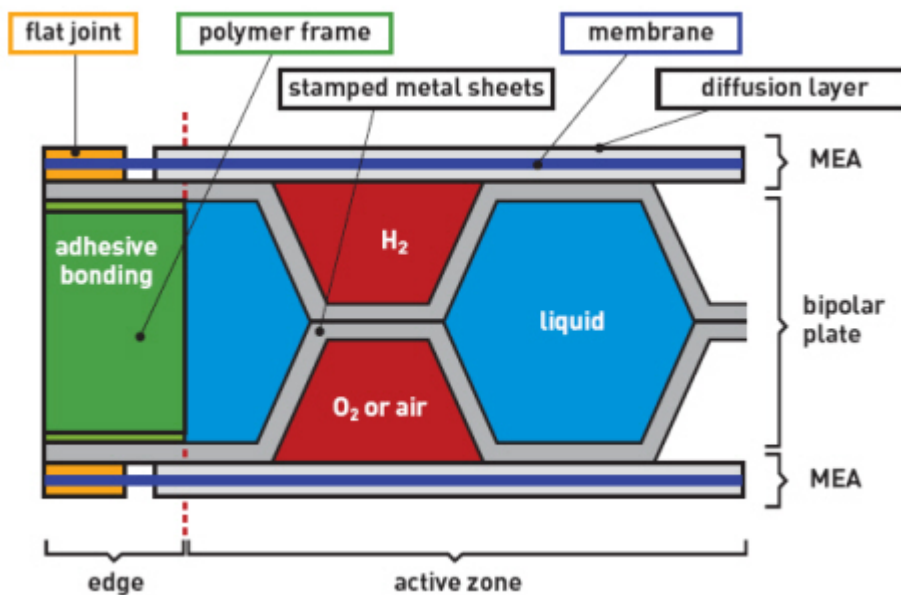


Figure 9.4: An innovative stamped metal sheets architecture

Research into the performance of the fuel cell stack flow-field is ongoing, with some recent achievements. For example, enhanced stack performances were achieved in Honda FCX Clarity fuel cell car by using the V-flow designs as shown in Figure 9.5. The Honda FCX clarity fuel cell stack using V-flow designs is 20% smaller, 30% lighter, and gives 14 kW more power output than the current FCX fuel cell stack [28].

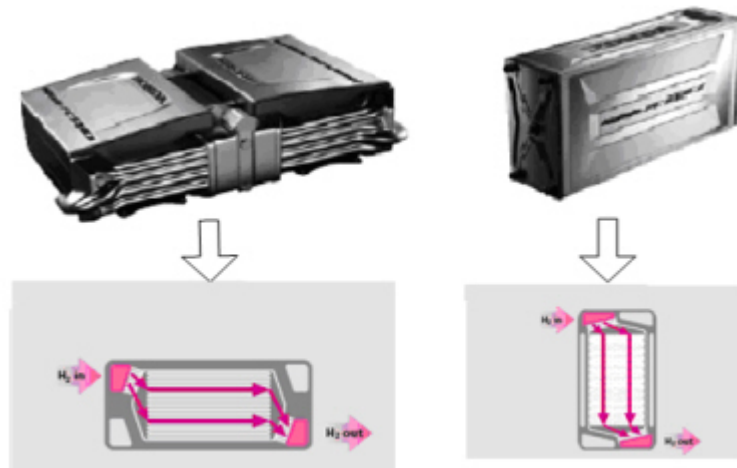


Figure 9.5: Honda FCX stack design (left) Vs. Clarity V-flow stack (right)

9.2.3 Balance of Plant (BOP)

Balance of plant consists of the remaining sub-systems, and components that comprise the fuel cell system. The balance of plant in a fuel cell system mainly contains an air compressor or blower, humidifier, pressure regulators, recirculation pump, and Fuel cell system Control Unit (FCU). Balance of plant makes fuel cell stack (module) run stably and safely under the predefined operation points, and provides the optimized boundary conditions for fuel cell control.

9.2.3.1 Air Compressor

The air compressor is a key component for air supply, especially for the high pressure PEM fuel cell system. There are many types of compressors for different FCS applications. Some available types of air compressors are shown in Figure 9.6. The selection of a compressor is driven by the FCS requirements. The specification of compressor is important for the whole FCS integration. The factors considered in the selection of a compressor include air flow, shaft power, pressure ratio, and efficiency. The comparison of different compressors and the relative performance characteristics are shown in Table 9.4.

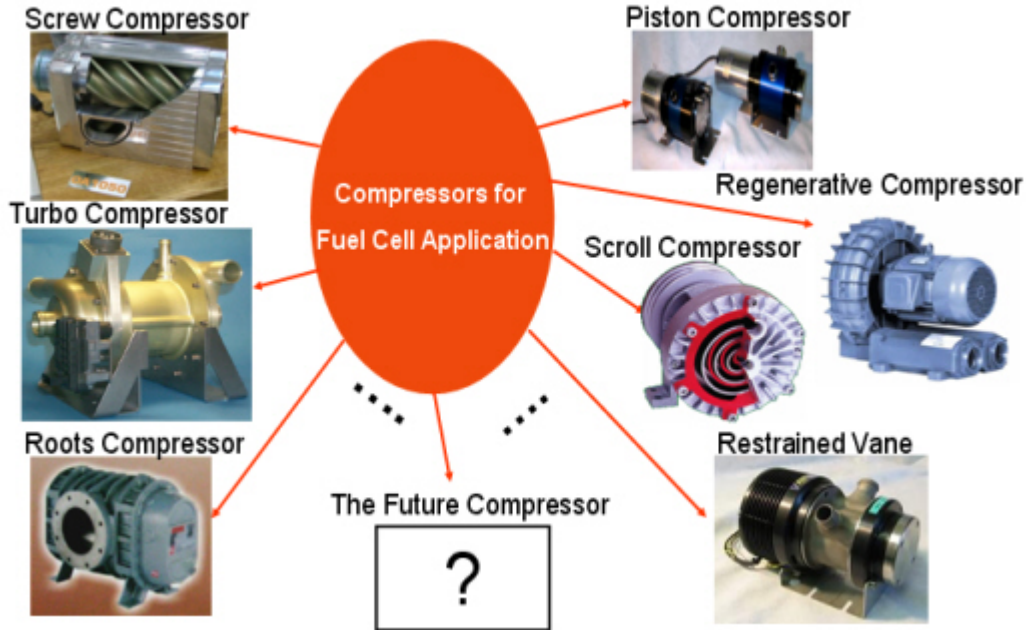


Figure 9.6: Available types of air compressors

	Flow	Pressure	Transients	Turndown	Efficiency	Packaging	Reliability	Noise	Cost
Restrained Vane	+	+	+	+	+	+	+	+	++
Twin Screw	++	++	0	+	0	+	-	-	0
Turbo	++	+	-	-	++	0	+	+	0
Scroll	+	+	+	+		-	+	0	0
Piston	0	++	+	++	+	-	+	+	-
Roots	++	0	0	0	-	+	+	0	0
Regenerative	+	-	-	-	-	0	+	+	+

Table 9.4: Comparison of different compressors

Besides the factors mentioned in Figure 9.4, other parameters such as transient behavior, noise, cost, etc. are also to be taken into account before finally selecting a compressor. Currently, various compressors can meet the requirements of FCS in different levels, but their energy consumption takes most of the parasitic losses. Reducing the energy consumption is the main research direction for the compressor suppliers.

9.2.3.2 Pressure Regulators

Pressure regulators are necessary to maintain appropriate pressure in the FCS. Due to the hydrogen pressure requirement in fuel cell stack, the regulator is necessary between the hydrogen tank with more than 35 MPa and inlet manifold of stack with 0.1-0.5 MPa. There are two regulators in the hydrogen delivery system. As shown in SFCV/Tongji working scope (see Fig 9.1), regulator number 1 contributes to reduce the high pressure (<25 MPa) to the max operation pressure. The regulator number 2 contributes to adjust the inlet pressure depending on the load requirements. It could be a proportional valve or follow-up valve. The hydrogen cylinder must be connected to the fuel cell via a pressurized hose connected to a pressure regulator, namely hydrogen regulator. The hydrogen regulator is designed to reduce the gas pressure, and controls the output pressure at a predefined value.

9.2.3.3 Humidifier

The humidifier monitors and maintains the level of humidity that the FCS needs to achieve peak operating efficiency. The humidifier performs this function by recovering some of the water from the electrochemical reaction, that occurs within the fuel cell stack, and recycling it for use in humidification. Especially in low temperature fuel cell systems, humidified gases (air and/or hydrogen) should be fed into the stack. Currently, there are different humidifiers for FCS applications, some of which are shown in Figure 9.7. The membrane humidifier and enthalpy wheel humidifier are the Gas-to-Gas (G/G) type. Its working principal is different to the water injection one.

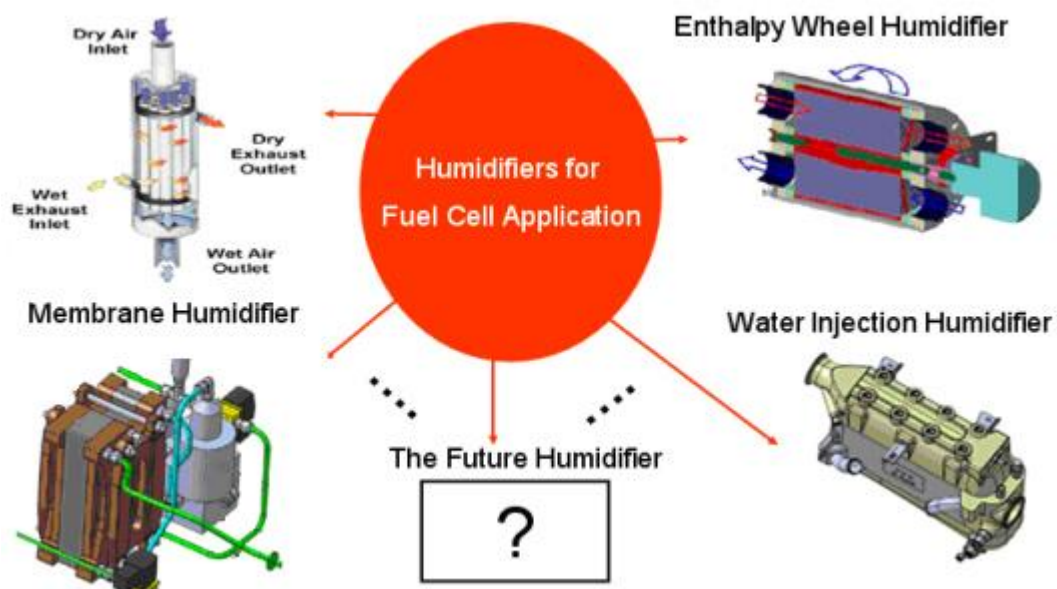


Figure 9.7: Available types of humidifiers

Even though the water injection humidifier has been used in a few fuel cell vehicles, this type of humidifier will be given up ultimately due to technical reasons. G/G humidifier would be more widely used in fuel cell vehicles. A shell-and-tube type G/G membrane humidifier consists of a bundle of membrane tubes arranged as a shell and tube heat exchanger as shown in Figure 9.8. The stack's exhausted air flows around the outside of the tubes. When dry inlet air flows through the inside of the bundle tubes, the air is humidified and absorbs heat from the stack's exhausted air. Therefore, the humidifying system can work without an additional water tank. Depending on the layout of flow directions of the inlet and the exhaust gas, two designs are possible: a parallel or a counter flow. The parallel flow design allows the dry and exhausted air to flow in the same direction, while the counter flow design allows them to flow in opposite directions.

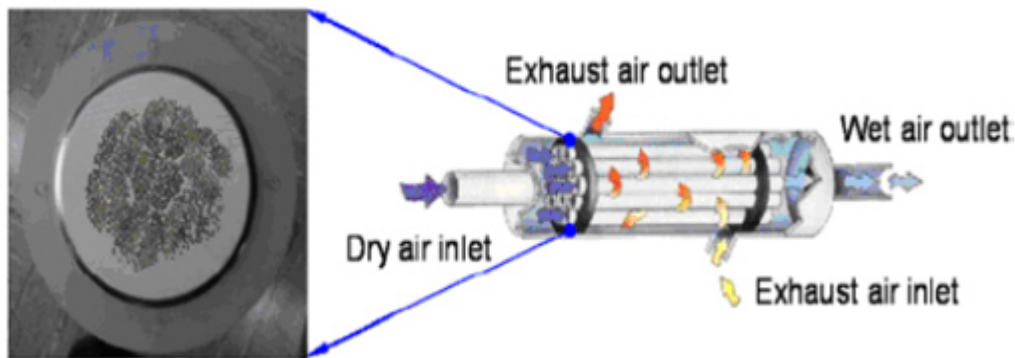


Figure 9.8: *Shell-and-tube type gas-to-gas membrane humidifier structure*

Currently, G/G humidifier is considered as the preferred humidifier for future development due the following features:

- More efficient method of humidification available
- Can achieve high degree of water transfer (over 85% of water content)
- Lesser or no electric energy required
- Humidifiers available to handle wide range of flows (<1 Standard Litre Per Minute (SLPM) up to 7,000 SLPM), temperatures (up to 130 °C) and pressures (up to 0.4 MPa)
- New low cost model available with molded shell and fittings

9.2.3.4 Recirculation Pump

The hydrogen recirculation pump delivers the unconsumed hydrogen back into the manifold of fuel cell stack in order to improve the utilization efficiency of hydrogen. The recirculation pump must satisfy the maximum hydrogen flow rate.

Considering a PEM fuel cell stack with $I_{max}=300$ A, the hydrogen stoichiometry $\lambda_H=1.5$ and number of the cells $n_{cell}=440$, the maximum corresponding residual hydrogen flow can be calculated (the hydrogen density ρ_{H_2} is known):

$$m_{H_2} = \frac{I_{max}}{2F} * 2 * n_{cell} * (\lambda_H - 1) * \frac{1}{\rho_{H_2}} \sim 8.3 \text{ l/min}$$

It is assumed that unused hydrogen is discharged into the ambient, the practical flow rate of recirculated hydrogen should be less than the residual one 8.3 l/min. The available pumps for hydrogen recirculation are shown in Figure 9.9.

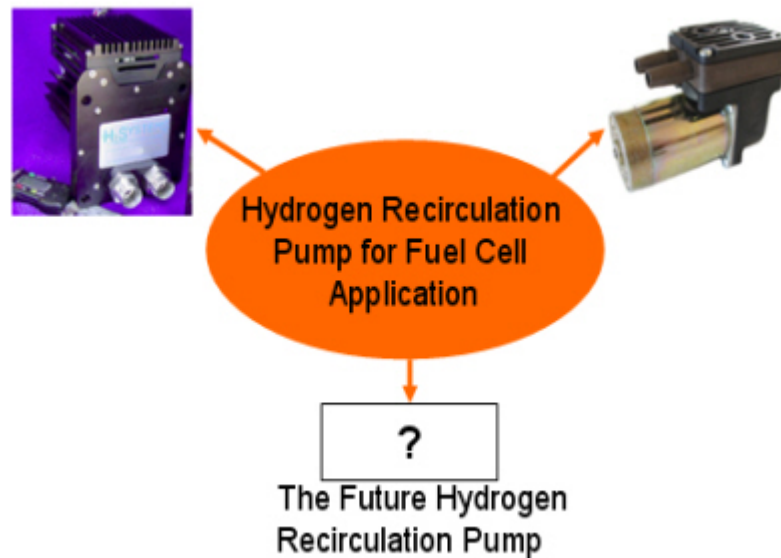


Figure 9.9: Available types of hydrogen recirculation pump

9.2.3.5 Fuel Cell System Control Unit

Fuel Cell system Control Unit (FCU) monitors and controls the fuel cell system under the right operation conditions. It mainly includes air compressor control box, recirculation pump control box, fuel cell system control module and Cell Voltage Monitoring (CVM). The air compressor control box receives the control signals from the fuel cell system control module, and it also sends the feedback signal (e.g. compressor rotation speed). The function of the hydrogen recirculation pump control box is to drive the pump. The speed of the pump is adjusted by fuel cell system control module. The fuel cell system control module is dedicated to send and receive various signals to determine the necessary control values. It also has interfaces (e.g. CAN or OBD) to communicate with the system controller (Vehicle Management System (VMS)) or diagnosing tools. The CVM monitors the individual cell voltage and gives warning signals to fuel cell system control module. Figure 9.10 and Figure 9.12 show the external and internal structure of FCU respectively.

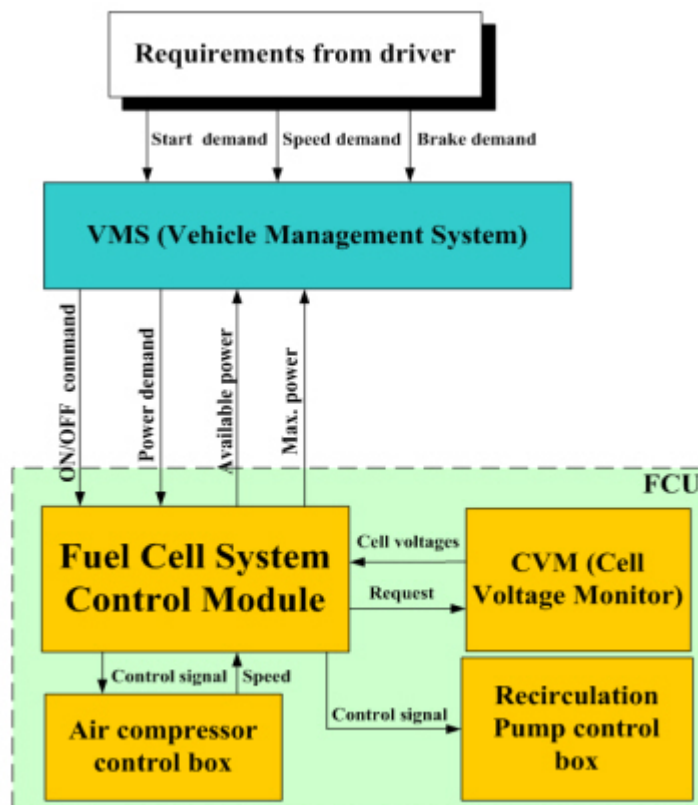


Figure 9.10: External of FCU

Pressure control is the main function of the fuel cell system control. Currently, the operation pressure of hydrogen is controlled electronically or mechanically (see Figure 9.11). As shown in Figure 9.11, the hydrogen operation pressure is adjusted by the pressure balance valve, and the pressure balance valve is controlled by inlet air pressure. In the bottom solution, in Fig 9.11,

the hydrogen operation pressure is adjusted by the proportional valve which is controlled by the pressure set point signal.

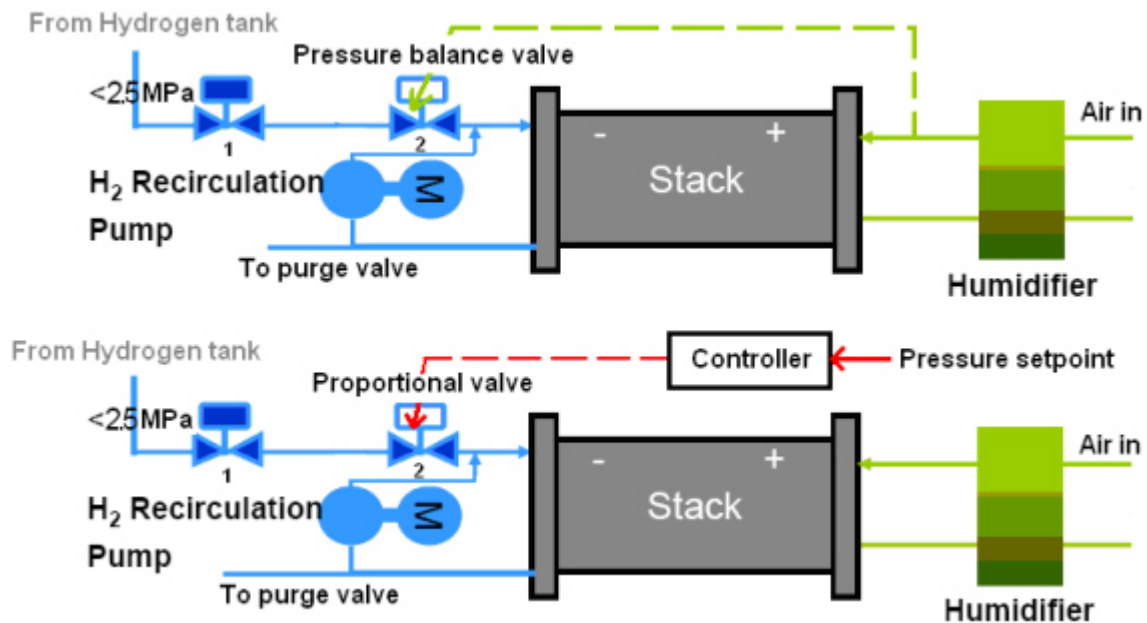


Figure 9.11: Two control methods of hydrogen operation pressure

The internal components of the FCU, as shown in detail in Figure 9.12, are the following:

1. Air module which mainly consists of air compressor and its driver
2. Hydrogen module which mainly consists of pressure regulator 2 and purge valve
3. Different valves and relays
4. Heat management module which mainly consists of radiator, electric fans and coolant pump.

The control signals are: air flow demand, hydrogen flow demand, switching commands and set-points of temperatures and pressure. The FCS is enabled to work, depending on the messages of "ON/OFF" and power demand from VMS. When the FCS has to start functioning, the predefined self-checking program is executed and the signals of status of fuel cell process are acquired through the sensors. FCS will send request message to CVM in order to obtain the individual cell voltages. Then, the controller gives out the control signals, based on the judgments of these states, and sends the available power messages back to VMS.

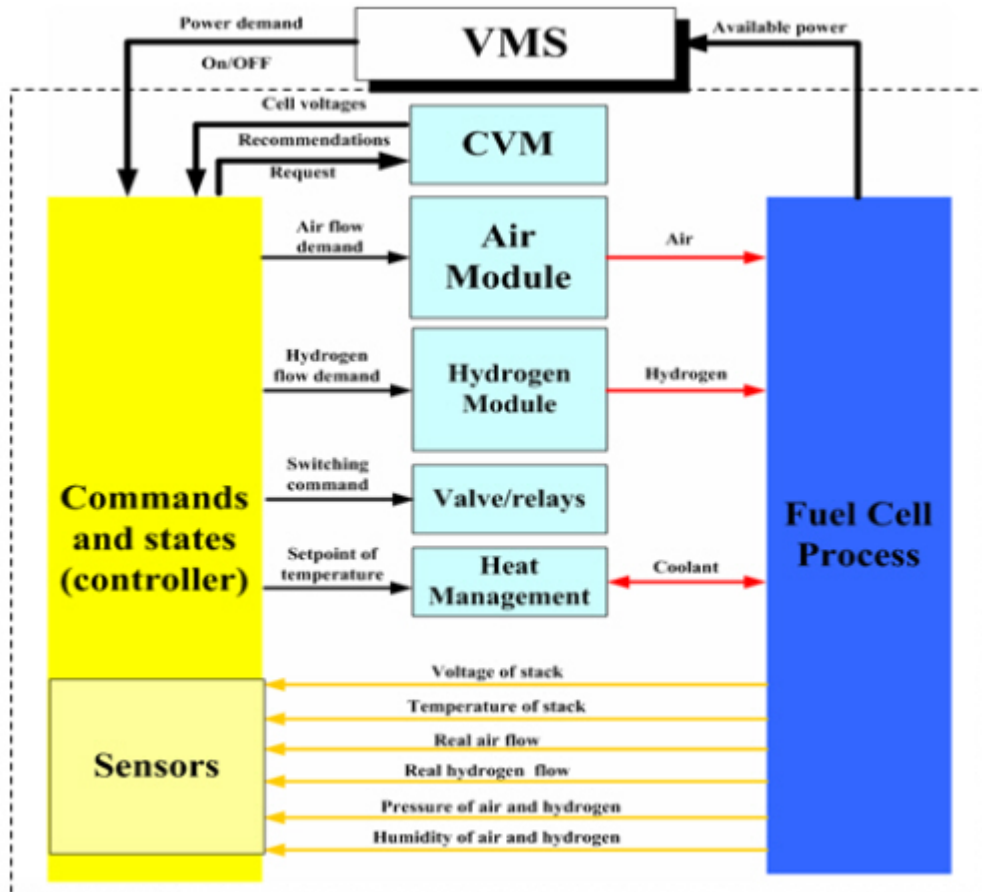


Figure 9.12: Internal of FCU

9.2.4 Miscellaneous Parts

The miscellaneous parts include air back-pressure valve, hydrogen purge valve and other parts. They play the necessary roles in FCS running. The pressure regulators consist of pressure reduction valve and pressure regulator, which is controlled electronically. An air back-pressure valve is necessary for adjusting air pressure in the FCM and installed at one outlet of G/G humidifier. It is electronically controlled as well. The hydrogen purge valve ejects the excessive hydrogen in order to avoid water flooding in the anode side. It is electronically controlled by the FCU frequently.

9.2.5 Operating Pressure

A fuel cell may be operated at an ambient pressure or it may be pressurized. The oxygen can be supplied to the fuel cell stack at a high pressure (>0.2 MPa) or at close to a low pressure (<0.2 MPa).

In a high pressurized system, the oxygen and/or hydrogen can be delivered to the fuel cell stack at a much higher rate. Thus, the system can achieve a faster dynamic response to the changing load than a low pressure system. A high-pressure fuel cell system uses a compressor, which requires smaller air intake manifold than that of a low pressure fuel cell system. So a high-pressure fuel cell can operate at a much higher current density, giving rise to a fuel cell stack with much higher power density. In transportation, operating at higher pressure is favored because of high power density. On the other hand, a high-pressure system requires more parasitic load. Hence, the overall efficiency of a high-pressure system is a trade-off result between higher stack voltage and higher parasitic consumption.

A low pressure system is more suitable for slowly varying loads. However, a low pressure system tends to be more reliable and durable since the fuel cell operates at lower current density with slower dynamic loads, and the stack assembly needs to withstand less pressure.

9.2.6 Operating Temperature

The fuel cell stack temperature is another parameter that may be selected and preset. Stacks can work under high temperature (90-120 °C) and low temperature (<90 °C), depending on the membrane materials. Low temperature fuel cell engines are widely used due to their quicker start-up, compact volume and lower weight, as compared to high temperature fuel cell engines. Low temperature fuel cell engines adopt the PFSA membrane. A Phosphoric Acid Doped Polybenzimidazole (PBI) membrane is often applied in high temperature fuel cell system. Compared to PBI membrane, a PFSA membrane costs less and is more reliable.

The heat management requirement in high temperature fuel cell engines is comparable to that in traditional internal combustion engines. Recent progress in the field of hydrogen/air PEM fuel cells is related to developing PEM fuel cells that operate at over 100 °C. There are several compelling reasons:

- Electrochemical kinetics for both electrode reactions are improved
- Water management
- Heat management is also simplified due to increased temperature gradient between stack and coolant
- CO tolerance of the stack is increased

Although there are many advantages in operating PEMFCs at high temperatures above 100 °C, there are still many major challenges. At higher operating temperatures, membrane dehydration and the subsequent decrease in proton conductivity is one of the major issues. Degradation of GDL, mechanical failure, and heat management failure are some of the other issues. [52]

9.2.7 Performance

Fuel cell system performance mainly depends on the following factors:

- Power density
- Cost
- Durability
- Cold start
- System efficiency

9.2.7.1 Power Density

Power density is a measure of the size of a fuel cell stack relative to its power. The higher the power density, the smaller the fuel cell stack can be for a given power level. The current status and 2015 forecast of volume power is shown in the Figure 9.13. It is considered that the key driving factors are novel flow field design, advanced manufacturing technology, and new materials application.

In the current status, the volumetric power density is estimated between 1.5 kW/l and 1.8 kW/l. In another six to eight years, the value may be improved to 2.25 kW/l ($\pm 10\%$). By 2020, unless there is a technology breakthrough the value is expected to improve marginally.

A similar trend is shown for the specific power in Figure 9.14. The same driving factors make the specific power higher than historical data. The 2015 forecast is 2.0 kW/kg ($\pm 10\%$). By 2020, the forecast is similar to that of volume power.

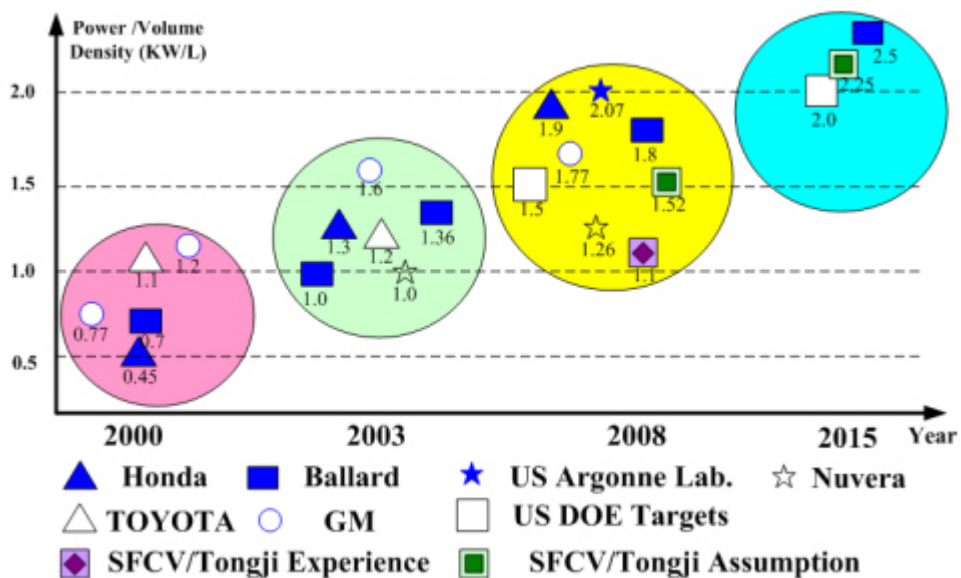


Figure 9.13: Volumetric power density (stack)- Current status and 2015 forecast

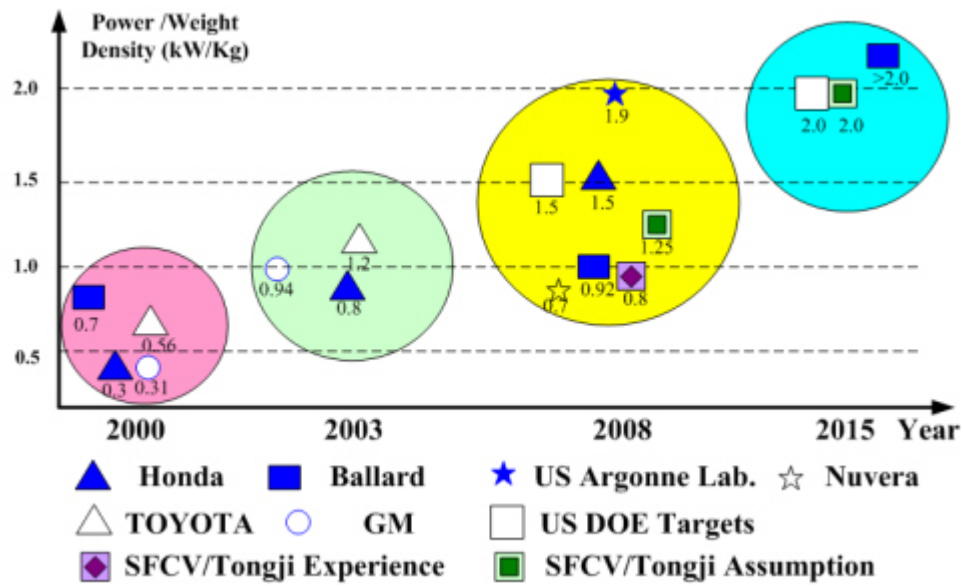


Figure 9.14: Specific power density (stack)- Current status and 2015 forecast

9.2.7.2 Cost

The cost is one of the key factors which impact the FCV actual commercialization. The cost ratio chart of a typical FCS with 80 kW net power is shown in Figure 9.15.

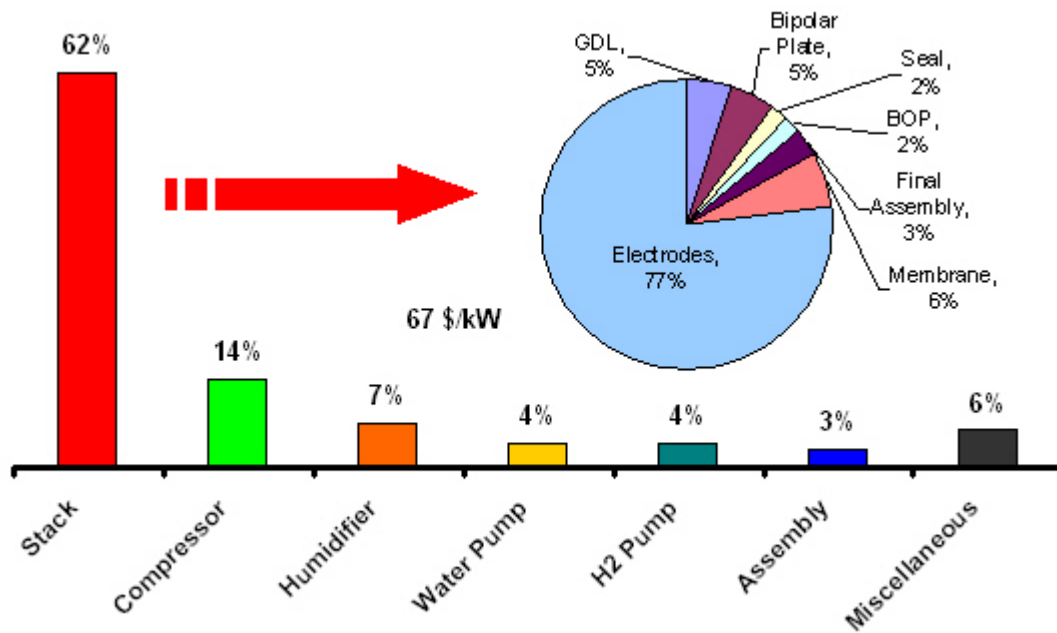


Figure 9.15: A typical FCS cost ratio

It can be seen that the stack cost is \$67 USD/kW and system cost \$108 USD/kW in 2006, as estimated by US Argonne Lab. But, a current purchasing price of a fuel cell stack is \$722 USD/kW - \$1446 USD/kW and a fuel cell system \$1446 USD/kW - \$2892 USD/kW for automotive applications.

Therefore, current average stack cost of \sim \$70 USD/kW and system cost of \sim \$110 USD/kW could be a rational estimation based on only material cost, without considering the losses during the manufacturing process and R&D costs. In 2015, it is estimated that stack cost will be \sim \$50 USD/kW and system cost will be \sim \$85 USD/kW, after the lower Pt loading technology and more requirements from markets. In 2020, there could be two possibilities: one is that the system cost can meet the requirements of automotive applications, and the cost would be around \$15 USD/kW; another is that the system cost will be \sim \$40 USD/kW which is lower than the US DOE's 2015 target \$45 USD/kW.

As well known, the cost of the FCS is mainly dependent on the Pt loading and the mass production of fuel cell vehicles. The efforts on reducing Pt loading are highlighted in the research. Figure 9.16 shows the historic data of Pt loading and outlook for 2015.

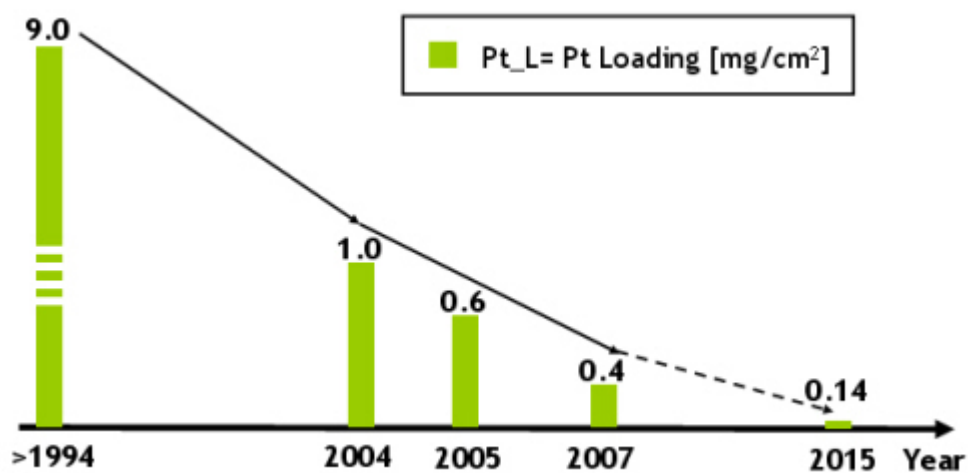


Figure 9.16: *Historic trend of Pt loading*

On the one hand, binary and tertiary catalysts, which can reduce Pt loading on the electrodes significantly, are considered as the promising alternative catalyst for fuel cell application, therefore $0.14 \frac{\text{mg}}{\text{cm}^2}$ Pt loading is possible in 2015, provided there are ongoing improvements on the catalyst. On the other hand, the R&D activities on non-Pt catalyst are still ongoing. Recent research activities on non-Pt catalysts have obtained great success. The new catalyst is less prone to CO contamination, and has comparable performance to a conventional design. [37]

9.2.7.3 Durability

In addition to cost and performance, long term stability of the fuel cell system is important. Often-quoted lifetime targets for fuel cells are 5,000 hours for automotive applications. The fuel cell systems must withstand these durations without significant changes in performance. Degradation mechanisms and component interactions as well as effects of operating conditions of a fuel cell are not fully understood. Since the lifetime of BOP currently is more than 5000 hours, the stack's durability determines the durability of FCS.

The average lifetime of a fuel cell stack is 2000-3000 hours. It is reported that the longest reported lifetime is 4000 hours. The future stack in 2015 or later must meet the requirement 5000 hours for automotive application. In order to reach this target, some collective efforts have been made by various industries and college research activities.

To improve the lifetime of stack, key influencing factors must be found and the corresponding solutions should be provided. After intensive research activities, the following factors were determined:

- Water management
- Fuel Cell Hydrogen and air starvation
- Degradation of cell components (mainly addressing the catalyst and membrane)

With engineering improvements made in the aforementioned criteria, it is expected that the system lifetime will be 5000 hours in 2015. In 2020, further investigations will be focused on the reliability of FCS.

9.2.7.4 Cold Start

Startup of a FCS in a sub-freezing environment, referred as "cold start", remains a significant challenge for automotive applications. At sub-zero temperatures, the water forms ice/frost, accumulating in the voids of the cathode catalyst layer. Once the open pores are filled completely with ice/frost, oxygen transport to the catalyst sites is blocked, and the fuel cell is shut down. Meanwhile, the oxygen reduction reaction (ORR) also produces heat that increases the temperature of the fuel cell. If the cell temperature can rise above the freezing point before the catalyst layer is filled with ice, the cold start is said to be successful [55]. The two methods widely used to address the cold-start are the following:

- Rapid heat up of cell/cell manifolds to prevent ice formation
- Heating of fluid/gas delivery systems.

As shown in Figure 9.17, the current fuel cell vehicles can cold-start at $-25\text{ }^{\circ}\text{C}$ to $-30\text{ }^{\circ}\text{C}$. However $-40\text{ }^{\circ}\text{C}$ is the basic requirement of automotive application. There are some ongoing efforts to improve the cold start capability of fuel cell engine. By 2015, the FCS can operate at $-40\text{ }^{\circ}\text{C}$, and by 2020 the cold start issue will not be a problem but the time of cold start initiation may be. One of the core areas of research is to initiate the FCS as quickly as possible.

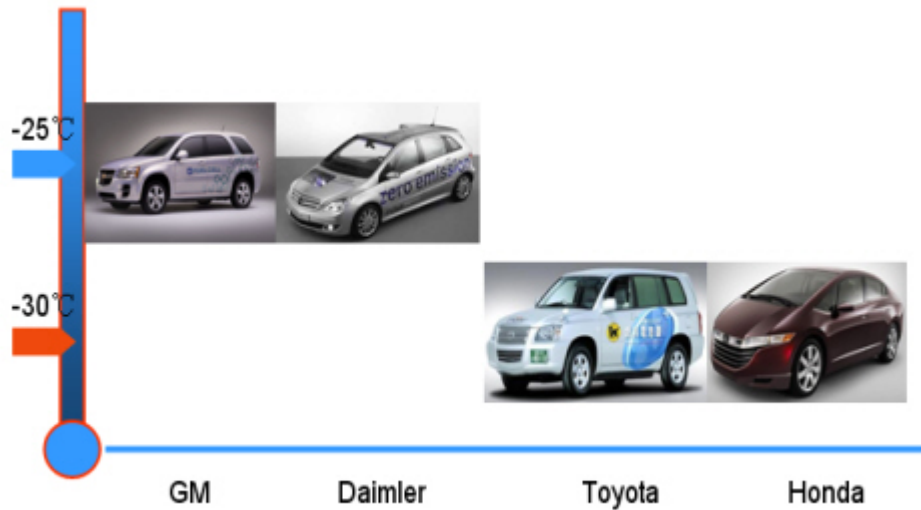


Figure 9.17: Fuel Cell vehicle's cold start temperatures

9.2.7.5 System Efficiency

System efficiency can be defined by the following equation:

$$n_{FCS} = \frac{F}{LHV_{H_2}} * \frac{I_{net}}{I_{gross}} * \frac{V_{stack}}{\lambda_{H_2}} = 0.805(1 - \alpha) * \frac{V_{cell}}{\lambda_{H_2}}$$

where,

$$\alpha = \frac{I_{aux}}{I_{gross}} = \frac{I_{gross} - I_{net}}{I_{gross}}$$

F - Faraday Constant

n_{cell} - Number of cells

LHV_{H_2} - Low heat Value of hydrogen

So, it can be seen that system efficiency is influenced by the ratio I_{aux} to I_{gross} , hydrogen stoichiometry λ_{H_2} and average voltage of cell V_{cell} .

9.2 Fuel Cell Technology

According to the equations of system efficiency, there are three major influencing factors:

- Ratio of the current consumed by auxiliary devices to gross current
- Average voltage of the cell
- Hydrogen stoichiometry

Hence, the efficiency can be enhanced by decreasing the parasitic losses (especially the air compressor consumption) and/or increasing the voltage of cells or stack. Reducing the compressor energy consumption has a greater influence on improving efficiency than improving the voltage of cell.

Currently, the FCS efficiency has a peak value (around 58%), and is about 45% at rated output power. In 2015, the peak value is expected to be around 60%, and would be 50% at rated output power. Figure 9.18 shows the current status and future 2015 estimate of FCS efficiencies. By 2020, it is assumed that there is less space for improving the system efficiency, and the system efficiency in 2020 could be enhanced up to 2% compared with the status in 2015.

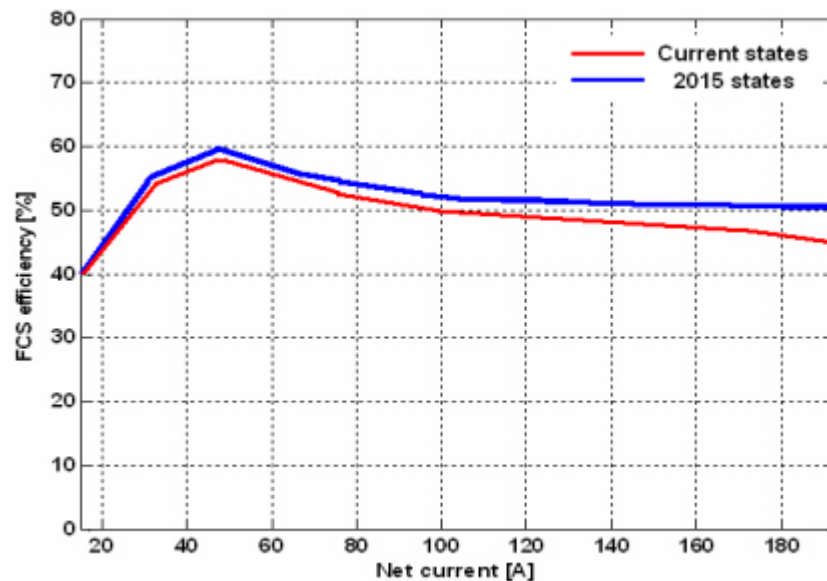


Figure 9.18: *Current status and future estimates of FCS efficiencies*

9.2.8 Mass Production Volume Forecast

Fuel cells fed by hydrogen have been applied to power vehicles for many years. With the annual decrease of the crude oil availability, and adverse effects on the environment due to vehicular exhaust emissions, hydrogen is considered as one of the regenerative and clean energy fuels to solve the crisis. Some OEMs have already developed and demonstrated Fuel Cell Vehicles (FCV). OEMs estimate that the commercialization of fuel cell system could be in the 2020 time frame.

Figure 9.19 shows the Ballard's forecast on the potential FCV market [19]. Figure 9.19 gives three possibilities with different commercial launch date: optimistic estimation with 2012, baseline with 2013 and pessimistic estimation with 2015. The FCV is in pre-commercial activities during 2005 to 2010 time frame.

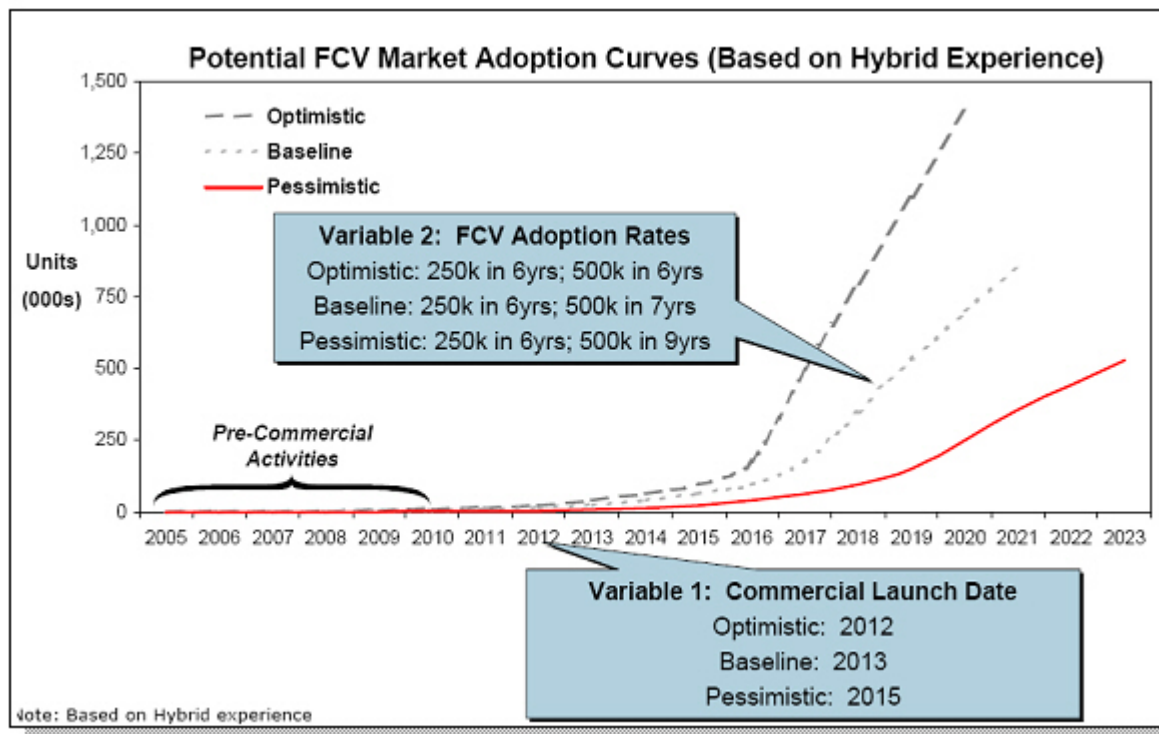


Figure 9.19: FCV commercialization scenarios from Ballard

A fuel cell commercialization scenario forecasted by the Japanese organization, New Energy industry technology Development Organization (NEDO) is shown in Figure 9.20. According to NEDO's forecast, the process of fuel cell commercialization is divided into three stages in the time frame: introduction, diffusion and penetration stages. The first stage will be finished in 5 years, and others in 10 years.

9.2 Fuel Cell Technology

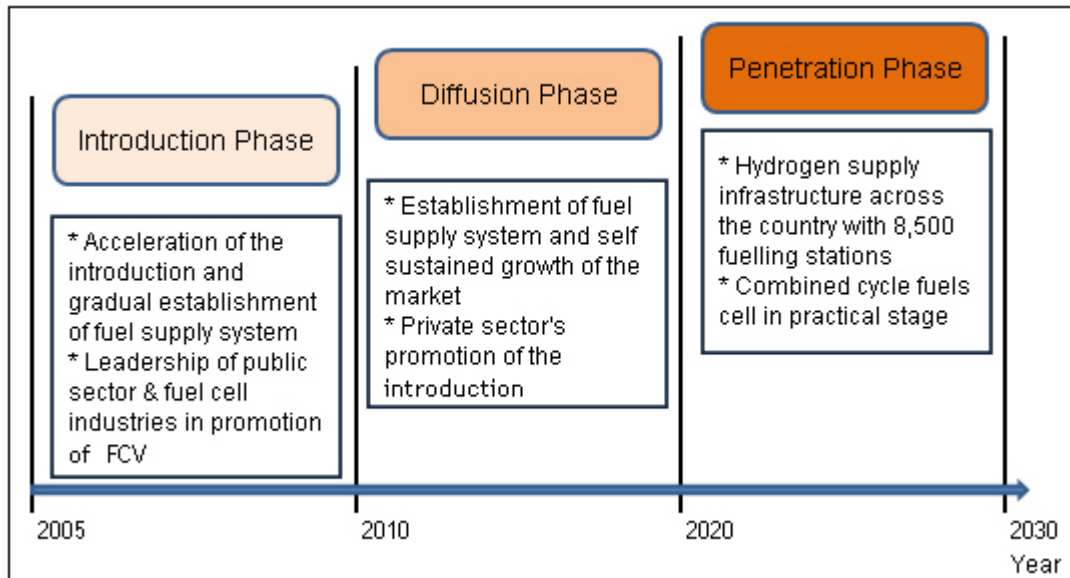


Figure 9.20: Fuel cell commercialization and diffusion scenarios from NEDO [57]

9.2.9 Cost Sensitivity

Fuel cell engine cost has not yet reached maturity, durability and manufacturing processes are being developed. Prototype technology is the basis for pricing projections made for 2015 limited volume production, and the production ramp up during the period after 2015. Predictions for cumulative fuel cell population can be seen in Figure 9.21.

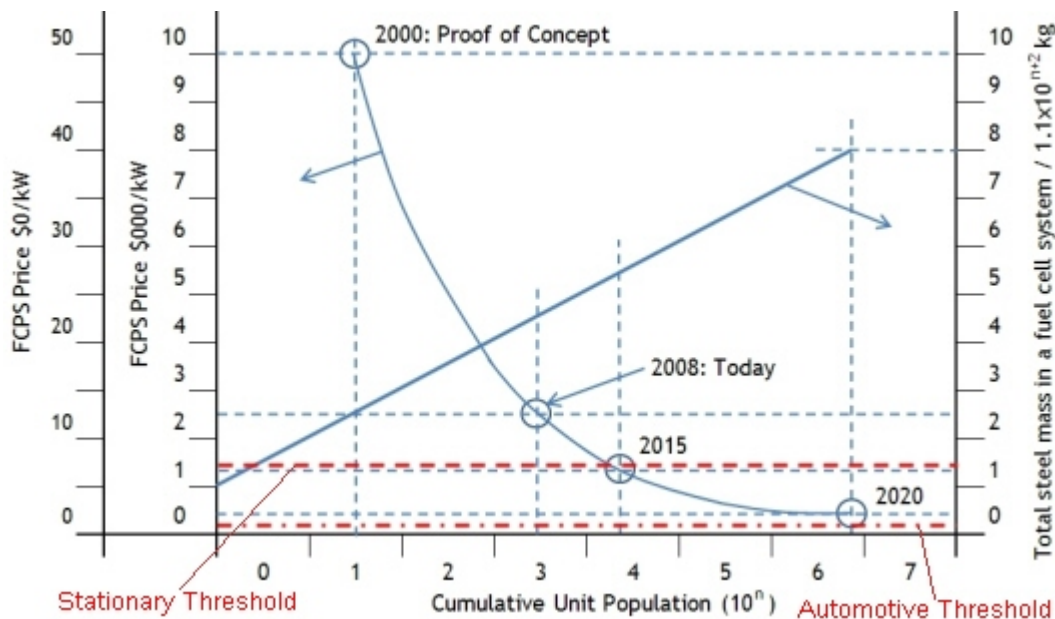


Figure 9.21: Mass production volume and steel usage [40]

From market studies and projects it can be assumed that Fuel Cell Engine volume ramp up may occur in the 2015 to 2020 time frame, thus making this technology a candidate for the Future Steel Vehicle concept development. It is not assumed, however, that costs will meet the automotive volume production threshold until 2020 at the earliest. In 2015, it is estimated that the cost of fuel cell systems cannot meet the requirements of automotive applications, and the requirements of stationary applications could be met. However, the cost will be reduced significantly compared with the previous status.

Some OEMs have announced their plan of mass production in the future. Honda may start mass production of its FCX Clarity fuel cell car within 10 years. "If we can bring costs down by a certain amount, I think we can start mass production" as stated by Honda's president Takeo Fukui in 2008 [27]. Daimler AG said that it plans to start mass production of fuel cell vehicles in less than 10 years. "By 2012 or 2015, we will be technologically well-advanced and in a position to produce cost-effective cars, comparable to those with other technologies" as stated by Christian Mohr dieck, Daimler's director of fuel cell system development, in 2007 [26]. GM will also increase production of its Chevy Volt PHEV car to low volume production as early as 2011 [14]. Based on the mass-production plans from OEMs, the fuel cell cars production is expected to increase dramatically, resulting in cost advantages in 2015.

9.2.10 Fuel Cell System Recommendations for FSV

The FCS proposed for the FSV program consists of Fuel Cell Module (FCM), air compressor, filter/muffler, G/G humidifier, pressure reduction valve, pressure regulator, recirculation pump, air back-pressure valve, hydrogen purge valve, FCU and other components. The proposed FCS dimensions and weights are shown in Table 9.5.

Key Components		Dimensions	Volume (Liter)	Weight (kg)
Fuel cell module		403mm × 372mm × 252mm	38	42.5
Air compressor		437mm × 93mm × 102mm	4.2	8.78
Filter/Muffler		Ø140mm × 280mm	4.3	2
G/G humidifier		Ø200mm × 411mm	11	6.08
Pressure Reduction valve (Regulator 1)		Ø63mm × 118mm	0.4	1
Pressure Regulator (Regulator 2)		Ø100mm × 300mm	2.4	2.7
H2 recirculation pump		Ø88mm × 266mm	1.6	10
Air back-pressure valve		Ø100mm × 65mm	0.5	2
Hydrogen purge valve		50mm × 50mm × 97mm	0.24	0.5
FCU	Compressor control box (including voltage converter)	190mm × 100mm × 120mm	2.28	10
	Recirculation pump control box	100mm × 150mm × 100mm	1.5	0.5
	Fuel cell system (engine) controller	145mm × 180mm × 30mm	0.8	0.5
Total			67.22	86.56

Table 9.5: Sizes and weight of proposed FCS

9.2.10.1 Proposed CAD models

The CAD model is designed for the proposed FCS in 2015. The tunnel mounting strategy of the fuel cell module and its BOP is considered in this model. The proposed layouts are shown in Figure 9.22 - Figure 9.25.

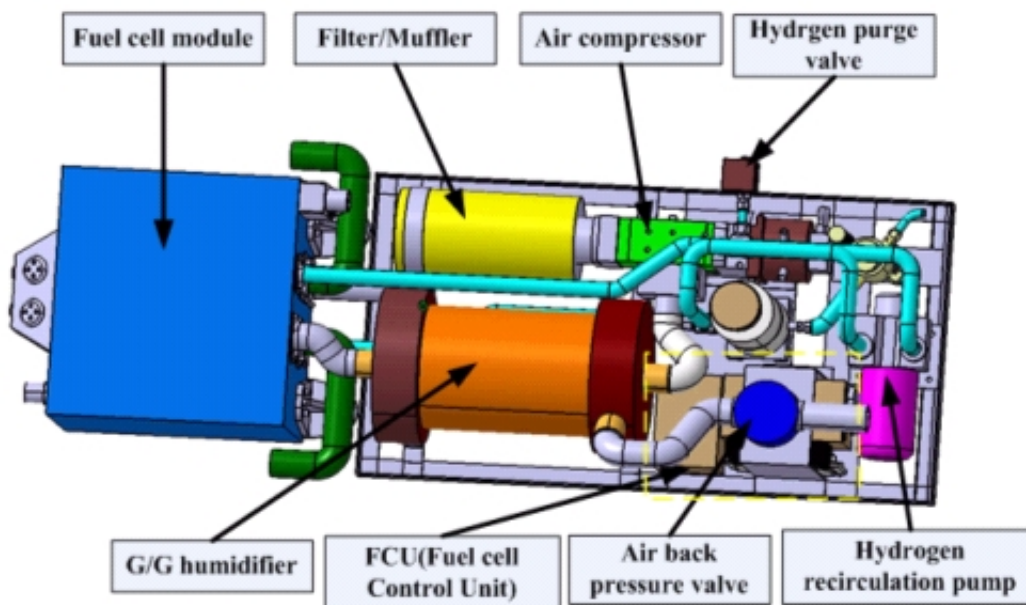


Figure 9.22: CAD model of proposed FCS (View 1)

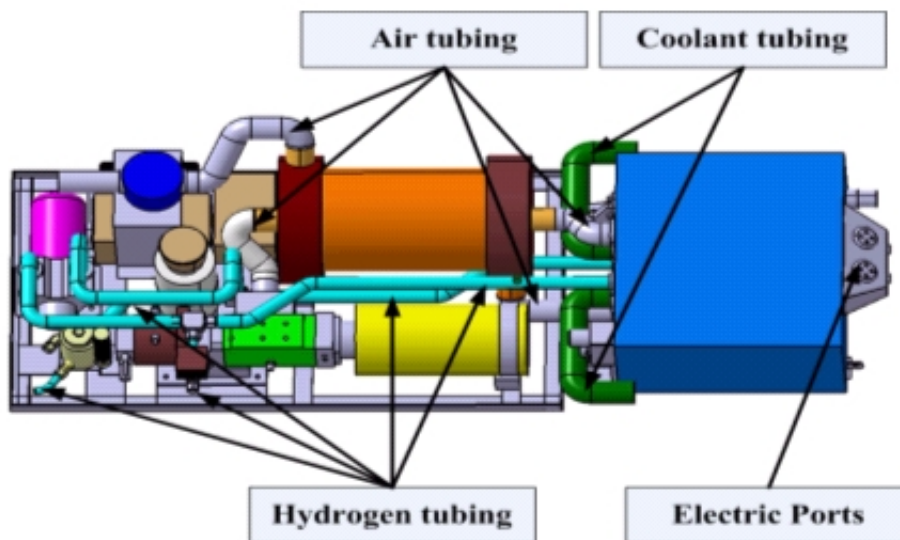


Figure 9.23: CAD model of proposed FCS (View 2)

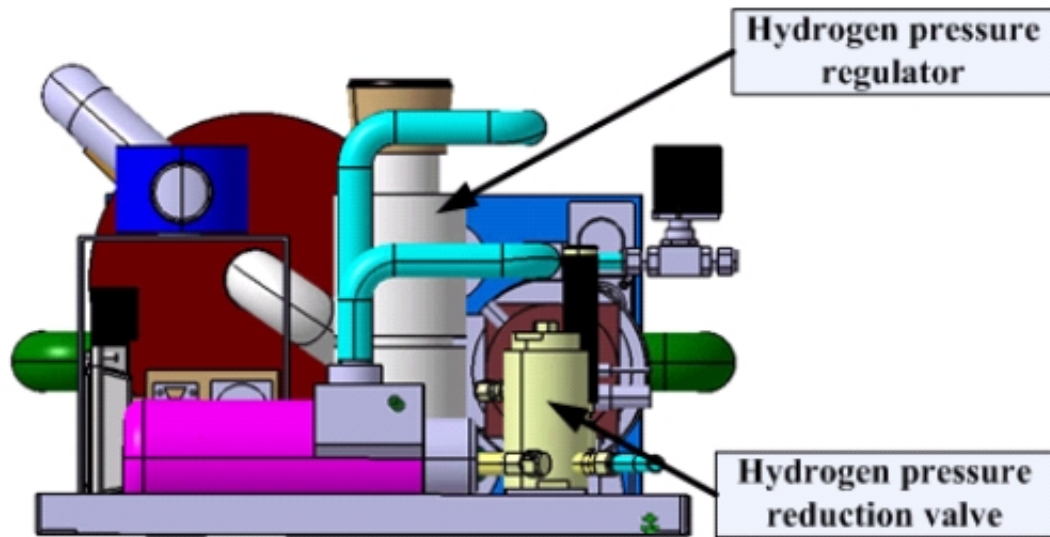


Figure 9.24: CAD model of proposed FCS (View 3)

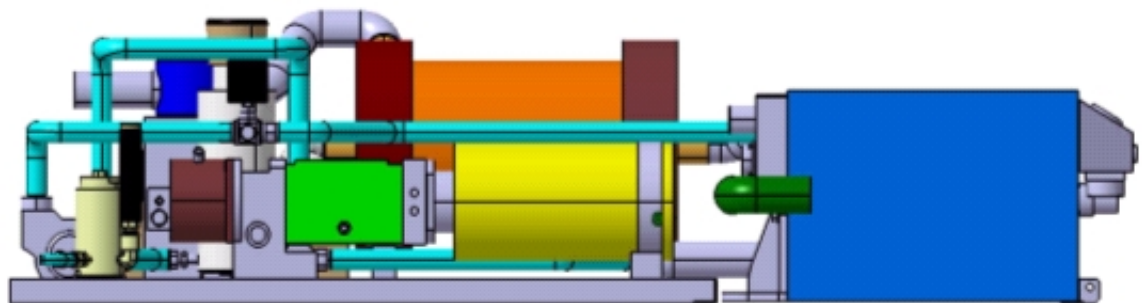


Figure 9.25: CAD model of proposed FCS (View 4)

9.2.10.2 Fuel Cell Module

The FCM (Fuel Cell Module) is the core component in the FCS. The key parameters are shown in Table 9.6.

No.	Parameters(Unit)	Value
1	Number of cells	440
2	Weight (kg)	42.5
3	Dimension	403mm × 372mm × 252mm
4	Volume (Liter)	38
5	Voltage at open circuit (V)	431
6	Max current (A)	220

Table 9.6: Fuel Cell Module key parameters

The front side of the Fuel Cell Module (FCM), where the electric output ports are located, is close to the power converter. The opposite one is close to its BOP. The FCM is installed on the chassis by the brackets. There are four mounting strategies as follows:

- The stack should be mounted at the resting feet on the bottom of the enclosure
- The fuel cell stack must be prevented from crash and impact load
- Vibration should be prevented as much as possible
- Electro-Magnetic Interference (EMI) should be avoided

9.2.10.3 Air Compressor

The air compressor is contributed to delivering the air to the FCM. Its key parameters are shown in Table 9.7.

No.	Parameters(Unit)	Value
1	Air flow (g/s)	4 – 90
2	Outlet pressure (MPa)	0.2 – 0.4
3	Weight (kg)	8.78
4	Dimension	437mm × 93mm × 102mm
5	Volume (Liter)	4.2
6	Max consumption (kW)	10

Table 9.7: Air compressor key parameters

The air compressor is mounted on the frame of the BOP. The main requirement of the air compressor's mounting strategy is to keep the mounting plane level for installation in order to make

the air compressor as horizontal as possible. The filter/muffler should be close to the compressor inlet. There are four mounting strategies for the air compressor:

- The compressor should be fixed to the bracket and bear equal force to the resting feet
- Special attention should be paid to the prevention of vibration transfer and resonance
- The pressure loss of the tubing leading out of the compressor should be minimized
- A chemical filter is required at the inlet of the air compressor. (which can remove the sulfur in the air)

9.2.10.4 G/G Humidifier

The G/G humidifier's purpose is to humidify the air. The key parameters are shown in Table 9.8.

No.	Parameters(Unit)	Value
1	Air flow (LSPM)	4000
2	Max air inlet pressure(MPa)	0.32
3	Air outlet relative humidity	80% – 100%
4	Weight(Kg)	6.08
5	Dimension	Ø200mm × 411mm
6	Volume(Liter)	11

Table 9.8: *Parameters of G/G humidifier*

G/G humidifier is installed on the frame of BOP. The main factor to be considered during its mounting process is to keep the body of humidifier horizontal. There are three mounting strategies as mentioned below:

- The tubing leading into and out of the humidifier should be as short as possible
- Heat insulation of the tubing leading into and out of the humidifier should be incorporated
- Heat insulation of the humidifier should be taken into account

9.2.10.5 Recirculation Pump

The principal function of the hydrogen recirculation pump is to circulate the excessive hydrogen partly return to the fuel cell stack. The key parameters are shown in Table 9.9.

No.	Parameters (Unit)	Value
1	Air flow (SLPM)	> 6
2	Voltage supply (V)	12
3	Power (W)	480
4	Pressure (MPa)	0.13 – 0.4
5	Weight (kg)	10
6	Dimension	Ø88mm × 266mm
7	Volume (Liter)	1.6

Table 9.9: *Recirculation pump key parameters*

The pump is installed close to FCU. The two major mounting strategies for recirculation pump is are the following:

- The vibration should be prevented
- The pressure loss in the hydrogen recirculation tubing should be minimized

The layout of miscellaneous parts can also be seen in Figure 9.22 and Figure 9.24.

9.2.11 Hydrogen Storage Systems

9.2.11.1 Liquid Hydrogen Storage (Cryogenic)

The storage density of liquid hydrogen (LH₂) is high, compared to other forms of hydrogen storage. Liquid hydrogen is delivered at about $-250\text{ }^{\circ}\text{C}$ into a highly insulated and low-pressure hydrogen gas tank as shown in Figure 9.26. The pressure relief system prevents tank over-pressurization due to heat transfer into the low temperature vessel. Heat exchangers are required to raise the gas temperature before it can be delivered to the fuel metering components of the hydrogen fuel cell system.

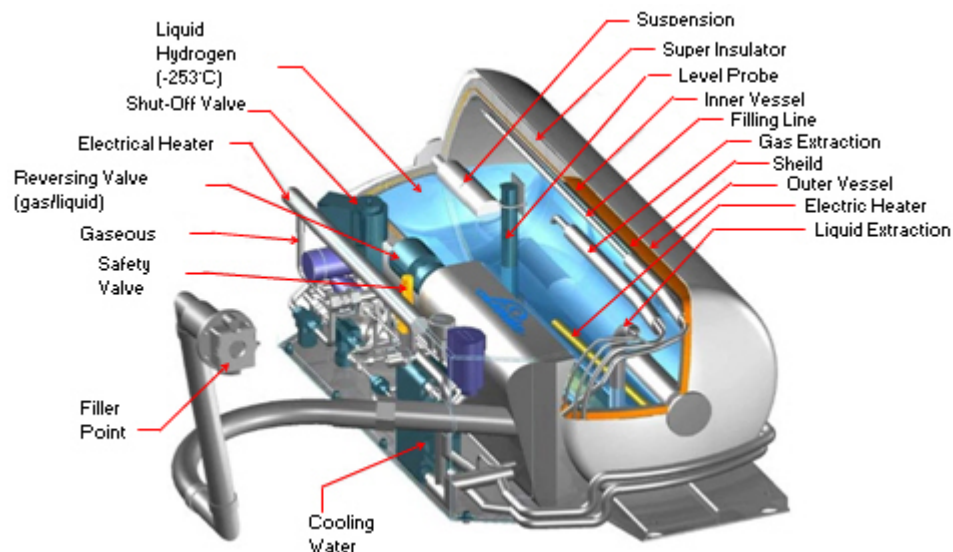


Figure 9.26: Liquid H₂ - tank system [29]

The tanks are made mostly from stainless steel components due to steel's corrosion protection and steel's compatibility with hydrogen. The estimated weight of a liquid hydrogen system is 15-25 kg per kg stored hydrogen. The estimated cost of a liquid hydrogen system is \$10,000 USD per kg stored hydrogen. Until 2008 there was no full vehicle validation of a LH₂ storage system. The long term durability of LH₂ storage system is not known, because a full vehicle validation has not been performed yet.

Some of the current LH₂ storage systems applications are:

- BMW 7 Series bio-fuel only production application with limited fleet
- 2001 - 2007 GM HyGen 3 fuel cell test vehicle fleet

Advantages

Following are the advantages of LH₂ storage systems:

- High storage density
- Potentially viable for mass production
- Commercially established cryogenic transport-trucks for distribution

Challenges

Following are the disadvantages of LH₂ storage systems:

- Size and weight similar to compressed gas storage systems
- Limited tank geometry options (cylindrical vessel shape is dominant)
- Hydrogen gas "boil-off" typically limits "in vehicle storage" to less than 2 weeks
- User unfriendly refueling equipment
- High fuel losses to cool supply line during refueling process

9.2.11.2 Metal Hydride Hydrogen Storage (Solid)

Metal-Hydride hydrogen is stored in a chemically dissolved state in a porous metal matrix, which is housed and protected by a composite reinforced pressure container as shown in Figure 9.27. Electric heating is required to achieve sufficient gas transfer for vehicle propulsion. The estimated weight of a metal hydride hydrogen storage system is over 30 kg per 1kg stored hydrogen. The cost and durability of this storage system is not known.

There are no known current applications of metal-hydride hydrogen storage systems. They are being tested in experimental systems and cars.

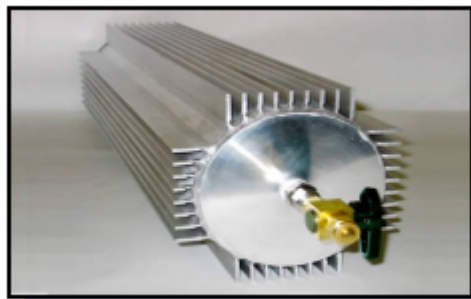


Figure 9.27: Metal hydride hydrogen storage

Advantages

Following are the disadvantages of metal hydride hydrogen storage systems:

- High storage density
- Compact packaging size for larger driving ranges

Challenges

Following are the disadvantages of metal hydride hydrogen storage systems:

- High weight of metal hydride material
- Limited dynamic charge / discharge rates
- Requires on-board energy management for refueling and de-fueling
- No automotive scale production development in progress

9.2.11.3 Compressed Hydrogen Gas Storage

Highly compressed gas is stored in one or multiple cylindrical vessels as shown in Figure 9.28. Pressure vessels are made from carbon fiber reinforced composite to reduce the overall weight. Valves and pressure regulators can be integrated. Gas pre-chilling may be used to allow fast fills in less than 5 minutes.



Figure 9.28: Cylindrical pressure vessels

The estimated weight of the compressed gas storage system is 30 kg per kg stored hydrogen for 70 MPa (Mega Pascal) (10,000 psi) systems (complete system with tanks, valves, regulators, sensors, mounting hardware). The estimated costs range from \$7,000 USD to \$12,000 USD per kg stored hydrogen.

Some full tank and valve development programs have been completed for compressed gas storage systems. Also, some vehicle tests have been completed by multiple OEM's and various certifications obtained in Europe, North America and Japan. So, the durability of the compressed gas storage system is not a big concern.

However, the raw material availability for manufacturing of this storage system is a concern because there is a limited carbon fiber availability for large-scale automotive production, due to rapidly rising market demand for medium and high strength fiber.

Advantages

Following are the advantages of compressed hydrogen gas storage systems:

- High storage density at 70 MPa (10,000 psi) (as shown in Figure 9.30)
- Safe technology well understood and already implemented
- Technology for 35 Mpa and 70 MPa developed, pressure level optimization possible (as shown in Figure 9.29 and Figure 9.30)
- Most economical and user friendly technology to date
- Commercially viable for mass production

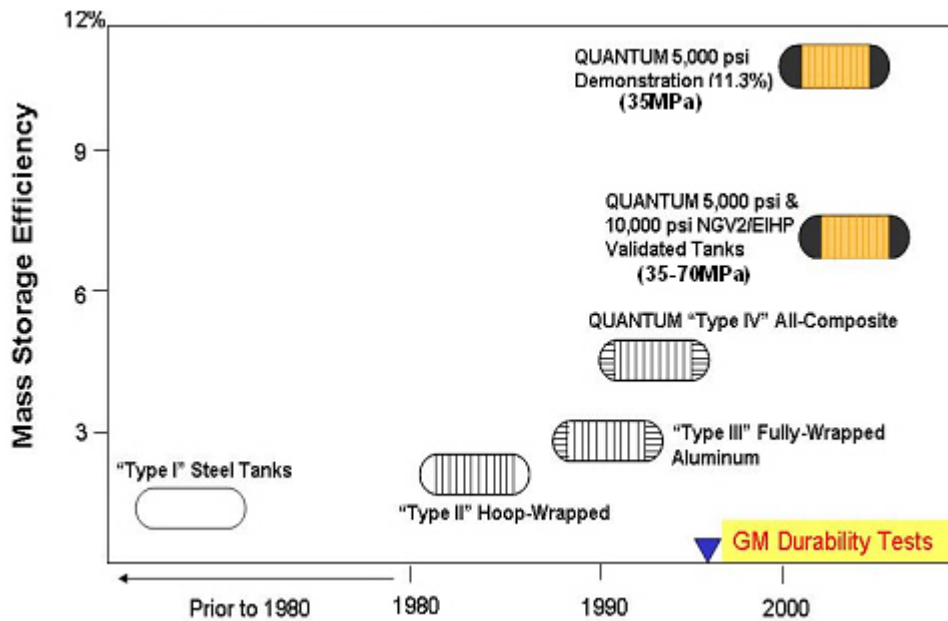


Figure 9.29: Gravimetric efficiency development trend for compressed gas vessels

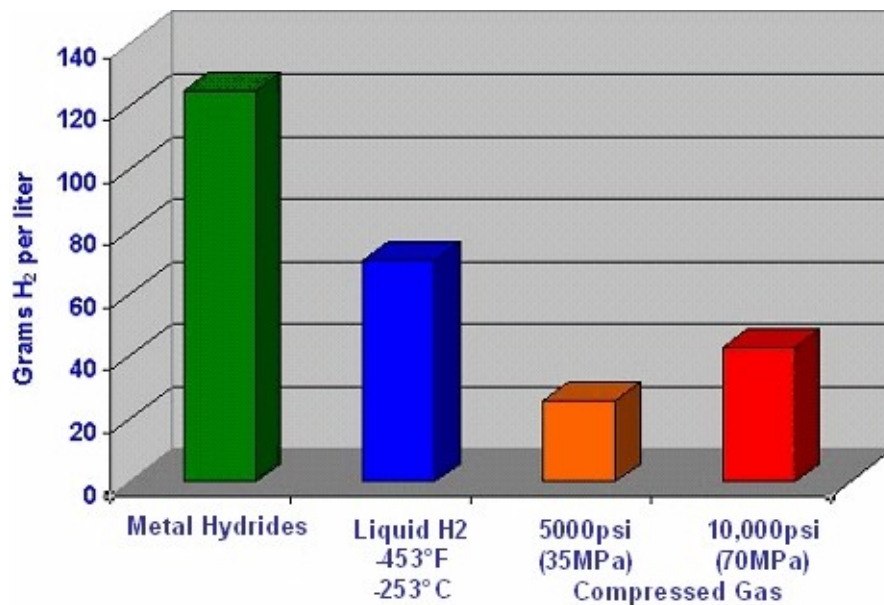


Figure 9.30: Different storage types and storage densities

Challenges

Following are the disadvantages of compressed hydrogen gas storage systems:

- Size and weight limit packaging freedom
- Carbon fiber material limited market supply/highly priced (approx. US \$30 USD/kg)
- High energy use in gas compression and chilling for refueling processes
- Low cost reduction potentials mainly due to carbon-fiber material

9.2.11.4 Implementation Forecast (2015)

Following are the forecasts for the implementation of different hydrogen storage systems by 2015:

- Liquid storage (Cryogenic)
 - Technology has already been abandoned by most OEM's
 - Very limited refueling infrastructure due to cost and complexity
- Metal hydride (Solid)
 - Very heavy and requires mainly cylindrical tanks, just like compressed gas tank shape
 - Refueling and de-fueling require thermal management and external heat sources
 - Extremely expensive, limited supply

- Technology is further researched in laboratory conditions only
- No known OEM roll-out plans
- Compressed Gas
 - Commercially viable technology 35 MPa and 70 MPa (5,000-10,000 psi)
 - Storage tanks present packaging challenges
 - High level of technical maturity
 - Proven durability, reliability and crash worthiness
 - Cost reduction dependent on carbon fiber pricing and large volume component manufacturing
 - Multiple OEMs plan fleet applications with 5,000 to 10,000 vehicles per year, expected at subsidized premium cost per car
 - Mass production technology and process development phase, (tanks and valves)
 - High pressure hydrogen tolerant steels needed in larger quantities required for valves, plumbing and fuel metering devices (alternatives to SS316L and A286)

9.2.11.5 Implementation Forecast (2020)

Following are the forecasts for the implementation of different hydrogen storage systems by 2020:

- Liquid storage (Cryogenic)
 - No vehicle integration anticipated
- Metal hydride (Solid)
 - Needs major weight, cost and performance improvements
 - No known OEM roll-out plans
- Compressed Gas
 - High volume production implementation phase, 100,000+ per year
 - Volume pricing with raw material suppliers to be achieved
 - OEM hydrogen storage system target price is \$1,000 USD per car (4-5 kg hydrogen, with valves sensors, regulator, bracket)
 - * not achievable without major raw material cost reductions
 - Carbon fiber cost alone has to be reduced from \$1,800 USD+ to below \$500 USD
 - Compressed gas refueling infrastructure will require substantial steel masses for compressors, mass storage and plumbing systems, trucks, pipelines, etc.

9.2.11.6 Recommendation for FSV

Based on the technology assessment, the compressed hydrogen gas storage system was recommended for the FSV program, since it is the most viable option for commercial use. The key attributes of the different storage systems that were compared are illustrated in Table 9.10. The technology for pressure level between 35 Mpa and 70 MPa is already available for the compressed hydrogen storage system. A single tank is preferred over multi tank option, due to factors such as cost, weight, and reliability. The pressure level chosen for the FSV is 70 Mpa. Tank mounting directly to the vehicle structure is favored for cost and weight reduction.

Factors	H ₂ Storage systems		
	Liquid H ₂	Compressed H ₂ gas	Metal hydride
Storage density	+	+	++
Mass production	+	+	
Size	-	-	+
Weight	+	+	-
Packaging	-	-	++
Commercial usage	+	++	-
User friendliness	-	++	
Technical maturity	-	++	-
Durability		++	
Cost	-	+	

(++) Good (+) Average (-) Poor (.) Not known

Table 9.10: H₂ storage system decision matrix

9.2.12 Hydrogen Refueling Infrastructure

9.2.12.1 Practical Considerations

A widespread adoption of fuel cell vehicles will need an adequate hydrogen refueling infrastructure. Mass distribution of hydrogen will be possible only upon availability of the following features:

- On-site compressor with high pressure cascade tanks
- Gas chilling system ($-20\text{ }^{\circ}\text{C}$ to $-40\text{ }^{\circ}\text{C}$) for "fast fill" supply to vehicle
- Substantial compressor systems needed for 70-87.5 MPa
- Steel cylinders required for transport and on-site bulk storage

The factors to be considered for a feasible hydrogen refueling structure are the following:

- Typical vehicle tank capacity : 3-5 kg hydrogen
- Expected fill time : less than 5 minutes
- Minimum station demand : 30-300 vehicles per day
- Average demand at station : 90-1,500 kg hydrogen per day
- Usable "tube trailer" capacity : < 200 kg hydrogen at 13.8 MPa

9.2.12.2 Future Hydrogen Refueling Options

Mobile On-Site Hydrogen Production and Dispensing Unit

A mobile on-site hydrogen production unit and dispensing unit consists of a rail mounted electrolyzer, a gas compressor and high-pressure storage vessels. These components allow continuous hydrogen generation from grid power. The vehicle fill equipment is integrated to the system. Such systems have been deployed for development support and military use. An example of such a system is shown in Figure 9.31



Figure 9.31: Mobile On-Site hydrogen production and dispensing unit

Transportable Hydrogen Compressor

Integrated gas compressor allows vehicle fills in about 10 to 30 minutes using hydrogen from industrial supply gas containers or tube trailers and grid power. Vehicle fill equipment is integrated. Systems have been deployed for development support and fleet operation. Compressor can be complemented with cascade tank storage and gas chilling system for higher capacity and faster fill times (less than 5 minutes). An example of such a system is shown in Figure 9.32



Figure 9.32: Transportable hydrogen compressor

Hydrogen Refueling Station

A commercial station with integrated gas compressor allows multiple vehicle fills using hydrogen from tube trailers and grid power. As compared to gasoline stations, more space is required to install above ground hydrogen storage and hydrogen fuel handling / delivery equipment. A typical prototype hydrogen refueling station is shown in Figure 9.33. The vehicle fill equipment is integrated into this system. Such systems have been deployed for development support and fleet operation.

A critical issue that needs to be tackled is the high electrical energy supply that is required to run an on-site hydrogen generation station.

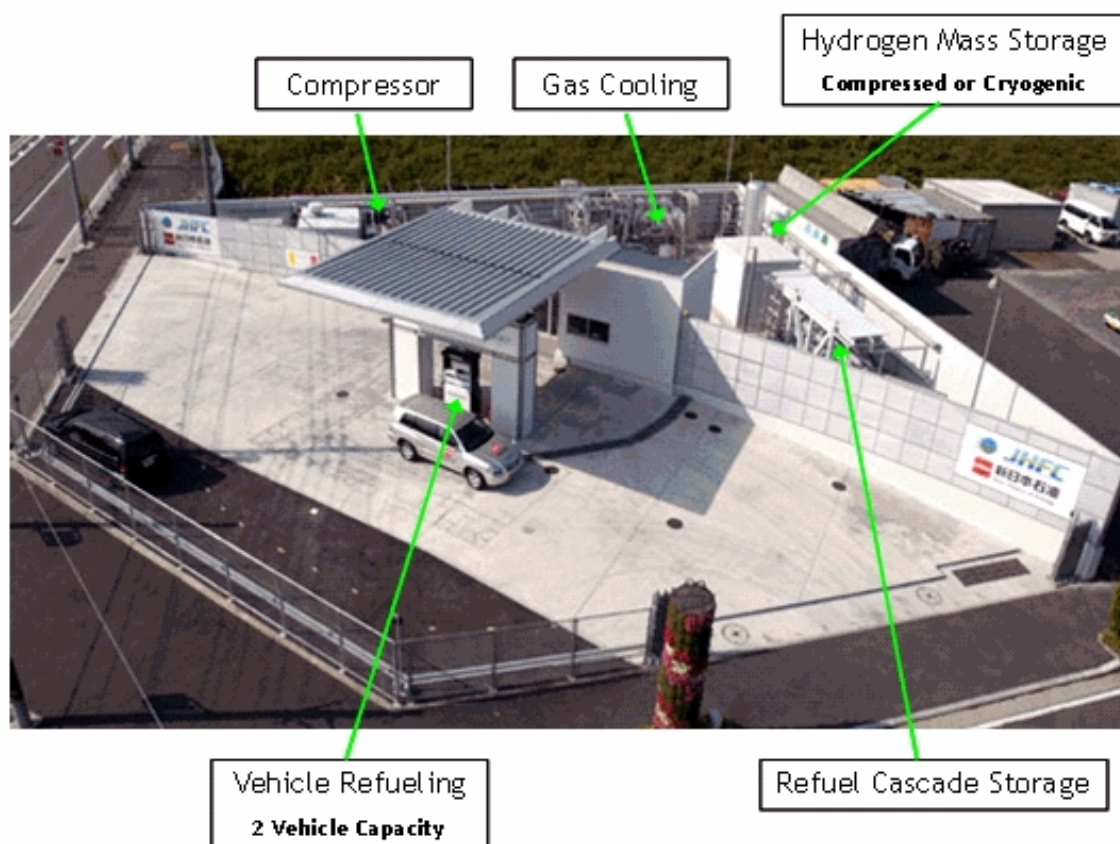


Figure 9.33: Typical prototype hydrogen refueling station for 1-20 fills per day

9.2.12.3 Conclusions

Typical refueling station would require ~ 0.4 to 7.5 "tube trailers" deliveries per day in order to be satisfy the need, therefore it would be impractical and cost prohibitive to implement a compressed

hydrogen system on a large-scale basis. The long-term solution for hydrogen distribution will have to rely on hydrogen pipelines, cryogenic hydrogen supply or local hydrogen production.

The "hydrogen refueling infrastructure" would require a substantial capital investment and varieties of steels. These steels would include:

- Stainless steel for valves, plumbing and instrumentation
- Gray iron for compressor technology
- Mild steels for cascade cylinders
- Miscellaneous steels for structure and enclosures

A high pressure hydrogen fuel storage and refueling infrastructure will require a broader spectrum of high strength and hydrogen compatible steels.

9.3 Battery Technology

9.3.1 Overview

In the past 10 years, rechargeable battery storage capacities have been rapidly improved upon by deploying new technologies for consumer products (cell phones, power tools, etc.). Some of these technologies have proven themselves with excellent product performance and reliability records. Automotive high voltage battery technology is typically utilizing the mass production technology for cylindrical cells, which are connected in series (strings) and parallel, to achieve the voltage levels and desired storage capacity. In order to increase durability and provide acceptable operation performance under extreme climate conditions (i.e. cold-start or continuous high output at high ambient temperatures), temperature control of individual cells and battery packs is one of the key areas to be further enhanced for automotive battery development .

The key automotive battery customers are shown in Figure 9.34 along with the market forecast until year 2015.

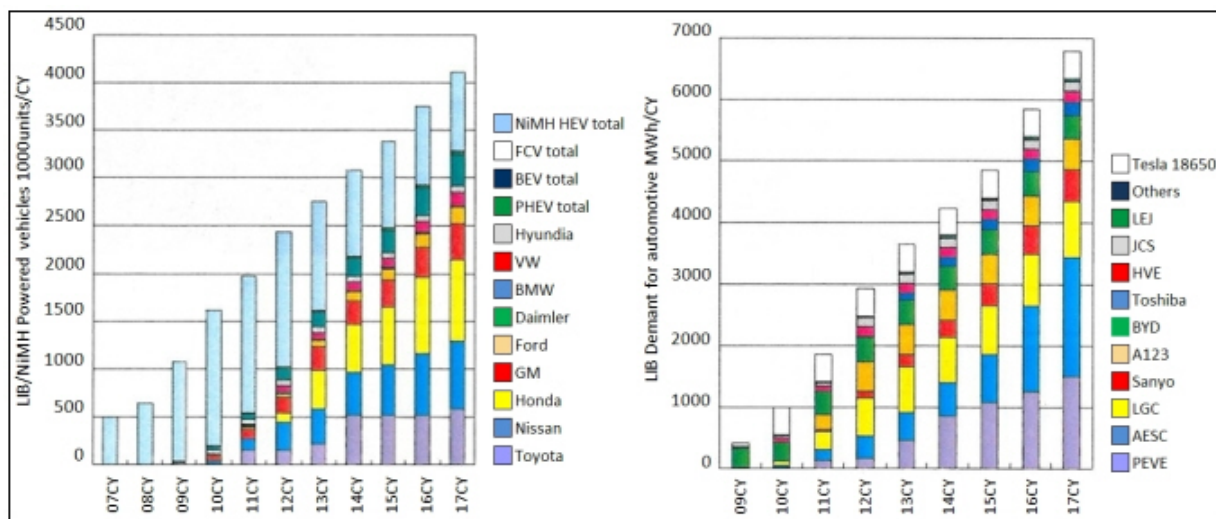


Figure 9.34: Automotive battery customers, suppliers and market forecasts

9.3.1.1 Battery Types

The different battery technologies currently used and under development for Hybrid or full electric automotive applications are the following.

- Nickel Metal Hydride (Ni-MH) - today's mainstream battery technology for automotive traction applications
- Lithium-Ion - cathode based on lithium compounds with materials such as cobalt, manganese, iron phosphate, aluminum, nickel, titanium, vanadium etc.

9.3 Battery Technology

- Cobalt-based technologies are dominant in low power applications (cellular phones, laptops etc.) due to high energy capacity
- Manganese based cells are used in high power applications (power tools)
- Iron phosphate based cells are used in high power applications (power tools)
- Other combinations of cathode materials are explored worldwide to achieve best compromise between the power, energy, safety and cost

9.3.1.2 Recommendations for FSV

For Phase-2 and Phase-3 of the FSV Program, it was recommended to use a battery technology that is safe, lightweight, and energy cost-efficient. The key attributes recommended for the FSV program, based on the technical assessment, are summarized in Table 9.11.

For the 2015 and forward time frame prismatic lithium-ion batteries using manganese oxide technology show great potential to meet automotive requirements. The large number of OEM Battery suppliers who heavily invest into this technology supports this. This technology is also supported by a large number of OEM battery suppliers.

Battery Technology Assessment				
		Status 2008	Prediction 2015-2020	Selection FSV
Dominating Technology		Ni-MH	Li-Ion	Li-Ion
Power Density	kW/kg	1.1	1-3	2.0
Energy Density	Wh/kg	45	90 - 170	130

Battery Pack Technology Assessment				
Capacity	kWh	10 (max)	1.5 - 40	2.3 - 35
Cost	\$ USD/ kWh	500	400-700	450

Future Steel Vehicle Concept				
	Capacity (kWh)	Weight (kg)	Volume (Liters)	Cost (\$ USD)
PHEV₂₀	5	58.2	47	\$2,346
PHEV₄₀	11.7	136.5	103	\$5,365
BEV	35	346.5	280	\$15,895
FCEV	2.3	27.3	25	\$1,503

Table 9.11: Battery recommendation for FSV

9.3.2 Nickel-Metal Hydride (NI-MH) Battery

Nickel-metal hydride is today's mainstream battery technology for automotive traction applications. A sample Nickel-metal hydride battery is shown in Figure 9.35



Figure 9.35: Sample Nickel-Metal Hydride battery

9.3.2.1 2008 Hybrid Vehicle Applications

- Toyota/Lexus, Honda, GM, Nissan

9.3.2.2 2008 Value Ratios (Cell)

- Cost : \$500 USD per kWh,
- Weight : 22 kg per kWh (45 Wh/kg)

9.3.2.3 Advantages

- More abuse tolerant than lithium-ion
- Commercially viable for mass production
- Well understood performance and life characteristics

9.3.2.4 Challenges

- Low power density resulting in an increase in battery size and weight

- Increasing raw material cost and limited long term availability
- Limited dynamic charge / discharge rate

9.3.3 Lithium-Ion Battery

In Lithium-Ion batteries, the cathode is based on lithium compounds with materials such as cobalt, manganese, iron phosphate, aluminum, nickel, titanium, vanadium etc. The key characteristics of Lithium-Ion batteries are the following:

- Highest electrochemical potential, energy density and power density of all known battery technologies
- Has already replaced Ni-MH in portable electronics, commercially available for power tool applications
- Most new hybrid vehicle prototypes use Li-Ion technology. Toyota aims to lower the cost of hybrid system by 30% and reduce the size of battery by 50%, by switching from Ni-MH to Li-Ion
- Lithium-ion chemistry allows recycling of most materials contained in an individual Battery cell
- Lithium is abundantly available, commercial exploitation improvements are required for significant cost reductions

9.3.3.1 Lithium-Ion Cobalt

Cobalt-based lithium-ion technologies are dominant in low power applications (cellular phones, laptops etc.) due to high energy capacity. There is no current hybrid vehicle applications for Lithium-Ion cobalt batteries. The technology has to be further developed for future OEM applications. A sample lithium-ion cobalt battery is shown in Figure 9.36.



Figure 9.36: *Sample lithium-ion cobalt battery*

The key characteristics of lithium ion-cobalt batteries are as follows:

- Commodity technology for consumer electronics - small cells (< 2 Ah)
- High energy density : 170 Wh/kg
- Low power density : 1000 W/kg
- Cost : \$500 USD/kg
- Safety issues - explosive failure mode
- In present form not suitable for automotive use due to safety problems
 - Research activities ongoing to improve the safety

9.3.3.2 Lithium-Ion Manganese

Manganese based cells are used in high power applications such as power tools. The key characteristics of Lithium Ion-Manganese batteries are as follows:

- Mass produced for power tool applications - larger cells (>2.9 Ah)
- High power density : 2000 W/kg
- High energy density : 120 Wh/kg
- High cell voltage : 3.8 V - 4.2 V
- Good safety - non explosive failure mode
- Lower raw material cost : \$400 USD/kg
- Calendar life and cycle life need further improvements

There is no current hybrid vehicle application for lithium-ion manganese batteries. The technology has to be further developed for future OEM applications.

9.3.3.3 Lithium-Ion Iron Phosphate

Iron Phosphate based cells are used in high power applications such as power tools. The key characteristics of lithium-ion phosphate batteries are as follows:

- Mass produced for power tools applications
- High power density: 2500 W/kg
- Lower energy density: 100 Wh/kg
- Lower cell voltage (3.3 V) - more cells needed for high voltage packs
- Cost : \$600 USD/kg
- Cells optimized for automotive use currently on the market
- Good safety - no explosive failure mode

There is no current hybrid vehicle applications for lithium-ion iron phosphate batteries. The technology has to be further developed for future OEM applications.

9.3.3.4 Other Li-Ion Technologies

- New technologies for power cells utilize mixed cathode materials such as mixtures of nickel, manganese and cobalt (NMC) compounds or nickel, cobalt and aluminum (NCA)
- Although these materials demonstrate good performance, there are still safety issues with cobalt and nickel
- The technologies using cathode materials other than cobalt, manganese or iron phosphate are in limited volume production or development stage
- More expensive materials and production processes required
- Energy density : 100 Wh/kg
- Power density : 2000 W/kg
- Cost : \$700 USD/kg

9.3.3.5 Lithium-Ion Cell Battery Designs

There are two different Lithium-Ion battery designs: Cylindrical cells design and prismatic cells design as shown in Figure 9.37 and Figure 9.38, respectively. Prismatic cells design are more viable for automotive applications due to its advantages in packaging and heat management, compared to cylindrical cells.

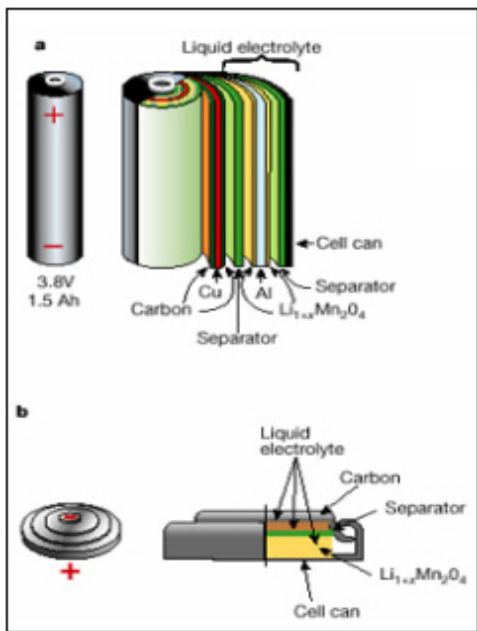


Figure 9.37: Cylindrical cells

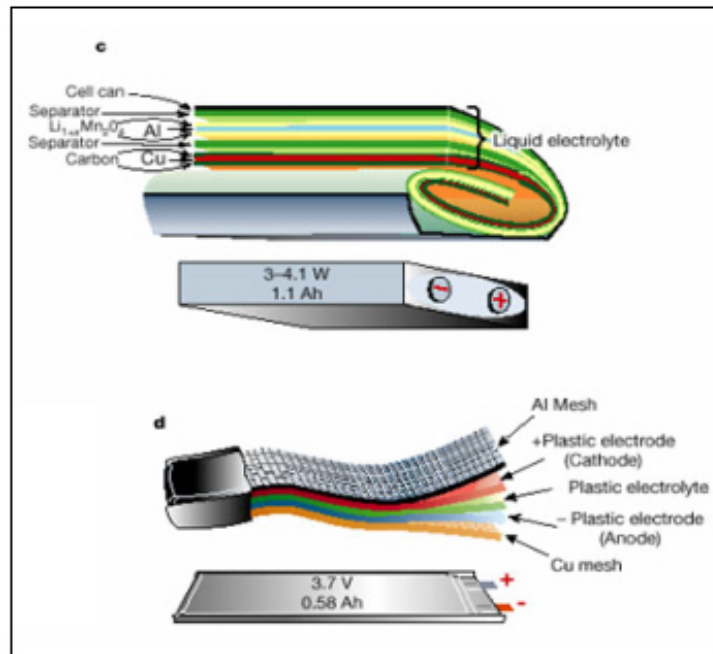


Figure 9.38: Prismatic cells

9.3 Battery Technology

9.3.4 Packaging

Automotive batteries utilizing cylindrical cells or prismatic cells are assembled in steps, starting with modules containing multiple cells (shown in Figure 9.39). These modules serve as building blocks for a "pack" which then is placed into an enclosure together with control devices for power delivery, cell protection and heat management. Besides having a stable and durable high-capacity battery cell composition, the key to battery durability lies in the power control and management of power input and output from the high-voltage battery pack. This may require external cooling from the vehicles air conditioning or a dedicated sub-system. The basic design and packaging concepts apply to both cylindrical and prismatic cell designs as shown in Figure 9.39.

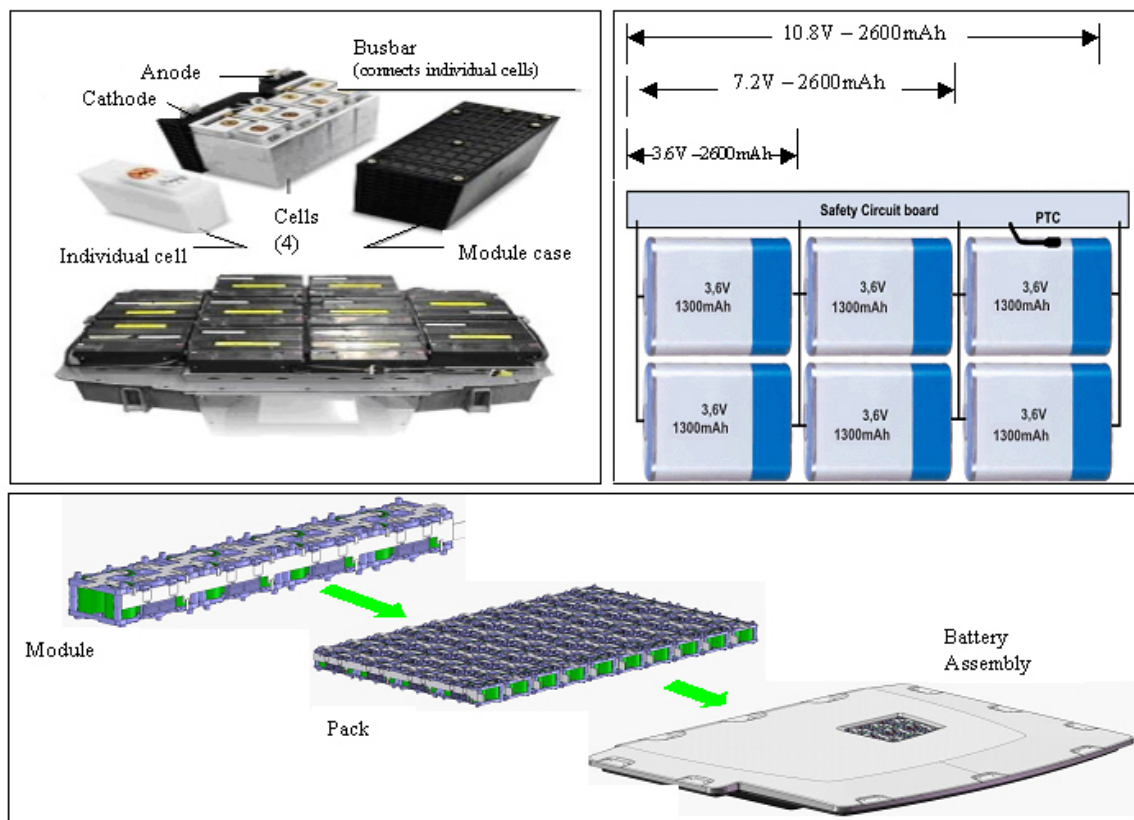


Figure 9.39: Basic design and packaging concepts

9.3.5 Future Trends

9.3.5.1 Nickel-Metal Hydride

The forecasts for the Nickel-Metal Hydride technology are the following:

- Market share will shrink due to lower energy density and higher weight
- Li-Ion batteries will be a more preferred technology by 2012
- Market share will be insignificant in the volume car after 2025
- The market share loss may be faster if the prices of nickel keep rising

9.3.5.2 Lithium-Ion

The forecasts for the Lithium-Ion technology are the following:

- Major market players will launch volume production 2011-2012 with cylindrical cells
- Initial market will be shared by lithium ferrite phosphate and lithium manganese oxide chemistries
- Cobalt and nickel based technologies (NMC, NCA) must demonstrate adequate safety
- Cell cost likely to drop to \$300 USD/kWh, battery management system costs will be in the range of \$100-200 USD/kWh (therefore the battery pack cost will be approximately \$450 USD/kWh)
- Service life expectation : 10 Years / 150,000 km / 3000 cycles will be met
- Li-Ion technology will dominate EV, HEV and FCV market
- Manufacturing capacity has to be established for increasing automotive and non-automotive markets.
- Highly automated large volume manufacturing processes and equipment for cylindrical cells will be further improved upon further improving cell consistency and reliability
- Probability of customized Prismatic cells for each application, therefore high production volumes will be required to make them commercially acceptable
- Production processes for large (automotive size) prismatic cells have to be optimized and validated
- Advancements in battery chemistry will focus on:
 - Durability and extreme operating condition improvements
 - Capacity increases
 - Cost reduction of battery materials and manufacturing processes

Lithium-Ion battery cell development is primarily occurring in Asia and North America. Production is mostly located in Asia. Some of the lithium-ion cell battery suppliers and the corresponding battery key characteristics are shown in Table 9.12.

9.3 Battery Technology

	Saft VL 30P	Valence	A123	GS Yuasa Battery	NEC	Panasonic	Sanyo	ALP
Chemistry	Nickel Cobalt	Iron phosphate	Iron phosphate	Manganese dioxide	Manganese dioxide	Manganese dioxide, nickel, cobalt	Manganese dioxide	Manganese dioxide
Specific Energy [Wh/kg]	100	90	90	45	Unknown (expect > 100)	Unknown (expect > 100)	Unknown (expect > 100)	> 130
Specific Power [W/kg]	1100	2000	3000	> 1500	Unknown (expect > 2500)	Unknown (expect > 2500)	Unknown (expect > 2500)	> 2500
Cost to Manufacture	High	High	Medium	High	Unknown	Unknown	Unknown	Low to Medium
Quality	Medium	Medium	Low - Medium	High	Expected to be high	Expected to be high	Expected to be high	High
Safety	Medium	High	High	High	Expected to be high	Expected to be high	Expected to be high	High
Hybrid Powertrain Design	Yes (with Johnson Controls input)	Some	Yes (with Cobasys input)	Unknown (expect yes)	Unknown (expect yes)	Unknown (expect yes)	Unknown (expect yes)	Yes

Table 9.12: Lithium-ion cell battery suppliers and key cell characteristics

9.3.6 Recommendations

Based on the technical assessment, representative cell densities in the range of 90-170 Wh/kg (energy density) and 1500-4000 W/kg (power density) were recommended as target values for 2015. Prismatic lithium-ion batteries using manganese-oxide technology show great potential to meet these requirements. Table 9.13 shows the key attributes compared by Quantum Technologies for the assessment.

	NiMH	Li-Ion Cobalt	Li-Ion Manganese	Li-Ion Iron Phosphate
Energy Density (Wh/kg)	-	++	+	+
Power Density (W/kg)	-	+	++	++
Cost (\$/kWh)	+	+	++	-
Safety	++	-	+	+

(++) Good (+) Average (-) Poor

Table 9.13: Battery decision matrix

9.3.6.1 Energy Density Comparison

The energy density of different battery technologies are shown in Figure 9.40. It can be seen that Li-Ion batteries have a higher energy density compared to the other available battery technologies. Also shown in Figure 9.40 is the recommended technology and densities for the FSV variants.

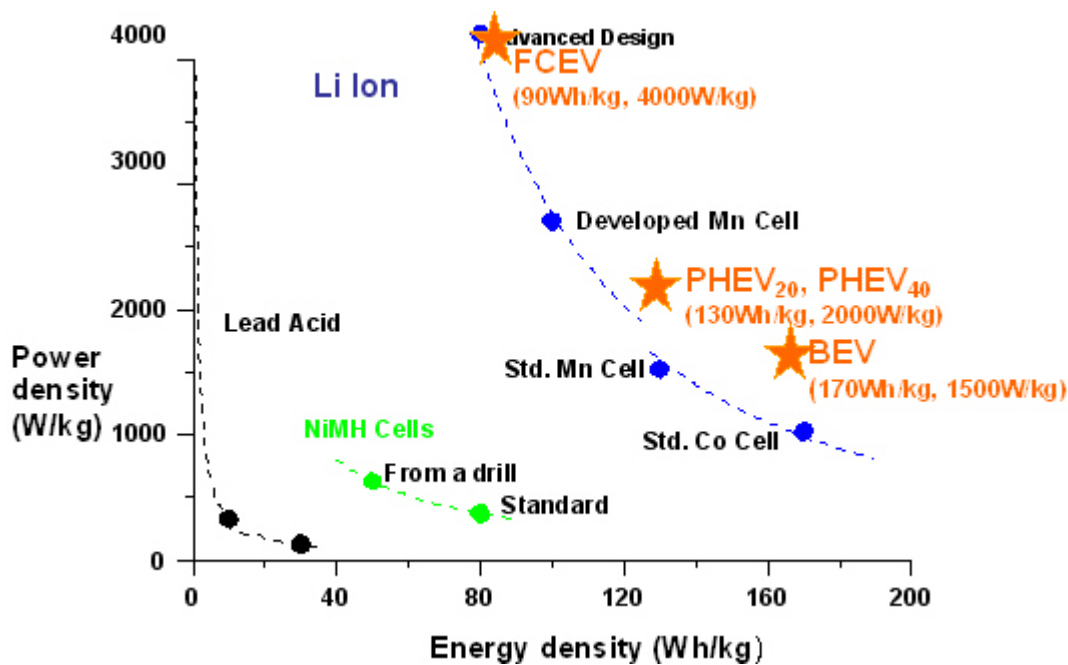


Figure 9.40: Energy density comparison

9.4 Ultra-Capacitor Technology

9.4.1 Overview

Ultra-capacitors have been evaluated instead of batteries in various hybrid vehicle development programs. Ultra-capacitors have very high dynamic electrical load handling capability and are less sensitive to harsh operating temperature conditions. Ultra-capacitors typically are produced as cylindrical coils using metal and isolating foils in layers as shown in Figure 9.41. Large capacitors are typically assembled similar to battery packs. They receive their high voltage charge from regenerative braking or from power inverters.



Figure 9.41: Sample ultra-capacitors

9.4.1.1 2008 Hybrid Vehicle Applications

- Honda fuel cell vehicle until 2007
- Experimental cars, trucks and buses

9.4.2 Energy and Power Density

Energy density of ultra-capacitors are lower than batteries as displayed in Figure 9.42, resulting in a lower vehicle driving range. Power density, in contrast, is very high allowing substantial power boosts in vehicle acceleration or power retrieval with regenerative braking.

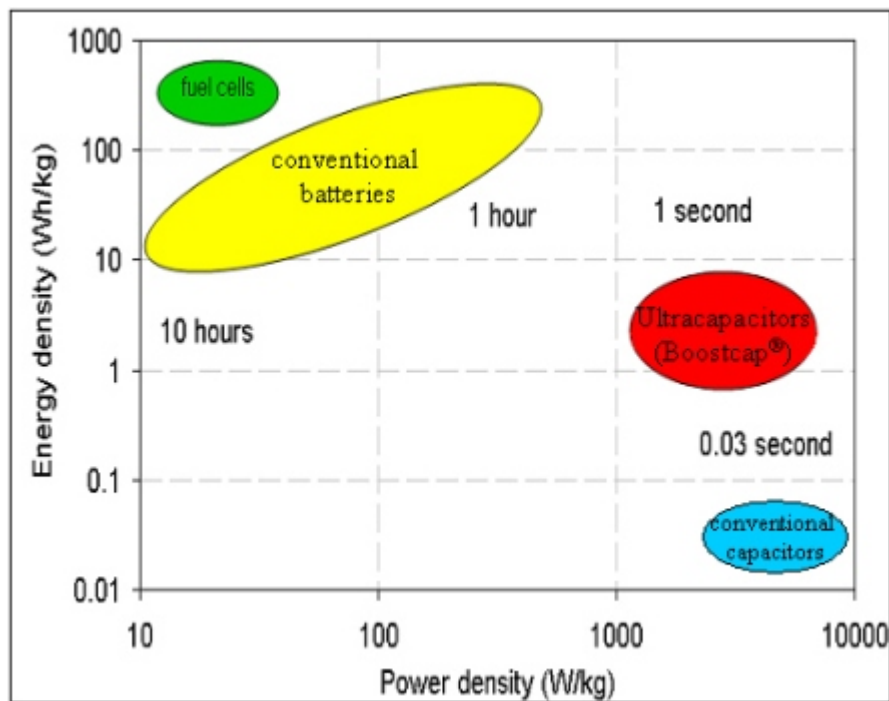


Figure 9.42: Energy density of ultra-capacitors [17]

By using ultra-capacitors in conjunction with bio-fuels or fuel cells, will reduce dynamic loads on either batteries or fuel cell subsystems. Thus using ultra-capacitors in combination with either batteries or fuel cell, increases their durability while the vehicle performance is enhanced. Figure 9.43 indicates how ultra-capacitors can be used to smooth power demand from the primary energy sources while also restoring energy upon vehicle deceleration. The net change in battery current when ultra-capacitor is used combination with battery is illustrated in Figure 9.44.

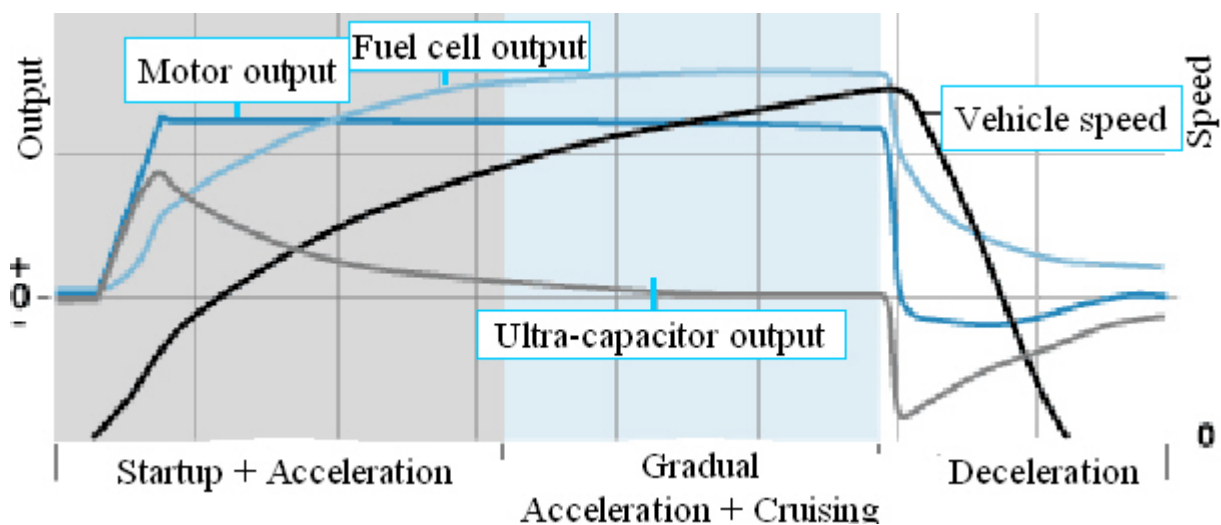


Figure 9.43: Power demand - combined usage of ultra-capacitor and another energy source [47]

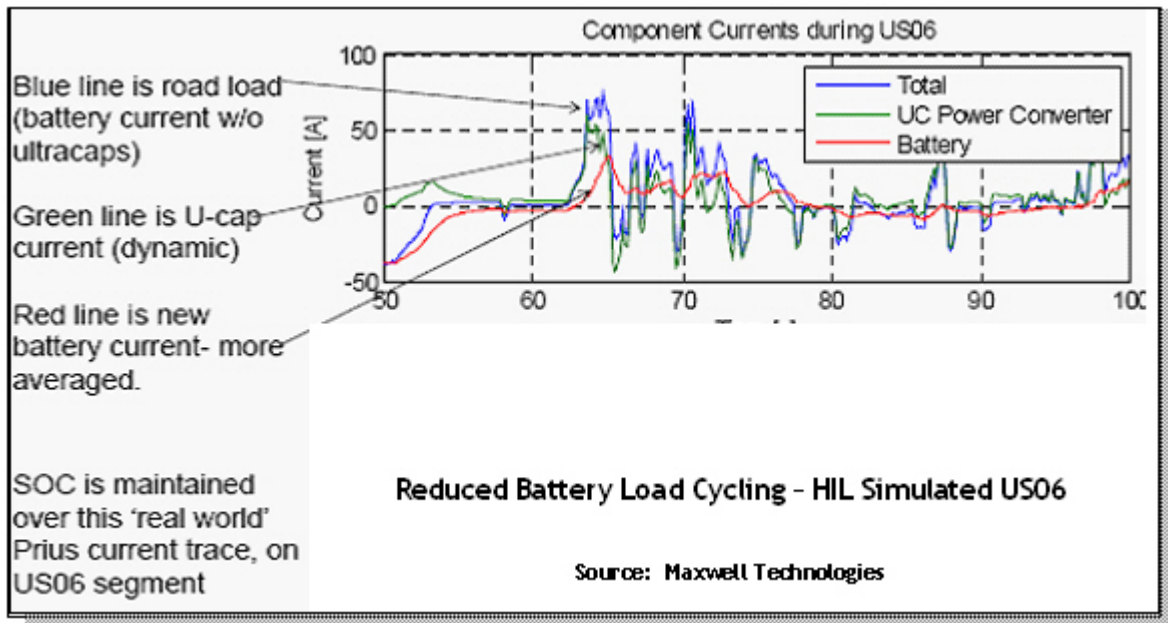


Figure 9.44: Current Vs time: net change in battery current

9.4.3 Performance Industry Targets

Figure 9.45 shows the current status of technology and the US Department of Energy (DOE) targets, which often represent a challenge to the established industry manufacturers.

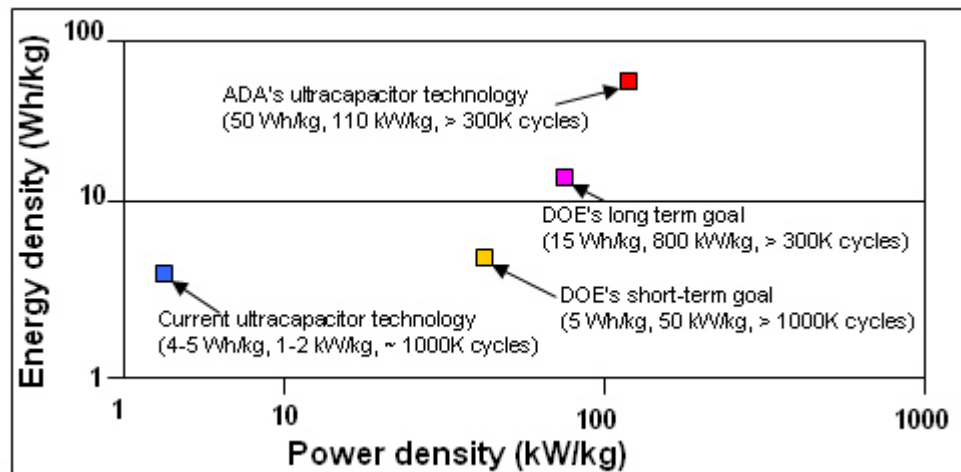


Figure 9.45: Current technology status and the US Department of Energy targets [62]

9.4.4 Packaging

The packaging of ultra-capacitors is similar to that in battery packs, where the cylindrical cells are arranged for high packaging density, while allowing cooling air to pass through the assembly. A typical ultra-capacitor packaging is shown in Figure 9.46. Protection of high-voltage components and control electronics need to be integrated.

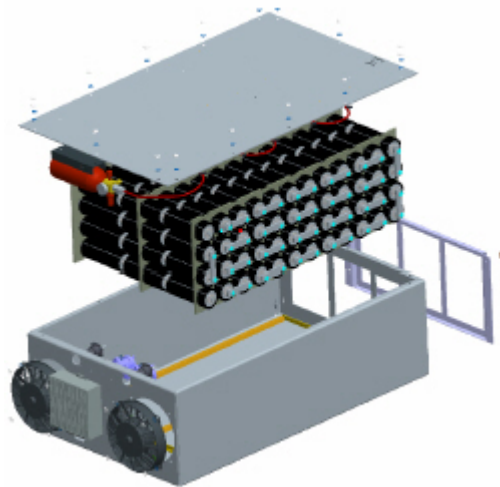


Figure 9.46: *Ultra-Capacitor packaging sample*

9.4.5 Advantages

Following are the advantages of ultra-capacitor technology:

- Capacitors deliver millions of cycles before failure, versus
 - Ni-MH batteries (10,000 cycles)
 - Lead acid batteries (1,000 cycles)
- 100% cold capacity (<-30 °C)
- Rapid charge/discharge for regenerative braking
- Can help reduce stress on battery packs
- 10x more specific power (W/kg) at very high voltages
- 10-20x more power delivery than lead-acid batteries
- "Green" technology , longer economic life than batteries when combined with an internal combustions engine

9.4.6 Disadvantages

Following are the disadvantages of ultra-capacitor technology:

- Energy stored per unit weight is considerably lower than that of a battery (see Figure 9.42)

9.4 Ultra-Capacitor Technology

- During discharge an ultra-capacitor will tend to fall below a given threshold voltage quicker than its battery counterpart. A DC-DC converter can be used to stabilize the voltage output, but leads to an additional weight, more complexity and reduced efficiency.
- Energy storage cost increase in combination with batteries
- Increased complexity & cost of power electronics
- Increased complexity in "state of charge" calculations
- Low-cost large volume manufacturing development is required

9.4.7 Future Trends (2015-2020)

Quantum technologies looked into two possible scenarios for future applications of ultra-capacitor technology, one being the ultra-capacitor as a primary energy storage, and the other being the ultra-capacitor as a secondary energy storage.

9.4.7.1 Ultra-Capacitors as Primary Storage

The following limitations have led to discontinuation of ultra-capacitors as the primary energy storage device in EVs and HEVs:

- Linear discharge voltage characteristic prevents use of all the available energy in some applications.
- Power only available for a very short duration.
- Low capacity.
- Low energy density. (6Wh/Kg)
- Cell balancing required for series chains.
- High self discharge rate. Much higher than batteries.

9.4.7.2 Ultra-Capacitors as Secondary Energy Storage: With Batteries

Even though ultra-capacitors are not preferred as the primary power source for EV and HEV applications, their advantages make them suitable for storing the energy from regenerative braking and for providing a booster charge in response to sudden power demands, in the applications such as:

- In specialty applications with frequent stop-and-go operation such as Mail delivery vehicles, city buses
- As supplement to battery packs to handle peak charge and discharge loads
- To extend battery life at reasonable weight impact
- To support and to optimize regenerative braking energy recovery

It should be noted however that while ultra-capacitors can be used as a secondary energy storage device, it is at the cost of considerable added weight and bulk of the system. Further, there is also additional complexity and costs due to the controls required to manage the two sources of energy.

9.4.8 Recommendations

Energy density is the most important required improvement for future success of ultra-capacitors. Currently, ultra-capacitors are not yet compact and light enough to be a practical universal replacement for batteries.

The costs of the ultra-capacitor and the required complex control mechanisms are the other hurdles to be overcome before adoption of ultra-capacitors as the energy storage solution for the FSV.

Due to the added cost, complexity, and the limited energy storage capability ultra-capacitors are not well suited for the FSV program. The emphasis of FSV program is on substantial electric only driving range (for all but the fuel cell vehicle powertrain variant). It is recommended to rely on battery packs for the primary energy storage alone and avoid weight/cost penalties by adding the ultra-capacitors to the design concept.

9.5 Internal Combustion Engine Technology

9.5.1 Overview

Internal Combustion Engine (ICE) technology is a very mature technology and well understood technology. The current fuels of choice for the light-duty vehicle market are gasoline and diesel, used with their respective engine types (Otto and Diesel cycle).

Following are some of the currently available advanced gasoline technologies:

- Atkinson cycle
- Direct injection
- Variable valve timing
- Turbo-charging
- Variable displacement

Some of the currently available diesel technologies are the following:

- Turbo-charging
- Selective Catalytic Reduction (SCR)

9.5.1.1 Recommendations for FSV

The internal combustion engine recommendations for Future Steel Vehicle program were based on the conclusions drawn from the technology assessment.

There is an increased engine thermal efficiency in an Atkinson cycle. However, it was not recommended for the FSV program because a bigger and heavier engine is required to produce the same power as that produced in an Otto cycle. Similarly, diesel engine was not recommended for the FSV program due to the cost and weight disadvantages.

Direct injection engines have significant advantages in fuel consumption, and a higher specific power output as compared to conventional engines. Direct injection engine technology is recommended for the FSV program.

The other gasoline engine technologies such as variable displacement, variable valve timing etc., result in improved engine power density and fuel economy efficiencies. However, there is an increase in power demand from the engine controller processor, due to these advancements, and there is a need for more sensors and more sophisticated engine control strategies. Therefore, these technologies were not considered due to the subsequent cost penalty of more sophisticated control electronics. The recommendations are summarized in Figure 9.47

	Unit	PHEV ₂₀	PHEV ₄₀
Fuel Type		Gasoline	Gasoline
Cycle		4-Stroke	4-Stroke
Fuel Injection		Direct	Direct
Aspiration		Natural	Natural
Displacement	L	1.0	1.4
Cylinders		3	4
Max Power	kW	50	70
Max Torque	Nm	90	125
Max Efficiency	%	36	36
Max Efficiency Range	kW	11 – 25	15 – 35
Specific Cost	\$/kW	21	21
Specific Power	kW/kg	0.59	0.59
Displacement Specific Power	kW/L	50	50
Physical Volume	L	53	74

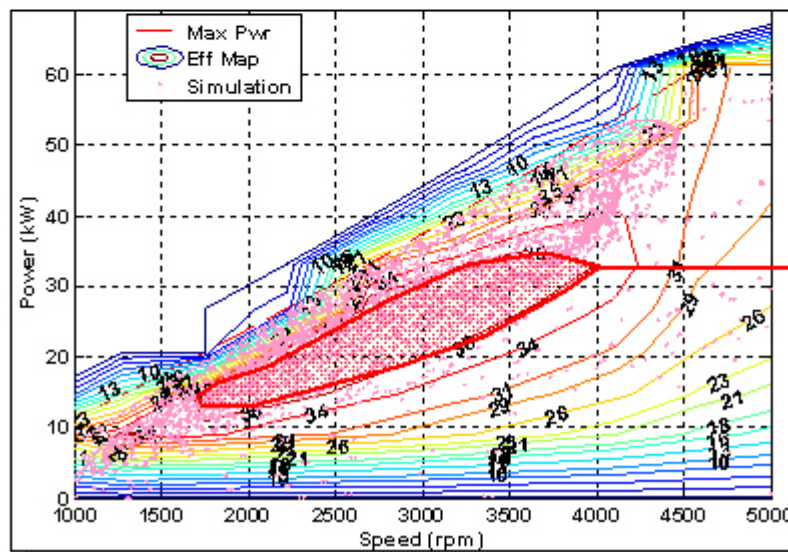


Figure 9.47: Internal combustion engine recommendations - PHEV₂₀ and PHEV₄₀

9.5.2 Gasoline Engine

Today, internal combustion engines in light-duty motor vehicles most commonly use the conventional "Otto" cycle. The four strokes of the Otto cycle are intake, compression, ignition, and exhaust as shown in Figure 9.48.

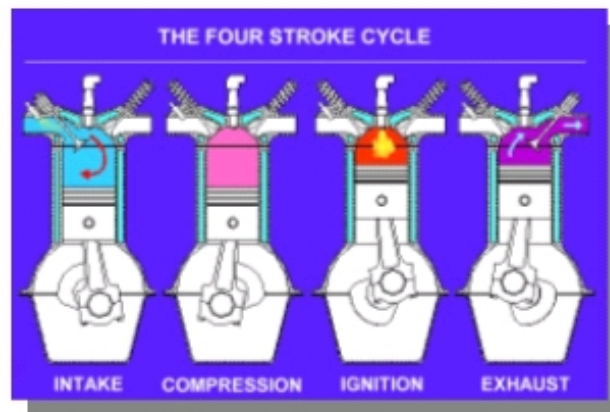


Figure 9.48: The four stroke cycle

9.5.2.1 Atkinson Cycle

The Atkinson cycle works on the same basic principle as the Otto cycle, with spark ignition of a compressed fuel/air mixture in the cylinder. However, in the Atkinson cycle the intake valves are left open during part of the compression stroke, effectively lowering the volumetric compression ratio. This makes it possible for a greater expansion ratio for a given compression ratio. The greater expansion ratio allows a higher efficiency as it extracts more of the heat energy from the combustion. The drawback is that it takes a larger engine to produce an equivalent amount of power, increasing the weight of the engine.

9.5.2.2 Direct Injection Gasoline Engine

In the direct injection engine, each cylinder receives fuel directly injected into the combustion chamber, combined with high pressure (>120 bar) fuel delivery. Therefore, the fuel delivery is more precise, and the liquid fuel evaporates directly in the cylinder during the compression stroke. The evaporation cools the fuel/air mixture resulting in a greater compression ratio without auto-ignition (knock). The greater compression ratios allow for greater expansion ratios, thus improving engine efficiency.

There is a 10% improvement in specific power, and a 20% improvement in fuel economy with direct injection technology, in comparison to conventional engine technology.

9.5.2.3 Variable Valve Timing

Camshaft phasing can be used to vary the amount and duration of valve lift on the intake and exhaust valves. This allows an engine to expand its torque and efficiency range. Hence, the variable valve timing technology improves torque and efficiency over a broader engine RPM range, and allows higher power output by improving torque at higher engine speeds.

9.5.2.4 Turbocharging

The turbocharging technology improves specific power 40%, depending on boost levels. When combined with direct injection, turbo-charging yields significant efficiency improvements. However, turbocharger components are costly to add to naturally aspirated engines. Further to cost, turbochargers require numerous additional systems to prevent damage to an engine, due to the increased stress and heat generated.

9.5.2.5 Variable Displacement

Variable displacement technology either isolates cylinders completely or changes the length of the compression stroke to accommodate various engine loads. This allows the engine to operate closer to its peak efficiency zone under a larger range of loads.

Even though variable displacement technology improves part load efficiency, the disadvantage of this technology is the added mechanical complexity.

9.5.3 Diesel Engine

The diesel engine is a compression ignition cycle where the fuel is injected into the combustion chamber and the heat of compression is sufficient to ignite the fuel/air mixture. Unlike gasoline, diesel generates enough heat when completely compressed to ignite itself and hence diesel engines do not require a spark plug. The compression pressure is directly related to the combustion as well. Diesel engines have a much higher compression pressure than gasoline engines. The higher compression pressure in diesels explains the difference in the methods of ignition used in gasoline and diesel engines. The reason for this higher pressure is that in a diesel engine, only air is compressed. The fuel is then directly injected into the cylinder by the high compression pressure, where the heat generated ignites the air/fuel mixture.

The efficiency of the diesel cycle is higher than the gasoline cycle because of the higher compression ratio and the higher temperature of combustion in a diesel engine. Therefore, the heat input in a diesel engine is at a higher average temperature. A gasoline engine cannot have the same compression ratio as a diesel engine, because fuel and air are mixed before they reach the cylinder, and they would explode before the piston reached the correct firing position, causing the engine to “knock” and not exploit the most efficient use of energy. Hence, a diesel engine is more cycle efficient than a gasoline engine.

Since the compression and expansion ratios of diesel engines are greater than that attained by gasoline engines, they are more thermally efficient and therefore generally have lower fuel consumption for a given power output than a gasoline engine. Diesel engines operate under lean (more air than necessary for combustion) conditions and therefore have a lower specific power output (kW/l) than gasoline engines, but a higher torque output (kNm), at a low RPM range, due to the high compression ratio.

However, the much higher compression ratio means diesel engines have to be heavier and more robust. Diesel engines are more expensive to build than gasoline engines.

9.5.3.1 Turbo-charging

Most diesel engines today and in the foreseeable future will be turbocharged. This allows a greater specific power output. Turbo-charging improves specific power $\sim 40\%$, depending on the boost level.

9.5.3.2 Selective Catalytic Reduction (SCR)

Since diesel engines do not pre-mix the fuel/air charge prior to combustion, the small fuel droplets injected into the combustion chamber burn locally at close to a stoichiometric ratio, causing local hot-combustion reactions. This stoichiometric combustion causes high NO_x levels in diesel exhaust. To make matters worse, the three-way catalysts used extensively on gasoline engines are only effective at removing NO_x at near zero excess oxygen levels in the exhaust. As

a diesel runs at a lean operating condition, the exhaust leaving the engine contains a lot of excess oxygen, making the destruction of NO_x very difficult.

Selective Catalytic Reduction (SCR) technology has been used for decades on large stationary power plants to remove excess NO_x from their exhaust stacks in the presence of excess oxygen. It injects small amounts of ammonia into the exhaust stream in the presence of a catalyst. The ammonia reacts with NO_x on the catalyst surface and reduces it to nitrogen gas and other harmless products. Up until a few years ago, this technology has been large, heavy, and expensive. Recently, SCR technology has been scaled down to fit on-board vehicles and has proven effective in allowing diesel engines to meet stringent emission standards when combined with particulate traps.

9.5.4 Future Trends

The following engine technologies are expected to be implemented by the year 2015:

- Vehicle weight and size reduction trend pushes engine designs towards smaller displacement, fewer cylinders and in-line configuration (to overcome packaging and NVH issues)
- Aggressive gasoline direct injection deployment anticipated due to emissions and fuel savings benefits
- Direct injection technology will likely displace Atkinson cycle technology achieving the same efficiency improvements without the size and weight penalty
- The anticipated power demand for plug-in hybrid vehicles is 80-110 kW for large volume production passenger cars
- Advanced technology will roll into lower price vehicles, but the cost balance between engine vs. hybrid technologies must be considered to preserve consumer acceptable vehicle price levels
- Variable valve timing technology will find broader implementation as the cost and weight penalties will decrease with increase in manufacturing volumes
- Hybrid and plug-in hybrid vehicles may trend away from variable valve timing, variable displacement, and high strength components as they have a limited speed range of operation and hybrid powertrain variants can be tuned to operate in a narrow efficiency band without the added cost of these technologies
- Continued efforts to optimize auxiliary systems power demand (AC, alternator, pumps etc.)
- Diesel engine cost penalty (two to three times) and their heavier weight makes it increasingly difficult to justify with increasing diesel fuel cost. Combination with hybrid powertrains is technically feasible, but commercial benefits may not justify implementation
- Variable geometry turbo deployment for performance vehicle technology may be difficult to package in smaller and mid-size cars along with hybrid technology, because of the potential for overheating issues with hybrid components

The following engine technologies are expected to be implemented by the year 2020:

- Based on current market share, vehicle down sizing trends will be regional with high potential in North America, medium potential in Europe and limited potential in Asia
- Homogeneous Charge Compression Ignition (HCCI) is expected to be introduced at moderate volumes

9.5.5 Alternative Energy Sources

The current fuels of choice for the light-duty vehicles are gasoline and diesel. However, with increase in the costs and dependency of oil based transportation fuels, and the environmental demands for lower CO₂ and other green-house-gas emissions, there is growing pressure to find viable fuel alternatives. Some of the potential alternative fuels that may be used in the future are:

- Natural gas
- Ethanol
- Propane (LPG)
- Bio-diesel
- Hydrogen

Each alternative fuel has its own challenges. Ethanol and bio-diesel are energy intensive to produce using state-of-the-art technologies. Hydrogen is energy intensive to generate from water or comes from fossil fuel sources. Propane and natural gas are both fossil fuels and it is debatable if there are any advantages to using these fuels over standard gasoline and/or diesel. Natural gas and hydrogen have storage challenges as each exists in a gaseous state under standard conditions and require expensive high-pressure tanks or cryogenic storage on the vehicle. These alternative fuels will likely have niche markets but is unlikely that any of them will have enough benefits to displace traditional gasoline or diesel fuel.

To use propane in vehicles, it is mixed with butane to produce Liquid-Petroleum-Gas (LPG). The advantage of LPG is that it is non-toxic, non-corrosive and free of tetra-ethyl lead or any additives. LPG also has a high octane rating (108 RON). LPG burns more cleanly than gasoline or diesel and is free of particulates. However LPG has limited availability and a lower energy density than either petrol or diesel, so the equivalent fuel consumption is higher.

Natural gas for use in vehicles is available as either “Compressed-Natural-Gas” (CNG) or “Liquefied-Natural-Gas” (LNG). The advantages of “CNG/LNG” include 60-90% less smog-producing pollutants, 30-40% less CO₂ and green-house-gas emissions as compared to gasoline, and is also less expensive to produce than gasoline. Similar to the use of LPG, there is a limited availability of CNG/LNG. The fuel consumption of vehicles using CNG/LNG is higher than that using gasoline/diesel or the other alternative fueled vehicles.

9.5.5.1 Bio-Fuels

Among the potential alternative energy sources, bio-fuel is becoming the preferred alternative. Unlike fossil fuels which are mined from the ground and refined into a liquid fuel or burned as a heat source, bio-fuel is any gas or liquid fuel which is manufactured from plant material (biomass) or their metabolic by-products, such as sugars.

Bio-fuel can generally be classified as: first, second or third generation bio-fuels.

- First generation fuels refer to bio-fuels made using food crops, from sugars and starches, vegetable oils and animal fats
- Second generation fuels are bio-fuels made using food crop waste, non-food crops, and is typically called "cellulosic bio-fuel"
- Third generation fuels are bio-fuels from algae, typically known as "algae fuel" or "oilgae"

The most commonly used bio-Fuels in the automotive industry belong to the first generation family. First generation bio-fuels are: Vegetable oils, bio-diesel, bio-Gas, solid bio-fuels, syngas and bio-alcohols such as: Ethanol, methanol, propanol, butanol and bio-butanol. The most popular bio-fuels used for transport needs are bio-diesel and Ethanol. In Europe more bio-diesel is used compared to ethanol in the USA.

US fuel consumption ratio (ethanol/bio-diesel) is 97.77/2.33% in favor of ethanol. This compares to ethanol/bio-diesel consumption ratio for the EU of 18.5 / 81.5% in favor of bio-diesel.

Member states in the European Union have jointly agreed to increase the amount of bio-fuel used for transportation by 10% by 2020. The USA is expected to increase the amount of bio-fuel used for transportation by 7.6% by 2030.

The projected increase in bio-fuel for transport needs in USA and European Commission is shown in Figure 9.49

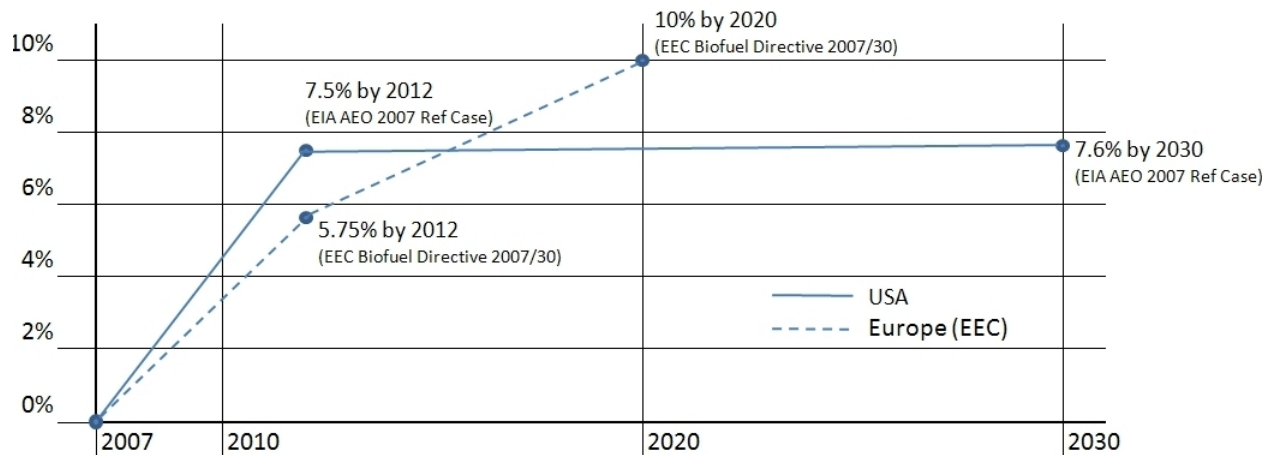


Figure 9.49: Projected increase of bio-Fuel in transport (USA and EC)

9.5.5.2 Ethanol



Ethanol using current production methods is a "first generation" bio-fuel that can be made from wide range of agricultural feedstock. Ethanol is typically manufactured from plants such as sugar cane, sugar beets, switch grass, corn, wheat and other biomass crops. Ethanol from corn, switch grass, wheat and other biomass crops are know as a "second generation" bio-fuel.

Ethanol is produced by the fermentation of sugars or by the hydration of ethylene from a petroleum based source. Today, the main focus is on using a pure "bio" process using starch and sugars from wide variety of crops.

E85 is a high-octane clean burning ethanol fuel that is a blend of 85% ethanol and 15% gasoline. Although E10, (10% ethanol / 90% gasoline), is available for vehicle use, E85 has now become the industry norm for an ethanol based fuel in the EU and US. Due to condensation "drops" of water in the fuel system, that will interrupt fuel flow, when using an ethanol-gasoline fuel mix, the fuel must exist in a "single phase". To eliminate engine stall, the fraction of water that an ethanol-gasoline fuel mix can contain without phase separation increases with the percentage of ethanol. Phase separation will not occur if the ethanol content is above 71%.

9.5.5.3 Ethanol Energy Balance

Energy balance is defined as the amount of energy it takes to produce fuel compared to the amount of energy that is created at the end of the manufacturing process. All biomass fuels go through a similar production process with one exception:

Growth → Harvest → Transport → Processing → Transport to the end user

The main difference is in the efficiency of the process related to the biomass used to produce ethanol. As shown in Table 9.14, it takes one unit of fossil fuel to produce 1.3 units of ethanol in the United States. The production of ethanol using sugar cane is more efficient than corn due to the energy content of sugar cane.

Country	Fuel Type	Energy Balance
USA	Corn Ethanol	1.3
Brazil	Sugar Cane Ethanol	8
Germany	Bio-Diesel	2.5

Table 9.14: *Energy balance table*

9.5.5.4 Ethanol Emissions

Calculating the CO₂ emissions from ethanol is far more complex than that from gasoline due to the method of production used to manufacture the fuel. When calculating the amount of CO₂ produced, one must consider the following variables:

- The CO₂ of growing the feedstock ^[1]
- The CO₂ produced by transporting the feedstock to the factory
- The CO₂ produced by processing the feedstock into ethanol
- The impact cost of the change in land use of the area where the fuel feedstock is grown
- The CO₂ produced by transportation of ethanol from the processing plant to its point of use
- The efficiency of ethanol compared with standard gasoline
- The amount of CO₂ produced at the tail pipe
- The benefits due to the production of useful by-products, such as cattle feed or electricity

CO₂ Released - Ethanol Production

Figure 9.50 shows the CO₂ released from the production of ethanol.

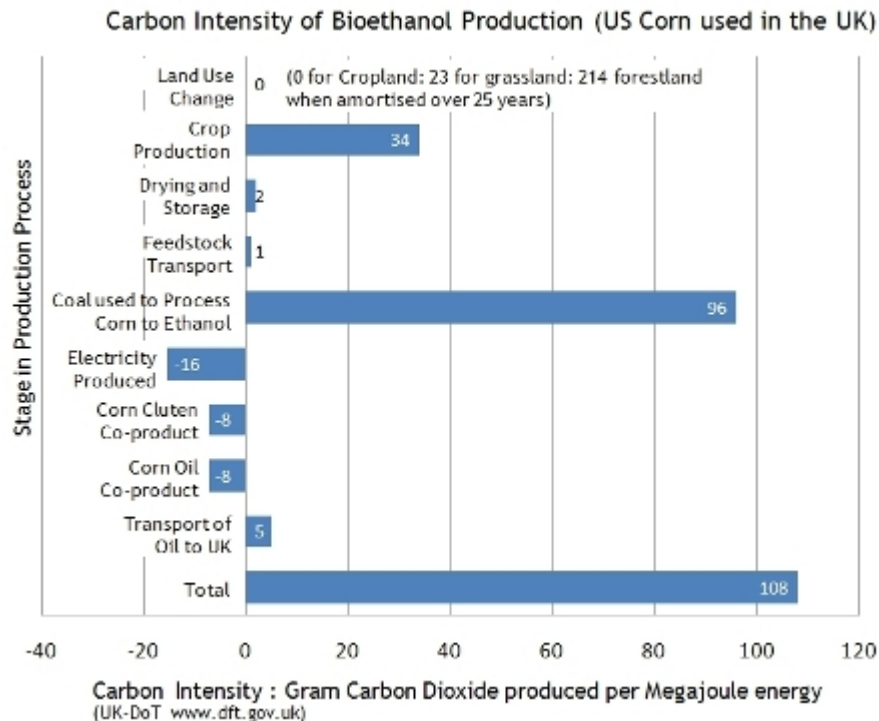


Figure 9.50: CO₂ released during ethanol production

¹Feedstock is defined as the required raw material substance used in a production process. In this case the feedstock is the raw material produced from the fermentation of cells to create ethanol.

CO₂ released - Different Feed stocks vs. Fossil fuels

Figure 9.51 shows the amount of released CO₂ from various bio-fuel feedstocks compared to that of fossil fuels (this is for production only and does not include the transport from the production facility to the pump or end user). It can be seen that the amount of CO₂ released depends on the feedstock used for production.

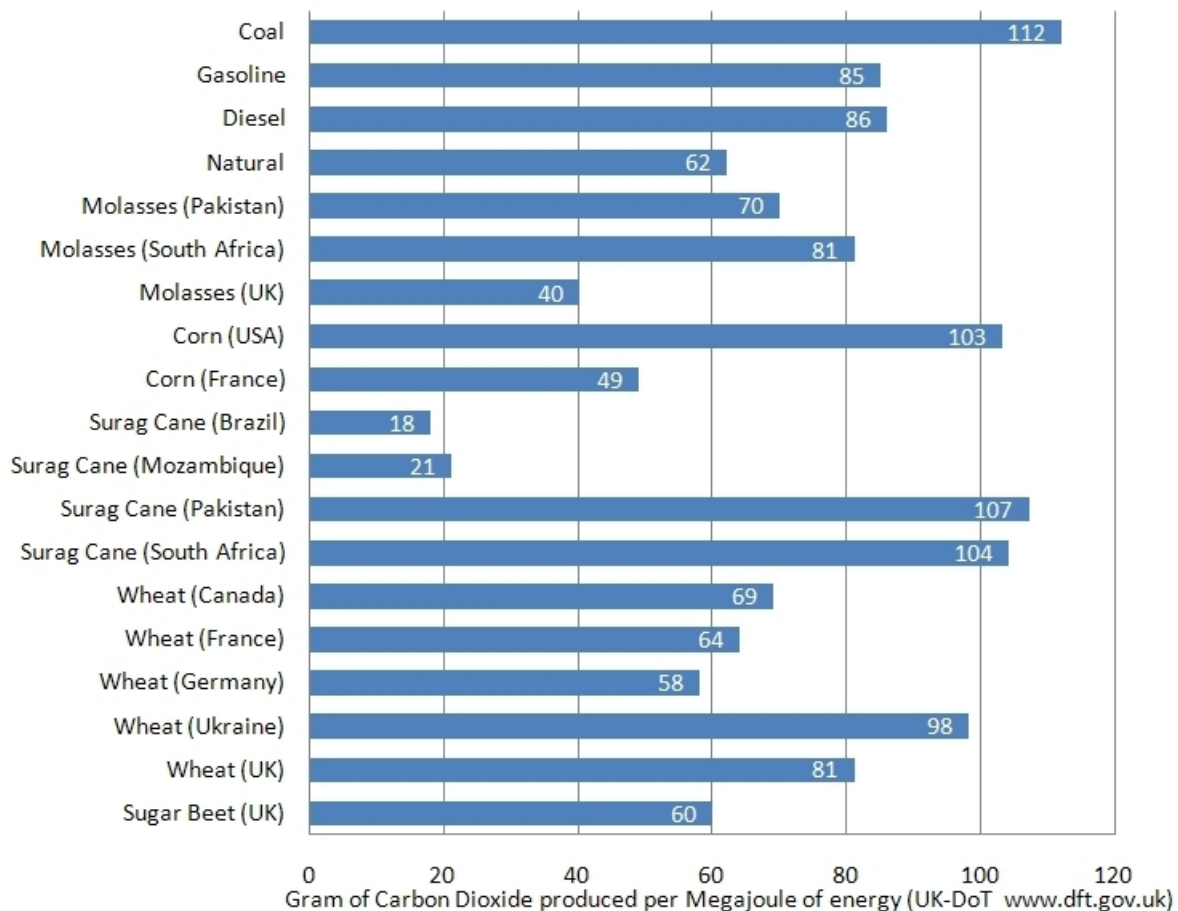


Figure 9.51: CO₂ released, bio-fuel feedstocks vs. fossil fuels

9.5.5.5 Advantages of Ethanol

- Engine efficiency
 - Ethanol is a high-octane fuel that can boost engine efficiency and performance
- Environmental
 - Renewable fuel helps to reduce the emissions of the end user. In some cases the production of ethanol from feedstocks result in a higher CO₂ emission than for gasoline Table 9.51. But the end result when we consider "Well-to-Wheel" results in an overall reduction compared to a vehicle using only gasoline.
- Energy security
 - Helps to reduce the dependency on fossil-based resources, OPEC and other oil exporting nations
- Low production costs
 - Ethanol is cost effective due to low productions cost. This tends to outweigh the fuel consumption penalty. It is possible to produce one gallon of ethanol for under USD \$1.00[15]. However this cost is dependent on possible future increases in feed stock costs, related to the competition for land for the growing of food stocks as the world population increases.
- Economy
 - Provides a economic boost to rural areas
- Feedstock availability
 - Ethanol can be produced from a number of different feedstocks
- Ethanol by-products
 - An ethanol by-product when using corn as a feedstock is "distillers grain" a valuable, high in protein animal feed stock. The sale of this by-product is used to offset the production costs of ethanol.

9.5.5.6 Disadvantages of Ethanol

- Fuel mix
 - Still needs to be mixed with some oil based products. Example, E10 (10% ethanol, 90% gasoline) & E85 (85% ethanol 15% gasoline)
- Fuel consumption

- Ethanol fueled vehicles have a higher fuel consumption (due to the fact that Ethanol contains approximately 34% less energy per unit volume than gasoline)
- Engine -
 - Ethanol based fuels cannot run in a vehicle without component modifications due to the corrosive nature of ethanol
- Emission transfer
 - Although ethanol based fuels are practically emission free at the tail pipe, there is a CO₂ and other greenhouse gas penalties due to feedstock processing and ethanol production (Table 9.51 and Table 9.50)
- Environmental
 - Large areas of land are being cleared for fuel-based crops resulting in the destruction of natural habitats, and a reduction in bio-diversity, this also results in a CO₂ absorption imbalance at the biomass level
- Food vs. fuel
 - As the demand for ethanol increases, more land is being replaced from food crops to fuel crops. This results in less food being available and higher food costs, and also effecting the cost of available feedstocks for the production of ethanol. This is a concern in industrialized nations, but of a greater concern to developing nations where the pressure for food is the greatest.

9.5.5.7 Conclusion

- Ethanol based fuel is energy efficient as indicated by its 1.3 to 8 energy balance, due to using different feedstocks
- In producing ethanol many different feedstocks can be used
- Ethanol reduces the dependency of fossil fuel (Gasoline)
- An ethanol by-product when produced from corn is called "distiller's grain" which is a high protein animal feed that yields more protein than generated from 1 acre/4,046 m² of soybean
- The production of ethanol needs to be carefully monitored in relationship to environmental issues (CO₂ & green house gases), change in land usage, food to fuel crops, loss of habitat and bio diversity, and the rise in food costs and the impact on developing nations

9.6 Transmission and Transaxle

9.6.1 Overview

For the purpose of the Future Steel Vehicle, only key highlights of the status of automotive transmission technology shall be discussed, as this technology is considered to continue to evolve only incrementally over the 2010 to 2020 time frame. Absolute efficiency gains are minimal compared to those gained from other technologies.

9.6.1.1 Transmission Types

Transmission types most frequently used and therefore discussed for the use in the Future Steel Vehicle are the following:

- Continuously Variable (CVT)
- Dual Clutch (DCT)
- 6-8 speed automatic transmission

Following are the key highlights of current automotive transmission technology:

- CVT transmissions are already produced in millions of units per year for small and large car applications
- Mechanical transmissions can be greater than 97% efficient
- Dual clutch and automatic planetary (6, 7, 8 speed) transmissions are gaining market share due to higher fuel efficiency, torque handling capability and driver comfort
- Transmission weight, size and cost must be considered when optimizing vehicle performance and efficiency

9.6.1.2 Recommendations for FSV

Based on the technology assessment, the different transmission types were compared based on the key attributes, namely: speed, performance, efficiency, durability, cost, as shown in Table 9.15.

Transmission Type	Speeds	Performance	Efficiency	Durability	Cost
Manual	4 - 5	+	++	+	+
Automatic Hydraulic	3 - 5	0	-	0	0
Automatic Planetary	6 - 8	+	++	+	-
Dual Clutch	6	+	++	+	-
Continuously Variable	- / -	+	+	+	+
(+) Good (0) Average (-) Poor					

Table 9.15: *Transmission comparison*

Considering performance, weight, cost and packaging attributes, the integrated traction drive concept offers the best compromise for the Future Steel Vehicle. The integrated traction concept is shown in Figure 9.52 [48]. By motor internal scaling and with different gear reductions it will be possible to support a modular powertrain design concept and thus reducing development and potential tooling cost at the same time. Engine PSAT simulations have shown that all FSV variants equipped with a single speed gear reduction integrated with the traction motor and differential are capable of achieving fuel economy and emissions targets while reducing overall vehicle weight, cost and complexity. Therefore, a multi-speed gear reduction is not proposed for the FSV program Phases 2 and 3.



Figure 9.52: *Integrated traction drive concept*

9.6.2 Continuously Variable Transmission (CVT)

9.6.2.1 Current applications

- Nissan, Audi, and others

9.6.2.2 Function

- Chain Drive CVT - Chain drive between variable diameter pulleys
- Toroidal CVT - Rollers between concave discs transmit torque at varying speed
- Electronically controlled transmission ratios for performance optimization and fuel economy

Figure 9.53 shows an example of a continuously variable transmission:

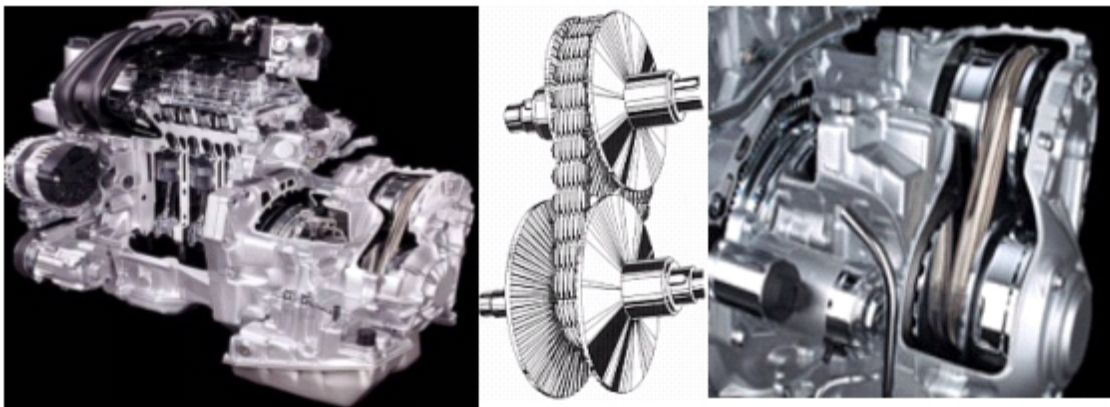


Figure 9.53: Chain drive CVT

9.6.2.3 Durability

- OEM validated for numerous passenger car applications in Asia, Europe and North America

9.6.2.4 Advantages

- Allows engine operation at peak fuel efficiency level
- Operates smoothly and quiet
- Low maintenance
- Packaging size fits in smaller cars

9.6.3 Dual Clutch Transmission (DCT)

9.6.3.1 Current applications

- Porsche, Nissan, BMW, Mercedes Benz, Lexus, and others

9.6.3.2 Function

- Multiple gear sets on two separate drive shaft sets
- Alternate engagement of two hydraulic clutches provide gear ratios
- Electronically controlled transmission shifting for optimization of performance and fuel economy

A sample dual clutch transmission is shown in Figure 9.54.



Figure 9.54: *Dual clutch transmission (DCT)*

9.6.3.3 Durability

- OEM validated for passenger car applications in Asia, Europe and North America

9.6.3.4 Advantages

- Designed for high powered internal combustion engine powertrain

9.6 Transmission and Transaxle

- Allows engine to run close to peak fuel efficiency in many operation conditions
- Helps increase of fuel efficiency while reducing CO₂ emissions
- Durability proven in multiple OEM validations and vehicle deployments

9.6.3.5 Challenges

- Added size, weight, cost and complexity for hybrids

9.6.4 6 - 8 Speed Automatic Transmission

9.6.4.1 Current applications

- BMW, Mercedes Benz, Lexus, and others

9.6.4.2 Function

- Multiple planetary gear sets and hydraulic clutches provide gear ratios
- Electronically controlled transmission shifting for optimization of performance and fuel economy

9.6.4.3 Durability

- OEM validated for numerous passenger car applications in Asia, Europe and North America

Figure 9.55 shows an example of a 6-8 Speed transmission.

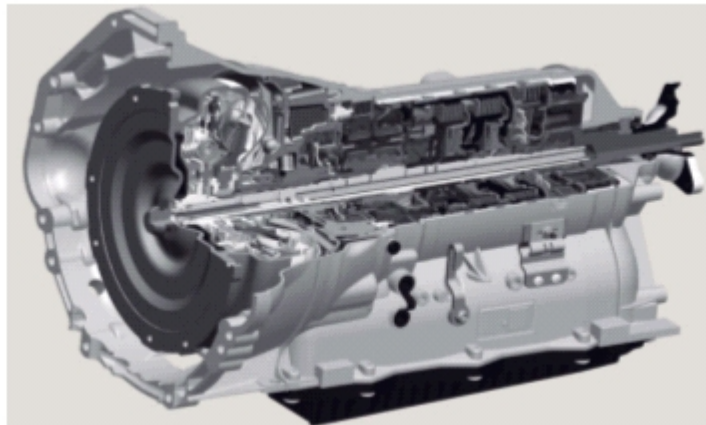


Figure 9.55: 6-8 speed transmission

9.6.4.4 Advantages

- Designed for a high power internal combustion engine powertrain
- Allows engine to run close to peak fuel efficiency in most driving conditions
- Helps increase of fuel efficiency while reducing CO₂ emissions
- Durability proven in multiple OEM validations and vehicle deployments
- Low maintenance

9.6.4.5 Challenges

- Added size and weight for hybrids
- Added complexity for hybrids
- Added costs

9.6.5 Future Trends

The future trends in the transmission technology expected by the years 2015-2020 are:

- Dual clutch and 6-8 speed automatic transmissions will displace manual and 3-5 speed automatic transmission in pure IC engine applications
- DCT and 6-8 Speed automatic integration in hybrids may be considered for high power applications such as larger cars and light trucks
- CVT package size and weight reduction can be expected in the range of 5 to 10%
- CVT efficiency improvements - 1 to 2% may be achieved
- Small light weight package of CVT is likely to be adopted in heavier duty hybrid vehicles, both for series and parallel-split configurations
- Heavy-duty applications including larger cars, trucks and SUVs will be equipped with dual-mode transmission / E-Motor combinations using an internal combustion engine as the primary power source. The dual-mode hybrid technology—developed with General Motors, BMW and Mercedes-Benz—incorporates two small electric motors into the four-speed automatic transmission. Enough power is generated by the electric motors to drive a vehicle in purely electric mode up to about 25 miles an hour.

9.6.6 High Voltage Generators and Traction Motors

To regulate speed and power, permanent magnets are electronically commutated to convert alternating electric current to direct current or vice versa, using variable voltage and variable frequency. The motor manufacturer ensures the generator and traction motors are a matched set and optimized for efficiency to their respective power inverters. Motors can also be integrated in the wheel hub to improve powertrain packaging or to integrate four-wheel-drive. Examples of wheel and traction motors can be seen in Figure 9.56.

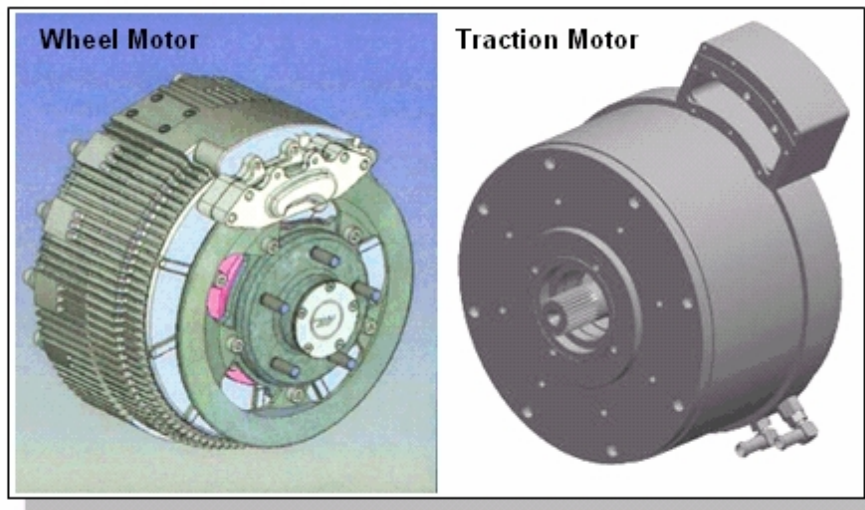


Figure 9.56: *Wheel and traction motor*

9.6.6.1 Design/Function Characteristics

High voltage generators/traction motors have the following characteristics:

- Permanent magnet type motor/generator drive systems
- Variable voltage and variable frequency electronics convert alternating electric current to direct current or vice versa (similar to an AC motor)
- Power electronics modulate voltage and frequency to control output power
- Highly efficient and reliable
- Generator operation for regenerative braking or engine operation in series hybrid
- Common input voltage range of 240-400 V
- Integration with transaxle and transmission unit possible
- Primary or secondary drive with wheel motors possible

9.6.6.2 Current applications

- Hybrid cars : Toyota Prius, Camry, GM Tahoe, Honda Accord, amongst others
- Electric cars : Tesla Roadster, GM Volt, Mitsubishi i-MiEV, amongst others

9.6.6.3 Recommendations Summary

Based on the technical assessment, the electric motor for the FSV program was recommended considering the following factors:

- Sized to provide maximum acceleration, grade ability, and top speed
- Peak efficiency is only available in a small operating space but technology is improving part load efficiencies
- Smaller motor is more efficient due to higher operating speed, but torque falls more rapidly as speed increases (electric motor efficiency is shown in Figure 9.58)

The recommendations are summarized in Table 9.16 and Table 9.17

	Units	Current	BEV	PHEV ₂₀	FCEV	PHEV ₄₀
Peak Power	kW	Varies	67	67	75	75
Continuous Power	kW	Varies	49	49	55	55
Max Torque	Nm	Varies	270	270	240	240
Max Efficiency	%	95	96	96	95	95
Specific Cost	\$/kW	40	26	26	26	26
Specific Power	kW/kg	1.2	1.63	1.63	1.63	1.63
Specific Power	kW/L	3.2	4.8	3.3	3.3	3.3
Physical Volume	L	Varies	14	14	23	23

Table 9.16: *Electric motor recommendations for FSV*

	Units	PHEV ₂₀	PHEV ₄₀
Peak Power	kW	65	70
Continuous Power	kW	50	63
Shaft Speed Range	rpm	1000 - 6000	1000 - 6000
Peak Shaft Torque	Nm	240	240
Weight	kg	40.6	45.5

Table 9.17: *Generator recommendations for FSV*

9.6.6.4 Performance

Traction motor and generator performance are typically rated in terms of both peak output power and continuous output power, both of which can vary significantly depending on manufacturer, size, and peak performance duration requirements.

Output power and weight ratings of some of the currently offered non-OEM motors are shown in Figure 9.57. Note that typically the peak power output is used in the motor designation, and continuous power frequently is only half of the rated peak power output. Due to heat dissipation from the motor internal components, water-cooling is utilized in many applications.

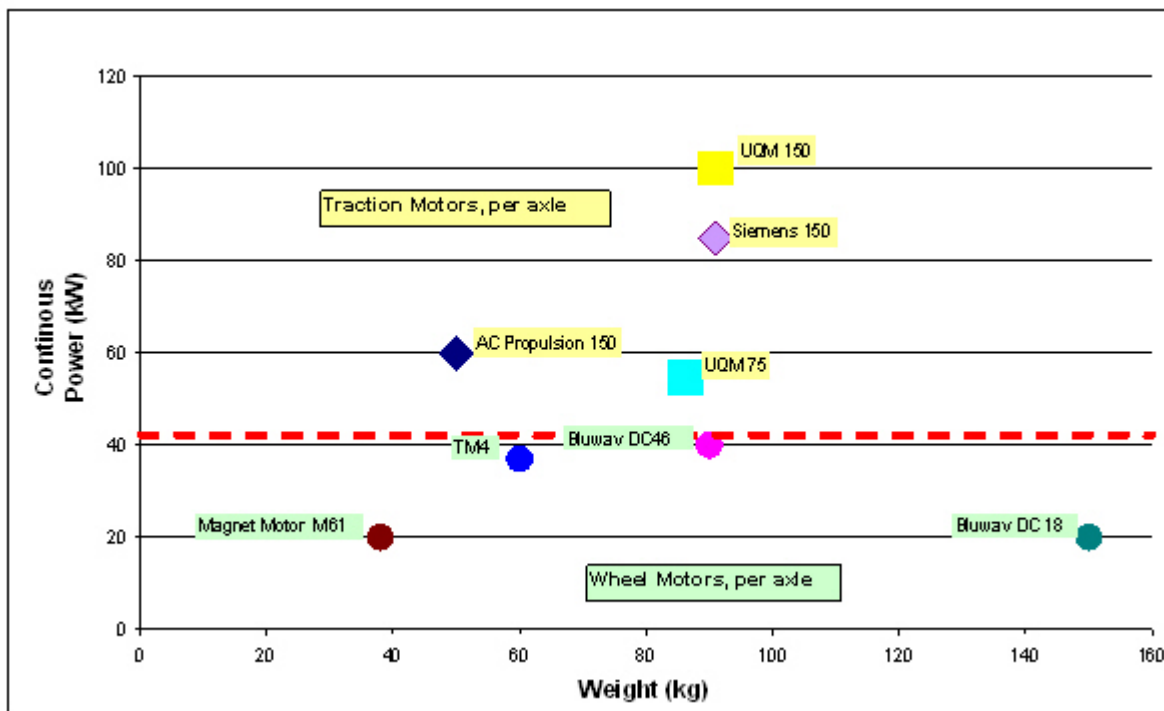


Figure 9.57: *Continuous power vs. weight*

9.6.6.5 Motor Efficiency

Electric motors transform more than 90% of energy input into propulsion, with respect to only 40%-50% for combustion engines. As illustrated in Figure 9.58, electric motors/generators are able to operate most efficiently in a narrow rpm range. Electric motor efficiency improvements are primarily extending the efficient operating range and power density. By focusing on magnet arrangement and coil designs, motor efficiency is optimized for the RPM operation range the unit will be spending most of its service life operating in. For larger speed ranges, multi-speed transmissions typically are used, especially if the motor is used as an auxiliary power supply in typical hybrid vehicle configurations. If the motor is required to provide full traction power, a single speed gear reduction may be sufficient.

Electric motors/generators are closely coupled with DC power inverter hardware and software for optimized performance, efficiency and electro-magnetic emission resistance. For power and speed regulation, permanent magnets are used to electronically commutate (converts alternating electric current to direct current or vice versa) using variable voltage and variable frequency.

Figure 9.58 shows a typical motor efficiency diagram. The graph illustrates the rpm ranges for normal driving conditions, in which a electric motor efficiently operates to make sufficient power available at various speed ranges.

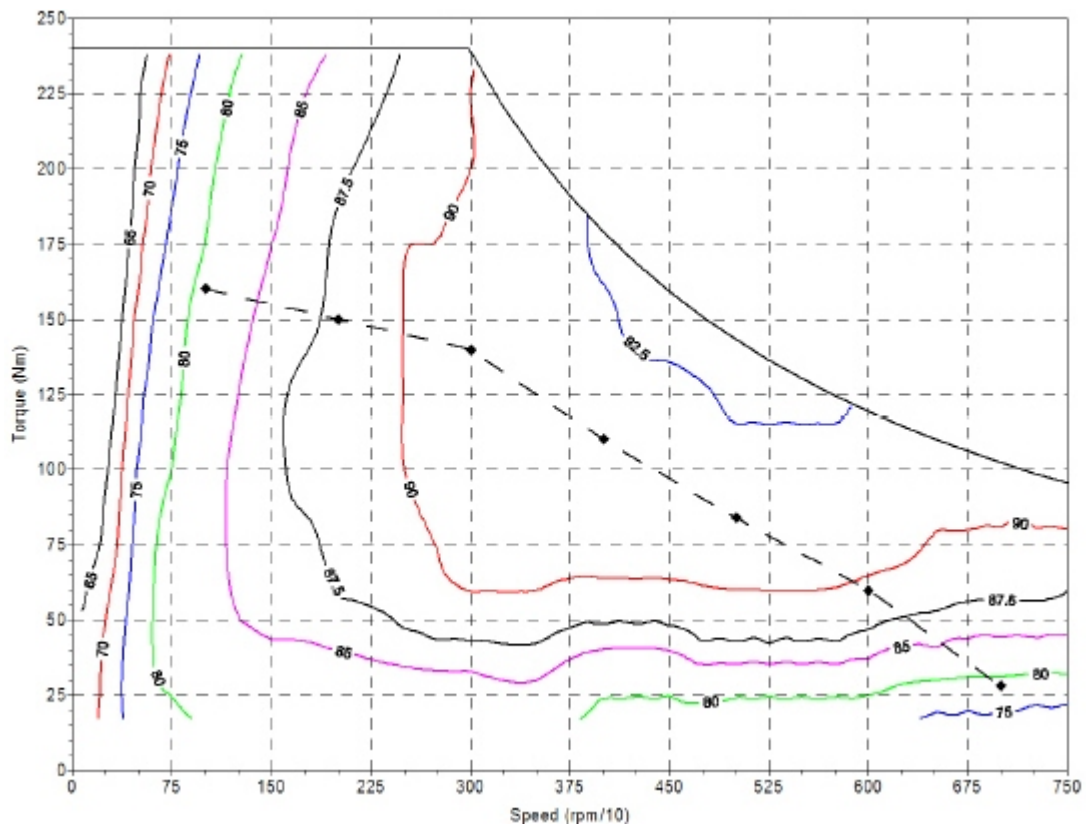


Figure 9.58: *Electric motor efficiency and speed range [25]*

9.6.7 Wheel Motor as Primary or Secondary Drive

9.6.7.1 Current Applications

- Vehicle prototypes and concepts only
- GM HyWire and Sequel, Mitsubishi i-MiEV
- Not readily available or fully developed

9.6.7.2 Advantages

- Integration of traction control and regenerative braking
- Improved performance and regenerative braking with smaller primary drive systems

9.6.7.3 Challenges

- Size and weight limiting power above 40 kW per axle (Insufficient for most passenger cars)
- Very high unsprung mass is detrimental to ride and handling
- Reduced motor speed range may limit vehicle acceleration vs. top speed
- Added weight, cost and complexity for redundant functionality for secondary drive
- Challenging development & validation with very harsh vibration, impact and environmental conditions
- Integration of disk brake assemblies
- More complex than traction motor, also resulting in additional costs

9.6.8 Traction Motor with Integrated Transaxle

Specifically for pure electric or Series hybrid vehicles, a compact unit has been introduced, combining the following functions into a single unit:

- Traction motor
- Single speed transmission (gear reduction)
- Differential and drive shafts

This design reduces packaging space, weight and, cost (in a high volume production scenario).

Significant output power and efficiency gains have been recently achieved with further improvements in motor design. Further technical advancements can be expected over the next 10 years.

Figure 9.59 shows Toyota's development progress in motor output and transmission size from the first to the second-generation hybrid drives. Both use an internal combustion engine as primary drive, but both also have limited driving potential in pure electric mode.

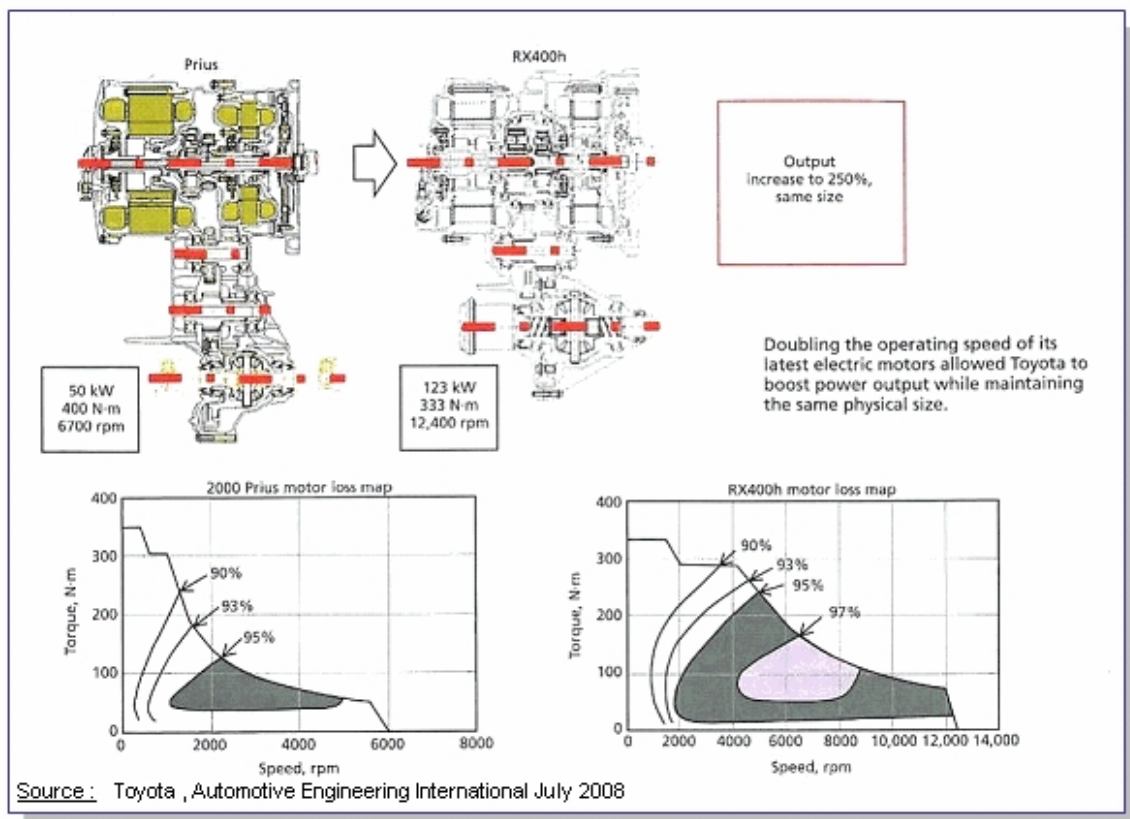


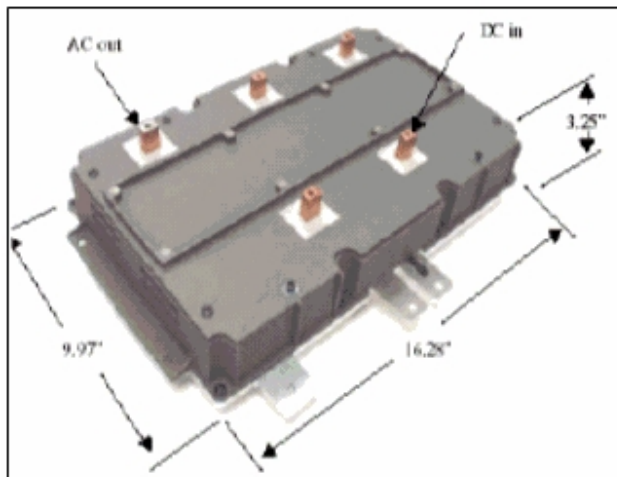
Figure 9.59: Toyota's development progress in motor output and transmission size from the first to the second-generation hybrid drives

9.6.9 Power inverter designs

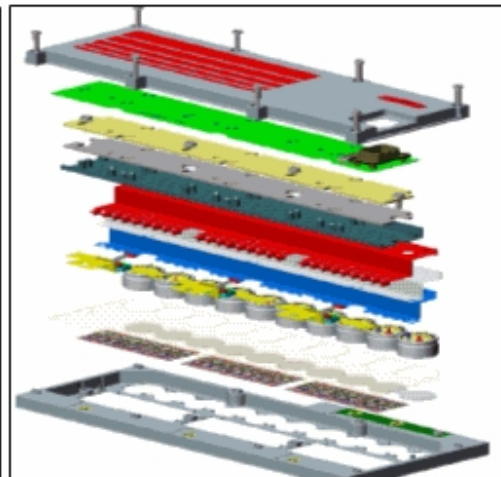
The power inverters are designed to match the selected traction motor, so as to optimize performance and efficiency of traction motors in dynamic and quasi-static operating conditions. The power inverter receives DC battery bus voltage fluctuating based on battery charge status and invert the DC current into a 3-phase AC current for the permanent magnet motor by employing power electronics. The AC output signal is manipulated both for voltage level and for frequency to control power delivery to the traction drive system, in response to driver inputs from the accelerator pedals. Examples of power inverter are shown in Figure 9.60

Essentially the same inverter technology also is used for the reverse power flow in regenerative brake operation. In this case, vehicle wheel speed and torque generate electrical power through the traction motor/generator, which is then a variable voltage and frequency input to the DC inverter. Power electronics are used to limit the mechanical to electrical power conversion to DC inverter output levels compatible with battery bus voltage and charge rate capabilities. When excess mechanical energy is available the integrated disk brakes system is engaged and the kinetic energy is converted to heat like in conventional vehicles.

The power inverters design and control strategy is tuned to reduce heat losses, to reduce any additional cooling loops in the vehicle. DC inverter technology is rapidly being optimized for improved packaging density, performance and control capability. Component pricing reduction is achieved through increased production volumes and higher integration density of the high power circuits.



Source: DOE, Semikron Inverter(450 V 55kW)



Source: DOE, Satcon Inverter (360 V 80kW)

Figure 9.60: *Power inverter designs*

9.6.10 Generator/Motor Recommendations for FSV

Due to the lack of gear reduction needed with escalating motor speeds, wheel motors do not offer sufficient power and may only have limited benefit from electric motor improvement achievements. System complexity and unresolved chassis and suspension tune-ability are further indicators that wheel motors may only be utilized in low power applications.

The Future Steel Vehicles, PHEV₂₀ and PHEV₄₀ both share a common size generator, which power ratings can be optimized per application. The generator is directly coupled via a "torsional vibration dampening coupling" to the crankshaft and flanged onto the engine housing. To avoid heat transfer from the engine to the generator housing, water-cooling is required for the temperature management of the generator. Sharing a common size generator will allow modular design integration thus reducing tooling and development cost in this program.

10.0 Steel Technologies

10.1 Summary

For the Future Steel Vehicle (FSV), a number of steel forming technologies will be adopted to take advantage of the benefits of Advanced High Strength Steel (AHSS), including the high strength martensites. Use of these steels result in a substantial mass savings by a reduction in material thickness with an increase in strength and part performance.

The FSV steel portfolio is utilized during the material selection process with the aid of full vehicle analysis using state-of-the-art software to determine material grade and thickness. From the steel portfolio, a primary formed blank or tube is produced, which is then formed to the final part geometry using a number of manufacturing processes.

10.2 Steel Grades Portfolio - FSV

The steel grades and thickness for the Future Steel Vehicle shall be determined using available steel from the WorldAutoSteel steel portfolio. The steel available ranges from “mild steel” to advanced high strength “martensitic steel”. The basic types are the following:

- Mild (Mild steel)
- BH (Bake Hardenable)
- IF (Interstitial Free)
- DP (Dual Phase)
- CP (Complex Phase)
- SF (Stretch Flange)
- FB (Ferrite Bainite)
- HT (Heat Treatable)
- HSLA (High Strength Low Alloy)
- TRIP (Transformed Induced Plasticity)
- MS (Martensitic)
- MnB (Boron)
- LIP (Light Induced Plasticity)

Table 10.1 shows the full range of steels available for the Future Steel Vehicle.

10.2 Steel Grades Portfolio - FSV

Item #	Steel Grade	Thickness (mm)		Gage Length	YS (Mpa) Min	YS (Mpa) Typical	UTS (Mpa) Min	UTS (Mpa) Typical	Tot EL (%) Typical	N-value Typical
		Min t	Max t							
1	Mild 140/270	0.6	2.3	A50	140	150	270	300	38-44	0.23
2	BH 210/340	0.64	2.79	A50	210	230	340	350	35-41	0.19
3	BH 260/370	0.64	2.79	A50	260		370		32-36	0.17
4	IF 260/410	0.6	2.3	A50	260	280	410	420	34-48	0.20
5	BH 280/400	0.6	2.8	A50	280	324	400	421	30-34	0.16
6	IF 300/420	0.6	2.3	A50	300		420		29-36	0.20
7	DP 300/500	0.5	2.5	A80	300	345	500	520	30-34	0.16
8	FB 330/450	1.8	3.0	A80	330	380	450	490	29-33	0.17
9	HSLA 350/450	0.5	3.0	A80	350	360	450	470	23-27	0.16
10	DP 350/600	0.6	2.5	A80	350	385	600	640	24-30	0.19
11	TRIP 350/600	0.6	2.3	A50	350	400	600	630	29-33	0.20
12	DP 400/700	1.27	3.2		400		700		19-25	0.14
13	TRIP 400/700	1.0	1.6		400		700		24-28	
14	HSLA 420/500	0.76	3.2		420	430	500	530	22-26	
15	FB 450/600	1.8	3.0	A80	450	530	560	605	18-23	0.11
16	TRIP 450/800	1.0	1.6	A80	450	550	800	825	26-32	0.24
17	TWIP 450/1000	1.2		A50M	450	496	1000	1102	50-54	0.41*
18	HSLA 490/600	0.75	3.2		490	510	600	630	20-25	0.13
19	CP 500/800	0.8	1.6	A80	500		800		10-14	
20	DP 500/800	0.6	2.3	A50	500	520	800	835	14-20	0.14
21	HSLA 550/650	0.75	3.2	A50	550	586	650	676	19-23	0.12
22	SF 570/640				570		640		20-24	0.08
23	SF 600/780	2.9	5	A50	600	650	780	830	20-24	
24	CP 700/800	1.5	3.0	A80	700	720	800	845	10-16	0.13
25	DP 700/1000	0.6	2.3	A50	700	720	1000	1030	12-17	0.09
26	CP 800/1000	0.8	3.0	A80	800	845	1000	1005	8-13	0.11
27	MS 950/1200	1.5	3.2	A50M	950	960	1200	1250	5-7	0.07
28	CP 1000/1200	0.8	2.3		1000	1020	1200	1230	8-10	
29	HF 1050/1500 (22MnB5)	1.0	2.5	A80	1050	1220	1300	1500	5-7	
	<i>Conventional Forming</i>	1.0	2.5	1.0 - 2.0	380		500		16-20	
	<i>Heat Treated after forming</i>	1.0	2.5	1.0	1050		1500		4-6	
30	MS 1150/1400	0.5	1.5		1150		1400			
31	MS 1250/1520	0.5	1.5	A50M	1250		1520		4-6	0.07
32	LIP 650			A80	270	300	650		55+	0.40*
33	LIP 780			A80	360	400	780		55+	0.35*

* Un-notched specimens, FSc = UTS + 345 (Mpa)
 Alternate approximation = 3.45*HB

Table 10.1: Range of steels available for FSV

10.3 Processing and Manufacturing Technology Portfolio - FSV

From the steel portfolio, a primary formed blank or tube is produced, and this can be from any of the following:

- Conventional single steel grade and thickness sheet
- Laser welded blank
- Laser welded tube, both constant and variable thickness
- Laser welded coils
- High-frequency induction welded tubes
- Variable walled tubes

From the primary formed blank or tube, a number of manufacturing processes can be utilized to produce the final part and include:

- Stamping
- Roll forming
- Hot stamping, both direct and in-direct
- Hydroforming

Figure 10.1 is a flow chart from the steel portfolio to the technology portfolio.

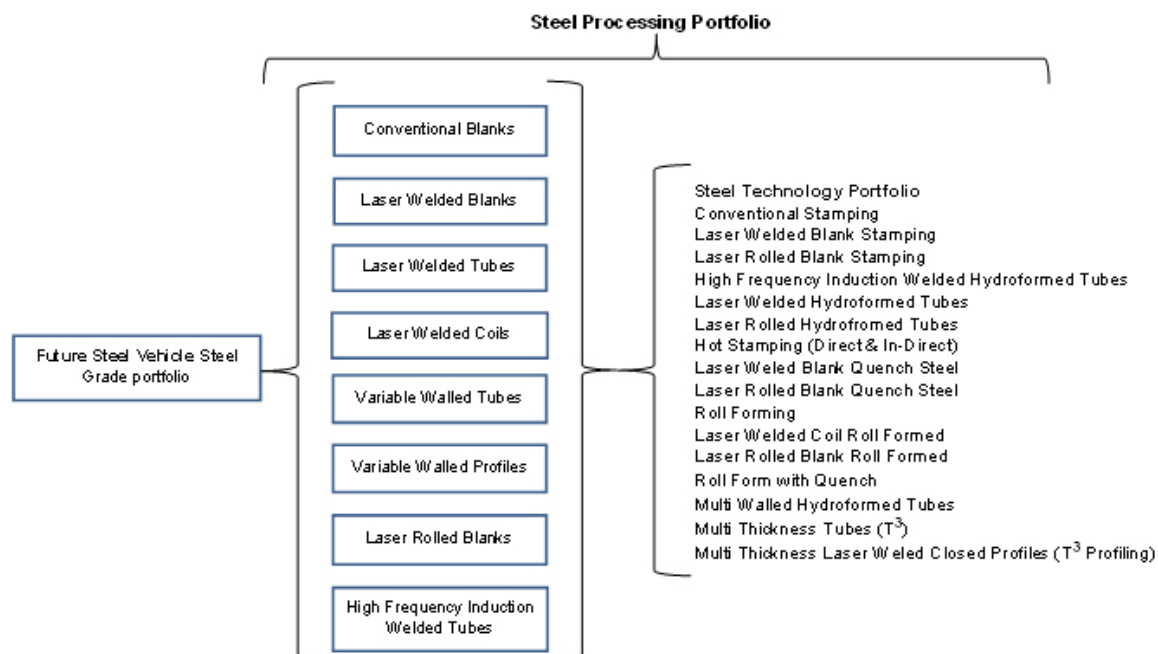


Figure 10.1: Steel portfolio to technology portfolio flow diagram

10.3.1 Laser Welded Blanks

In an automotive application, a laser welded blank is two or more steel sheets butt-welded together to form a new single blank. This blank can contain individual parts of differing material grades or thickness.

Laser blank technology allows for the positioning of these material grades in areas where higher performance is required, such as in the lower A-pillar area on a body side panel. This technology also allows for a reduction in panel thickness in non-critical areas, thus contributing to an overall mass reduction of the part. Figure 10.2 shows an example of a laser weld blank used for a body side panel. [1]



Figure 10.2: Laser welded blank to final stamping example

10.3.1.1 Welding Methods

The welded blank can be welded by using a number of methods such as:

- Laser welding
- Resistance mash-seam welding
- High-frequency induction welding
- Electron beam non-vacuum welding

Each of the above has specific attributes that are dependent on the finished part geometry and strength requirements. Length of weld and material thickness is critical. Some methods rely on a high quality edge condition while others only have straight line welding capabilities. All these factors influence the selection of the welding method.

10.3.1.2 Laser Welding

- Can weld non-straight edges
- Long weld length requires a higher edge alignment and quality
- Minimum panel thickness to be welded: 0.7 mm
- Maximum panel thickness to be welded: 3.0 mm
- Maximum material thickness ratio: 3:1

10.3.1.3 Resistance Mash-Seam Welding

- Can only weld in straight line
- Edge preparation not critical
- Minimum panel thickness to be welded: 0.7 mm
- Maximum panel thickness to be welded: 3.0 mm
- Combined total material thickness to be welded: 5.0 mm (T1 + T2)
- Maximum material thickness ratio: 3:1

10.3.1.4 High Frequency Induction Welding

- Edge condition not critical
- Minimum panel thickness to be welded: 0.7 mm
- Maximum panel thickness to be welded: 2.5 mm
- Maximum material thickness ratio: 2.5:1

10.3.1.5 Beam Welding

- Weld length only limited by blank holding equipment
- Higher speed welding process than all other methods
- Can weld non-straight edges
- Edge condition is critical
- Minimum panel thickness to be welded: 0.7 mm
- Maximum panel thickness to be welded: 6.0 mm
- Maximum material thickness ratio: 3:1

10.3.1.6 Advantages

There are a number of advantages for a laser welded blank of a conventional single grade and part thickness such as:

- Superior structural strength and rigidity than parts produced with conventional methods
- Higher strength parts of the blank can replace as needed
- Consolidation of parts, where one blank can replace a number of different parts
- Lower vehicle and part weight
- Reduced steel usage
- Improved safety
- Elimination of reinforcement parts
- Elimination of assembly processes
- Reduction in capital spending for stamping and spot-welding equipment
- Reduced inventory costs
- Improved dimensional integrity (fit and finish)
- Increase in vehicle strength and rigidity
- Achievement of high performance objectives with lower total costs
- Reduction in Noise, Vibration, and Harshness (NVH)
- Elevated customer-perceived quality

10.3.2 Laser Welded Coil

Laser welded coil is a process of producing a continuous coil of steel from individual separate coils of varying steel grades and thickness. The basic process takes separate coils of steel, prepares the coil edges for laser welding and re-coils the strip, making it ready for stamping by the end user. Figure 10.3 shows the laser welding coil production process.

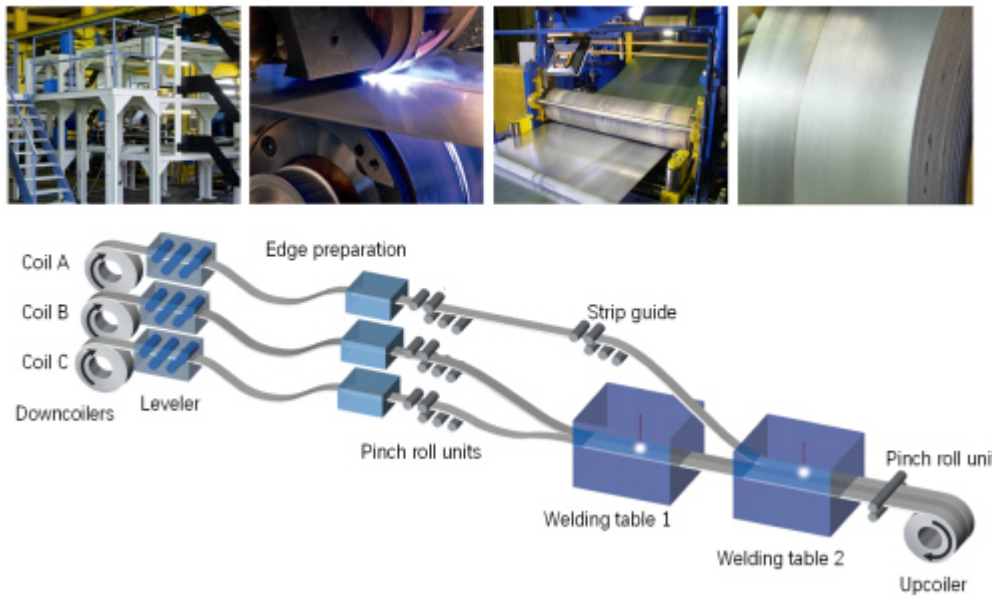


Figure 10.3: *Laser Welded Coil production process*









Current coil technology dictates the requirement of tonnage, strip width and coil outside diameter, for each downcoiler and final upcoiler for the final laser welded strip. Table 10.2 shows the tonnage and coil recommendations for the individual downcoilers and upcoiler. Coil width of 1,600 mm with a maximum of 25 tonnes will be available from May 2009.

Coiler	Tonnage	Strip Width [mm]	Coil OD/ID [mm]
Lower downcoiler	10.0	up to 1,000	max. 2,000 / 508
Middle downcoiler	10.0	up to 1,000	max. 2,000 / 508
Upper downcoiler	10.0	up to 800	max. 2,000 / 508
Upcoiler	25.0	1,600	ID 508 or 610

Table 10.2: *Tonnage and coil recommendations*

Table 10.3 shows the material combinations that can be used or are under development for laser welded coils.

Material Grade	DC 04	MHZ 340	DX 56	DK-P 34/60*	DK-P 45/78*	DK-P 60/98*	1.4301**	1.4509***	MBW 1500*	FB-W 450*
DC 04	✓	✓	✓	—	—	—	✓	—	—	✓
MHZ 340	✓	✓	✓	—	—	—	✓	—	—	✓
DX 56	✓	✓	✓	—	—	—	✓	—	—	✓
DK-P 34/60*	—	—	—	✓	✓	✓	—	—	—	—
DK-P 45/78*	—	—	—	✓	✓	✓	—	—	—	—
DK-P 60/98*	—	—	—	✓	✓	✓	—	—	—	—
1.4301**	✓	✓	✓	—	—	—	✓	✗	—	—
1.4509***	✓	✓	✓	—	—	—	✗	✗	—	—
MBW 1500*	—	—	—	—	—	—	—	—	✓	—
FB-W 450*	✓	✓	✓	—	—	—	—	—	—	✓

 Carbon Steel	 Heat Treat Steel	 Successfully produced
 Dual Phase Steel	 Fine Grain Steel	 Development ongoing
 Stainless Steel		 Not yet produced

* ThyssenKrupp Product
 ** Austenitic stainless steel
 *** Ferritic stainless steel

Table 10.3: Material combinations laser welded coils

10.3.2.1 Potential Usages

Potential use of a laser welded coil in an automotive application, using a progressive die-stamping process, include the following:

1. Roof frames
2. Roof bows
3. Side members
4. Reinforcements
5. Seat cross members
6. Exhaust systems

Figure 10.4 shows the examples of usages in automotive applications. [2]



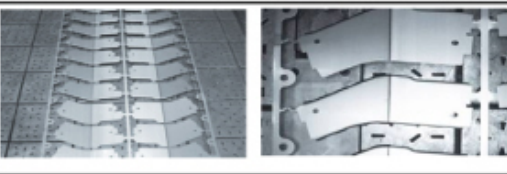


Roof frames	
Side members	
Reinforcements	
Seat cross members	
Exhaust systems out of stainless steel	

Figure 10.4: Examples of usages in automotive applications

10.4 Laser Welded Rolled Tubes

Laser welded rolled tubes is a method of producing a tube that is specifically suited to hydroforming. This process maximizes the residual ductility for post tube bending and hydroforming. The tube blank is produced by a pressing operation and laser welding the joint, rather than the conventional roll forming process. The rolled tubes are cut from the width of a coil. The coil can then be laser welded, giving different material grades or thickness. The press operation then gradually forms the tube into a circle, which is then passed to a laser welding operation. [3]

The hydroforming process typically requires a relatively thin walled tube. Conventional tubes used for hydroforming have a D/t ratio of 75, whereas the rolled tube can reach a D/t ratio of up to 250, with diameters ranging from 50 mm to 250 mm and thickness ranging from 0.6 mm to 3 mm. Figure 10.5 shows the possible rolled tube dimensions.

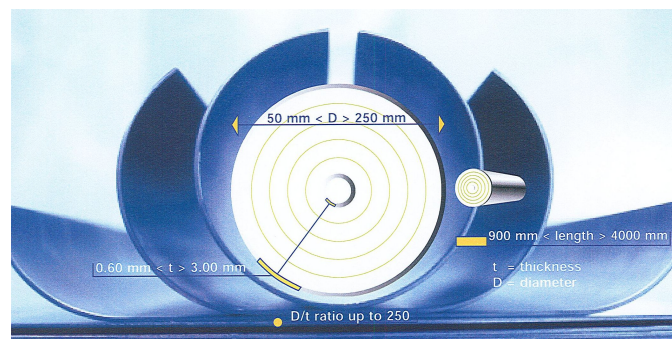


Figure 10.5: Possible rolled tube dimensions

In addition to a circular tube, a tapered tube can be produced. Length of this tube can be up to 1000 m with a diameter ratio of 30%. This gives an additional advantage over a conventional roll formed tube. Figure 10.6 shows the rolled tapered tube dimensions.

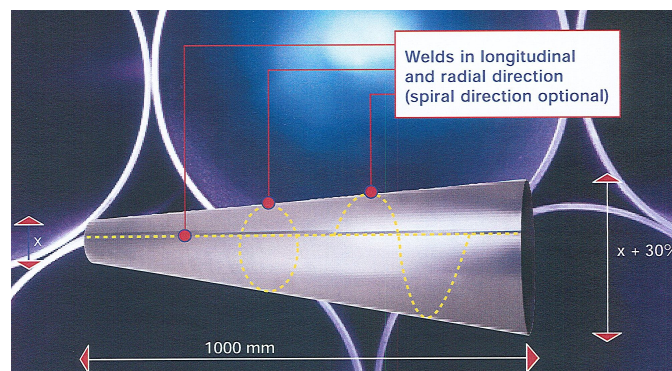


Figure 10.6: Rolled tapered tube dimensions

10.4.0.2 Product Guidelines

Current product guidelines with today's rolled blank technology are listed below:

- Current strip widths: 350 mm to 800 mm.
- Strip widths up to 1500 mm are under investigation and are expected to be available in the near future
- Maximum material variation: +/-50% (e.g. 1.0 mm to 2.0 mm)
- Maximum profile thickness: 3-4 mm (depending on strip width and material)
- Minimum transition length: 1.0 mm / 100 mm
- Material thickness tolerance: +/-0.05 mm
- Standard profile position tolerance: +/-5.0 mm

10.4.0.3 Material Portfolio

Material portfolio for laser welded blanks are listed below:

- Mild steel ($160 \text{ MPa} < R_p^{[1]} < 220 \text{ MPa}$)
- Higher strength steel ($220 \text{ MPa} < R_p < 300 \text{ MPa}$)
- Micro alloy high strength steel ($300 \text{ Mpa} < R_p < 500 \text{ Mpa}$)
- Boron alloyed AHSS (uncoated only)
- Dual phase steel (under development)

Laser welded blank mechanical properties are at a maximum "Rp" difference between thickness sections of +100 MPa, depending on profile and material grade. The laser welded rolled blank process can accommodate both hot-dip and electro-zinc galvanized coatings without impacting product performance.

10.4.0.4 Automotive Applications

Automotive applications suited for laser welded rolled tubes include the following:

- Front longitudinal
- A/B-pillar reinforcements
- Instrument panel support beam
- Rocker reinforcement

¹Rp - Strength Value

- Front/rear sub frame
- Front/rear bumper beam

10.4.0.5 Advantages

There are many advantages in using a laser welded rolled tube over a conventional roll formed tube such as the following:

- Weight reduction
- Reduction in number of parts by component consolidation
- High diameter to thickness ratio, up to 250 compared to 75 for a roll formed tube
- Possible to form a conical tube
- Laser welded coils can be used
- Improved formability, in many cases annealing is not necessary
- Excellent corrosion resistance when using galvanized materials
- Class-A surface quality is possible
- Different materials can be used (steel-steel, steel-stainless steel, steel-aluminum)

10.5 Multiwall Tube (T³)

Multiwall T³ is a proprietary process by which the wall thickness is varied along the length of a single piece formed tube according to the structural requirements of the design application using high strength low alloy (HSLA) steel. The Multiwall tube wall thickness can vary on either the inside or outside of the tube. [4]

Figure 10.7 is an example of Multiwall tube, and Figure 10.8 is an example of a Multiwall tube with varying thickness.



Figure 10.7: *Multiwall T³ Tube*

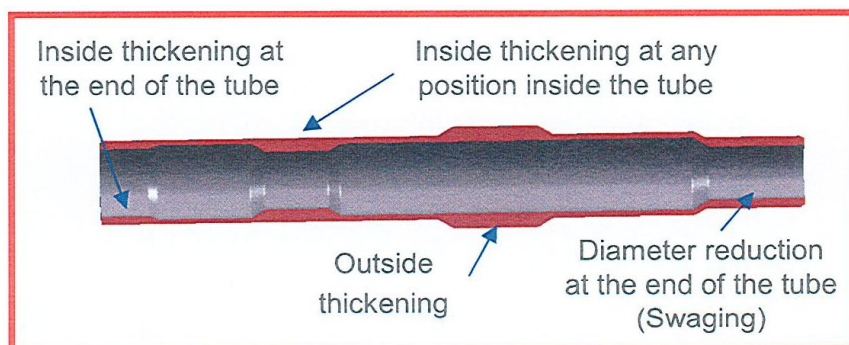


Figure 10.8: *Multiwall T³ Tube with varying thickness*

As Multiwall is a cold working process, any material appropriate to cold forming can be used. Multiwall T³ tubes can be produced with material ranging from low carbon steel to dual phase (DP780) steels. There is continuing development being undertaken to use boron based Advanced High Strength Steel (AHSS), and other alloyed heat treatable steels for Multiwall applications. Figure 10.9 shows the range of materials that can be used for Multiwall T³.

10.5 Multiwall Tube (T^3)

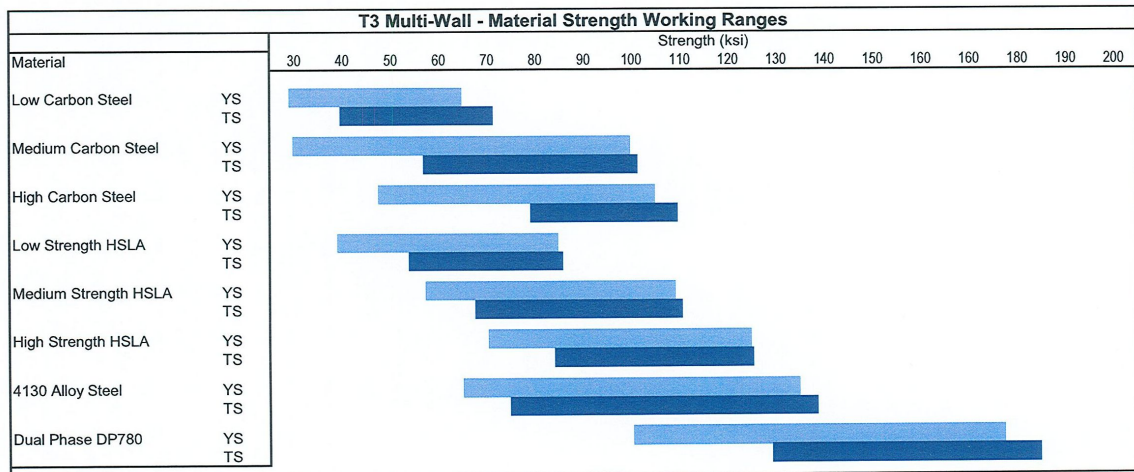


Figure 10.9: Range of materials that can be used for Multiwall T^3 tubes

10.5.0.6 Advantages

Some of the benefits of using Multiwall T^3 tubes are the following:

- Mass savings, typically up to 30% over conventionally stamped parts
- Design flexibility, material can be added where needed
- Improvement in part yield strength due to cold working of the parts in the Multiwall process
- Improved NVH performance
- Less scrap
- Part consolidation is possible
- Part cost reduction and the elimination of the need of using a laser welded blank
- Part strength and formability properties can be adjusted by selective heat treatment
- Multiwall tube is ideally suited to be hydroformed

10.5.1 MultiWall Tube (T^3 Profiling)

Multiwall T^3 profiling is process by a closed profile is produced with varying wall thickness using a laser welded blank of conventional and advanced high strength steels. [22]

Figure 10.10 shows the principle for the production of a closed Multiwall thickness profile.

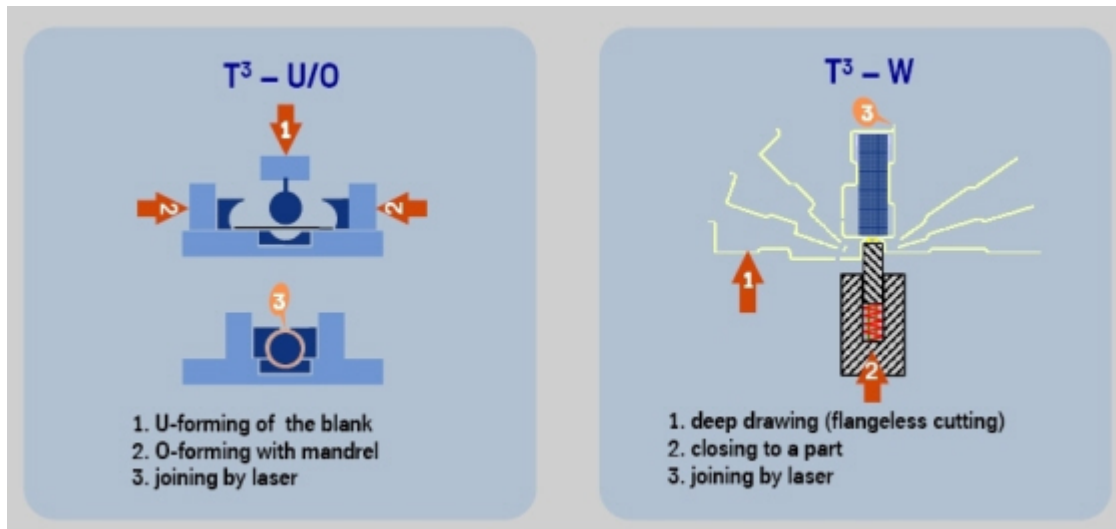


Figure 10.10: T^3 profiling manufacturing principle

Generally most parts of a "shell" type construction can be replaced using a T^3 profile intensive structure. Part consolidation is also possible using this process.

T^3 profiling can be used for the following automotive applications:

- Longitudinal members
- Instrument panel support beam
- A-pillar
- Underbody cross members

There are also addition advantages of using T^3 profiled parts related to other manufacturing techniques, this include:

- Part performance
- Part weight
- The packaging of part in the vehicle design
- Use of differing material gauges

10.5 Multiwall Tube (T^3)

Table 10.4 shows some of the advantages of using a T^3 profiled part compared to hydroforming and conventional "shell" type part.

	T^3 (U/O; W)	Hydroforming	Conventional shell parts
Performance	++	+	=
Weight	++	++	-
Package	++	++	=
Grades	++	=	++

Table 10.4: T^3 profiling advantages matrix

With a T^3 profiled part there are a number of restrictions that apply to T^3 - U/O (Circular) and T^3 - W (multi shaped) process. Table 10.5 shows the restrictions between the T^3 - U/O and T^3 - W process.

	T^3 - U/O	T^3 - W
Geometry	<ul style="list-style-type: none"> ○ Mean structured parts ○ Only slight bends possible ○ Geometric dimensions mainly restricted by machine park (force, size, handling ect.) ○ Only simple shaped beads and embossings possible 	<ul style="list-style-type: none"> ○ Plane and straight turn - over area needed ○ Turn – over area depends on grade ; the higher the grade, the wider the area ○ Restrictions according to the conventional deep drawing
Grades	<ul style="list-style-type: none"> ○ Less restrictions; from conventional deep drawing grades up to high strength steels 	<ul style="list-style-type: none"> ○ Less restrictions; from conventional deep drawing grades up to high strength steels
Process	<ul style="list-style-type: none"> ○ Inserting and extraction mandrel ○ Process time increase 	<ul style="list-style-type: none"> ○ Pre - form has to be precise with less variation

Table 10.5: Restrictions between the T^3 - U/O and T^3 - W process

10.6 Vibration Damping Steel Sheets and NVH

Vibration Damping Steel Sheets (VDSS) have sandwich structures with intermediate layers of resin as shown in Figure 10.11. [5][4]

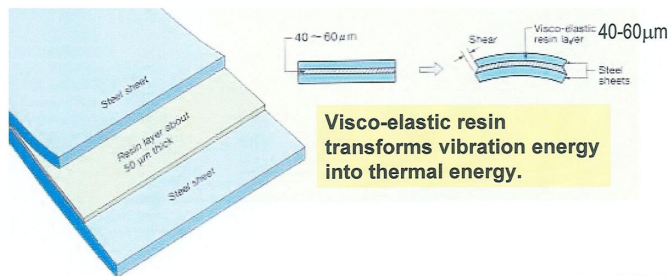


Figure 10.11: Construction of vibration damping steel

The most important characteristics of VDSS for inner panels of automotive vehicles are the vibration damping properties, press formability and spot weldability. Stamping formability of VDSS is strongly influenced by the adhesive strength of the core resin. Higher adhesive strength gives better stamping formability. Figure 10.12 shows the addition of metal particles for electric conductivity.

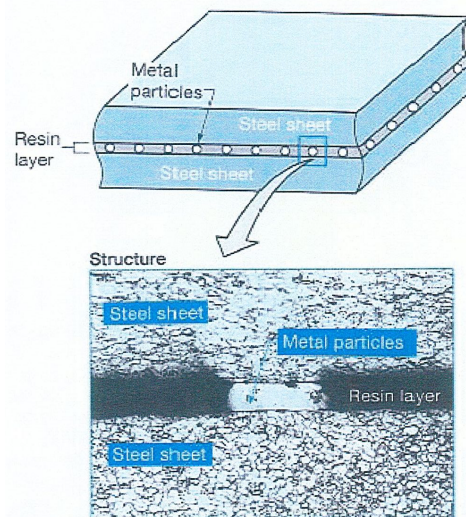


Figure 10.12: Vibration damping body-structure

10.6 Vibration Damping Steel Sheets and NVH

VDSS for inner parts of automotive vehicles can be directly spot welded, similar to ordinary steel sheets. Spot weldability of VDSS depends upon the amount and the size of the metal powder in the resin layer, and spot weldability in this case is not dependent on the kind of the steel sheet used. Figure 10.13 shows the vibration damping effect over time when using VDSS against a conventional steel panel.

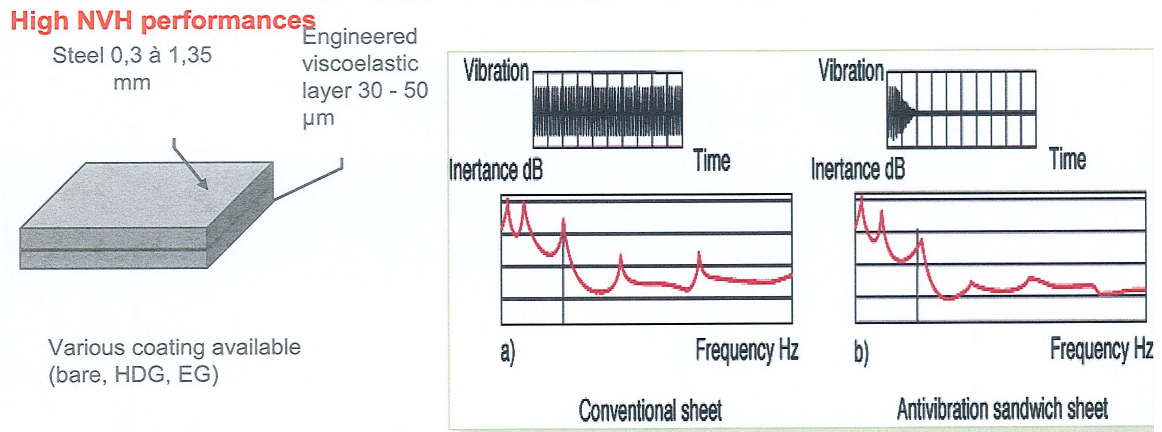


Figure 10.13: *Vibration damping effect over time*

10.6.1 Advantages

Apart from the obvious advantages related to NVH and sound damping, there is an added weight reduction potential by the elimination of sound deadener materials and mastics applied to the interior of the vehicle.

10.6.2 Automotive Application

Typical automotive applications include body-structure and powertrain:

Body-structure panels include:

- Dash panel
- Floor panels
- Wheelhouse

Powertrain panels include:

- Engine oil pan
- Engine covers

Figure 10.14 shows the examples of body-structure panels suitable for vibration damping steel and Figure 10.15 shows the examples of powertrain parts suitable.

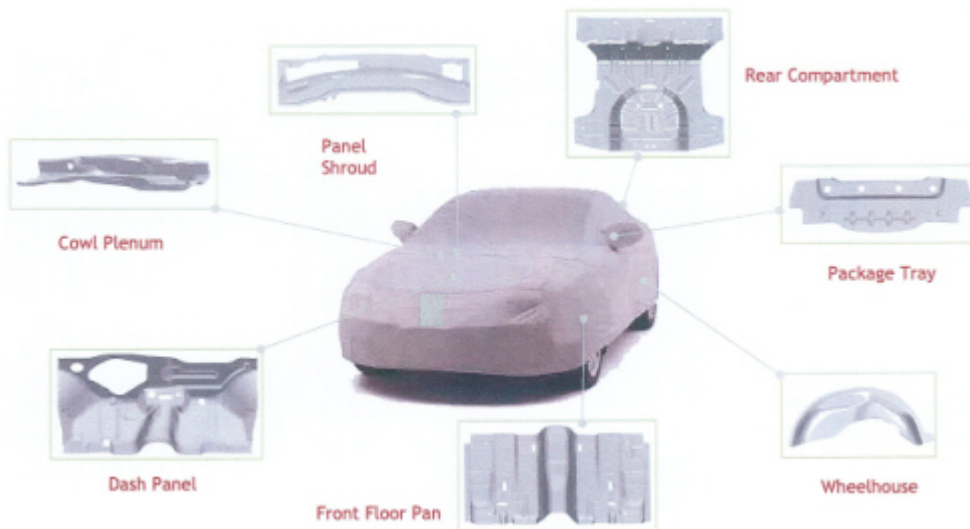


Figure 10.14: Steel structure panels suitable for vibration damping steel



Figure 10.15: Powertrain parts suitable for vibration damping steel

10.7 Laser Arc Hybrid Welding

Laser Arc Hybrid Welding combines the advantages of laser and arc welding, producing deep penetration welds with good tolerance to joint fit-up. The laser source can be CO₂, Nd:YAG, or Yb fiber laser, and can be used with a MIG/MAG, TIG or plasma arc welding. The two sources are usually combined so that the laser and arc operate in a single, elongated process zone. [6][4]

Figure 10.16 shows the hybrid welding process.

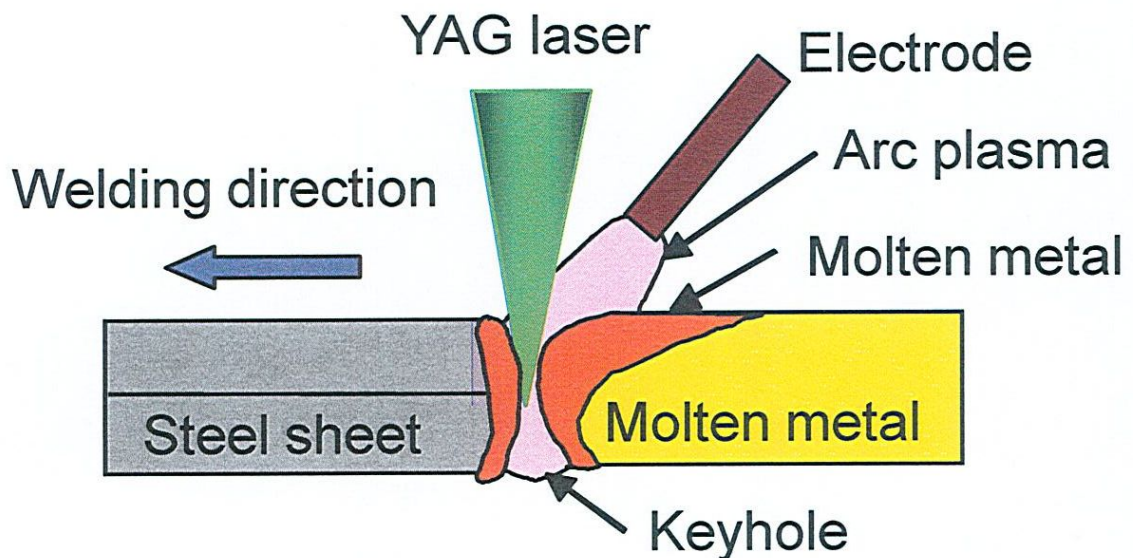


Figure 10.16: Laser Arc Welding Process

Figure 10.17 shows transition from conventional spot weld to lap and butt welding.

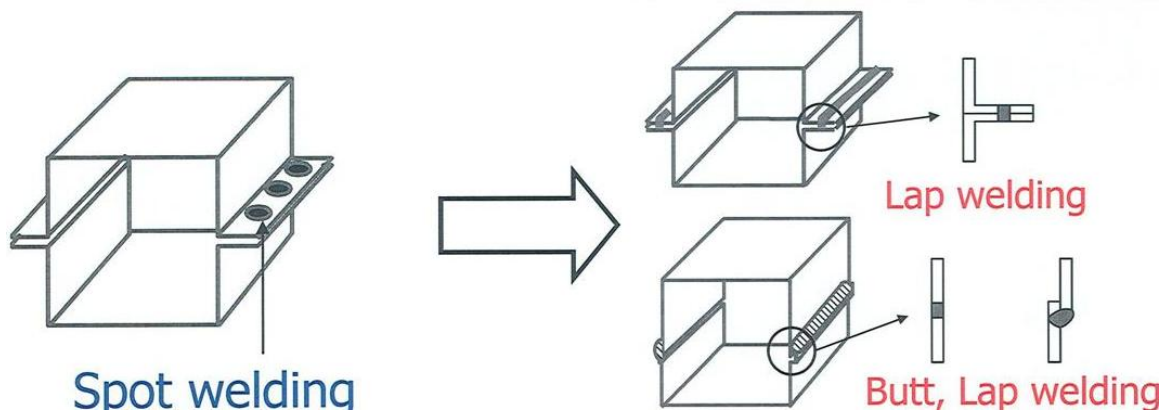


Figure 10.17: Transition using Laser Arc Welding

A number of different material grades can be welded together using the laser arc welding process. But there are some limitations related to material gage. Table 10.6 shows materials that can be successfully welded using the laser arc process.

MATERIAL	IF	HSLA	DP	TRIP	CP	Boron	Martensite
IF	X						
HSLA	X	X					
DP	X	X	X				
TRIP							
CP							
Boron							
Martensite	X	X	X				X

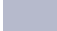
 These grades can be welded
 X Experimentally confirmed

Table 10.6: *Material combinations for laser welded coils*

10.7.1 Advantages

The laser arc hybrid welding process can replace the conventional spot welding of parts giving a number of advantages such as the following:

- Good gap bridging ability
- Gap tolerance wider than for laser welding
- Higher welding speeds compared to laser or spot welding, up to 5 m/min for a butt weld
- Improved weldability when welding zinc coated steels
- High weld joint strength for both static and fatigue strength
- Better weld burn through, as compared to laser welding

10.7.2 Limitations

Limitations on material gage when using the laser arc process are the following:

- Butt weld restricted to a 3:1 thickness ratio
- Butt welding maximum/minimum gages: 5.0 mm / 0.6 mm
- Lap and fillet weld maximum gage: 5 mm

10.8 High Frequency Induction Welded Tubes

High frequency induction welding is widely employed for longitudinal seam welding of small scale tubes and pipes due to its relatively high processing speed and efficiency.

10.8 High Frequency Induction Welded Tubes

Figure 10.18 shows a typical high frequency induction welded tube mill.

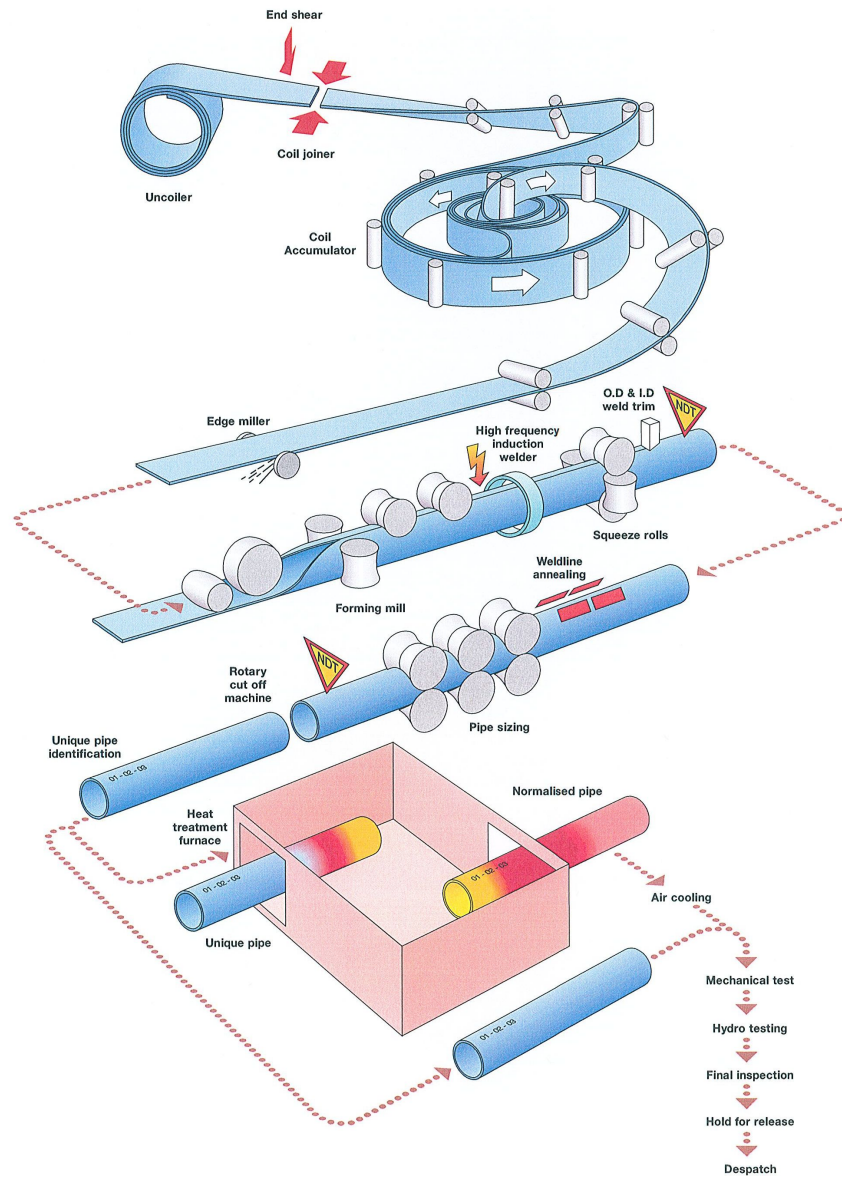


Figure 10.18: High-frequency induction welded tube mill

Tubes of a number of material grades can be produced using the high-frequency induction welding process, the grades ranging from lower grades of steel, with development being undertaken using Advanced High Strength Steel (AHSS), up to Dual Phase (DP) 980. Figure 10.19 shows materials that can be high-frequency induction welded, and the diameter to thickness ratio related to various material strengths.

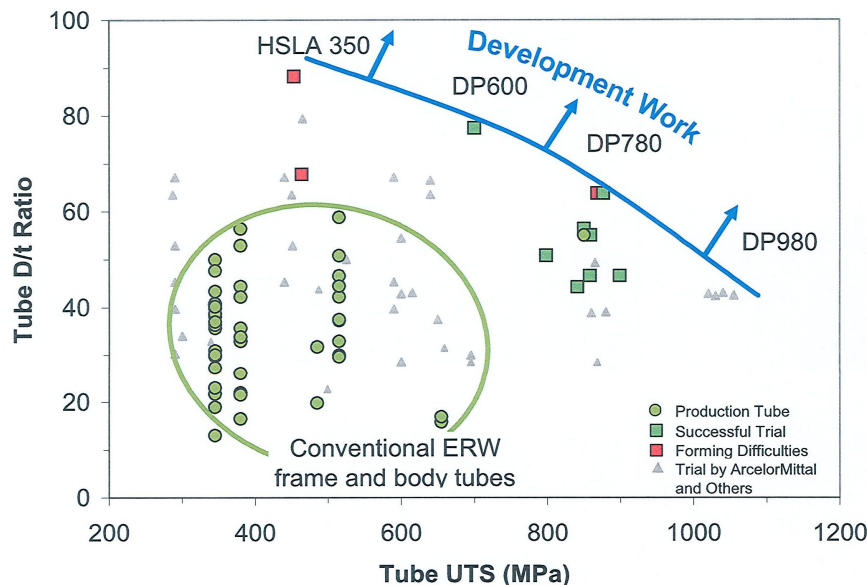


Figure 10.19: High frequency induction welded materials and D/T ratio

Thin walled tube outside diameter from 25 mm - 150 mm is possible. Tube thickness is commonly defined by diameter / thickness (D/T) ratio. D/T ratio depends on steel strength but is also influenced by the manufacturing tooling design.

10.8.1 Automotive Application

A high-frequency induction welded tube is ideally suited to the hydroforming process. Some of the automotive applications include the following:

- Engine cradles
- Seating frames and other seating components
- Anti-sway bars
- A-B pillar
- Rocker reinforcements

Figure 10.20 shows automotive applications using high-frequency welded tubes.

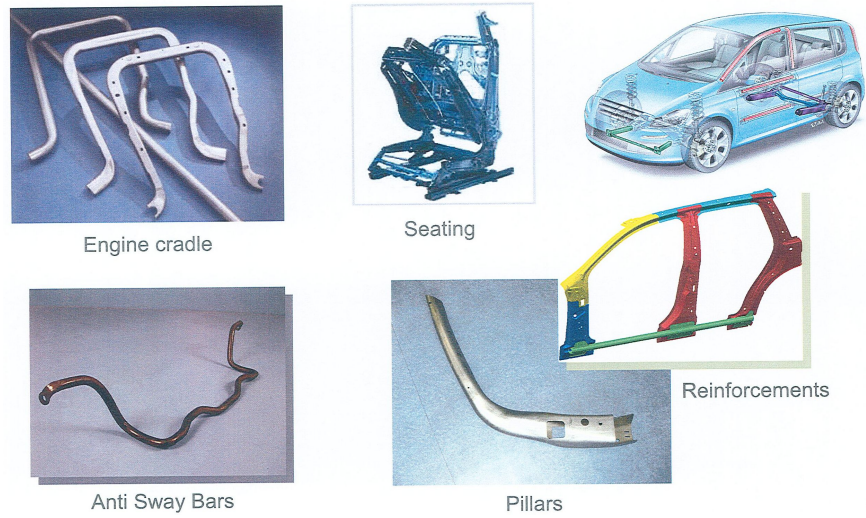


Figure 10.20: Automotive application using high-frequency welded tubes

10.9 Roll Forming

Roll forming is a continuous bending operation using a steel strip which is passed through a series of rolls each performing an incremental bend, until the final profile is achieved. This can then be left as an open profile, in the case of a vehicle roof bow, or seam welded to form a tube. This is a high speed process and is ideally suited to parts produced in large quantities. [7]

Figure 10.21 shows the roll forming process.

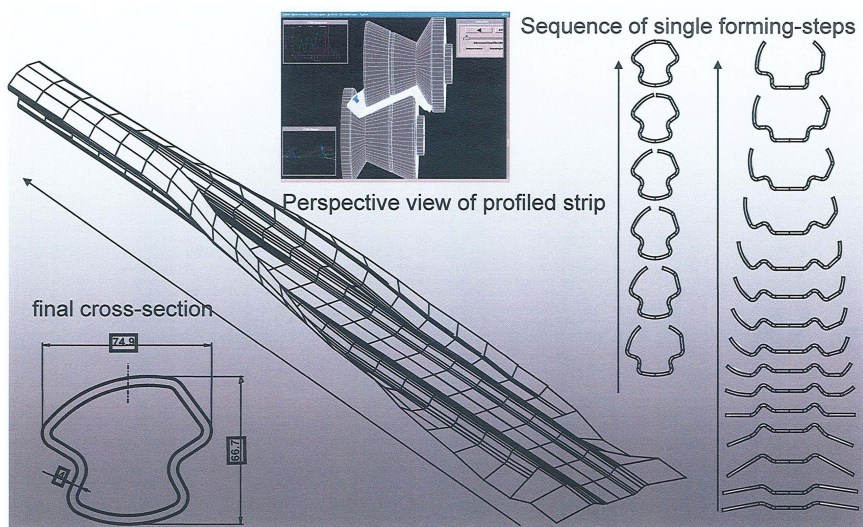


Figure 10.21: *Roll forming process*

10.9.1 Roll Forming Process

A typical roll forming process would consist of the following:

- Decoiler and leveler
- Loop station
- Roll form mill
- Welder, if roll forming a tube
- Calibration mill
- Cutting unit

Figure 10.22 shows a typical roll forming machine.

10.9 Roll Forming

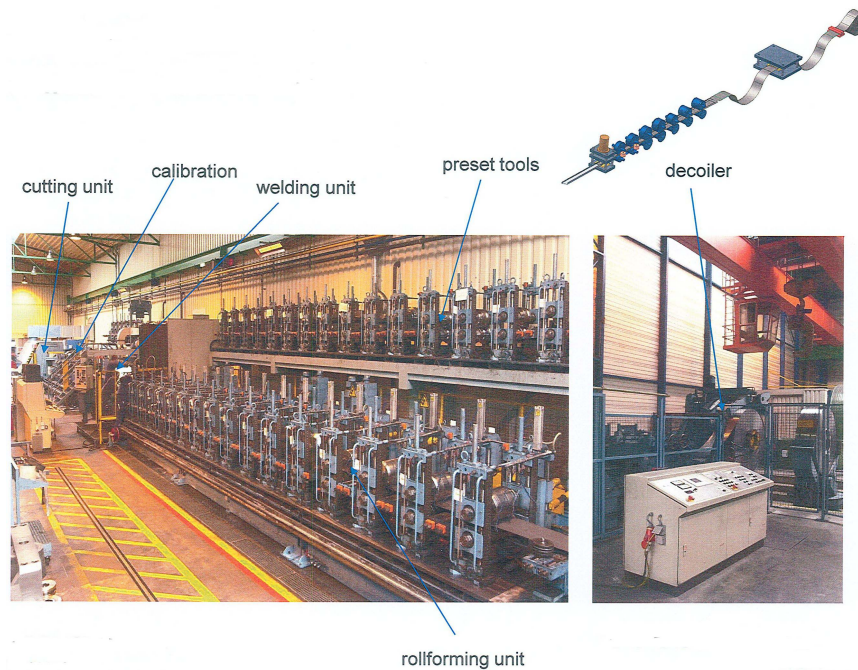


Figure 10.22: *Roll forming machine*

10.9.2 Advantages

Roll formed parts have a number of advantages over conventionally produced parts.

- High-speed process, with speeds up to 75 m/min are possible
- High-volume process
- Secondary operations can be done at the same time, e.g., punching, notching, welding etc.
- Part can be curved by using "stretchbending"
- Provides close tolerances which remain uniform from part to part
- Infinite number of profiles possible
- Low tooling costs
- Low piece cost
- Low maintenance costs
- Roll forming makes uniform and accurately dimensioned parts
- Parts are produced with little handling, minimizing labor costs

10.10 Hot Stamping (Direct and In-Direct)

Due to the increase in vehicle crash requirements, the use of Advanced High Strength Steel (AHSS) in the vehicle structure is increasing. These higher requirements can generally be met by the cold stamping process and by increasing the component gauge. However, this results in an unacceptable weight increase. [7][8]

Cold stamping is acceptable when using material grades up to 1000 MPa for stamping of relatively simple shapes. When higher material grades are required, AHSS grades are used. This poses a challenge to the stamping process used, because of their limited formability, excessive springback, and the need of increasing complex part geometry. To successfully form parts when using AHSS, a hot stamping process is utilized. Direct and in-direct hot stamping can provide structural parts with advanced high-strength. [7][8]

Future Steel Vehicle Steel Portfolio grade of 22MnB5 is used.

Part properties range from:

- Yield Strength (YS): 1050 to 1200 Mpa
- Ultimate Tensile Strength (UTS): 1350 to 1600 Mpa
- Elongation: 5 to 8x

10.10.1 Direct Versus In-Direct Process

The main difference in the two processes is that with the in-direct process, the part can be cold stamped to 100% of its final geometry prior to heating, and then press hardened in the final cooled die.

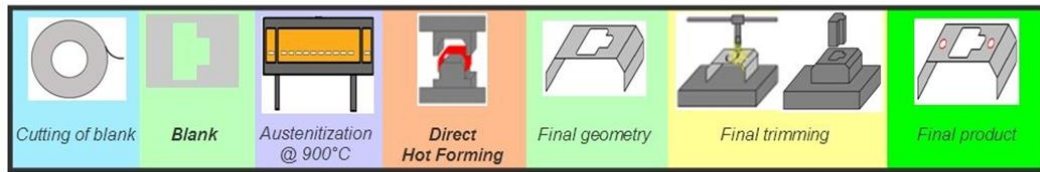
10.10.1.1 Advantages

- 100% part geometry can be achieved at the cold stamping stage
- Some part geometry adjustment can be made in the final press hardening die
- Final trimming of part is not required after process is complete, thus reducing part scrap
- Good shape and length tolerances on large parts (>2.0 m)
- Complex part geometry possible

Figure 10.23 shows direct and in-direct hot stamping processes.

10.10 Hot Stamping (Direct and In-Direct)

Direct Hot-Forming



Indirect Hot-Forming

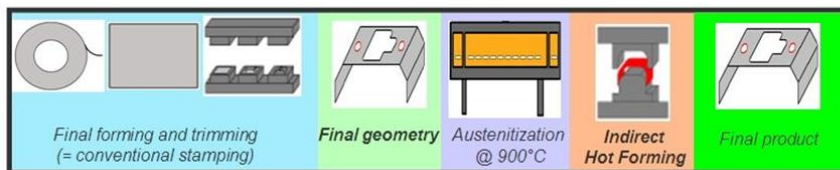


Figure 10.23: Direct and In-Direct hot stamping process

10.10.2 Properties

In the majority of cases with the in-direct hot stamping of part, no final trimming operation is necessary. However a trim operation may be added to the process dependent on part geometry and complexity. This additional process would be added after the in-direct hot forming operation and the final part stage of the process. This additional process would have an impact to the overall part process time and tooling and piece cost.

Figure 10.24 shows direct and in-direct processed steel properties (elongation vs. tensile strength) diagram.

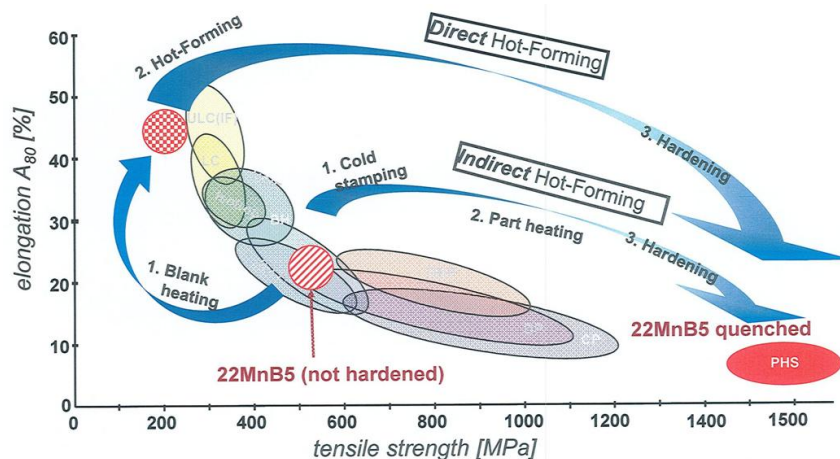


Figure 10.24: In-Direct processed steel properties (elongation vs. tensile strength)

10.10.3 Material Grades

Laser welded blanks with different material grades and thickness can be used for a hot stamping process. Steel grades and thickness that gives weight saving potential are as follows:

- 22MnB5 - High Strength Low Alloy (HSLA)
- 1.2 - 1.6 mm
- 1.3 - 1.5 mm
- 1.2 - 2.0 mm
- 1.6 - 2.0 mm
- 2.0 - 2.0 mm
- 1.7 - 2.5 mm

A laser welded blank used for hot stamping with 22MnB5 can be welded without any specific restriction to the following steel grades:

- HSLA (High Strength Low Alloy)
- DP (Dual Phase)
- CP (Complex Phase)
- TRIP (Transformed Induced Plasticity)
- MS (Martensitic)

10.10.4 Guidelines

The part geometry should be designed to take into account specific guidelines when using hot stamping, whether it is a direct or in-direct process. These guidelines [8] are:

- Direct hot stamping part geometry is achieved in a "one hit" operation
- In-direct hot stamping part geometry is achieved at the cold forming stage which is not a "one hit" operation
- Direct hot stamping part cannot have any "die lock" conditions that would require "slides" to be added to the die
- In-direct hot stamping utilizes a cold stamping stage, therefore the die can be of a conventional multi-stage type with slides if necessary
- Minimum recommended section width of 8 mm

10.10 Hot Stamping (Direct and In-Direct)

- Minimum inside corner radii of 5 mm
- Minimum draft angle of 3°
- Punch clearance of 15% of sheet thickness
- Shearing clearance of 10% of sheet thickness

10.10.5 Automotive Application

Hot stamped parts are ideally suited for the following automotive applications [8], [22], [7]:

- A/B/C pillars
- Rocker reinforcements
- Front & rear impact beams
- Front & rear headers
- Roof bows
- Center tunnel panels
- Seat cross members

10.11 Hydroforming

Hydroforming is a process of forming either a sheet or tube by the application of pressurized fluid in a closed die. [9]

In tube hydroforming, there are two major practices:

1. High pressure - tube is fully enclosed in a die prior to pressurization of the tube
2. Low pressure - tube is slightly pressurized to a fixed volume during the closing of the die

In tube hydroforming, pressure is applied to the inside of a tube that is held by dies with the desired cross sections and forms. When the dies are closed on the tube, the ends are sealed and the tube is filled with hydraulic fluid, the internal pressure causes the tube to conform to the die. Punches may also be incorporated in the forming die to punch holes in the work piece during the forming process.

Low pressure hydroforming simply re-shapes tubes, producing a very good shape, but is not as useful if better cross-section definition is required. High-pressure hydroforming, totally changes the tube shape and alters the length to circumference ratio by up to 50%. It gives very good tolerance control, being a highly robust process.

Figure 10.25 shows differences between high and low pressure hydroforming.

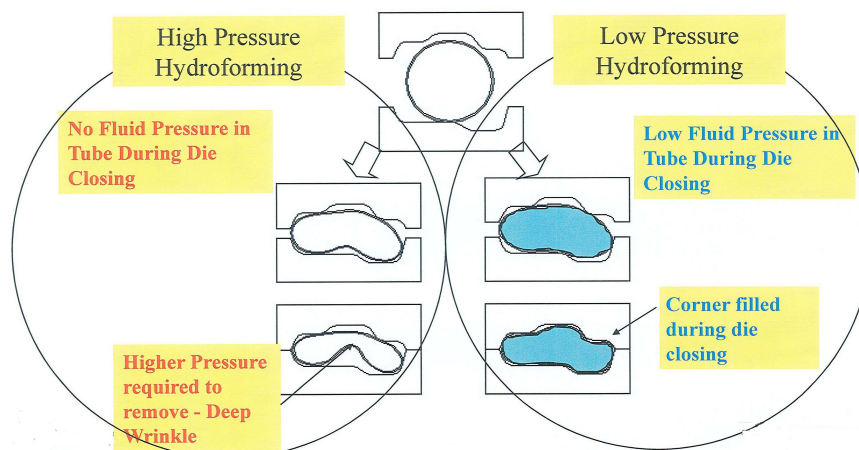


Figure 10.25: Low and high-pressure hydroforming differences

Tube hydroforming can be used to consolidate parts giving the added advantage of part weight reduction. Figure 10.26 shows the comparison between a hydroformed tube against a profile that is MIG welded together, and a profile that has spot welded flanges.

10.11 Hydroforming

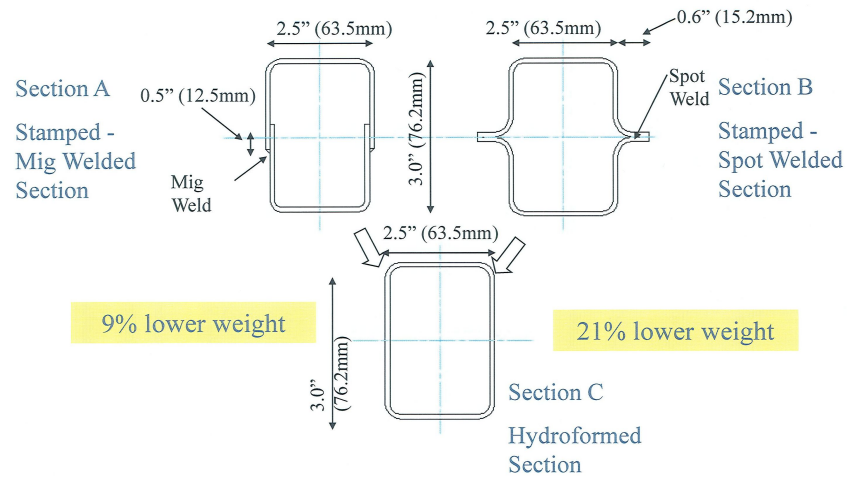


Figure 10.26: Hydroformed section comparison

Hydroforming can utilize the advantages given by laser welded tubes (both straight and conical), Multiwall T³ tubes, and extruded profiles. Figure 10.27 shows types of profiles that can be used in the hydroforming process.

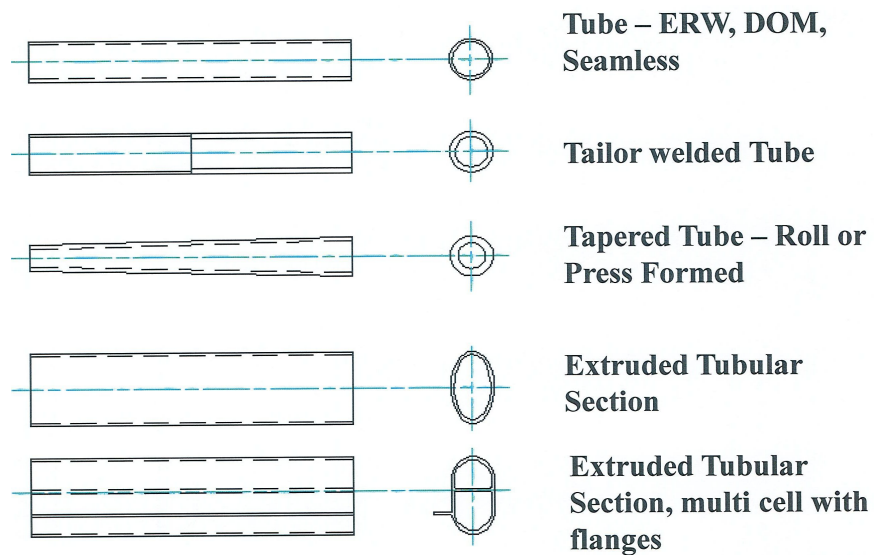


Figure 10.27: Profiles that can be used in hydroforming process

10.11.1 Guidelines

Dependent on the part final geometry, it may be necessary to perform a pre-bending / pre-forming operation. Figure 10.28 shows general guidelines for these operations, and Figure 10.29 shows guidelines for section expansion.

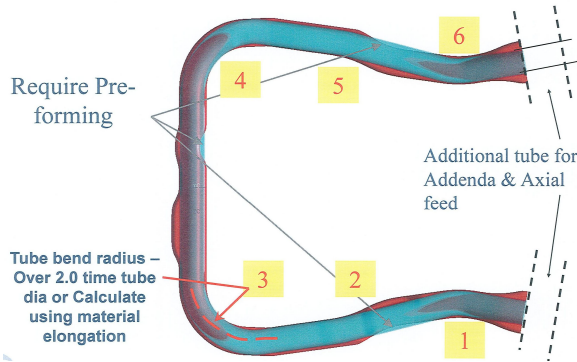


Figure 10.28: Pre-bending and pre-forming guidelines

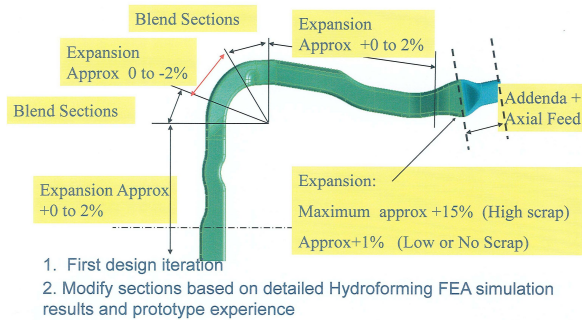


Figure 10.29: Section expansion guidelines

10.12 Stamping Advanced High Strength Steel

When stamping Advanced High Strength Steels (AHSS) in a conventional die, the part geometry needs to make allowances for the properties of the material. Integral to the design process when using AHSS, is the impute of CEA/FEA modeling and formability studies. Recommendations from these studies should be integrated into the final part geometry.

Primarily the increased strength leads to a tendency for greater springback than would be expected when using a lower strength steel. As the material strength increases, the part geometry has to be designed accordingly to avoid an unsatisfactory part.

10.12.1 Springback

Springback in the part can be a major issue when stamping AHSS. Springback can occur in the form of panel twist, side wall curl, under or over crown, side wall springback, and flange springback. This is a result of residual elastic recovery and is caused by the part material properties, stamping process and part geometry. To reduce the effect of springback, the part sidewall angles need to be designed "more open" for spring back allowances as material strength increases.

The recommended side wall angles for a range of materials are the following:

- DP-350 (6-degrees)
- DP-850 (8-degrees)
- DP-1000 (10-degrees)
- TRIP-450/800 (10-degrees)

Depressions or beads along the side wall and edge flange relief notches may also be added to help in minimizing springback.

10.12.2 Part Corner Radii

Apart from side wall angles, the part corner radii also impact the final part quality. These radii need to be increased from the norm used for lower strength steels. The minimum corner radii for advanced high strength steel, DP-600, is 3 x material thickness. This needs to be increased for higher strength materials.

10.12.3 Open Ended Profiles

The part geometry should equalize the depth of the part and length-of-line in the cross section, and lengthwise sections as much as possible. Longitudinal rails, cross members and pillars should be designed as open ended channels.

10.12.4 Surface Depressions

Where ever possible, dependent on the final part geometry and design requirements, any depression should be designed to be parallel to the main surface. Particular attention should be made to length-of-line as this may cause deformation of adjacent surface.

10.12.5 Flanged Holes

When a flanged hole is required, the length of the flange from the corner radii tangent line should be kept to 2 mm if possible. The flange open angles should follow the recommendations made to side wall angles.

10.12.6 Surface Transitions

For advanced high strength steel, any surface transition should be as gradual as possible to avoid buckles and twists in the part. Flange edge radii should be made as large as possible to avoid splits. [10]

10.13 Joining Strategy

A variety of techniques are possible for joining Advanced High Strength Steel (AHSS) such as the following:

- Resistance spot welding
- Laser welding
- Adhesive bonding
- Mechanical joining
- Hybrid joining

The selection of the joining strategy adopted should be evaluated against each method's advantages, part and joint design. Additionally inputs from CAE/FEA analysis and assembly engineering should be considered. Figure 10.30 shows types of joining methods used for a body-structure.

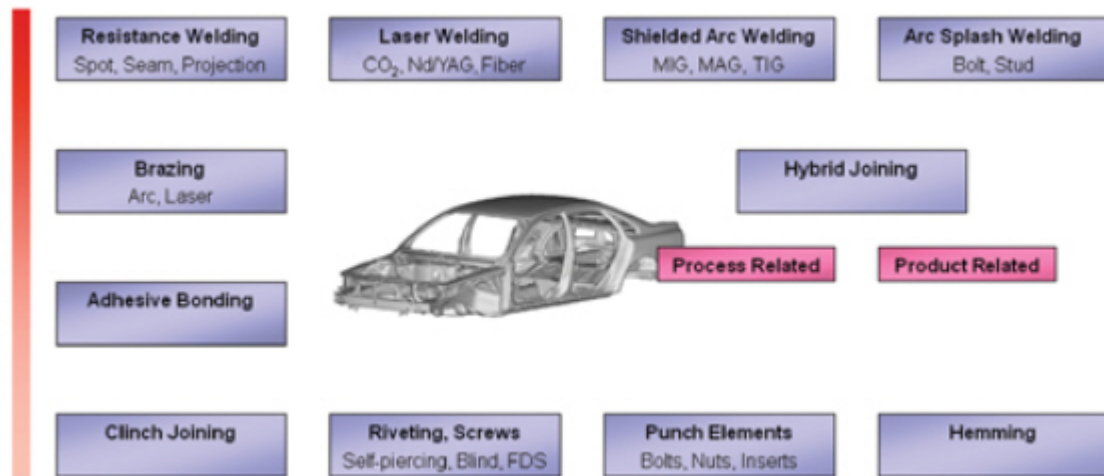


Figure 10.30: Types of joining methods used for a body-structure

10.13.1 Resistance Spot Welding

Any type of AHSS (CP, DP, TRIP), either coated or uncoated can be spot welded. This is the same process as for welding mild steel, except that the electrode force should be increased by 20%. As the material yield strength increases the electrode force increases.

Weld flange length should be designed to accommodate a standard 16 mm diameter spot weld electrode with 3 mm clearance between the electrode and any vertical surface feature. Generally a 6 mm weld nugget is generated, with the distance between center of nugget to the flange edge to be a minimum of 6 mm. Spot welding should only be used in a 2 or 3 panel thickness application. Panel thickness ratio is dependent on the grade of AHSS used, each joint condition should be evaluated with the assistance of assembly and welding engineering.

10.13.2 Laser Welding

Laser welding is a non-contact process that directs laser outputs of 2-10 kW into a very small area. This means that power levels in excess of 10^3 - 10^5 W-mm⁻² are produced on the surface of the parts to be welded. The laser beam makes a “keyhole” and the liquid steel solidifies behind the traversing beam, leaving a narrow weld and a heat affected zone. The weld is approximately 1 mm wide and the surrounding material is not distorted. Because the weld bead is small, there is usually no need for finishing or re-working, thus reducing the costs. In the case of zinc-coated steels, the narrow weld also means that it is protected by the sacrificial galvanic corrosion in the adjacent zinc layers. As access for welding is required from one side only, many different joint configurations are possible than were previously available.

In addition to the other advantages of using laser welding, there is a benefit from the process due to the narrow weld bead resulting in the reduction of the weld flange, thus leading to a vehicle weight savings. The width of the weld flange is dependent on the type of laser head used, and should be determined after consultation with welding engineering. Flange to flange clearance is more critical than for spot welding, so part quality should be monitored during the forming process.

10.13.3 Adhesive Bonding

In a vehicle body-structure, practically all components can be bonded using industrial structural adhesives. The benefits of structural adhesives are particularly evident when different materials need to be bonded to each other. This is even more important when dealing with a mix of lightweight construction materials, where bonding would not be possible without adhesives. For example a typical mid-sized vehicle requires approximately 4,000 weld points. It is possible to replace more than half of these with adhesive joints, hence reducing vehicle costs and mass.

The following steps should be followed when using adhesives combined with spot welding or other mechanical joining methods: application of adhesive, clamping, and then spot welding or mechanical joining. Weld/mechanical joining bonding is typically a three step process as shown in Figure 10.31.

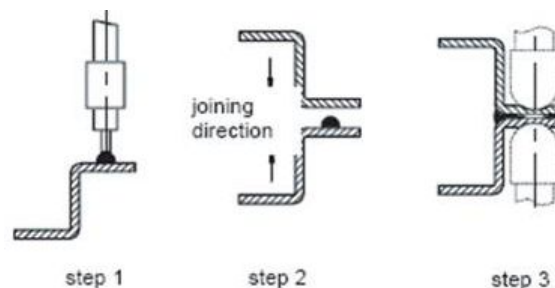


Figure 10.31: *Weld bonding process*

10.13.3.1 Adhesive Bead Length

Bead lengths less than 50 mm should be avoided due to application variations. Stop-start bead lengths should also be avoided.

10.13.3.2 Spot Weld Spacing

The distance between individual spot welds or mechanical fasteners should be no greater than 100 mm. At distances greater than 100 mm additional means may be necessary to ensure joint compression during adhesive curing. This is of particular importance when the adhesive is cured during the vehicle paint system, where the steel panel may result in a no bond condition between the steel and adhesive due to thermal expansion in the e-coat oven.

10.13.3.3 Joint Gaps

The ideal joint gap for the most effective adhesive bonding is 0.2-0.5 mm. Joint strength is greatly reduced with joint gaps lower than 0.1 mm or greater than 1.4 mm, these two extremes should be avoided.

10.13.3.4 Steel Substrate

Zinc coatings are required on steel to prevent adhesive under-cutting in corrosive environments. Galvannealed coatings are not recommended for bonding applications where joint integrity is necessary in dynamic loading conditions. Galvannealed steels can be used for stiffness, fatigue and durability conditions.

10.13.4 Mechanical Joining

Generally, mechanical joining of panels refers to the use of "Self Piercing Rivets" (SPR). Figure 10.32 shows an example of self piercing rivet.



Figure 10.32: Self Piercing Rivet

Self Piercing Riveting is a cold forming process used to join two or three layers of material by

driving a rivet through the top layers of material, and upsetting the rivet in the lower layer without piercing the lower material. The self piercing rivet head can be manually positioned and operated, by mounting the rivet head on a robot arm for a fully automated operation. Figure 10.33 shows the self piercing riveting process.

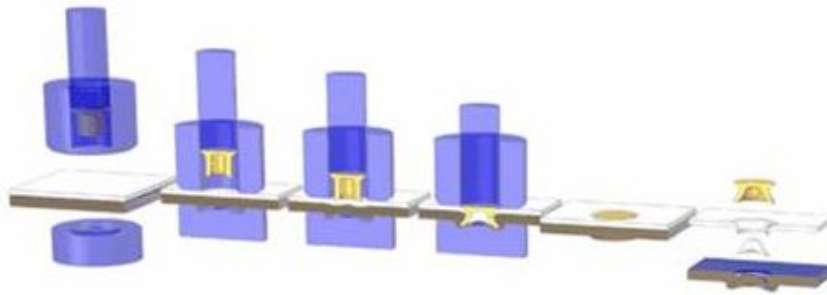


Figure 10.33: *Self Piercing Rivetting Process*

Total material stack-up depends on the material specification used, but generally ranges from 0.6 mm to 10.0 mm, two or three layer material thickness is feasible. Flange width is dependent on the material thickness stack-up. The higher this is, the larger the rivet diameter needs to be. When joining a flange, for example a window opening, follow the guide lines required for a spot weld flange. When joining parts that do not have a flange condition, the only clearance issue is concerning the diameter of the setting head. The surface at the site of the rivet needs to be flat normal to the axis of the rivet and should have a minimum additional clearance of 5.05 mm to any surface feature.

10.13.5 Hybrid Joining

Hybrid joining of panels is a combination of two or more fastening methods, and is employed to attach similar or dissimilar materials. One example is a mechanically fastened joint (i.e., bolted or riveted) that is also bonded with adhesive. These types of joints could provide a compromise between a familiar mechanical attachment that has proven reliability, and the reduction of problematic issues such as stress concentrations and crack sites introduced by using mechanical fasteners with polymeric composites. The use of hybrid joining could also lead to other benefits such as increased joint rigidity, contributing to overall stiffness gains and a reduction of vehicle mass.

Additionally, the use of adhesives in conjunction with mechanical fasteners could significantly reduce stress concentrations, which serve as locations for crack propagation. Hybrid joining methods can also provide additional joint integrity to allow increased spacing between fasteners or welds.

For details on joining flange sizes & panel-to-panel gaps see sections above. Additional information on joining guide lines can be obtained from:

- WorldAutoSteel AHSS guidelines Section 3, (Joining).
- Auto/Steel Partnership (A/S P) Future Generation Passenger Compartment, (Joining Sensitivity).
- Auto/Steel Partnership (A/S P) Automotive Steel Design Manual (Revision 6.1, 2002)
- Auto/Steel Partnership (A/S P) Weld Bond Adhesive Guidelines

11.0 Other Advanced Technologies

11.1 Drive-by-Wire

11.1.1 Overview

As a part of this engineering assessment on drive by wire systems as viable options for mainstream production on FSV1 and FSV2 by 2020, four types of Drive-by-Wire systems were looked at:

1. Brake-by-Wire
2. Throttle-by-Wire
3. Steer-by-Wire
4. Active suspension (By-Wire control)

Based on its research, the FSV engineering team strongly believes that of the four systems, only Brake-by-Wire and Throttle-by-Wire are viable production oriented technologies, as these provide a mass savings of approximately 3 kg, and packaging advantages that significantly change the front end structure of the vehicle while overcoming its current design challenges.

“By-Wire-Systems” require a robust and reliable 42 V battery system, available on FSV-1 and FSV-2 high performance and high voltage batteries. This technology provides a means for the FSV team to arrive at a much optimized front-end packaging while reaping the other benefits of such a system.

At present, there are “partial” Brake-by-Wire systems that have some type of fail-safe hydraulic backup built into the system that provides minimal braking (limp home condition) in case of a complete electrical failure in the vehicle and/or the Brake-by-Wire system. However, all future developmental work currently being undertaken in terms of fault tolerant electronics in this regard lead us to conclude that a complete Brake-by-Wire system with no hydraulic backup shall be a production technology of the future (2020).

With the timeframe that FSV-1 and FSV-2 vehicles are targeted for production, the FSV engineering team believes that steer by wire is not a viable technology due to its inherent challenges in terms of safety and reliability of the system, and its fault tolerance. As can be seen in figure 9.2, the sizes of the components required are similar to a conventional steering system

and the use of Steer-by-Wire does not lead to any significant mass saving. It is well regarded that at present, the use of a steering wheel is essential for providing the sensory tactile feedback of the car's tire contact with the road (road feel) that is especially necessary during high-speed driving, allowing the driver to make steering adjustments based on his perception of the car's contact with the road. In the case of Steer-by-Wire, this is accomplished with either a tactile-feedback device (see section 9.2.7.2), or a similar stiff structural mounting as a conventional hydraulic assisted steering system, to transmit (control) vibrations at the steering wheel for the perfect balance of "road feel", without harshness. The apparent lack of a mass savings in a Steer-by-Wire system is not the main factor why the FSV engineering team believes that Steer-by-Wire is not a viable technology, but rather it's need for further development of robust failsafe and redundant systems. (See section 9.2.9.1)

On the FSV structure, the positioning of the steering rack will not yield any additional packaging gains as the front length has been reduced to the minimum required to meet the 5-star crash rating.

Advantages of Drive-by-Wire Systems

- The systems react more quickly, and thus are more responsive than their mechanical equivalent
- No non-linearities and losses due to friction and flexing of materials
- Performance increases due to increase in responsiveness
- Very versatile, more efficient vehicle packaging space
- Faster electronic actuators are lighter and take up less room
- Costs less than current alternative
- Diagnostic capabilities are inherently increased
- Vehicles have fewer parts, thus reducing the cost and time of assembly

11.1.2 Types of By-Wire Systems

- Steer-by-Wire
- Brake-by-Wire
- Throttle-by-Wire (Cruise control systems)
- Active suspension (By-Wire control)

See Figure 11.1 for applications of "By-Wire" systems.

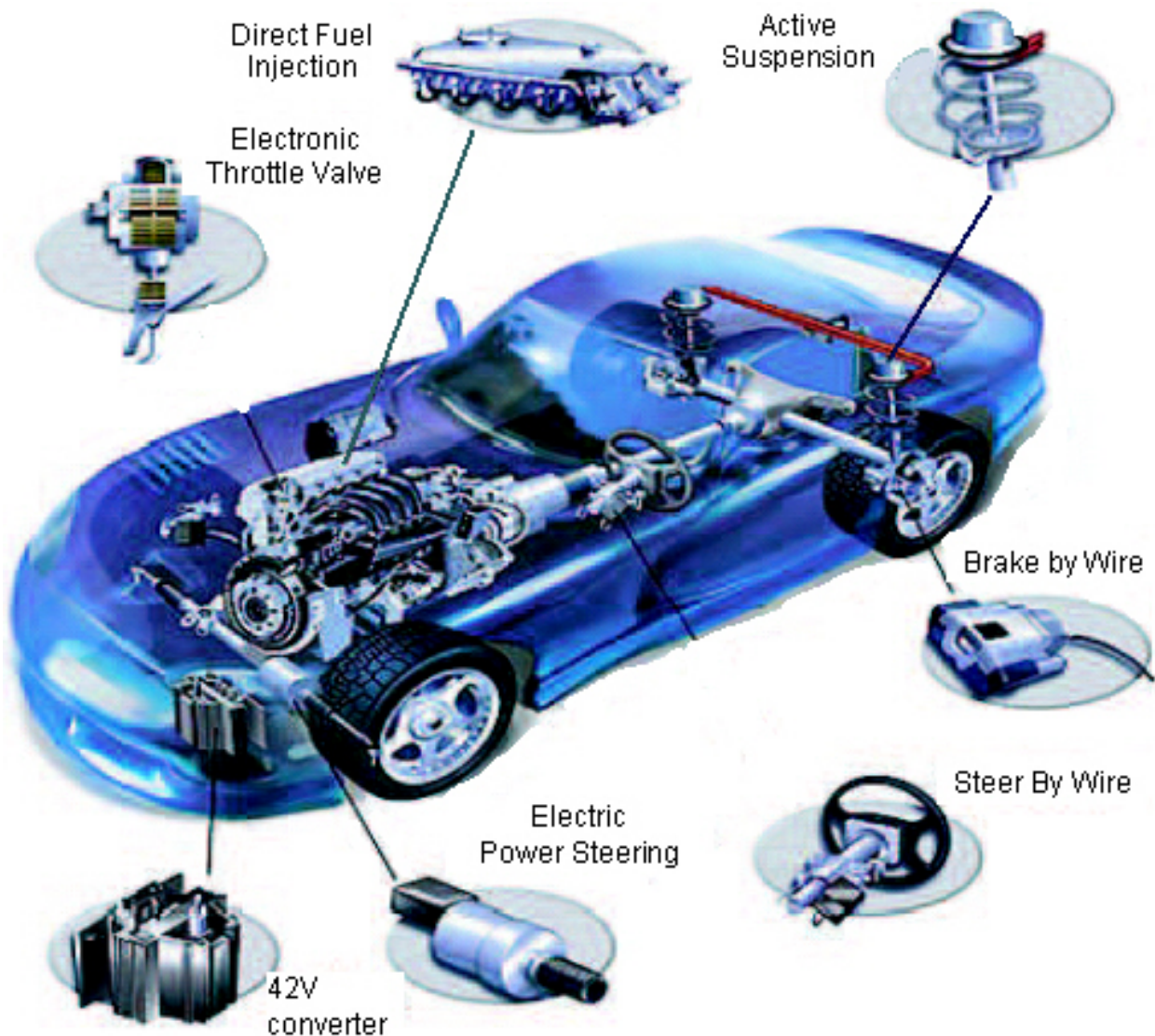


Figure 11.1: Automotive applications for by-Wire technology. Credit: Motorola

Among these above mentioned systems, Throttle-by-Wire and shock (suspension) control have been proven, tested and accepted by the automotive industry today.

The newer and more safety critical technologies like Steer-by-Wire and Brake-by-Wire are under development, and this technology assessment concentrates on the pros and cons of such a system and its implementation challenges into the mainstream automotive production cycle.

11.1.3 Assessment Scope

This document is a technical description of the Steer-by-Wire and Brake-by-Wire technology. It discusses system architectures, redundancy, sensors, actuators, and their implementation together with the effect these have on safety and performance.

The final implementation of each of these technologies is application specific and must take into account the high level of safety and robustness required while providing high performance and feel.

The steering and brake systems in a vehicle are safety critical systems. The risk must be minimized while achieving a sensible and cost effective solution.

Since the main incentive to introduce Steer-by-Wire and Brake-by-Wire from the current well understood mechanical components is to improve safety and operational efficiencies, their By-Wire replacements must exceed all parameters of conventional system performance in a lightweight design.

These electronic systems are designed to have multiple redundant systems with no single point of failure for all components, including sensors, actuators, and control & power systems. For such systems, it may be worth looking at aerospace and military approaches where in order to detect a failure and continue to operate safely, a desired dependability of 10^{-9} ^{[1][2]} is preferred, and only dual and triplex systems can provide that required level of failure detection and recovery performance.

¹The Failures in Time (FIT) rate of a device is the number of failures that can be expected in one billion (10^9) hours of operation.

²In practice, the closely related Mean Time To Failures (MTTF) is more commonly expressed and used for high quality components or systems. MTTF is an important specification parameter in all aspects of high importance engineering design

11.2 Steer-by-Wire

11.2.1 Overview

The Steer-by-Wire system works by replacing the conventional mechanical steering system with an electronically controlled system. Instead of relying on a mechanical shaft that connects the steering wheel to the steering rack, steer by wire consists of sophisticated sensors that closely tracks the position of the steering wheel relative to the vehicle wheels. It then sends this information to the Electronic Control Module (ECM) which in turn sends the appropriate signal to the steering actuator which moves the driven wheels accordingly. This is superior to a mechanically operated system for the following reasons:

- Steer-by-Wire reduces the number of mechanical parts in the steering system. This means greater accuracy and theoretically, no service requirements (no hydraulic fluid)
- The greater accuracy not only improves the driving experience by increasing responsiveness, but also increases the safety of the vehicle. This is achieved by the system being interfaced with other safety systems like electronic stability control which can offer more control over the vehicle in terms of over-steer and under-steer (as compared to the typical user input)
- One of the most attractive benefits of Steer-by-Wire is its Active Steering^[3] capability, which when supplied with continuous knowledge of a vehicle's dynamic behavior, can be used to modify the vehicle's handling dynamics
- Another benefit of Steer-by-Wire is the availability of steering torque information from the actuator current. Because part of the steering effort goes toward overcoming the tire self-aligning moment, which is related to the tire forces and, in turn, the vehicle motion, knowledge of steering torque indirectly leads to a determination of the vehicle's dynamic behavior, the essential element of any vehicle dynamics control system
- Finally, with Steer-by-Wire, previously fixed characteristics like steering ratio and steering effort are now infinitely adjustable to optimize steering response and feel

³Active Steering is an automotive technology which varies the degree that the wheels turn in response to steering wheel inputs. The steering system electronic response time to sensory inputs is less responsive at lower vehicle speeds and more responsive at higher vehicle speeds, allowing for quick response of the driven wheels to steering wheel inputs. This is in direct contrast to the steering power boost assist function, which provides more boost at lower speeds to reduce steering efforts, and less boost at faster speeds.

11.2.2 General Requirements for Steer-by-Wire

- Must be reliable and responsive
- Controller must demonstrate a complete control of the steering system
- Packaging must be compact and non-intrusive
- Must provide adequate feedback (road feel) to the driver

11.2.2.1 Conventional Steering vs. Steer-by-Wire

The major hardware changes required to convert a conventional steering system to a Steer-by-Wire system is shown in Figure 11.2.

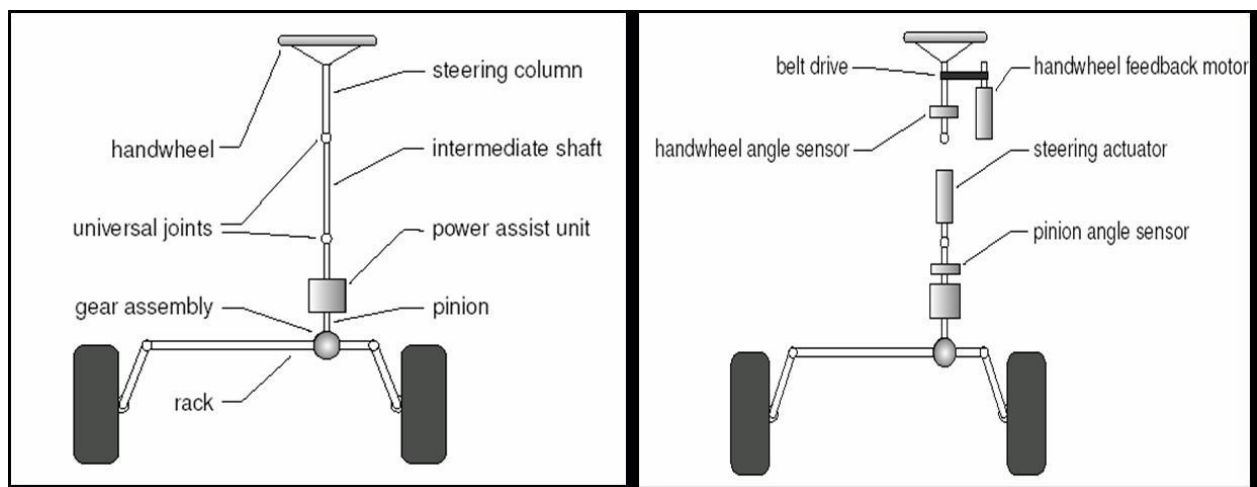


Figure 11.2: *Conventional steering vs. Steer-by-Wire*

11.2.2.2 Required Hardware for Steer-by-Wire

Sensors:

- Steering position and velocity, both at steering wheel and road wheels
- Torque measurement devices for both steering and road wheels (for force feedback)
- Sensors used for lateral acceleration, yaw rate, etc.

Actuators:

- Electronic Control Unit (ECU)

See Figure 11.3 and Figure 11.4 for typical Steer-by-Wire schematic and system hardware.

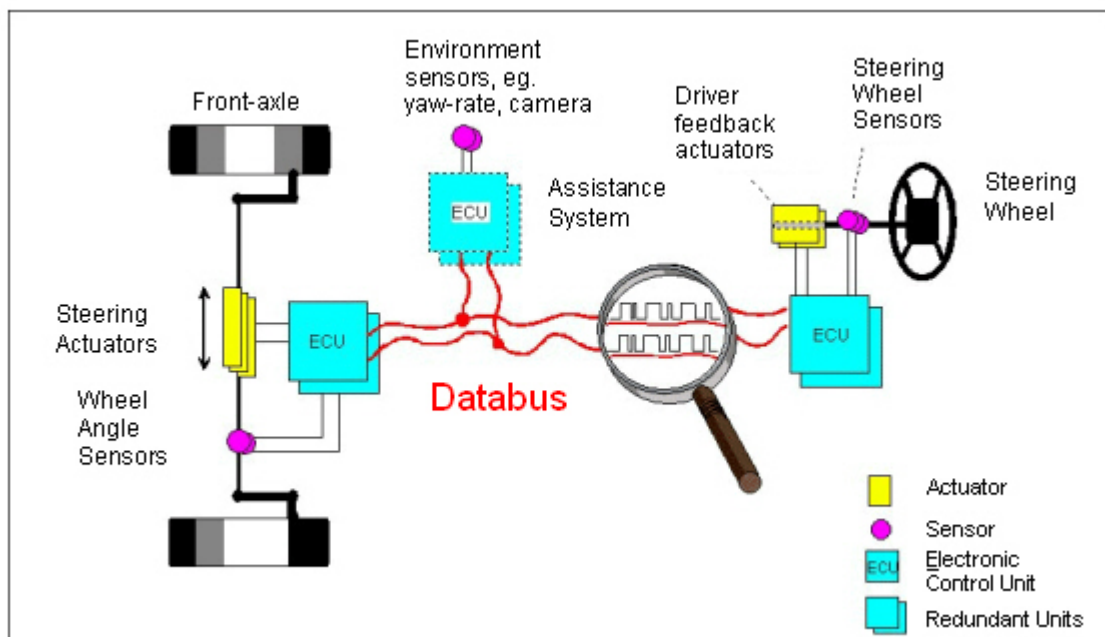


Figure 11.3: Typical Steer-by-Wire schematic

11.2 Steer-by-Wire

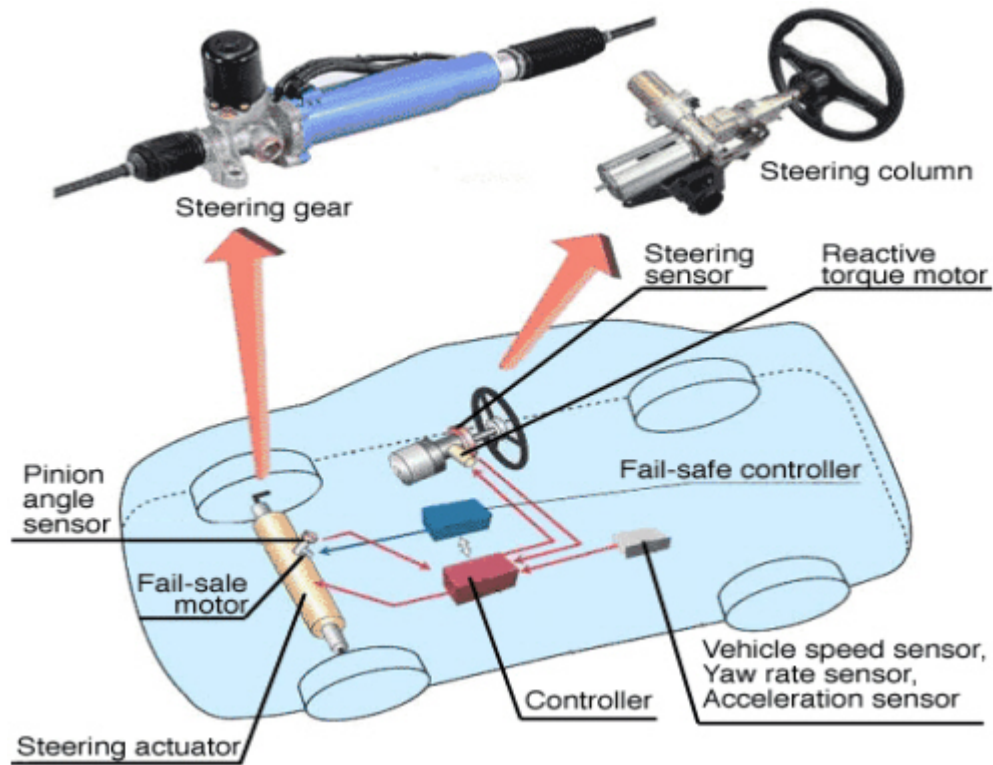


Figure 11.4: Typical Steer-by-Wire system (with hardware)

11.2.3 Types Of Steer-by-Wire Systems

Steer-by-Wire systems are classified into two types based on their actuation methods. Both of these systems differ from a conventional system in the fact that they both have no mechanical connection from the steering column to the steering rack. The two types of actuation methods are:

- Electric/Electro-mechanical
- Hydraulic

11.2.3.1 Electric/Electro-Mechanical

Replace input from the steering column into the steering rack with an electric actuator and, either a separate actuator mounted on the steering rack controlling both wheels as shown in Figure 11.5, or with a single electric actuator mounted at both front wheels, providing independent control of each road wheel as shown in Figure 11.6.

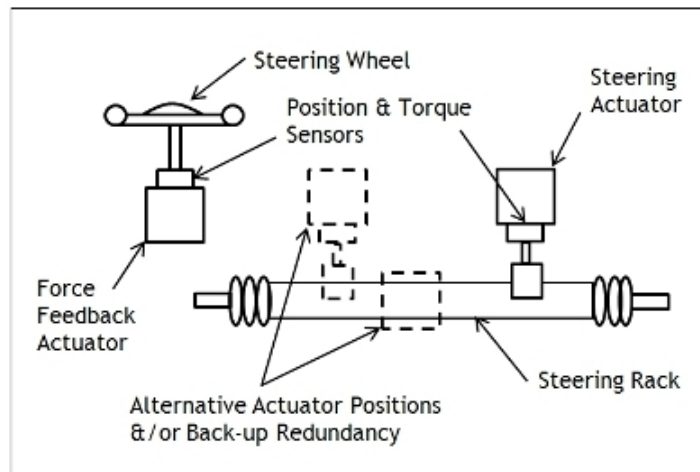


Figure 11.5: *One motor controls both wheels via a steering rack*

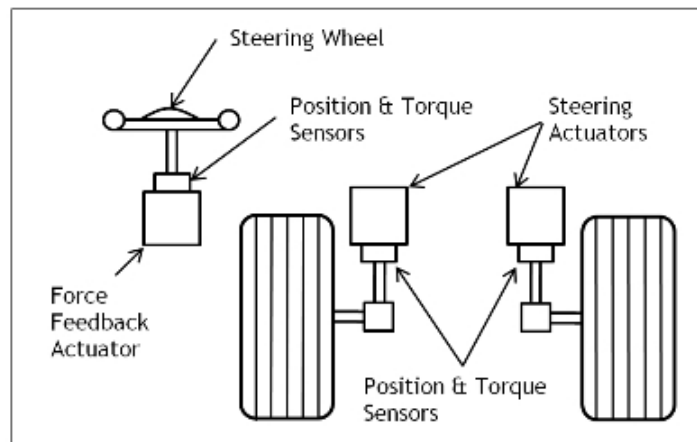


Figure 11.6: *Individual actuators control each wheel*

Advantages

- Easy method of modifying a vehicle from a conventional system to Steer-by-Wire, by removing a conventional hydraulic system's pump and hoses, and replacing the steering rack with a new electrically driven actuator, and a new steering column with an electric

11.2 Steer-by-Wire

- actuator, which has no mechanical connection to the steering rack
- Increase in fuel economy, resulting from the elimination of parasitic losses that a conventional hydraulic pump has on a car engine

Disadvantages

- As compared to a conventional system, there are possible packaging constraints due to the large electric actuators on the steering column and rack.

11.2.3.2 Hydraulic Only Actuation Method

Power assisted steering racks provide the steering actuation with a series of hydraulic control valves to provide control over the rack position, as shown in Figure 11.7.

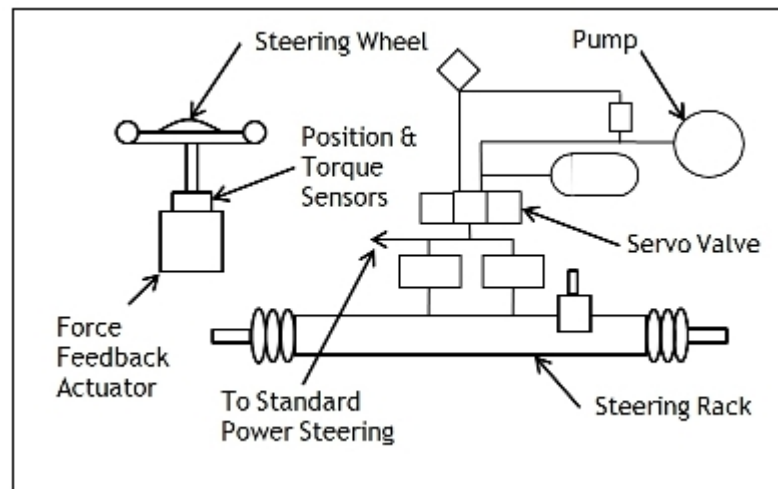


Figure 11.7: *Hydraulic only method*

Advantages

- Easy method of modifying a vehicle from a conventional system to Steer-by-Wire, by replacing the steering column with a new column that uses an electric actuator, and has no mechanical connection to the steering rack. Also needed is a modified hydraulic steering rack with a servo valve which provides a control feedback loop to the steering column

Disadvantages

- As compared to a conventional system, possible weight and packing constraints due to the large electric actuator fitted to the steering column, and the addition of a servo valve and other hydraulic control components located on the steering rack

11.2.3.3 Actuators

Steer by Wire requires the use of actuators for two reasons:

- To provide correct positioning and sufficient force to control the steering rack
- To provide meaningful feedback to the driver via the steering wheel

This is currently achieved by the use of high voltage (42 V) DC motors. Redundancy would not be required for the feedback but is definitely required for the steering actuation which could be achieved through a number of solutions including twin motors connected via a gearbox.

There are two main requirements with respect to a power supply for Steer-by-Wire technology:

- Sufficient power for steering
- Redundancy

The main power system has to be of higher voltage than the currently available 12 V supply (either a 24 V or a 42 V), and the redundancy can be achieved by using the vehicle's conventional 12 V battery (albeit at a reduced performance level).

11.2.4 Real Time Performance & Reliability Requirements

Car manufacturers looking to replace conventional steering systems with Steer-by-Wire systems, must satisfy stringent real time performance and reliability requirements. An automotive Steer-by-Wire system is a safety critical system and manufacturers should make sure that a Steer-by-Wire system in a production car has a very small probability of failure.

Although regulating organizations have not established a specific automotive requirement on probability, the 10^{-9} [4][5] failures/hour requirement for the aircraft industry applies. The reliability, (probability that a system will fulfill the service a user expects), is computed with the Mean Time To Failure (MTTF) $\frac{1}{e}$ (where "e" is the failure rate) according to the failure distribution: $R(t)=P(\frac{1}{e}>t)$. So, depending on the mission phase of the vehicle, the safety of the system can sometimes be considered the same as the reliability of the system. For the given MTTF of the components (sensors, computers, network links, actuators) and their redundancy, static reliability analysis can give the total reliability of the Steer-by-Wire system.

⁴The Failures in Time (FIT) rate of a device is the number of failures that can be expected in one billion (10^9) hours of operation.

⁵In practice, the closely related Mean Time To Failures (MTTF) is more commonly expressed and used for high quality components or systems. MTTF is an important specification parameter in all aspects of high importance engineering design

11.2.5 Mean Time to Failure Greater Than Life of the Vehicle

In fact, a Steer-by-Wire system is also time-critical and its reaction time directly impacts the safety of the car. For instance: The delay introduced by a Steer-by-Wire system between the driver's request and the activation of the wheels can be considered as a performance measure until a certain threshold value is reached, and then considered as a dependability measure after the threshold value is reached, since in this case the driver loses all control of the vehicle.

The illustration in Figure 11.8 shows the pure delay introduced by the Steer-by-Wire system between hand wheel requests, to the reaction of the driver's request by front axle actuators. It also shows the total response time of the system, which is the sum of the hand wheel request time and front axle response time divided into the pure delay and mechatronics delay time.

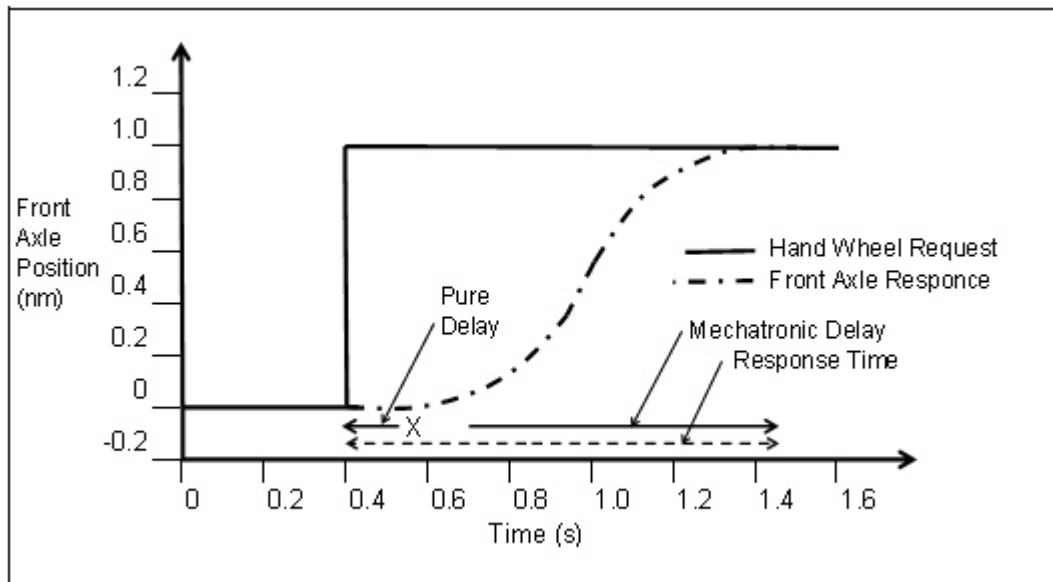


Figure 11.8: Delay introduced by Steer-by-Wire

The mechatronic delay is the time required for the actuator to reach front axle position, and pure delay is directly related to the delay in processing time by the CPU and other network delays.

11.2.6 Response Time

The evaluated criterion is called Quality of Service (QoS) as perceived by the user depending on the response time of the system, which may also impact the safety of the system.

Table 11.1 shows the comparison of a conventional mechanical steering system as compared to Steer-by-Wire systems in terms of pure delay time and QoS score.

Steering System Configuration	Pure Delay (ms)	Score N
Mechanical System	0	11.23
Steer by Wire	5	11.21
Steer by Wire	10	11.19
Steer by Wire	15	11.15
Steer by Wire	20	11.13
Steer by Wire	25	11.1
Steer by Wire	30	11.05
Steer by Wire	35	11
Steer by Wire	50	10.9
Steer by Wire	100	10.45

Table 11.1: *Conventional mechanical steering system versus Steer-by-Wire systems*

After the critical limit is reached for the pure delay, the system becomes unsafe for operation.

All these factors make it even more important to evaluate the real time performance of the Steer-by-Wire system and not only the reliability factor of 10^{-9} [6][7].

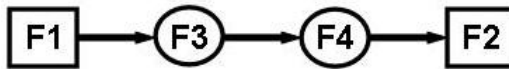
⁶The Failures in Time (FIT) rate of a device is the number of failures that can be expected in one billion (10^9) hours of operation.

⁷In practice, the closely related Mean Time To Failures (MTTF) is more commonly expressed and used for high quality components or systems. MTTF is an important specification parameter in all aspects of high importance engineering design

11.2.7 Tactile Feedback Control

11.2.7.1 Functional Architecture

There are four main functions identified in considering the functionality of “turning the wheels according to the user’s will”:



They are defined as:

- F1:** Hand wheel position acquisition (sensor)
- F2:** Front axle activation (actuator)
- F3:** Hand wheel measure treatment (ECU)
- F4:** Front axle order computation (ECU)

In most electrical systems, an encoder or similar sensor detects steering wheel movements, direction, magnitude, speeds, etc, and sends inputs to an onboard controller. It interprets the signals and then commands the electro-mechanical actuators to turn the wheels accordingly.

Position sensors on the actuators close the feedback loop with the controller, ensuring the vehicle wheels match steering commands.

Without the traditional mechanical steering link, however, developers of by-Wire controls discovered early on that the loss of tactile feedback often degraded control. It caused problems such as over or under-steer and compromised safety. Overcoming this drawback often requires a Tactile-Feedback Device (TFD) that connects to the steering wheel and mimics the feel of mechanical systems. For example, a TFD can increase steering effort to tell the operator he’s hit an obstruction by vibrating the steering wheel to indicate mechanical failure.

TFD’s can incorporate vehicle warning systems, end stops (end of-travel indication), and variable effort steering to enhance control, minimize over-steer and under-steer, and improve safety. Furthermore, ongoing efforts to develop standards and common vehicle interfaces may cut engineering and operator training costs.

11.2.7.2 Tactile Feedback

In “By-Wire systems”, optical or magnetic Hall-effect encoders or potentiometer-resistive sensors near the wheels or suspension will sense motion. The controller receives the data and, in turn, drives the TFD. Tactile feedback algorithms modulate the torque an operator feels as a function of steering wheel rotational position, velocity, acceleration, wheel position and speed, and so on.

There are two potential ways to achieve this feedback control:

- Magnetically Responsive (MR)
- Variable Rate Steering (VRS)

11.2.7.3 Magnetically Responsive Tactile Feedback Type Devices (MR)

Design engineers have several options when it comes to TFDs. For instance, feedback based on proportional Magnetically Responsive (MR) technology is used in lift trucks and marine propulsion systems. MR-based TFDs offer advantages over torque generating devices such as electromagnetic friction brakes and motors. For example, MR feedback generates smooth torque with no stick-slip or cogging, and the units tend to be smaller and consume less power. Better energy efficiency improves fuel economy on conventional vehicles and extends run time and battery life on all electric ones.

Inside MR-based TFDs, a coil generates a magnetic field that spans the gap between a rotor and stationary pole (stator). A magnetically responsive material fills the gap between rotor and pole.

If there is no magnetic field present, the rotor turns freely inside the housing. When the coil is energized, however, the magnetic field causes the iron particles to form molecular “chains”. The result is torque on the output shaft proportional to the input current. The response takes about 10 ms, permitting fine control of torque output. This gives designers the possibility of a wide range of control. For instance, steering “feel” can be fairly light, almost free spinning, or offer moderate resistance. Vehicle manufacturers also specify the number of turns from full left to full right.

When the steering actuators reach their travel limits, the controller increases current and torque in the TFD so the driver cannot turn the wheel any further, or the system can generate a different tactile feel, such as pulsing.

11.2.7.4 Variable Rate Steering

Another option is variable rate steering. It offers more-precise control at low speeds. An industrial truck, for instance, might offer two or three steering wheel turns, lock to lock, for maneuvering at low speeds. The TFD automatically adjusts the range to six or more turns for less sensitivity at high speeds. This helps prevent violent turns and rollovers.

Likewise, the system can be programmed to limit the change rate of steering, regardless of how quickly the operator might turn the steering wheel, the controller limits how fast the wheels respond to prevent loss of control.

TFDs can also simulate inertia. Quickly turning from full left to full right requires some effort to overcome inertia in mechanical systems. Electrical steering without TFD does not have that sensation. But applying a ramping, varying current to the TFD will simulate the inertia found in mechanical systems.

11.2.8 Regulatory Requirements for Steering Performance

ECE Regulation 79.01 is predominantly a European regulation for certification of vehicle steering performance. This regulation has now been accepted by a number of other nations who either accept this regulation in its originality or have their own regulation that is widely based on ECE R79.01.

ECE R79.01 has been recently updated to include clauses allowing the use of Steer-by-Wire systems on passenger vehicles and trucks.

The excerpt below is taken directly out of the regulation.

“The intention of the regulation is to establish uniform provisions for the layout and performance of steering systems fitted to vehicles used on the road. Traditionally the major requirement has been that the main steering system contains a positive mechanical link between the steering control, (normally the steering wheel), and the road wheels in order to determine the path of the vehicle. The mechanical link, if amply dimensioned, has been regarded as not being liable to failure.

Advancing technology, coupled with the wish to improve occupant safety by elimination of the mechanical steering column, and the production advantages associated with easier transfer of steering control between left and right hand drive vehicles, has led to a review of the traditional approach and the regulation is now amended to take account of the new technologies.

Accordingly, it will now be possible to have steering systems in which there is not any positive mechanical connection between the steering control and the road wheels”.

11.2.9 Conclusions

After reviewing the two different technologies in detail, the engineering assessment lead us to the conclusion that Steer-by-Wire will not be a viable “production ready” technology by 2020. The conclusion was based on the following facts:

1. Steer-by-Wire requires a very high degree of redundancy built into the system in order for the system to be as robust as the current mechanical system. Such a system requires more development and testing
2. Such a system will require high speed communication protocols capable of data transfer rates of about $10 \frac{MB}{s}$ (current industry standard is $2 \frac{MB}{s}$). New communication protocols capable of handling such high speed data transfers are very few (Flexray, TTCAN) and are in their early stages of development
3. Systems like steering control require a very precise tactile feedback to the driver and require intensive development and testing
4. Most OEMs have looked into this technology and have “prototypes”, but have not announced any plans of mainstream production using this technology in the near future
5. The weight savings on this type of system is negligible, and does not impose a radical change to the vehicle structure

11.3 Brake-by-Wire

Brake-by-Wire is a next generation braking system designed to stop vehicles by using electrical signals, rather than by a hydraulic system as used on most conventional brake systems today. See Figure 11.9 for layout of a conventional and future EMB brake system.

Brake-by-Wire eliminates all brake fluids and hydraulic lines as well as most mechanical parts customarily associated with brakes and is replaced with a system controlled by small computer chips.

Brake-by-Wire technology has been under development within various OEMs for some time now and seems like a viable technology for production by 2020. We base our conclusion on these following facts:

1. Brake-by-Wire had been used on premium vehicles (Mercedes) for a few model years and discontinued. The system relied on a hydraulic backup (redundancy system), in case of electrical system failure. This leads us to believe that the technology has a few “bugs” that needs to be worked out in the next few years
2. A few brake suppliers have developed and tested this technology and believe it is production ready (Siemens, Continental Teves, TRW Automotive)
3. Elimination of the brake booster offers a significant advantage in terms of engine compartment packaging and weight savings

11.3.1 Types Of Brake-by-Wire Systems

- Electro Hydraulic Braking (EHB) – Hydraulic backup present
- Electro-mechanical Braking (EMB) – No hydraulic backup present
- Hybrid Braking – Combination of conventional braking and EMB
- Electronic Wedge Braking (EWB) - Siemens developed (uses 12 V)

11.3.2 Advantages Of Brake-by-Wire Systems

- Shorter braking and stopping distances because of multi-point sensor feedback and control
- Optimized braking and stability behavior due to interaction with braking/stability systems listed below
- No pedal vibration during ABS mode (Anti-lock Braking System)
- Improved crash avoidance because of better vehicle control
- Improved packaging, less installation effort, because there is no hydraulic components to install
- Can be easily networked with future traffic management systems
- Capable of realizing all required braking and stability functions such as:
 - ABS - Anti-lock Braking Systems
 - EBD - Electronic Brake-force Distribution system

11.3 Brake-by-Wire

- TCS - Traction Control Systems
- ESC - Electronic Stability Control
- BAS - Brake Assist Systems
- ACC - Adaptive Cruise Control systems

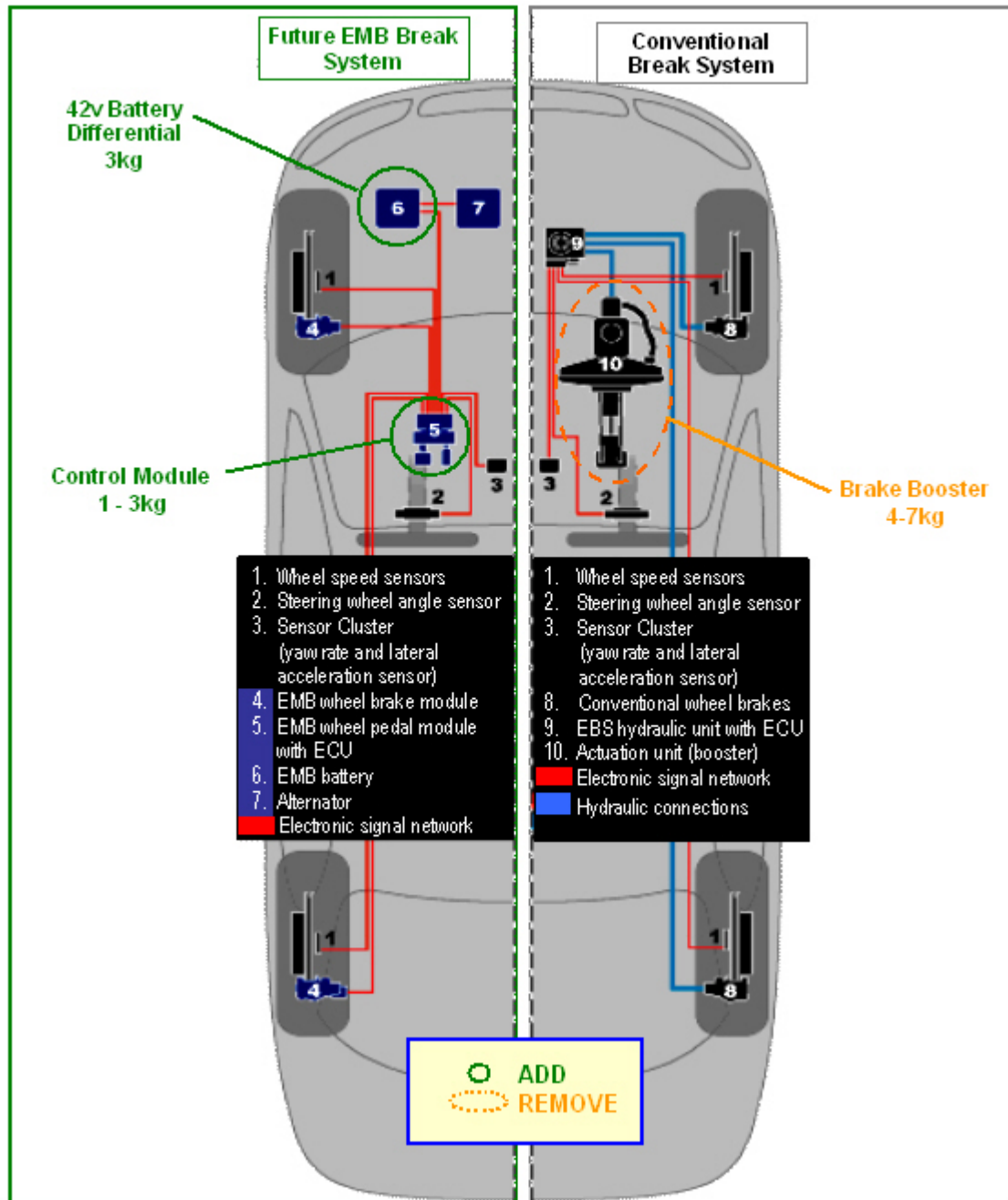


Figure 11.9: Conventional and future EMB brake system [11]

11.4 Current Challenges to the Auto Industry

As far as the industry is concerned, it is only a matter of time before Drive-by-Wire becomes standard. But some safety experts are questioning the wisdom of this radical change. They point out that Fly-by-Wire has a bumpy track record. [New Scientist, 8 Nov. 2003]

Drive-by-Wire is harder to implement in cars rather than in airplanes because of costs and the fact that the system may need continuous scheduled maintenance, as in the aviation industry. Also Fly-by-Wire in airplanes needs less precision than that of Drive-by-Wire systems in automobiles.

Drive-by-Wire may have to be proven first in a secondary system, such as the parking brake, before consumers grow more comfortable with the idea of replacing the traditional primary control systems in their vehicles. [Business Wire, 12 Dec. 2002]

Steer-by-Wire for cars is much harder to implement because of costs, reliability without maintenance and required steering precision in the range of < 1 cm.

Conventional servo power steering is the pre-runner of Steer-by-Wire; however, power steering is on an electro-mechanical basis and has a physical connection between the steering wheel and front wheels.

11.4.1 Costs

One of the biggest challenges to the growth and acceptance of Steer-by-Wire systems has been the cost, or perceived cost, according to Markus Plankensteiner, consortium coordinator for the TTA-Group based in Vienna, Austria. The group, a cross-industry consortium researching highly dependable time-triggered systems^[8], is developing certifiable architectures for By-wire systems that will not need mechanical backup for on road use. The objective is to develop global guidelines that enhance reliability, interoperability, and safety of Steer-by-Wire systems, which should speed adoption and lower costs.

Leading tractor, construction machinery, forklift manufacturers, and suppliers have committed significant time and money to developing common platforms. More than 20 companies and organizations have teamed up in the Steer-by-Wire working group, including vehicle manufacturers such as John Deere, Liebherr, and Volvo Wheel Loader, and system suppliers such as Dana, Eaton and Sauer Danfoss.

⁸TTP (Time-Triggered Protocol) is an open and modular control system platform technology that supports the design of upgradeable, reusable and easy-to-integrate systems. As a time-triggered fieldbus, it can significantly impact the design of modern electronics and control system architectures for next-generation vehicles and industrial applications.

11.4.2 Application of By-Wire Systems

According to officials at Danaher Motion Systems, a manufacturer of electric-vehicle controls, there is a common misconception that By-Wire systems are still experimental and expensive. The reality is that the technology is proven. For instance, By-Wire systems have been used for more than two decades on 20 ton forestry tractors. And as more people use them, costs continue to decline.

Lord Corp. recently worked with Linde Material Handling UK to develop programmable TFDs for high-fidelity “feel” in all electric active reach trucks with Steer-by-Wire control. During development, Linde recognized that the vehicles were unsafe without tactile feedback to the driver through the steering wheel. Although the company considered using electric motors, they rejected the idea based on cost, size, weight, and energy-consumption. Instead, it selected an MR device that could send realistic feedback to the operator.

Sister-company Fenwick-Linde S.A.R.L., based in France, also relies on Steer-by-Wire technology for a full line of all electric lift trucks. According to company officials, Lord Corp.’s TFD improves control and safety by simulating the resistive torque of wheel end-of-turn, so the operator “feels” where the wheels are located.

11.4.3 Throttle-by-Wire in Current Cars

Currently Drive-by-Wire applications are being used to replace the throttle cable system on newly developed cars such as:

- Toyota Land Cruiser
- Peugeot
- Holden Barina and Holden Astra
- Renault Clio
- Land Rover
- Nissan Patrol, X-Trail and Pulsar models
- BMW
- Mercedes-Benz
- VW Golf and Caravelle

11.4.4 By-Wire (Active) Suspension Systems In Current Cars

There have been a number of vehicles produced over the years which have employed production proven By-Wire suspension technology. A few examples are:

- 1991 Infiniti Q45
- 1993 Cadillac, several models with road sensing suspension.
- 1996 Jaguar XK8 “CATS”
- 1997 Jaguar XJ “CATS”
- 1999 Mercedes-Benz CL-Class
- 1999+ Lexus LX470
- 2002+ Jaguar S-Type “CATS” (S-Type R model)
- 2002 BMW 7-Series
- 2002 Cadillac Seville STS, first MagneRide
- 2003 Mercedes-Benz S-Class
- 2003 Chevrolet Corvette, some Cadillacs and other GM vehicles with MagneRide
- 2004 - 2007 Volvo S60R
- 2004 - 2007 Volvo V70R
- 2008 + Audi TT Magnetic Ride

11.5 Drive-by-Wire Concept Cars

Prototype cars employing Steer-by-Wire systems designed by Toyota Motor Corp., Nissan Motor Co., Ltd., Suzuki Motor Corp., and Fuji Heavy Industries Ltd. (FHI) filled the site of the 39th Tokyo Motor Show in 2005.

11.5.1 SKF - Bertone

SKF, who is best known as a leading supplier of wheel bearings, is also a pioneer in adapting aerospace Fly-by-Wire technology to future automotive applications.

The Bertone concept car, which first debuted at the 2002 Geneva auto Show, was created around SKF's prototype Steer-by-Wire, Brake-by-Wire and unique throttle control systems to illustrate the design freedom and possibilities these new technologies offer.

The SKF Steer-by-Wire system uses a "smart" electro-mechanical steering actuator instead of a conventional rack and pinion gear. The electric actuator that moves the rack to either side is wrapped around the rack for a very compact design. There is no power steering pump, no pressure hoses, no steering shaft and no physical connection between the driver's hands and the front wheels. Sensors on the steering yokes send the driver's steering inputs to a processor, which monitors and controls the position of the front wheels.

A feedback loop keeps the wheels and steering inputs in sync with one another, while redundant circuits provide a failsafe backup should anything go wrong.

The bright orange Novanta concept car (see Figure 11.10) has a futuristic yet contemporary look that is more evolutionary than revolutionary. The car is built on a Saab 9-5 chassis with a 3.0 I V6 engine and automatic transmission. It's fully drivable (unlike many concept cars).



Figure 11.10: Novanta concept car

Bertone-SKF “Filo” is a next generation prototype which is a complete “By-Wire” vehicle. All of the Filo’s “By-Wire” systems were developed and manufactured by SKF.

The Filo employs two power supply levels, the conventional 12 V and the emerging 42 V. The clutch and gearshift are on the conventional supply level, and systems with higher power requirements, such as steering and braking, are 42 V.

Filo’s driver’s control - the “Guida” - incorporates an active feedback system within the yokes of the steering arrangement. This system gives the driver “feel”. Running in a closed loop with the steering SEMAU (Smart Electro-Mechanical Actuating Unit) and sensors on the yokes, a high-torque motor provides the Filo’s driver with tactile feedback on steering-angle and road surface changes.



Figure 11.11: Bertone-SKF “Filo”

11.5.2 Toyota Fine-X

The Toyota Fine-X (Figure 11.12) is a concept car created by Toyota and first introduced at the 2005 Tokyo Motor Show.

The Toyota Fine-X is a hybrid concept that combines a hydrogen fuel cell system with electric in-wheel motors, and a four-wheel independent steering system that allows the vehicle to turn on the spot.

A Drive-by-Wire system connects the driver's controls to actuators that operate vehicle functions. In front-axle/rear-axle turning mode, the vehicle can be turned around from the front or rear, which makes maneuverability easier when parallel parking.

In directional change mode, continuously variable steering of the front and rear wheels allows a change of direction of almost the entire length of the vehicle in four directions. This feature allows for U-turns while coming out of parallel parking.

The on-the-spot turning mode allows for convenient 360-degree turning on the vertical axis.



Figure 11.12: Toyota's 'Fine-X'

11.5.3 Suzuki Ionis

The Suzuki Ionis (See Figure 11.13) is a hydrogen concept minivan that made its first public appearance at the Tokyo Auto Show in October of 2005.

The major advancement that has been made in the Suzuki Ionis is making the fuel cell itself much smaller and positioning it underneath the cabin floor. This means that the interior space in the car is optimized for a comparably larger cabin. The Suzuki Ionis, at only 134 inches long, can seat four adults comfortably.

Another major advancement in the Suzuki Ionis is the use of By-Wire technology, created by General Motors. By-Wire technology allows all the functions that normally clutter up the area around the driver, such as the steering column and gearshift, to be controlled by the push of a button. Features that are controlled with By-Wire include the brakes, throttle, and steering. This frees up even more space in the car, allowing passengers to get the most room for the size of the car.



Figure 11.13: Suzuki Ionis

11.5.4 FHI - IVX-II

Fuji Heavy Industries Ltd. (FHI), a global manufacturer of transportation and aerospace-related products and the maker of Subaru automobiles, announced the major features of its vehicles and technologies, exhibited at the 39th Tokyo Motor Show in 2005.

Fuji's IVX-II (Intelligent Vehicle X, "X" symbolizes the infinite) is the next generation of intelligent vehicle which is ensuring driving pleasure, comfort, and advanced safety. Enhanced pleasurable driving, while its integrated preventive safety functions help the car automatically avoid dangers, and restores it to a safe driving position.

The IVX-II utilizes the next generation of By-Wire chassis control technology for vehicle control. See Figure 11.14.



Figure 11.14: FHI - IVX-II

11.5.5 Nissan EA2 Concept

The Nissan EA2 concept car (see Figure 11.15) featuring “X-by-Wire” technology was announced in April 2008. The EA2’s X-by-Wire technology uses wires and electrics to control the steering, braking and transmission. The EA2 is built on the first generation Murano crossover SUV platform.

The adoption of Steer-by-Wire and Brake-by-Wire systems has resulted in an interior length of 2,600 mm - 110 mm more than a conventional model. The Steer-by-Wire steering also helps improve ingress and egress through the use of a smaller diameter yet still easy to use steering wheel.

The Shift-by-Wire system allows for the installation of a movable center console, making it easier to move between the driver and front passenger seats.

The Brake-by-Wire system reduces pedal travel through the use of an electrical system instead of boosters, links and hydraulic cylinders, freeing up more interior space.

X-by-Wire also helps to reduce vehicle weight, resulting in gains in performance, economy and emissions.



Figure 11.15: Nissan EA2 concept

11.5.6 Mazda Washu

The Mazda Washu, Japanese for “Eagle’s Wing”, (see Figure 11.16) is an innovative six seat concept that represents a new genre of vehicles, was unveiled at the 2003 North American International auto show.

Eliminating the need for a traditional steering shaft, Steer-by-Wire technology also makes it possible to neatly store the steering wheel inside the instrument panel when the vehicle is parked.

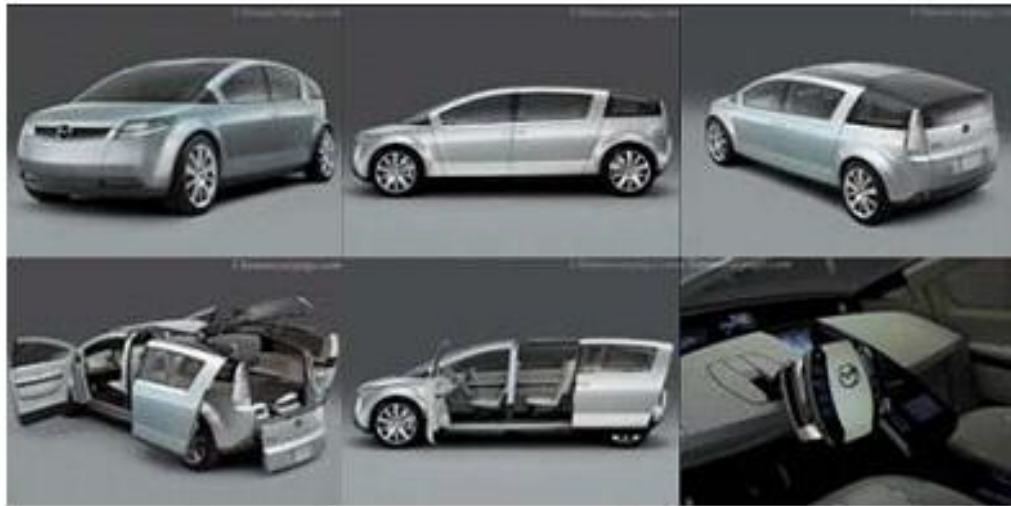


Figure 11.16: *Mazda Washu*

11.6 Low Rolling Resistance Tires (LRRT)

11.6.1 Overview

Low-rolling resistance tires are designed to improve the fuel efficiency of a vehicle by minimizing the heat energy wasted as the tire rolls down the road. Approximately 5-15% of the fuel consumed by a typical car is used to overcome rolling resistance. A 2003 California Energy Commission[59] (CEC) preliminary study estimated that adoption of low-rolling resistance tires could save 1.5-4.5% of all gasoline consumption. The rolling resistance coefficient (RRC) is the value of the rolling resistance force divided by the wheel load. A lower coefficient means the tires will use less energy to travel. The Society of Automotive Engineers (SAE) has developed test practices to measure the RRC of tires. These tests (SAE J1269 and SAE J2452) are commonly performed on new tires. When measured by these standard test practices, most new passenger tires have reported RRCs ranging from 0.008 to 0.014.

LRRT provide less resistance on the road compared to other tires.

Rolling resistance is affected by:

- Tire design and construction
- Rubber compounds
- Tire inflation
- Roadway surface
- Vehicle suspension alignment

11.6.2 Role of LRRT in Fuel Consumption

Each 10% reduction in tire rolling resistance leads to an increase of approximately 2% in fuel savings, [36] depending on driving conditions and vehicle type.[65]

For example, a typical driver who drives 24,140 km a year (15,000 miles) at $8.50 \frac{\text{km}}{\text{l}}$ ($20 \frac{\text{m}}{\text{g}}$) would purchase 2,839 l per year (750 gallons). With a 2% fuel savings, the fuel saved would be about 56.78 l (15 gallons) for a savings of US \$64 per year or US \$1.12/l (\$4.25/gal). Assuming the life of the LRRTs is 3 years, the total savings would be US \$192.

Overall in the USA alone, consumers will save \$470 million annually at current retail prices or \$1.4 billion over the three year lifetime of a typical set of replacement tires.[41]

11.6.3 Tread Wear, Traction and Temperature Resistance Labeling

Uniform Tire Quality Grade standard (UTQG)[24] originated from the Department of Transportation (DOT) and NHTSA to provide useful information to consumers when purchasing new tires based on the relative tread wear, traction and temperature resistance.

The UTQG test is conducted by independent testing companies, however NHTSA can inspect the tire manufacturer's data and can penalize the OEMs if inconsistent data is found. Based on test data results, the grade is assigned and must be labeled on the sidewall of a tire. See Figure 11.17 for UTQG tire labeling.

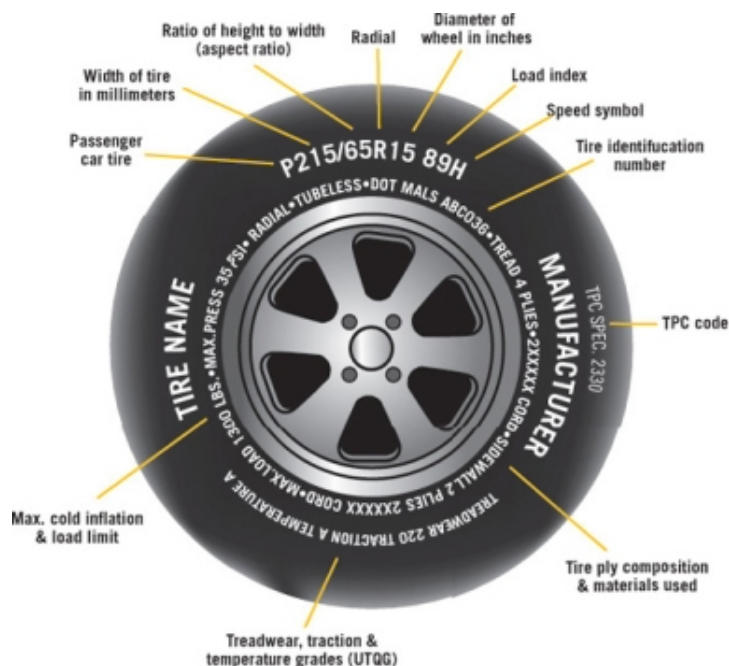


Figure 11.17: Uniform tire quality grade standard (UTQG) labeling

11.6.4 LRRT - Tread Wear

UTQG tread wear grades are based on a standardized road test course used for monitoring tires. The tires are run for 11,587 km (7200 miles) on a 644 km (400 mile) test track loop, along with a Course Monitoring Tire (CMT). The CMT is made to be used as a reference standard to which tires that run on the test course are compared. CMT tires are specially designed and built to American Society for Testing and Materials (ASTM) standard E1136, to have particularly narrow limits of variability. At every 1287 km (800 miles), the tires are checked for pressure and alignment on the vehicle. At the end of the test, the tires wear is measured. A grade of 100 would indicate the tire tread would last as long as the test CMT, 200 would indicate the tread would last

twice as long as the test CMT, etc. Generally a higher tread wear grade has a higher roll resistance coefficient (RRC). See Figure 11.18 for RRC and UTQG correlation.

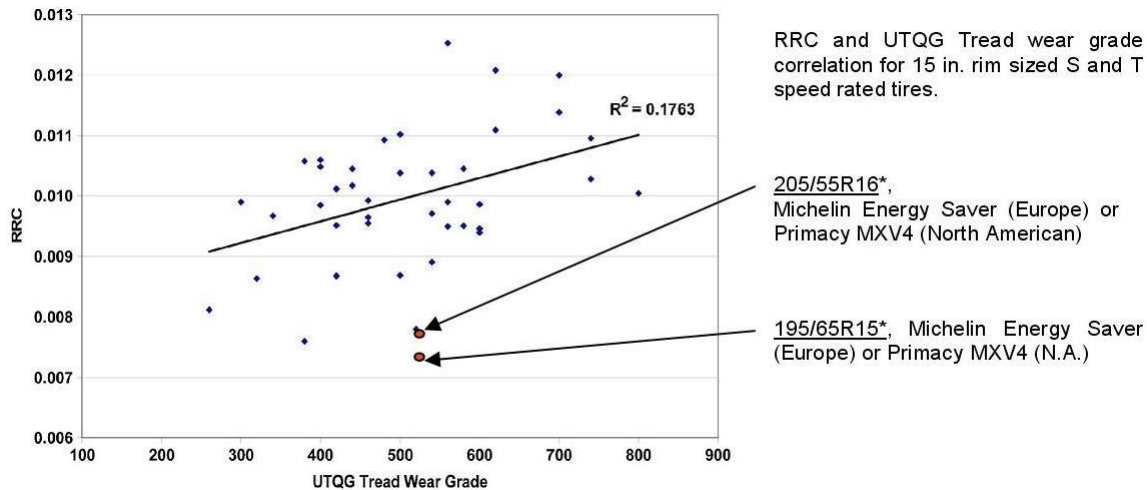


Figure 11.18: RRC and UTQG tread wear grade correlation

11.6.5 LRRT - Traction

UTQG traction grades are based on the tire's straight line wet coefficient of traction as the tire skids across the specified test surfaces. Properly inflated tires are mounted on an instrumented axle of a "skid trailer" which is pulled behind a truck at a constant speed of $64.37 \frac{\text{km}}{\text{h}}$ (40 mph) over wet concrete and asphalt test surfaces. During the test, the skid trailer's brakes are applied, momentarily locking them while the axle sensors measure the tire's coefficient of friction and braking g-forces as it slides across the test surfaces. The lower the traction grade, the lower the g-force measurement, hence the less resistance to rolling. Tire manufacturers design tires to exhibit a blend of performance characteristics for a particular application. The combination of all these design factors has an effect on the RRC.

The highest of the ratings is "AA", followed by "A", "B" and "C". See Table 11.2 for UTQG traction grades.

Traction Grades	Asphalt g-Force	Concrete g-Force
AA	Above 0.54	0.41
A	Above 0.54	0.35
B	Above 0.54	0.26
C	Less than 0.38	0.26

Table 11.2: UTQG traction grades

11.6.6 LRRT - Temperature Resistance

UTQG temperature resistance ratings, measures how well the tire can dissipate heat at high speed. If the tire is not capable of handling heat build up, the tire will have destructive effects. “A” is the highest rating, and follows by “B” and “C”. See Table 11.3 for UTQG tire temperature resistance rating.

Temperature Grade	Speed (mph)
A	Over 115
B	100 - 115
C	85 - 100

Table 11.3: *UTQG temperature resistance*

11.6.7 LRRT - Chemical Compound

A tire’s treads are the single most important factor for traction and rolling resistance. Carbon Black (CB) has a long history in the development of tire treads. Traditionally CB is used as a reinforcing filler for tire treads. In 1992, Michelin pioneered the development of adding silica to tire tread for the purpose of reducing rolling resistance.[33] However, to make silica tread compounds adhere to CB, it is necessary to add silane, which is a coupling or bonding agent, so silica can bond to CB. The tire tread is composed of carbon black (60-70%) + silica (20-25%) + silanes (8-10%).

Even though silane is a great coupling agent for holding silica to tire tread, silane emits ethanol, a green-house gas. The ethanol is released during the tire manufacturing process and on the road. Recently, one chemical company, Momentive Performance Materials, came up with the breakthrough of using NXT Z Silane[31] agents which emits zero ethanol.

11.6.8 European Emission Rating on Tires

At the beginning of 2011, tires are required to have emission ratings listed on new tire labels [32] for the purpose of energy performance in terms of CO₂ mass per kilometer of distance traveled ($\frac{g(CO_2)}{km}$) with the highest rating of “A” to the lowest of “G”. See Figure 11.19 for an example of a European CO₂ emission ratings label (translated from French).

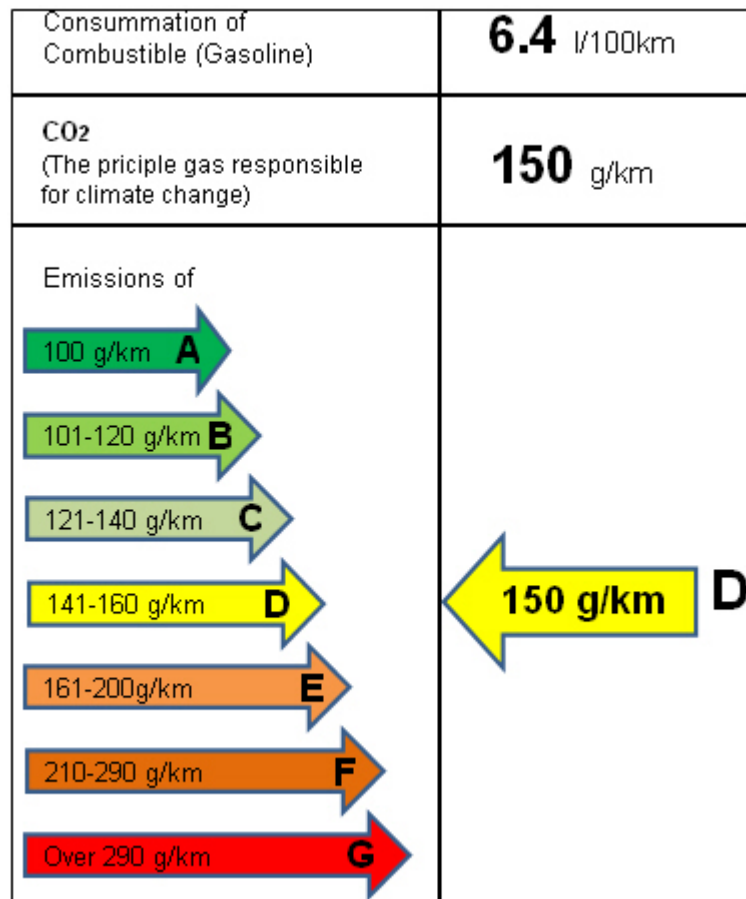


Figure 11.19: European CO₂ emission rating label

11.6.9 North American Emission Rating on Tires

New cars are generally equipped with low-rolling resistance tires that offer better fuel economy. This helps auto manufacturers to meet their Corporate Average Fuel Economy standards (CAFE). However, no requirements are currently placed on replacement tires. Therefore, if you want to purchase fuel-efficient replacement tires, you must research to figure out which tires have low rolling resistance. See Figure 11.20 for passenger tire shipments in the US.

Early in 2009, a rolling resistance grading system (RRGS) will be instituted for tires sold in

11.6 Low Rolling Resistance Tires (LRRT)

California [50], requiring manufacturers to provide rolling resistance coefficient information to customers. According to the California Energy Commission, they are currently collecting rolling resistance data. Information on the rating system will be available to consumers in 2009.[46] See Figure 11.21 for tire rolling resistance values.

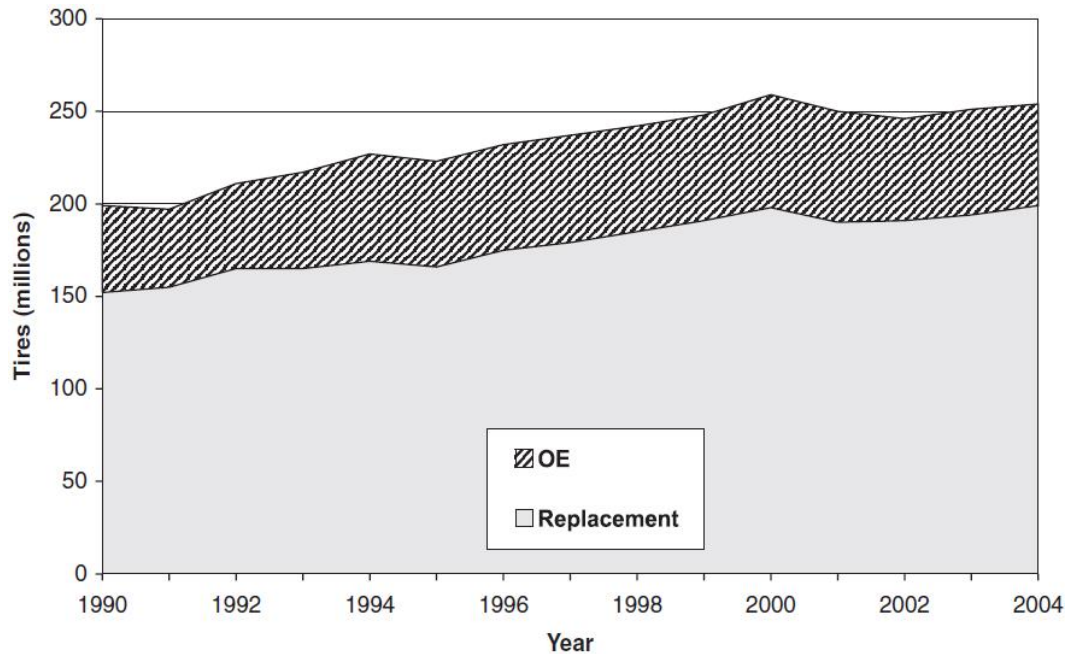


Figure 11.20: Passenger tire shipment in US - OE / replacement

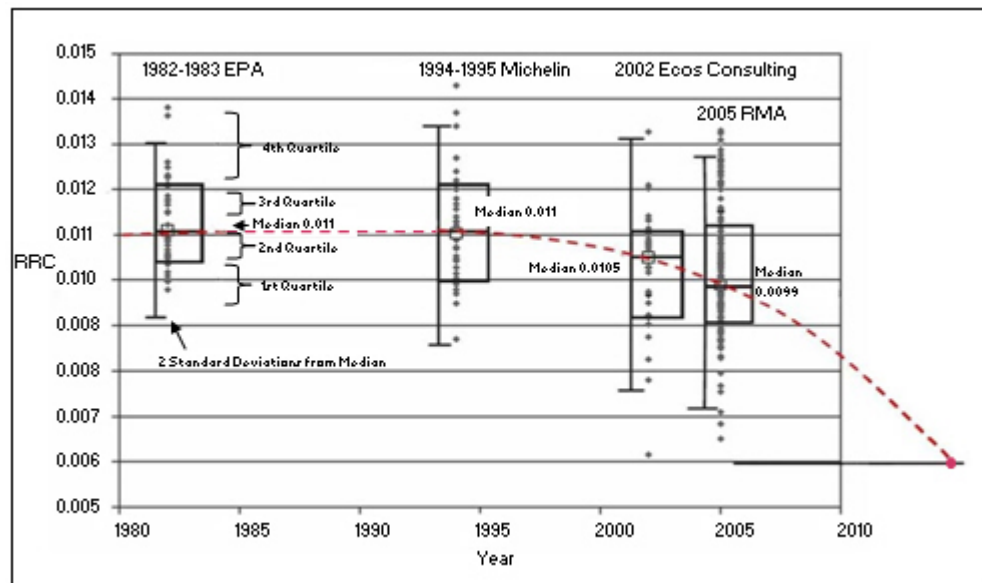


Figure 11.21: Tire rolling resistance values trend

11.6.10 Conclusions

By 2015 to 2020, low-rolling resistance tire technology will have advanced to a stage where rolling coefficients of 0.006 to 0.008 will be a norm.

Improved tire marking with rolling resistance coefficient information for California, and $\frac{\text{g}(\text{CO}_2)}{\text{km}}$ for Europe will increase consumer awareness for energy efficient replacement tires.

11.7 Future Lightweight Technologies

11.7.1 Overview

Investigations of new automotive technologies on the horizon were investigated to assess the impact of mass reduction and packaging space implications without sacrificing vehicle function or safety. The reduction in trim and component mass generally leads to a total reduction in the vehicle's mass and also a reduction of body structure mass (Mass Compounding)⁹.

The following automotive technologies were investigated:

- Glazing
- LED lighting
- Instrument panel displays
- Light weight seating

Table 11.4 below illustrates the component weight savings compared between conventional vehicles and the proposed Future Steel Vehicle thus proving the FSV's considerable advantage.

Item	Generic Weight [kg]	FSV Weight [kg]	Mass Savings [%]
Glazing	44	31	29.5
Lighting	10	6.3	37
I/P Display	2.2	0.2	91
Seating	65	42	35.4
Totals	121.2	79.5	

Mass Savings [kg]	41.7
--------------------------	-------------

Table 11.4: *Component weight savings - Conventional vehicles versus Future Steel Vehicle*

The mass compounding effect of a 41.7 kg weight savings on the vehicle and body is a mass reduction of 10 kg on the body-structure.

⁹Mass compounding is the incremental change in a vehicle sub-system (ie; brakes, suspension) mass for a unit change in gross vehicle mass. When one major sub-system changes (ie; vehicle powerplant) with either an increase or decrease in mass, this has a ripple effect throughout the vehicle. Other components/sub-systems need to be resized, increasing or decreasing the vehicle mass accordingly.

11.7.2 Automotive Glazing

11.7.2.1 Automotive Glazing Regulations

Apart from each OEM's internal specifications, there are a number of regulations that are applicable to automotive glazing, such as:

- FMVSS 205 (USA)
- CMVSS 205 (Canada)
- ECE R43 (Europe)
- GB-9656-96 CCC (China)

Note: FMVSS limits the use of alternative (polycarbonate) and normal (tempered/laminated) glazing materials to side and rear glazing as long as they fulfill all of the FMVSS criteria.

11.7.2.2 Types of Automotive Glazing

There are generally three (3) materials used for automotive glazing:

- Tempered glass
- Laminated glass (glass /plastic layer/ glass)
- Polycarbonate

Each material has its own advantages and disadvantages. See Figure 11.22 for typical automotive glass application.

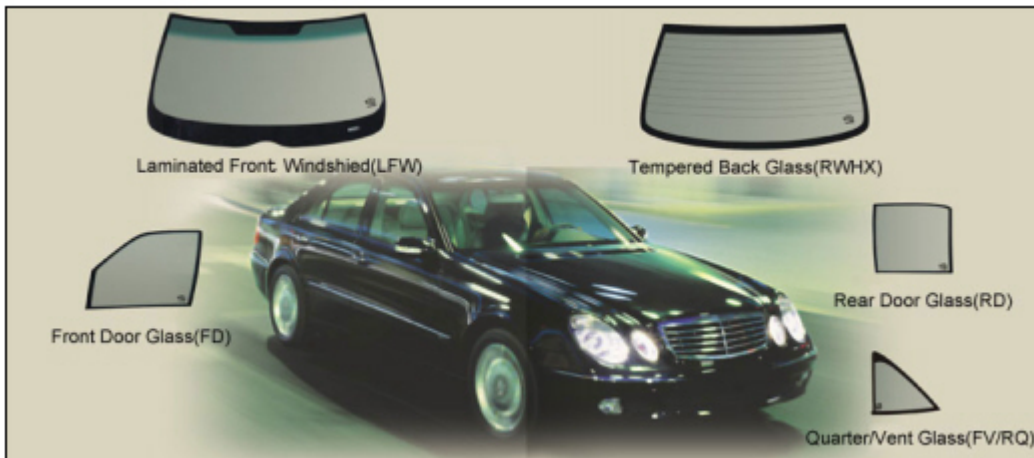


Figure 11.22: *Glass panels typical for a vehicle manufactured in 2008*

11.7.2.3 Comparison of Tempered Glass & Laminated Glass

Most vehicles on the road contain tempered glass in their side, rear and roof window openings. In accidents, this tempered glass shatters and breaks, causing lacerations and other injuries and opening up portals through which occupants can be fully or partially ejected.

The expanding usage of laminated glass in high-end luxury vehicles not only is making clear the benefits of laminated glass, but also the ease with which laminated glass could be substituted for tempered glass in passenger cars, pickups and SUVs. Laminated glass is multi-layered while tempered glass is a single sheet as illustrated in Figure 11.23.

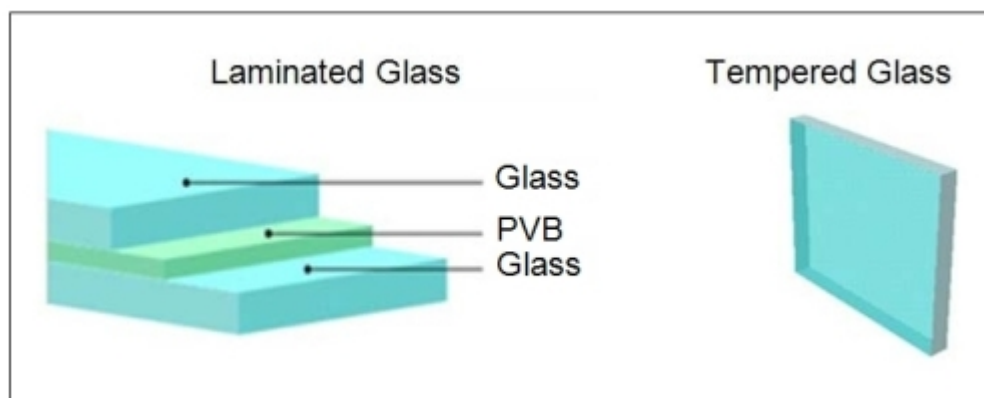


Figure 11.23: *Tempered vs. laminated glass*

Laminated glass is required in windshields and has been used in the windshields of every car sold in the US and Europe for decades. Laminated glass is not required in other window locations, and car makers typically have relied on the use of tempered glass for those window locations. Only high-end luxury vehicles are now being offered with all-round laminated glazing. Laminated glass consists of two pieces of glass bonded together with a plastic inner layer, typically consisting of polyvinyl butyral (“PVB”).

In a collision, the glass will fracture but the PVB interlayer holds the fragments together and in place in the window opening. The PVB interlayer serves to hold the glass in place, which, in turn, acts to contain occupants by preventing ejections. Even after severe accidents, windshields typically remain in place. Ejections through windshields are largely a thing of the past.

Tempered glass, in contrast, consists of a single layer of heat treated glass. When tempered glass breaks in a collision, the entire piece of glass shatters and the fragments fly about. When this happens, the flying glass fragments can cause lacerations and other injuries, while the window opening becomes a potential portal of ejection.

Laminated Glass

Laminated glass offers a number of benefits such as the ability to combine a number of advantageous mechanical properties of both mediums. See Table 11.5.

Glass	PVB Plastic Layer
Mechanically robust	Energy absorbent
Stiffness	No catastrophic breakage
Chemical & physically durable	Ability to carry heating and/or antenna wires

Table 11.5: *Combined benefits of laminated glass*

The interface between the glass and plastic layer allows the integration of other components such as:

- Thin film systems
- Additional plastic films
- The addition of environmentally sensitive sensors

See Table 11.6 and Table 11.7 for a comparison of laminated windshields (acoustical vs. conventional) and laminate vs. polycarbonate for side glass applications. Laminated glass is now used in all the following glazing applications.

- Windshields
- Side drop glass
- Rear quarter glass
- Rear/back glass
- Sunroof glass

Windshield construction	Density kg/m ³	Thickness mm	Weight	
			gms	lbs
Acoustical windshield				
Glass layer #1	2.4	2.3	8280	18.25
PVB layer	1.06	45	1813	3.99
Glass layer #2	2.4	1.7	6120	13.48
Conventional windshield				
Glass layer #1	2.4	2.3	8280	18.25
PVB layer	1.06	30	1208	2.66
Glass layer #2	2.4	2.3	8280	18.24
Weight savings of acoustical over a conventional windshield			1556	3.43
Glass density ranges from 2.2 to 2.8				2.4 kg/m ³
PVB density is fixed at:				1.06 kg/m ³
Windshield size (Area)				1.5 m ³

Table 11.6: Acoustical windshield weight savings calculator

Side glass construction	Density kg/m ³	Thickness mm	Weight	
			gms	lbs
Laminate glass				
Glass layer #1	2.4	1.8	2592	5.71
PVB layer	1.06	0.64	407	0.9
Glass layer #2	2.4	1.8	2592	5.71
Polycarbonate glass				
	2.4	4.3	6192	13.64
Number of window installation positions				4
Weight savings of laminate over polycarbonate			2390	5.27
Glass density ranges from 2.2 to 2.8				2.4 kg/m ³
PVB density is fixed at:				1.06 kg/m ³
Windshield size (Area)				0.6 m ³

Table 11.7: Side glass laminate weight savings calculator

11.7.2.4 Polycarbonate Glazing

While polycarbonate has not gained a foothold in the US, it is regularly used in Europe, and with the modern trend for panoramic roofs, polycarbonate is becoming the preferred material.

One of the largest limitations is the performance related to the durability of aging glass, specifically abrasion/scratching issues, and the effects of UV radiation. However, with the advent of PECVD (Plasma Enhanced Chemical Vapor Disposition) the application of protective coatings give a comparable durability performance to glass.

PECVD (Plasma Enhanced Chemical Vapor Disposition) performance features are:

- Glass like abrasion resistance
- Wiper capability
- Extended weathering resistance
- Scratch resistance
- Acceptable polycarbonate / body structure bonding

To protect polycarbonate from the effects of UV radiation, an additional hard silicon coat is added.

Other advantages over laminated glass are:

- Overall reduction in weight of 40-50% over laminated glass, resulting in improved fuel economy
- Can be injection molded in to complex shapes
- Can be produced with differing colors, color patterns & textures
- Will not shatter, providing excellent occupant protection
- Extremely durable, thereby improving vehicle security

11.7.2.5 Conclusions

Polycarbonate glazing offers an even greater weight savings over laminated glazing. While polycarbonate cannot be used for windshields in the US, recent technology developments in Europe have produced a virtually unbreakable polycarbonate windshield achieving a weight savings of 40-50% over a conventional laminated glass windshield. A Polycarbonate windshield would give an approximate weight savings of between 7.1 kg (17.8 lbs) and 8.9 kg (22 lbs) over the same size laminate windshield. For the side-drop glass, polycarbonate would give an approximate weight savings of between 2.5 kg (5.4 lbs) and 3.1 kg (6.8 lbs) over the same size laminate side glass. Even though polycarbonate for automotive glazing is still under development, the general opinion is that this technology will be available during the life time of this program.

Typical glass mass per vehicle:

- Laminate glass for windshield, side, & rear - 44 kg
- Laminate acoustical glass for windshield, side & rear - 39 kg
- Laminate windshield, with polycarbonate side & rear - 31 kg
(This option is recommended for FSV)
- Polycarbonate windshield, side & rear - 23 kg

Note: Laminated windshield side & rear calculated from an actual vehicle, (Mazda-3).

11.7.3 Lighting & Displays

A typical headlamp module weighs approximately 3.2 kg (7 lbs), per side, depending on vehicle style. Due to the fact that the headlamp module, contains the main beam, spot lamps, and the turn indicator lamp, there is potential weight saving opportunities using LED technology. See Figure 11.24 for a typical headlamp module.

Tail lamp modules typically weigh approximately 1.8 kg (4 lbs) per side, and are also dependent on vehicle style. Unlike LED headlamps, there is a possibility of up to a 50% weight savings by using LED lighting technology for tail lamps over a conventional tail lamp design. This is because a headlamp module requires a large background reflector to project light, unlike a tail lamp that does not need to project light.



Figure 11.24: Headlamp module

11.7.3.1 LED Lighting

LED (Light Emitting Diodes) were first applied to the automotive market in the late 1990's in the "Center High Mount Stop Lamps" (CHMSL). By 2004 approximately 40% of all vehicles (cars & trucks) worldwide featured LED based CHMSL's. However, the worldwide penetration of LED based rear-stop and turn-signal/tail lamp assemblies only reached 4% and was limited to "high end" vehicles.

In 2008, the Audi A8 became the world's first car in which all exterior lighting functions of the headlamp & tail lamp were realized using LED technology. This included:

- Low/high beam
- Turn signal
- DRL (Daylight Running Lights)
- Position lights
- Rear stop lamp
- Vehicle lighting

While current vehicle styling trends tend to have larger headlamp systems with more lights, the

weight penalty can be offset by using modern lighting technologies.

New vehicle lighting systems that are being introduced today include, LED tail lamps, and LED headlamps combined with HID (High Intensity Discharge) lamps. These together result in a positive weight savings together with a major improvement in system performance. See Figure 11.25 and Figure 11.26.



Figure 11.25: 2008 - Audi A8 with full LED head & tail lamps



Figure 11.26: 2008 Cadillac Escalade w/ LED/ HID headlamps LED tail lamps

11.7.4 LED Lighting – Advantages & Disadvantages

Some advantages for using LED vehicle lighting:

- LED's produce more light per watt than incandescent lamps
- Consumes less energy than conventional lighting systems
- LED's can emit light of an intended color without the need of filters
- Flexible packaging of LED's can be utilized to focus light
- LED's do not change color when in a dimming mode
- LED's are ideal for frequent on-off applications like turn-signals
- Being a solid-state component, they are difficult to damage by external shock
- Relative long life, estimated to be up to 50,000 hours of useful life
- Quick light-up to full brightness, typically less than 100 ns (Phillips Lumileds)
- LED's do not contain any environmental contaminants

Some disadvantages of using LED's:

- Currently, LEDs are generally more expensive to produce per lumen than conventional lighting technology
- Performance can be affected by ambient temperature, and heat sinking is required to maintain long life
- LED's must be supplied with the correct current, and need a regulated power supply
- Concern that blue & white LED's can exceed safe limits for "Blue-Light Hazard" as defined by eye safety specifications (ANSI/ESNA RP-27.1-05)

11.7.5 Conclusion

LEDs when used for exterior vehicle lighting can save both weight and energy.

Weight

Headlamp and tail lamp assemblies for a vehicle with conventional lighting typically weigh 10 kg (22 lbs for Lh & Rh parts). When using LED lighting, a weight savings in the order of 3.7 kg (8.2 lbs) can be realized.

Energy

Due to the overall efficiency of LED lighting over conventional lighting, the average energy consumption is approximately 10% of that used for a conventional lighting system.

Note: Both weight and energy savings are dependent on the vehicle lighting configuration.

11.7.6 Lightweight Interior Displays

With vehicle occupants of the future demanding increasingly more vehicle and navigation information, together with entertainment outputs, the evolution of the modern instrument panel will become increasingly more complex and heavy. See Figure 11.27 for a lightweight interior display, and Figure 11.28 for evolution of the complexity of the instrument cluster towards a driver information system.



Figure 11.27: Interior with lightweight instrument cluster display

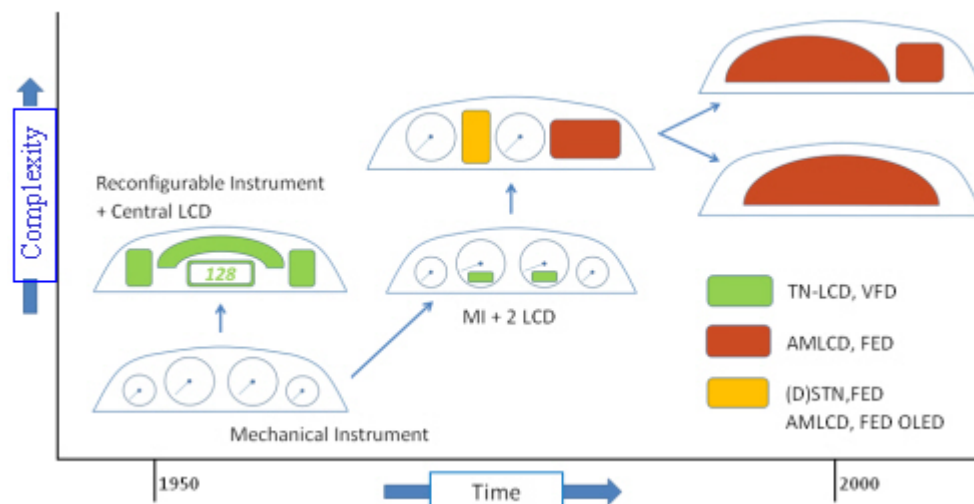


Figure 11.28: Evolution of the complexity of the instrument cluster

In an effort to reduce weight and energy, and to cope with increasing vehicle data and driver & passenger expectations, the use of flat screen technology is a viable option for the future, (year 2020). This technology will be readily available by the year 2020.

11.7.6.1 Flat Screen Displays

Flat screen displays are produced by using:

- LCD (Liquid Crystal Display)
- PM-OLED (Passive Matrix-Organic Light Emitting Diode)
- AM-OLED (Active Matrix-Organic Light Emitting Diode)

LCDs have been used in vehicles for a number of years mainly for navigation and entertainment screens, PM/AM-OLED is an emerging technology, but is expected to surpass LCD technology in the future. Figure 11.29 shows reconfigurable instrument cluster concepts.

All three technologies offer a number advantages over a conventional instrument display, these being:

- Weight savings: Conventional instrument clusters weigh approx 2.2 kg compared to approx 0.75 kg for a LCD screen and approx 0.2 kg for an OLED display
- Manufacturing cost savings
- Common part can be used for different vehicle platform models
- No moving parts
- End user customer configuration



Figure 11.29: *Reconfigurable instrument cluster concepts [39] [47]*

Flat, solid state screens offer the driver & passenger a number of benefits, the main one being reconfigurable displays (“Smart” technology). This technology allows the screen to be programmed at the end of the manufacturing line or even in the field and display data can be changed instantly from imperial to metric units at a touch of a button. Smart technology utilizes multiplex communication technology, that allows instrument control technology for several instruments in the instrument cluster over a single wire, which leads to additional weight savings. Subliminal suggestions can also be programmed (slow change in display color) to signal external environmental changes like freezing roads or exceeding the speed limit.

PM/AM-OLED (Passive/Active-Organic Light Emitting Diode) displays offer a number of additional advantages over LCD displays. See Figure 11.30.



Figure 11.30: PM/AM-OLED displays

Organic Light-Emitting Diode (OLED) displays are:

- Are referred to as “electronic paper” due to their thin construction
- Robust design - OLED are shock resistant
- Viewing angle - can be viewed up to 160 degrees
- Production advantages - Up to 50% cheaper to produce than LCDs
- Speed - Lighter and faster than a LCD screen
- Can be attached to a curved surface.

11.7.6.2 Displays Conclusion

Due to the construction of the OLED display, a significant weight and energy savings can be achieved when using a P/A-OLED (Passive/Active-Organic Light Emitting Diode) over a convention instrument panel display (cluster).

Weight

The weight of a conventional instrument cluster is approximately 2.2 kg (4.8 lbs). When this is replaced with a OLED (electronic paper) display, a weight reduction in the order of 2.0 kg (4.3 lbs) could be achieved. This does not take into account the use of “Smart” communication technology, which can result in further weight savings.

Energy

Typically, a conventional instrument panel requires approximately 120 Watts to operate, with a peak load of 480 Watts, dependent on the panel’s complexity. An OLEN display would require an estimated operating load of 10 Watts with a peak requirement of 50 Watts. This results in a possible energy savings of approximately 90% over a conventional instrument panel.

11.7.7 Light Weight Seat Systems

A conventional fully optioned front seat can weigh approximately 30 kg (66 lbs) and is composed of the following components:

- Seat frame
- Seat tracks
- Recliner and hardware lumbar supports
- Headrest restraints and side impact airbags
- Any applicable wiring/motors attributed to heated and/or electric seating

Today's All-Belt To Seat (ABTS) consists of a metal frame, electrical wiring harness, electrical hardware, and foam/trim. There are opportunities for manufactures to realize mass reduction all these areas. See Figure 11.31 and Figure 11.32.



Figure 11.31: *The front seat frame structure consists of 65 to 70% of total seat mass*

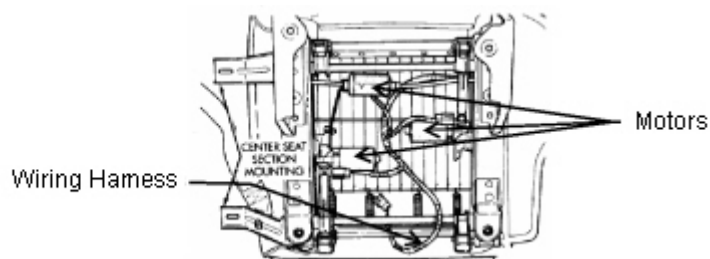


Figure 11.32: *The rear seat frame structure consists of 70 to 80% of the total seat mass*

Where applicable, the remaining 20% driver's total seat mass is in the electrical wiring harness and motors.

11.7.8 Lightweight Seating

In an effort to improve fuel economy, engineers are looking into several areas to reduce weight without sacrificing comfort and performance. See Figure 11.33.

11.7.8.1 Seat Frame Construction

Front Seat Improvements:

Seating suppliers such as Lear, are developing new seat frames using hydroform manufacturing methods with higher-grade steels. This process can reduce the seat frame mass by nearly 0.6 kg while increasing its stiffness by nearly 30%. These advancements are engineered to save mass which in turn will save on fuel consumption.

Rear Seat Improvements:

Because rear seats are anchored on the floor and mounted to the vehicle chassis, the performance is less demanding. Therefore, manufacturers are looking into various types of high-strength plastic composites. These composites may consist of polymer materials with steel reinforcements.

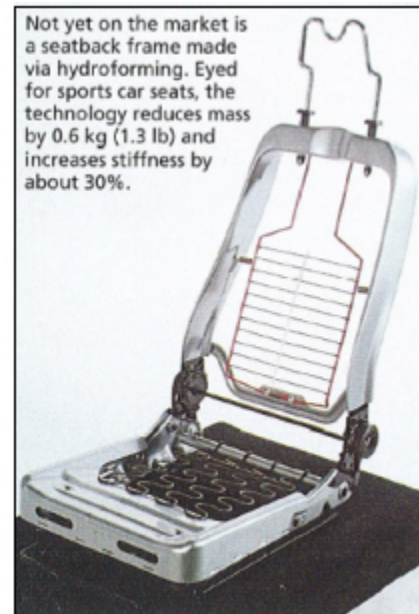


Figure 11.33: Seatback frame made via hydroforming

11.7.8.2 Seat Accessories

Electrical Wiring Harnesses

Electrical wiring harnesses are becoming more complex as the demand for safety and comfort features increases. In order to reduce wiring harness mass, suppliers are using Local Interconnect Network (LIN) cables in place of traditional wiring harnesses. This technology will provide for all the features in the seat system to be linked together in one controller unit with its monitor, and be mounted at a single interface. See Figure 11.34.

Seat Cushions

The VT foam used in the “Slim Seat” design from Johnson Controls, Inc, offers up to a 40% improvement in vibration absorption, resulting in a smoother more comfortable ride. By using this high-tech foam, seat cushion thickness can be reduced from the typical 50 mm to 30 mm, without a decrease in comfort. Taking advantage of this VT foam will enable the seat to weigh less and provide additional space for interior packaging.

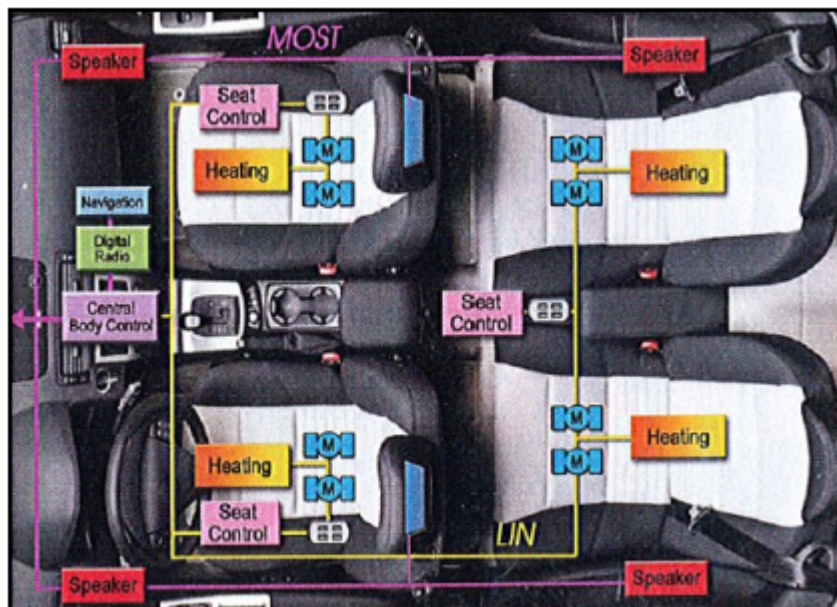


Figure 11.34: *Electrical wiring harnesses*

Our FSV front seats, at 15 kg each, will be a light weight design. It has a high strength steel frame and is hydro-formed. Structural polypropylene foam will replace conventional metal wiring support.

Our FSV rear bench seat is weight 12 kg. It consists mostly of polyurethane foam and bonding material because we are taking advantage of the raised floor pan as a bottom support, and the vehicle’s rear structural panel as a back support.

11.8 Auxiliary Equipment

As a part of this engineering assessment, the FSV engineering team studied the impact of auxiliary loads on the vehicles performance and All Electric Range (AER) by incorporating new automotive technologies slated to be available for production by the year 2020.

A major portion of the auxiliary load comes from the vehicle's air conditioning system. Reducing this load significantly affects the vehicles performance and range. A number of new technologies will be available for mainstream production for FSV-1 and FSV-2 by 2020 that will help reduce this parasitic load and provide FSV-1 and FSV-2 with an enhanced performance and range. Reducing and optimizing A/C load may be the most efficient way of designing the battery and propulsion system and arrive at a very balanced (in terms of cost and size) design, while achieving the set performance targets. Studies have shown that peak A/C loads can reduce the range of an electric vehicle by as much as 38%.

In this study, we recommend a combination of proven methods and systems for FSV-1 and FSV-2 to achieve its performance targets while maintaining an optimized propulsion system.

- Advanced glazing (Solar reflective glass)
- Cabin ventilation (Solar sunroof panels)
- Electric driven A/C compressor

11.8.1 Auxiliary Systems

A typical electric and/or hybrid electric vehicle has two types of electric load requirements [56]: Propulsion loads, which are required to propel the vehicle forward (engine, motor, inverter), and non-propulsion loads, which are auxiliary loads such as A/C, heater, lighting, suspension, etc. . .

With the increase in electric/electronic content in current vehicles, the onboard electric power requirements for non-propulsion loads are likely to increase from 1 kW to 5 kW. For electric and hybrid vehicles, the propulsion loads are likely to be on the order of 100 kW peak in the near future. See Table 11.8 for peak and average auxiliary power system requirements.

Electric Loads	Peak Power [kW]	Average Power [kW]	
Electric vehicle/ hybrid electric vehicle propulsion	30-100	10-30	Propulsion loads
Fuel-cell electric vehicle air compressor	12	8	
Active suspension	12	0.36	Non-Propulsion loads
Integrated starter generator	4-8	2-4	
Electric AC compressor	4	1	
Variable engine valve	3.2	1	
Heated catalytic converter	3	0.1	
Heated windscreen	2.5	0.25	
Electric power steering	1.5	0.1	
Engine cooling fan (ICE)	0.8	0.4	
Engine coolant pump (ICE)	0.5	0.4	

Table 11.8: Peak and average power requirements

Until recently, little has motivated automakers to find ways to reduce the impact of air conditioning on fuel economy. Reducing the weight of a mid-sized vehicle's air-conditioning system by 9.1 kg (20 lbs) results in about a $0.04 \frac{\text{km}}{\text{l}}$ ($0.1 \frac{\text{m}}{\text{g}}$) increase in fuel economy on the current combined city/highway test.

Simulation results show the impact of auxiliary loads on a conventional vehicle and on a high fuel economy vehicle for the SC03 drive cycle using ADVISOR[60] (ADvanced Vehicle SimulatOR). See Figure 11.35.

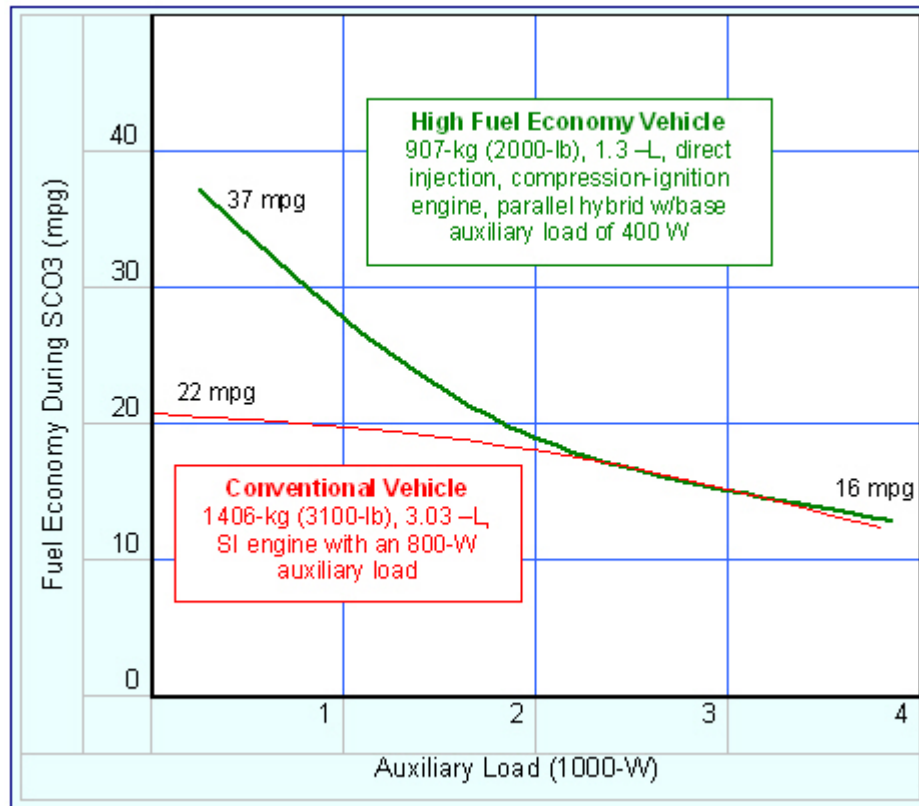


Figure 11.35: Fuel economy impacts of auxiliary loads [18]

11.8.2 Climate Control

11.8.2.1 Auxiliary Loads - Impact on Fuel Economy

Vehicle air-conditioning systems are sized to provide adequate cool down time for peak cooling loads with a solar load of $\frac{1\text{kW}}{\text{m}^2}$ and 49°C ambient temperature.

Such conditions can lead to cabin surface temperatures of more than 121°C and cabin air temperatures higher than 82°C.

The power necessary to operate a vehicles air-conditioning compressor is significant (about 4 kW peak power). A/C power can be greater than the engine power required to move a mid-sized vehicle at a constant speed of $56\frac{\text{km}}{\text{h}}$ (35 mph). A 400 Watt load on a conventional engine[60] can decrease the fuel economy by about $0.4\frac{\text{km}}{\text{l}}$ ($1\frac{\text{m}}{\text{g}}$). See Table 11.9 and Table 11.10.

Auxiliary Power:	500 W	1500 W		2500 W		3500 W	
Drive cycle	Range km (mi)	Range km (mi)	Change from 500W Case	Range km (mi)	Change from 500W Case	Range km (mi)	Change from 500W Case
FUDS	175.9 (109.3)	147.7 (91.8)	-16%	125.5 (78.0)	-29%	108.9 (67.7)	-38%
HWFET	183.6 (114.1)	167.5 (104.1)	-9%	154.0 (95.7)	-16%	142.1 (88.3)	-23%
US06	116.0 (72.1)	107.6 (66.9)	-7%	102.5 (63.7)	-12%	95.3 (59.2)	-18%
SC03	174.3 (108.3)	146.9 (91.3)	-16%	126.8 (78.8)	-27%	11.2 (69.1)	-36%

Table 11.9: EV-range simulation results

Auxiliary Power:	500 W	1500 W		2500 W		3500 W	
Drive cycle	Fuel Use (L/100 km) Fuel Economy (mpg)	Fuel Use (L/100 km) Fuel Economy (mpg)	Change from 500 W Case	Fuel Use (L/100 km) Fuel Economy (mpg)	Change from 500 W Case	Fuel Use (L/100 km) Fuel Economy (mpg)	Change from 500 W Case
FUDS	5.45 (43.2)	6.51 (36.1)	19% (-16%)	7.69 (30.6)	41% (-29%)	9.03 (26.0)	66% (-40%)
HWFET	4.88 (48.3)	5.18 (45.4)	6% (-6%)	5.48 (42.9)	12% (-11%)	5.84 (40.3)	20% (-16%)
US06	6.64 (35.4)	6.94 (33.9)	5% (-4%)	7.30 (32.2)	10% (-8%)	7.70 (30.6)	16% (-12%)
SC03	5.96 (39.5)	6.91 (34.1)	16% (-10%)	7.96 (29.5)	34% (-19%)	9.38 (25.1)	57% (-28%)

Table 11.10: HEV - Fuel economy range simulation results

11.8.2.2 Conclusions

A steady state A/C load of 1 kW-1.5 kW will cause the range of a BEV to reduce by an average of 16%, and fuel economy of a HEV to reduce by an average of 18%, while peak loads of 3 kW or more, reduces the range of an BEV by as much as 38% and fuel economy of a HEV by 19%.

11.8.3 Future Technologies to Reduce Climate Control Load

1. Solar panel roofs
2. Solar Reflective Paint (SRP)
3. Advanced (solar reflective) glazing
4. Parked car ventilation
5. More efficient A/C compressors

Since the A/C system in a vehicle is sized to reduce the interior temperature to an acceptable level after a hot soak, technologies such as solar reflective glass and paint can reduce the thermal load on vehicle interior temperatures, and fuel use[21].

11.8.3.1 Solar Panel Roof

Another method that produces reasonable savings on A/C loads is by adding a convex solar roof to hybrid cars. With the solar roof, the Toyota Prius can operate up to 32 km (20 miles) per day in electric mode thus improving fuel economy by up to 29%. The solar modules are rated at 200-300 Watts, and this power is utilized to charge a supplemental battery. See Figure 11.36.



Figure 11.36: Solar roof - Toyota Prius

11.8.3.2 Solar Reflective Paint

Solar reflective paint (SRP) is considered one of the most effective technologies to reduce energy consumption for cooling buildings, and is expected to mitigate the “heat island” effect in urban areas. When applied to automobiles, preliminary measurements showed that a rise of body reflectivity of 67.3% reduces the fuel consumption for cooling by half, as illustrated in Figure 11.37.

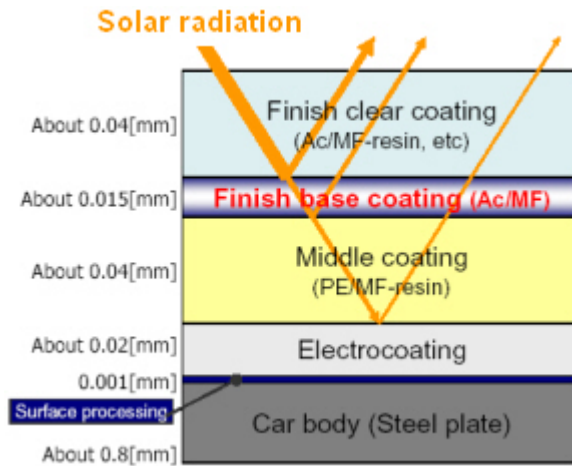


Figure 11.37: Standard automobile paint composition

The cooling loads measured on two identical vehicles, one with Solar Reflective Paint (SRP)[51] and one with a conventional paint, is shown in Figure 11.38.

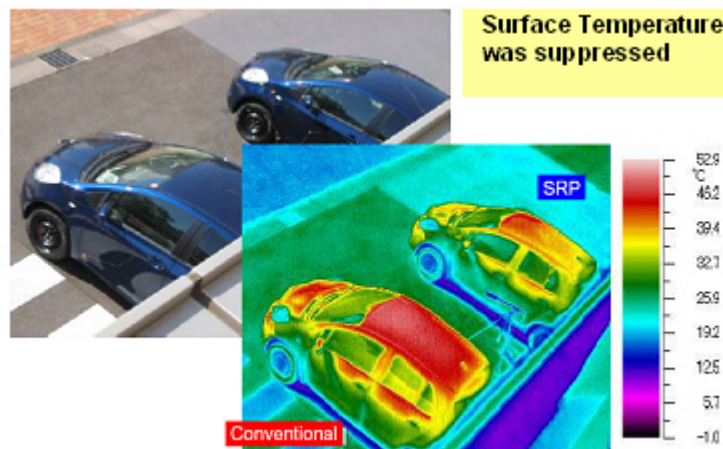


Figure 11.38: Surface temperature

SRP is a suitable technology for automobiles, which have a very small heating load and do not use A/C when heating. SRP slightly improves the actual fuel efficiency about 0.2% to 0.9%. SRP reduces air temp inside cars only by 1.6°C - 3.9°. Therefore, SRP is not a FSV intent technology.

11.8.3.3 Advanced Glazing

Solar gains (loading) on a vehicle interior, increases the strain on a vehicles air-conditioning system, resulting in more fuel being used to overcome the parasitic loading of the air-conditioning compressor on the engine. Advanced glazing is one technology that can be employed to reduce solar loading. Advanced windshields, such as PPG's Sungate, effectively reduce transmission of ultraviolet (UV) and infrared (IR) solar radiation into the vehicle compartment. This technology provides for reduced solar loading on the vehicle interior and hence, a lower vehicle interior temperature as compared to conventional windshields.

Figure 11.39 compares the transmissivity of the Sungate windshield (purple lower curve) with that of a conventional windshield (blue upper curve).

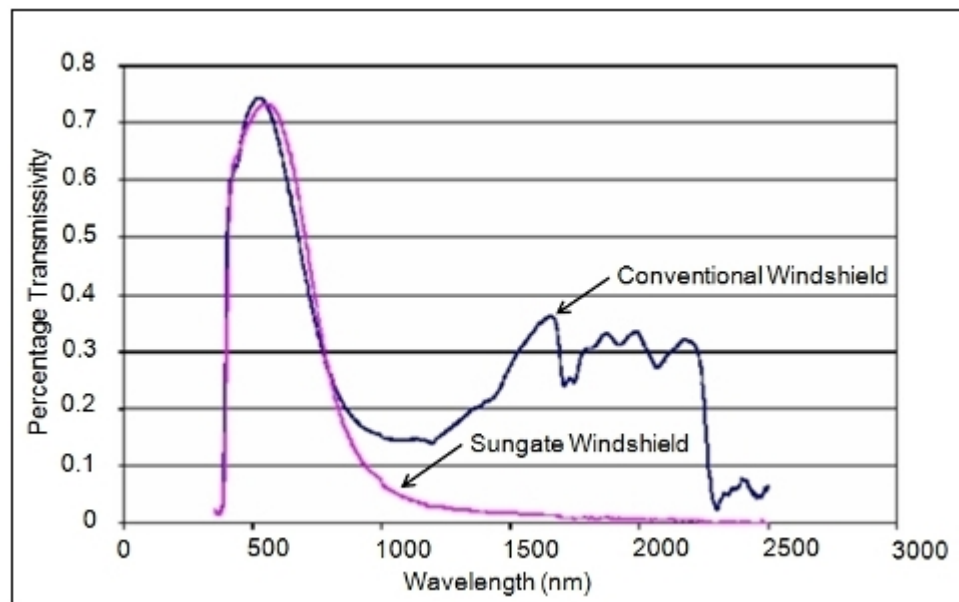


Figure 11.39: Comparison of transmissivity

Automotive Windshields

The solar gains, (loading) in the vehicle are decreased by 27% if the standard front windshield (Solex) is replaced with the Sungate windshield. If the A/C compressor is proportionally downsized, the Sungate windshield can increase the fuel economy of a mid-sized sedan by about 1.5% over the SFTP^[10] drive cycle and by about 3.5% over the SCO3^[11] drive cycle. Sungate EP automotive glass is an advanced version of the original infrared (IR) reflective Sungate windshield. According to the National Renewable Energy Laboratory (NREL) study, Sungate EP glazing can reduce front seat temperatures by 15°C (27°F) and air breath temperatures by 9°C (16°F), thus reducing the air conditioners workload, along with fuel consumption and carbon dioxide emissions. Previous research showed drivers could save up to 4% in annual fuel costs using the Sungate windshield, which is featured on several current Mercedes-Benz and BMW models. See Table 11.11.

Test Condition	Solar Gain
Opaque	1
Sungate - New low-E glass windshield	1.66
Solargreen - Standard EU windshield	1.81
Solex - Standard US windshield	1.93

Table 11.11: *Automotive windshields*

11.8.3.4 Parked Car Ventilation

Webasto Sunroofs has developed a ventilation product called “Solar Tilt/Slide Sunroof”[30]. (See Figure 11.12) and Figure 11.36. The benefits and features of this ventilation system are as follows:

- The solar cells integrated in the sunroof generate electricity, which powers the car’s blower continuously while the car is parked
- Used in conjunction with the car’s own blower, this solar roof can reduce the temperature inside the car by up to 20°C in summer conditions

Because there is nearly five times as much solar energy available in summer as in winter, the solar ventilation and battery maintenance features complement each other perfectly due to the car’s interior not being overheated; the A/C works much more efficiently and saves on fuel.

It is the intent of the FSV Engineering Team, to use a parked car ventilation system on the FSV.

¹⁰Supplemental Federal Test Procedure or “drive cycle” over which cars are driven for emissions evaluation

¹¹A supplemental FTP procedure to simulate emissions associated with the use of air conditioning units.

Technical data		Reference List
Number of cells	28	V W Phaeton, Passat
Cell material	Monocrystalline silicon	Audi A8, A6, A4
Current (A)	3	Mercedes-Benz E-Class
Output (Wp)	>36.7	Skoda Superb
Solar cell efficiency	>16%	Lancia Thesis

Table 11.12: Parked car ventilation table

11.8.3.5 Advanced A/C Compressors

Gasoline Powered A/C Compressors with Idle Stop

Gasoline/Electric hybrid vehicles are beginning to employ a different approach to powering the compressor on the air conditioning (A/C) system. Manufacturers currently employ three types of compressor technology.

1. Gasoline powered A/C compressors with idle stop
2. Electric A/C compressors
3. Dual scroll hybrid A/C compressors

Used in 2001 - 2004 Prius, Camry. See Figure 11.40.

Type:

- Engine Belt Driven with “idle stop” (engine shuts off during idling)

Advantages:

- During “idle stop”, A/C compressor load on engine is absent

Disadvantages:

- During “idle stop”, no cooling of the passenger cabin is possible, leading to customer dissatisfaction. Since the compressor is belt driven, “idle stop” is automatically disabled when A/C load is higher



Figure 11.40: Gasoline engine/belt-driven A/C compressor

Electric A/C Compressors

Used in 2004 and later model Prius. See Figure 11.41.

Type:

- Typically, on series and some parallel hybrid vehicles, the A/C compressor is powered by an electric motor with an integrated inverter and controls, to drive the air conditioning compressor

Advantages:

- No engine drag, (with its resulting negative effect on fuel economy)
- Can provide cooling at all times (unless state of charge on the battery is low)

Disadvantages:

- High current draw from batteries thus reducing EV range (not a viable option for parallel hybrids)

The electric compressor is a FSV intent technology.



Figure 11.41: Electric compressor

Dual Scroll Hybrid A/C Compressors

Used in: 2006 and later Honda vehicles. See Figure 11.42.

Type:

- Honda's approach to solving the idle stop/air conditioning issue is a "hybrid", using a conventional 75cc belt driven scroll compressor in the front, and a smaller 15cc electric scroll compressor in the rear

Advantages:

- Better efficiency and A/C load handling characteristics
- Can provide cooling at all times (unless state of charge on the battery is low)

Disadvantages:

- Unit cost and complexity



Figure 11.42: Dual scroll hybrid compressor

11.8.3.6 Vehicle Results

The combination of solar reflective glass (all locations), solar powered ventilation, and solar reflective paint resulted in significant temperature reductions.

- The breath air temperature was reduced 12.0°C
- The seat surface temperature was reduced 10.0°-12.0°C
- The dashboard temperature was reduced 16.8°C
- Windshield temperature was reduced 20.4°C

Solar reflective roof only:

- The 6.7°C (44°F) cooler roof temperature did not have a significant impact on the interior temperature

Solar powered ventilation only:

- With the air being pulled out of the vehicle, the reduction in temperatures was significant, thus reducing the air and seat temperatures 5.6°C (42°F)

Cabin air re-circulation:

- After reducing the peak thermal load and the solar gain, the next most important approach to minimizing air conditioning loads is to reduce the amount of outside air brought in for ventilation. It is more effective to condition re-circulated cabin air than to treat very cold or very hot air from outside the cabin. Generally, only 1.2 kW is needed to maintain the cabin air at 30°C above ambient using 100% re-circulated air, versus 4.5 kW that will be needed if 100% outside air is used

11.8.3.7 Conclusion

The air conditioning system is the single largest auxiliary load on a vehicle by nearly an order of magnitude. Conventional air conditioning loads can reduce EV range and HEV fuel economy by nearly 40% depending on the size of the air conditioner and the driving cycle. The peak cabin soak temperature must be reduced if a smaller air conditioning system is to be used. Advanced glazing and cabin ventilation during soak conditions are effective ways to reduce the peak cabin temperature. A combination of these technologies reduced breath air temperature by 12°C, seat temperature by 11°C and windshield temperature by 20°C.

Solar Reflective Paint is effective in reducing external surface temperatures but studies have shown it to be ineffective in reducing interior cabin temperatures.

Vehicle simulation results have shown that a 30% reduction in thermal load results in a 26% reduction in fuel used for A/C.

What does this mean to the average consumer?

For a real world scenario, consider the following assumptions, and Figure 11.43:

- Type of vehicle: PHEV₄₀
- Usable energy (50% SOC): 8 kWh
- Residence: Phoenix, AZ
- Daily commute: 60 minutes
- Time of year: Mid-August
- Ambient temperature: 44°C (110°F)
- Average interior temp: 65°C (149°F)
- The vehicle has been parked outside for 8 hours
- The A/C compressor peak load is 4 kW for 20 minutes, and the steady-state load is 1 kW for the next 40 minutes of the trip - **conventional setup**
- The A/C compressor peak load is 1 kW for 20 minutes, and the steady state load is 1 kW for the next 40 minutes of the trip - **with discussed strategy**

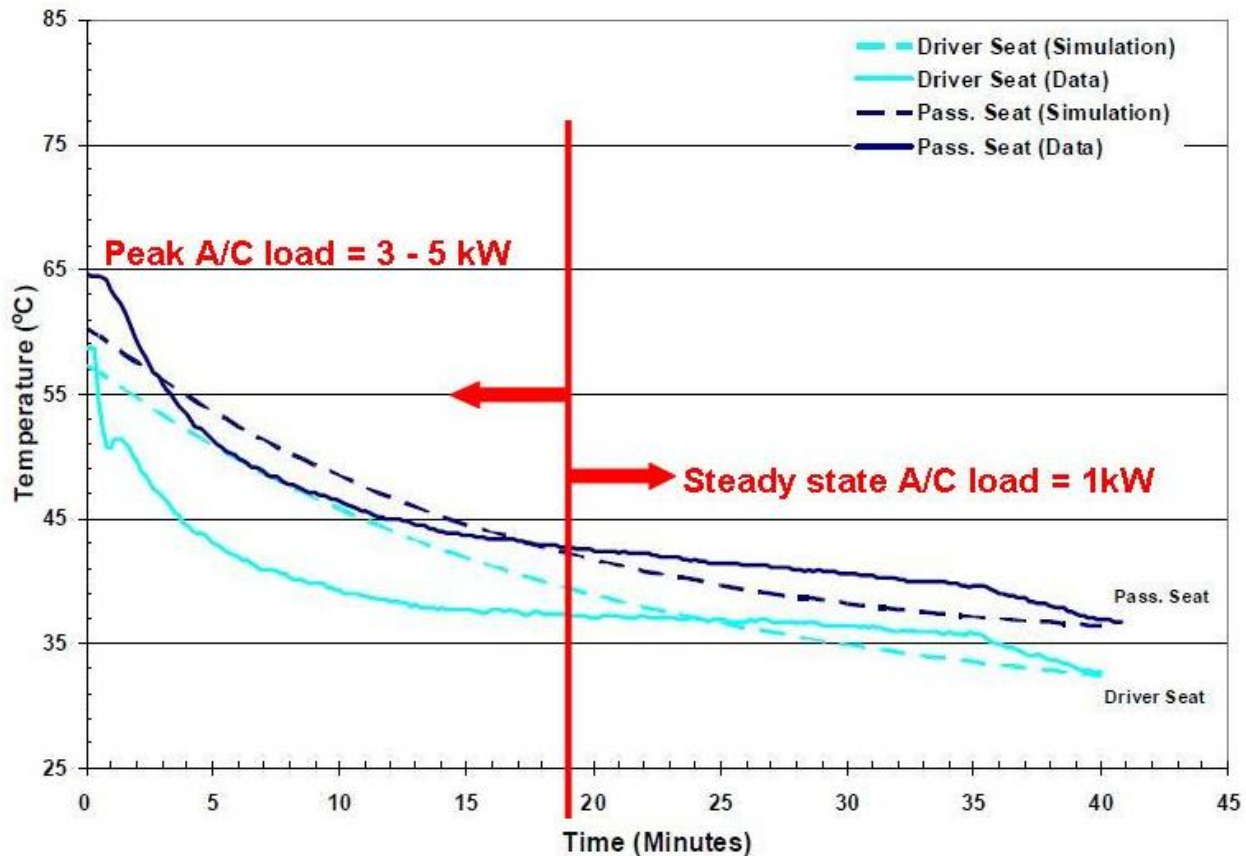


Figure 11.43: Air conditioning loads (temperature vs. time)

11.8 Auxiliary Equipment

Energy required for the first 20 minutes of the trip =

$$4 \text{ kW} \times 20/60 \text{ h} = 1.33 \text{ kWh}$$

$$(1 \text{ kW} \times 20/60 \text{ h} = 0.33 \text{ kWh})$$

Energy required for the next 40 minutes of the trip =

$$1 \text{ kW} \times 40/60 \text{ h} = 0.7 \text{ kWh}$$

$$(1 \text{ kW} \times 40/60 \text{ h} = 0.7 \text{ kWh})$$

Energy lost due to A/C =

$$1.33 \text{ kWh} + 0.7 \text{ kWh} = 2.03 \text{ kWh} (\sim 16.1 \text{ km} (\sim 10 \text{ miles}) \text{ of All Electric Range - (AER))}$$

$$0.33 \text{ kWh} + 0.7 \text{ kWh} = 1.03 \text{ kWh} (\sim 0.8 \text{ km} (\sim 5 \text{ miles}) \text{ of AER})$$

Actual AER of the vehicle $64.37 \text{ km} - 16.1 \text{ km} = 48.27 \text{ km}$ ($40 - 10 = 30$ miles)

Actual AER of the vehicle $64.37 \text{ km} - 0.8 \text{ km} = 63.57 \text{ km}$ ($40 - 5 = 35$ miles)

With the above calculations, the following conclusions are ascertained:

PHEV₄₀ is actually reduced to a PHEV₃₀

PHEV₄₀ is actually only reduced to a PHEV₃₅

12.0 FSV Structure Design Methodology

12.1 Overview

12.1.1 FSV Development Process

The design and development process used for the Future Steel Vehicle program is shown in Figure 12.1. The Auto/Steel Partnership (A/SP) projects, Future Generation Passenger Compartment (FGPC) Phases 1 & 2, have previously validated the major portions of this design and development process for an existing structure. This form of optimization is referred to as 3G Optimization, representing full shape, material and gauge (geometry, grade and gauge) optimization. Building on this work, the FSV program will first define the optimum load path of a clean sheet design by blocking out the initial structure. This type of optimization is called Topology Optimization. It will then continue with the previous proven methods developed by FGPC Phases 1 & 2.

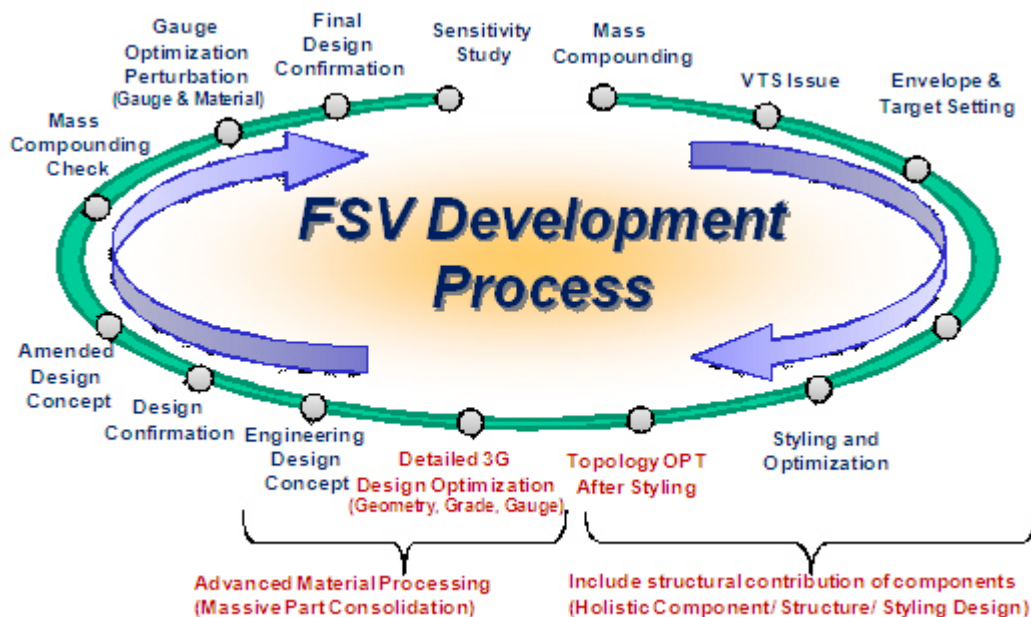


Figure 12.1: Detailed FSV development process

12.1.2 FSV Pilot Project Development Process

The FSV pilot project development process is shown in Figure 12.2. The complete FSV development process is significantly more detailed than the pilot project. But, a majority of the tasks within the FSV Development process have already been proven by both FGPC projects. It is only the integration of Topology Optimization into the whole process that has not previously been considered. Hence, the focus of the FSV pilot project was Topology Optimization and its integration to the overall development process.

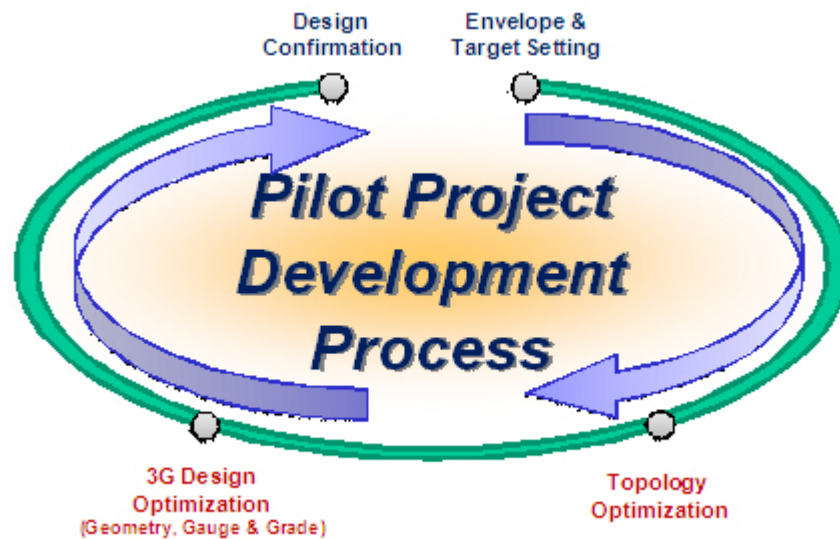


Figure 12.2: Pilot project development process

12.1.3 Objective

The first objective of FSV pilot project was to validate the proposed optimization methodology that will be used in the FSV program.

The second objective was to apply the same optimization methodology to the A/SP Lightweight Front End (LWFE) front rail to establish any additional mass savings. Figure 12.3 illustrates a summary of the LWFE program. The project started with the donor vehicle front rail and created three optimized concepts: a Laser Welded Blank (LWB) and two Tailor Welded Tube (TWT) concepts. The LWB concept was the baseline geometry for the pilot project.

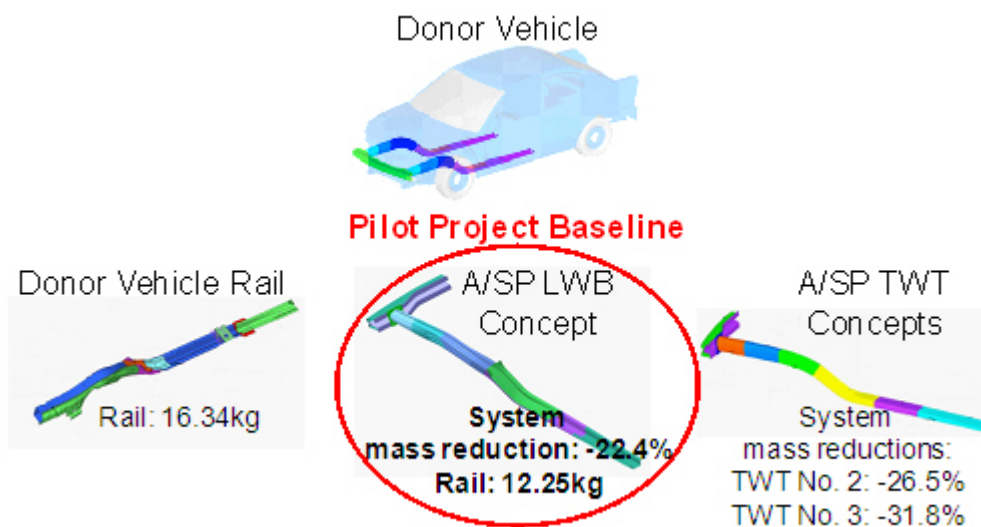


Figure 12.3: *LWB concept - pilot project baseline*

12.1.4 Optimization Methodology

As shown in Figure 12.4 the optimization methodology involved the following steps:

- Block out design envelope
- Topology Optimization
- Parameterize Geometry
- Detailed 3G Optimization: Geometry (Shape), Grade (material) & Gauge

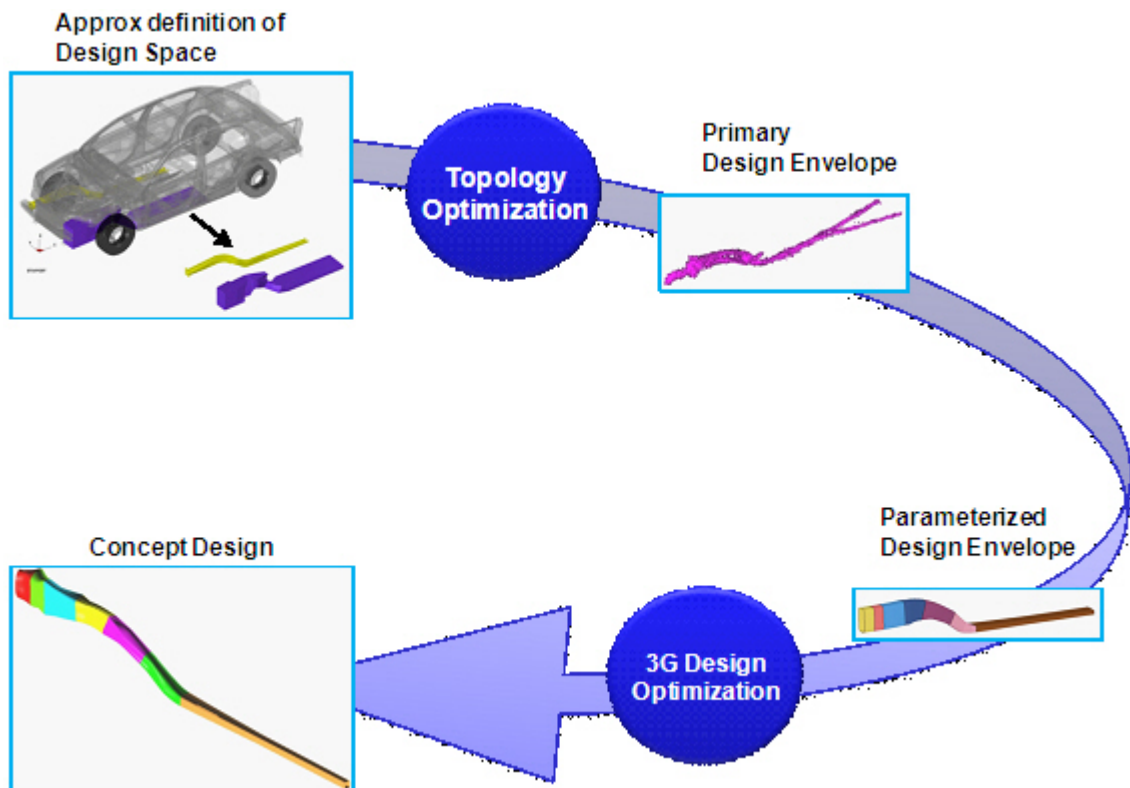


Figure 12.4: Optimization methodology overview

Following were the optimization load cases considered:

- US-NCAP zero degree front crash
- IIHS Front Impact 40% Offset Deformable Barrier (ODB)
- Static stiffness
 - Torsion
 - Bending

12.2 Baseline Model

The donor vehicle model as received was a full LS-Dyna crash model of approximately 310,000 elements. The donor vehicle model and front rail model are shown in Figure 12.5.

Front rail mass = 12.25 kg (A/SP LWFE-LWB)

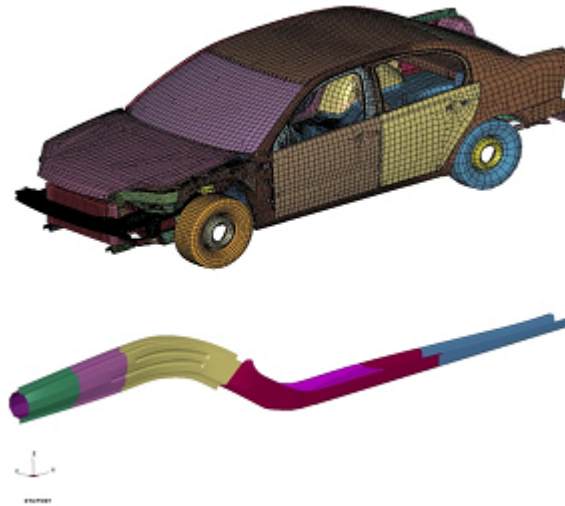


Figure 12.5: *Model as received (front rails shown for clarity)*

In order to assess the baseline model performance, CAE analysis was conducted on the donor vehicle model for the following test procedures:

- US-NCAP zero degree front crash
- IIHS front crash 40% ODB

Also, the following static stiffnesses were calculated for the baseline model.

- Torsion
- Bending

12.2.1 Baseline Performance

12.2.1.1 US-NCAP Zero Degree Front Crash

Boundary Conditions

The impact barrier is represented as a fixed rigid wall positioned so that it almost contacts the front tip of the front bumper at the start of the simulation. The ground is also represented as a rigid wall positioned at the very lowest points of the tires. The performance of the vehicle structure was verified under NCAP loading. The vehicle is impacted into a rigid wall at an initial velocity of 35 mph.

Results

The CAE test setup and results are shown in Figure 12.6.

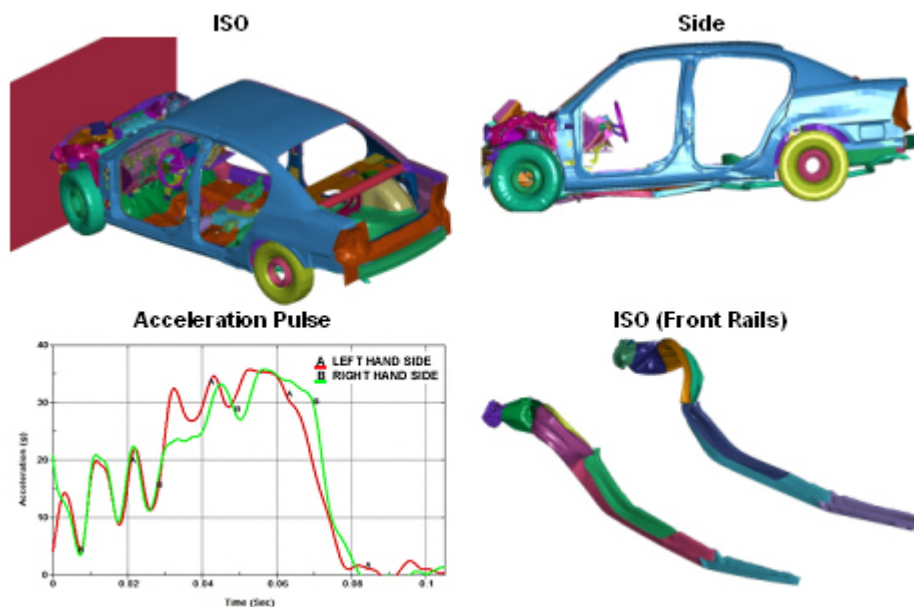


Figure 12.6: NCAP - deformed plots & acceleration

Maximum B-Pillar Pulse

The maximum B-pillar pulses were the following:

- Left hand side: 36 g
- Right hand side: 36 g

12.2.1.2 IIHS Front Crash 40% ODB

Boundary Conditions

The vehicle impacts a deformable barrier, offset 10% from centerline (40% overlap), at 40 mph.

Results

The CAE test results are shown in Figure 12.7 and Figure 12.8^[1].

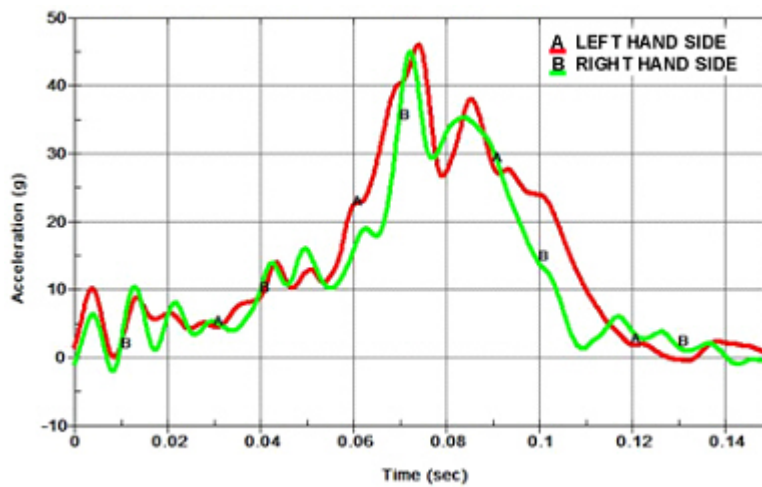


Figure 12.7: *Rocker acceleration pulse*

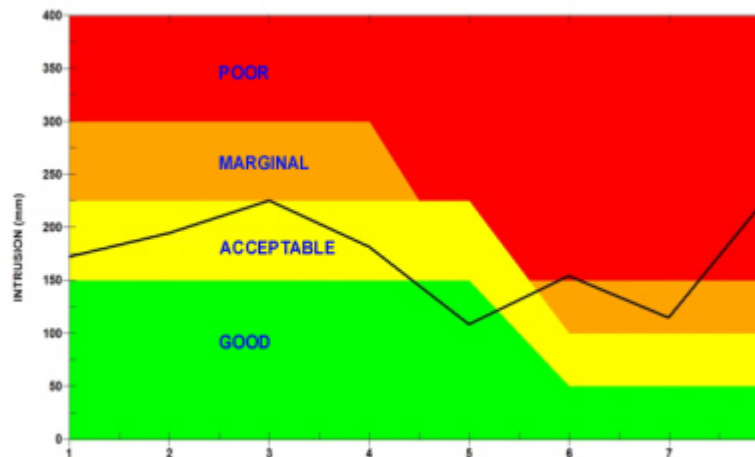


Figure 12.8: *IIHS intrusion performance*

¹1: Footwell, 2:Left Toe, 3:Center Toe, 4:Right Toe, 5:Brake Pedal, 6:Left IP, 7:Right IP, 8:Door

12.2.1.3 Static Stiffness

Boundary Conditions

Following were the boundary conditions:

- Torsion: Vehicle is held at the rear stock towers and front bumper. A couple is applied to the front shock towers.
- Bending: Vehicle is supported at all four shock towers, a load is applied in the vertical (negative z-direction) to the rocker at the front door opening.

Results

The CAE test results are shown in Figure 12.9.

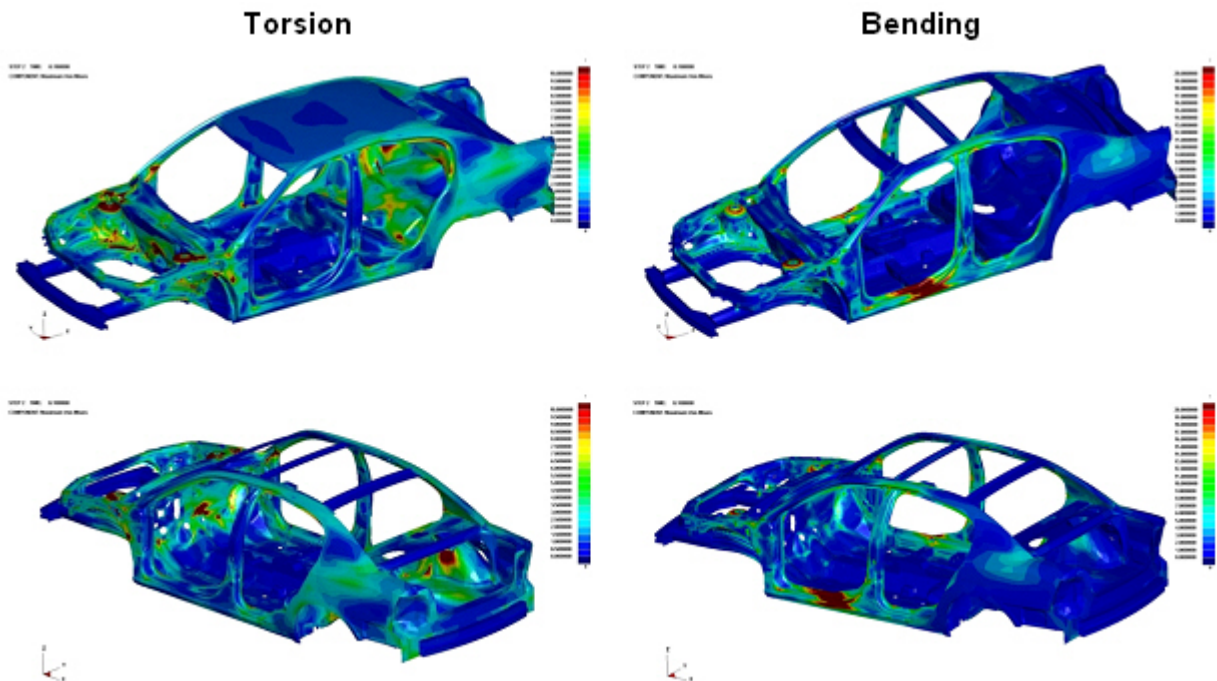


Figure 12.9: Static stiffness

Following were the stiffness values attained from CAE analysis results (shown in Figure 12.9):

- Torsion: $17,788 \frac{\text{Nm}}{\text{deg}}$
- Bending: $12,122 \frac{\text{N}}{\text{mm}}$

12.2.1.4 Performance Summary

The performance summary of the baseline model is shown in Table 12.1.

LOADCASE	PERFORMANCE	
NCAP Front Impact	Max B-Pillar Pulse	
	Left Hand Side	36g
	Right Hand Side	36g
IIHS Front Impact 40% ODB	IIHS Peak Intrusion	
	Left Toe pan	15 cm
	Center Toe pan	20 cm
	Right Toe pan	24 cm
	A-B Pillar Closure	19 cm
Static Stiffness	Torsion	17,788 Nm/deg
	Bending	12,122 N/mm

Table 12.1: *Baseline model performance summary*

12.3 Topology Optimization

The Topology Optimization began by defining the design space available to the optimization as shown in Figure 12.10. This represented the extreme packaging volume that the optimization can use. The new front rail must fit within this space.

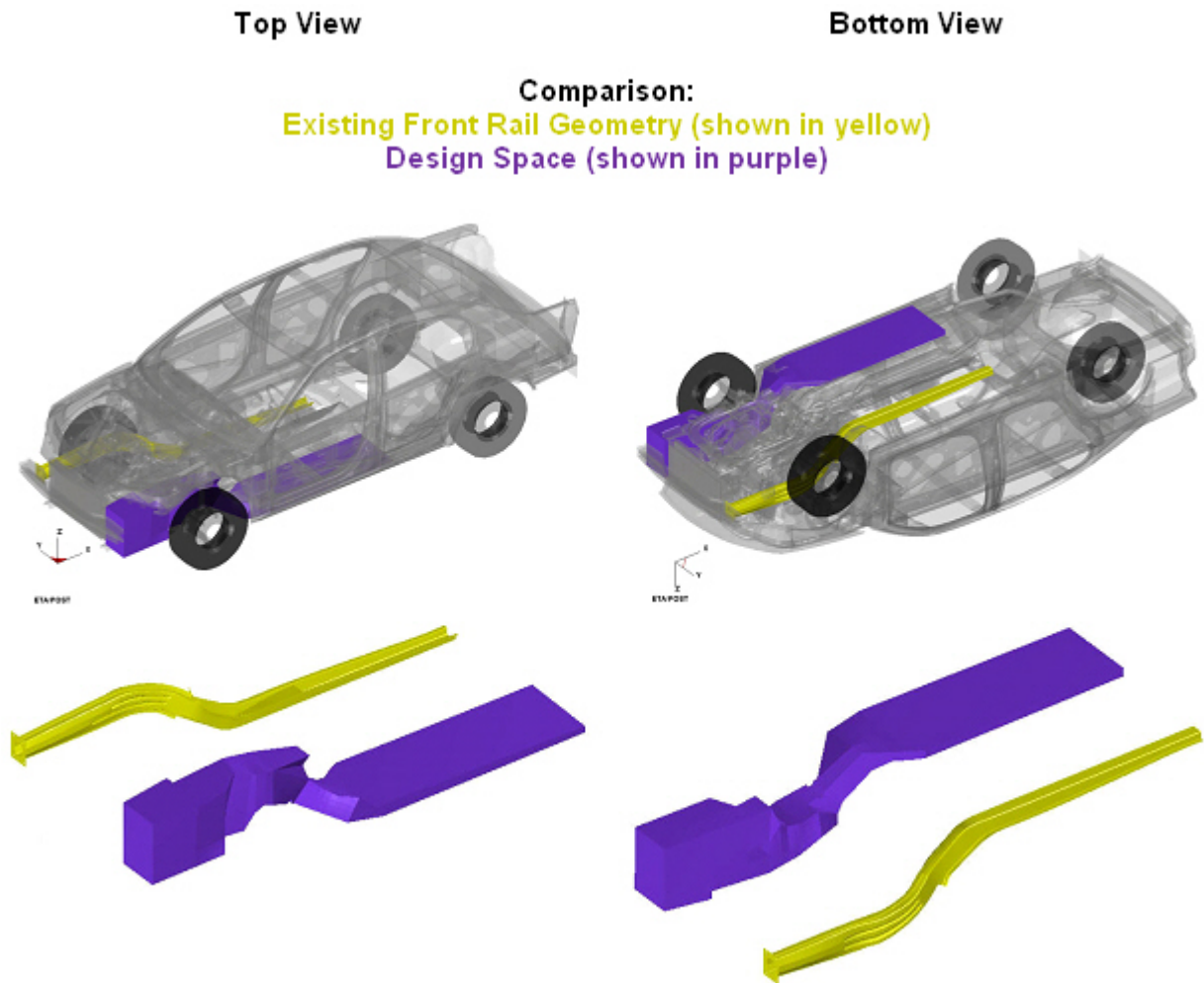


Figure 12.10: Design space

Calibration of the Donor Vehicle used a full vehicle dynamic crash model. However, Topology Optimization is based on static analysis and so an analogous static loading of the dynamic impact was applied to a de-coupled sub-model of the front rail. Figure 12.11 shows a direct comparison of the front rail deformed shapes for both the full vehicle dynamic analysis and the de-coupled static analysis.

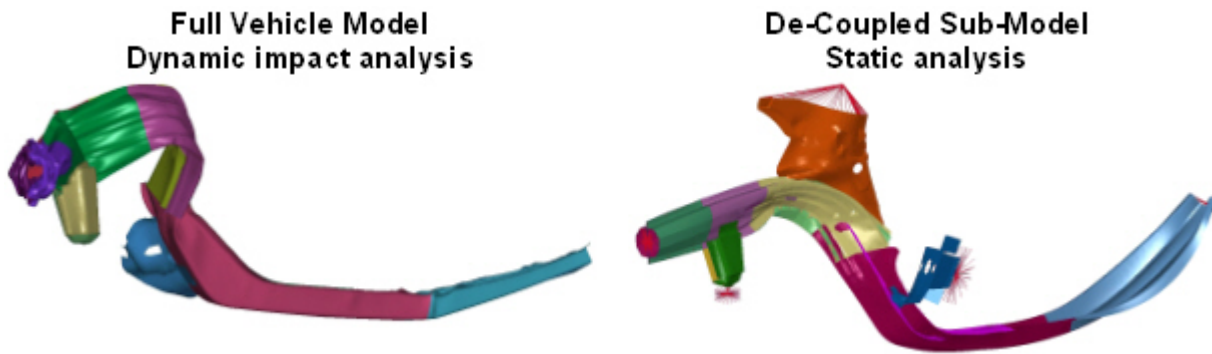


Figure 12.11: Comparison between full-vehicle dynamic & de-coupled static deformed shapes

Figure 12.12 shows the results of the Topology Optimization in combination with the Design Space (in light red) & original rail (in green). The Topology Optimization provided an insight into what the structure desires, free from the traditional design thought process. The optimal load path could now be used as the base for the 3G (Geometry, Grade & Gauge) Optimization. However, it should be noted that although Topology Optimization may seem quite straight forward, it is in fact a subtle iterative process.

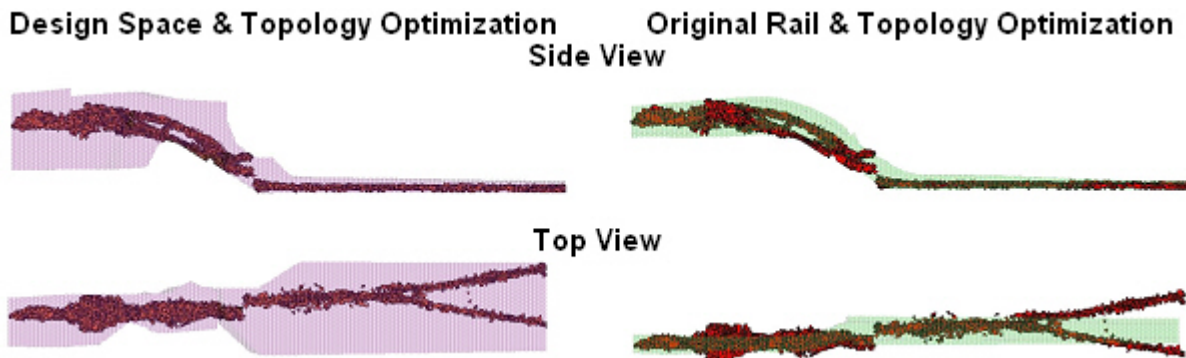


Figure 12.12: Topology Optimization results shown in combination with the design space (in light red) & original rail (in green)

12.4 3G Optimization

12.4.1 Background

3G Optimization represents full shape, material and gauge (Geometry, Grade & Gauge) optimization. At its core the process is the fully automated interface between the multi-dimensional optimization, simulation and parametric modeling. The multi-dimensional optimization controls the process as it conducts its search through the design space. It creates a design iteration which it submits to the simulation software for analysis. It then reviews the analysis results, compares these to the design objectives and the previous search history to develop a new design proposal. Any geometry changes it deems necessary are created by the parametric modeler. Once the new design proposal is complete, the optimization submits it for analysis to begin the next cycle of optimization. Figure 12.13 illustrates the 3G Optimization interface.

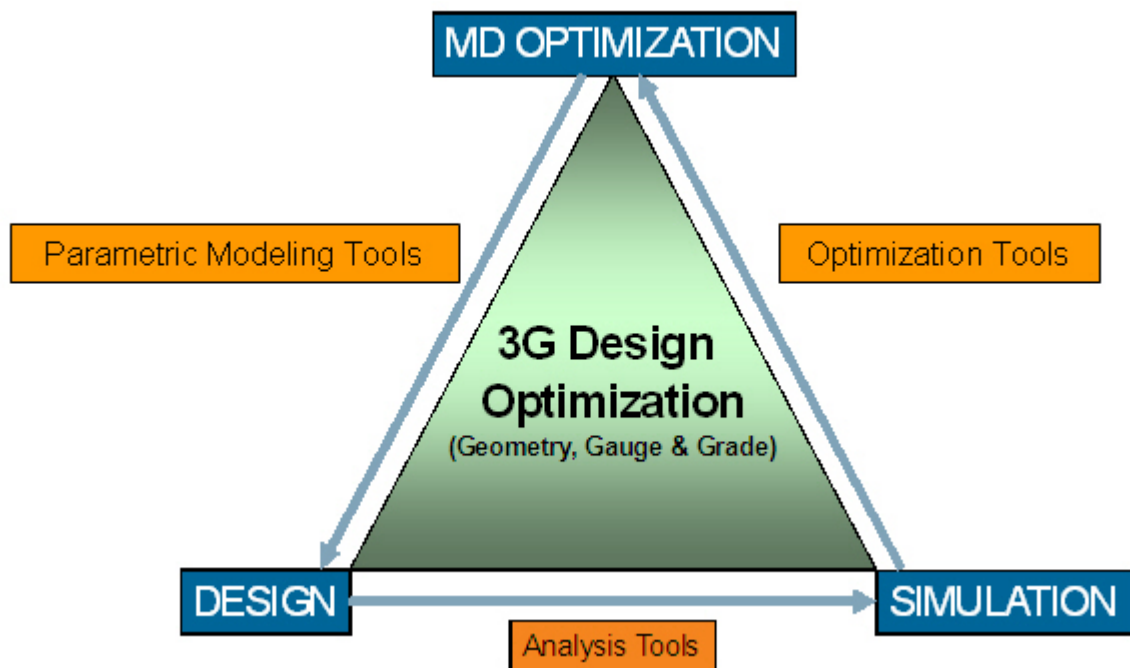


Figure 12.13: 3G Optimization - key interfaces

12.4.2 Load Path Parameterization

The first step to setting up the 3G Optimization was to parameterize the load path by defining a series of cross-sections through the load path. At each section, the optimization will be able to vary its dimensions, thus locally defining its shape. It was therefore necessary to define not only the location and number of cross-sections but also the boundary parameters that the optimization can control.

Figure 12.14 shows sections cut through both the load path and design space. For reference, Figure 12.15 includes the original front rail in place.

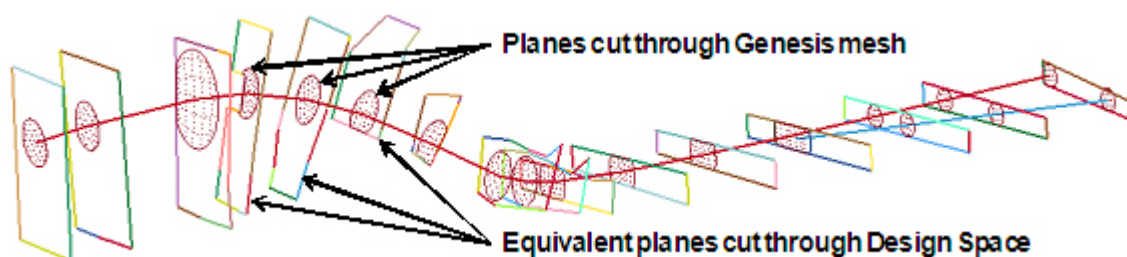


Figure 12.14: *Cross-sections through the Topology Optimization's load path mesh & design space*

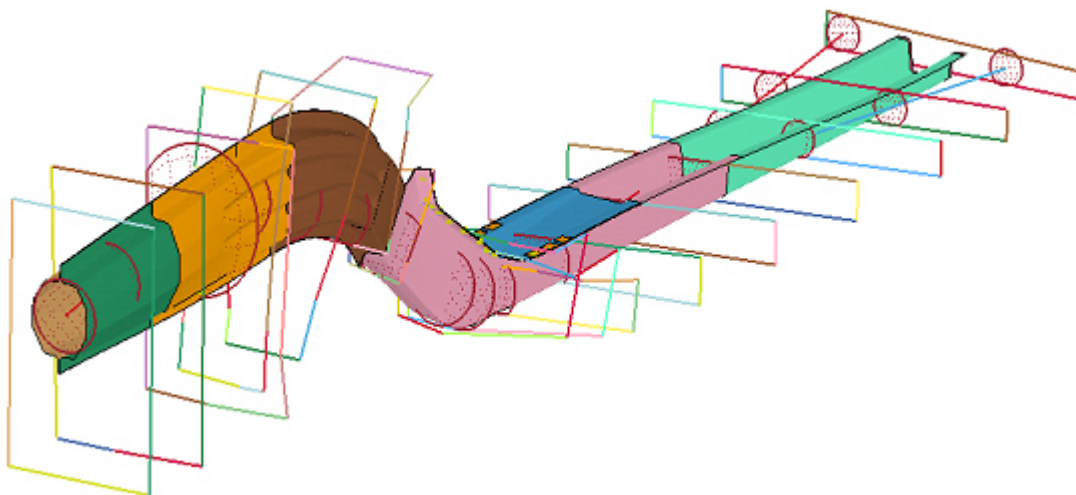


Figure 12.15: *Original front rail shown in combination with cross-sections through the design space*

After reviewing the deformed shapes from the initial calibration NCAP and IIHS Front Crash analysis, it was decided to add additional cross-sections at the front of the rail, cross-sections 1→12 and use fewer cross-sections for the rear portion, sections 13→15 (as shown in Figure 12.16 & Figure 12.17).

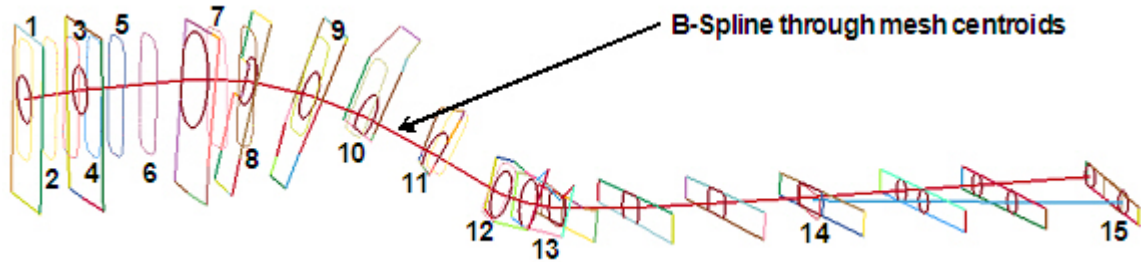


Figure 12.16: Finalized cross-sections through the Topology Optimization's loadpath mesh & design space

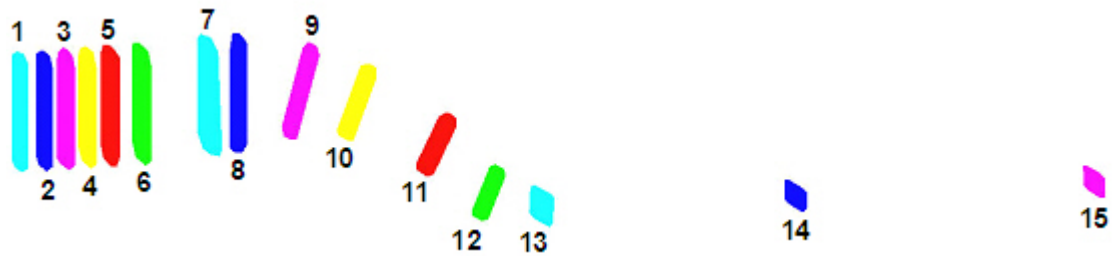


Figure 12.17: Finalized cross-sections

Once the number and location of the cross-sections were defined, the parameterization continued with the definition of the control points for each section, as shown in Figure 12.18.

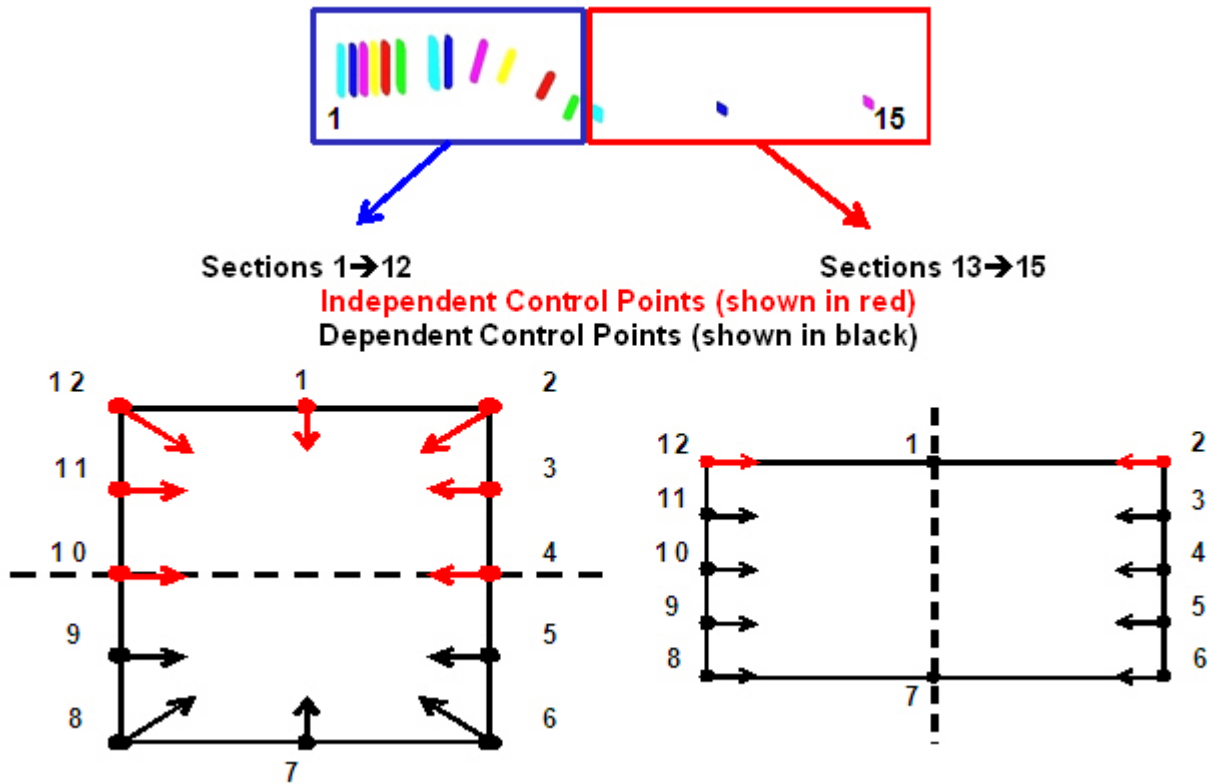


Figure 12.18: Parameterization of cross-sections

The shape of each cross-section is defined by twelve control points, as shown in Table 12.2. The independent control points are free to move within the plane of the cross-section. A dependent control point must follow its corresponding independent point's movement. Limits to a cross-section's shape change were set so that the maximum size of the section was the outer limit of the design space, from here the optimization was free to reduce the perimeter by up to 40% or 60% of the outer boundary.

CROSS-SECTION	CONTROL POINTS	
01→12	Independent	1, 2, 3, 4, 10, 11, 12
	Dependent	5, 6, 7, 8, 9
13→15	Independent	2, 12
	Dependent	1, 3, 4, 5, 6, 7, 8, 9, 10, 11

Table 12.2: Control points

In addition to shape changes, the optimization was able to independently select both material and gauge along the length of the rail. Table 12.3 lists the material and allowable gauge range available to the optimization. Figure 12.19 shows the regions in which this choice was available (Note: The rail's shape variables are shown at the maximum size for each section, the outer limit of the design space).

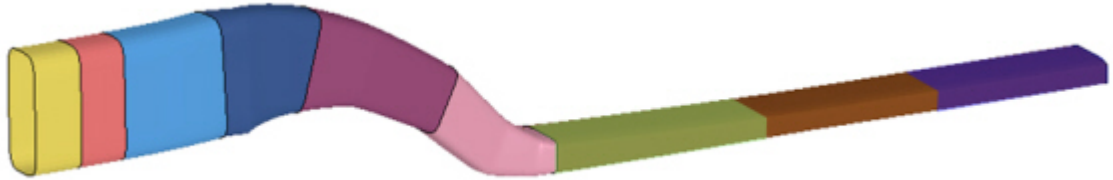


Figure 12.19: *Material & gauge parameterization*

MATERIAL	GAUGE RANGE
DP350/600	0.6 →2.3mm
DP500/800	0.6 →2.3mm
DP700/1000	0.6 →2.3mm

Table 12.3: *Material & gauge variables*

12.4.3 Problem Statement

The 3G optimization problem statement is shown in Table 12.4.

Maximize:	Mass Reduction
Subject to:	Section Force \leq 35kN
By Varying:	Cross-sectional Shape (106 variables)
Material:	DP350/600, DP500/800, DP700/1000 (9 variables)
Gauge:	0.6 → 2.3 mm (9 variables)

Table 12.4: *3G Optimization problem statement*

12.5 Final Design

The final optimized design of the FSV front rail is shown in Figure 12.20. The material and corresponding gauge selections are shown in Table 12.5.

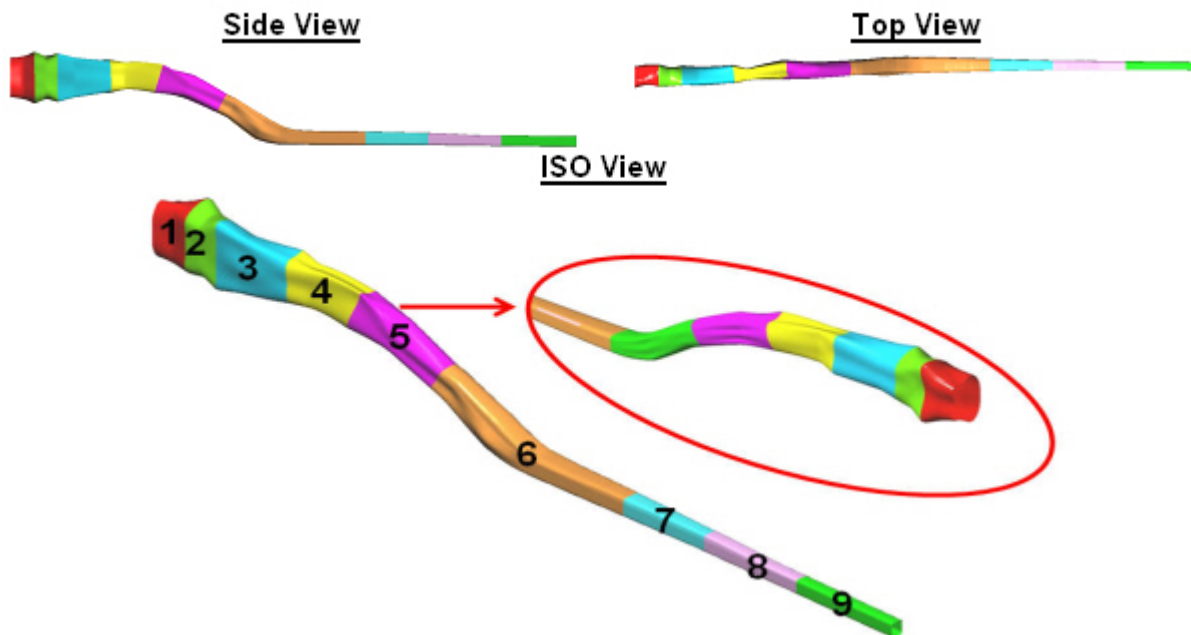


Figure 12.20: *Final design*

CROSS-SECTION	MATERIAL	GAUGE [mm]	MASS [kg]
1	DP350/600	1	0.48
2	DP500/800	1	0.46
3	DP700/1000	0.7	0.64
4	DP500/800	1.5	0.99
5	DP700/1000	2	1.58
6	DP700/1000	2.3	3.53
7	DP700/1000	1.5	0.69
8	DP700/1000	0.8	0.37
9	DP700/1000	0.6	0.26
		TOTAL	8.98

Table 12.5: *Final design - material & gauge selections*

The mass of the FSV optimized front rail was 8.98 kg (27% reduction in weight compared to A/SP LWFE-LWB). The comparison of the FSV optimized front rail to the A/SP LWFE-LWB is shown in Figure 12.21.

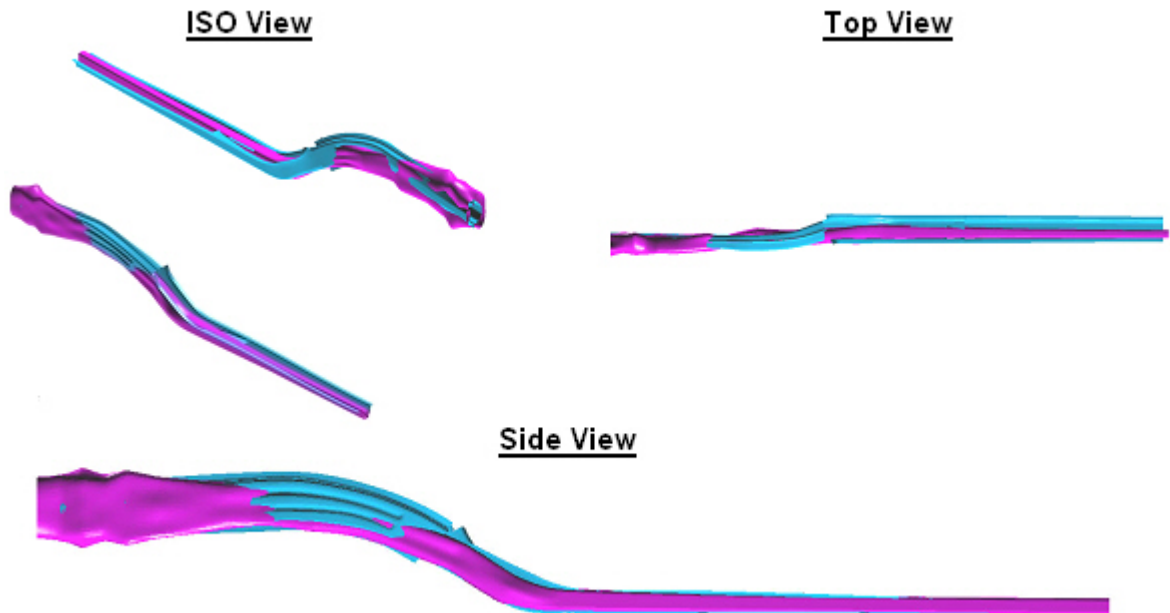


Figure 12.21: Final design (in purple) shown in combination with original rail (in blue)

Figure 12.22 shows the FSV optimized front rail combination of the Topology Optimization.

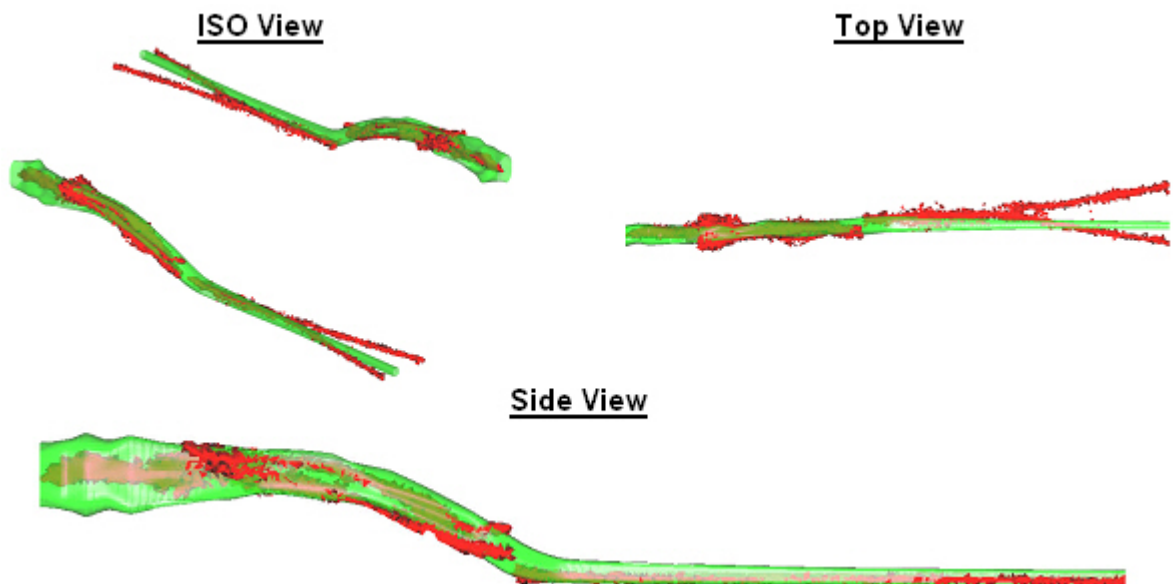


Figure 12.22: Design (in green) shown in combination with Topology Optimization (in red)

12.6 Final Validation

The final optimized design was validated for the test procedures: US-NCAP zero degree front crash and IIHS front crash 40% ODB. The static stiffnesses (torsion and bending) were calculated for the final optimized design, and compared to those of the baseline model.

12.6.1 US-NCAP Zero Degree Front Crash

The CAE results of the US-NCAP zero degree front crash procedure is shown in Figure 12.23.

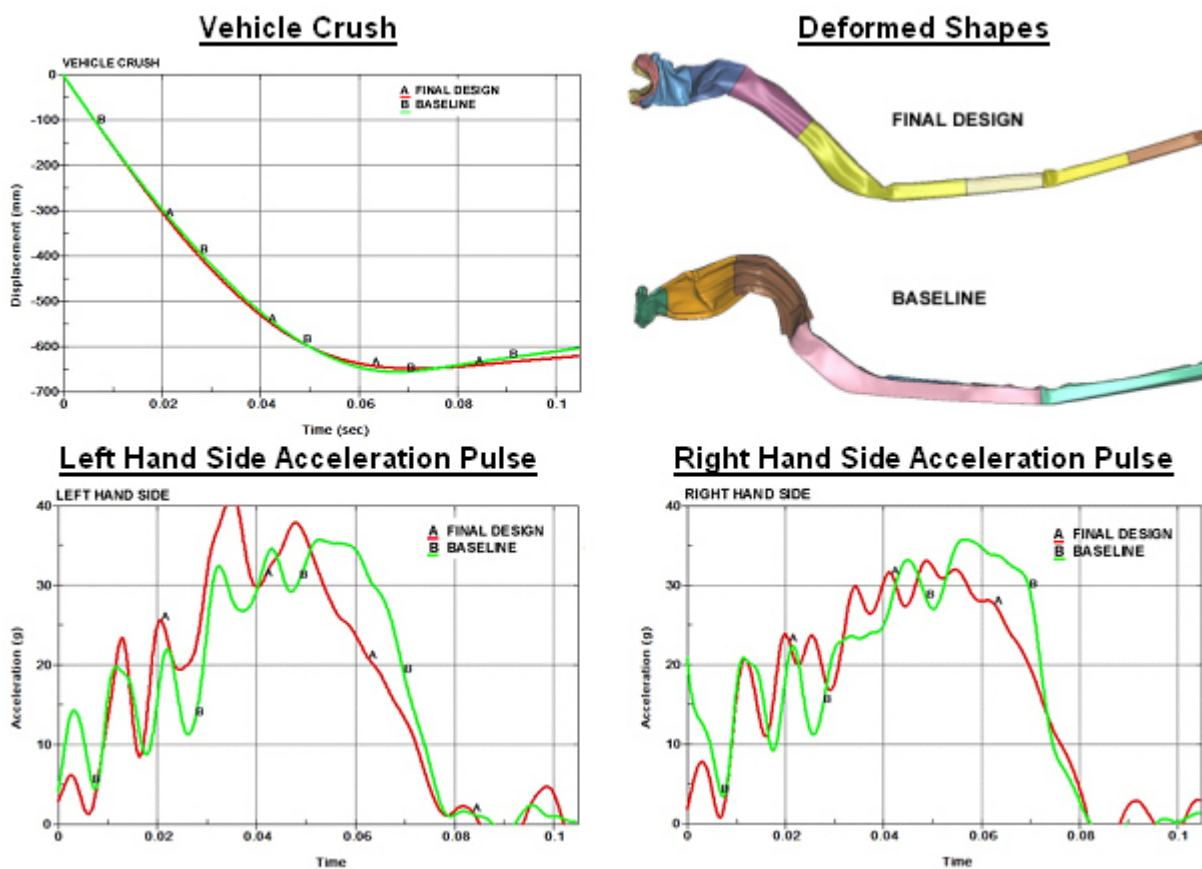


Figure 12.23: NCAP - final design & original rail - deformed plots & Acceleration

The donor vehicle and the final design models are shown in Figure 12.24.

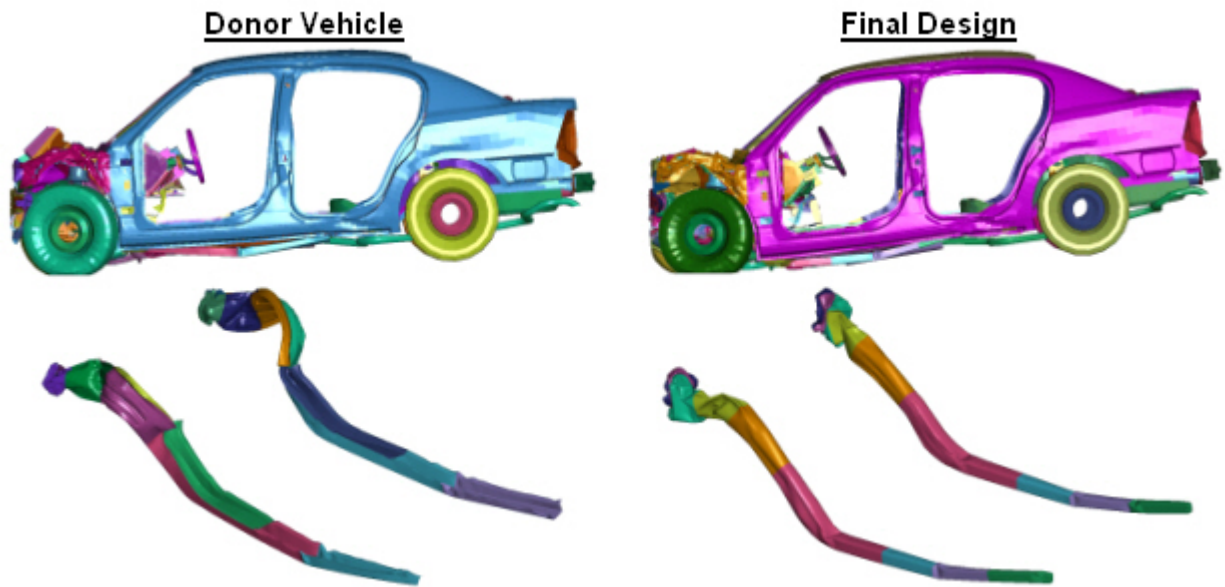


Figure 12.24: NCAP - donor vehicle & final design

12.6.2 IIHS Front Crash 40% ODB

The IIHS front 40% offset crash was analysed on the final design as shown in Figure 12.25. The corresponding results of the CAE analysis is shown compared to the baseline design in Figure 12.26.

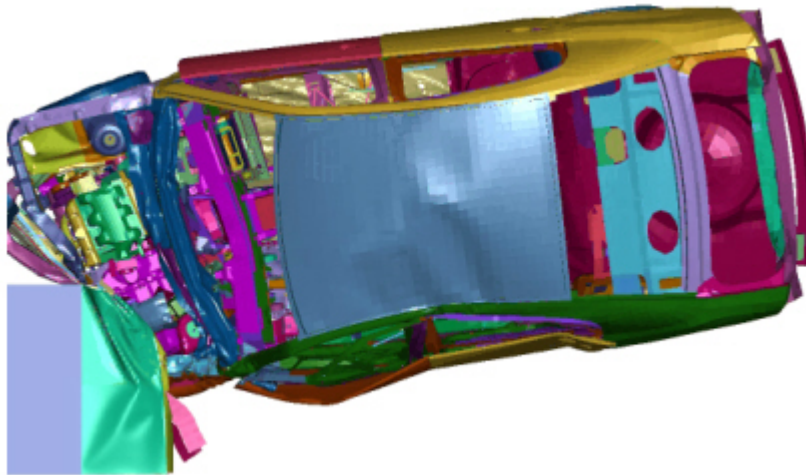


Figure 12.25: IIHS front 40% offset crash procedure

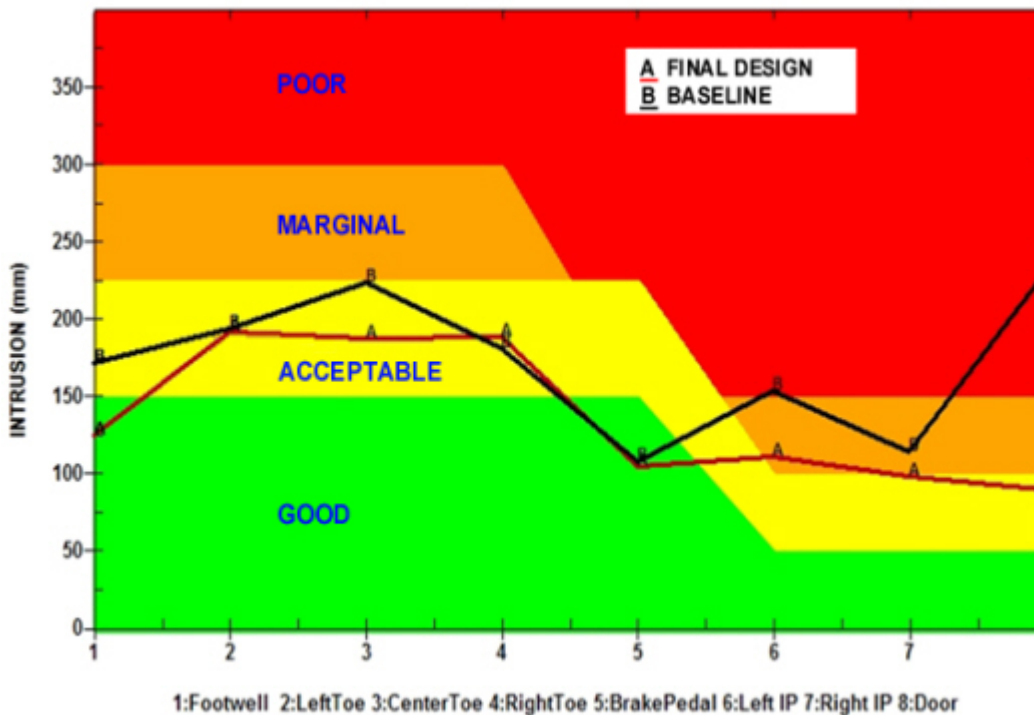


Figure 12.26: IIHS front impact 40% offset crash results- donor vehicle & final design

12.6.3 Static Stiffness

Following were values attained from CAE analysis results (shown in Figure 12.27).

- Torsion: $17,094 \frac{\text{Nm}}{\text{deg}}$ (Baseline: $17,788 \frac{\text{Nm}}{\text{deg}}$)
- Bending: $11,870 \frac{\text{N}}{\text{mm}}$ (Baseline: $12,122 \frac{\text{N}}{\text{mm}}$)

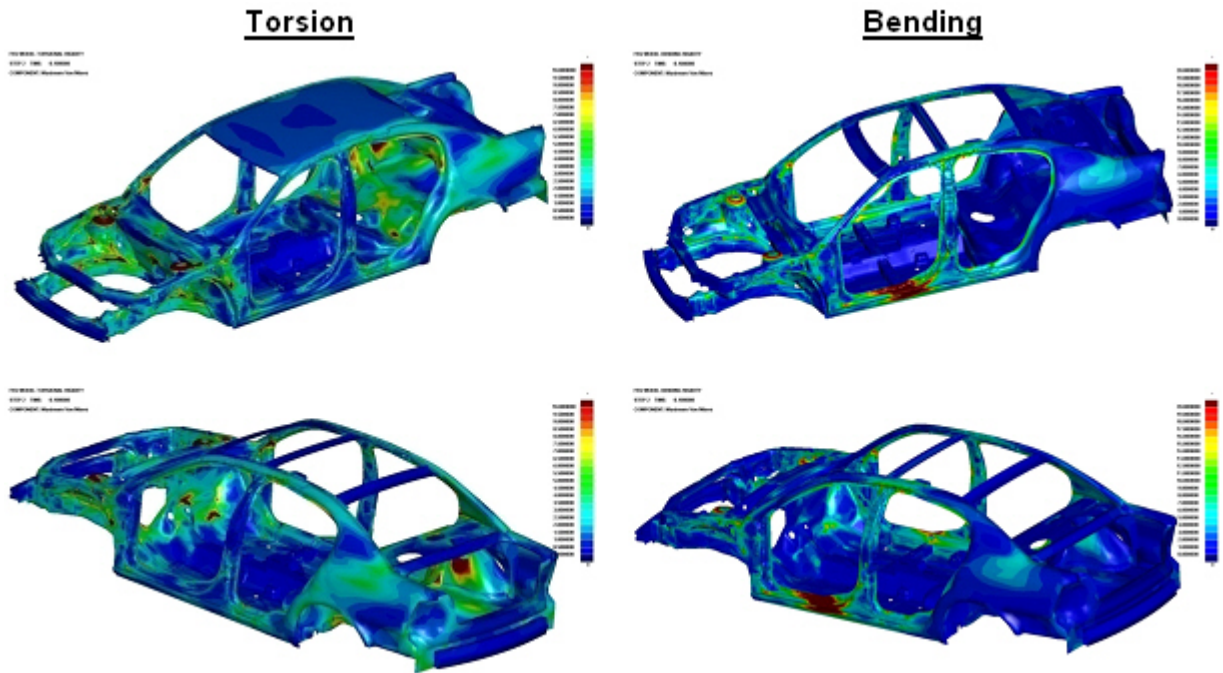


Figure 12.27: Static stiffness

12.7 Conclusion

The proposed design optimization method (Topology and 3G) proved to be effective for the FSV pilot project. The final FSV optimized front rail design realized a mass savings of 27% and 45%, as compared to the LWFE-LWB (A/SP optimized design) and the donor vehicle front rail, respectively (as shown in Figure 12.28).

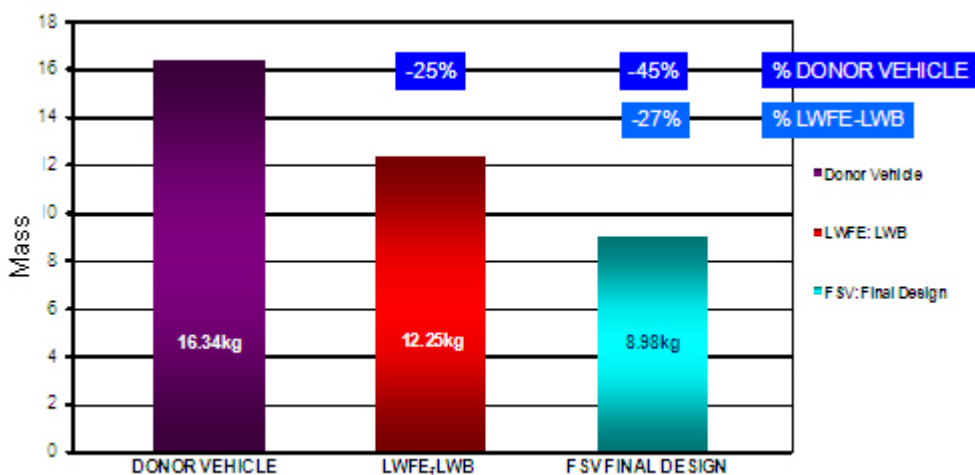


Figure 12.28: Front rail: donor vehicle, LWFE & LSV pilot project comparison

12.8 Manufacturability

The optimization did not consider any manufacturability constraints. The only objective of the optimization was to identify what the structure sought, free from any additional considerations.

The circumferential variation along the length of the rail is shown in Figure 12.29 and the corresponding dimensions are listed in Table 12.6.

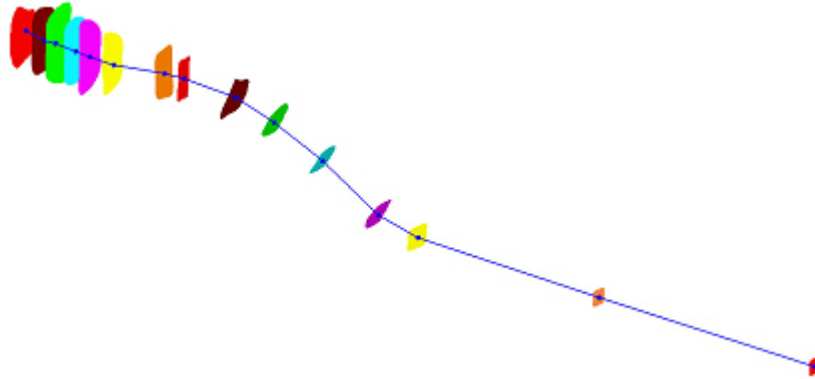


Figure 12.29: Final design - cross-sectional variation along rail

CROSS-SECTION	PERIMETER		SECTION-DISTANCE [mm]
	[mm]	[% Change]	
1	483.5	-	
2	522.5	8%	61
3	612.3	17%	58
4	514.7	-16%	60
5	550.8	7%	47
6	471.2	-14%	76
7	429.2	-9%	165
8	347.1	-19%	65
9	382.4	10%	159
10	325.4	-15%	138
11	290.4	-11%	172
12	304.5	5%	212
13	269.1	-12%	134
14	173.6	-35%	603
15	158	-9%	720

* % change in perimeter from previous cross-section

** Distance between section centroids

Table 12.6: Final design - cross-sectional variation along rail

Based upon the analysis shown in Table 12.6 a hydro-formed tube was considered as a potentially viable concept.

Figure 12.30 shows the equivalent tube diameters corresponding to the cross-sectional changes along the length of the final design. Using these equivalent diameters, the circumferential strain was calculated along the length of the hydro-formed tube as shown in Figure 12.31.

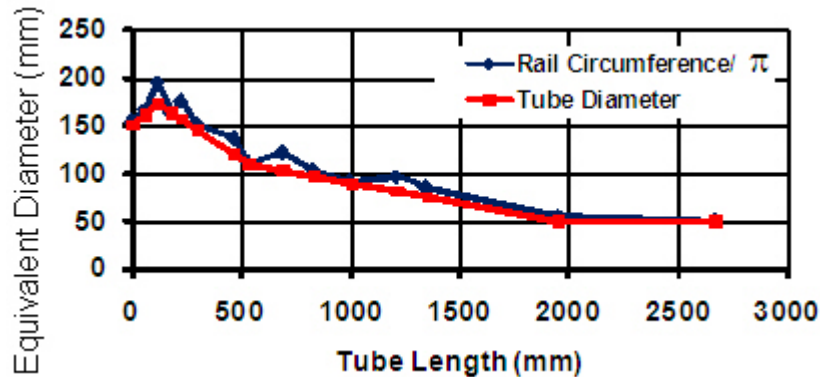


Figure 12.30: *Final design hydroformed tube concept - equivalent diameters*

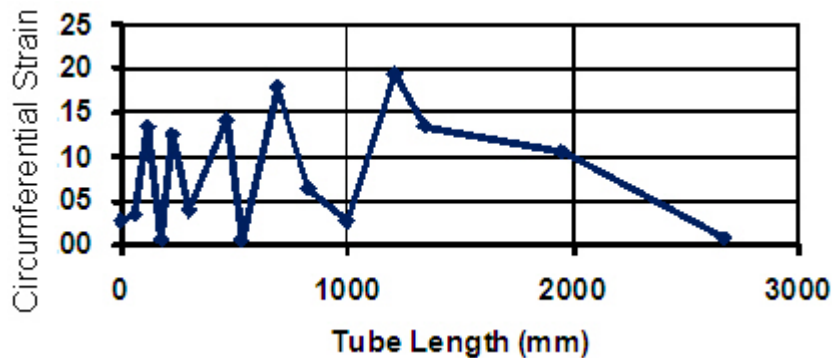


Figure 12.31: *Final design hydroformed tube concept - circumferential strain*

Substituting TRIP450/780 for DP500/800 and TRIP650/980 for DP700/1000, Figure 12.32 shows a potential hydro-formed tube concept based on the results of this optimization. This is only a potential concept and it is recognized that there could be design modifications necessary based on manufacturing feasibility and costs.

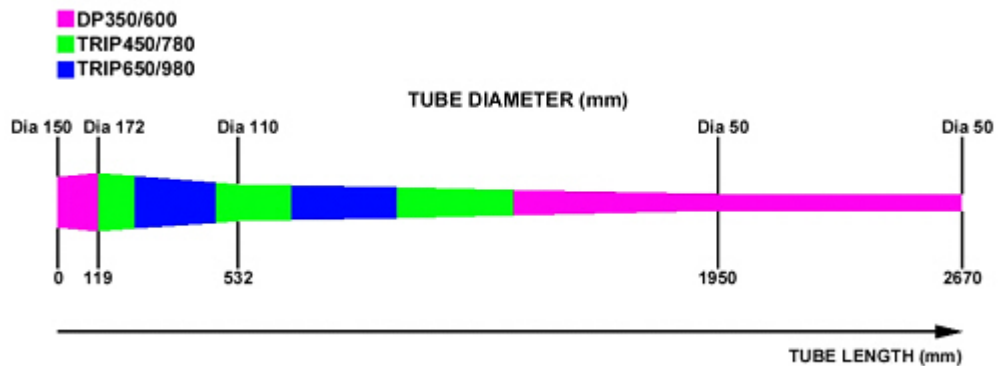


Figure 12.32: *Final design hydroformed tube concept - geometry & material*

The approach for the FSV program will be similar to that of the FSV front rail. However, appropriate manufacturing constraints will be applied to the optimization process accordingly.

12.9 3G Optimization Process

The 3G optimization used the HEEDS search algorithm to conduct an efficient search for optimized designs, in a fraction of the time it would take to perform a few manual design iterations.

12.9.1 HEEDS Search Algorithm

The key characteristics of the HEEDS search algorithm are the following:

- Hybrid
 - Blend of 'methods' used simultaneously, not sequentially
 - Multiple optimization methodologies used; evolutionary methods, simulated annealing, response surface methods, gradient methods & more
 - Takes advantage of best attributes of each approach
 - Global & local search performed together
- Adaptive
 - Each 'method' adapts itself to the design space
 - Master controller determines the contribution of each 'method' to the search process
 - Efficiently learns about design space & effectively searches even very complicated spaces
- Both single and multi-objective capabilities

12.9.2 How HEEDS Works

The basic steps of the HEEDS algorithm are shown in Figure 12.33. At the beginning of an optimization study, HEEDS creates an initial set of randomly generated designs. HEEDS evaluate the performances of the designs, either sequentially or in parallel. As the assessments are completed, HEEDS post-processes each design's performance to determine its constraint and objective function values. Aimed with the results of each design's performance and its search history to date, HEEDS uses an adaptive strategy that combines aspects of multiple search techniques to create a new set of designs for evaluation.

Figure 12.34 shows the Hybrid Adaptive Search strategy used by HEEDS. This intelligent search process is then repeated over a number of cycles while searching for the optimal design. The number of designs required to find the optimal depends on the total number of design variables considered and on the nature of the response, whether it is smooth, noisy, multi-modal, discontinuous, etc.

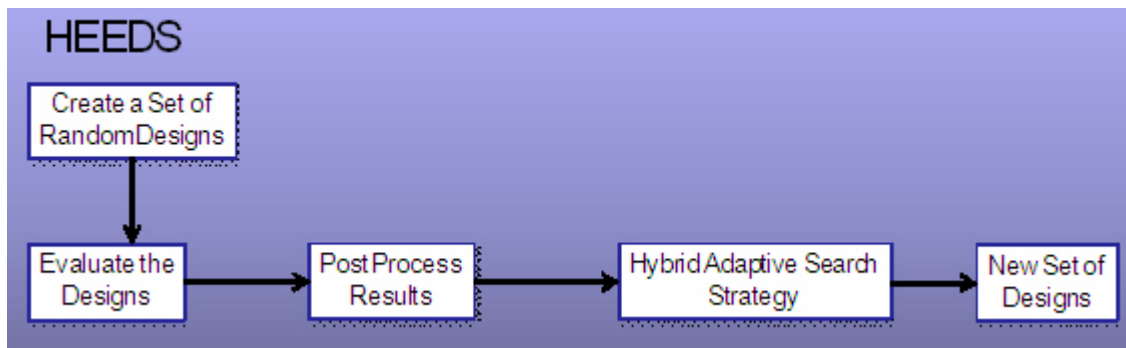


Figure 12.33: HEEDS Algorithm - basic loop

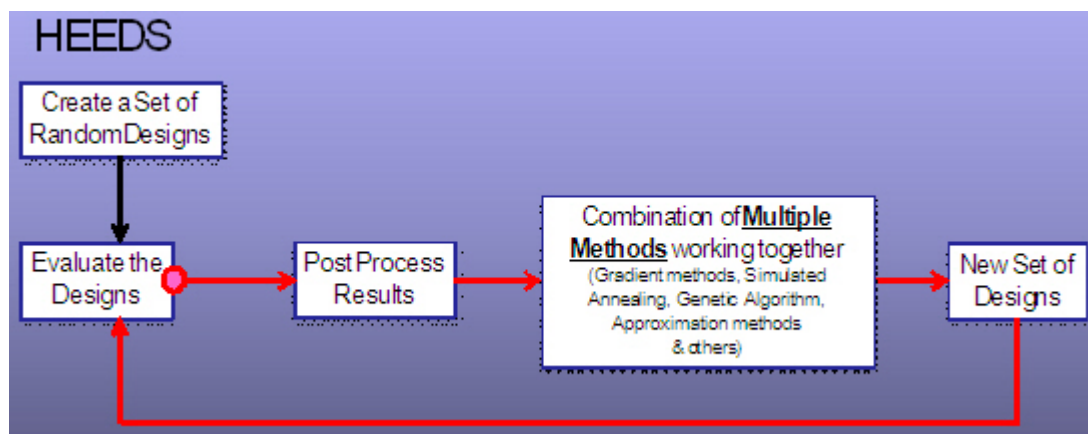


Figure 12.34: Hybrid Adaptive Search Strategy

As a general rule of thumb, previous experience can be used to identify the approximate minimum number of design evaluations required. Such an approximation is shown in Figure 12.35.

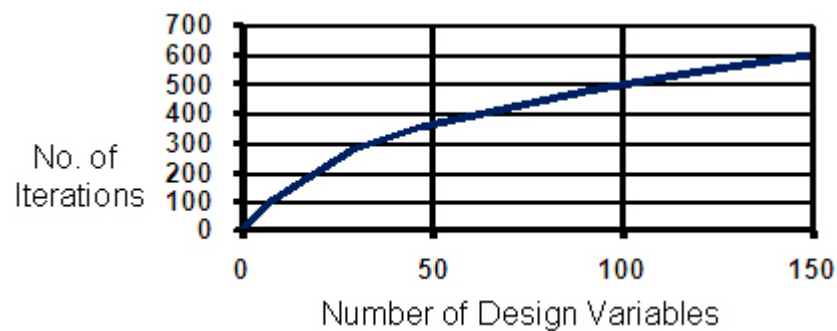


Figure 12.35: Estimate for recommended number of design iterations

The minimum number of design evaluations is also dependent on the amount of time available for the optimization. HEEDS will tune its search in order to find the best design within the number of evaluations allowed. However, if the number of iterations considered is much smaller than the recommended minimum, it could result in a sub-optimal solution.

Once the number of design evaluations has been estimated, the likely amount of time required for the optimization can be predicted, as shown in Table 12.7. This will depend upon the time required to perform each evaluation, which itself will depend on the number of load cases considered and runtime for each evaluation. If there are five load cases to be considered, this may require five individual analysis to be performed for each evaluation.

$$\text{Total Time} = \frac{(\text{No of Evaluations}) \times (\text{Time for each Evaluation})}{(\text{No of Evaluations run in Parallel})}$$

Example:					
One Design Iteration Time	=	2 Days	Total Number of Iterations	=	200
In Series			In Parallel (10 Machines)		
Total Time	=	400 Days	Total Time	=	40 Days

Table 12.7: *Time calculation*

There are three ways that the optimization runtime can be reduced. The first is to reduce the number of design evaluations required. This will depend on the efficiency of the search methodology. In multiple benchmark studies, HEEDS has been shown to be one of the most efficient search methods available over a broad class of optimization problems. The second is to execute multiple design evaluations simultaneously, in parallel. The third way is to reduce the runtime of each individual analysis. This can be achieved by simplifying the model, running the analysis in parallel on multiple CPUs and by running the analysis for the shortest possible duration, for example to peak displacement at 100 ms rather than final spring back at 300 ms.

Once started, when is it appropriate to stop the optimization? Obviously, the theoretical goal would be to find the global optimal solution. However, without prior knowledge this is impossible. The practice goal is thus the best possible solution, which may be the global best, within the available time. There are numerous convergence criteria available to detect optimization stagnation within HEEDS but probably the best method is interrogation of the optimization results by the user themselves.

As an example of HEEDS search efficiency consider the following example;

- 50 design variables
- Each variable has 10 possible choices (a relatively small number)
- Total number of possible designs = 1050
- Odds of finding the optimal solution by luck: 1 in 1050
- Odds of winning the Mega Millions Lottery: 1 in 1.758
- HEEDS can usually find an optimal or near optimal solution within 100–500 iterations, depending on the problem

12.9.3 3G Optimization Applied to FSV Pilot Project

12.9.3.1 Optimization Response

Figure 12.36 shows the mass response during the optimization. Each individual evaluation is shown as a blue point. The current best design is shown in the red “staircase” line. Blue points below this line are not feasible designs. Note, this may also be true for some of the blue points above this line too. As the number of evaluations increase, the bandwidth of the mass variation decreases, approaching a practical optimal design at about 700 designs.

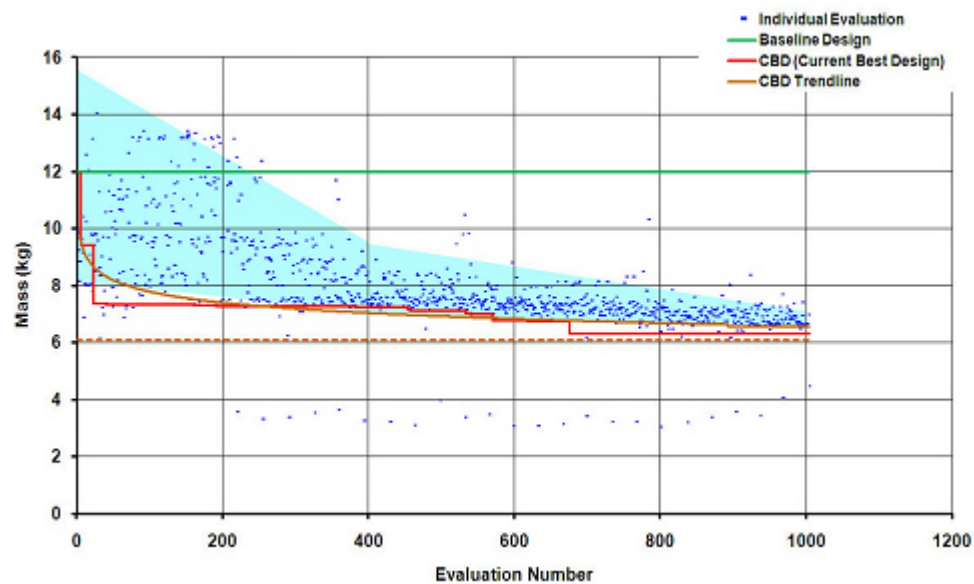


Figure 12.36: Mass during optimization

Figure 12.37 and Figure 12.38 show the variation in material and gauge choice for the current best design during the optimization. In most cases the optimization has identified the best material and gauge choice for each section early in the process.

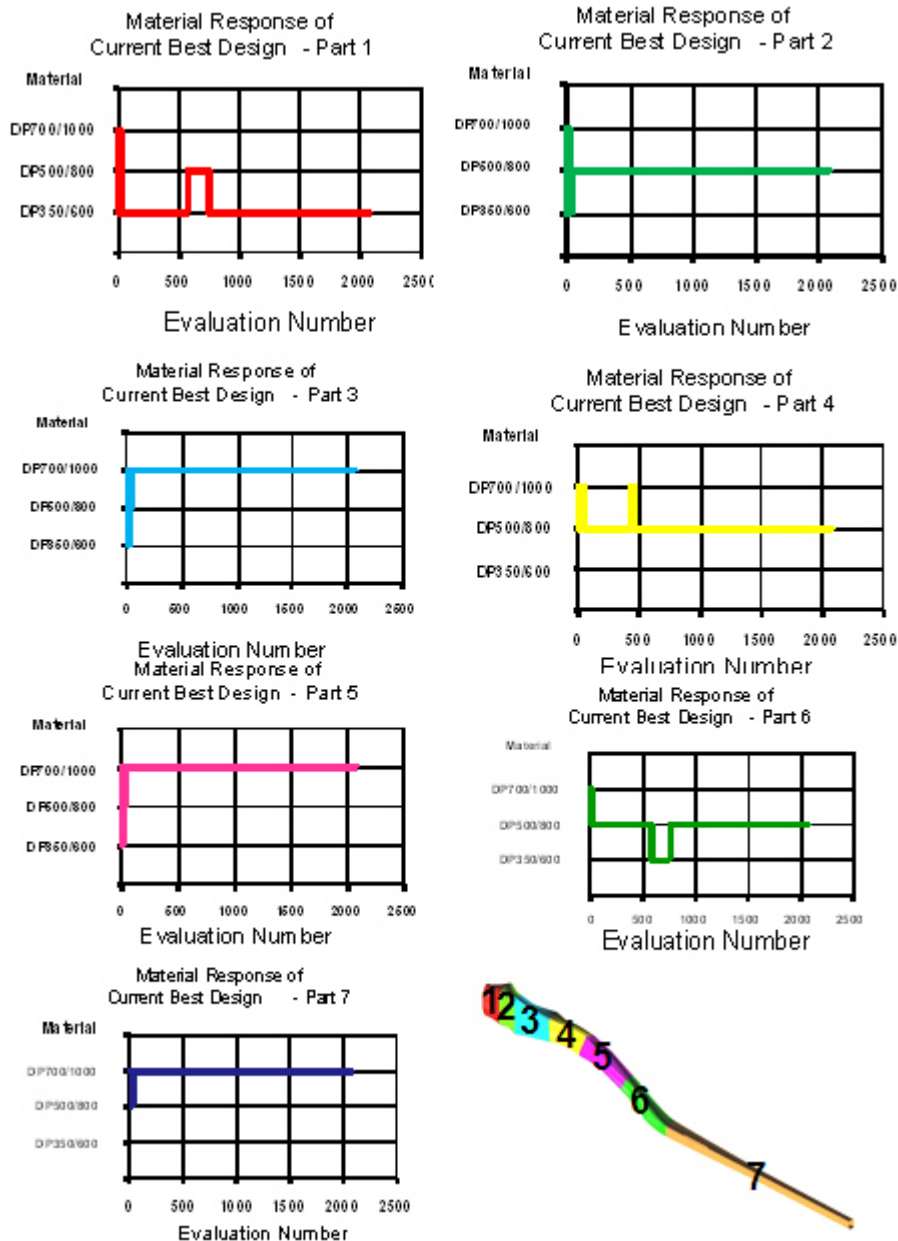


Figure 12.37: Plot of performance - 143 feasible designs within 10% mass of optimal, material choices

12.9 3G Optimization Process

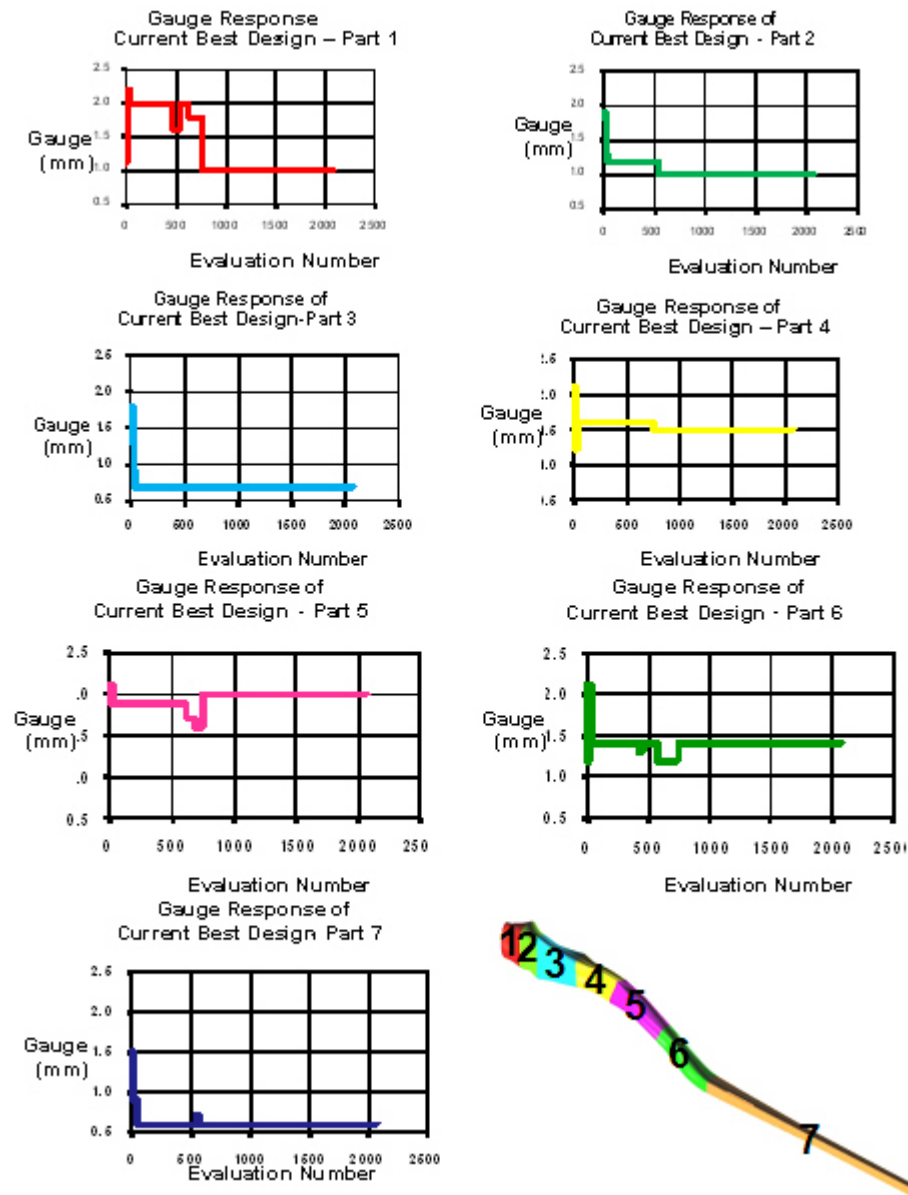


Figure 12.38: Plot of performance - 143 feasible designs within 10% mass of optimal, gauge choices

12.9.3.2 Feasible Designs

In total 2079 individual designs were evaluated, of which 968 were considered feasible. A feasible design is one that achieved section forces of less than 35 kN. Figure 12.39 illustrates the range of performance and material and gauge choices for all feasible designs (Note the variation in mass for these designs).

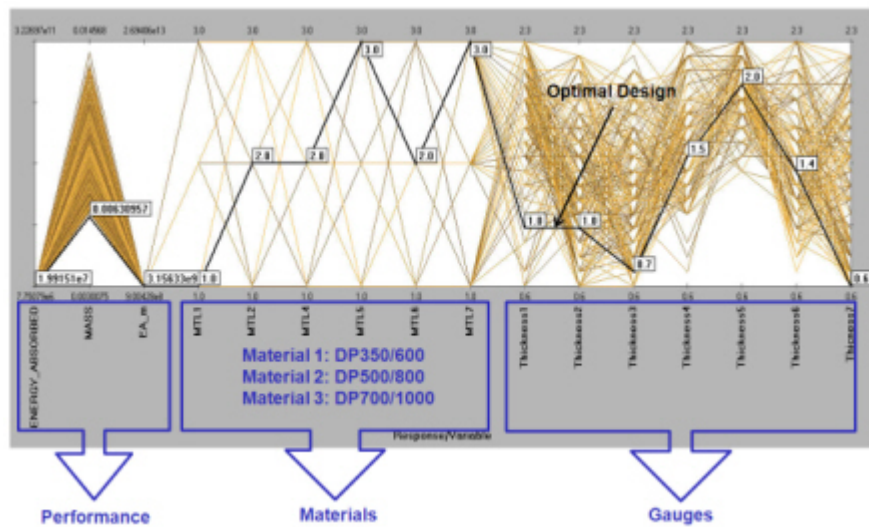


Figure 12.39: Performance, material & gauge choice for all 968 feasible designs

Figure 12.40 shows the same data but for the 143 feasible designs within 10% mass of the optimal. Note the significantly smaller range of choices.

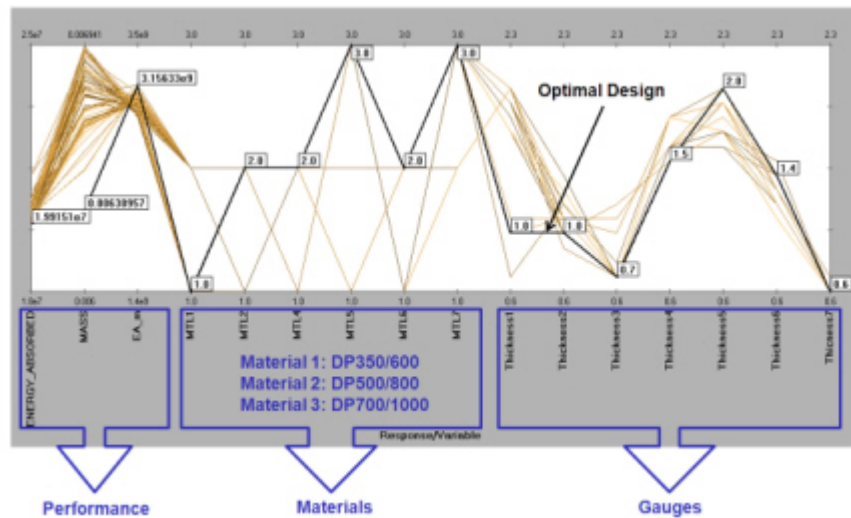


Figure 12.40: Performance, material & gauge choice for 143 feasible designs within 10% mass of optimal

Bibliography

- [1] Auto Steel Partnership (AS-P), Tailored Steel Product Alliance (TSPA), American Iron and Steel Institute(AISI).
- [2] Thyssenkrupp March 2009.
- [3] Corus Automotive.
- [4] ArcelorMittal.
- [5] Nippon Steel.
- [6] JFE Steel Corporation.
- [7] Voestalpine.
- [8] Severstal International.
- [9] EDAG Inc. - USA.
- [10] Auto/Steel Partnership (A/SP).
- [11] Continental teves.
- [12] greencarcongress.com.
- [13] <http://auto.howstuffworks.com/fuel-efficiency/alternative-fuels/fuel-cell6.htm>.
- [14] <http://gm-volt.com/2007/11/07/fuel-cell-chevy-volt-for-production-in-2011/>.
- [15] <http://www.coskata.com>.
- [16] <http://www.optics.rochester.edu>.
- [17] Maxwell technologies.
- [18] Nrel/cp-540-28960.
- [19] Office for the study of automotive transportation (umtri), jd power, monitor analysis.
- [20] Polkinsight china.
- [21] Reduction in vehicle temperatures and fuel use from cabin ventilation-solar reflective paint

- and solar reflective glazing. Technical report, NREL.
- [22] Thyssenkrupp steel ag.
- [23] Toyota.
- [24] Uniform tire quality grade (utqg) standards.
- [25] Uqm technologies.
- [26] www.autospies.com/news/daimler-mass-production-of-fuel-cell-cars-by-2015-22062.
- [27] www.bloomberg.com/app/news/2008.
- [28] www.honda.com.
- [29] www.linde.com.
- [30] www.webasto.us.com.
- [31] New nxt z free silane. Technical report, Momentive Performance Materials Company, March 2007.
- [32] Michelin's green meters press kit. Technical report, Michelin (www.michelingreenmeter.com), October 30th 2007.
- [33] September 2nd 1992.
- [34] AS/P. Mass compounding program.
- [35] Autodata and EIA World's. Transportation energy data book, ed. 26, table 4.6, 2007.
- [36] Dennis Candido; John Sheerin; Tony Brinkman; Don Amos; Dave Chapman; Red Hermann; Sanat Bhavsar. Rma presentation to ciwmb special waste committee. Technical report, Rubber Manufacturers Association: Michelin; Continental; Goodyear; Bridgestone; Cooper; Pirelli; Yokohama, March 9th 2005.
- [37] Douglas R. MacFarlane Bjorn Winther-Jensen. High rates of oxygen reduction over a vapor phase-polymerized pedot electrode, science, 2008.
- [38] Donald S. Cameron. Fuel cells – science and technology. Platinum Metal Rev. 49(1), 2005, 2005.
- [39] Ford Motor Company.
- [40] Vairex corporation. Fuel cell manufacturing costs - trends and cost reduction strategies. Seminar and Exposition, 2007.
- [41] Marion G. Pttinger; Joseph D. Walter; John D. Eagleburger. A commented synopsis of the report of the committee for the national tire efficiency study. Technical report, TSTCA, vol. 35 No. 2, April - June 2007.

- [42] General Motors Corp. et al. Well to wheel energy use and greenhouse gas emissions of advanced fuel/vehicle systems - north american analysis, executive summary report. Technical report, Argonne National Laboratory, Transportation Technology Research and Development Center, 2001.
- [43] Orest L. Adrianowycz. et .al. Next generation bipolar plates for automotive pem fuel cells, annual progress report (doe usa), 2007.
- [44] S. Plotkin et al. Hybrid vehicle technology assessment: Methodology, analytical issues, and interim results. Technical report, Argonne National Laboratory Report ANL/ESD/02-2, Argonne II, 2001.
- [45] V. Freyermuth et al. Comparison of powertrain configurations for plug-in hev's from a fuel economy perspective. Technical report, SAE Paper 2008-01-0461, 2008 World Congress, Detroit MI., 2008.
- [46] Terry Gettys. Passion for an airless future; sae technical report no. 1-113-6-86. Technical report, SAE Automotive Engineering International, June 2005.
- [47] Honda.
- [48] Honda. Automotive engineering international, July 2008.
- [49] Kurt Zenz House. The limits of energy storage technology. Bulletin of Atomic scientists, 20th January 2009.
- [50] Craig Noble; Roland Hwang. California adopts world's first fuel-efficient tires law. Technical report, National Resources Defense Council (nrinfo@nrdc.org), October 2nd 2003.
- [51] Tomohiko Ihara. Solar reflective coating to an automobile reduces cooling load and fuel consumption. Technical report, AIST.
- [52] al. Jialu Zhang, et. High temperature pem fuel cells, journal of power sources, 2006.
- [53] Shuo-Jen Lee. Stainless steel bipolar plates, power sources, 2005.
- [54] C.E. Thomas; B.D. James; F.D. Lomax and I.F. Kuhn. Integrated analysis of hydrogen passenger vehicle transportation pathways. Technical report, Report final draft prepared by Directed Technologies, Inc. (Subcontract No. AXE-6-16685-01) for the National Renewable Energy Laboratory, Golden, CO., March, 1998.
- [55] Hua Meng. Numerical studies of cold-start phenomenon in pem fuel cells, electrochimica acta., 2008.
- [56] Dr. John Shen; Dr. Abdul Masrur; Dr. Vijay K. Garg; John Monroe. Optimal power management and distribution in automotive systems. *Handbook of Automotive Power Electronics and Motor Drives by Ali Emadi*, page 98, 2005.
- [57] Koji Nakui. Japanese fuel cell and hydrogen programs initiatives hydrogen-fuel cell based energy systems workshop, vienna, 2004.

- [58] DOE Hydrogen Program. Water transport exploratory studies - annual progress report, 2007.
- [59] Chris Calwell; Ecos Consulting; My Ton; Travis Reeder. Green seal's choose green. Technical report, Green Seal Environmental Partners, Inc., March 2003.
- [60] R. Farrington; J. Rugh. Impact of vehicle air-conditioning on fuel economy - tailpipe emissions and electric vehicle range. Technical report, National Renewable Laboratory; Golden CO. USA, September 2000.
- [61] Nigel Sammes. Fuel cell technology. Springer, 2006.
- [62] Ada Technologies.
- [63] C.E. Thomas. Pngv-class vehicle analysis: Task 3 final report. Technical report, Prepared by Directed Technologies, Inc. for the National Renewable Energy Laboratory, Golden, CO., March, 1999.
- [64] TLD Workshop. Iea. Paris, 07/6/11-12.
- [65] www.autobloggreen.com. Michelin, inc. video of Irrt's vs. non-Irrt's. Technical report, Frankfurt Auto Show, 2007.

List of Figures

2.1	Phase 1 - Engineering study: content & methodology	4
2.2	Conventional ICE front-end	7
2.3	FSV Electric drive front-end	7
2.4	Compact Electric Drive	8
2.5	Front-end rail	8
2.6	PHEV ₂₀ powertrain layout	9
2.7	BEV underbody	10
2.8	FSV-2 (PHEV ₄₀)	11
2.9	FSV-2 - FCEV	12
2.10	FSV fuel economy and CO ₂ emissions	18
2.11	FSV-1 Pump-to-Wheel CO ₂ emissions	20
2.12	FSV-1 Well-to-Wheel CO ₂ emissions	21
2.13	FSV-2 Pump-to-Wheel CO ₂ emissions	22
2.14	FSV-2 Well-to-Wheel CO ₂ emissions	23
2.15	Fuel stack assembly	27
3.1	Global Auto Market - small car sales & share	37
3.2	Breakdown of car market by segments (India)	39
3.3	Breakdown of car market by segments (China)[20]	40
3.4	Mini-Vehicle market in Japan	41
3.5	Suzuki WagonR - most popular mini car in Japan	42
3.6	Annual vehicle sales in Europe	43
3.7	New passenger car registration	43
3.8	US car and light truck sales (new vehicle) with average gasoline price [35]	44
3.9	Rapid change in market structure [23]	45
3.10	Future forecast of vehicle technologies	47
3.11	Toyota Prius plug-in hybrid	54
3.12	Toyota's new 516-mile range fuel cell vehicle	54
3.13	Sept 2010 - Chevrolet Volt	55
3.14	Late - 2009 Saturn Vue	55
3.15	Chevrolet Equinox	55
3.16	Ford flex-fuel plug-in hybrid electric vehicle	56
3.17	Dodge EV	57
3.18	Jeep EV	58
3.19	Chrysler EV	58
3.20	Mitsubishi innovative Electric Vehicle (i-MiEV)	59

3.21	2008 Honda FCX Clarity	60
3.22	Hyundai i-Blue fuel cell electric vehicle	61
3.23	2010 Mazda Premacy Hydrogen RE hybrid	62
3.24	Volvo C30 ReCharge concept	63
3.25	Volvo C30 concept powertrain	63
3.26	Nissan EV - Electric Vehicle	64
3.27	TATA Indica	65
3.28	Peugeot	66
3.29	F3DM plug-in hybrid	67
3.30	Fisker Karma	68
3.31	Tesla Roadster	69
3.32	Project Better Place business plan	70
3.33	Project Better Place powertrain	71
3.34	Project Better Place mule vehicle	71
3.35	Vehicles selected for benchmark	73
3.36	2009 Mitsubishi i-Miev	74
3.37	Future Steel Vehicle-1	74
3.38	2009 Mitsubishi i-Miev	75
3.39	Future Steel Vehicle 1	75
3.40	Material usage	76
3.41	2009 Mitsubishi i-MiEV	77
3.42	FSV-1 BEV	77
3.43	i-MiEV electric drive components	78
3.44	FSV-1 electric drive components	78
3.45	i-Miev 16 kWh Li-ion battery	79
3.46	FSV 35 kWh Li-ion battery	79
3.47	i-MiEV traction motor	80
3.48	FSV-1 BEV traction motor	80
3.49	i-MiEV underhood	81
3.50	FSV underhood	81
3.51	i-MiEV rear	81
3.52	FSV rear	81
3.53	i-MiEV front suspension	82
3.54	FSV front suspension	82
3.55	i-Miev rear suspension	82
3.56	FSV rear suspension	82
3.57	i-MiEV wheel	83
3.58	FSV-1 wheel	83
3.59	i-MiEV front	84
3.60	i-MiEV rear	84
3.61	i-MiEV cargo space	84
3.62	FSV-1 front	84
3.63	FSV-1 rear	84
3.64	FSV-1 cargo space	84

3.65	i-MiEV instrument cluster	85
3.66	i-MiEV transmission shifter	85
3.67	Underbody structure	86
3.68	2009 Honda FCX Clarity	87
3.69	Future Steel Vehicle-2	87
3.70	Honda Clarity exterior dimensions	88
3.71	FSV-2 exterior dimensions	88
3.72	Honda Clarity material usages	89
3.73	Honda Clarity layout	91
3.74	FSV-2 layout	91
3.75	Honda Clarity battery	92
3.76	Honda Clarity fuel cell module	92
3.77	Honda Clarity traction motor	92
3.78	FSV-2 FCEV battery	92
3.79	FSV-2 FCEV fuel cell module	92
3.80	FSV-2 FCEV traction motor	92
3.81	Honda Clarity battery location	93
3.82	FSV-2 FCEV battery location	93
3.83	Honda Clarity battery	93
3.84	FSV-2 FCEV battery	93
3.85	Honda Clarity fuel cell stack location	94
3.86	FSV-2 FCEV fuel cell stack location	94
3.87	Honda Clarity fuel cell stack	94
3.88	FSV-2 FCEV fuel cell stack	94
3.89	Honda Clarity hydrogen tank	95
3.90	FSV-2 FCEV hydrogen tank	95
3.91	Honda Clarity motor	96
3.92	FSV-2 FCEV Traction motor	96
3.93	Honda Clarity radiator	97
3.94	FSV-2 radiator	97
3.95	Honda Clarity - packaging	98
3.96	FSV-2 - packaging	98
3.97	Honda Clarity underhood	99
3.98	FSV-2 FCEV underhood	99
3.99	Honda Clarity front suspension	100
3.100	FSV-2 FCEV front suspension	100
3.101	Clarity rear suspension	100
3.102	FSV-2 FCEV rear suspension	100
3.103	Honda Clarity wheel	101
3.104	FSV-2 Wheel	101
3.105	Honda Clarity front	102
3.106	Honda Clarity rear	102
3.107	Honda Clarity cargo space	102
3.108	FSV-2 front	102

3.109	FSV-2 rear	102
3.110	FSV-2 cargo Space	102
3.111	Honda Clarity instrument cluster	103
3.112	Honda Clarity shifter	103
3.113	Honda Clarity interior materials	104
3.114	Honda Clarity climate controlled seats	104
3.115	2010 Chevrolet Volt	106
3.116	FSV-2 PHEV ₄₀	106
3.117	Chevrolet Volt exterior dimensions	107
3.118	FSV-2 PHEV ₄₀ exterior dimensions	107
3.119	Chevrolet Volt - material usages	108
3.120	Powertrain packaging - Chevrolet Volt (top) & FSV-2 (bottom)	109
3.121	Chevrolet Volt 16 kWh battery	110
3.122	Chevrolet Volt 111 kW motor	110
3.123	Chevrolet Volt 1.4 L IC engine	110
3.124	FSV-2 PHEV ₄₀ 11.7 kWh battery	110
3.125	FSV-2 PHEV ₄₀ 75 kW motor	110
3.126	FSV-2 PHEV ₄₀ 1.4 L IC engine	110
3.127	Chevrolet Volt battery location	111
3.128	FSV-2 PHEV ₄₀ battery layout	111
3.129	Chevrolet Volt 16 kWh battery	111
3.130	FSV-2 11.7 kWh battery	111
3.131	Chevrolet Volt 1.4 L ICE	112
3.132	FSV-2 1.4 L ICE	112
3.133	Chevrolet Volt motor location	113
3.134	FSV-2 PHEV ₄₀ motor location	113
3.135	Chevrolet Volt- 111 kW motor	113
3.136	FSV-2 75 kW motor	113
3.137	Chevrolet Volt front suspension	114
3.138	FSV-2 front suspension	114
3.139	Volt rear suspension	114
3.140	FSV-2 rear suspension	114
3.141	Volt wheel	115
3.142	FSV-2 wheel	115
3.143	Chevrolet Volt rear	116
3.144	FSV-2 rear	116
3.145	Mercedes Blue-Zero concept vehicles	117
3.146	Vehicle Range Comparison - FSV & Mercedes Blue-Zero	118
3.147	Mercedes Blue-Zero powertrain layout	119
3.148	Mercedes Blue-Zero floor height	120
3.149	Mercedes E-Cell - powertrain layout	121
3.150	Mercedes F-Cell - powertrain layout	122
3.151	Mercedes E-Cell+ - powertrain layout	123
3.152	Mercedes Blue-Zero wheel covers	124

3.153	FMVSS 208 - 56 $\frac{\text{km}}{\text{h}}$ (35 mph) 0-degree frontal impact	127
3.154	FMVSS 208 - Hybrid III 5th female	128
3.155	FMVSS 208 - Hybrid III 50th male	128
3.156	FMVSS 214P Anthropomorphic Test Device (ATD)	129
3.157	Current - 54 $\frac{\text{km}}{\text{h}}$ side crabbed barrier	129
3.158	Additional - 32 $\frac{\text{km}}{\text{h}}$ 75 degree rigid pole test	129
3.159	Roof crush resistance	130
3.160	Electronic Stability Control system (ESC)	131
3.161	IIHS - New side barrier to simulate crash into a SUV	132
3.162	IIHS - New bumper impact tests	133
3.163	Pedestrian protection requirements Phase 1	135
3.164	Pedestrian protection requirements Phase 2	135
3.165	Pedestrian protection requirements Phase 1 and 2	135
3.166	Adult occupant protection	136
3.167	Child occupant protection	136
3.168	Pedestrian impact protection	137
3.169	Rear Impact - Whiplash protection	137
3.170	Safety assist	138
3.171	Actual and projected GHG emissions for new passenger vehicles: 2002-2018	142
3.172	New proposed fuel economy label	143
3.173	CO ₂ emission vs. vehicle mass	146
3.174	Chinese fuel economy standards	148
3.175	US emissions	153
3.176	Year of implementation of each of the EURO standards	156
3.177	Year of implementation of each of these EURO standards in Asia	157
4.1	BEV	165
4.2	FCEV	166
4.3	PHEV Series hybrid vehicle	167
4.4	PHEV Parallel hybrid vehicle	168
4.5	PHEV Parallel-Split hybrid vehicle	169
5.1	Future Steel Vehicle size comparisons	177
5.2	Future Steel Vehicle size comparison with competitive vehicles	177
5.3	FSV exterior dimensions	178
5.4	FSV interior dimensions	179
5.5	Conventional ICE front-end	181
5.6	FSV - electric drive front-end	181
5.7	FSV- front-end comparison	182
5.8	Honda Clarity electric drive	182
5.9	FSV front rail	183
5.10	Powertrain mass	185
5.11	Powertrain sub-system cost	185
5.12	FSV-1 Battery Electric Vehicle	186
5.13	BEV underbody	192

5.14	BEV packaging	192
5.15	2009 Mitsubishi i-Miev	193
5.16	2009 Mitsubishi i-MiEV	193
5.17	Future Steel Vehicle	193
5.18	FSV-1 PHEV ₂₀	198
5.19	PHEV ₂₀ layout	203
5.20	PHEV ₂₀ underbody	204
5.21	FSV-2 PHEV ₄₀	209
5.22	PHEV ₄₀ layout	214
5.23	FSV-2 FCEV	219
5.24	FCEV layout	224
5.25	FSV powertrain key parameters comparison	230
6.1	Motor vertical	235
6.2	Motor Horizontal in front of axle	236
6.3	Inverter and controller - front	237
6.4	Motor- Rear of axle, inverter - on top	238
6.5	Integrated motor - generic	239
6.6	Integrated motor - evolved	239
6.7	Electric drive- final design and packaging	240
6.8	Single large rectangular battery pack	241
6.9	additional pack under the hood	242
6.10	T shaped battery pack	243
6.11	Packaging in vehicle	243
6.12	More refined T-shaped battery	244
6.13	Packaging in vehicle	244
6.14	Battery pack with minimized areas	245
6.15	Packaging in vehicle	245
6.16	Battery pack w/under seat pods	246
6.17	Packaging in vehicle	246
6.18	Battery pack - Assembly	247
6.19	FSV-1 sub-pack (78 cells)	248
6.20	35 kWh pack(6 sub-packs)	248
6.21	FSV-1 battery pack in vehicle	248
6.22	FSV-1 35 kWh /66 kWh I pack	249
6.23	Packaging in vehicle	249
6.24	FSV-1 66 Kwh (500 km) pack	250
6.25	FSV-1 Packaging in vehicle	250
6.26	Fuel cell components	251
6.27	Packaging overview with tanks	251
6.28	Stack repositioned with modified tanks	252
6.29	Fuel cell stack under the rear seat	253
6.30	Fuel cell stack in the tunnel	254
6.31	FCEV with Tongji fuel cell model	255
6.32	Design of the FCEV with structure	255

6.33	Front engine/generator configuration	256
6.34	Rear Engine - Horizontal	257
6.35	Fuel tank and battery locations	257
6.36	Rear engine - vertical	258
6.37	Rear engine with fuel tank and battery	258
6.38	Rear Engine - 17° tilt	259
6.39	New 1.4 L 4-cylinder engine/generator	260
6.40	PHEV ₄₀ 45° orientation layout	260
6.41	Upper control arm / Lower trailing arm (sprung)	261
6.42	Upper control arm (sprung) / Lower trailing arm	262
6.43	Upper Control Arm (sprung) / Lower control arm	263
6.44	Upper control arm / Lower control arm (sprung)	265
6.45	Leaf spring design	266
6.46	McPherson strut (sprung) / Lower trailing arm	267
6.47	Conventional McPherson strut	268
6.48	Twist Beam or Torsion Beam	270
6.49	Passive wheel	271
6.50	Trailing arm with 2 camber links	272
6.51	Double wishbone	273
6.52	Chapman strut / McPherson strut	274
6.53	H-arm with camber control link	275
6.54	FSV suspension - front and rear	277
6.55	Camber angle versus wheel travel	278
6.56	Toe change versus wheel travel- front	279
6.57	Toe change versus wheel travel - rear	279
7.1	Battery energy density versus specific energy	282
7.2	Redox potential of elements [64]	283
7.3	Negative electrode materials for rechargeable Li-cells	284
7.4	Positive electrode materials for rechargeable Li-cells	284
7.5	NEDO Li-ion battery targets	285
7.6	FSV BEV recommended specification	288
7.7	FSV BEV battery pack (NEDO3 target)	289
7.8	35 kWh, 250 km range FSV 2015-2020	291
7.9	35 kWh (250 km) or 66 kWh (500 km)	291
7.10	66 kWh (500 km) NEDO3 2030 target battery pack	291
7.11	FSV motor with cooling cavity	293
7.12	FSV motor & transmission cutaway	296
7.13	FSV motor with cooling	296
7.14	FSV motor cooling flow diagram	296
7.15	FSV BEV energy balance	297
7.16	FSV BEV motor torque versus RPM	298
7.17	FSV BEV motor torque versus RPM - Acceleration	298
7.18	FSV BEV motor torque versus RPM - Constant speed grade climb	299
7.19	FSV BEV power demand at 10% grade	299

7.20	Energy density (power/weight)	301
7.21	Power density (power/Volume)	301
7.22	FSV fuel cell system packaging	302
8.1	Total life cycle assessment	306
8.2	Well-to-Pump efficiency fuel production cycle (US)	308
8.3	Well-to-Pump fuel production GHG CO ₂ emissions (US)	308
8.4	FSV fuel economy and CO ₂ emissions versus other technologies	310
8.5	US EPA UDDS cycle	311
8.6	Japan 10-15 cycle	312
8.7	EU NEDC Drive cycle	312
8.8	FSV-1 Pump-to-Wheel CO ₂ emissions	314
8.9	FSV-1 Well-to-Wheel CO ₂ emissions	315
8.10	FSV-2 Pump-to-Wheel CO ₂ emissions	316
8.11	FSV-2 Well-to-Wheel CO ₂ emissions	317
8.12	Well-to-Wheel Energy Efficiency	318
8.13	Conventional technologies Well-to-Wheel energy efficiency	319
8.14	Advanced technologies Well-to-Wheel energy efficiency (non-renewable energy source)	320
8.15	BEV Well-to-Wheel energy efficiency (renewable energy source)	320
8.16	FSV-1 Well-to-Wheel energy usage	321
8.17	FSV-2 Well-to-Wheel energy usage	321
9.1	SFCV/Tongji's working scope	325
9.2	Arrangement of major cell components in a fuel cell stack [16]	327
9.3	Bipolar plates alternative materials for PEM fuel cell application	330
9.4	An innovative stamped metal sheets architecture	330
9.5	Honda FCX stack design (left) Vs. Clarity V-flow stack (right)	331
9.6	Available types of air compressors	332
9.7	Available types of humidifiers	333
9.8	Shell-and-tube type gas-to-gas membrane humidifier structure	334
9.9	Available types of hydrogen recirculation pump	335
9.10	External of FCU	336
9.11	Two control methods of hydrogen operation pressure	337
9.12	Internal of FCU	338
9.13	Volumetric power density (stack)- Current status and 2015 forecast	340
9.14	Specific power density (stack)- Current status and 2015 forecast	341
9.15	A typical FCS cost ratio	341
9.16	Historic trend of Pt loading	342
9.17	Fuel Cell vehicle's cold start temperatures	344
9.18	Current status and future estimates of FCS efficiencies	345
9.19	FCV commercialization scenarios from Ballard	346
9.20	Fuel cell commercialization and diffusion scenarios from NEDO [57]	347
9.21	Mass production volume and steel usage [40]	348
9.22	CAD model of proposed FCS (View 1)	350

L

9.23	CAD model of proposed FCS (View 2)	350
9.24	CAD model of proposed FCS (View 3)	351
9.25	CAD model of proposed FCS (View 4)	351
9.26	Liquid H ₂ - tank system [29]	355
9.27	Metal hydride hydrogen storage	356
9.28	Cylindrical pressure vessels	357
9.29	Gravimetric efficiency development trend for compressed gas vessels	358
9.30	Different storage types and storage densities	359
9.31	Mobile On-Site hydrogen production and dispensing unit	363
9.32	Transportable hydrogen compressor	363
9.33	Typical prototype hydrogen refueling station for 1-20 fills per day	364
9.34	Automotive battery customers, suppliers and market forecasts	366
9.35	Sample Nickel-Metal Hydride battery	368
9.36	Sample lithium-ion cobalt battery	369
9.37	Cylindrical cells	372
9.38	Prismatic cells	372
9.39	Basic design and packaging concepts	373
9.40	Energy density comparison	376
9.41	Sample ultra-capacitors	377
9.42	Energy density of ultra-capacitors [17]	378
9.43	Power demand - combined usage of ultra-capacitor and another energy source [47]	378
9.44	Current Vs time: net change in battery current	379
9.45	Current technology status and the US Department of Energy targets [62]	379
9.46	Ultra-Capacitor packaging sample	380
9.47	Internal combustion engine recommendations - PHEV ₂₀ and PHEV ₄₀	384
9.48	The four stroke cycle	385
9.49	Projected increase of bio-Fuel in transport (USA and EC)	391
9.50	CO ₂ released during ethanol production	393
9.51	CO ₂ released, bio-fuel feedstocks vs. fossil fuels	394
9.52	Integrated traction drive concept	398
9.53	Chain drive CVT	399
9.54	Dual clutch transmission (DCT)	400
9.55	6-8 speed transmission	402
9.56	Wheel and traction motor	404
9.57	Continuous power vs. weight	406
9.58	Electric motor efficiency and speed range [25]	407
9.59	Toyota's development progress in motor output and transmission size from the first to the second-generation hybrid drives	409
9.60	Power inverter designs	410
10.1	Steel portfolio to technology portfolio flow diagram	414
10.2	Laser welded blank to final stamping example	415
10.3	Laser Welded Coil production process	418
10.4	Examples of usages in automotive applications	420

10.5	Possible rolled tube dimensions	421
10.6	Rolled tapered tube dimensions	421
10.7	Multiwall T ³ Tube	424
10.8	Multiwall T ³ Tube with varying thickness	424
10.9	Range of materials that can be used for Multiwall T ³ tubes	425
10.10	T ³ profiling manufacturing principle	426
10.11	Construction of vibration damping steel	428
10.12	Vibration damping body-structure	428
10.13	Vibration damping effect over time	429
10.14	Steel structure panels suitable for vibration damping steel	430
10.15	Powertrain parts suitable for vibration damping steel	430
10.16	Laser Arc Welding Process	431
10.17	Transition using Laser Arc Welding	431
10.18	High-frequency induction welded tube mill	433
10.19	High frequency induction welded materials and D/T ratio	434
10.20	Automotive application using high-frequency welded tubes	435
10.21	Roll forming process	436
10.22	Roll forming machine	437
10.23	Direct and In-Direct hot stamping process	439
10.24	In-Direct processed steel properties (elongation vs. tensile strength)	439
10.25	Low and high-pressure hydroforming differences	442
10.26	Hydroformed section comparison	443
10.27	Profiles that can be used in hydroforming process	443
10.28	Pre-bending and pre-forming guidelines	444
10.29	Section expansion guidelines	444
10.30	Types of joining methods used for a body-structure	447
10.31	Weld bonding process	448
10.32	Self Piercing Rivet	449
10.33	Self Piercing Rivetting Process	450
11.1	Automotive applications for by-Wire technology. Credit: Motorola	454
11.2	Conventional steering vs. Steer-by-Wire	457
11.3	Typical Steer-by-Wire schematic	458
11.4	Typical Steer-by-Wire system (with hardware)	459
11.5	One motor controls both wheels via a steering rack	460
11.6	Individual actuators control each wheel	460
11.7	Hydraulic only method	461
11.8	Delay introduced by Steer-by-Wire	463
11.9	Conventional and future EMB brake system [11]	469
11.10	Novanta concept car	473
11.11	Bertone-SKF "Filo"	474
11.12	Toyota's 'Fine-X'	475
11.13	Suzuki Ionis	476
11.14	FHI - IVX-II	477
11.15	Nissan EA2 concept	478

11.16	Mazda Washu	479
11.17	Uniform tire quality grade standard (UTQG) labeling	481
11.18	RRC and UTQG tread wear grade correlation	482
11.19	European CO ₂ emission rating label	484
11.20	Passenger tire shipment in US - OE / replacement	485
11.21	Tire rolling resistance values trend	485
11.22	Glass panels typical for a vehicle manufactured in 2008	488
11.23	Tempered vs. laminated glass	489
11.24	Headlamp module	494
11.25	2008 - Audi A8 with full LED head & tail lamps	495
11.26	2008 Cadillac Escalade w/ LED/ HID headlamps LED tail lamps	495
11.27	Interior with lightweight instrument cluster display	497
11.28	Evolution of the complexity of the instrument cluster	497
11.29	Reconfigurable instrument cluster concepts [39] [47]	498
11.30	PM/AM-OLED displays	499
11.31	The front seat frame structure consists of 65 to 70% of total seat mass	500
11.32	The rear seat frame structure consists of 70 to 80% of the total seat mass	500
11.33	Seatback frame made via hydroforming	501
11.34	Electrical wiring harnesses	502
11.35	Fuel economy impacts of auxiliary loads [18]	505
11.36	Solar roof - Toyota Prius	507
11.37	Standard automobile paint composition	508
11.38	Surface temperature	508
11.39	Comparison of transmissivity	509
11.40	Gasoline engine/belt-driven A/C compressor	511
11.41	Electric compressor	512
11.42	Dual scroll hybrid compressor	512
11.43	Air conditioning loads (temperature vs. time)	514
12.1	Detailed FSV development process	516
12.2	Pilot project development process	517
12.3	LWB concept - pilot project baseline	518
12.4	Optimization methodology overview	519
12.5	Model as received (front rails shown for clarity)	520
12.6	NCAP - deformed plots & acceleration	521
12.7	Rocker acceleration pulse	522
12.8	IIHS intrusion performance	522
12.9	Static stiffness	523
12.10	Design space	525
12.11	Comparison between full-vehicle dynamic & de-coupled static deformed shapes	526
12.12	Topology Optimization results shown in combination with the design space (in light red) & original rail (in green)	526
12.13	3G Optimization - key interfaces	527
12.14	Cross-sections through the Topology Optimization's load path mesh & design space	528

12.15	Original front rail shown in combination with cross-sections through the design space	528
12.16	Finalized cross-sections through the Topology Optimization's loadpath mesh & design space	529
12.17	Finalized cross-sections	529
12.18	Parameterization of cross-sections	530
12.19	Material & gauge parameterization	531
12.20	Final design	532
12.21	Final design (in purple) shown in combination with original rail (in blue)	533
12.22	Design (in green) shown in combination with Topology Optimization (in red)	533
12.23	NCAP - final design & original rail - deformed plots & Acceleration	534
12.24	NCAP - donor vehicle & final design	535
12.25	IIHS front 40% offset crash procedure	536
12.26	IIHS front impact 40% offset crash results- donor vehicle & final design	536
12.27	Static stiffness	537
12.28	Front rail: donor vehicle, LWFE & LSV pilot project comparison	538
12.29	Final design - cross-sectional variation along rail	539
12.30	Final design hydroformed tube concept - equivalent diameters	540
12.31	Final design hydroformed tube concept - circumferential strain	540
12.32	Final design hydroformed tube concept - geometry & material	541
12.33	HEEDS Algorithm - basic loop	543
12.34	Hybrid Adaptive Search Strategy	543
12.35	Estimate for recommended number of design iterations	543
12.36	Mass during optimization	545
12.37	Plot of performance - 143 feasible designs within 10% mass of optimal, material choices	546
12.38	Plot of performance - 143 feasible designs within 10% mass of optimal, gauge choices	547
12.39	Performance, material & gauge choice for all 968 feasible designs	548
12.40	Performance, material & gauge choice for 143 feasible designs within 10% mass of optimal	548

List of Tables

2.1	FSV-1 and FSV-2 vehicle capacity	5
2.2	Powertrain options & performance	6
2.3	FSV-1 mass estimates (all in kg)	13
2.4	FSV-2 mass estimates (all in kg)	14
2.5	Cost of ownership, FSV-1	15
2.6	Cost of ownership, FSV-2	16
2.7	FSV fuel economy and CO ₂ emissions table	17
2.8	Well-to-Pump results (electricity generation)	19
2.9	Powertrain mass, cost, fuel consumption, and GHG emissions	24
2.10	Battery recommendation for FSV	26
2.11	Fuel cell recommendation for FSV	28
2.12	Electric motor recommendations for FSV	29
2.13	Internal Combustion Engine Recommendations - PHEV ₂₀ and PHEV ₄₀	30
2.14	Component weight savings - conventional vehicles versus Future Steel Vehicle	32
2.15	FSV wheels & tires	33
2.16	Estimated mass, cost and fuel economy impacts	34
2.17	CO ₂ emission requirements	35
3.1	Japan 2008 car taxation	42
3.2	OEM announcements	48
3.3	Battery electric vehicles	49
3.4	Battery electric vehicles	50
3.5	Battery electric vehicles	50
3.6	Fuel cell electric vehicles	51
3.7	Plug-in hybrid electric vehicles	52
3.8	Plug-in hybrid electric vehicles	53
3.9	i-MiEV data table	59
3.10	Prototype vehicle specifications	71
3.11	General specifications - FSV & Mitsubishi i-Miev	74
3.12	Battery specifications	79
3.13	Motor specifications	80
3.14	Tire & wheel specifications - i-MiEV and FSV-1	83
3.15	Interior specifications	84
3.16	General specifications - FSV & Honda FCX Clarity	87
3.17	Honda Clarity - mass savings	90
3.18	Layout - key points	91

Q

3.19	Battery specifications	93
3.20	Fuel Cell specifications	94
3.21	Hydrogen tank specifications	95
3.22	Motor specifications	96
3.23	Tire & wheel specifications - 2009 Honda Clarity and FSV-2	101
3.24	Interior specifications	102
3.25	General specifications - FSV-2 PHEV ₄₀ & Chevrolet Volt	106
3.26	Battery specifications - FSV-2 PHEV ₄₀ & Chevrolet Volt	111
3.27	ICE specifications - FSV-2 PHEV ₄₀ & Chevrolet Volt	112
3.28	Motor specifications - FSV-2 PHEV ₄₀ & Chevrolet Volt	113
3.29	Tire & wheel specifications - 2009 Chevy Volt and FSV-2	115
3.30	Interior specifications - - FSV & Chevrolet Volt	116
3.31	Mercedes Blue-Zero Dimensions comparison with FSV	118
3.32	General specifications - FSV (BEV) & Mercedes E-Cell	121
3.33	General specifications - FSV (FCEV) & Mercedes F-cell	122
3.34	General specifications - FSV (PHEV ₄₀) & Mercedes E Cell+	123
3.35	Estimated mass, cost and fuel economy impacts	126
3.36	Timeframe of adoption into the Indian regulatory standards	139
3.37	CO ₂ emission requirements	141
3.38	Average miles per gallon	144
3.39	Test cycle - JCO8 (cold and hot), applicable from March 2011	147
3.40	2015 fuel economy requirement for all fuels	147
3.41	Implementation timeline	150
3.42	US EPA - emission limits	151
3.43	CARB emission limits	152
3.44	US/CARB implementation timeline	153
3.45	European emission standards for gasoline	156
3.46	Vehicle Classification	159
3.48	USA vehicle classification	160
3.49	China vehicle classification	162
3.50	India vehicle classification	163
4.1	Industry perspectives	171
4.2	Vehicle design parameters for PHEV ₄₀ series & parallel-split	173
4.3	PHEV decision matrix	174
5.1	Future Steel Vehicle	176
5.2	FSV vehicle dimensions	178
5.3	FSV vehicle dimensions	179
5.4	FSV-1 and FSV-2 vehicle capacity	180
5.5	Powertrain options & performance	184
5.6	FSV-1 BEV estimated mass (kg)	187
5.7	BEV - Powertrain and fuel system mass & cost	187
5.8	Vehicle design parameters for BEV	189
5.9	BEV - Powertrain design parameters	190

5.10	BEV - Vehicle performance results	191
5.11	Mitsubishi i-MiEV data	194
5.12	Bill of materials : FSV-1 - EV	197
5.13	FSV-1 PHEV ₂₀ estimated mass (kg)	199
5.14	FSV-1 PHEV ₂₀ - Powertrain and fuel system mass & cost	199
5.15	Vehicle design parameters for PHEV ₂₀	201
5.16	Powertrain design parameters - PHEV ₂₀	201
5.17	Vehicle performance results - PHEV ₂₀	202
5.18	Bill of materials : FSV-1 - PHEV ₂₀	208
5.19	FSV-2 PHEV ₄₀ estimated mass (Kg)	210
5.20	FSV-2 PHEV ₄₀ - Powertrain and fuel system mass & cost	210
5.21	Vehicle design parameters PHEV ₄₀	212
5.22	Powertrain design parameters - PHEV ₄₀	212
5.23	Vehicle performance results - PHEV ₄₀	213
5.24	Bill of materials : FSV-2 - PHEV ₄₀	218
5.25	FSV-2 FCEV estimated mass (Kg)	220
5.26	FSV-2 FCEV - Powertrain and fuel system mass & cost	220
5.27	Vehicle design parameters FCEV	222
5.28	Powertrain design parameters - FCEV	222
5.29	Vehicle performance results - FCEV	223
5.30	Bill of materials : FSV-2 - FCEV	228
5.31	Vehicle simulation results summary	229
5.32	Fuel economy and emissions	231
5.33	Cost of ownership - FSV-2	232
5.34	Cost of ownership - FSV-1	233
6.1	FSV-1 BEV battery specifications	248
6.2	FSV-1 Battery specs with NEDO3 targets	250
6.3	Front suspension design - Decision matrix	276
6.4	Rear suspension design - Decision matrix	276
7.1	Battery recommendation for FSV	281
7.2	Current cell technology	281
7.3	Energy storage limits [49]	286
7.4	FSV-1 BEV battery specifications (new pack)	287
7.5	FSV-1 BEV battery specifications (end of life)	287
7.6	FSV-1 BEV final battery specifications (end of life)	287
7.7	FSV-1 Battery specs with NEDO3 targets	289
7.8	Battery case study results	290
7.9	FSV battery shape assessment	292
7.10	Electric motor recommendations for FSV	293
7.11	DOE motor and power electronics targets	294
7.12	FSV motor and gasoline ICE	294
7.13	FSV motor & transmission case studies	295
7.14	Fuel Cell recommendation for FSV	300

8.1	Selected facts and figures 2002 (Source: US Department of Transportation - Federal Highway Administration)	305
8.2	Well-to-Pump results (electricity generation)	307
8.3	FSV fuel economy and CO ₂ emissions table	309
8.4	Pump-to-Wheel GHG CO ₂ emissions	313
9.1	Types of fuel cells and applications	323
9.2	Main suppliers of fuel cell stack and system	324
9.3	Fuel cell recommendation for FSV	326
9.4	Comparison of different compressors	332
9.5	Sizes and weight of proposed FCS	349
9.6	Fuel Cell Module key parameters	352
9.7	Air compressor key parameters	352
9.8	Parameters of G/G humidifier	353
9.9	Recirculation pump key parameters	354
9.10	H ₂ storage system decision matrix	361
9.11	Battery recommendation for FSV	367
9.12	Lithium-ion cell battery suppliers and key cell characteristics	375
9.13	Battery decision matrix	376
9.14	Energy balance table	392
9.15	Transmission comparison	397
9.16	Electric motor recommendations for FSV	405
9.17	Generator recommendations for FSV	405
10.1	Range of steels available for FSV	413
10.2	Tonnage and coil recommendations	418
10.3	Material combinations laser welded coils	419
10.4	T ³ profiling advantages matrix	427
10.5	Restrictions between the T ³ - U/O and T ³ - W process	427
10.6	Material combinations for laser welded coils	432
11.1	Conventional mechanical steering system versus Steer-by-Wire systems	464
11.2	UTQG traction grades	482
11.3	UTQG temperature resistance	483
11.4	Component weight savings - Conventional vehicles versus Future Steel Vehicle	487
11.5	Combined benefits of laminated glass	490
11.6	Acoustical windshield weight savings calculator	491
11.7	Side glass laminate weight savings calculator	491
11.8	Peak and average power requirements	504
11.9	EV-range simulation results	506
11.10	HEV - Fuel economy range simulation results	506
11.11	Automotive windshields	510
11.12	Parked car ventilation table	511
12.1	Baseline model performance summary	524

12.2	Control points	530
12.3	Material & gauge variables	531
12.4	3G Optimization problem statement	531
12.5	Final design - material & gauge selections	532
12.6	Final design - cross-sectional variation along rail	539
12.7	Time calculation	544